frontiers | Research Topics

Soil microorganisms under ecological planting

Edited by
Ming Liu, Muhammad Saleem and Jia Liu

Coordinated by
Pengfa Li

Published in
Frontiers in Microbiology

ISSN 1664-8714
ISBN 978-2-8325-3299-7
DOI 10.3389/978-2-8325-3299-7

About Frontiers

Frontiers is more than just an open access publisher of scholarly articles: it is a pioneering approach to the world of academia, radically improving the way scholarly research is managed. The grand vision of Frontiers is a world where all people have an equal opportunity to seek, share and generate knowledge. Frontiers provides immediate and permanent online open access to all its publications, but this alone is not enough to realize our grand goals.

Frontiers journal series

The Frontiers journal series is a multi-tier and interdisciplinary set of open-access, online journals, promising a paradigm shift from the current review, selection and dissemination processes in academic publishing. All Frontiers journals are driven by researchers for researchers; therefore, they constitute a service to the scholarly community. At the same time, the *Frontiers journal series* operates on a revolutionary invention, the tiered publishing system, initially addressing specific communities of scholars, and gradually climbing up to broader public understanding, thus serving the interests of the lay society, too.

Dedication to quality

Each Frontiers article is a landmark of the highest quality, thanks to genuinely collaborative interactions between authors and review editors, who include some of the world's best academicians. Research must be certified by peers before entering a stream of knowledge that may eventually reach the public - and shape society; therefore, Frontiers only applies the most rigorous and unbiased reviews. Frontiers revolutionizes research publishing by freely delivering the most outstanding research, evaluated with no bias from both the academic and social point of view. By applying the most advanced information technologies, Frontiers is catapulting scholarly publishing into a new generation.

What are Frontiers Research Topics?

Frontiers Research Topics are very popular trademarks of the *Frontiers journals series*: they are collections of at least ten articles, all centered on a particular subject. With their unique mix of varied contributions from Original Research to Review Articles, Frontiers Research Topics unify the most influential researchers, the latest key findings and historical advances in a hot research area.

Find out more on how to host your own Frontiers Research Topic or contribute to one as an author by contacting the Frontiers editorial office: frontiersin.org/about/contact

Soil microorganisms under ecological planting

Topic editors

Ming Liu — Institute of Soil Science, Chinese Academy of Sciences (CAS), China

Muhammad Saleem — Alabama State University, United States

Jia Liu — Jiangxi Academy of Agricultural Sciences (CAAS), China

Topic coordinator

Pengfa Li — Nanjing Agricultural University, China

Citation

Liu, M., Saleem, M., Liu, J., Li, P., eds. (2023). *Soil microorganisms under ecological planting*. Lausanne: Frontiers Media SA. doi: 10.3389/978-2-8325-3299-7

Table of contents

frontiers | Frontiers in Microbiology

TYPE Editorial
PUBLISHED 08 August 2023
DOI 10.3389/fmicb.2023.1227230

OPEN ACCESS

EDITED AND REVIEWED BY
Trevor Carlos Charles,
University of Waterloo, Canada

*CORRESPONDENCE
Ming Liu
✉ mliu@issas.ac.cn

RECEIVED 22 May 2023
ACCEPTED 17 July 2023
PUBLISHED 08 August 2023

CITATION
Li P, Liu J, Saleem M and Liu M (2023) Editorial: Soil microorganisms under ecological planting. *Front. Microbiol.* 14:1227230. doi: 10.3389/fmicb.2023.1227230

Editorial: Soil microorganisms under ecological planting

Pengfa Li[1,2], Jia Liu[3], Muhammad Saleem[4] and Ming Liu[1,5]*

[1]State Key Laboratory of Soil and Sustainable Agriculture/Institute of Soil Science, Chinese Academy of Sciences, Nanjing, China, [2]Department of Microbiology, College of Life Sciences, Nanjing Agricultural University/Key Laboratory of Agricultural and Environmental Microbiology, Ministry of Agriculture and Rural Affairs, Nanjing, China, [3]National Engineering and Technology Research Center for Red Soil Improvement/Institute of Soil & Fertilizer and Resources & Environment, Jiangxi Academy of Agricultural Sciences, Nanchang, China, [4]Department of Biological Sciences, Alabama State University, Montgomery, AL, United States, [5]University of Chinese Academy of Sciences, Nanjing/University of Chinese Academy of Sciences, Beijing, China

KEYWORDS

soil sustainability, plant productivity, crop rotation, intercropping, soil microorganism, element cycle, plant-microbe interactions

Editorial on the Research Topic
Soil microorganisms under ecological planting

As the global human population is expected to reach nine billion by 2050, ensuring stable and sufficient food, poultry, and fiber supplies is a major challenge. To increase food production, chemical fertilizers and pesticides have been widely used in agriculture, but they have caused serious harm to the environment and human health. Therefore, it is urgent to adopt sustainable agricultural practices that can improve and maintain crop yield and quality. One such practice is ecological planting, which combines traditional methods of crop rotation, intercropping, or relay intercropping with modern agricultural technology, based on the growth rhythm of different crops on a unit area of land. This way, natural and biological resources, such as light, heat, water, and fertilizer, can be used more efficiently and fully to achieve higher yield and economic and ecological benefits.

Soil microorganisms link above-ground and below-ground ecosystems and play an important role in soil nutrient cycling, soil-borne disease control, and other ecosystem processes. Ecological planting can increase above-ground plant diversity and subsequently influence below-ground microorganisms. However, the effects of above-ground crops on below-ground microorganisms are still unclear and contradictory. For example, how microorganisms drive the cycling of C, N, P, S, and other elements or pollutants under different cropping patterns is a cutting-edge topic that is far from clear. Moreover, the complex plant–microbe interactions, such as the relationship between plant disease, soil-borne phytopathogens, and plant-beneficial microbes, under ecological planting remain poorly understood.

In this Research Topic, 13 articles were published, providing a deeper understanding of microbial response, process, and function under ecological planting. We aim to elucidate the response of the under-ground microbial process and ecological function, the interaction mechanisms between beneficial microbes and pathogens, and the changes in microbial community and metabolites under different cropping patterns with different management strategies. These findings will advance our understanding of soil microbial ecological processes and functions under ecological planting.

Xiang et al. studied the effects of green manure (hairy vetch) and peanut straw on soil fertility, peanut yield, and the AMF community in Ultisol dryland. The study found that the application of green manure improved soil nutrients and peanut yield and promoted the positive feedback relationship between peanut and the AMF community by increasing

soil AMF abundance and network stability. In rice cultivation, leguminous crop rotation can increase soil productivity, but little is known about the role of microorganisms in soil productivity under leguminous crop rotation. Xia et al. found that Chinese milk vetch rotation can enrich key microbial groups with potential phosphorus dissolution ability, increase soil available phosphorus content, and ultimately increase crop yield. The appropriate amount of Chinese milk vetch instead of chemical fertilizer can also improve the nitrogen cycle function of key ecological bacterial communities in soil (Lv et al.). Reasonable nitrogen application and organic agriculture, including Chinese milk vetch returning, can also effectively improve soil microbial diversity and soil fertility in wheat–rice rotation (Xu et al.).

Besides the farmland ecosystem, Sun et al. studied soil microbial changes under the *Cinnamomum camphora* canopy and between *C. camphora* trees. The study showed that *C. camphora* planting can improve soil fertility in subtropical regions and promote the transformation of soil microbial communities from *oligotrophic* (K-strategy) to *eutrophic* bacteria (r-strategy). The effects of canopy nitrogen addition and understory management on soil microbial communities in Chinese fir forests were also investigated. The results showed that short-term canopy nitrogen addition changed soil bacterial and fungal communities, leading to a stronger response in the surface and middle soil layers than in the deep soil layer, while understory removal may enhance the effect on soil bacterial abundance (Xi et al.).

Regarding the inhibition of soil-borne diseases and the elimination of soil pollution, studies have found that when tomato plants are infected by pathogens, some harmful biological pathways such as quorum sensing are significantly enriched, while some beneficial biological pathways such as streptomycin biosynthesis are depleted. These findings extend our understanding of plant–microbe interactions and provide new clues for understanding the underlying mechanisms of interactions between plant microbial communities and pathogens (Kuang et al.). Li Q.-M. et al. found that rotation significantly changed the composition of bacterial and fungal communities, increased potentially plant-beneficial fungi, and reduced the relative abundance of potentially phytopathogenic fungi. You et al. found that *Glomus mosseae* affected the rhizosphere microbial community by regulating soil properties and greatly enhanced the cadmium remediation ability of *Solanum nigrum*.

With respect to biological network interactions and microbial and metabolite interactions, a 10-year field experiment revealed that the potential predation pressure of nematodes on bacteria may enhance bacterial abundance, which in turn has a positive effect on carbon fixation. The interaction between nematodes and microorganisms plays an important role in regulating carbon dynamics under the return of organic matter (Shi et al.). Li M. et al. found that different compounds in root exudates were the main driving factors affecting the microbial community in the *Populus* rhizosphere. The key taxa of the rhizosphere microbial community are very important for maintaining the rhizosphere stability. Root exudates had a stronger effect on key bacteria than on dominant bacteria and fungi. Zhang et al. found that the use of enzymatic fermented soybean fertilizer can improve soil nutrition, regulate related microbial communities, and have a positive impact on the lipid metabolites of new tea shoots, which provides feasible technical guidance for the use of soybean as an advanced fertilizer to produce high-quality tea.

Moreover, the effects of habitat fragmentation on soil microbial biomass, diversity, and community assembly under two typical plants in the mainland–island system were also investigated (Wu et al.).

For future research on microbial processes under ecological planting, the following aspects should also be considered. First, unraveling the complex plant–microorganism interaction mechanisms under the ecological planting pattern. Second, developing and optimizing ecological planting strategies for the synergistic improvement of soil quality and plant productivity. Third, understanding the transformation of soil carbon and carbon sequestration and emission reduction under ecological planting in the context of climate change. Fourth, achieving the One Health concept for soil, plants, microorganisms, the environment, and human health by using ecological planting.

Author contributions

PFLi and MLiu revised the manuscript and wrote the final version of the manuscript. All authors listed have made a substantial, direct, and intellectual contribution to the work and approved it for publication.

Funding

This work was funded by the National Key Research and Development Program of China (Nos. 2022YFD1900603 and 2021YFD1901201), the National Natural Science Foundation of China (No. 42177294), the Key Research and Development Program of Jiangxi Province (No. 20212BBF63007), the China Agriculture Research System of MOF and MARA (No. CARS-22), the Jinggangshan Agricultural Hi-tech District Project (No. 20222-051261), and the Central Guidance for Local Science and Technology Development Projects (No. 20231ZDD02003).

Acknowledgments

We thank Prof. Xiaoyan Ma from Beijing Institute of Technology for his advice in the writing.

Conflict of interest

The authors declare that the research was conducted in the absence of any commercial or financial relationships that could be construed as a potential conflict of interest.

Publisher's note

frontiers | Frontiers in Microbiology

TYPE Original Research
PUBLISHED 23 August 2022
DOI 10.3389/fmicb.2022.992823

OPEN ACCESS

EDITED BY
Ming Liu,
Institute of Soil Science (CAS), China

REVIEWED BY
Lei Xu,
Heilongjiang Bayi Agricultural University, China
Yang Jian,
Ningbo University, China

*CORRESPONDENCE
Zhaotang Ding
dzttea@163.com

SPECIALTY SECTION
This article was submitted to Microbe and Virus Interactions with Plants, a section of the journal Frontiers in Microbiology

RECEIVED 13 July 2022
ACCEPTED 04 August 2022
PUBLISHED 23 August 2022

CITATION
Zhang S, Sun L, Shi Y, Song Y, Wang Y, Fan K, Zong R, Li Y, Wang L, Bi C and Ding Z (2022) The application of enzymatic fermented soybean effectively regulates associated microbial communities in tea soil and positively affects lipid metabolites in tea new shoots.
Front. Microbiol. 13:992823.
doi: 10.3389/fmicb.2022.992823

The application of enzymatic fermented soybean effectively regulates associated microbial communities in tea soil and positively affects lipid metabolites in tea new shoots

Shuning Zhang[1], Litao Sun[2], Yujie Shi[1], Yujie Song[1], Yu Wang[1], Kai Fan[1], Rui Zong[3], Yusheng Li[4], Linjun Wang[5], Caihong Bi[6] and Zhaotang Ding[1,2]*

[1]Tea Research Institute, Qingdao Agricultural University, Qingdao, China, [2]Tea Research Institute, Shandong Academy of Agricultural Sciences, Jinan, China, [3]Qingdao Hexie Biotechnology Co., Ltd., Qingdao, China, [4]Shandong Agricultural Technology Extension Center, Jinan, China, [5]Weihai Agricultural and Rural Affairs Service Center, Weihai, China, [6]Linyi Agricultural Technology Extension Center, Linyi, China

Compared with traditional organic fertilizer, fermented soybean is a better fertilizer resource in tea plantations. The application of organic fertilizer is a feasible practice to mitigate the soil degradation caused by the overuse of chemical fertilizers, which can effectively regulate soil microbial communities in tea plantations. However, the effects of fermented soybean on soil microbial communities, soil metabolites and metabolites in tea new shoots have not been systematically demonstrated, and their interactions have never been studied. Here, we investigated the responses of the soil microbial community, soil metabolites and metabolites of tea new shoots to urea fertilization (UF), naturally fermented soybean fertilization (NFS) and enzymatic fermented soybean fertilization (EFS), and analyzed the relationships between soil microbes, soil metabolites and metabolites in tea new shoots. The results showed that soil bacterial communities were dominated by *Pseudomonas*, *Romboutsia*, *Candidatus_Nitrosotalea* and *Helicobacter*, and soil fungal communities were dominated by *Peziza*, *Fusarium*, *Candida* and *Cheilymenia* at the genus level. In EFS, bacterial genera (*Glutamicibacter* and *Streptomyces*) and fungal genera (*Candida* and *Actinomucor*) presented high abundances, which were correlated with soil carbohydrate and lipid including D-Mannitol, D-Sorbitol, 9,12-Octadecadienoic acid and (Z)-13-Docosenoic acid. Enzymatic fermented soybean fertilization also affected the lipid metabolites in tea new shoots. Glycerolipids and glycerophospholipids significantly increased in EFS, which positively correlated with some soil microbial communities. Besides, the application of fermented soybean fertilizer could increase the contents of TP, AP and AK, which were also important environmental factors affecting

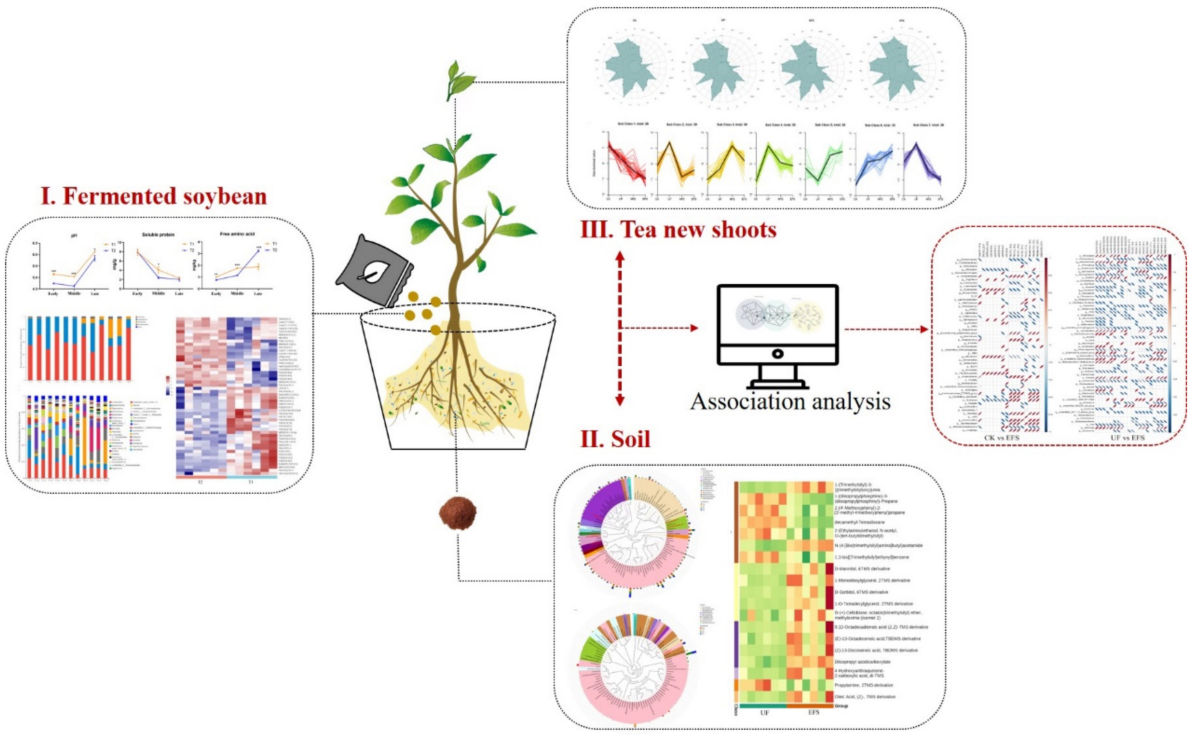

GRAPHICAL ABSTRACT

the structure of soil microbial community in tea plantation. It was concluded that fermented soybean fertilization could improve soil nutrition, regulate associated microbial communities, and positively affect lipid metabolites in tea new shoots. This study not only explores the relationships between soil microbes and metabolites in tea plants, but also provides feasible technical guidance to cultivate high-quality tea using soybean as high-grade fertilizer.

KEYWORDS

tea, fermented soybean, fertilization, microbial communities, metabolite profiling

Introduction

Tea (*Camellia sinensis* (L.) Kuntze) is a perennial evergreen leaf-used economic plant. Its internal rich metabolites confer tea elegant flavors and healthy function (Wachira et al., 2013). The tea taste was influenced by well-characterized non-volatile metabolites including polyphenols, flavonoids, theanine and alkaloids, and the source of tea aroma was volatile metabolites including terpenoids, phenylpropanoids and fatty acid derivatives (Yang et al., 2013; Daglia et al., 2014). Among them, lipid was the main contributor to the generation of flavor and aroma compounds in tea leaves. The oxidation products of free fatty acids including (Z)-3-hexenol, its esters and (E)-2-hexenal principally contribute to the fresh odor of green tea (Ho et al., 2015). The changes of lipids in tea plants could affect the formation of aroma-generating compounds and thus the final tea quality (Liu et al., 2017). In addition, plants and their microbiome were highly interlinked and might have co-evolved to function as integrated ecologies (Pang et al., 2021). Soil microbiomes, as the second genome of plants, could provide

plants with microbe-derived metabolites and traits (Pascale et al., 2020). Some microbiomes could assist the plant in nutrient absorption, pathogen resistance and growth promotion (Turner et al., 2013). Kudjordjie et al. (2019) and Maggini et al. (2020) reported that the key microbiomes played important roles in promoting the growth and development of maize and echinacea plants. Korenblum et al. (2020) investigated that rhizosphere bacteria could trigger the systemic exudation of acyl sugars and changed the leaf metabolites and transcriptomes in tomato plants (Korenblum et al., 2020). In tea plants, the tea microbiome has shown that it could help the plant with soil nutrient acquisition and stress management. Arbuscular Mycorrhizal Fungi (AMF) and some beneficial microorganisms could colonize in tea roots, which was beneficial to tea growth by increasing the contents of amino acids, protein, caffeine, and polyphenols (Bag et al., 2022).

Soil is a complex bioreactor and a nutrition stronghold of microbial communities. Thousands of bacteria and fungi coexisted in soil using various organic carbon sources (Fierer, 2017). Soil is also the main hub of fertilizer transportation and can act directly on plant roots (Edwards et al., 2015; Bonanomi et al., 2018). In recent years, tea industry had increasingly moved toward refinement, modernization and intensification. More and more tea farmers applied heavy chemical fertilization for high yield and quality components in tea plantations, which could cause environment problems and soil degradation (Ni et al., 2018; Yang et al., 2018). It could finally cause inhibit tea growth and affect the tea quality and yield (Fung et al., 2008; Arafat et al., 2019). So, the organic fertilizer was applied as direct and effective management in tea plantations to realize the synchronization of nutrient supply and quality improvement of tea plants. Soybean was an excellent choice with rich in high-quality plant protein, which was usually used as organic fertilizer in tea plantations of China. In agricultural production, soybeans should need a solid fermentation process before application, which could improve the effective utilization. However, it might lead to some problems such as malodorous gas volatilization and inadequate conversion (Gupta et al., 2018). Currently, the addition of enzymes and bacteria could accelerate the fermentation processes and reduce the risk of fermentation failure (Park et al., 2010). Lee et al. (2014) and Park and Kim (2020) reported that the effects of various microbial starters on volatile and non-volatile metabolites during soybean fermentation, indicating biotransformation in fermentation had the potential to improve the soybean nutritional value. Therefore, enzymes and bacteria were applied in soybean fermentation to obtain better fertilizer effects.

In recent years, the direct analyses of microbial communities using high-throughput sequencing technology have become more and more accurate and effective. The combination of microbiome research and multi-omics methods has deepened our understanding of the relationships between microbiomes and plants. However, it is far from enough to pay attention to the single effect of soil nutrition and tea quality improvement after organic fertilization in tea plantation, which seriously ignores the relationships between the underground and aboveground parts of tea plants. The interactions of soil microbiomes, soil metabolites and metabolites in tea new shoots remain unclear. In this study, we investigated microbial communities and metabolites in soybean in the naturally fermented way and enzymatic fermented way. After fertilization, we studied the effects of naturally fermented soybean fertilization and enzymatic fermented soybean fertilization on soil microbial communities, soil metabolites and metabolites of tea new shoots by using 16S and ITS rRNA sequencing, GC-MS, and UPLC-MS, respectively. We also analyzed the relationships of key microbial communities, key metabolites in soil and metabolites of tea new shoots. This study provided feasible technical guidance for fermented soybean application in tea plantation. In addition, exploring the microbial communities related to the metabolites of tea new shoots can also have potential contributions to tea flavor improvement.

Materials and methods

Soybean fermentation and collection

The experiment was conducted in Qingdao, Shandong Province, China (36° 18' N, 120° 7' E) in 2020. Fermented soybeans were prepared in plastic barrels with 50 L. The diameter of the barrel bottom is 38 cm, and the height is 58 cm. Before fermentation, each barrel needs to be cleaned and air dried. In this experiment, we used natural fermentation (T1) and enzyme fermentation (T2) to ferment soybean. Firstly, 5 kg soybeans and 9 L sterile water were added to each fermentation barrel. Soybean and water were fully mixed in the ratio of 1:1.8. The enzyme preparation was a mixed powder with bacteria and enzymes (the number of effective viable bacteria $\geq$ 20 billion/g and the total enzyme activity > 10,000 u/g). The main bacteria were *Saccharomycetes*, *Lactobacillus*, *Brevibacterium* and *Bacillus licheniformis*, and the enzymes mainly included cellulase, lipase and neutral xylanase. This was added to the soybean at a 2‰ ratio based on the total weight of soybeans and water. The whole fermentation process was facultative anaerobic fermentation, which lasted for 21 days. At 3, 12, and 21 days, fermented soybeans were collected at random under aseptic conditions. Then, each sample with six replications was divided into two parts, one part was stored at 4°C to determine its physical and chemical properties, and the other part was frozen at −80°C to determine its bacterial composition and metabolites.

Fermented soybean sampling and analysis

Microbial DNA was extracted from fermented soybean using the E.Z.N.A.® soil DNA Kit (Omega Bio-Tek, Norcross, GA, United States). The final DNA concentration and purification were determined by NanoDrop 2000 UV–vis spectrophotometer (Thermo Scientific, Wilmington, NC, United States), and DNA quality was checked by 1% agarose gel electrophoresis. The V3–V4 hypervariable regions of the bacterial 16S rRNA gene were amplified with primers 338Fand 806R by thermocycler PCR system (GeneAmp 9700, ABI, Foster City, CA, United States). PCR amplification and Illumina MiSeq sequencing were performed according to previous methods (Zhang et al., 2020c).

UHPLC-MS analysis of fermented soybean was performed on a Thermo UHPLC system equipped with an ACQUITY BEH C18 column (100 mm × 2.1 mm i.d, 1.7 μm; Waters, Milford, MA, United States). Firstly, the metabolites were extracted using a 400 μl methanol: water (4:1, v/v) solution. The mixture was allowed to settle at −20°C and treated by a high throughput tissue crusher Wonbio-96c (Shanghai Wanbo Biotechnology Co., Ltd., Shanghai, China). The samples were placed and centrifugated, and the supernatant was carefully transferred to sample vials for LC-MS/MS analysis. The mobile phases consisted of 0.1% formic acid in water (solvent A) and 0.1% formic acid in acetonitrile: isopropanol (1:1, v/v; solvent B). Then, the mass spectrometric data were collected using a Thermo UHPLiC-Q Exactive Mass Spectrometer equipped with an electrospray ionization (ESI) source operating in either positive or negative ion mode. After UPLC-TOF/MS analyses, the raw data were imported into the Progenesis QI 2.3 (Nonlinear Dynamics, Waters, Milford, MA, United States) for peak detection and alignment. Finally, quality control and data annotation were performed.

Pot experiment

The experiment was conducted in Qingdao, Shandong Province, China (36°18′N, 120°7′E) in 2020. A 2-year-old tea seeding of "*Zhongcha 108*" [*C. sinensis* (L.) O. Kuntze] were planted in plastic pots with 28 cm diameter and 18 cm high. Four tea plants were in each pot. The soil was brown loam with a pH of 5.92, soil organic matter of 36.92 g/kg and total nitrogen content of 1.13 g/kg. The environmental conditions in the greenhouse were as followed: the temperature was 26°C/20°C (day/night), air humidity was 55% and light time lasted 12 h per day. The experiment consisted of four treatments: control (CK), urea fertilization (UF), naturally fermented soybean fertilization (NFS) and enzymatic soybean fertilization (EFS). Each treatment consisted of six replicates. The application of nitrogen content was based on the previous study (Yang et al., 2018). 3 g urea was applied to each pot in UF, and 20 g fermented soybean was applied to each pot in NFS and EFS. The fertilizer position was 5 cm on the side of each tea seedling and 10 cm in depth. Finally, the fertilizer holes were covered with topsoil and watered adequately. One month after fertilization, the soil and tea new shoots were sampled 1 month after fertilization. Soil samples were divided into two parts: one part was frozen quickly in liquid nitrogen and stored at −80°C until the microbial communities and soil metabolites were analyzed, and the other part was dried naturally in the room and then analyzed for physicochemical indexes. Tea new shoots were frozen quickly in liquid nitrogen and stored at -80°C until metabolites were analyzed.

Soil sampling and analysis

Microbial DNA was extracted from soil using the E.Z.N.A.® soil DNA Kit (Omega Bio-Tek, Norcross, GA, United States). DNA concentration was detected by agarose gel electrophoresis PCR amplification was performed. The V4 hypervariable regions of the bacterial 16S rRNA gene were amplified with primers 515F and 806R by thermocycler PCR system (GeneAmp 9700, ABI, United States), and the ITS1 hypervariable regions of the fungal ITS gene were amplified with primers ITS5-1737F and ITS2-2043R. The purified amplicons were pooled and constructed using TruSeq® DNA PCR-Free Sample Preparation Kit library construction Kit. The constructed libraries were quantified by Qubit and Q-PCR and then sequenced by NovaseQ6000.

GC-MS analysis of soil was performed on Agilent 7890B gas chromatograph coupled to a 7000D mass spectrometer with a DB-5MS column (30 m length × 0.25 mm i.d. × 0.25 μm film thickness, J&W Scientific, Folsom, CA, United States). Firstly, the freeze-dried soil materials were crushed using a mixer mill (MM 400, Retsch) with a zirconia bead for 1.5 min at 30 Hz. 500 mg powder was diluted to a 500 μl with methanol: isopropanol: water (3:3:2 V/V/V), vortexed for 3 min and ultrasound for 30 min. The extracts were centrifuged at 12,000 r/min under 4°C for 3 min. Then, helium was used as the carrier gas, at a flow rate of 1 ml/min. Injections were made in the front inlet mode with a split ratio of 10:1 and the injection volume was 1 μL. The oven temperature was held at 40°C for 1 min and then raised to 100°C at 20°C/min, raised to 300°C at 10°C/min, and held at 300°C for 5 min. All samples were analyzed in scan mode. The injector inlet and transfer line temperatures were 250 and 280°C, respectively. Finally, quality control and data annotation were performed.

Tea new shoots sampling and analysis

The extracts and determination of each sample were performed by Wuhan Metware Biotechnology Co., Ltd., China[1] using a UPLC-MS/MS system (UPLC, SHIMADZUNexera X2; MS, Applied Biosystems 4500 Q TRAP) equipped with an Agilent SB-C18 (1.8 μm, 2.1 mm × 100 mm). Firstly, tea new shoots were freeze-dried by the vacuum freeze-dryer and crushed by a mixer mill. 100 mg of lyophilized powder were dissolved with 1.2 ml 70% methanol solution and placed in a refrigerator at 4°C overnight. Following centrifugation at 12,000 rpm for 10 min, the extracts were filtrated (SCAA-104, 0.22 μm pore size; ANPEL, Shanghai, China[2]) before UPLC-MS/MS analysis. The mobile phase consisted of solvent A, pure water with 0.1% formic acid, and solvent B, acetonitrile with 0.1% formic acid. Sample measurements were performed with a gradient program that employed the starting conditions of 95% A and 5% B. Within 9 min, a linear gradient to 5% A, 95% B was programmed, and a composition of 5% A, 95% B was kept for 1 min. Subsequently, a composition of 95% A and 5.0% B was adjusted within 1.10 min and kept for 2.9 min. The flow velocity was set as 0.35 ml per minute; The column oven was set to 40°C; The injection volume was 4 μl. The effluent was alternatively connected to an ESI-triple quadrupole-linear ion trap (QTRAP)-MS. Quality control and data annotation were performed according to previous methods.

Statistical analysis

One-way analysis of variance (ANOVA) with Duncan's test was used to determine significant differences ($p < 0.05$) among soybean nutrition analysis, soil properties and enzyme activities, as well as the relative abundance of microbial taxa. The LDA Effect Size algorithm used the non-parametric factorial Kruskal Wallis sum rank test to detect microbial groups with significant abundance differences. The Circos graph was used to visualize the composition of microbial communities using Circos-0.67-7 software.[3] The HCA (hierarchical cluster analysis) results of samples and metabolites were presented as heatmaps with dendrograms, while Pearson correlation coefficients (PCC) between samples were calculated by the cor function in R and presented as only heatmaps. Both HCA and PCC were carried out by R package. For HCA, normalized signal intensities of metabolites (unit variance scaling) are visualized as a color spectrum. Significantly regulated metabolites between groups were determined by VIP and absolute Log_2FC (fold change). VIP values were extracted from the OPLS-DA result containing score plots and permutation plots were generated using the R package MetaboAnalyst. The data was log transform (log_2) and mean centering before OPLS-DA. To avoid overfitting, a permutation test (200 permutations) was performed. The heatmaps about metabolites were normalized by unit variance scaling and processed "pheatmap" in R software, and the heatmaps about the correlation between differential metabolites and microorganisms were normalized by unit variance scaling and processed "corrplot" in R software. All statistical analyses were performed using the R platform (version3.5.0).

1 https://www.metware.cn
2 http://www.anpel.com.cn/
3 http://circos.ca/

Results

Effects of different fermentation methods on soybean fermentation

To evaluate the effects of different fermentation ways on soybean, we analyzed the pH value and nutrition contents at the early, middle and late stages of fermentation. In the whole fermentation process, the pH value of T2 was significantly lower than that of T1. As the fermentation process went on, the content of soluble protein in soybean gradually decreased, while the content of free amino acids gradually increased. The content of free amino acids in T2 was significantly higher than that in T1 at the late stage of fermentation (**Supplementary Figure 1A**). In addition, we also analyzed the contents of amino acids in fermented soybean. In two fermentation ways, the contents of tyrosine and histidine were relatively higher, and the contents of cystine and serine were lower than the other amino acids. The contents of 20 amino acids in T2 were significantly higher than that in T1 (**Supplementary Figure 1B**). At the last stage of fermentation, the nutrients in soybean were fully decomposed. So, the following analysis was focused on soybean in the late stage of fermentation.

To analyze the changes of bacterial communities in fermented soybeans, we studied the composition and structure of bacterial communities at the phylum and genus level using 16S rRNA gene sequencing. At the phylum level, *Firmicutes*, *Proteobacteria*, *Bacteroidota* and *Actinobacteriota* were the dominant phyla in fermented soybean (**Supplementary Figure 2A**). At the genus level, *Lactobacillus*, *Ignatzschineria*, *Peptoniphilus*, *Enterococcus* and *Bacteroides* were the dominant genus in fermented soybean (**Supplementary Figure 2B**). In addition, we also studied the key bacterial communities that could explain the differences between natural fermentation and enzymatic fermentation using linear discriminant analysis of effect size (LEfSe; **Supplementary Figure 2C**). Overall, the bacterial communities with significant differences in T2 were different from that in T1. Specifically, significant enrichments of *Proteobacteria, Firmicutes* and *Bacteroidota* were in T2. *Proteobacteria* included *g_Ralstonia*, *g_norank_f_norank_o_Enterobacterales*, *o_Sphingomonadales*, *o_Rhizobiales* and *c_Alphaproteobacteria*. *Firmicutes* included

TABLE 1 The physicochemical properties of soils after fermented soybean fertilization.

	pH	OM g/kg	TN g/kg	TP g/kg	TK g/kg	AN mg/kg	AP mg/kg	AK mg/kg	Ca g/kg	Mg g/kg	Na g/kg	Cu mg/kg	Zn mg/kg
CK	6.68 ± 0.11a	93.77 ± 35.13b	2.55 ± 0.40c	0.64 ± 0.20b	14.03 ± 1.03a	70.16 ± 7.99c	131.20 ± 34.34b	285.53 ± 13.62b	3.86 ± 0.37a	2.68 ± 0.03ab	1.64 ± 0.24a	18.22 ± 8.07a	83.62 ± 6.41a
UF	5.19 ± 0.16c	175.52 ± 82.59ab	4.76 ± 1.71ab	0.82 ± 0.18b	11.26 ± 2.01a	186.50 ± 8.16a	158.77 ± 48.40b	371.37 ± 92.03b	3.85 ± 0.40a	2.42 ± 0.12ab	1.60 ± 0.06a	10.81 ± 3.09a	74.88 ± 4.38ab
NFS	6.21 ± 0.14b	192.29 ± 27.38ab	5.97 ± 2.20a	0.93 ± 0.11ab	8.39 ± 4.98a	146.64 ± 11.10b	245.17 ± 33.21ab	436.27 ± 45.00ab	3.71 ± 0.40a	2.29 ± 0.42c	1.87 ± 0.76a	12.08 ± 3.30a	72.33 ± 3.96b
EFS	6.31 ± 0.14b	209.37 ± 47.40a	4.91 ± 1.22ab	1.25 ± 0.18a	11.69 ± 0.99a	125.46 ± 13.37b	410.42 ± 147.52a	695.27 ± 176.77a	3.60 ± 0.20a	2.84 ± 0.30a	1.88 ± 0.89a	14.43 ± 5.37a	78.10 ± 4.16ab

Values with the same letter are not significantly different ($p < 0.05$).
CK, control experiment; UF, urea fertilization; NFS, naturally fermented soybean fertilization; EFS, enzymatic fermented soybean fertilization.

g_Peptoniphilus, *g_Gallicola*, *g_Bacillus*, *g_Erysipelothrix* and *g_Leuconostoc*. *Bacteroidota* included *g_Bacteroides*, *f_Bacteroidaceae*, *g_Dysgonomonas* and *g_Sphingobacterium*. Therefore, the species of bacterial community with high abundances did not change significantly, but the internal structure of the bacterial community changed significantly in soybean with enzymatic fermentation.

To reveal the marked differences of metabolites in fermented soybeans, lipid metabolites were performed. A total of 247 lipid molecular species were identified in fermented soybean. The Euclidean distance coefficient method was used to visualize the lipid metabolites with significant differences between natural fermentation and enzymatic fermentation in soybeans (**Supplementary Figure 3A**). According to the selecting criteria of fold change, VIP value and *p*-value (fold change $\geq$ 1.5 and fold change $\leq$ 0.67; VIP $\geq$ 1; $p < 0.05$), 22 lipid metabolites exhibited significant up-regulation in EFS including glycerophospholipids [PA(18:0/16:0), PA(24:0/18:2), PA(16:0/18:3), LPMe(14:0), PMe(16:0/18:3), PMe(18:2/23:0) and PG(18:3e/18:1)], glycerolipids [DGMG(18:2), MGDG(16:0/12:2), MGDG(18:1/29:2), MGDG(18:2/10:0), MG(18:3), TG(27:0/18:0/18:2) and DG(15:0/18:1)], and sphingolipid [Cer(m17:1/18:2), Cer(d17:1/17:0 + O), Cer(d18:1/18:2 + 2O), Cer(t18:1/18:0 + 2O), Cer(t18:1/18:0 + 2O), Cer(t17:1/16:0 + O), CerG2GNAc1(m19:1/18:3) and Hex2Cer(d23:0/18:2)]. To explore the correlations between metabolites and bacterial communities in fermented soybeans, we used spearman coefficient to calculate the correlation coefficient and determined the statistically significant correlation through rank correlation test (**Supplementary Figure 3B**). The relative abundances of *Bacillus*, *Bacteroides*, *Gallicola*, *Leuconostoc* and *Neoscardovia* were positively correlated with ceramides, while the relative abundances of *Acinetobacter*, *Cronobacter*, *Enterobacter*, *Rummeliibacillus* and *Microvirgula* were negatively correlated with ceramides. Glycerolipid metabolites [DG(18:1/23:0), DG(18:1/24:0), DG(19:1/18:1), DG(16:0e/20:1), TG(4:0/18:1/18:2), TG(16:0/6:0/18:2) and TG(20:1/18:2/18:3)] showed opposite correlation with ceramide metabolites.

Effects of fermented soybean on soil environmental factors and microbial communities

To evaluate the soil physicochemical indexes after fermented soybean fertilization, we analyzed the nutrient contents and enzyme activities in tea soils (**Tables 1**, **2**). Compared with CK, soil pH values in UF, NFS and EFS significantly reduced, but the pH value was the lowest in UF, at 5.19. The contents of TP, AP and AK significantly increased in soils after fermented soybean fertilization, especially in enzymatic fermented soybean fertilization. In addition, soybean fertilization stimulated the

TABLE 2 The activities of some enzymes in soils after fermented soybean fertilization.

	S-ACP (nmol/h/g)	S-UE (μ g/d/g)	S-CAT (μ mol/h/g)	S-CL (μ g/d/g)	S-ACPT (μ g/h/g)	S-SC (mg/d/g)
CK	1387.62 ± 313.27b	783.83 ± 52.79c	739.73 ± 52.07ab	303.78 ± 32.17a	16.45 ± 8.29b	29.85 ± 1.11c
UF	1073.41 ± 45.67b	1017.27 ± 107.68bc	744.50 ± 62.76ab	322.42 ± 47.68a	32.90 ± 14.15ab	29.62 ± 2.06c
NFS	2687.83 ± 92.49a	1258.29 ± 149.95ab	687.37 ± 81.87b	344.58 ± 107.54a	63.45 ± 19.70a	56.24 ± 6.74a
EFS	2718.61 ± 733.84a	1418.29 ± 124.51a	821.88 ± 42.32a	488.32 ± 245.45a	60.67 ± 8.23a	45.77 ± 3.88b

Values with the same letter are not significantly different ($p < 0.05$).
CK, control experiment; UF, urea fertilization; NFS, naturally fermented soybean fertilization; EFS, enzymatic fermented soybean fertilization.

activities of some enzymes, including solid-sucrase (S_SC), solid-acid phosphatase (S_ACP), solid-urease (S_UE) and solid-acid protease (S_ACPT).

To analyze the microbial composition in the soils after fermented soybean fertilization, we aligned the dominant OTUs with the Silva 119 and Unite database at the phylum and genus levels (Figure 1). In bacterial communities, the dominant phyla were *Proteobacteria*, *Bacteroidota*, *Firmicutes*, *Acidobacteriota* and *Actinobacteriota*. The dominant genera were *Pseudomonas*, *Romboutsia*, *Candidatus_Nitrosotalea*, *Helicobacter*, *Bryobacter* and *Bradyrhizobium* (Figure 1A). In fungal communities, the dominant phyla were *Ascomycota*, *Mortierellomycota*, *Rozellomycota*, *Glomeromycot* and *Mucoromycota*. The dominant genera were *Peziza*, *Fusarium*, *Candida*, *Cheilymenia*, *Mortierella* and *Dactylonectria* (Figure 1B). To further confirm the differences of microbial communities at the genus level, we used the *t*-test test to select microbial communities with significant differences in soils. Microbial communities with significant differences were shown in red color (Figure 1). In bacterial communities, *Glutamicibacter*, *Oligoflexus*, *Luteolibacter*, *Dyadobacter*, *Streptomyces* and *Occallatibacter* presented high abundances in EFS. In fungal communities, *Candida* and *Actinomucor* presented high abundances in EFS.

To explore the influences of soil environmental factors on soil bacterial communities, we analyzed the relationships between dominant genus and soil properties using spearman correlation (Figure 2). In terms of soil properties, AP, AK, TP and pH were important environmental factors in soils. The results showed that the soil AP was significantly related to the relative abundances of *Pseudomonas* and *Chitinophaga*. The soil AK was significantly related to the relative abundances of *Pseudomonas*, *Glutamicibacter* and *Croynebacterium*. The soil TP was significantly related to the relative abundances of *Pseudomonas, Pseudolabrys, Pedobacter, Novosphingobium, Glutamicibacter, Chitinophaga, Croynebacterium* and *Candidatus_solibacter*. The soil pH was significantly related to the relative abundances of *Nitrosospira*, *Brevundimonas*, *Rhodanobacter and Stenotrophomonas*. In terms of soil enzymic activities, S_ACP, S_ACPT, S_SC and S_UE were important environmental factors in soils. The results showed that the S_ACP, S_ACPT and S_UE were strongly associated with *Chitinophaga, Glutamicibacter* and *Pseudomonas*. The S_SC was strongly associated with *Chitinophaga, Novosphingobium and Pseudomonas*.

Effects of fermented soybean on soil metabolites

To elucidate the metabolic changes in soils after fermented soybean fertilization, we detected and screened out metabolites with significant differences in soils. The S-plot of the OPLS-DA model was used to maximize the discrimination among EFS treatment and other treatments, including CK vs EFS, UF vs EFS and NFS vs EFS (Figure 3A). The results showed that two treatments of these three contrast groups were located, respectively, on the positive and negative sides of the x-axis, indicating that the OPLS-DA model was a goodness of fit as a predictive model to evaluate the variation in metabolite profiles. Firstly, soil metabolites with different fertilizations were distributed into 4 clusters by k-means cluster analysis (Figure 3B). The contents of metabolites in cluster 4 of NFS and EFS were higher than in CK and UF. In cluster 4, 16 metabolites were found including lipid, carbohydrate, organic acid and amino acid. Soil metabolites with significant differences were further screened out. In total, 106 metabolites were detected in soils. Compared with CK, there were 21 metabolites with significant differences in EFS (Figure 3C). Therein, lipid, carbohydrate and acid substances were significantly up-regulated including (Z)-13-Docosenoic acid, 9,12-Octadecadienoic acid, D-Mannitol, D-Sorbitol, 1-O-Tetradecylglycerol, 1-Monooleoylglycerol and oleic acid, etc. Compared with UF, 19 metabolites with significant differences in EFS (Figure 3D). Therein, lipid, carbohydrate and acid substances were significantly up-regulated, including (Z)-13-Docosenoic acid, 9,12-Octadecadienoic acid, D-Mannitol, D-Sorbitol and oleic acid, etc. Compared with NFS, there were no metabolites with significant differences in EFS. In addition, we analyzed the correlations between microbial communities with significant differences and metabolites in soil (Figures 4, 5). Compared with CK, carbohydrate, organic acid and lipid substances established close relationships with soil bacterial communities in EFS (Figure 4A). *Comamonas*, *Cupriavidus*, *Kribbella*, *Achromobacter*, *Sumerlaea* and

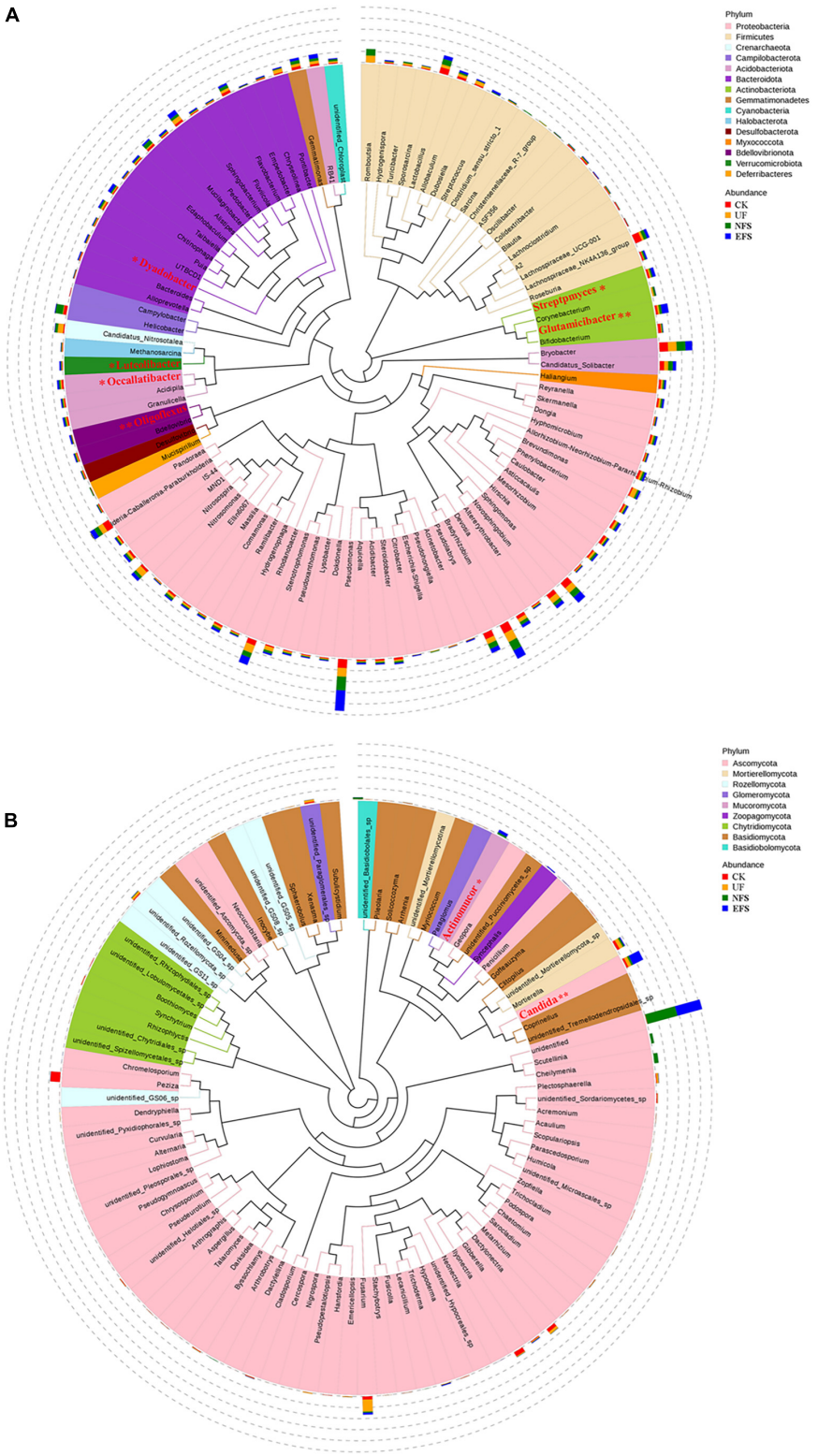

FIGURE 1
The composition of microbial communities in soil with fermented soybean fertilization. **(A)** The phylogenetic tree of soil bacterial communities. **(B)** The phylogenetic tree of soil fungal communities.

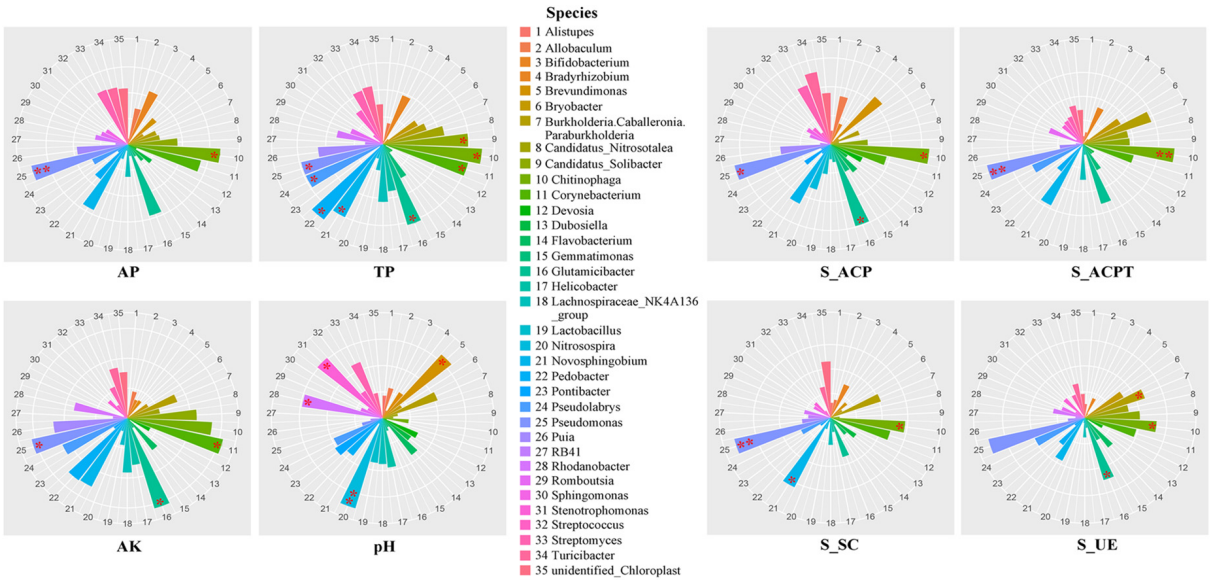

FIGURE 2
The rose diagrams of relationships between soil key properties and bacterial communities in soils with fermented soybean fertilization.

Methanomassiliicoccus were positively correlated with carbohydrate and oleic acid including D-Mannitol, D-Sorbitol and oleic acid. *Cellulomonas* and *Methanomassiliicoccus* were positively correlated with lipid including 9,12-Octadecadienoic acid (Z, Z)- and (Z)-13-Docosenoic acid. Compared with NFS, carbohydrate and lipid substances also established close relationships in EFS (**Figure 4B**). *Actinospica*, *Arthrobacter*, *Flavihumibacter*, *Rhodobacter* and *Terrimicrobium* were positively correlated with carbohydrates, while *Parapusillimonas*, *Rhodopseudomonas* and *Thalassobaculum* were negatively correlated with carbohydrates including D-Mannitol and D-Sorbitol. *Actinospica*, *Arthrobacter* and *Terrimicrobium* were positively correlated with lipid, while *Rhodopseudomonas* was negatively correlated with lipid including 9,12-Octadecadienoic acid (Z, Z)-, (Z)-13-Docosenoic acid and Diisopropyl azodicarboxylate. In fungal communities, compared with CK, carbohydrate and lipid substances established close relationships with fungal communities in EFS (**Figure 5A**). *Candida* was positively correlated with (Z)-13-Docosenoic acid. *Mucor* and *Stachylidium* were positively correlated with 9,12-Octadecadienoic acid (Z, Z)- and (Z)-13-Docosenoic acid, while *Cystofilobasidium* and *Cephalotrichum* were negatively correlated with these two lipid metabolites. *Candida, Penicillium, Myriococcum*, *Mucor* and *Stachylidium* were positively correlated with D-Mannitol and D-Sorbitol, while *Rhizophlyctis, Talaromyces, Microascus, Cystofilobasidium*, *Torula,* and *Chaetosphaeria* were negatively correlated with these two carbohydrate metabolites. Compared with UF, carbohydrate and lipid substances established close relationships with soil fungal communities in EFS (**Figure 5B**). *Volutella*, *Mucor* and *Stachylidium* were positively correlated with 9,12-Octadecadienoic acid (Z, Z)- and (Z)-13-Docosenoic acid, while *Metarhizium*, *Stachybotrys*, *Lophiostoma*, *Microascus*, *Cystofilobasidium, Gaeumannomyces, Acrocalymma* and *Peltigera* were negatively correlated with these lipid metabolites. *Volutella* and *Mucor* were positively correlated with D-Mannitol and D-Sorbitol, while *Stachybotrys, Peltigeta, Rhizophagus, Chaetosphaeria, Acrocalymma* and *Gaeumannomyces* were negatively correlated with these carbohydrate metabolites.

Effects of fermented soybean on metabolites of tea new shoots

To reveal the metabolic changes of tea new shoots under fermented soybean fertilization, we screened the differential metabolites of tea shoots by UPLC-MS. Firstly, the OPLS-DA analysis was used to maximize the discrimination among EFS treatment and other treatments, including CK vs EFS, UF vs EFS and NFS vs EFS (**Supplementary Figure 4A**). The metabolite profiles indicated that enzymatic soybean fertilization was discriminated from control, urea fertilization. Compared with CK, 111 metabolites were identified including 79 up-regulated and 32 down-regulated metabolites. A total of 79 up-regulated metabolites were from lipids, amino acids and their derivatives, phenolic acids, tannins and terpenoids (**Supplementary Figure 5A**). Compared with UF, 149 metabolites were identified including 77 up-regulated and 72 down-regulated metabolites. There were 77 up-regulated metabolites from tannins, lipids

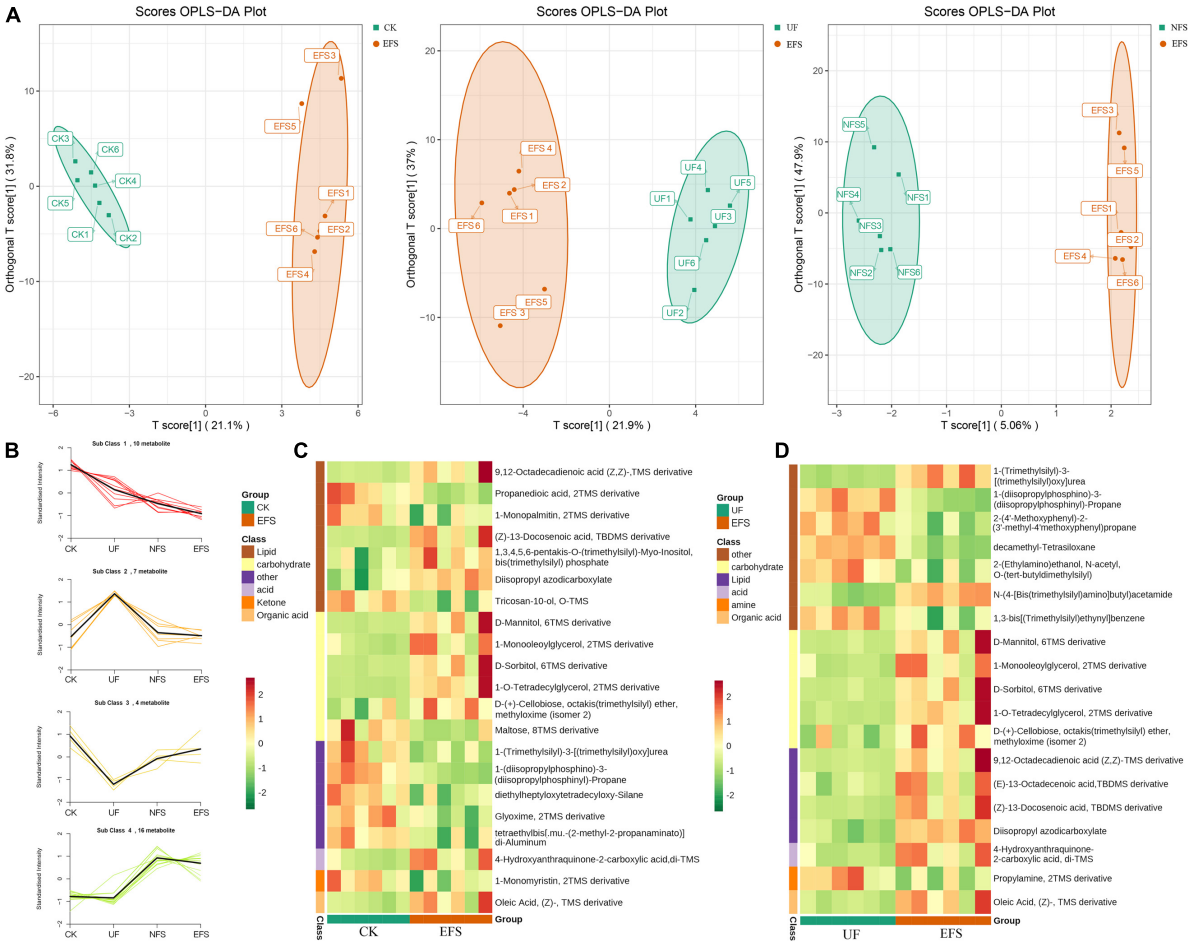

FIGURE 3
The differential metabolites of soil with fermented soybean fertilization. **(A)** The OPLS-DA analysis of soil metabolites. **(B)** The K-means cluster analysis of lipid molecules in tea soils. **(C)** The heatmap of soil differential metabolites in CK vs EFS group. **(D)** The heatmap of soil differential metabolites in UF vs EFS group.

and terpenoids (Supplementary Figure 5B). Compared with NFS, 22 metabolites were identified including 13 up-regulated and 9 down-regulated metabolites (Supplementary Figure 5C). 13 up-regulated metabolites mainly existed in lipids [PE (18:3/18:3 + O3), PE (oxo-11:0/16:0) and 1-Linoleoylglycerol-3-O-glucoside], phenolic acids (cinnamic acid, feruloyl syringic acid and Salicylic acid), Terpenoids (ursolic acid) and flavonoids (galangin-7-O-glucoside). Among them, lipid metabolites in tea new shoots were focused on in this study.

The OPLS-DA analysis was used to explore the clustering of CK vs EFS, UF vs EFS and NFS vs EFS groups (Supplementary Figure 4B). A total of 695 lipid species were identified, spanning five major lipid categories including 27 fatty acids (FA), 157 glycerophospholipids (GP), 422 glycerolipids (GL), 86 sphingolipids (SL), and 3 prenol lipids (PR). These lipid compounds can be further attributed to 27 subclasses mainly including 219 triacylglycerols (TG), 77 diacylglycerols (DG), 39 phosphatidylethanolamines (PE), 34 monogalactosyldiacylglycerols (MGDG), 32 ceramides (Cert), 31 phosphatidylglycerols (PG), 29 digalactosyldiacylglycerols (DGDG), 27 free fatty acids, 26 cer, 26 sulfoquinovosyl diacylglycerols (SQDG), 25 HexCer and 21 lysophosphatidylcholines (LPC; Figure 6A). The radar charts showed that the proportions of lipid metabolites in 27 categories were different in CK, UF, NFS and EFS (Figure 6B). Lipid metabolites in tea new shoots under different fertilizations were distributed into 7 clusters by using k-means cluster analysis (Figure 6C). The contents of lipid in cluster 3, 5, and 6 of NFS and EFS were higher than in CK and UF. Especially in clusters 5 and 6, the number of lipid metabolites in EFS was more than that in NFS. In cluster 5, 28 lipid metabolites were found including 32% DG, 18% HexCer, 14% TG, 14% LPE and 11% LPC. In cluster 6, 33 lipid metabolites were found including 32% DG, 24% TG, 9% LPC and 9% ADGGA. To compare the advantages of enzymatic fermented soybean fertilization, we carried out an in-depth analysis of the NFS vs EFS group.

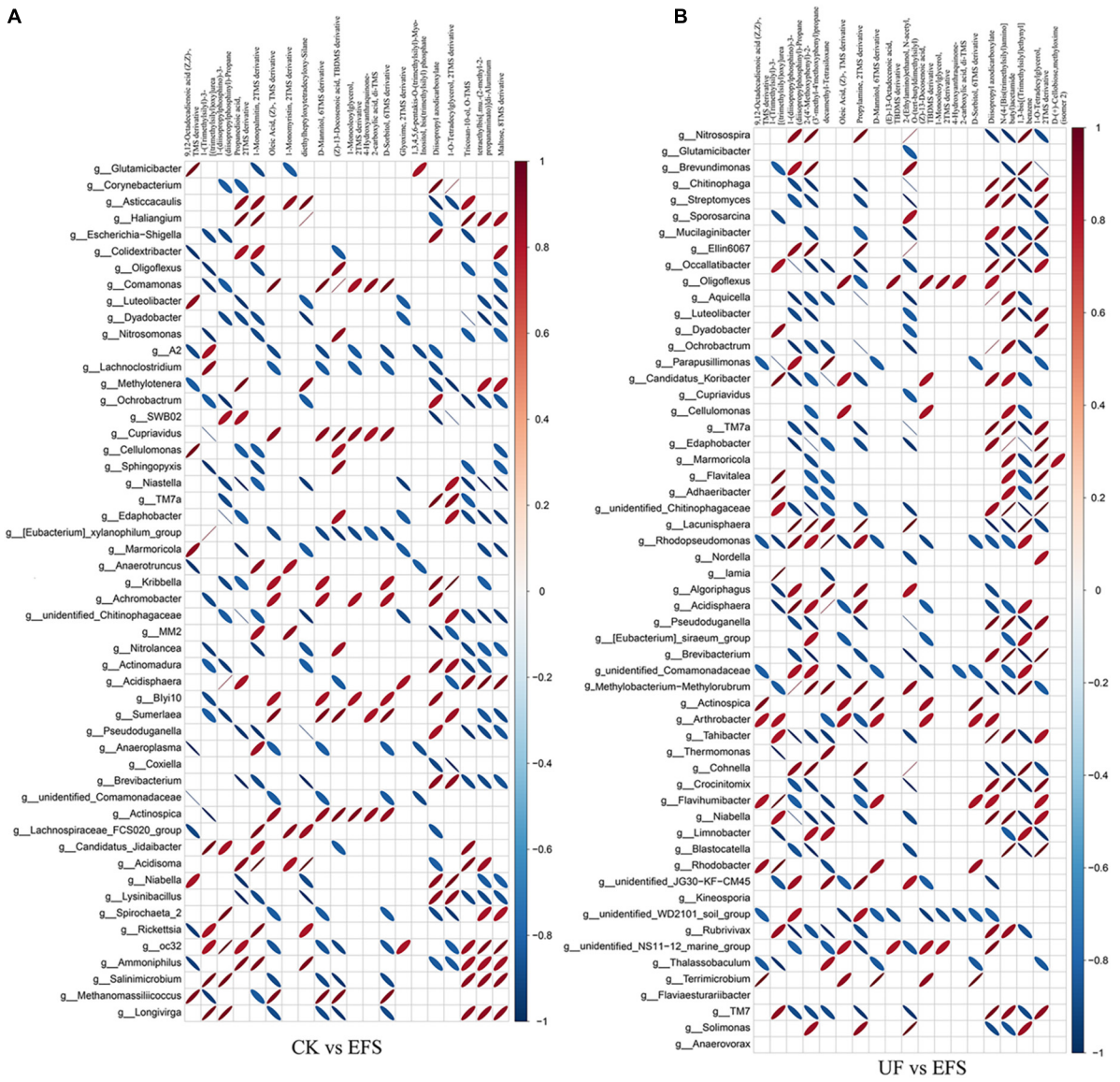

FIGURE 4
The ellipse heatmap of relationships between soil bacterial communities and soil metabolites. **(A)** The relationship of soil bacterial communities and soil metabolites in CK vs EFS group. **(B)** The relationship of soil bacterial communities and soil metabolites in UF vs EFS group.

Lipid metabolites with significant differences were selected using heatmaps and violin plot (Figure 7). 6 lipid metabolites exhibited significant up-regulation in EFS including HexCer [t18:1/27:0(2OH)], Cer (d18:1/26:0), DG (16:0_22:5), TG (10:0_12:0_14:0), TG (18:2_16:3_18:3) and SQDG (18:0_19:1), which focused on glycerolipids and ceramides (Figure 7A). The contents of these metabolites were shown in Figure 7B.

To further explore the relationships between soil microbial communities and metabolites in tea new shoot, we also analyzed their correlations using the Spearman coefficient (Figures 8, 9). In CK vs EFS group, glycerolipids (DG, DGTS and LDGTS) and glycerophospholipids (PE, PI and PMeOH) closely interacted with soil bacterial communities (Figure 8A). DG(18:2_22:1), DGTS(16:0_18:2) and LDGTS[(16:0, 18:1, 18:2, 18:3)] were positively correlated with *Dyadobacter*, *Nitrolancea* and *Pseudoduganella*, while these metabolites were negatively correlated with *Haliangium* and *Acidisoma.* PE[(16:0_16:3), (16:2_18:3) and (18:1_16:3)], PI[(15:0_16:1) and (16:1_17:1)] and PMeOH[(16:0_18:2), (18:2_18:2) and (18:2_18:3)] were positively correlated with *Colidextribacter, Anaeroplasma, Acidisoma, Rickettsia, Salinimicrobium* and *Longivirga,* while these metabolites were negatively correlated with *Glutamicibacter*, *Cellulomonas*, *Sphingopyxis*, *Nitrolancea*, *Actinospica* and *Methanomassiliicoccus*. In UF vs EFS group,

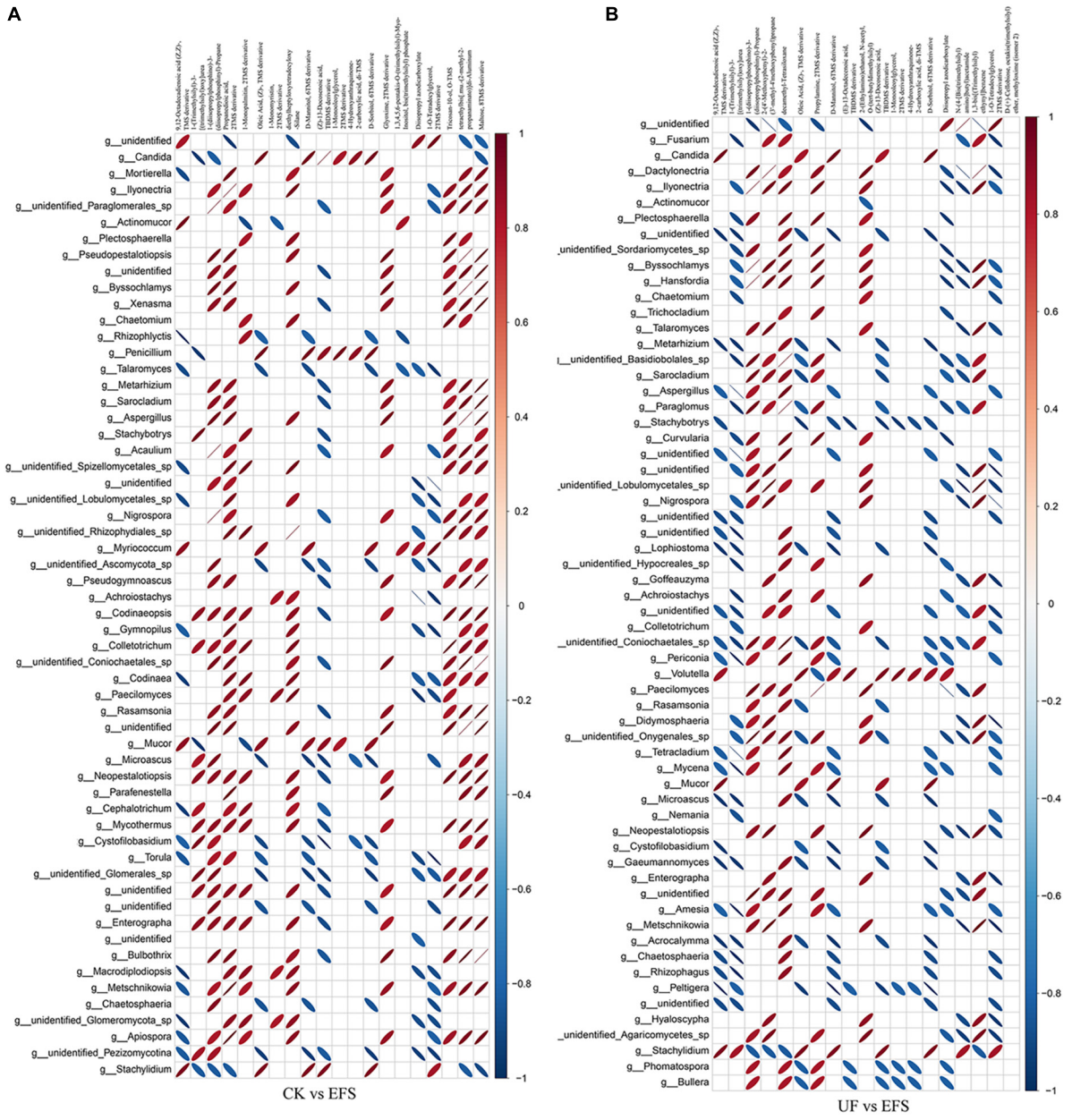

FIGURE 5
The ellipse heatmap of relationships between soil fungal communities and soil metabolites. **(A)** The relationship of soil fungal communities and soil metabolites in CK vs EFS group. **(B)** The relationship of soil fungal communities and soil metabolites in UF vs EFS group.

sphingolipids (Cer) and glycerophospholipids (PG and PMeOH) closely interacted with soil bacterial communities (Figure 8B). Cer [(d18:1/22:0), (d18:2/22:1), (t18:0/21:0(2OH)), (t18:0/22:0(2OH)), (t18:0/23:0(2OH)), (t18:0/24:0(2OH)), (t18:1/20:0(2OH)) and (t18:1/26:0(2OH))] were positively correlated with *Nitrosospira*, *Brevundimonas*, *Ellin6067*, *Lacunisphaera, Cohnella* and *Solimonas,* while these metabolites were negatively correlated with *Chitinophaga, Streptomyces, Mucilaginibacter, Ochrobactrum, TM7a, Edaphobacter, Pseudoduganella, Brevibacterium, Crocinitomix* and *TM7*. PG[(16:1_16:1), (16:1_18:3), (18:2_16:1) and (18:3_18:4)] and PMeOH[(16:0_18:2), (16:0_18:3), (18:2_18:2) and (18:2_18:3) were positively correlated with *Nitrosospira, Cohnella, Lacunisphaera* and *Solimonas,* while these metabolites were negatively correlated with *Glutamicibacter*, *Chitinophaga*, *Streptomyces, Nordella, Pseudoduganella, Brevibacterium and Crocinitomix.* In NFS vs EFS group, Cer(d18:1/26:0) and LDGTS (18:3) closely interacted with soil bacterial communities

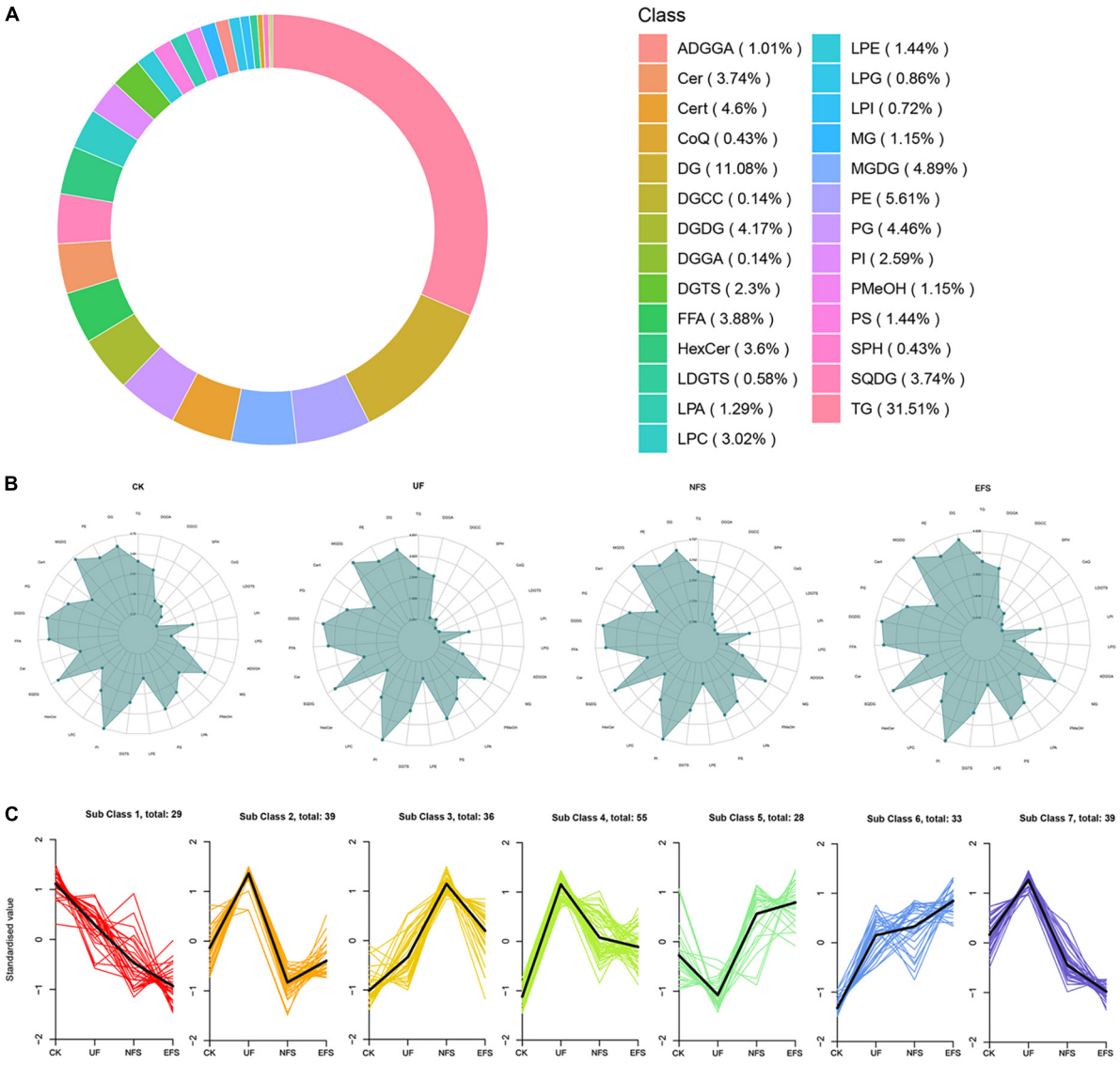

FIGURE 6
The sub-classes of lipid molecules in tea new shoots. **(A)** The count ring of lipid classes and proportion. **(B)** The radar charts of lipid classes in tea new shoots. **(C)** The K-means cluster analysis of lipid molecules in tea new shoots.

(Figure 8C). Cer(d18:1/26:0) was positively correlated with *Caulobacter*, *Flavitalea*, *Pseudoduganella* and *Brevibacterium*. LDGTS (18:3) was positively correlated with *Coxiella* and *Rhizorhapis*. In fungal communities, DG, DGTS and LDGTS were negatively correlated with *Plectosphaerella*, *Chaetomium*, and *Colletotrichum* in CK vs EFS group. PE, PI and PMeOH were positively correlated with *Srachybotrys*, *Codinaeopsis*, *Collectotrichum*, *Neopestalotiopsis*, *Cephalotrichum* and *Enterographa* in CK vs EFS group (Figure 9A). In UF vs EFS group, Cer and PG were positively correlated with *Dactylonetria*, *llyonectria*, *Nigrospora*, *Goffeauzyma*, *Neopestalotiopsis*, *Enterographa* and *Hyaloscypha* (Figure 9B). In NFS vs EFS group, Cer(d18:1/26:0) and LDGTS(18:3) closely interacted with soil fungal communities (Figure 9C). Cer(d18:1/26:0) was positively correlated with *Annulohypoxylon*, *Torula* and *Paraphaeosphaeria*. LDGTS (18:3) was positively correlated with *Coprinellus* and *Geminibasidium*.

Discussion

Soybean nutritional contents, microbial communities and metabolites changed during the fermentation process. The pH value was considered as an important indicator for reflecting the fermentation process and microbial activity (Jiang et al., 2020). In the soybean silage fermentation, all treatments

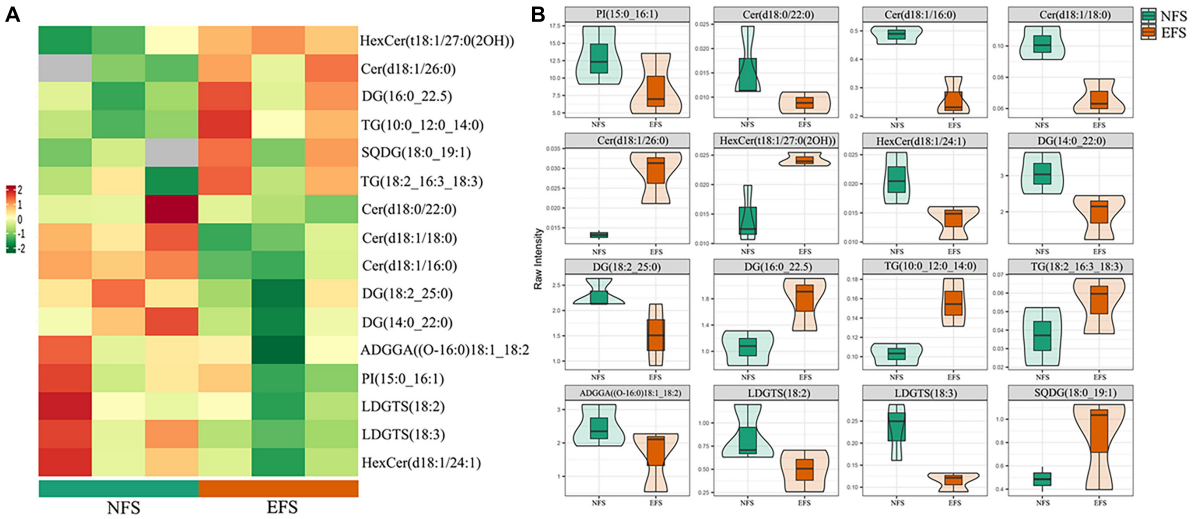

FIGURE 7
The differential lipid metabolites of tea new shoots in NFS vs EFS group. **(A)** The heatmap of differential metabolites in tea new shoots. **(B)** The violin plot of differential metabolites in tea new shoots.

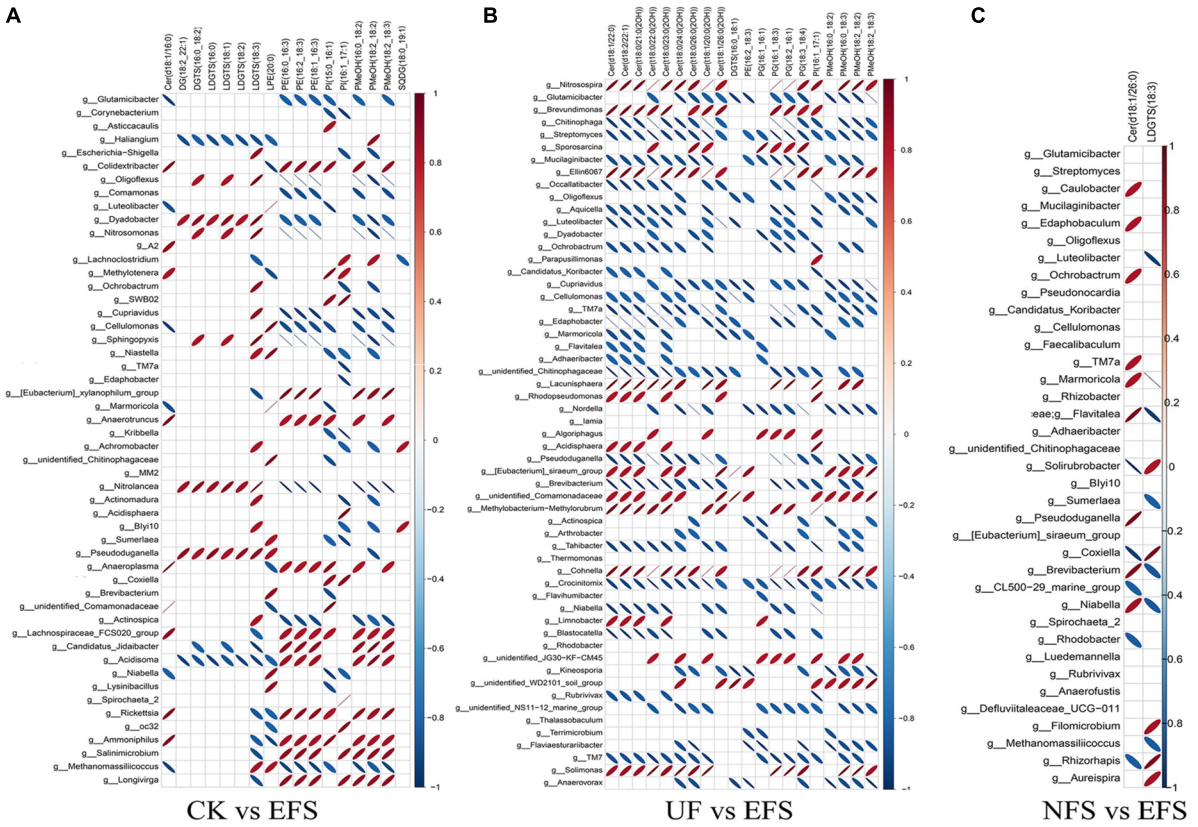

FIGURE 8
The ellipse heatmap of relationships between bacterial communities and metabolites in tea new shoots. **(A)** The relationship of bacterial communities and metabolites in CK vs EFS group. **(B)** The relationship of bacterial communities and metabolites in UF vs EFS group. **(C)** The relationship of bacterial communities and metabolites in NFS vs EFS group.

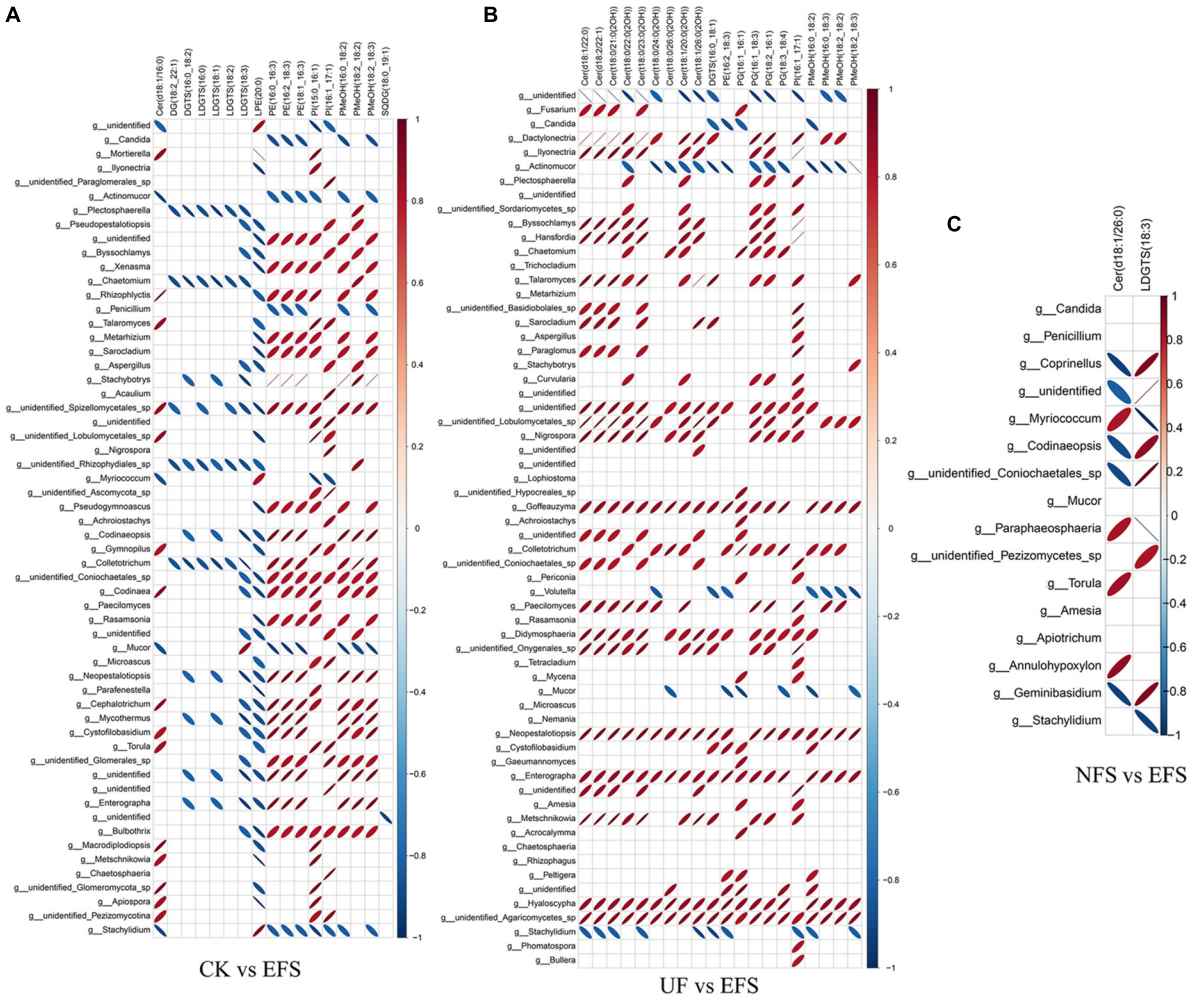

FIGURE 9
The ellipse heatmap of relationships between soil fungal communities and metabolites in tea new shoots. **(A)** The relationship of fungal communities and metabolites in CK vs EFS group. **(B)** The relationship of fungal communities and metabolites in UF vs EFS group. **(C)** The relationship of fungal communities and metabolites in NFS vs EFS group.

showed lower pH values than the control treatment, and the addition of lactic acid bacteria and molasses led to the highest pH drop (Ni et al., 2017). In the sainfoin silage fermentation, wilted sainfoin and inoculated sainfoin all had low pH and high concentration of lactic acid (Dongmei et al., 2020). Our results also showed that the pH of enzymatic fermented soybean was significantly lower than that of naturally fermented soybean, indicating that the addition of enzymes and bacteria could provide a slightly acidic environment for soybean fermentation (**Supplementary Figure 1**). It was more conducive to the decomposition of macromolecular nutrients and the improvement of the nutritional value of fermented soybean (Nguyen et al., 2022). These small molecular substances produced by decomposition were beneficial to the growth of tea plants, among which the amino acids produced such as tyrosine, histidine and lysine played positive roles in the growth of tea plants. However, previous studies have not reported the changes of microbial community and metabolite reaction during soybean fermentation, which were easy to be ignored. *Firmicutes*, *Proteobacteria* and *Bacteroidetes* were the main dominant phyla in different fermentations (Jin et al., 2019; Zhang et al., 2020a), which was consistent with our results. Our results also showed that *Enterobacter* and *Bacillus* were significantly enriched in enzymatic fermented soybean (**Supplementary Figure 2**). *Bacillus* was the key contributor to degrading organic components in the process of fertilizer fermentation, especially lignocellulosic biomass. *Enterobacter* could excrete acetoin, which was an important physiological metabolite and a quality indicator of fermented products (Xiao and Ping, 2007; Chen et al., 2010). Metabolic differences in soybean could be triggered by bacterial communities in different soybean fermentation processes. During the fermentation of

soybean, microbial hydrolases were released and then the complex macromolecules of soybean were degraded into monosaccharides, amino acids and short-chain fatty acids such as palmitic acid, 9,12-octadecanoic acid and stearic acid, etc. (Gupta et al., 2018). Fermentation also affected and changed the lipid content, and then the nutritional composition of soybeans including lipid and protein increased in soybean after fermentation (Nguyen et al., 2022). The contents of phospholipids, fatty acids from neutral lipids and free fatty acids significantly increased after soy sauce fermentation (Zou et al., 2019). In our study, lipid metabolites in EFS were focused on and analyzed to explore the advantages of enzymatic soybean fertilization. The results showed that lipid metabolites accounted for a large proportion of the up-regulated metabolites in soybeans with enzymatic fermentation, such as palmitic acid, oleamide and 11-oxohexadecanoic acid. The obtained findings have demonstrated the role and impact of enzymes and bacteria addition on lipid metabolites formed during soybean fermentation. Therefore, enzymes and bacteria jointly promoted the transformation of macromolecules and increased fermentation efficiency to rapid application in tea plantations.

Enzymatic soybean fertilization improved soil nutrition and altered soil microbial community. Soil environmental factors played important roles in changing the structure of soil microbial communities. In previous studies, soil pH, AN and OM were the key factors altering the microbial communities after organic fertilization (Gu et al., 2019; Zhang et al., 2020b). Our results showed that the contents of TP, AP, and AK significantly increased in soils after enzymatic fermented soybean fertilization, and the activities of S_SC and S_ACP also increased (**Tables 1**, **2**). Due to the tea soil being acidic, phosphorus was easy to combine with iron and aluminum to form insoluble compounds with low mobility. The application of enzymatic fermented soybean could make soil enzymes more active and provide a sufficient material basis for the growth and development of microorganisms. The changes of soil conditions led to the release of nutrients and the inhibition of soil pathogens, which further changed soil microorganisms and soil metabolites. In the present study, *Pseudomonas* was the main species in tea soil, and the abundances of *Glutamicibacter* and *Streptomyces* were higher in soil with enzymatic fermented soybean fertilization. *Pseudomonas* bacteria functioned as a keystone group in soils to mediate complex microbiome-plant feedback and had positive effects on multiple plant growth and phytohormone production through hormonal signaling (Jousset et al., 2017; Finkel et al., 2020; Zhuang et al., 2020). *Glutamicibacter* could tolerate a wide pH range and take a variety of organic substances as carbon sources and showed multiple potential plant growth-promoting traits, including nitrogen fixation and phosphorus dissolution (Feng et al., 2017; Sheng et al., 2018). The functions of *Streptomyces* mainly focused on improving the absorption of nutrients by plants, promoting plant growth, and improving the ability of plants to deal with biotic and abiotic stresses (Jacob et al., 2018; Wu et al., 2018). The results showed that the dominant bacterial communities in tea soil were different from that in fermented soybean fertilizer, indicating that the beneficial microbes in fertilizer did not directly participate in soil improvement and tea growth, but these microbes were guided to promote and activate the resident plant growth-promoting microbes already existing in the rhizosphere of tea plants. In addition, the enrichment of soil nutrients caused substantial shifts in both primary and secondary metabolism within the microbial community, leading to changes in soil functioning (Brown et al., 2022). In this study, lipid (9,12-Octadecadienoic acid), carbohydrate (D-Mannitol and D-Sorbitol) and acid substances were significantly up-regulated in soil with fermented soybean (**Figure 3**). Carbohydrates were also key metabolites in soil microorganisms, functioning as metabolic substrates and structural cell components (Reardon et al., 2018). D-Mannitol and D-Sorbitol could serve as carbohydrate reserves to store power, transfer compounds, and enhance the growth of plants, fungi and bacteria under stress. A higher concentration of sorbitol could increase microbial diversity and the addition of mannitol could enhance some enzyme activities (Yu et al., 2016). Therefore, fermented soybean fertilization was conducive to shaping an active network of nutrients, microorganisms and metabolites in the soil, which could provide a good soil environment and rich material basis for the growth of tea plants.

Enzymatic soybean fertilization affected the lipid metabolism of tea new shoots, which was closely related to soil microorganisms. Microorganisms were essential for plant growth and had potential benefits in plant secondary metabolism and stress resistance such as promoting photosynthesis, osmotic regulation and antioxidant enzymatic activities (Gabriel et al., 2017; Xiong et al., 2020). As important biomolecules, lipids were represented as precursors of tea aroma and contributed to the tea sensory quality. They could produce many volatile compounds through oxidation and degradation (Ho et al., 2015). Previous studies were focused on lipid components and changes according to different processing procedures of tea (Li et al., 2017, 2019, 2021). However, the lipid profile in tea depends not only on the manufacturing process but also on the fertilizer management in tea plantations. In the present study, glycerolipids accounted for the largest proportion in tea new shoots (**Figure 6**). In differential metabolites, glycerolipids and glycerophospholipids significantly increased in EFS (**Figure 7**). Glycerolipids made up a large proportion of plant lipids. Glycerolipids and triacylglycerols in the endoplasmic reticulum could be assembled into fatty acids. The composition of glycerolipids was strongly influenced by plant nutrients. In the model plant system *Arabidopsis*, lipid biosynthesis was significantly

affected by nitrogen nutrition, while lipid remodeling was regulated by phosphorus starvation (Kong et al., 2013; Pant et al., 2015). Our results also showed that glycolipids levels positively correlated with some soil bacteria, indicating changes in soil nutrients and bacterial communities jointly influence lipid changes in tea new shoots. In addition, ceramide [mainly Cer (d18:1/26:0)] closely interacted with soil microbial communities in comparison with the naturally fermented soybean fertilization in enzymatic fermented soybean fertilization. Sphingolipids were not only bio-active components of cells with signal transduction function (Worrall et al., 2008), but also the second messenger of plant defense mechanisms participating in various plant stress responses (Markham et al., 2013; Michaelson et al., 2016). Ceramide was the key intermediate of the sphingolipid metabolism pathway, and its synthesis was the starting point of biosynthesis in various complex sphingolipid compounds (Hou et al., 2016). It was proved that sphingolipids had been shown in other crops to be conducive to establishing a mutually beneficial symbiotic relationship between plants and fungi (Fabienne et al., 2011). It also might exist this special beneficial relationship in tea plants according to our results, which could induce the defense response of tea plants and improve the adaptability and disease resistance of tea plants. Further research should focus on the relationships between soil microbiomes and tea lipid metabolites using rhizosphere environment, root secretions and endophytes, etc.

Conclusion

Our results highlighted the effects of fermented soybean application on soil nutrients, soil microbial communities, soil metabolites, and metabolites in tea new shoots. Compared with urea fertilization, fermented soybean significantly increased the contents of TP, AP, and AK, which were also important environmental factors affecting soil microbial community in tea plantation. Moreover, soil microbial communities had close relationships with soil metabolites and tea new shoots metabolites after enzymatic fermented soybean fertilization. It provides technical support for the rational use of fermented soybean and is of great significance to reduce the amount of chemical fertilizer to protect the soil ecological environment in the tea plantation.

Data availability statement

The datasets presented in this study can be found in online repositories. The names of the repository and accession numbers can be found below: https://www.ncbi.nlm.nih.gov/, PRJNA863478, PRJNA863595, and PRJNA863609.

Author contributions

SZ carried out the experiment, collected and analyzed the data, and wrote the manuscript. ZD, LS, and YW raised the hypothesis, designed the experiment, and directed the study. YSh and YSo participated in material preparation and collected sample data. KF directed the laboratory work. RZ, YL, LW, and CB guided and popularized the fertilization technology. All authors contributed to the study and approved the final version.

Funding

This work was supported by the Significant Application Projects of Agriculture Technology Innovation in Shandong Province (SD2019ZZ010), the Technology System of Modern Agricultural Industry in Shandong Province (SDAIT-19-01), the Special Foundation for Distinguished Taishan Scholar of Shangdong Province (No. 201712057), the Livelihood Project of Qingdao City (19-6-1-64-nsh), and the Project of Agricultural Science and Technology Fund in Shandong Province (2019LY002, 2019YQ010, and 2019TSLH0802).

Acknowledgments

We would like to thank all authors for their valuable discussions.

Conflict of interest

RZ was employed by Qingdao Hexie Biotechnology Co., Ltd.

The remaining authors declare that the research was conducted in the absence of any commercial or financial relationships that could be construed as a potential conflict of interest.

Publisher's note

Supplementary material

The Supplementary Material for this article can be found online at: https://www.frontiersin.org/articles/10.3389/fmicb.2022.992823/full#supplementary-material

SUPPLEMENTARY FIGURE 1
Nutrition analysis of soybean during the fermentation process. **(A)** The changes of physicochemical properties in fermented soybean. **(B)** The contents of 20 amino acids in fermented soybean.

SUPPLEMENTARY FIGURE 2
The composition of bacterial communities in fermented soybean. **(A)** The histogram of bacterial composition in fermented soybean at the phylum level. **(B)** The histogram of bacterial composition in fermented soybean at the genus level. **(C)** The LDA Effect Size algorithm of bacterial communities with significant differences in fermented soybean.

SUPPLEMENTARY FIGURE 3
The differential lipid molecules of fermented soybean. **(A)** The heatmap of differential metabolites in soybeans with two fermentations. **(B)** The relationships of bacterial communities and lipid metabolites in soybeans.

SUPPLEMENTARY FIGURE 4
The OPLS-DA analysis of tea new shoots metabolites. **(A)** The OPLS-DA analysis of tea new shoots metabolites. **(B)** The OPLS-DA analysis of lipid metabolites in tea new shoots.

SUPPLEMENTARY FIGURE 5
The differential lipid metabolites of tea new shoots in CK vs EF **(A)**, UF vs EF **(B)** and SF vs EF **(C)** group.

References

Arafat, Y., Tayyab, M., Khan, M., Chen, T., Amjad, H., Awais, S., et al. (2019). Long-term monoculture negatively regulates fungal community composition and abundance of tea orchards. *Agronomy* 9, 466–473. doi: 10.3390/agronomy9080466

Bag, S., Mondal, A., and Banik, A. (2022). Exploring tea (Camellia sinensis) microbiome: Insights into the functional characteristics and their impact on tea growth promotion. *Microbiol. Res.* 254:126890. doi: 10.1016/j.micres.2021.126890

Bonanomi, G., Lorito, M., Vinale, F., and Woo, S. L. (2018). Organic Amendments, Beneficial Microbes, and Soil Microbiota: Toward a Unified Framework for Disease Suppression. *Annu. Rev. Phytopathol.* 56, 1–20. doi: 10.1146/annurev-phyto-080615-100046

Brown, R. W., Chadwick, D. R., Bending, G. D., Collins, C. D., Whelton, H. L., Daulton, E., et al. (2022). Nutrient (C, N and P) enrichment induces significant changes in the soil metabolite profile and microbial carbon partitioning. *Soil Biol. Biochem.* 172:108779. doi: 10.1016/j.soilbio.2022.108779

Chen, J., Chen, Q., Guo, Q., Ruan, S., Hui, R., Gu, Q., et al. (2010). Simultaneous determination of acetoin and tetramethylpyrazine in traditional vinegars by HPLC method. *Food Chem.* 122, 1247–1252. doi: 10.1016/j.foodchem.2010.03.072

Daglia, M., Antiochia, R., Sobolev, A. P., and Mannina, L. (2014). Untargeted and targeted methodologies in the study of tea (*Camellia sinensis L.*). *Food Res. Int.* 63, 275–289. doi: 10.1016/j.foodres.2014.03.070

Dongmei, X., Ding, Z., Wang, M., Jie, B., and Ke, W. (2020). Characterization of the microbial community, metabolome and biotransformation of phenolic compounds of sainfoin (Onobrychis viciifolia) silage ensiled with or without inoculation of Lactobacillus plantarum. *Bioreso. Technol.* 316:123910. doi: 10.1016/j.biortech.2020.123910

Edwards, J., Johnson, C., Santos-Medellín, C., Lurie, E., and Sundaresan, V. (2015). Structure, variation, and assembly of the root-associated microbiomes of rice. *Proc. Nat. Acad. Sci.U.S.A.* 112, 911–920. doi: 10.1073/pnas.1414592112

Fabienne, M., Véréna, P., Olivier, A., Virginie, P., Alexandra, H., Gueunier, M., et al. (2011). Fungal lipochitooligosaccharide symbiotic signals in arbuscular mycorrhiza. *Nature* 469, 58–63. doi: 10.1038/nature09622

Feng, W., Wang, T., Bai, J., Ding, P., and Xing, K. (2017). Glutamicibacter halophytocola sp. nov., an endophytic actinomycete isolated from the roots of a coastal halophyte, Limonium sinense. *Mirobiol. Soc.* 67, 1120–1125. doi: 10.1099/ijsem.0.001775

Fierer, N. (2017). Embracing the unknown: Disentangling the complexities of the soil microbiome. *Nat. Rev. Microbiol.* 15, 579–590. doi: 10.1038/nrmicro.2017.87

Finkel, O., Salas-González, I., Castrillo, G., Conway, J., and Dangl, J. (2020). A single bacterial genus maintains root growth in a complex microbiome. *Nat. Rev. Microbiol.* 587, 103–108. doi: 10.1038/s41586-020-2778-7

Fung, K., Carr, H., Zhang, J., and Wong, M. (2008). Growth and nutrient uptake of tea under different aluminum concentrations. *J. Sci. Food Agric.* 88, 1582–1591. doi: 10.1002/jsfa.3254

Gabriel, C., Teixeira, P., Paredes, S., Law, T., Lorenzo, L., and Jeffery, D. (2017). Root microbiota drive direct integration of phosphate stress and immunity. *Nature* 543, 513–518. doi: 10.1038/nature21417

Gu, S., Hu, Q., Cheng, Y., Bai, L., Liu, Z., Xiao, W., et al. (2019). Application of organic fertilizer improves microbial community diversity and alters microbial network structure in tea (Camellia sinensis) plantation soils. *Soil Tillage Res.* 195:104356. doi: 10.1016/j.still.2019.104356

Gupta, S., Lee, J., and Chen, W. (2018). Analysis of Improved Nutritional Composition of Potential Functional Food (Okara) after Probiotic Solid-State Fermentation. *J. Agric. Food Chem.* 66, 5373–5381. doi: 10.1021/acs.jafc.8b00971

Ho, C., Zheng, X., and Li, S. (2015). Tea aroma formation. *Food Sci. Hum. Well.* 4, 9–27. doi: 10.1016/j.fshw.2015.04.001

Hou, Q., Ufer, G., and Bartels, D. (2016). Lipid signalling in plant responses to abiotic stress. *Plant Cell Environ.* 39, 1029–1248. doi: 10.1111/pce.12666

Jacob, S., Sajjalaguddam, R., and Sudini, H. (2018). Streptomyces sp. RP1A-12 mediated control of peanut stem rot caused by Sclerotium rolfsii. *J. Integr. Agr.* 17, 892–900. doi: 10.1016/S2095-3119(17)618161

Jiang, K., Tang, B., Wang, Q., Xu, Z., and Lei, P. (2020). The bio-processing of soybean dregs by solid state fermentation using a poly γ-glutamic acid producing strain and its effect as feed additive. *Bioreso. Technol.* 291:121841. doi: 10.1016/j.biortech.2019.121841

Jin, W., Zhang, Z., Zhu, K., Xue, Y., Xie, F., Mao, S., et al. (2019). Comprehensive Understanding of the Bacterial Populations and Metabolites Profile of Fermented Feed by 16S rRNA Gene Sequencing and Liquid Chromatography-Mass Spectrometry. *Metabolites* 9, 239–252. doi: 10.3390/metabo9100239

Jousset, A., Bienhold, C., Chatzinotas, A., Gallien, L., Gobet, A., Kurm, V., et al. (2017). Where less may be more: How the rare biosphere pulls ecosystems strings. *ISME J.* 11, 853–862. doi: 10.1038/ismej.2016.174

Kong, Y., Chen, S., Yang, Y., and An, C. (2013). ABA-insensitive (ABI) 4 and ABI5 synergistically regulate DGAT1 expression in Arabidopsis seedlings under stress. *FEBS Lett.* 587, 3076–3082. doi: 10.1016/j.febslet.2013.07.045

Korenblum, E., Dong, Y., Szymanski, J., Panda, S., and Aharoni, A. (2020). Rhizosphere microbiome mediates systemic root metabolite exudation by root-to-root signaling. *Proc. Nat. Acad. Sci.U.S.A.* 117:201912130. doi: 10.1073/pnas.1912130117

Kudjordjie, E., Sapkota, R., Steffensen, S. K., Fomsgaard, I. S., and Nicolaisen, M. (2019). Maize synthesized benzoxazinoids affect the host associated microbiome. *Microbiome* 7, 59–76. doi: 10.1186/s40168-019-0677-7

Lee, S., Seo, M. H., Oh, D. K., and Lee, C. H. (2014). Targeted metabolomics for Aspergillus oryzae-mediated biotransformation of soybean isoflavones, showing variations in primary metabolites. *Biosci. Biotech Bioch.* 78, 167–174. doi: 10.1080/09168451.2014.877827

Li, J., Hua, J., Yuan, H., Deng, Y., and Jiang, Y. (2021). Investigation on green tea lipids and their metabolic variations during manufacturing by nontargeted lipidomics. *Food Chem.* 339:128114. doi: 10.1016/j.foodchem.2020.128114

Li, J., Hua, J., Zhou, Q., Dong, C., Wang, J., Deng, Y., et al. (2017). Comprehensive lipidome-wide profiling reveals dynamic changes of tea lipids during manufacturing process of black tea. *J. Agric. Food Chem.* 65, 10131–10140. doi: 10.1021/acs.jafc.7b03875

Li, P., Zhu, Y., Lu, M., Yang, C., Xie, D., Tan, J., et al. (2019). Variation patterns in the content of glycosides during green tea manufacturing by a modification-specific metabolomics approach: Enzymatic reaction promoting an increase in the glycosidically bound volatiles at the pan firing stage. *Food chem.* 279, 80–87. doi: 10.1016/j.foodchem.2018.11.148

Liu, M., Burgos, A., Ma, L., Zhang, Q., Tang, D., and Ruan, J. (2017). Lipidomics analysis unravels the effect of nitrogen fertilization on lipid metabolism in tea plant (Camellia sinensis L.). *BMC Plant Biol.* 17:165. doi: 10.1186/s12870-017-1111-6

Maggini, V., Mengoni, A., Bogani, P., Firenzuoli, F., and Fani, R. (2020). Promoting Model Systems of Microbiota-Medicinal Plant Interactions. *Trends Plant Sci.* 25, 3–5. doi: 10.1016/j.tplants.2019.12.013

Markham, J., Lynch, D., Napier, J., Dunn, J., and Cahoon, E. (2013). Plant sphingolipids: Function follows form. *Curr. Opin. Plant Biol.* 16, 350–357. doi: 10.1016/j.pbi.2013.02.009

Michaelson, L., Napier, J. A., Molino, D., and Faure, J. (2016). Plant sphingolipids: Their importance in cellular organization and adaption. *BBA-Mol. Cell Biol. Lipids* 1861, 1329–1335. doi: 10.1016/j.bbalip.2016.04.003

Nguyen, T., Lapoin, W., Young, M., and Nguyen, C. H. (2022). Changes in Fermented Soybean Nutritional Content Generated Under the Different Fermentation Conditions by Bacillus Subtilis. *Waste Biomass Valorization* 13, 563–569. doi: 10.1007/s12649-021-01501-2

Ni, K., Shi, Y. Z., Yi, X. Y., Zhang, Q. F., Fang, L., Ma, L. F., et al. (2018). Effects of long-term nitrogen application on soil acidification and solution chemistry of a tea plantation in China. *Agr. Ecosyst. Environ.* 252, 74–82. doi: 10.1016/j.agee.2017.10.004

Ni, K., Wang, F., Zhu, B., Yang, J., Zhou, G., Pan, Y., et al. (2017). Effects of lactic acid bacteria and molasses additives on the microbial community and fermentation quality of soybean silage. *Bioreso. Tech.* 238, 706–715. doi: 10.1016/j.biortech.2017.04.055

Pang, Z., Chen, J., Wang, T., Gao, C., Li, Z., Guo, L., et al. (2021). Linking Plant Secondary Metabolites and Plant Microbiomes: A Review. *Front. Plant Sci.* 12:621276. doi: 10.3389/fpls.2021.621276

Pant, B. D., Burgos, A., Pant, P., Cuadros-Inostroza, A., Willmitzer, L., and Scheible, W. R. (2015). The transcription factor PHR1 regulates lipid remodeling and triacylglycerol accumulation in Arabidopsis Thaliana during phosphorus starvation. *J. Exp. Bot.* 66, 1907–1918. doi: 10.1093/jxb/eru535

Park, M. K., Cho, I. H., Lee, S., Choi, H., Kwon, D., Kim, Y. S., et al. (2010). Metabolite profiling of Cheonggukjang, a fermented soybean paste, during fermentation by gas chromatography-mass spectrometry and principal component analysis. *Food Chem.* 122, 1313–1319. doi: 10.1271/bbb.100269

Park, M. K., and Kim, Y. S. (2020). Comparative metabolic expressions of fermented soybeans according to different microbial starters. *Food chem.* 305:125461. doi: 10.1016/j.foodchem.2019.125461

Pascale, A., Proietti, S., Pantelides, I. S., and Stringlis, I. A. (2020). Modulation of the Root Microbiome by Plant Molecules: The Basis for Targeted Disease Suppression and Plant Growth Promotion. *Front. Plant Sci.* 10:1471. doi: 10.3389/fpls.2019.01741

Reardon, P. N., Walter, E. D., Marean-Reardon, C. L., Lawrence, C. W., Kleber, M., and Washton, N. M. (2018). Carbohydrates protect protein against abiotic fragmentation by soil minerals. *Sci. Rep.* 8:813. doi: 10.1038/s41598-017

Sheng, Q., Feng, W., Zhang, Y., Wang, T., Xiong, Y., and Ke, X. (2018). Diversity of bacterial microbiota of coastal halophyte Limonium sinense and amelioration of salinity stress damage by symbiotic plant growth-promoting actinobacterium Glutamicibacter halophytocola KLBMP 5180. *Appl. Environ. Microb.* 84:e1533–e1518. doi: 10.1128/AEM.01533-18

Turner, T. R., James, E. K., and Poole, P. S. (2013). The plant microbiome. *Genome Biol.* 14, 209–219. doi: 10.1186/gb-2013-14-6-209

Wachira, F. N., Kamunya, S., Karori, S., Chalo, R., and Maritim, T. (2013). *The Tea Plants: Botanical Aspects. Tea in Health and Disease Prevention*. Amsterdam, NL: Elsevier, 3–17.

Worrall, D., Liang, Y. K., Alvarez, S., Holroyd, G. H., Spiegel, S., Panagopulos, M., et al. (2008). Involvement of sphingosine kinase in plant cell signalling. *Plant J.* 56, 64–72. doi: 10.1111/j.1365-313X.2008.03579

Wu, Q., Mi, N., Liu, W., Ren, J., Rao, Y., Jie, C., et al. (2018). Omics for understanding the mechanisms of Streptomyces lydicus A01 promoting the growth of tomato seedlings. *Plant Soil* 431, 129–141. doi: 10.1007/s11104-018-3750-2

Xiao, Z., and Ping, X. (2007). Acetoin metabolism in bacteria. *Crit. Rev. Microbiol.* 33, 127–140. doi: 10.1080/10408410701364604

Xiong, Y., Li, X., Wang, T., Gong, Y., Zhang, C., Xing, K., et al. (2020). Root exudates-driven rhizosphere recruitment of the plant growth-promoting rhizobacterium Bacillus flexus KLBMP 4941 and its growth-promoting effect on the coastal halophyte Limonium sinense under salt stress. *Ecotox. Environ. Safe.* 194:110374. doi: 10.1016/j.ecoenv.2020.110374

Yang, Z., Baldermann, S., and Watanabe, N. (2013). Recent studies of the volatile compounds in tea. *Food Res. Int.* 2, 585–599. doi: 10.1016/j.foodres.2013.02.011

Yang, X., Ni, K., Shi, Y., Yi, X., Zhang, Q., Fang, L., et al. (2018) Effects of long-term nitrogen application on soil acidification and solution chemistry of a tea plantation in China. *Agric. Ecosyst. Environ.* 252, 74–82. doi: 10.1016/j.agee.2017.10.004

Yu, H., Si, P., Shao, W., Qiao, X., Yang, X., Gao, D., et al. (2016). Response of enzyme activities and microbial communities to soil amendment with sugar alcohols. *Microbiologyopen* 5, 604–615. doi: 10.1002/mbo3.355

Zhang, S., Wang, Y., Sun, L., Qiu, C., and Ding, Z. (2020c). Organic mulching positively regulates the soil microbial communities and ecosystem functions in tea plantation. *BMC Microbiol.* 20:103–116. doi: 10.1186/s12866-020-01794-8

Zhang, C., Gao, Z., Shi, W., Li, L., and Zhou, B. (2020a). Material conversion, microbial community composition and metabolic functional succession during green soybean hull composting. *Bioreso. Tech.* 316:123823. doi: 10.1016/j.biortech.2020.123823

Zhang, S., Sun, L., Wang, Y., Fan, K., and Ding, Z. (2020b). Cow manure application effectively regulates the soil bacterial community in tea plantation. *BMC Microbiol.* 20:190–201. doi: 10.1186/s12866-020-01871-y

Zhuang, L., Yan, L., Wang, Z., Yu, Y., Zhang, N., Yang, C., et al. (2020). Synthetic community with six *Pseudomonas* strains screened from garlic rhizosphere microbiome promotes plant growth. *Microbial. Biotechnol.* 14, 488–502. doi: 10.1111/1751-7915.13640

Zou, M., Zhu, X., Li, X., and Zeng, X. (2019). Changes in lipids distribution and fatty acid composition during soy sauce production. *Food Sci. Nutr.* 7, 764–772. doi: 10.1002/fsn3.922

frontiers | Frontiers in Microbiology

TYPE Original Research
PUBLISHED 26 September 2022
DOI 10.3389/fmicb.2022.1002459

OPEN ACCESS

EDITED BY
Fayuan Wang,
Qingdao University of Science and Technology, China

REVIEWED BY
Janusz Blaszkowski,
West Pomeranian University of Technology, Poland
Pengfa Li,
Nanjing Agricultural University, China
Yangquanwei Zhong,
Northwestern Polytechnical University, China

*CORRESPONDENCE
Jia Liu
liujia422@126.com
Yuji Jiang
yjjiang@issas.ac.cn

†These authors have contributed equally to this work

SPECIALTY SECTION
This article was submitted to Microbe and Virus Interactions with Plants, a section of the journal Frontiers in Microbiology

RECEIVED 25 July 2022
ACCEPTED 29 August 2022
PUBLISHED 26 September 2022

CITATION
Xiang X, Zhang J, Li G, Leng K, Sun L, Qin W, Peng C, Xu C, Liu J and Jiang Y (2022) Positive feedback between peanut and arbuscular mycorrhizal fungi with the application of hairy vetch in Ultisol. *Front. Microbiol.* 13:1002459. doi: 10.3389/fmicb.2022.1002459

Positive feedback between peanut and arbuscular mycorrhizal fungi with the application of hairy vetch in Ultisol

Xingjia Xiang[1,2†], Jinyi Zhang[1,2†], Guilong Li[3,4], Ke Leng[1,2], Luyuan Sun[3,4], Wenjing Qin[3,4], Chunrui Peng[3,4], Changxu Xu[3,4], Jia Liu[3,4*] and Yuji Jiang[5*]

[1]School of Resources and Environmental Engineering, Anhui University, Hefei, China, [2]Anhui Province Key Laboratory of Wetland Ecosystem Protection and Restoration, Hefei, China, [3]Soil and Fertilizer and Resources and Environment Institute, Jiangxi Academy of Agricultural Sciences, Nanchang, China, [4]Key Laboratory of Acidified Soil Amelioration and Utilization, Ministry of Agriculture and Rural Affairs, Nanchang, China, [5]State Key Laboratory of Soil and Sustainable Agriculture, Institute of Soil Science, Chinese Academy of Sciences, Nanjing, China

Multiple agricultural practices are being applied to increase crop yield in order to overcome the food shortage. Green manure has emerged as an appropriate practice to improve soil fertility and crop yield. However, the potential functions of arbuscular mycorrhizal fungi (AMF) in the below-ground ecosystems following the application of green manure in Ultisols remain largely unexplored. In this study, qPCR and high-throughput sequencing were used to investigate the response of AMF abundance and communities in different treatment groups, i.e., control (without fertilization), mineral fertilization (NPK), mineral fertilization with returning peanut straw (NPKS), and with green manure (hairy vetch; NPKG). The NPKG treatment significantly increased soil fertility compared to other treatment groups. Compared with control, the NPK, NPKS, and NPKG treatments increased peanut yield by 12.3, 13.1, and 25.4%, respectively. NPKS and NPKG treatments significantly altered the AMF community composition decreased the AMF diversity and increased AMF abundance compared to the control. The AMF network of the NPKG treatment group showed the highest complexity and stability compared to other treatment groups. The structural equation modeling revealed that the application of hairy vetch improved soil nutrients and peanut yield by increasing the soil AMF abundance and network stability. Overall, the results suggested that the application of hairy vetch might trigger positive feedback between the peanut and AMF community, contributing to fertility and yield improvement in the dryland of Ultisol.

KEYWORDS

AMF community, hairy vetch, soil fertility, peanut yield, sequencing

Introduction

Ultisol, one of the most important soil types, occupies approximately 21% land area of China. Over time, high-strength and long-term farming in Ultisol have adversely impacted the ecosystem in the form of soil acidification, fertility depletion, and a decline in crop yield (Xiang et al., 2020). However, the use of organic materials (e.g., animal excreta) in agriculture practices effectively alleviates these adverse effects. The application of animal excreta to agricultural soil increased soil fertility and suppressed plant pathogens (Shahbaz et al., 2017). However, deleterious effects of animal excreta application, such as the enrichment of heavy metals and residual antibiotics have gained increasing attention (Sager, 2007; Yan et al., 2022). Thus, suitable and sustainable agricultural practice in Ultisol demands urgent investigation.

Crop straw and green manure are important renewable organic resources (Zhou et al., 2019). Maize and rice straw returning improved soil nitrogen content (Akhtar et al., 2018) and contributed to the accumulation of soil organic carbon (Lee et al., 2020; Dutta et al., 2022). However, the direct return of peanut straw to the field might result in soil-borne diseases and obstacles in continuous cropping (Li et al., 2014). Thus, the effects of returning composted peanut straw to the agroecosystem should be investigated further. Peanuts are planted in mid-late April and harvested at the end of August in South China. Monoculture is commonly practiced in Ultisols due to severe seasonal drought. The 8-month peanut planting interval provides enough time and space for planting green manure (Xiang et al., 2021). Planting green manure triggered long-term effects such as improving soil quality, and immediate effects such as the increasing supply of available nutrients for subsequent crops (Mohanty et al., 2020; Ansari et al., 2022).

Soil microbes are involved in several functions in agroecosystems, such as nutrient availability, pathogen control, and resilience to abiotic stresses (de Vries et al., 2020; Chen et al., 2021). The application of crop straw and green manure to the field triggered changes in soil microbial diversity and biomass (Xiang et al., 2021). Besides, the application of green manure improved soil fertility and crop production by activating the functions of below-ground soil microbes (Khan et al., 2020). Recently, microbial network analysis was particularly useful to statistically identify the key microbial taxa that regulate the microbial functions in the below-ground ecosystem (Banerjee et al., 2018; Yuan et al., 2021). However, few studies have explored key taxa involved in the regulation of agroecosystem using network analysis following returning crop straw and planting green manure.

Arbuscular mycorrhizal fungi (AMF) are present in the roots of plants and live in mutualistic symbiosis with most plants. AMF also improved the absorption of nutrients for plants in exchange for carbohydrates (Smith and Read, 2008). In addition, AMF improved the soil structure and increased ecosystem functions by decreasing nutrient loss from leaching (van der Heijden, 2010; Martin et al., 2012). Mineral fertilization directly increased soil fertility to decrease the dependence of plants on their AMF partners. This phenomenon might shift the relationship between the plants and AMF from mutualism to parasitism (Kiers et al., 2011). However, the previous study has shown that the addition of pig manure increased the AMF biomass (Jiang et al., 2020) and richness (Liu et al., 2020). However, the response of the AMF communities to the application of green manure and crop straw remains largely unknown in the Ultisol.

In this study, we evaluate the effects of green manure and peanut straw on soil fertility, crop yield, and AMF communities in the dryland of Ultisol using qPCR and sequencing (Illumina MiSeq). Hairy vetch (*Vicia villosa Roth* L.) was selected as the experimental green manure. Peanut straw was composted for 8 months and then returned to the field. This study aimed to investigate the effects of (a) composted straw and green manure on soil fertility and peanut yield, (b) composted straw and green manure on the AMF communities and key taxa within the AMF network, and (c) feedback among AMF, soil fertility, and peanut yield following different agricultural practices in Ultisol.

Materials and methods

Experimental design

The experimental site is located at the Comprehensive Experimental Station of red soil (28°10′59″N, 106°35′11″E, 50 m), Dongxiang County, Jiangxi Province, China. The soil type was classified as Ultisol. This region experiences a typical subtropical warm and humid monsoon climate. The annual average temperature and precipitation are 18°C and 2,180 mm, respectively. This experiment was established in 2014. The soil properties before the experiments were as follows: 5.34 pH, 7.69 g kg^{-1} organic C, 1.02 g kg^{-1} total N, 85.9 mg kg^{-1} alkaline N, 0.68 g kg^{-1} total P, and 12.7 mg kg^{-1} available *P*.

The experiments included four treatment groups with six replicates, i.e., (a) without fertilizer (control), (b) mineral fertilization (NPK), (c) mineral fertilization with returning composted peanut straw (NPKS), and (d) mineral fertilization with planting green manure (NPKG). Peanut straw was removed in the control, NPK, and NPKG treatment groups. Composted peanut straw was plowed into the soil 2 weeks before the next peanut planting. Dry straw is about 1,300 kg $ha^{-1}yr^{-1}$ in NPKS treatment. Green manure was applied at a seeding rate of 20 kg ha^{-1} in mid-October every year with a yield of around 2×10^4 kg $ha^{-1}yr^{-1}$ in NPKG treatment. The green manure was cut into 5 cm small pieces and plowed into the soil 2 weeks before the next peanut planting. The field site was used to cultivate peanuts (cv. Yueyou 256). Peanuts were sown in a row at a spacing of 40 cm and a whole spacing of 20 cm.

Two seeds were planted in each cave, and the planting density was about 1.25×10^5 points hm^{-2}. The peanut seedlings were planted in mid-April, and they ripened in mid to late August.

The application rates of mineral fertilizers to peanuts were: 135 kg ha^{-1} urea (containing 46.4% N), 81 kg ha^{-1} calcium superphosphate (containing 12.0% P_2O_5), and 135 kg ha^{-1} potassium chloride (containing 60.0% K_2O). The 50% of N and K fertilizers were broadcasted as basal application, while the other 50% was applied at the peanut needle stage. All *P* fertilizers were applied as basal fertilizers. Basal fertilizer was thoroughly incorporated into the soil by plowing one day before the peanut plantation.

Soil sampling

Rhizospheric soils were sampled at the pod stage on 15 July 2017. One composite rhizospheric soil sample was taken from each plot consisting of five randomly selected peanut plants. After gently pulling out the peanuts, we tap the entire root system to dislodge all the loose soil and the remaining soil was collected as a rhizospheric soil sample (Smalla et al., 2001).

Soil chemical properties analyses

The soil water suspension (1:2.5 wt/volume) was shaken for 30 min, and then the pH of the soil water solution was determined. The potassium dichromate oxidation method was used to determine soil organic carbon (SOC). Total nitrogen (TN) was determined using an elemental analyzer (multi-EA 5,000, Jean, Germany). The molybdenum blue colorimetry method was used for measuring total phosphorus (TP) (Bowman, 1988). Alkaline nitrogen (AN) (Ai et al., 2017) was determined using the alkaline hydrolysis diffusion method. Available phosphorus (AP) (Stahlberg, 1980) was extracted using sodium bicarbonate and AP content was determined using the molybdenum blue colorimetric method.

DNA extraction

The soil DNA was extracted from 0.5 g of soil using the Fast DNA® SPIN Kit (MP Biomedicals, Santa Ana, CA, USA) according to the manufacturer's instructions.

Quantitative real-time PCR for arbuscular mycorrhizal fungi abundance

Primer pair AMV4.5NF/AMDGR were used to determine AMF abundance by CFX96 Optical Real-Time Detection System (Bio-Rad, Laboratories Inc., Hercules, CA, USA). Each PCR reaction was carried out in a 25 μl qPCR reaction mixture containing 12.5 μl SYBR® Premix Ex Taq (TliRNaseH Plus, 2×, Takara Bio, Japan), 0.5 μl PCR forward and reverse primers (both 10 μM), 2 μl DNA template, and 9.5 μl double distilled water (ddH_2O). Quantitative real-time PCR reactions were set to 95°C for 5 min, followed by 35 cycles of 95°C for 30 s, 58°C for 30 s, and 72°C for 1 min. The melting curve analysis showed excellent specificity of the qPCR with an efficiency of 98.5% ($R^2 = 0.9997$).

PCR and amplicon library preparation

The PCR was performed in a 50-μL reaction mixture and the mixture contained a concentration of 1.25 mM deoxynucleoside triphosphate, 15 μM of forward and reverse primers (i.e., AMV4.5NF/AMDGR) in each, 2 U of Taq DNA polymerase (TaKaRa, Japan). Each PCR reaction mixture contained 1 μl of DNA as a template. The cycling parameters were as follows: 35 cycles of 95°C for 45 s, 58°C for 45 s, and 72°C for 1 min, with a final extension at 72°C for 10 min.

Bioinformatics analysis

Raw data were processed using qiime2-2020.2 (Bolyen et al., 2019). The deblur algorithm was used to filter poor-quality sequences (Amir et al., 2017). Then, the chimeras of amplicon sequence variants (ASVs) were filtered using vsearch (Rognes et al., 2016). All singleton ASVs were removed. Annotations for ASV were conducted by classify-sklearn using the MaarjAM database (Öpik et al., 2010). A subset of 21,000 sequences was randomly selected per sample for further analysis.

Statistical analysis

The differences in the AMF index (i.e., AMF abundance, AMF richness, and the dominant taxa) and soil properties among different treatments were tested using one-way ANOVA. Canonical analysis of principal coordinates (CAP), ANOSIM, and RDA analyses were conducted using the R v.4.0.4 software. The primary factors affecting AMF abundance, diversity, and relative abundance of dominant taxa were determined using the Random Forest model (Trivedi et al., 2016). The differences in AMF species were detected using STAMP 2.1.3 software among treatment groups. The co-occurrence network was performed using high-frequency ASVs (>3 samples) with robust (Spearman's $r > 0.6$ or < -0.6), and significant ($P < 0.05$) Benjamini–Hochberg multiple testing correction. Topological features (i.e., average degree, natural connectivity, and the average clustering coefficient) were determined using the igraph

package in R v.4.0.4 software. The structural equation modeling (SEM) was performed using the lavaan package in R v.4.0.4 software to assess the direct and indirect contributions of abiotic (soil nutrient) and biotic (AMF index) variables to peanut yield.

Results

Soil properties and peanut productivity

Different agricultural practices triggered significant changes in the soil properties (**Table 1**). The soil pH in NPKS and NPKG treatment groups was decreased to 4.97 and 4.71, respectively, compared to control (pH 5.21). Besides, the NPKG treatment significantly increased soil fertility levels. Compared to control, peanut yield was significantly increased by 12.3% in NPK, 13.1% in NPKS, and 25.4% in NPKG (**Table 1**).

Soil arbuscular mycorrhizal fungi abundance and alpha-diversity

The NPKS and NPKG treatments increased AMF abundance by 10.9 times and 12.2 times, respectively, while NPK treatment had little effect on the AMF abundance compared to the control (**Figure 1A**). The AMF abundance was significantly correlated with the soil pH, SOC, and AN (**Supplementary Figure 1**). Compared with the control, the NPK, NPKS, and NPKG treatments significantly decreased the AMF richness, and the lowest AMF richness was observed in the NPKG treatment group (**Figure 1B**). The ASV richness was significantly correlated with the soil pH and soil nutrient contents (**Supplementary Figure 1**).

Soil arbuscular mycorrhizal fungi community composition

The organic application significantly altered the soil AMF community composition. However, mineral fertilization had little impact on the AMF community composition (**Figure 2** and **Supplementary Figure 2**). The shifts in the AMF community composition were driven by practice-mediated changes in the soil pH and nutrients (**Figure 2**). At the order level, compared to control, the NPK and NPKG treatments decreased and increased the relative abundance of Glomerales, respectively (**Supplementary Figure 3**). The NPKG treatment decreased the relative abundances of Diversisporales and Paraglomerales compared to the control (**Supplementary Figure 3**). At the family level, compared to the control, the NPKS and NPKG treatments significantly increased the relative abundance of Glomeraceae and decreased the relative abundance of Claroideoglomeraceae. The relative abundances of Acaulosporaceae and Gigasporaceae were significantly increased in the NPK treatment group and decreased in the NPKG treatment group compared to the control (**Supplementary Figure 4**). The STAMP analysis showed that NPKS treatment significantly decreased the relative abundance of *Claroideoglomus*, and NPKG treatment significantly increased the relative abundance of *Glomus* and decreased the relative abundance of *Claroideoglomus* and *Acaulospora* (**Supplementary Figure 5**).

Characteristics of co-occurrence networks

The soil AMF network was investigated for each agricultural practice separately in this study (**Figure 3**). The lower number of nodes (e.g., taxa) and edges (interactions among taxa) were found in the networks of control, NPK, and NPKS treatment groups. The network of NPKG consisted of a higher number of nodes and edges. The average degree and the average clustering coefficient in the NPKG network were also considerably higher than in the other three networks. The NPKG network exhibited higher robustness and stability than the other three networks (**Supplementary Figure 6**). Furthermore, the topological characteristics of the sub-network within Glomeraceae were also significantly higher in the NPKG treatment group than in other treatment groups (**Supplementary Figure 7**).

The effect of abiotic and biotic variables on yield

The SEM analysis demonstrated that the application of green manure was associated with a higher AMF abundance, network complexity, and relative abundance of *Glomus* (**Figure 4**). Specifically, planting green manure improved the soil nutrient level indirectly by increasing the AMF abundance and the relative abundance of *Glomus*. Soil nutrients, AMF network complexity, and relative abundance of *Glomus* showed a significant and positive correlation with the peanut yield (**Figure 4**).

Discussion

Previous studies have shown that the application of green manure improved fertility and yield (Mohanty et al., 2020; Ansari et al., 2022; **Table 1**). In this study, shifts in certain AMF taxa might be crucial to improving the yield in addition to increasing soil fertility following the application of hairy vetch (Bonanomi et al., 2020). Soil AMFs are beneficial for the absorption of soil nutrients (de Gruyter et al., 2022). The Glomeraceae showed the highest P uptake efficiency

TABLE 1 The summary of the main soil properties and peanut yield.

Variables	Control	NPK	NPKS	NPKG
Soil pH	5.21 ± 0.10a	5.29 ± 0.17a	4.97 ± 0.14b	4.71 ± 0.20c
Soil organic carbon (g kg^{-1})	7.82 ± 0.30b	7.64 ± 0.37b	8.00 ± 0.47b	10.6 ± 0.37a
Total nitrogen (g kg^{-1})	0.99 ± 0.04b	0.95 ± 0.05b	0.96 ± 0.05b	1.20 ± 0.05a
Total phosphorus (g kg^{-1})	0.67 ± 0.02b	0.74 ± 0.06ab	0.67 ± 0.10b	0.75 ± 0.03a
Alkaline nitrogen (mg kg^{-1})	86.4 ± 4.50b	90.0 ± 2.01b	91.3 ± 2.77b	128 ± 16.8a
Available phosphorus (mg kg^{-1})	13.1 ± 1.68bc	16.0 ± 3.06b	11.9 ± 2.69c	23.4 ± 2.18a
Peanut yield (kg ha^{-1})	2864 ± 192.9c	3217 ± 174.3b	3240 ± 224.7b	3591 ± 278.3a

The values in brackets represent the standard deviation of the mean. Letters following numbers represent significant differences from one-way ANOVA with Duncan's HSD comparisons ($P < 0.05$).

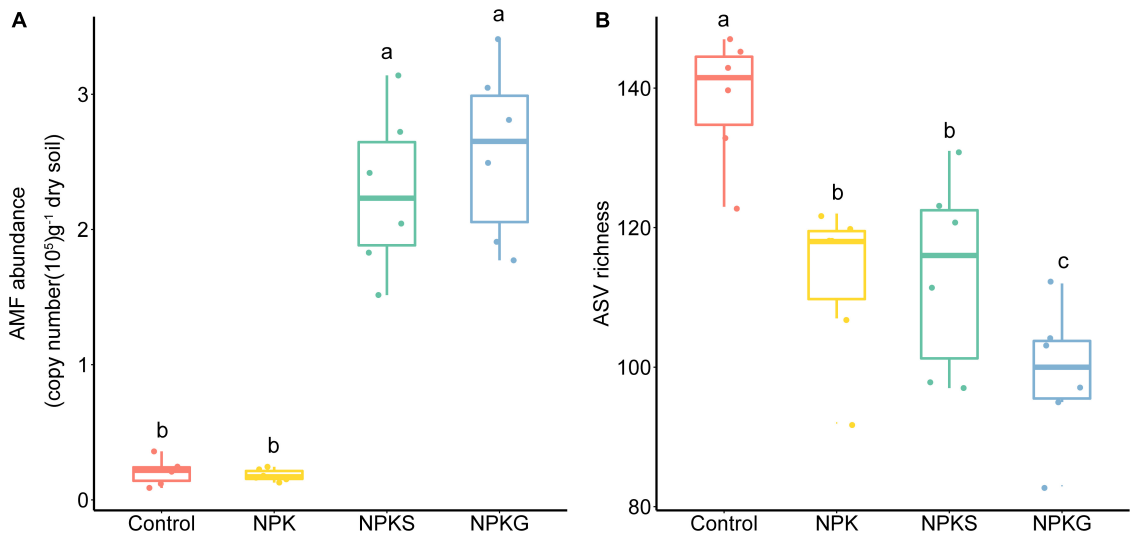

FIGURE 1
The variation of arbuscular mycorrhizal fungi (AMF) abundance **(A)** and ASV richness **(B)** in the soil among different treatments. The bottom and top of the box denote the first and third quartiles; the band inside the box denotes the median. Letters represent significant differences from the one-way ANOVA with Tukey's HSD comparisons ($P < 0.05$).

and antagonistic activities against plant pathogens (Kaur et al., 2022). However, Gigasporaceae showed a negative impact on the plant growth potential (Li et al., 2008). In this study, the application of hairy vetch increased the relative abundance of Glomeraceae and decreased the relative abundance of Gigasporaceae (**Supplementary Figure 4**). These results indicated that the application of hairy vetch might benefit the agricultural ecosystem by optimizing soil AMF taxa and regulating below-ground AMF functions.

The AMF could recruit soil saprotrophs to decompose organic matter following organic amendment (Xiang et al., 2015; Frey, 2019; Wang et al., 2021). Especially, the AMF genus *Glomus* might act as a conduit to transport plant-derived monosaccharides from the roots to the soil aggregates (Johnson et al., 2002; Jeewani et al., 2021), which might regulate soil saprotrophs for the transformation of organic matters. In this study, the application of hairy vetch significantly increased the relative abundance of *Glomus* (**Supplementary Figure 5**). This demonstrates that certain beneficial taxa (i.e., *Glomus*) might accelerate organic degradation to increase mineral fertilizers levels following the application of hairy vetch (**Table 1**).

Previous studies have shown the negative response of AMF diversity to nutrient enrichment (Alguacil et al., 2010; Camenzind et al., 2014; **Figure 1B** and **Supplementary Figure 1**). However, the decreased microbial diversity did not completely reflect the loss of ecological functions due to the functional redundancy of the microbes (Louca et al., 2018; Frew et al., 2022). Moreover, previous studies have shown that the primary driver of soil multifunctionality was microbial biomass/abundance rather than microbial diversity (Garland et al., 2021; Wang et al., 2021; Frew et al., 2022). In line with the previous studies, planting hairy vetch significantly increased the soil AMF abundance (Jiang et al., 2021; **Figure 1A**). A higher AMF abundance could result in the degradation of organic matter to release mineral nutrients for plants (Treseder and Cross, 2006; **Figure 4**).

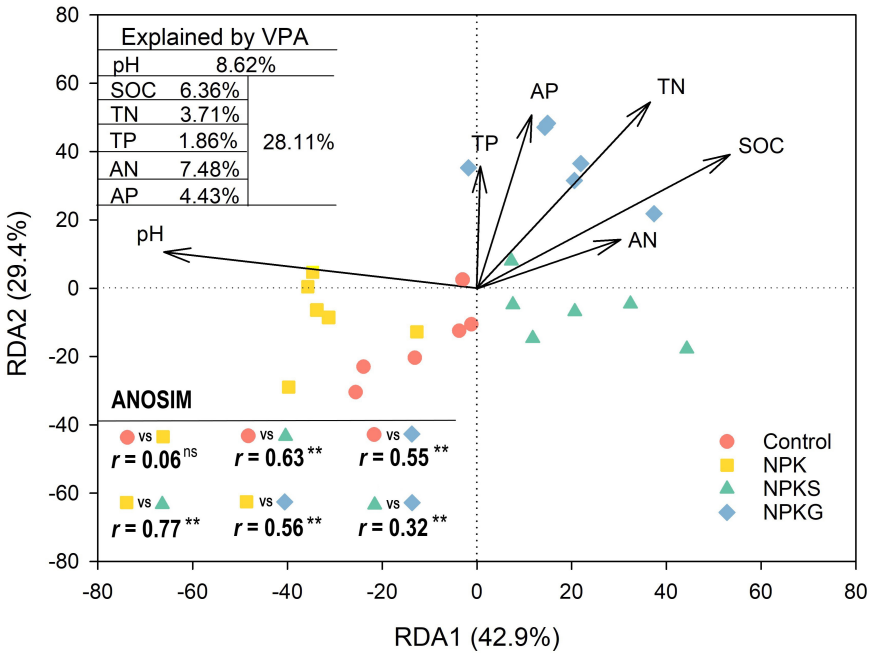

FIGURE 2
Redundancy analysis (RDA) plot showing AMF community composition across different treatments. Differences in the soil AMF community composition among different treatments were determined using Analyses of Similarities (ANOSIM). The explanation rate for each factor is placed in the upper left corner. SOC, soil organic carbon; TN, total nitrogen; AN, alkaline nitrogen; AP, available phosphorus; and TP, total phosphorus. $^{**}P < 0.01$.

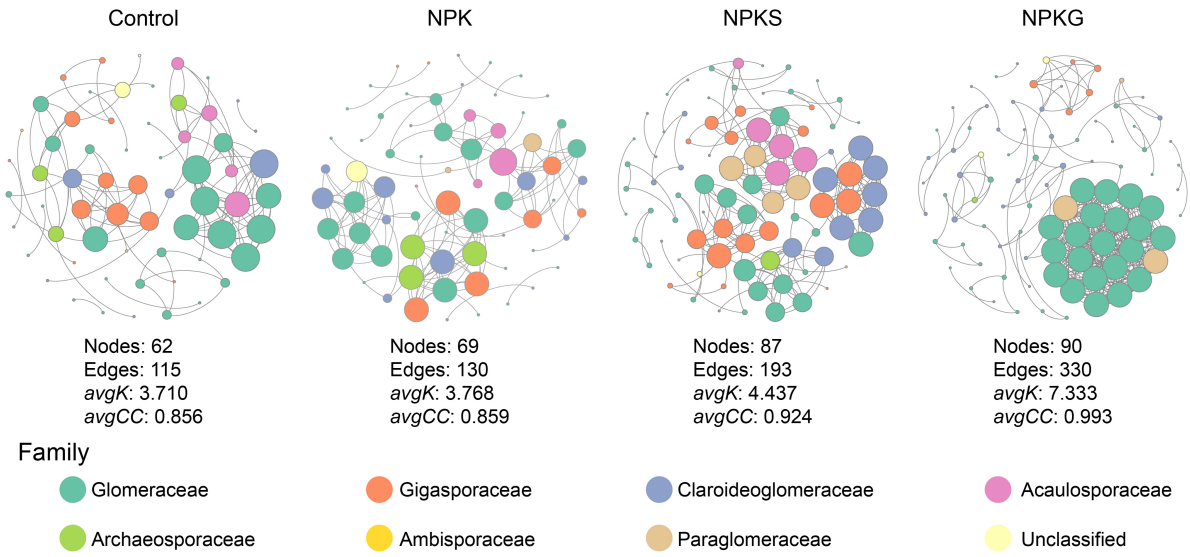

FIGURE 3
Co-occurrence AMF network for each treatment. Each node in the figure represents an amplicon sequence variant (ASV), and the size of the point represents the degree of the node.

The soil microbial networks reveal the microbial structure and their response to environmental fluctuations (Wagg et al., 2019; Yuan et al., 2021). This study showed that the application of hairy vetch had a significantly more intricate network than other treatments (**Figure 3**). Previous studies have shown that the networks with more sophisticated architecture were more stable to environmental fluctuations and might support higher ecosystem multifunctionality (Wagg et al., 2019).

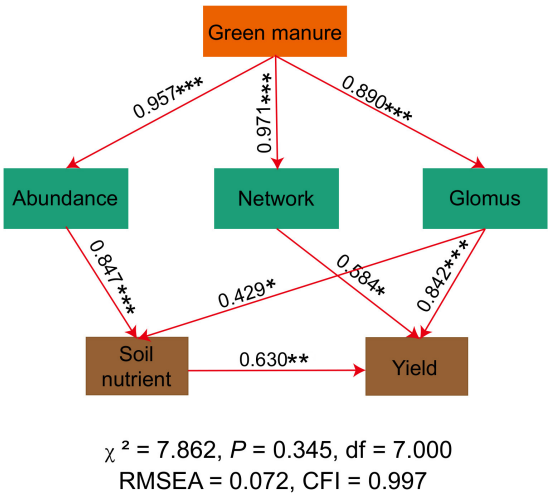

FIGURE 4
The structural equation model shows the relationships among AMF index, soil nutrient, and crop yield. The solid line represents a significant relationship, and the dotted line represents an insignificant relationship. *, **, and *** in the figure represents significance at the probability of 0.05, 0.01, and 0.001 level, respectively. All variances attributable to the constrained factor and the significance of the factor are portrayed at the bottom of the plot.

Thus, the application of hairy vetch might increase the complexity of the soil AMF network to strengthen below-ground multifunctionality, contributing to nutrient level and crop productivity.

In this study, the effects of returning composted straw on the soil nutrients and peanut yields were not remarkable compared to the application of hairy vetch (**Table 1**). The peanut straw showed a higher carbon content and lower nitrogen and phosphorus contents (Zhou et al., 2019). More nutrient loss occurred after nearly 8 months of composting. Thus, returning composted straw might not be an appropriate practice in the dryland of Ultisol. Besides, the application of the hairy vetch increased AMF abundance and optimized AMF community structure to increase soil nutrients and peanut yields (**Figures 1–4** and **Table 1**). However, the results of this study also demonstrated that the soil pH decreased sharply following planting green manure. Thus, attention should be paid to the negative effect of soil acidification following the long-term application of green manure.

Conclusion

This study demonstrated the differential feedback between peanut and their AMF partners in different agricultural practices. Planting hairy vetch significantly increased the AMF abundance, and network complexity, and optimized soil AMF taxa, contributing to the nutrient and yield improvement in the dryland of Ultisol. The application of hairy vetch might trigger positive feedback to strengthen the mutualism between crops and their AMF partners in the agroecosystem. In addition, returning peanut straw, without increasing nutrient levels but triggering soil acidification, might be an inappropriate practice in Ultisol. Overall, this study added to a growing body of knowledge on underlying feedback between plants and their AMF partners following different practices in Ultisol. However, there are certain limitations to this study. The AMF infection rate which could evaluate the feedback between plant and AMF was not measured. As the application of leguminous green manure increased the soil nitrogen content, we did not clarify the role of microbes within nitrogen cycling following the application of hairy vetch. These limitations should be addressed in future studies.

Data availability statement

The datasets presented in this study can be found in online repositories. The names of the repository/repositories and accession number(s) can be found in the article/**Supplementary material**.

Author contributions

JZ, JL, and XX designed the experiments. JZ, GL, KL, LS, WQ, and CP completed the field sampling. JZ, GL, and XX performed the data analysis and prepared the figures. JZ and GL wrote the manuscript. YJ, CX, JL, and XX contributed to the revision of manuscript. All authors contributed to the article and approved the submitted version.

Funding

This work was supported by the National Key Research and Development Program of China (No. 2021YFD1901201-05), China Agriculture Research System of MOF and MARA (No. CARS-22), the National Natural Science Foundation of China (Nos. 31801989, 41661052, and 32060333), the Natural Science Foundation of Anhui Province (No. 2008085MC62), and Anhui University Scientific Research Foundation (No. S020118002/038).

Acknowledgments

We thank Miss Lele Jin from Anhui University for her help in data analysis.

Conflict of interest

The authors declare that the research was conducted in the absence of any commercial or financial relationships that could be construed as a potential conflict of interest.

The reviewer PL was currently organizing a research topic with one of the author JL.

Publisher's note

All claims expressed in this article are solely those of the authors and do not necessarily represent those of their affiliated organizations, or those of the publisher, the editors and the reviewers. Any product that may be evaluated in this article, or claim that may be made by its manufacturer, is not guaranteed or endorsed by the publisher.

Supplementary material

The Supplementary Material for this article can be found online at: https://www.frontiersin.org/articles/10.3389/fmicb.2022.1002459/full#supplementary-material

References

Ai, Z. M., He, L. R., Xin, Q., Yang, T., Liu, G. B., and Xue, S. (2017). Slope aspect affects the nonstructural carbohydrates and C: N: P stoichiometry of Artemisia sacrorum on the Loess Plateau in China. *Catena* 152, 9–17. doi: 10.1016/j.catena.2016.12.024

Akhtar, K., Wang, W. Y., Ren, G. X., Khan, A., Feng, Y. Z., and Yang, G. H. (2018). Changes in soil enzymes, soil properties, and maize crop productivity under wheat straw mulching in Guanzhong, China. *Soil Till. Res.* 182, 94–102. doi: 10.1016/j.still.2018.05.007

Alguacil, M. M., Lozano, Z., Campoy, M. J., and Roldán, A. (2010). Phosphorus fertilization management modifies the biodiversity of AM fungi in a tropical savanna forage system. *Soil Biol. Biochem.* 42, 1114–1122. doi: 10.1016/j.soilbio.2010.03.012

Amir, A., McDonald, D., Navas-Molina, J. A., Kopylova, E., Morton, J. T., Zech, et al. (2017). Deblur rapidly resolves single-nucleotide community sequence patterns. *mSystems* 2, e191–e116. doi: 10.1128/mSystems.00191-16

Ansari, M. A., Choudhury, B. U., Layek, J., Das, A., Lal, R., and Mishra, V. K. (2022). Green manuring and crop residue management: Effect on soil organic carbon stock, aggregation, and system productivity in the foothills of Eastern Himalaya (India). *Soil Till. Res.* 218:105318. doi: 10.1016/j.still.2022.105318

Banerjee, S., Schlaeppi, K., and van der Heijden, M. G. A. (2018). Keystone taxa as drivers of microbiome structure and functioning. *Nat. Rev. Microbiol.* 16, 567–576. doi: 10.1038/s41579-018-0024-1

Bolyen, E., Rideout, J. R., Dillon, M. R., Bokulich, N. A., Abnet, C. C., Caporaso, J. G., et al. (2019). Reproducible, interactive, scalable and extensible microbiome data science using QIIME 2. *Nat. Biotechnol.* 37, 852–857. doi: 10.1038/s41587-019-0209-9

Bonanomi, G., De Filippis, F., Zotti, M., Idbella, M., Cesarano, G., Abd-ElGawad, A., et al. (2020). Repeated applications of organic amendments promote beneficial microbiota, improve soil fertility and increase crop yield. *Appl. Soil Ecol.* 156:103714. doi: 10.1016/j.apsoil.2020.103714

Bowman, R. A. (1988). A rapid method to determine total phosphorus in soils. *Soil Sci. Soc. Am. J.* 52, 1301–1304. doi: 10.2136/sssaj1988.03615995005200050016x

Camenzind, T., Hempel, S., Homeier, J., Horn, S., Velescu, A., Rillig, M. C., et al. (2014). Nitrogen and phosphorus additions impact arbuscular mycorrhizal abundance and molecular diversity in a tropical montane forest. *Glob. Change Biol.* 20, 3646–3659. doi: 10.1111/gcb.12618

Chen, Q. L., Hu, H. W., He, Z. Y., Cui, L., Zhu, Y. G., and He, J. Z. (2021). Potential of indigenous crop microbiomes for sustainable agriculture. *Nat. Food* 2, 233–240. doi: 10.1038/s43016-021-00253-5

de Gruyter, J., Weedon, J. T., Elst, E. M., Geisen, S., van der Heijden, M. G., and Verbruggen, E. (2022). Arbuscular mycorrhizal inoculation and plant response strongly shape bacterial and eukaryotic soil community trajectories. *Soil Biol. Biochem.* 165:108524. doi: 10.1016/j.soilbio.2021.108524

de Vries, F. T., Griffiths, R. I., Knight, C. G., Nicolitch, O., and Williams, A. (2020). Harnessing rhizosphere microbiomes for drought-resilient crop production. *Science* 368, 270–274. doi: 10.1126/science.aaz5192

Dutta, A., Bhattacharyya, R., Chaudhary, V. P., Sharma, C., Nath, C. P., Parmar, B., et al. (2022). Impact of long-term residue burning versus retention on soil organic carbon sequestration under a rice-wheat cropping system. *Soil Till. Res.* 221:105421. doi: 10.1016/j.still.2022.105421

Frew, A., Antunes, P. M., Cameron, D. D., Hartley, S. E., Johnson, S. N., Bennett, A. E., et al. (2022). Plant herbivore protection by arbuscular mycorrhizas: A role for fungal diversity? *New Phytol.* 233, 1022–1031. doi: 10.32942/osf.io/g6c3j

Frey, S. D. (2019). Mycorrhizal fungi as mediators of soil organic matter dynamics. *Annu. Rev. Ecol. Evol. S.* 50, 237–259. doi: 10.1146/annurev-ecolsys-110617-062331

Garland, G., Edlinger, A., Banerjee, S., Degrune, F., Rillig, M. C., van der Heijden, M. G. A., et al. (2021). Crop cover is more important than rotational diversity for soil multifunctionality and cereal yields in European cropping systems. *Nat. Food* 2, 28–37. doi: 10.1038/s43016-020-00210-8

Jeewani, P. H., Luo, Y., Yu, G. H., Fu, Y. Y., He, X. H., Xu, J. M., et al. (2021). Arbuscular mycorrhizal fungi and goethite promote carbon sequestration *via* hyphal-aggregate mineral interactions. *Soil Biol. Biochem.* 162:108417. doi: 10.1016/j.soilbio.2021.108417

Jiang, S. T., An, X. R., Shao, Y. D., Kang, Y. L., Chen, T. S., Shen, Q. R., et al. (2021). Responses of Arbuscular Mycorrhizal Fungi Occurrence to Organic Fertilizer: A meta-analysis of field studies. *Plant Soil* 469, 89–105. doi: 10.1007/s11104-021-05153-y

Jiang, Y. J., Luan, L., Hu, K. J., Liu, M. Q., Chen, Z. Y., Sun, B., et al. (2020). Trophic interactions as determinants of the arbuscular mycorrhizal fungal community with cascading plant-promoting consequences. *Microbiome* 8, 1–14. doi: 10.1186/s40168-020-00918-6

Johnson, D., Leake, J. R., Ostle, N., Ineson, P., and Read, D. J. (2002). In situ$_{13}CO^2$ pulse-labelling of upland grassland demonstrates a rapid pathway of carbon flux from arbuscular mycorrhizal mycelia to the soil. *New Phytol.* 153, 327–334. doi: 10.1046/j.0028-646X.2001.00316.x

Kaur, S., Campbell, B. J., and Suseela, V. (2022). Root metabolome of plant-arbuscular mycorrhizal symbiosis mirrors the mutualistic or parasitic mycorrhizal phenotype. *New Phytol.* 234, 672–687. doi: 10.1111/nph.17994

Khan, M. I., Gwon, H. S., Alam, M. A., Song, H. J., Das, S., and Kim, P. J. (2020). Short term effects of different green manure amendments on the composition of main microbial groups and microbial activity of a submerged rice cropping system. *Appl. Soil Ecol.* 147:103400. doi: 10.1016/j.apsoil.2019.103400

Kiers, E. T., Duhamel, M., Beesetty, Y., Mensah, J. A., Franken, O., Bucking, H., et al. (2011). Reciprocal rewards stabilize cooperation in the mycorrhizal symbiosis. *Science* 333, 880–882. doi: 10.1126/science.1208473

Lee, J. H., Lee, J. G., Jeong, S. T., Gwon, H. S., Kim, P. J., and Kim, G. W. (2020). Straw recycling in rice paddy: trade-off between greenhouse gas emission

and soil carbon stock increase. *Soil Till. Res.* 199:104598. doi: 10.1016/j.still.2020.104598

Li, H. Y., Smith, F. A., Dickson, S., Holloway, R. E., and Smith, S. E. (2008). Plant growth depressions in arbuscular mycorrhizal symbioses: Not just caused by carbon drain? *New Phytol.* 178, 852–862. doi: 10.1111/j.1469-8137.2008.02410.x

Li, X. G., Ding, C. F., Zhang, T. L., and Wang, X. X. (2014). Fungal pathogen accumulation at the expense of plant-beneficial fungi as a consequence of consecutive peanut monoculturing. *Soil Biol. Biochem.* 72, 11–18. doi: 10.1016/j.soilbio.2014.01.019

Liu, J., Zhang, J., Li, D. M., Xu, C. X., and Xiang, X. J. (2020). Differential responses of arbuscular mycorrhizal fungal communities to mineral and organic fertilization. *MicrobiologyOpen* 9:e00920. doi: 10.1002/mbo3.920

Louca, S., Polz, M. F., Mazel, F., Albright, M. B., Huber, J. A., Parfrey, L. W., et al. (2018). Function and functional redundancy in microbial systems. *Nat. Ecol. Evol.* 2, 936–943. doi: 10.1038/s41559-018-0519-1

Martin, S. L., Mooney, S. J., Dickinson, M. J., and West, H. M. (2012). The effects of simultaneous root colonisation by three Glomus species on soil pore characteristics. *Soil Biol. Biochem.* 49, 167–173. doi: 10.1016/j.soilbio.2012.02.036

Mohanty, S., Nayak, A. K., Swain, C. K., Dhal, B. R., Kumar, A., and Behera, K. K. (2020). Impact of integrated nutrient management options on GHG emission, N loss and N use efficiency of low land rice. *Soil Till. Res.* 200:104616. doi: 10.1016/j.still.2020.104616

Öpik, M., Vanatoa, A., Vanatoa, E., Moora, M., Davison, J., Zobel, M., et al. (2010). The online database MaarjAM reveals global and ecosystemic distribution patterns in arbuscular mycorrhizal fungi (Glomeromycota). *New Phytol.* 188, 223–241. doi: 10.1111/j.1469-8137.2010.03334.x

Rognes, T., Flouri, T., Nichols, B., Quince, C., and Mahé, F. (2016). VSEARCH: a versatile open source tool for metagenomics. *PeerJ* 4:e2584. doi: 10.7717/peerj.2584

Sager, M. (2007). Trace and nutrient elements in manure, dung and compost samples in Austria. *Soil Biol. Biochem.* 39, 1383–1390. doi: 10.1016/j.soilbio.2006.12.015

Shahbaz, M., Kuzyakov, Y., Maqsood, S., Wendland, M., and Heitkamp, F. (2017). Decadal nitrogen fertilization decreases mineral-associated and subsoil carbon: A 32-year study. *Land Degrad. Dev.* 28, 1463–1472. doi: 10.1002/ldr.2667

Smalla, K., Wieland, G., Buchner, A., Zock, A., Parzy, J., Berg, G., et al. (2001). Bulk and rhizosphere soil bacterial communities studied by denaturing gradient gel electrophoresis: plant-dependent enrichment and seasonal shifts revealed. *Appl. Environ. Microb.* 67, 4742–4751. doi: 10.1128/AEM.67.10.4742-4751.2001

Smith, S. E., and Read, D. J. (2008). *Mycorrhizal Symbiosis*, 3rd Edn. London, UK: Academic Press.

Stahlberg, S. (1980). A new extraction method for estimation of plant-available P, K and Mg: a trial application in Swedish cultivated soils. *Acta Agr. Scand.* 30, 93–107. doi: 10.1080/00015128009435700

Treseder, K. K., and Cross, A. (2006). Global distributions of arbuscular mycorrhizal fungi. *Ecosystems* 9, 305–316. doi: 10.1007/s10021-005-0110-x

Trivedi, P., Delgado-Baquerizo, M., Trivedi, C., Hu, H., Anderson, I. C., Singh, B. K., et al. (2016). Microbial regulation of the soil carbon cycle: Evidence from gene- enzyme relationships. *ISME J.* 10, 2593–2604. doi: 10.1038/ismej.2016.65

van der Heijden, M. G. A. (2010). Mycorrhizal fungi reduce nutrient loss from model grassland ecosystems. *Ecology* 91, 1163–1171. doi: 10.1890/09-0336.1

Wagg, C., Schlaeppi, K., Banerjee, S., Kuramae, E. E., and van der Heijden, M. G. (2019). Fungal-bacterial diversity and microbiome complexity predict ecosystem functioning. *Nat. Commun.* 10, 1–10. doi: 10.1038/s41467-019-12798-y

Wang, T., Duan, Y., Liu, G. D., Shang, X. W., Liu, L. F., Fang, W. P., et al. (2021). Tea plantation intercropping green manure enhances soil functional microbial abundance and multifunctionality resistance to drying-rewetting cycles. *Sci. Total Environ.* 15:151282. doi: 10.1016/j.scitotenv.2021.151282

Xiang, X. J., Adams, J. M., Qiu, C. F., Qin, W. J., Chen, J. R., Liu, J., et al. (2021). Nutrient improvement and soil acidification inducing contrary effects on bacterial community structure following application of hairy vetch (*Vicia villosa Roth* L.) in Ultisol. *Agr. Ecosyst. Environ.* 312:107348. doi: 10.1016/j.agee.2021.107348

Xiang, X. J., Gibbons, S. M., Yang, J., Kong, J. J., Sun, R. B., and Chu, H. Y. (2015). Arbuscular mycorrhizal fungal communities show low resistance and high resilience to wildfire disturbance. *Plant Soil* 397, 347–356. doi: 10.1007/s11104-015-2633-z

Xiang, X. J., Liu, J., Zhang, J., Li, D. M., Xu, C. X., and Kuzyakov, Y. (2020). Divergence in fungal abundance and community structure between soils under long-term mineral and organic fertilization. *Soil Till. Res.* 196:104491. doi: 10.1016/j.still.2019.104491

Yan, X. T., Zhai, Y. Q., Cai, Y. Y., Guo, Z., Zhang, Q. Q., and Ying, G. G. (2022). Hypothetical scenarios estimating and simulating the fate of antibiotics: Implications for antibiotic environmental pollution caused by manure application. *Sci. Total Environ.* 822:153177. doi: 10.1016/j.scitotenv.2022.153177

Yuan, M. M., Guo, X., Wu, L. W., Zhang, Y., Xiao, N. J., Zhou, J. Z., et al. (2021). Climate warming enhances microbial network complexity and stability. *Nat. Clim. Change* 11, 343–348. doi: 10.1038/s41558-021-00989-9

Zhou, G. P., Cao, W. D., Bai, J. S., Xu, C. X., Zeng, N. H., Rees, R. M., et al. (2019). Non-additive responses of soil C and N to rice straw and hairy vetch (*Vicia villosa Roth* L.) mixtures in a paddy soil. *Plant Soil* 436, 229–244. doi: 10.1007/s11104-018-03926-6

frontiers | Frontiers in Microbiology

TYPE Original Research
PUBLISHED 12 October 2022
DOI 10.3389/fmicb.2022.1015936

OPEN ACCESS

EDITED BY
Jia Liu,
Jiangxi Academy of Agricultural Sciences (CAAS), China

REVIEWED BY
Xiaofeng Xu,
San Diego State University, United States
Xinhou Zhang,
Nanjing Normal University, China

*CORRESPONDENCE
Jianping Wu
jianping.wu@ynu.edu.cn
Shaofei Jin
jinsf@tea.ac.cn

SPECIALTY SECTION
This article was submitted to Microbe and Virus Interactions with Plants, a section of the journal Frontiers in Microbiology

RECEIVED 10 August 2022
ACCEPTED 20 September 2022
PUBLISHED 12 October 2022

CITATION
Xi D, Jin S and Wu J (2022) Soil bacterial community is more sensitive than fungal community to canopy nitrogen deposition and understory removal in a Chinese fir plantation. *Front. Microbiol.* 13:1015936. doi: 10.3389/fmicb.2022.1015936

Soil bacterial community is more sensitive than fungal community to canopy nitrogen deposition and understory removal in a Chinese fir plantation

Dan Xi[1,2], Shaofei Jin[3]* and Jianping Wu[4,5]*

[1]Lushan Botanical Garden, Chinese Academy of Sciences, Jiujiang, China, [2]College of Forestry, Fujian Agriculture and Forestry University, Fuzhou, China, [3]Department of Geography, Minjiang University, Fuzhou, China, [4]Yunnan Key Laboratory of Plant Reproductive Adaptation and Evolutionary Ecology, Institute of Biodiversity, Yunnan University, Kunming, China, [5]Key Laboratory of Soil Ecology and Health in Universities of Yunnan Province, School of Ecology and Environmental Sciences, Yunnan University, Kunming, China

Soil microorganisms are key regulators for plant growth and ecosystem health of forest ecosystem. Although previous research has demonstrated that soil microorganisms are greatly affected by understory nitrogen (N) addition, little is known about the effects of canopy N addition (CNA) and understory management on soil microorganisms in forests. In this study, we conducted a full designed field experiment with four treatments: CNA (25 kg N ha^{-1} $year^{-1}$), understory removal (UR), canopy N addition, and understory removal (CNAUR) (25 kg N ha^{-1} $year^{-1}$), and control in a Chinese fir plantation. High-throughput sequencing and qPCR techniques were used to determine the abundance, diversity, and composition of bacterial and fungal communities in three soil layers. Our results showed that CNA increased bacterial diversity in the 10–20 cm soil layer but decreased bacterial abundance in the 20–40 cm soil layer and fungal diversity in the 0–10 cm soil layer. UR increased bacterial abundance only in the 20–40 cm soil layer. CNA, not UR significantly altered the compositions of soil bacterial and fungal community compositions, especially in the 0–20 cm soil layer. CNA sharply reduced the relative abundance of copiotrophic taxa (i.e., taxa in the bacterial phylum Proteobacteria and the orders Eurotiales and Helotiales in the fungal phylum Ascomycota) but increased the relative abundance of oligotrophic taxa (i.e., in the bacterial phylum Verrucomicrobia). RDA analysis revealed that soil pH, DON, and DOC were the main factors associated with the variation in bacterial and fungal communities. Our findings suggest that short-term CNA changes both soil bacterial and fungal communities, with stronger responses

in the surface and middle soil than in the deep soil layer, and that UR may enhance this effect on the soil bacterial abundance. This study improves our understanding of soil microorganisms in plantations managed with understory removal and that experience increases in N deposition.

KEYWORDS

canopy N deposition, understory removal, microbial community, bacterial diversity, Chinese fir plantation

Introduction

Deposition of active nitrogen (N) has dramatically accelerated because of anthropogenic activities (Galloway et al., 2004; Yu et al., 2019), and the effects of N deposition on terrestrial ecosystems have been widely investigated (Chen et al., 2015; Wu et al., 2019; Lu X. K. et al., 2021; Peguero et al., 2021). Most of the previous studies on the effects of N deposition on forests involved the experimental addition of N fertilizer to the forest floor (e.g., Krumins et al., 2009; Wu et al., 2019; Lu X. K. et al., 2021; Peguero et al., 2021) or a natural N-deposition gradient (Zechmeister-Boltenstern et al., 2011). With natural N deposition in forests, the quantity of N reaching the floor can be reduced by an interception with the canopy and the understory. In studies of N deposition in forests, such interception and retention have largely been ignored (Liu et al., 2020; Tian et al., 2020), likely resulting in overestimates of the effects of N deposition on forest ecosystems. Moreover, recent studies have indicated that forest canopies can intercept 30 to 85% of N deposition (Houle et al., 2015; Liu N. et al., 2018; Liu et al., 2020; Wang X. et al., 2021) and that elevated N deposition does not adversely affect microorganisms (Liu et al., 2020), fauna (Tian et al., 2020) or carbon (C) processing in the soil (Lu X. F. et al., 2021). Previous studies have also reported that canopy N addition (CNA) increased the species richness of the shrub layer (Tian et al., 2019) and increased the size of xylem tracheids of dominant broadleaf species (Jiang et al., 2018). These studies suggest the effects of N addition differ depending on where the N is added (i.e., directly to the forest floor or to the canopy). Overall, our understanding of how CNA affects forest ecosystems is incomplete.

Soil microorganisms are important regulators of nutrient cycling and litter decomposition processes (Zeng et al., 2016) that greatly affect plant growth and ecosystem health (Wall et al., 2015). It is well known that soil microorganisms are sensitive to environmental change and that increases in N deposition are likely to change soil microbial communities by altering nutrient availability (Ma et al., 2020). Many studies have reported that N deposition significantly affects soil microbial biomass, diversity, and community composition in subtropical forests (Mo et al., 2008; Liu et al., 2015; Li et al., 2016; Wang et al., 2018; Tian et al., 2019; Wu et al., 2019) and in temperate and boreal forests (Boot et al., 2016). In contrast, a recent study found that the soil microbial community was not influenced by N addition in a tropical rainforest (Li P. et al., 2019). As noted earlier, however, most studies of the response of soil microorganisms to increasing N deposition in forest ecosystems have involved N addition to the forest floor (e.g., Mo et al., 2008; Li et al., 2016; Wu et al., 2019; Wang J. P. et al., 2021), and only three studies have determined how the soil microbial community responds to CNA (Shi et al., 2016, 2018; Zhao et al., 2020). Research is needed to clarify how soil microbial communities in forests respond to CNA. In addition to being affected by how N is added, the response of soil microorganisms to N addition can be affected by forest or stand type (Zechmeister-Boltenstern et al., 2011; Zhou et al., 2017). Shi et al. (2016) reported that the effect of CNA on soil microbial biomass differed between subtropical and temperate forests. Fan and Hong (2001) found that the canopies of coniferous species, like those of broadleaf species, also intercepted substantial proportions of N before N reached the soil. Whether the response of the soil microbial community to CNA in conifer forests is similar to that in broadleaf forests has yet to be investigated.

Understory vegetation removal is an important silviculture practice in plantation ecosystems (Wang T. et al., 2021). The understory is removed to reduce competition between tree and understory species and increase lumber production (Wu et al., 2011; Wang et al., 2014). On the other hand, removing understory vegetation also alters soil temperature and moisture (Xiong et al., 2008; Wang et al., 2014; Giuggiola et al., 2018) and nutrient availability, which greatly affect soil microorganisms. Several studies reported that understory removed reduced soil microbial biomass due to the increased soil temperature or reduced substrate availability in subtropical forests (Xiong et al., 2008; Wu et al., 2011; Zhao et al., 2013; Wan et al., 2019), and one study found that soil microbial properties were not significantly affected by understory removal (Urcelay et al., 2010). It, therefore, remains unclear how understory removal influences the soil microbial community. By increasing N availability, N addition was previously found to enhance forest understory regeneration (Trentini et al., 2018). Removal of understory plants is likely to increase the proportion of N deposition that reaches the floor and thereby increase soil N availability, which is likely to stimulate or

suppress microbial activity and consequently result in changes in microbial biomass, diversity, and community composition. Previous phospholipid fatty acids (PLFAs) analyses indicated a reduction in fungal biomass after understory N addition and understory removal in subtropical plantations (Zhao et al., 2013; Lei et al., 2018). However, these previous studies did not indicate which specific microbial groups were affected by N addition and understory removal.

Plantations of Chinese fir (*Cunninghamia lanceolata*) have been widely planted in the subtropical regions of China due to the tree's ecological and economic value (Li R. S. et al., 2019). As previously indicated, understory plants are usually removed from these plantations to increase timber quality and production (Li R. S. et al., 2019), and these subtropical regions have higher N deposition than other regions in China (Yu et al., 2019). Although the effects of N addition or understory removal on soil microorganisms have been studied in plantations, the data are mostly limited to the surface/subsurface soil layer (<20 cm) (Wu et al., 2011, 2019; Lei et al., 2018; Li R. S. et al., 2019) even though nutrient levels are known to change with soil depth (Liu D. et al., 2018; Kang et al., 2021). It remains unclear how the soil microbial community at different soil depths is affected by the interaction of N deposition and understory removal in Chinese fir plantations. A better understanding of the effects of N deposition, understory removal, and soil depth on soil fungi and bacteria will help clarify the mechanisms affecting nutrient availability in these plantations. Understanding the changes in microbial diversity and community structure in these soil layers could also contribute to forest management.

This study performed a 5-year CNA and understory removal experiment on a Chinese fir plantation. The objectives were to determine whether CNA, understory removal, or their interaction affected the abundance, diversity, and structure of soil bacterial and fungal communities in different soil layers and identify which factors were associated with these effects. We tested three hypotheses: (1) short-term CNA would not significantly affect microbial communities in surface or deeper soil layers due to the substantial interception of N by the canopy (Shi et al., 2016); (2) by reducing the belowground input of C, understory removal would affect the bacterial community more than the fungal community because nutrient demand and metabolic activities are lower for fungi than bacteria (Zhou et al., 2017); and (3) changes in the composition of soil microbial communities will be associated with different soil properties in different soil layers.

Materials and methods

Site description

This study was carried out at the Guanzhuang National Forestry Farm (117°43′ E, 26°30′ N) in Sanming City, Fujian Province, China. The region has a subtropical monsoon climate. The average annual temperature and precipitation are 18.8–19.6°C and 1,606–1,650 mm, respectively, and the soil is classified as acrisol (Wu et al., 2019).

The Chinese fir plantation used in this study was established in 2008 on a 4-ha site with homogenous conditions. At the start of the experiment in June 2013, the dominant understory plants were *Bambusa chungii* and *Dicranopteris dichotoma* (accompanied by *Smilax china* and *Melastoma dodecandrum*); the mean fir tree height and diameter at breast height were 5.11 m and 7.34 cm, respectively; the average contents of total organic carbon (TOC) and total nitrogen (TN) in the soil surface layer were 33.37 and 1.91 kg^{-1}, respectively; and the mean pH was 4.44 (Lei et al., 2018).

Experimental design

Eight plots (15 m × 15 m for each plot), four plots with N addition treatments and four plots without N addition, were randomly selected. A 5-m × 10-m understory removal subplot was established in each plot. As a result, the experiment included two levels of N addition (±) and two levels of understory removal (±) in a factorial design that resulted in four treatments: no N addition and no understory removal (control, CK); understory removal without N addition (UR, 0 kg N ha^{-1} $year^{-1}$); CNA without understory removal (CNA, 25 kg N ha^{-1} $year^{-1}$); and canopy N addition plus understory removal (CNAUR) (25 kg N ha^{-1} $year^{-1}$). Adjacent plots were separated by a 3- to 8-m wide buffer strip to prevent cross-contamination. To add N to a plot, the required quantity of NH_4NO_3 (269 g) was dissolved in 15 L of water, and the solution was sprayed onto the tree canopy using a previously described spraying system (Lei et al., 2018). Control plots received an equivalent volume of water without NH_4NO_3. Plots were treated once every 2 months starting in June 2014 and continuing until sampling in April 2019. All understory plants were manually removed in UR and CNAUR plots at the start of the experiment, and germinating understory plants in UR and CNAUR plots were manually removed every 2 months.

Sample collection and analyses

In April 2019, eight soil cores (3.5 cm diameter) were randomly collected at depths of 0–10, 10–20, and 20–40 cm in each plot and were combined to yield one composite sample per depth per plot. Litter was removed from the soil surface before the cores were taken. The fresh soil samples were passed through a 2-mm sieve. Visible roots and stones were carefully removed before each composite soil sample was divided into three parts. One part was used for the determination of soil moisture and contents of soil ammonium (NH_4^+), nitrate

(NO_3^-), microbial biomass carbon (MBC) and microbial biomass nitrogen (MBN), and dissolved organic carbon (DOC) and dissolved organic nitrogen (DON). Another part was air-dried to the determination of soil pH and contents of TOC, TN, and available phosphorus (AP). The third part was stored at −80°C for microbial molecular analysis.

Soil TOC and TN contents were measured with an element analyzer (Vario isotope cube, Germany). Soil NH_4^+ and NO_3^- contents were determined with a chemical analyzer (SmartChem 200, Italy). Soil MBC and MBN were analyzed using a chloroform fumigation-extraction method. Soil DOC and TDN were extracted with a 0.5 M K_2SO_4 solution and were measured with a total organic analyzer (TOC-V CPH, Japan); DON was calculated by subtracting inorganic N (NH_4^+ and NO_3^-) from TDN. Soil pH was measured in a 1:2.5 (w/v) mixture of soil and deionized water with a pH meter. Soil moisture was determined by the gravimetrical weight method by drying fresh soil at 105°C to a constant weight. Soil AP was extracted with a 0.05 M NH_4F–0.01 M HCl solution and was determined with the colorimetrical molybdate blue method.

DNA extraction, PCR amplification, and sequence processing

Microbial DNA was extracted from 0.5-g subsamples of fresh soil samples using the PowerSoil DNA Isolation Kit (MO Bio Laboratories Inc., Carlsbad, CA, USA) according to the manufacturer's protocols. The final DNA concentration and purification were determined with a NanoDrop 2000 UV-vis spectrophotometer (Thermo Scientific, Wilmington, DE, USA), and DNA quality was checked by 1% agarose gel electrophoresis.

The V3–V4 hypervariable region of the bacterial 16S rRNA gene was amplified using paired primers 338F (5′-ACTCCTACGGGAGGCAGCA-3′) and 806R (5′-GGACTACHVGGGTWT CTAAT-3′) by a PCR thermal cycler (GeneAmp 9700, ABI, Cambridge, MA, USA). The PCR amplification procedure for bacteria was as follows: 95°C for 3 min; followed by 29 cycles of 30 s at 95°C for denaturation, 30 s at 55°C for annealing, and 45 s at 72°C for extension; and a final extension at 72°C for 10 min. The rDNA internal transcribed spacer (ITS) region 1 of fungi was amplified using the primers ITS1F (5′-CTTGGTCATTTAGAGGAAGTAA-3′) and ITS2R (5′-GCTGCGTTCTTCATCGATGC-3′). The PCR amplification procedure was as follows: initial denaturation at 95°C for 3 min; followed by 37 cycles at 95°C for 30 s, 55°C for 30 s, and 72°C for 45 s; and a final extension at 72°C for 10 min. The PCR products of both bacteria and fungi were further purified, quantified, and finally sent for sequencing on an Illumina MiSeq PE300 platform at Majorbio Bio-Pharm Technology Co., Ltd., Shanghai, China. The bacterial and fungal gene sequences were deposited in NCBI under accession number SRP264464.

High-quality sequences were obtained by filtering the raw reads with the three criteria reported by Wu et al. (2019). Sequences with >97% similarity were clustered to the same operational taxonomic units (OTUs) using UPARSE software (version 7.1) (Edgar, 2013). The taxonomy of each bacterial and fungal OTU was determined by the RDP classifier (version 2.11),[1] and the selected representative sequences were implemented in the SILVA database (Release138)[2] and the UNITE database (Release 8.0)[3] for identification of bacteria and fungi, respectively. The Chao 1 index, the Shannon Index, and the number of observed OTUs were calculated to assess the alpha-diversity of the bacterial and fungal community in each sample.

Quantitative PCR for bacteria and fungi

qPCR was used to determine the absolute abundance of bacterial 16S rRNA and fungal ITS genes. The target primers for bacteria and fungi were the same primers used for the PCR amplification process described in the previous section. The PCR reactions were carried out using an ABI Real-time 7500 system (Applied Biosystems, Waltham, MA, USA) and SYBR Green Premix (TaKaRa Bio Inc., Shiga, Japan). The PCR protocol for both bacteria and fungi involved an initial denaturation at 94°C for 5 min; followed by 30 cycles at 94°C for 30 s, 55°C for 30 s, and 72°C for 30 s; and a final extension at 72°C for 5 min. All qPCR reactions in each DNA sample were run in triplicate. Ten-fold serial dilutions of a plasmid containing the full-length target genes were used to generate the standard curves for quantitative PCR. The 16S rRNA and ITS gene abundances in all samples were expressed as copies per gram of dried soil.

Statistical analysis

Statistical analyses were carried out with the SPSS 16.0 software package for Windows (SPSS Inc., Chicago, IL, USA). One-way ANOVAs were used to determine differences in physicochemical properties, microbial biomass (C and N), gene abundance, diversity indexes, and dominant community species among treatments in each soil layer; when ANOVAs were significant, means were compared by the LSD method. Two-way ANOVAs were used to assess the effects of CNA, understory removal on soil physicochemical properties and microbial communities in each soil layer. Pearson correlation analysis was used to examine the relationships between microbial abundance and diversity with soil properties, and a heatmap

1 http://sourceforge.net/projects/rdp-classifier/
2 http://www.arb-silva.de
3 http://unite.ut.ee/index.php

of microbial community composition at the order level and soil properties was generated using the "corrplot" package in R (version 4.0.5). Differences in the structure of bacterial and fungal communities among treatments were examined using principal coordinate analysis (PCoA) with non-parametric multivariate statistical methods (ADONIS). The relationships between microbial community properties and soil properties in each soil layer were assessed by redundancy analysis (RDA) with the Mantel test in the "vegan" package of R software (version 4.0.5). The structure equation model (SEM) was performed in the "piecewiseSEM" package (Lefcheck, 2016). All effects at $p < 0.05$ were considered statistically significant, and all analyses were performed using R software (R version 4.0.5).

Results

Soil physicochemical properties

The following properties within each soil layer were unaffected by the treatments: pH, soil moisture, TOC, TN, NH_4^+, NO_3^-, and DOC (**Table 1**). Soil AP content in the 0–10 cm layer was lower for the CNA treatment than for the CK treatment (**Table 1**). A similar pattern was found for DON content in the 20–40 cm layer. Two-way ANOVAs showed that CNA and UR did not influence soil physicochemical properties in different soil layers, whereas their statistical interactions (CNA × UR) had a marginal effect on soil AP and DON (**Supplementary Table 1**).

Gene abundance and microbial biomass carbon and nitrogen

Abundance was higher for the bacterial 16S rRNA gene (range = 1.97×10^8 to 2.61×10^9 copies g^{-1} soil) than for the fungal ITS gene (range = 4.01×10^6 to 4.46×10^7 copies g^{-1} soil) (**Figures 1C,D**). In the 0–20 cm soil layer, microbial gene abundances were not significantly affected by the treatments. However, in the 20–40 cm soil layer, bacterial gene abundance was significantly higher for the UR treatment than for the CK, UN, or CNAUR treatments (**Figure 1C**). Moreover, two-way ANOVAs demonstrated that bacterial gene abundance in this soil layer was significantly affected by CNA, UR, or their interaction (**Figure 1C**; **Supplementary Table 2**). In addition, bacterial gene abundance was negatively correlated with MBC and MBN in the 10–20 cm soil layer (**Figure 2**).

Soil MBC but not MBN was significantly affected by the CNA and UR treatments (**Figures 1A,B**). In the 10–20 cm layer, soil MBC content was significantly higher for the UR treatment than for the CK or the CNAUR treatment. In the 20–40 cm layer, soil MBC content was significantly lower for the CNA treatment than for the CK treatment. The statistical interaction between CNA and UR was significant for soil MBC in the 10–40 cm layer (**Figure 1A**; **Supplementary Table 2**).

Soil bacterial and fungal diversity

The number of OTUs and the Chao1 and Shannon indices were used to assess microbial diversity. For bacteria, the number of OTUs and the Chao1 index did not significantly differ among the treatments in any soil layer (**Figures 3A,B**). However, the Shannon index for bacteria in the 10–20 cm soil layer was significantly higher for the CNAUR treatment than for the CK treatment (**Figure 3C**). For fungi, the number of OTUs did not significantly differ among the treatments in any soil layer (**Figure 3D**). The Chao1 index for fungi was significantly higher in the CK treatment than in the CNAUR treatment in the 0–10 cm soil layer (**Figure 3E**). The Shannon index for fungi was significantly lower in the CNA treatment than in the other treatments in the 0–10 cm soil layer; it did not differ among the treatments in the 10–20 cm soil layer and was significantly higher in the CNA treatment than in the CNAUR treatment in the 20–40 cm soil layer (**Figure 3F**). Overall, the effects of CNA and UR on bacterial and fungal diversity differed among the soil layers (**Figure 3**; **Supplementary Table 2**). In addition, the Shannon index and the number of OTUs for bacteria were negatively related to soil TN and DON in the 10–20 cm layer (**Figure 2**). Similar negative correlations for bacteria were observed between soil DOC and the Chao 1 index, the OTU number in the 10–20 cm layer, and between DOC and the Shannon index in the 20–40 cm layer. For fungi, in contrast, the Chao 1 index and the OTU number were positively correlated with soil DOC and AP in the 0–10 cm layer and with TC in the 20–40 cm layer; the Shannon index was negatively correlated with soil pH, soil moisture, TOC, and TN in the 10–20 cm layer (**Figure 2**).

Composition of bacterial and fungal communities

The following seven major bacterial phyla (relative abundance >1%) were identified across treatments and accounted for >94% of the bacterial community: Proteobacteria, Acidobacteria, Chloroflexi, Actinobacteria, Planctomycetes, Verrucomicrobia, and WPS_2 (**Figure 4**). The bacterial phyla in different soil layers were affected by CNA and UR (**Supplementary Table 2**). For example, CNA significantly increased the relative abundances of Verrucomicrobia and Chlamydiae in the 0–20 cm layer (**Figures 4A,B**) and Chloroflexi in the 10–40 cm layer (**Figures 4B,C**) but significantly decreased the relative abundances of Proteobacteria and Actinobacteria in the 10–20 cm layer (**Figure 4B**). A decrease in Proteobacteria relative abundance and an increase

TABLE 1 Soil properties under different treatments.

Soil layer (cm)	Treatment	pH	Soil moisture (%)	TOC ($g\ kg^{-1}$)	TN ($g\ kg^{-1}$)	NH_4^+-N ($mg\ kg^{-1}$)	NO_3^--N ($mg\ kg^{-1}$)	DON ($mg\ kg^{-1}$)	DOC ($mg\ kg^{-1}$)	AP ($mg\ kg^{-1}$)
0–10	CK	4.33 (0.04) a	24.41 (0.87) a	23.67 (2.04) a	1.29 (0.08) a	11.80 (2.54) a	1.89 (0.44) a	16.77 (1.22) a	560.9 (65.4) a	10.34 (1.74) a
	UR	4.36 (0.08) a	24.12 (0.96) a	24.38 (2.96) a	1.31 (0.15) a	8.24 (1.27) a	1.61 (0.31) a	16.26 (0.85) a	551.3 (44.4) a	7.10 (1.07) ab
	CNA	4.38 (0.04) a	24.18 (0.86) a	20.37 (1.75) a	1.05 (0.10) a	7.36 (0.98) a	1.21 (0.32) a	17.16 (1.36) a	531.2 (52.6) a	6.49 (0.15) b
	CNAUR	4.41 (0.04) a	24.87 (1.06) a	27.27 (3.24) a	1.47 (0.22) a	9.05 (1.82) a	1.26 (0.08) a	17.46 (4.22) a	520.7 (81.8) a	8.60 (1.41) ab
10–20	CK	4.39 (0.02) a	22.73 (0.45) a	14.86 (2.03) a	0.91 (0.11) a	4.56 (0.06) a	1.58 (0.45) a	19.47 (1.76) a	587.1 (53.2) a	5.20 (0.95) a
	UR	4.33 (0.02) a	22.38 (1.16) a	14.92 (1.45) a	0.93 (0.09) a	5.31 (0.56) a	1.18 (0.21) a	17.52 (1.48) a	578.0 (53.5) a	3.47 (0.54) a
	CNA	4.37 (0.04) a	21.34 (0.94) a	12.47 (1.17) a	0.78 (0.08) a	4.43 (0.91) a	1.16 (0.15) a	16.01 (1.10) a	544.1 (51.5) a	3.36 (0.26) a
	CNAUR	4.36 (0.02) a	22.13 (0.68) a	13.67 (1.21) a	0.83 (0.09) a	5.08 (0.81) a	0.88 (0.16) a	16.98 (1.64) a	593.2 (63.1) a	3.80 (0.78) a
20–40	CK	4.32 (0.06) a	19.09 (0.45) a	8.24 (0.74) a	0.55 (0.05) a	2.91 (0.44) a	1.58 (0.19) a	14.39 (1.35) a	498.1 (81.8) a	2.42 (0.70) a
	UR	4.34 (0.01) a	20.59 (1.57) a	7.90 (1.04) a	0.57 (0.09) a	3.14 (0.39) a	1.44 (0.32) a	10.93 (1.20) ab	510.2 (63.9) a	2.32 (0.41) a
	CNA	4.34 (0.01) a	19.29 (0.76) a	8.18 (0.99) a	0.54 (0.04) a	3.72 (1.73) a	1.74 (0.59) a	10.20 (0.55) b	453.1 (71.9) a	1.36 (0.17) a
	CNAUR	4.18 (0.13) a	17.51 (1.13) a	8.29 (1.39) a	0.57 (0.09) a	2.69 (0.50) a	0.72 (0.10) a	11.68 (1.36) ab	427.7 (69.5) a	3.36 (1.71) a

Data are presented as mean and standard errors (in brackets) for replicates ($n = 4$). Different letters within columns indicate significant differences among treatments in the same soil layer.

10.3389/fmicb.2022.1015936

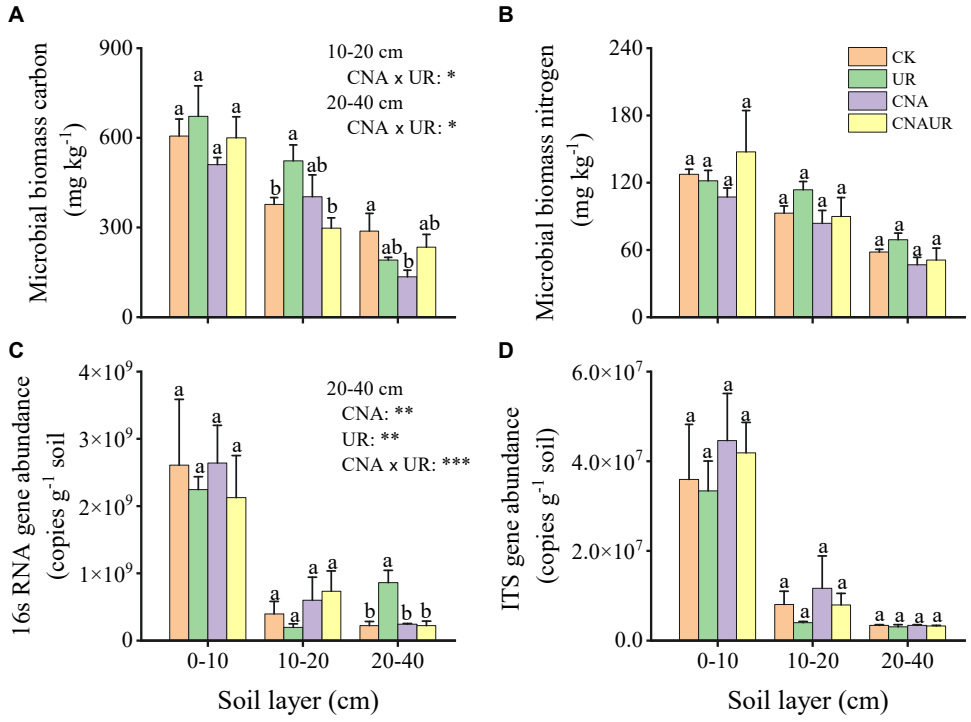

FIGURE 1

Contents of microbial biomass C **(A)** and N **(B)** and gene abundances of bacteria **(C)** and fungi **(D)** in three soil layers as affected by four treatments, i.e., two levels (±) of canopy N addition (CNA) and two levels (±) of understory removal (UR), and the statistical interaction CNA × UR. Treatments are described in **Table 1**. Values are means + SE. In each plot, means with different letters are significantly different at $p < 0.05$. *, **, and *** indicate significance at $p < 0.05$, 0.01, and 0.001, respectively.

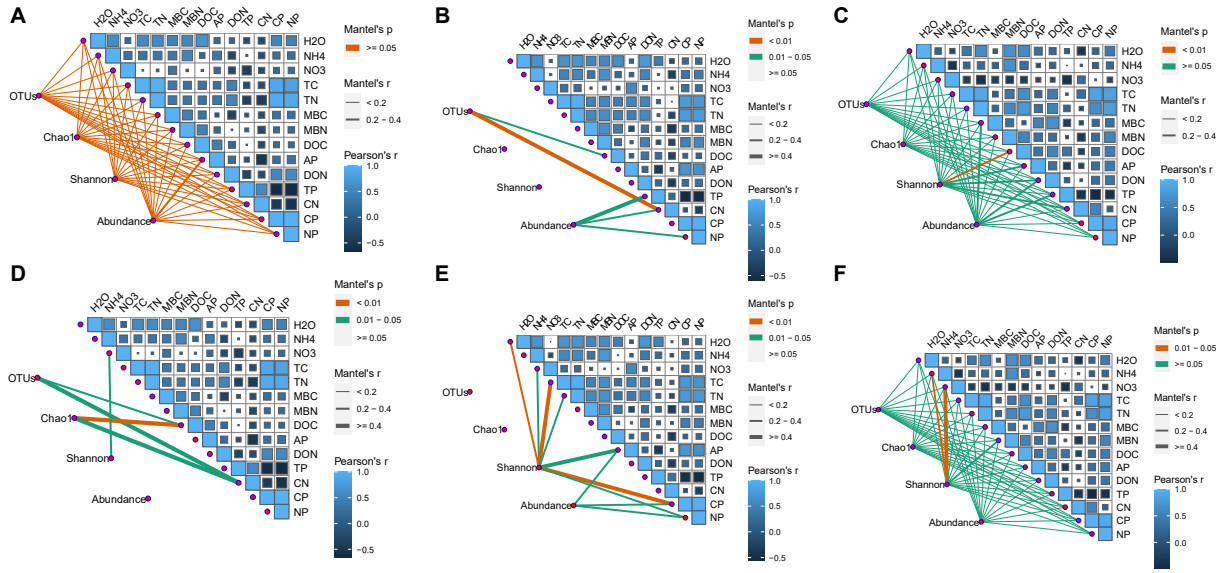

FIGURE 2

Correlations among soil chemical parameters and bacterial **(A–C)** and fugal **(D–F)** diversity indexes (OTUs, Chao1, Shannon, and gene abundance) in different soil layers, 0–10 cm **(A,D)**, 10–20 cm **(B,E)**, and 20–40 cm **(C,F)**. The correlation coefficients of each soil chemical parameter are presented by area size of squares, smaller area lower correlation, and vice versa. The level of correlations between microbial index and soil chemical variables is indicated by line thickness; the correlations are indicated by the line color; red and blue colors indicate positive and negative correlation, respectively.

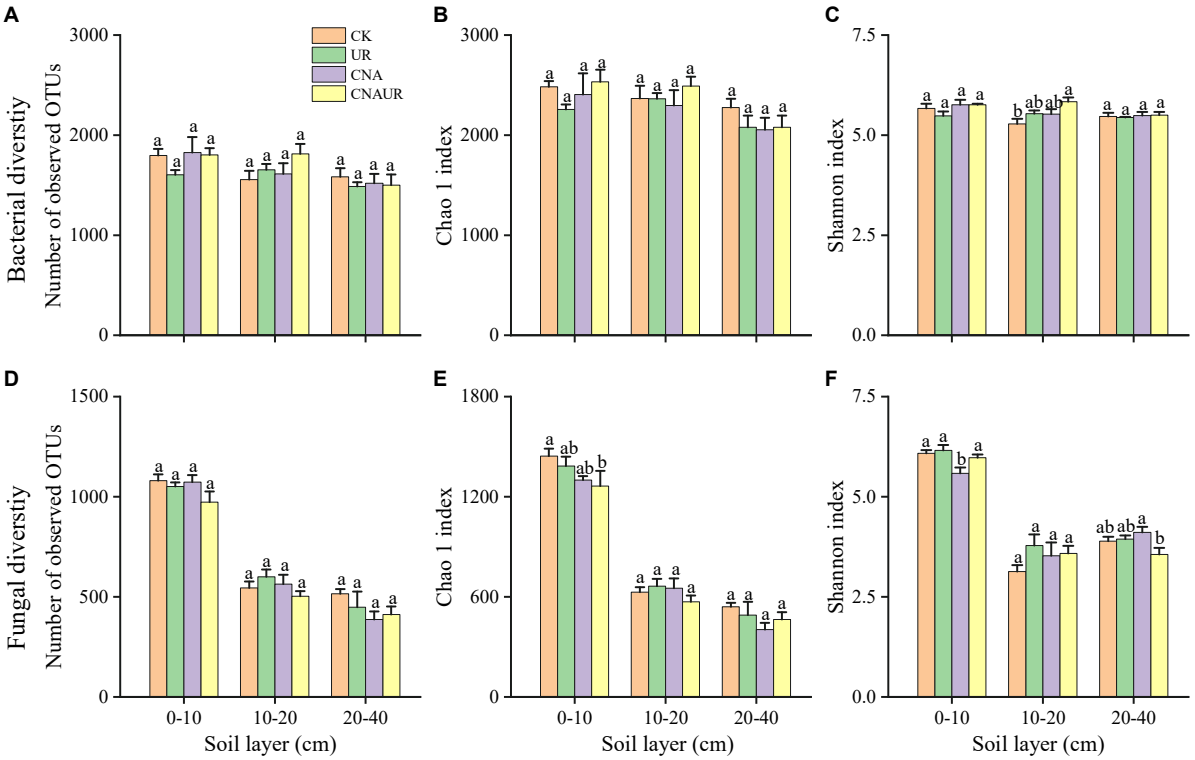

FIGURE 3
Diversity indices of bacteria **(A–C)** and fungi **(D–F)** in three soil layers as affected by four treatments (treatments are described in **Table 1**). Values are means ± SE. In each plot, means with different letters are significantly different at $p < 0.05$.

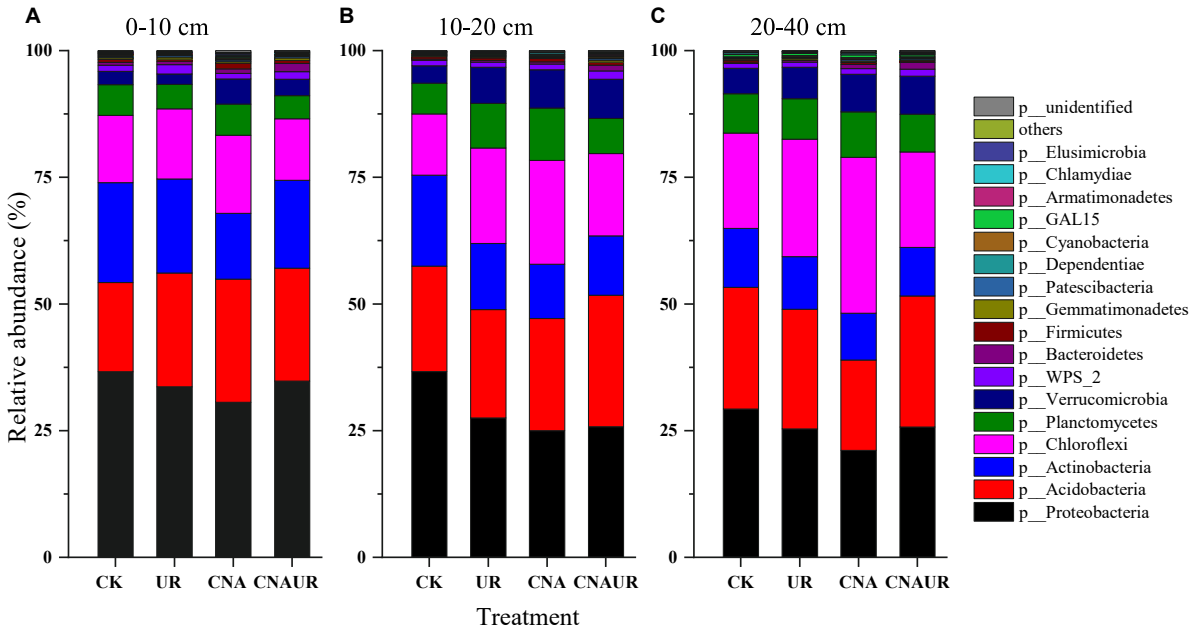

FIGURE 4
Relative abundance of soil bacterial community at the phyla level under treatments (treatments are described in **Table 1**) in three soil layers, 0–10 cm **(A)**, 10–20 cm **(B)**, 20–40 cm **(C)**. Those phyla that represent >0.1% of the bacterial community abundance are named, while those that represent <0.1% of the bacterial community abundance are referred to as "others."

in Chloroflexi relative abundance were also observed for the UR treatment in the 10–40 cm soil layer (Figures 4B,C). In addition, the relative abundances of Chloroflexi and Planctomycetes in the 10–20 or 20–40 cm soil were affected by the statistical interaction between CNA and UR (Supplementary Table 2).

The two most dominant phyla of fungi in all soil layers were Ascomycota (relative abundance = 36.1–87.5%) and Basidiomycota (5.7–15.3%); the less abundant phyla included Mortierellomycota (0.14–4.3%) and Mucoromycota (0.13–1.3%) (Supplementary Figure 1). The phylum Glomeromycota (0.85–1.30%) was only found in the 0–10 cm soil layer (Supplementary Figure 1A). Among the detected sequences, there were 45.8–48.7% and 29.0–36.3% of sequences unidentified in the 10–20 and 20–40 cm soil layer, respectively (Supplementary Figures 1B,C), although good coverage of sequences was in the range of 0.98–1.0 in these soil layers. Archaeorhizomycetales, Eurotiales, and Agaricales were the three most dominant orders of fungi in the 0–10 cm soil layer (Figure 5A). However, GS31, Tremellales, and Archaeorhizomycetales including unclassified p_Ascomycota were the dominant fungi in the 10–40 cm soil layer (Figures 5A,B). Moreover, CNA significantly decreased the relative abundances of order Archaeorhizomycetales, Eurotiales, Helotiales, and Venturiales, and the interaction of CNA and UR affected the relative abundance of Mortierellales in the 0–10 cm soil layer (Supplementary Table 4). In contrast, UR significantly increased the relative abundance of Mortierellales in the 10–20 cm layer (Supplementary Table 4) and decreased the relative abundance of Mortierellales and Chaetothyriales in the 20–40 cm layer (Supplementary Table 4). In addition, UR and the CNA × UR interaction significantly affected the relative abundance of the phylum Mortierellomycota in the 0–20 cm soil layer, while CNA significantly decreased the relative abundance of the phylum Mucoromycota in the 20–40 cm layer (Supplementary Table 3).

Factors associated with bacterial and fungal community composition

The PCoA analysis showed that the soil bacterial community structure in the 10–20 cm layer was significantly shifted by CNA and UR treatment (Supplementary Figure 2B, PERMANOVA test, $R^2 = 0.31$, $p = 0.013$). In particular, the bacterial community composition was different with the CNA treatment than with the CK treatment. RDA analysis revealed that the first two RDA axes explained 16.1% of the variance in the bacterial community and that soil DON ($F = 3.9$, $p = 0.008$) followed by soil moisture and DOC were the most important factors associated with bacterial community composition in the 10–20 cm layer (Figure 6). However, soil TN ($F = 2.3$, $p = 0.011$) had the largest effect on the bacterial community in the 0–10 cm layer, and soil pH ($F = 5.5$, $p = 0.038$) and DOC ($F = 4.3$, $p = 0.002$) were the two important factors to bacterial community composition in the 20–40 cm soil layer (Figures 6A,C). Together, the RDA 1 and RDA 2 axes accounted for 40.22% of the variance in the 0–10 cm layer and 42.7% of the variance in the 20–40 cm layers. The SEM analysis showed that soil pH, DOC, and DON explained 29.00% of variance in the bacterial community (Supplementary Figure 3). In addition, the relative abundances were negatively correlated with pH for the orders Frankiales and Elsterales but were positively correlated with pH for the order Streptomycetales. Positive correlations were observed between NH_4^+ and Myxococcales and Solirubrobacteriales and between AP and Rhizobiales and Acetobacterales in the 0–10 cm layer (Figure 7). In the 10–20 cm layer, Elsterales and Corynebacteriales were positively correlated with soil moisture and DON; Streptomycetales were positively correlated with TC, TN, and DON; and Acidobacteriales and Myxococcales were negatively correlated with all soil parameters except NO_3^- and AP. In the 20–40 cm layer, Rhizobiales, Elsterales, and Corynebacteriales were positively correlated with DOC and DON, and Gemmatales were positively correlated with TC and TN but were negatively correlated with AP (Figure 7B). Negative correlations were also found between Betaproteobacteriales and NO_3^- and between norank taxa of phyla WPS.2 and class AD3 and TOC and TN.

Unlike the bacterial community, fungal community composition significantly differed among treatments in the 0–10 cm soil layer (Supplementary Figure 4A, PERMANOVA test, $R^2 = 0.24$, $p = 0.034$). In this layer, the fungal community composition was significantly associated with soil DOC ($p = 0.002$) and pH ($p = 0.004$), and in the RDA, the two axes (RDA 1 and RDA 2) were explained for 26.89% of the variation (Figure 8). The SEM analysis showed that soil pH, DOC, and DON explained 47.00% of variance in the bacterial community (Supplementary Figure 3). Moreover, the relative abundance of Helotiales was negatively correlated with pH but was positively correlated with DOC. Negative correlations were also observed between the relative abundance of Archaeorhizomycetales and TN, between the relative abundance of Geminibasidiales and AP, and between the relative abundance of Capnodiales and TOC, TN, and DON (Figure 7E). In contrast, the relative abundances of Botryosphaeriales, GS31, Glomerales, and Orbiliales were positively correlated with AP, soil moisture, DON, and pH, respectively. Although the treatments did not change fungal community composition in the 10–40 cm layer (Supplementary Figure 4), soil DOC ($F = 1.4$, $p = 0.024$) and pH ($F = 1.6$, $p = 0.008$) were closely related to fungal community composition in the 10–20 and 20–40 cm layer, respectively (Figures 8A,C). In the 10–20 cm layer, the relative abundances of Archaeorhizomycetales, GS31, and Tremellales were positively correlated with NH_4^+, DOC, and pH, respectively, but the relative abundance of an unidentified phylum of Ascomycota was negatively correlated with TOC, TN, soil moisture, and DON. Negative correlations were also

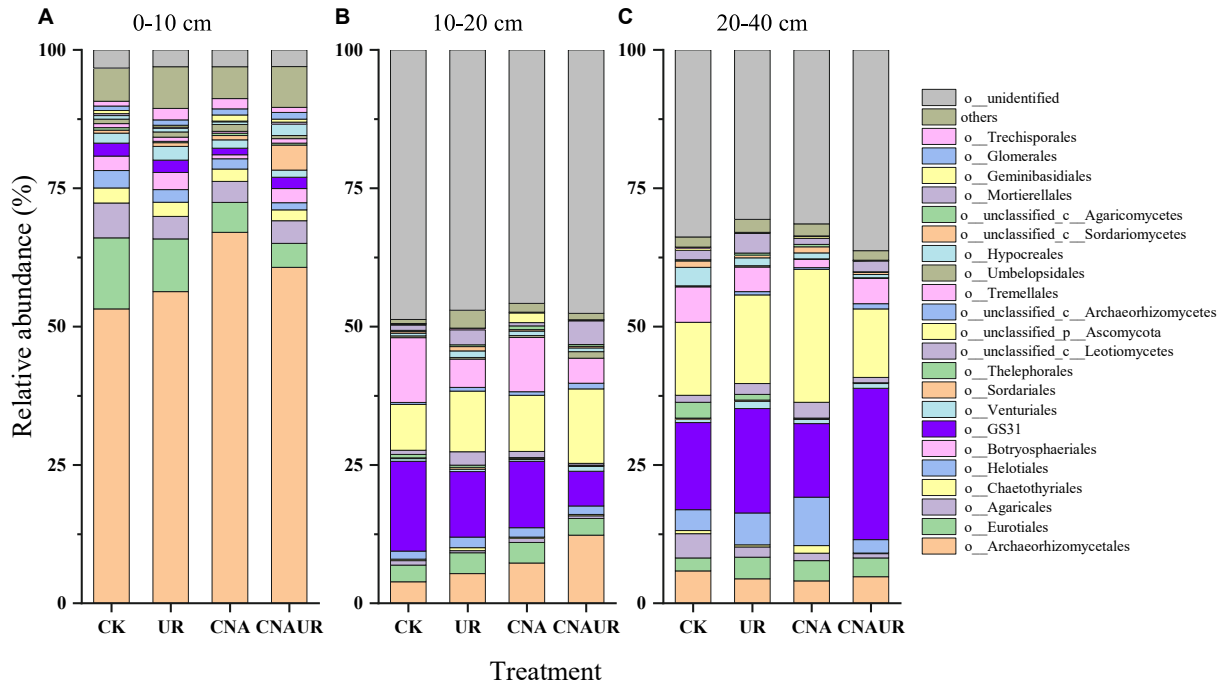

FIGURE 5
Relative abundance of soil fungal community at the order level under treatments (treatments are described in **Table 1**) in three soil layers, 0–10 cm **(A)**, 10–20 cm **(B)**, and 20–40 cm **(C)**. Those orders that represent >0.1% of the fungal community abundance are named, while those that represent <0.1% of the fungal community abundance are referred to as "others."

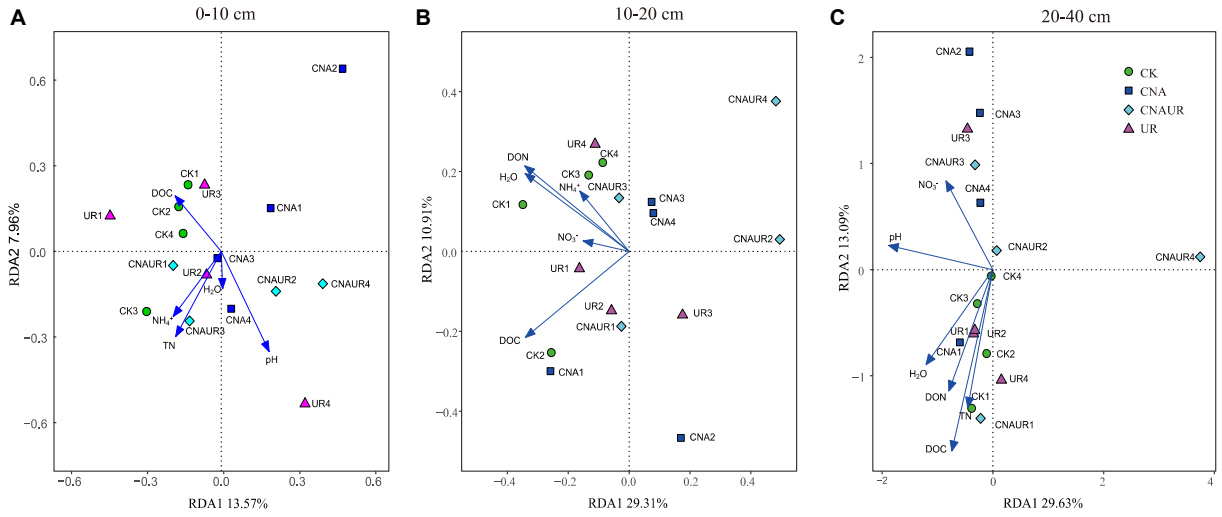

FIGURE 6
Redundancy analysis (RDA) of the relationship between bacterial community composition at the operational taxonomic (OTU) level and soil physicochemical properties across treatments in three soil layers, 0–10 cm **(A)**, 10–20 cm **(B)**, and 20–40 cm **(C)**.

found between the relative abundances of Mortierellales and unclassified taxa of the phylum Archaeorhizomycetes and NO_3^- and between the relative abundance of Venturiales and TOC. In the 20–40 cm layer, however, the relative abundances of Agaricales and Thelephorales were positively correlated with NH_4^+, TOC, DON, respectively, and the relative abundances of Archaeorhizomycetales, an unidentified phylum of Ascomycota, and an unidentified class of Leotiomycetes were negatively correlated with pH, DOC, and DON, respectively (**Figure 7F**).

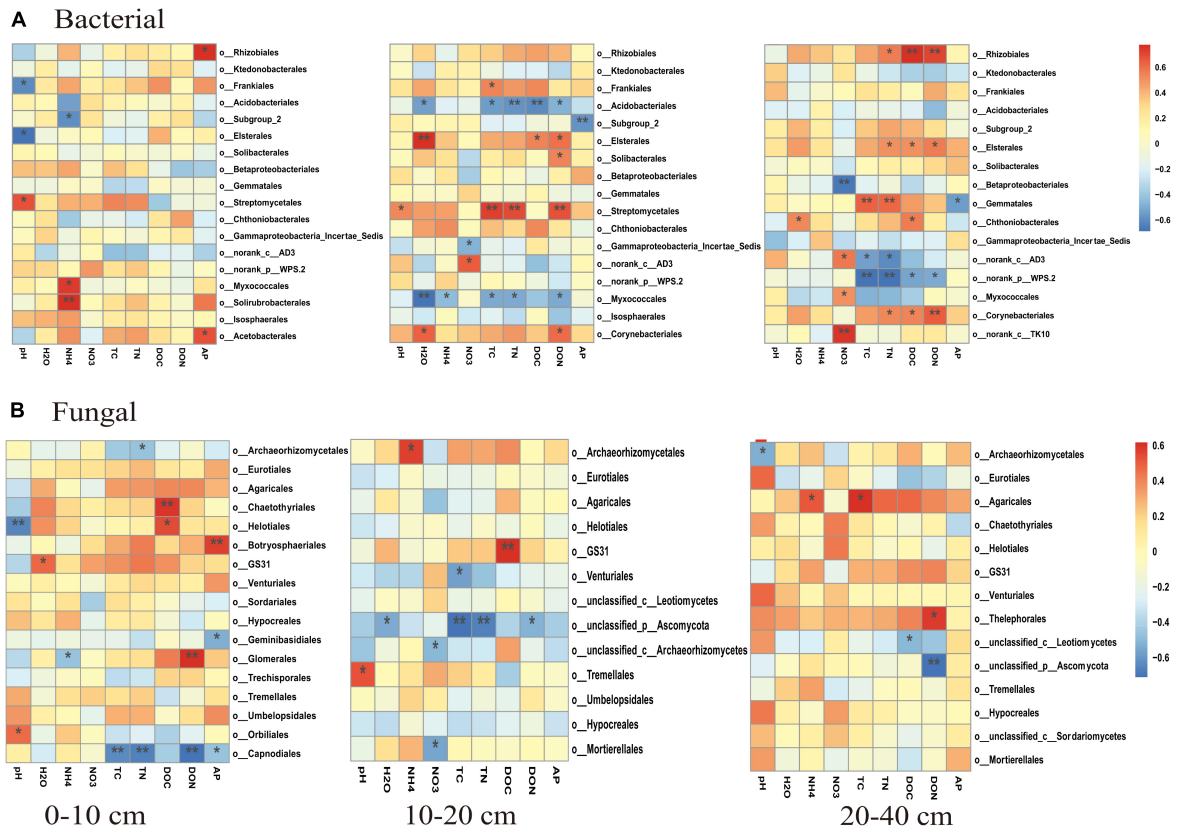

FIGURE 7
Correlations (as indicated by Pearson correlation coefficients) between soil properties and relative abundances of major bacterial taxa (>1.0%, **A–C**) and fungal taxa (>0.5%, **D–F**) at the order level in different soil layers. Blue indicates a negative correlation, and red indicates a positive correlation; the strength of the color indicates the strength of the correlation. * and ** indicate significant correlations at $p < 0.05$ and 0.01, respectively.

Discussion

Effects of canopy N addition and understory removal on microbial abundance

In the present study, the abundance of bacteria but not of fungi was affected by CNA (**Figure 1**), which was partly consistent with our first hypothesis but was inconsistent with previous results obtained with understory N addition (Wang J. P. et al., 2021) and with CNA (Zhao et al., 2020). In mixed deciduous forests in China, N addition significantly decreased the abundance of bacteria and fungi in two studies (Shi et al., 2016; Wang J. P. et al., 2021) but increased the abundance of fungi in a third study (Zhao et al., 2020). These conflicting results may be due to differences in soil pH and nutrient availability. In general, N addition reduces soil pH, resulting in changes in soil microbial communities because pH greatly affects soil bacterial and fungal abundance in subtropical forest soils (Zhao et al., 2013; Wang et al., 2018). Wang J. P. et al. (2021) observed that a decrease in microbial abundance was associated with a decrease in soil pH after 6 years of N addition. Moreover, the increased N availability due to N deposition reduced the N limitation on the growth of soil fungi (Zhao et al., 2020). In the current study, soil pH did not significantly differ between CNA and CK treatments in all three soil layers. Two reasons may explain the short-term experimental period and the canopy interception. However, the CNA treatment significantly decreased the soil DON content in the 20–40 cm layer (**Figure 1C**; **Table 1**). Like the decrease in soil DON, bacterial abundance decreased mainly in the 20–40 cm layer. This finding was further supported by the significant decrease in MBC content in the CNA treatment.

Contrary to the effect of CNA, removing understory plants significantly increased bacterial abundance in the deep soil (**Figure 1C**), which partly supported our second hypothesis. Researchers previously reported that the removal of the understory increased the soil temperature and N supply and reduced the soil water content (Wang et al., 2014; Giuggiola et al., 2018; Fang et al., 2021), which are important factors affecting microbial growth (Kamble et al., 2013). For instance,

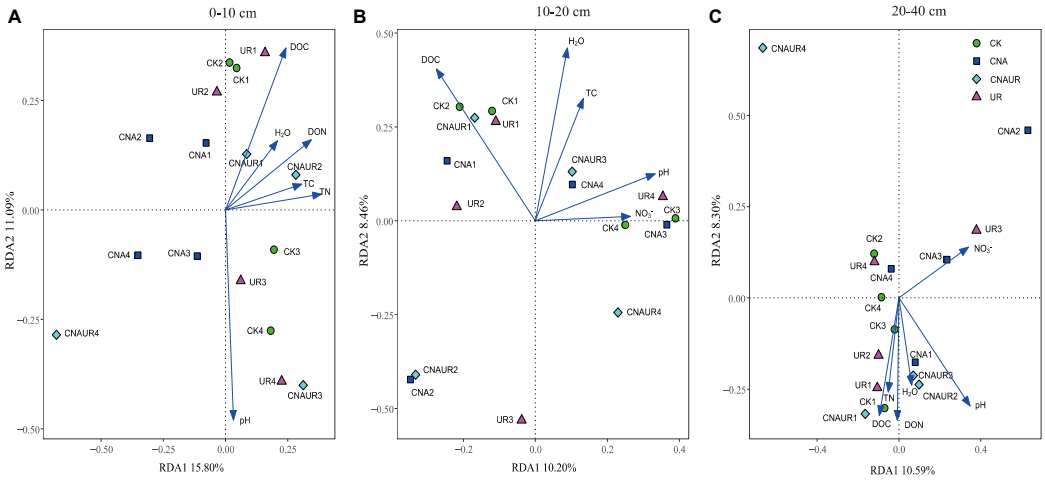

FIGURE 8
Redundancy analysis (RDA) of the relationship between fungal community composition at the operational taxonomic (OTU) level and soil physicochemical properties across treatments in three soil layers, 0–10 cm **(A)**, 10–20 cm **(B)**, and 20–40 cm **(C)**.

studies in *Eucalyptus* plantations showed that understory removal reduced microbial biomass in the surface soil (Wu et al., 2011; Zhao et al., 2013). However, in the current study, soil moisture and available N content did not differ between the UR and CK treatments and were not correlated with bacterial or fungal abundance (**Figure 2**). Xiong et al. (2008) also found that understory removal did not greatly affect soil physical and chemical properties in a subtropical *Acacia mangium* plantation in China. In the current study, we speculate that understory removal may have increased the soil temperature and thereby increased litter decomposition in the deep soil, thereby increasing the supply of C for microbial growth; C is considered the most limiting nutrient for soil microorganisms (Demoling et al., 2007). Although soil temperature was not measured in this study, a significant increase in soil MBC content with the UR treatment was observed in the 10–20 cm layer. Moreover, the ratio of active soil C to total C in response to understory removal had been previously observed to increase with soil depth (Xi et al., 2021). We also found that CNA × UR interaction significantly influenced the bacterial abundance and MBC content in the 20–40 cm soil layer, suggesting that soil microbial biomass and especially bacterial biomass were more sensitive to the treatments in the deep soil than in the surface soil.

Effects of canopy N addition and understory removal on microbial diversity

Previous studies have indicated that N addition increases, decreases, or does not affect microbial diversity (Allison et al., 2007; Freedman et al., 2015; Nie et al., 2018; Li P. et al., 2019; Wu et al., 2019; Wang J. P. et al., 2021). For instance, N addition significantly decreased soil microbial diversity in a northern hardwood forest (Freedman et al., 2015) and in subtropical forests (Li et al., 2016; Nie et al., 2018; Wu et al., 2019) but increased bacterial and fungal diversity in a natural subtropical forest (Wang J. P. et al., 2021). Another study reported that soil bacterial diversity did not respond to N addition in two tropical rainforests (Li P. et al., 2019). In the current study, CNA increased bacterial diversity in the 10–20 cm layer but reduced fungal diversity in the 0–10 cm layer (**Figure 3D**; **Supplementary Table 2**). This finding was contrary to our first hypothesis and was inconsistent with Zhao et al. (2020), who found that canopy addition of N increased soil fungal diversity. A possible explanation for the inconsistency is the difference in forest type, i.e., the current study was conducted in a coniferous forest, and the study of Zhao et al. (2020) was conducted in a deciduous forest. Previous reports suggested that soil microorganisms seem to be more strongly influenced by coniferous trees than by deciduous trees (White et al., 2005), and that the effect of N deposition on the soil microbial community could differ depending on tree species (Zechmeister-Boltenstern et al., 2011). Similarly, microbial properties were reported to be more sensitive to N addition in a subtropical broadleaf forest than in a temperate deciduous forest, and the difference was attributed to the differences in the soil buffering systems (Shi et al., 2016). Additional evidence that forest type helps explain why CNA increased soil fungal diversity in Zhao et al. (2020) but not in the current study is provided by the pH data. In Zhao et al. (2020), the soil pH of the deciduous forest was significantly decreased by 5 years of CNA, but the same duration and level of CNA did not significantly affect soil pH or other soil chemical properties in the current study (**Table 1**; **Supplementary Table 1**). Interestingly most

negative correlations between the Shannon index, soil pH, NO_3^- content, and TN content were observed in the 10–20 cm soil layer (**Figure 2**), suggesting that soil depth may be an important factor regulating microbial diversity in response to N addition. Overall, the current and previous results suggest that the responses of microbial diversity to CNA may depend on forest type and soil layer.

Contrary to our expectations, understory removal had minor effects on bacterial and fungal diversity (**Figure 3**; **Supplementary Table 2**). In previous studies, understory removal reduced the input of labile C into the oil (Chen et al., 2019), thereby affecting the microbial activity and community composition (Demoling et al., 2007; Wan et al., 2019). In the current study, however, understory removal did not alter the contents of soil DOC and available N (i.e., NH_4^+, NO_3^-, and DON). Other researchers also found that understory removal did not change the soil DOC content (Wu et al., 2011) or the hydrolyzable N content (Xiong et al., 2008). We infer that understory removal in the current study did not affect the availability of substrates for soil microorganisms. In addition, we observed that soil fungal diversity was significantly lower in the 20–40 cm soil layer with the CNAUR treatment than with the CNA treatment (**Figure 3F**) and that a strong statistical interaction was found between CNA and UR (**Supplementary Table 2**). A possible explanation is that removing understory plants after N addition reduced the competition for nutrients between roots and microorganisms in the deep soil and increased soil N availability. The increase in N availability could reduce fungal diversity (Cox et al., 2010). A trend for DON content supports that explanation to increase in the CNAUR treatment in the 20–40 cm soil layer (**Table 1**).

Composition of the microbial community in response to canopy N addition and understory removal

There were significant differences in the microbial communities among treatments in the current study, especially in the surface and middle soil layers (**Supplementary Figures 2**, **3**). Furthermore, RDA analysis suggested that soil DON was a key factor affecting the composition of the bacterial community in the 10–20 cm layer (**Figure 6B**), while soil pH and DOC were key factors affecting the composition of the fungal community in the 0–10 cm layer (**Figure 8A**). The findings are consistent with our third hypothesis and with the results of Kang et al. (2021), who found that changes in the composition of soil microbial communities were associated with different factors in different soil layers.

Contrary to our first hypothesis, short-term (5 years) CNA significantly influenced the composition of soil bacterial and fungal communities (**Supplementary Figures 2**, **3**). This finding supported most studies of understory N addition (Freedman et al., 2015; Wang T. et al., 2021) but was inconsistent with Shi et al. (2016), who found that CNA did not change the composition of soil microbial communities in a subtropical or temperate forest. The difference in experimental duration might explain this inconsistency. Soil samples were collected after 2 years of CNA in Shi et al. (2016) but after 5 years of CNA in the current study. Zhao et al. (2020) recently found that the composition of the soil fungal community was altered after 5 years of CNA in the same site as that studied by Shi et al. (2016). Moreover, the response of microbial taxa to CNA differed among soil layers in the current study (**Figures 4**, **5**; **Supplementary Tables 2**, **4**). It is generally accepted that with increases in resource availability, the abundance of copiotrophic taxa (i.e., Proteobacteria, Actinobacteria, and Ascomycota) increases, whereas the abundance of oligotrophic taxa (e.g., Verrucomicrobia and Basidiomycota) decrease (Fierer et al., 2012; Ho et al., 2017; Wu et al., 2019; Zhao et al., 2020; Wang J. P. et al., 2021). Li et al. (2016) also found that experimental N deposition increased the abundance of copiotrophic soil microorganisms. In the current study, however, CNA caused a decrease in the abundance of Proteobacteria and Actinobacteria in the 10–20 cm layer, an increase in the abundance of Verrucomicrobia in the 0–20 cm layer, and no significant changes in the abundances of fungal phyla (**Figure 4**; **Supplementary Figure 1**; **Supplementary Table 2**). The differences might be explained by the relationships between soil factors and single taxa at a finer taxonomic scale than used in the current study because physiological traits can vary greatly within a single microbial phylum (Ho et al., 2017; Wang J. P. et al., 2021). The latter explanation was supported by our finding that some fungal taxa at the order level were especially sensitive to N addition in the current study, as evidenced by significant reductions in the relative abundances of Eurotiales, Helotiales, and Venturiales in the surface soil in response to the CNA treatment (**Figure 5**; **Supplementary Figure 1**; **Supplementary Table 3**). Our correlation heatmap further indicated that soil factors had different correlations with single microbial taxa at the order level in different soil layers (**Figure 7**). For example, the relative abundance of the order Rhizobiales, as a potential N fixer, was positively correlated with AP in the surface soil and with DON and DOC in the deeper soil (**Figure 7**). The latter finding was inconsistent with Wang J. P. et al. (2021), who found that the abundance of Rhizobiales was negatively correlated with soil NH_4^+ and NO_3^-. The CNA treatment resulted in a sharp decrease in AP content in the surface soil (**Table 1**). Together, these findings suggest that reducing the availability of P, CNA may inhibit the decomposition of organic matter in the surface soil and consequently cause the nutrient limits for microbes in middle and deep soils due to reducing the carbon source input.

Relative to CNA, understory removal had less effect on the composition of the soil microbial communities at the OTU level (**Supplementary Figures 2**, **3**). This result was inconsistent with results obtained from a eucalyptus plantation (Wu et al., 2011; Zhao et al., 2013). The latter studies found that understory removal changed soil microbial communities (as indicated by the ratio of fungal biomass to bacterial biomass) and that the changes were associated with soil temperature and water content. In the present study, the small effect of understory removal on soil microbial communities was associated with the failure of understory removal to change soil physical and chemical properties (**Table 1**). The possible explanation is the difference in acquiring resources among microbial species (Coleman et al., 2002). Because single taxa of bacteria or fungi within orders but not phylum were found to have positive or negative correlations with soil parameters (**Figure 7**), another possible reason for the failure of understory removal to significantly affect soil microbial communities is that dominant understory species (*B. chungii* and *D. dichotoma*) represent relatively insufficient resources for soil bacteria and fungi. Studies in eucalyptus plantations indicate that the litter of *D. dichotoma* has a high ratio of lignin to nitrogen and a low decomposition rate (Zhao et al., 2011; Liu et al., 2012). We also found that the composition of the bacterial community was more affected by the statistical interaction of CNA and understory removal in the middle soil layer than in the surface or deeper soil layer (**Supplementary Table 3**). Overall, our results suggest that understory removal and its interaction with CNA had slight effects on the composition of the bacterial community in surface and middle soil layers. Additional studies are needed on the long-term effects of understory removal on the composition of bacterial and fungal communities in different soil layers.

Conclusion

The current study demonstrated that bacterial abundance in the deep soil layer was decreased by CNA but increased by understory removal. Furthermore, the diversity and composition of soil bacterial and fungal communities were affected more by CNA than by understory removal, and the effects depended on the soil layer. In the surface soil layer, CNA increased bacterial diversity and altered bacterial community structure. In contrast, CNA decreased fungal diversity and changed fungal community composition in the middle soil layer. Soil pH, DOC, and DON were associated with the responses of bacterial and fungal communities to the treatments in the different soil layers. In addition, the bacterial community in the surface soil was also influenced by the statistical interaction between CNA and UR. Our results indicate that the soil bacterial community was more sensitive than the fungal community to CNA and understory removal in the short term.

Data availability statement

The original contributions presented in this study are included in the article/**Supplementary material**, further inquiries can be directed to the corresponding authors.

Author contributions

DX and JW performed the field experiments. DX and SJ performed the statistical analysis. DX wrote the first draft of the manuscript. All authors contributed to the conception and design of the study and manuscript revision, read, and approved the submitted version.

Funding

This work was financially supported by the National Natural Science Foundation of China (41703068, 31570444, and 41701099), the start-up funding of Minjiang University (32304307), Natural Science Foundation of Fujian Province, China (Grant No. 2022J011140), Central Government Guides Local Projects (Grant No. 2020L3024), and Fujian Forestry Science and Technology Research Project (2022FKJ02).

Conflict of interest

The authors declare that the research was conducted in the absence of any commercial or financial relationships that could be construed as a potential conflict of interest.

Publisher's note

Supplementary material

The Supplementary Material for this article can be found online at: https://www.frontiersin.org/articles/10.3389/fmicb.2022.1015936/full#supplementary-material

References

Allison, S. D., Hanson, C. A., and Treseder, K. K. (2007). Nitrogen fertilization reduces diversity and alters community structure of active fungi in boreal ecosystems. *Soil Biol. Biochem.* 39, 1878–1887. doi: 10.1016/j.soilbio.2007.02.001

Boot, C. M., Hall, E. K., Denef, K., and Baron, J. S. (2016). Long-term reactive nitrogen loading alters soil carbon and microbial community properties in a subalpine forest ecosystem. *Soil Biol. Biochem.* 92, 211–220. doi: 10.1016/j.soilbio.2015.10.002

Chen, H., Li, D. J., Gurmesa, G. A., Yu, G. R., Li, L. H., Zhang, W., et al. (2015). Effects of nitrogen deposition on carbon cycle in terrestrial ecosystems of China: A meta-analysis. *Environ. Pollut.* 206, 352–360. doi: 10.1016/j.envpol.2015.07.033

Chen, Y. Q., Cao, J. B., Zhao, J., Wu, J. P., Zou, X. M., Fu, S. L., et al. (2019). Labile C dynamics reflect soil organic carbon sequestration capacity: Understory plants drive topsoil C process in subtropical forests. *Ecosphere* 10:e02784. doi: 10.1002/ecs2.2784

Coleman, D., Fu, S. L., Hendrix, P., and Crossley, D. (2002). Soil foodwebs in agroecosystems: Impacts of herbivory and tillage management. *Eur. J. Soil Biol.* 38, 21–28. doi: 10.1016/S1164-5563(01)01118-9

Cox, F., Barsoum, N., Lilleskov, E. A., and Bidartondo, M. I. (2010). Nitrogen availability is a primary determinant of conifer mycorrhizas across complex environmental gradients. *Ecol. Lett.* 13, 1103–1113. doi: 10.1111/j.1461-0248.2010.01494.x

Demoling, F., Figueroa, D., and Bååth, E. (2007). Comparison of factors limiting bacterial growth in different soils. *Soil Biol. Biochem.* 39, 2485–2495. doi: 10.1016/j.soilbio.2007.05.002

Edgar, R. C. (2013). UPARSE: Highly accurate OTU sequences from microbial amplicon reads. *Nat. Methods* 10, 996–998. doi: 10.1038/nmeth.2604

Fan, H. B., and Hong, W. (2001). Estimation of dry deposition and canopy exchange in Chinese fir plantations. *Forest Ecol. Manage.* 147, 99–107. doi: 10.1016/S0378-1127(00)00469-2

Fang, X. M., Wang, G. G., Xu, Z. J., Zong, Y. Y., Zhang, X. L., Li, J. J., et al. (2021). Litter addition and understory removal influenced soil organic carbon quality and mineral nitrogen supply in a subtropical plantation forest. *Plant Soil* 460, 527–540. doi: 10.1007/s11104-020-04787-8

Fierer, N., Leff, J. W., Adams, B. J., Nielsen, U. N., Bates, S. T., Lauber, C. L., et al. (2012). Cross-biome metagenomic analyses of soil microbial communities and their functional attributes. *Proc. Natl. Acad. Sci. U.S.A.* 109, 21390–21395. doi: 10.1073/pnas.1215210110

Freedman, Z. B., Romanowicz, K. J., Upchurch, R. A., and Zak, D. R. (2015). Differential responses of total and active soil microbial communities to long-term experimental N deposition. *Soil Biol. Biochem.* 90, 275–282. doi: 10.1016/j.soilbio.2015.08.014

Galloway, J. N., Dentener, F. J., Capone, D. G., Galloway, J. N., Dentener, F. J., Capone, D. G., et al. (2004). Nitrogen cycles: Past, present, and future. *Biogeochemistry* 70, 153–226.

Giuggiola, A., Zweifel, R., Feichtinger, L. M., Vollenweider, P., Bugmann, H., Haeni, M., et al. (2018). Competition for water in a xeric forest ecosystem - Effects of understory removal on soil micro-climate, growth and physiology of dominant Scots pine trees. *Forest Ecol. Manag.* 409, 241–249. doi: 10.1016/j.foreco.2017.11.002

Ho, A., Lonardo, D. P. D., and Bodelier, P. L. E. (2017). Revisiting life strategy concepts in environmental microbial ecology. *FEMS Microbiol. Ecol.* 93:fix006. doi: 10.1093/femsec/fix006

Houle, D., Marty, C., and Duchesne, L. (2015). Response of canopy nitrogen uptake to a rapid decrease in bulk nitrate deposition in two eastern Canadian boreal forests. *Oecologia* 177, 29–37. doi: 10.1007/s00442-014-3118-0

Jiang, X. Y., Liu, N., Lu, X. K., Huang, J. G., Cheng, J., Guo, X. L., et al. (2018). Canopy and understory nitrogen addition increase the xylem tracheid size of dominant broadleaf species in a subtropical forest of China. *Sci. Total Environ.* 642, 733–741. doi: 10.1016/j.scitotenv.2018.06.133

Kamble, P. N., Rousk, J., Frey, S. D., and Baath, E. (2013). Bacterial growth and growth-limiting nutrients following chronic nitrogen additions to a hardwood forest soil. *Soil Biol. Biochem.* 59, 32–37. doi: 10.1016/j.soilbio.2012.12.017

Kang, E. Z., Li, Y., Zhang, X. D., Yan, Z. Q., Wu, H. D., Li, M., et al. (2021). Soil pH and nutrients shape the vertical distribution of microbial communities in an alpine wetland. *Sci. Total Environ.* 774:145780. doi: 10.1016/j.scitotenv.2021.145780

Krumins, J. A., Dighton, J., Gray, D., Franklin, R. B., Morin, P. J., and Roberts, M. S. (2009). Soil microbial community response to nitrogen enrichment in two scrub oak forests. *Forest Ecol. Manag.* 258, 1383–1390. doi: 10.1016/j.foreco.2009.06.046

Lefcheck, J. S. (2016). piecewiseSEM: Piecewise structural equation modeling in R for ecology, evolution, and systematics. *Methods Ecol. Evol.* 7, 573–579. doi: 10.1111/2041-210X.12512

Lei, X. M., Shen, F. F., Lei, X. C., Liu, W. F., Duan, H. L., Fan, H. B., et al. (2018). Assessing influence of simulated canopy nitrogen deposition and under-story removal on soil microbial community structure in a *Cunninghamia lanceolata* plantation. *Biodivers. Sci.* 26, 962–971. doi: 10.17520/biods.2018033

Li, P., Shen, C. C., Jiang, L., Feng, Z. Z., and Fang, J. Y. (2019). Difference in soil bacterial community composition depends on forest type rather than nitrogen and phosphorus additions in tropical montane rainforests. *Biol. Fertil. Soils* 55, 313–323. doi: 10.1007/s00374-019-01349-8

Li, R. S., Zheng, W. H., Yang, Q. P., Zhang, W. D., Chi, Y. G., Wang, P., et al. (2019). The response of soil respiration to thinning was not affected by understory removal in a Chinese fir (*Cunninghamia lanceolata*) plantation. *Geoderma* 353, 47–54. doi: 10.1016/j.geoderma.2019.06.025

Li, Q., Song, X. Z., Gu, H. H., and Gao, F. (2016). Nitrogen deposition and management practices increase soil microbial biomass carbon but decrease diversity in Moso bamboo plantations. *Sci. Rep.* 6:28235. doi: 10.1038/srep28235

Liu, D., Huang, Y. M., An, S. S., Sun, H. Y., Bhople, P., and Chen, Z. W. (2018). Soil physicochemical and microbial characteristics of contrasting land-use types along soil depth gradients. *Catena* 162, 345–353. doi: 10.1016/j.catena.2017.10.028

Liu, L., Gundersen, P., Zhang, W., Zhang, T., Chen, H., and Mo, J. M. (2015). Effects of nitrogen and phosphorus additions on soil microbial biomass and community structure in two reforested tropical forests. *Sci. Rep.* 5:14378. doi: 10.1038/srep14378

Liu, N., Wu, S. H., Guo, Q. F., Wang, J. X., Cao, C., and Wang, J. (2018). Leaf nitrogen assimilation and partitioning differ among subtropical forest plants in response to canopy addition of nitrogen treatments. *Sci. Total Environ.* 637-638, 1026–1034. doi: 10.1016/j.scitotenv.2018.05.060

Liu, T., Mao, P., Shi, L. L., Eisenhauer, N., Liu, S. J., Wang, X. L., et al. (2020). Forest canopy maintains the soil community composition under elevated nitrogen deposition. *Soil Biol. Biochem.* 143:107733. doi: 10.1016/j.soilbio.2020.107733

Liu, Z. F., Wu, J. P., Zhou, L. X., Lin, Y. B., and Fu, S. L. (2012). Effect of understory fern (*Dicranopteris dichotoma*) removal on substrate utilization patterns of culturable soil bacterial communities in subtropical *Eucalyptus* plantations. *Pedobiologia* 55, 7–13. doi: 10.1016/j.pedobi.2011.07.014

Lu, X. K., Vitousek, P. M., Mao, Q. G., Gilliam, F. S., Luo, Y. Q., Turner, B. L., et al. (2021). Nitrogen deposition accelerates soil carbon sequestration in tropical forests. *Proc. Natl. Acad. Sci. U.S.A.* 118:e2020790118. doi: 10.1073/pnas.2020790118

Lu, X. F., Kuang, Y. W., Mou, L. Y., Hou, E. Q., Fu, S. L., and Li, J. (2021). Canopy mitigates the effects of nitrogen deposition on soil carbon-related processes in a subtropical forest. *Sci. Total Environ.* 757:143847. doi: 10.1016/j.scitotenv.2020.143847

Ma, S. H., Chen, G. P., Tian, D., Du, E. Z., Xiao, W., Jiang, L., et al. (2020). Effects of seven-year nitrogen and phosphorus additions on soil microbial community structures and residues in a tropical forest in Hainan Island, China. *Geoderma* 361:114034. doi: 10.1016/j.geoderma.2019.114034

Mo, J. M., Zhang, W., Zhu, W. X., Gundersen, P., Fang, Y. T., Li, D. J., et al. (2008). Nitrogen addition reduces soil respiration in a mature tropical forest in southern China. *Glob. Chang. Biol.* 14, 403–412. doi: 10.1111/j.1365-2486.2007.01503.x

Nie, Y. X., Wang, M. C., Zhang, W., Ni, Z., Hashidoko, Y., and Shen, W. J. (2018). Ammonium nitrogen content is a dominant predictor of bacterial community composition in an acidic forest soil with exogenous nitrogen enrichment. *Sci. Total Environ.* 624, 407–415. doi: 10.1016/j.scitotenv.2017.12.142

Peguero, G., Folch, E., Liu, L., Ogaya, R., and Penuelas, J. (2021). Divergent effects of drought and nitrogen deposition on microbial and arthropod soil communities in a Mediterranean forest. *Eur. J. Soil Biol.* 103:103275.

Shi, L. L., Zhang, H. Z., Liu, T., Mao, P., Zhang, W. X., Shao, Y. H., et al. (2018). An increase in precipitation exacerbates negative effects of nitrogen deposition on soil cations and soil microbial communities in a temperate forest. *Environ. Pollut.* 235, 293–301. doi: 10.1016/j.envpol.2017.12.083

Shi, L. L., Zhang, H. Z., Liu, T., Zhang, W. X., Shao, Y. H., Ha, D. L., et al. (2016). Consistent effects of canopy vs. understory nitrogen addition on the soil exchangeable cations and microbial community in two contrasting forests. *Sci. Total Environ.* 553, 349–357. doi: 10.1016/j.scitotenv.2016.02.100

Tian, Y., Lu, H. F., Wang, J., Lin, Y. B., Campbell, D. E., and Jian, S. G. (2019). Effects of canopy and understory nitrogen addition on the structure and eco-exergy of a subtropical forest community. *Ecol. Indic.* 106:105459.

Tian, Y., Tao, L. B., Wang, J., Lu, H. F., Zhou, L. X., Campbell, D. E., et al. (2020). Canopy and understory nitrogen additions did not significantly change the community structure of soil fauna under a mature subtropical forest. *Sci. Total Environ.* 718:137438.

Trentini, C. P., Villagra, M., Gomez Pamies, D., Bernava Laborde, V., Bedano, J. C., and Campanello, P. I. (2018). Effect of nitrogen addition and litter removal on understory vegetation, soil mesofauna, and litter decomposition in loblolly pine plantations in subtropical Argentina. *Forest Ecol. Manag.* 429, 133–142.

Urcelay, C., Díaz, S., Gurvich, D. E., Chapin, F. S. I. I. I., Cuevas, E., and Domínguez, L. S. (2010). Mycorrhizal community resilience in response to experimental plant functional type removals in a woody ecosystem. *J. Ecol.* 97, 1291–1301.

Wall, D. H., Nielsen, U. N., and Six, J. (2015). Soil biodiversity and human health. *Nature* 528, 69–76.

Wan, S. Z., Liu, Z. F., Chen, Y. Q., Zhao, J., Ying, Q., and Liu, J. (2019). Effects of lime application and understory removal on soil microbial communities in subtropical *Eucalyptus* L'Hér, Plantations. *Forests* 10:40338.

Wang, C., Lu, X. K., Mori, T., Mao, Q. G., Zhou, K. J., Zhou, G. Y., et al. (2018). Responses of soil microbial community to continuous experimental nitrogen additions for 13 years in a nitrogen-rich tropical forest. *Soil Biol. Biochem.* 121, 103–112. doi: 10.1016/j.soilbio.2018.03.009

Wang, F. M., Zou, B., Li, H. F., and Li, Z. (2014). The effect of understory removal on microclimate and soil properties in two subtropical lumber plantations. *J. For. Res.* 19, 238–243.

Wang, X., Wang, B., Wang, C. Z., Wang, Z. H., Li, J., Jia, Z., et al. (2021). Canopy processing of N deposition increases short-term leaf N uptake and photosynthesis, but not long-term N retention for aspen seedlings. *New Phytol.* 229, 2601–2610. doi: 10.1111/nph.17041

Wang, J. P., Shi, X. Z., Zheng, C. Y., Suter, H., and Huang, Z. Q. (2021). Different responses of soil bacterial and fungal communities to nitrogen deposition in a subtropical forest. *Sci. Total Environ.* 755:142449. doi: 10.1016/j.scitotenv.2020.142449

Wang, T., Xu, Q., Gao, D., Zhang, B., Zuo, H., and Jiang, J. (2021). Effects of thinning and understory removal on the soil water-holding capacity in Pinus massoniana plantations. *Sci. Rep.* 11, 2045–2322.

White, C., Tardif, J. C., Adkins, A., and Staniforth, R. (2005). Functionaldiversity of microbial communities in the mixed boreal plain forest of central Canada. *Soil Biol. Biochem.* 37, 1359–1372. doi: 10.1016/j.soilbio.2004.12.007

Wu, J. P., Liu, W. F., Zhang, W. X., Shao, Y. H., Duan, H. L., Chen, B. D., et al. (2019). Long-term nitrogen addition changes soil microbial community and litter decomposition rate in a subtropical forest. *Appl. Soil Ecol.* 142, 43–51. doi: 10.1016/j.apsoil.2019.05.014

Wu, J. P., Liu, Z. F., Wang, X. L., Sun, Y. X., Zhou, L. X., Lin, Y. B., et al. (2011). Effects of understory removal and tree girdling on soil microbial community composition and litter decomposition in two Eucalyptus plantations in South China. *Funct. Ecol.* 25, 921–931. doi: 10.1111/j.1365-2435.2011.01845.x

Xi, D., Weng, H. D., Hu, Y. L., and Wu, J. P. (2021). Effects of canopy N addition and understory removal on soil organic carbon fractions in a Chinese fir plantation. *Acta Ecol. Sin.* 41, 8525–8534. doi: 10.5846/stxb202008162130

Xiong, Y. M., Xia, H. P., Li, Z. A., Cai, X. A., and Fu, S. L. (2008). Impacts of litter and understory removal on soil properties in a subtropical Acacia mangium plantation in China. *Plant Soil* 304, 179–188. doi: 10.1007/s11104-007-9536-6

Yu, G. R., Jia, Y. L., He, N. P., Zhu, J. X., Chen, Z., Wang, Q. F., et al. (2019). Stabilization of atmospheric nitrogen deposition in China over the past decade. *Nat. Geosci.* 12, 424–429.

Zechmeister-Boltenstern, S., Michel, K., and Pfeffer, M. (2011). Soil microbial community structure in European forests in relation to forest type and atmospheric nitrogen deposition. *Plant Soil* 343, 37–50. doi: 10.1007/s11104-010-0528-6

Zeng, J., Liu, X., Song, L., Lin, X., Zhang, H., Shen, C., et al. (2016). Nitrogen fertilization directly affects soil bacterial diversity and indirectly affects bacterial community composition. *Soil Biol. Biochem.* 92, 41–49. doi: 10.1038/ismej.2011.159

Zhao, A., Liu, L., Chen, B., Fu, W., Xie, W., Xu, T., et al. (2020). Soil fungal community is more sensitive to nitrogen deposition than increased rainfall in a mixed deciduous forest of China. *Soil Ecol. Lett.* 2, 20–32. doi: 10.1007/s42832-020-0026-6

Zhao, J., Wan, S., Fu, S., Wang, X., Wang, M., Liang, C., et al. (2013). Effects of understory removal and nitrogen fertilization on soil microbial communities in Eucalyptus plantations. *Forest Ecol. Manag.* 310, 80–86. doi: 10.1016/j.foreco.2013.08.013

Zhao, J., Wang, X., Shao, Y., Xu, G., and Fu, S. (2011). Effects of vegetation removal on soil properties and decomposer organisms. *Soil Biol. Biochem.* 43, 954–960. doi: 10.1016/j.soilbio.2011.01.010

Zhou, Z. H., Wang, C. K., Jiang, L. F., and Luo, Y. Q. (2017). Trends in soil microbial communities during secondary succession. *Soil Biol. Biochem.* 115, 92–99. doi: 10.1016/j.soilbio.2017.08.014

frontiers | Frontiers in Microbiology

TYPE Original Research
PUBLISHED 09 December 2022
DOI 10.3389/fmicb.2022.1063340

OPEN ACCESS

EDITED BY
Muhammad Saleem,
Alabama State University,
United States

REVIEWED BY
Kai Feng,
Research Center for Eco-environmental Sciences (CAS), China
Yang Yang,
Northwest A&F University, China

*CORRESPONDENCE
Dima Chen
chendima@ctgu.edu.cn
Jianping Wu
jianping.wu@ynu.edu.cn

SPECIALTY SECTION
This article was submitted to Microbe and Virus Interactions with Plants, a section of the journal Frontiers in Microbiology

RECEIVED 07 October 2022
ACCEPTED 18 November 2022
PUBLISHED 09 December 2022

CITATION
Wu Y, Wang B, Wu L, Liu S, Yue L, Wu J and Chen D (2022) Fifty-year habitat subdivision enhances soil microbial biomass and diversity across subtropical land-bridge islands.
Front. Microbiol. 13:1063340.
doi: 10.3389/fmicb.2022.1063340

Fifty-year habitat subdivision enhances soil microbial biomass and diversity across subtropical land-bridge islands

Ying Wu[1,2,3], Bing Wang[3], Liji Wu[3], Shengen Liu[3], Lingyan Yue[3], Jianping Wu[1,2]* and Dima Chen[3]*

[1]Yunnan Key Laboratory of Plant Reproductive Adaptation and Evolutionary Ecology, Yunnan University, Kunming, China, [2]Key Laboratory of Soil Ecology and Health in Universities of Yunnan Province, School of Ecology and Environmental Science, Yunnan University, Kunming, China, [3]Engineering Research Center of Eco-Environment in Three Gorges Reservoir Region of Ministry of Education, China Three Gorges University, Yichang, China

Although habitat loss and subdivision are considered main causes of sharp declines in biodiversity, there is still great uncertainty concerning the response of soil microbial biomass, diversity, and assemblage to habitat subdivision at the regional scale. Here, we selected 61 subtropical land-bridge islands (with small, medium, and large land areas) with a 50-year history of habitat subdivision and 9 adjacent mainland sites to investigate how habitat subdivision-induced unequal-sized patches and isolation affects biomass, diversity, and assemblages of soil bacteria and fungi. We found that the soil bacterial and fungal biomass on all unequal-sized islands were higher than that on mainland, while soil bacterial and fungal richness on the medium-sized islands were higher than that on mainland and other-sized islands. The habitat subdivision-induced increases in microbial biomass or richness were mainly associated with the changes in subdivision-specified habitat heterogeneities, especial for soil pH and soil moisture. Habitat subdivision reduced soil bacterial dissimilarity on medium-sized islands but did not affect soil fungal dissimilarity on islands of any size. The habitat fragment-induced changes in soil microbial dissimilarity were mainly associated with microbial richness. In summary, our results based on the responses of soil microbial communities from subtropical land-bridge islands are not consistent with the island biogeographical hypotheses but are to some extent consistent with the tradeoff between competition and dispersal. These findings indicate that the response of soil microbial communities to habitat subdivision differed by degree of subdivision and strongly related to habitat heterogeneity, and the distribution of microbial diversity among islands is also affected by tradeoff between competition and dispersal.

KEYWORDS

community assembly, habitat subdivision, mainland-island system, island biogeography, soil microbial diversity, habitat heterogeneity

Introduction

How habitat loss and fragmentation affects biodiversity and ecosystem functions is an important topic in ecological research (Lindenmayer and Fischer, 2007; Haddad et al., 2015; Si et al., 2016). Empirical studies in macro ecosystem commonly emphasize that habitat loss has triggered negative effects on biodiversity, while the effects of habitat fragmentation *per se* (hereafter termed habitat subdivision) are still large uncertainties (Haddad et al., 2015; May et al., 2019). Habitat subdivision is a landscape-level reconfiguring that subdividing a single large of habitat into several smaller areas involves multidimensional effects on biodiversity (Ewers and Didham, 2006; Lindenmayer and Fischer, 2007). The most intuitive effects are derived from increase of habitat patches, decrease of habitat area, changes of isolation, and even novel ecological boundaries (Ewers and Didham, 2006; Haddad et al., 2017; Bueno and Peres, 2019). It is still controversial to clarify the impacts of habitat subdivision due to its divergent changes in configuration (Villard and Metzger, 2014). The habitat amount hypothesis holds that the effect of habitat subdivision is consistent with the effect of habitat amount changes (Haddad et al., 2017). However, increased researches have demonstrated that the impacts of habitat area reduction and isolation changes caused by habitat subdivision on biodiversity cannot be replaced by the impacts of habitat amounts (Haddad et al., 2017; Deane et al., 2022). Therefore, habitat subdivision induced changes of geometric properties may strongly influence biodiversity and ecosystem functions directly and indirectly (Deane et al., 2022). The geometric effects of habitat subdivision on soil microbial biomass and diversity are especially unclear due to the substantial mismatch between habitat subdivision scale and microbial habitat area or diffusion capacity (Baas-Becking, 1934; Finlay, 2002). Furthermore, few studies have focused on the responses of soil microbial biomass and diversity to long-term (e.g., more than 50 years) habitat subdivision (Peay et al., 2007; Vannette et al., 2016), despite the important contribution of soil microorganisms to ecosystem functions (van der Heijden et al., 2007; Delgado-Baquerizo et al., 2016).

Habitat subdivision may alter soil microbial biomass and diversity at a regional scale by changing patch sizes and isolation, and soil abiotic and biotic factors (Peay et al., 2007; Vannette et al., 2016; Fanin et al., 2018; Li et al., 2020b). It is generally considered that the distribution pattern of microorganisms is completely different from that of macroorganisms due to the high species number, high diffusion ability, and small size of microorganisms (Baas-Becking, 1934; Finlay, 2002; Si et al., 2016; Zeng et al., 2019). Nonetheless, studies have increasingly indicated that unequal-sized patches and diffusion limitation caused by habitat subdivision are main factors affecting soil microbial diversity (Peay et al., 2007; Vannette et al., 2016; Li et al., 2020b). A study conducted in a lava-fragmented landscape, for example, showed that root-associated fungal communities were affected by fragmented area (Vannette et al., 2016), which was consistent with the theory concerning the relationship between species and area relationship based on macroorganisms (Macarthur and Wilson, 1963, 2016). Researchers have also suggested that changes in soil microbial biomass and diversity after habitat subdivision could be explained by other theories, such as island biogeographical theory (Macarthur and Wilson, 1963, 2016) and the regional similarity hypothesis (Mouquet and Loreau, 2002), which states that community changes result from the interaction between dispersal and species competition. In addition, the changes in the soil environment and biotic interactions caused by habitat subdivision can also greatly affect soil microbial diversity (van der Heijden et al., 2007; Fierer, 2017; Li et al., 2020b). The area of fragmented habitat, for example, can affect soil bacterial diversity through soil moisture (Li et al., 2020b) and can affect root-associated fungal communities through their host plants (Vannette et al., 2016). Landscape ecologists have therefore suggested that future habitat fragmentation studies should assess the effects of unequal-size patches and isolation (Wilson et al., 2016).

Explaining the effects of habitat subdivision on species and communities is difficult because of the ecosystem differences in connectivity, habitat area, and heterogeneity (Si et al., 2016; Wilson et al., 2016; Zeng et al., 2019). For example, habitat subdivision studies often involve hidden uncertainties related to incomplete diffusion barriers (e.g., corridors) or large-scale matrix changes (e.g., fire and logging); such uncertainties make it difficult to generalize about the effects of habitat subdivision on biodiversity (Wardle et al., 1997; Haddad et al., 2015; Wilson et al., 2016; Kardol et al., 2018). Simplified experimental studies, such as mesocosm or microcosm experiments (Åström and Bengtsson, 2011; Delgado-Baquerizo et al., 2018), cannot provide a complete understanding of the natural response of biodiversity to habitat subdivision. As an alternative to mesocosm and microcosm experiments, islands provide a more natural system for studying basic problems of ecology and evolution (Wardle et al., 1997; Losos and Ricklefs, 2009; Kardol et al., 2018), and land-bridge islands in particular are ideal model systems for testing the consequences of habitat subdivision (Si et al., 2016; Wilson et al., 2016; Zeng et al., 2019). In the case of land-bridge islands, the fragmented habitats are surrounded by water with a high-contrast heterogeneity, which severely limits the dispersal of certain taxa (Wilson et al., 2016). On the other hand, land-bridge island system is also a natural laboratory for verifying theory of island biogeography (Wilson et al., 2016; Li et al., 2020b). However, only a few studies have explored the distribution patterns of soil microorganisms among islands (Li et al., 2020b). Larger islands may lead to higher soil microbial diversity due to higher soil environmental heterogeneity, however, there is still doubt whether landscape-scale habitat heterogeneity can match the scale threshold of soil microorganisms (Bru et al., 2011; Fierer, 2017).

In the current study, we used mainland-island system to explore two questions: (1) examine effects and process of unequal-sized patches and isolation after habitat subdivision on soil microbial biodiversity in fragmented islands *via* comparing soil microbial biodiversity and composition among mainland fragmented into small islands, mainland fragmented in to medium

islands, and mainland fragmented in to large islands; (2) verify island biogeographic theory and heterogeneity hypothesis *via* finding major factors that affect soil microbial diversity and composition among islands. The islands, which are located in Jiangxi Province, China, were created in 1972 when Zhelin Reservoir was established (Supplementary Figure S1). In 2020, after the islands had experienced nearly 50 years of habitat subdivision, we assessed the soil bacterial and fungal communities and soil abiotic variables on 61 land-bridge islands and 9 adjacent mainland sites. We categorized the 61 land-bridge islands into three types based on land area (small, medium, and large), and we also characterized the attributes of each island (e.g., distance to mainland, perimeter to area ratio, and island shape index). We hypothesize that: (1) soil microbial biomass and diversity would be lowest when mainland fragmented into small-sized islands because small patches may be too small to sustain a local population (Debinski and Holt, 2000); (2) soil microbial biomass and diversity may be not suitable for island biogeography theory but support other theories such as habitat heterogeneity hypothesis because of the mismatch between fragmented scale and micro-habitat scale (Sonnier et al., 2014) or dispersal-competition tradeoff (Mouquet and Loreau, 2002).

Materials and methods

Study sites

The Zhelin Reservoir is located at 29°03′-29°18′N and 115°04′-115°40′E in northwest Jiangxi Province, China (Supplementary Figure S1). In 1972, the Zhelin Reservoir was created by the damming of the middle reaches of the Xiushui River; with the rise of water level, thousands of islands were created in the reservoir (Lu et al., 2013). The Zhelin Reservoir is dominated by a subtropical monsoon climate, and subtropical evergreen broadleaf forest is the native vegetation. The mean annual precipitation ranges from 1,461 to 1,582 mm, and the mean annual temperature ranges from 17.3 to 17.5°C. In December of 2021, about 50 years after reservoir establishment, we selected 61 land-bridge islands and 9 mainland sites with minimal human interference. The elevation of islands and mainland sites ranged from 56 to 135 m above sea level (mean water depth is above 55 m), and the dominant tree species are *Cyclobalanopsis glauca* and *Pinus massoniana*. The climatic datasets during 1979–2022 from three stations around our study sites showed that mainland and three types of islands had similar historical climate conditions.

Measurement of land-bridge island attributes

We digitized the map of the Zhelin Reservoir from Google Earth™ and calculated the area and perimeter of all 1,080 islands using ArcGIS 10.2 (ESRI, Inc., Redlands, CA, United States). Based on the position, area, and perimeter of these islands, we randomly selected 61 islands. To explain the effects of unequal-sized patches after habitat subdivision, we classified the 61 islands into three "area types": small islands (< 1 ha, $n = 15$), medium islands (> 1, < 5 ha, $n = 31$), and large islands (> 5 ha, $n = 15$). The 9 mainland sites were on the north (4 sites) and south (5 sites) riverbanks. The distance of each land-bridge island to the mainland and to the nearest island was calculated in R version 3.6.3 (R Core Team, R, 2017). More specifically, the distance to mainland was calculated from each island to the north or south riverbank (that is distance to nearest coastline) *via* the dist2Line function in the 'geosphere' package, and the distance to the nearest island was calculated *via* the gdit function in the 'Imap' package. We also calculated the ratio of the perimeter to the area and the island shape index ($S=P/[2\times(\pi\times A)]^{0.5}$) for each island (Yu et al., 2012).

Soil sampling and analysis and soil microbial community analysis

Soil samples were collected from all land-bridge islands and mainland sites in December 2020. Three evenly spaced, concentric circles from the center to the edge of each island were designated for soil sampling; the radii of the circles (i.e., sampling lines) increased with island size, and the outermost circles were at least 10 m from the island edge. Soil samples were also collected from 9 mainland sites that had minimum human interference and that were located on both sides of the reservoir. At each mainland site, three evenly spaced sampling lines were designated; each line was 50 m long, was perpendicular to the reservoir bank, and extended from the highest to the lowest altitude. For each island and mainland sampling line, we collected five soil samples by taking 7-cm-diameter soil cores in the topsoil (0–10 cm); these were mixed to yield one composite sample per line and three samples per land-bridge island and mainland site. After roots were removed, the fresh soil samples were passed through a 2-mm-mesh sieve. One part of the soil sample was aired-dried and used for analysis of soil pH with a 1:2.5 (soil: water) suspension, soil organic carbon (SOC) using the Walkley-Black modified acid-dichromate $FeSO_4$ titration method, total soil nitrogen (TN) using micro-Kjeldahl digestion, and total soil phosphorus (TP) using the H_2SO_4-$HClO_4$ fusion method (Chen et al., 2016, 2019). The other part of each moist soil sample was used for determining soil moisture and the soil microbial properties.

Soil bacterial and fungal biomasses were estimated by phospholipid fatty acid (PLFA) analysis (Chen et al., 2016, 2019), which were extracted using 8 g freeze-dried soil for each sampling. Biomasses (nmol g^{-1} of dry soil) were determined according to PLFAs specific to bacteria (i14:0, i15:0, a15:0, i16:0, 16:1ω7c, i17:0, a17:0, cy17:0, 17:1ω8, 18:1ω7c, 18:1ω9, and cy19:0) and fungi (18:2ω6,9). The bacterial to fungal biomass ratio (B:F ratio) was also calculated. For assessment of soil bacterial and fungal diversity and composition, soil DNA was extracted from a 0.5-g

soil sample using the FastDNA® Spin Kit for Soil (MP Biomedical, Solon, OH). We targeted the V3-V4 region of bacterial 16S rRNA gene *via* 338F-806R primers and the ITS sequence of the fungal gene *via* ITS1-ITS2 primers using an Illumina MiSeq platform (San Diego, CA, United States). Demultiplexed paired-end fastq files were used to complete downstream processing using QIIME2 with the DADA2 denoising method (Callahan et al., 2016). After sequences were trimmed (to remove adapters) and truncated (to remove sequences with low quality), we filtered amplicon sequencing variants (ASVs) that had <0.01% relative abundance or that only appeared in three samples. The taxonomy of each gene sequence was analyzed by the Naive Bayes Classifier algorithm against the Silva database (Silva 138) for bacteria and the Unite database (Unite 8.2) for fungi (Abarenkov et al., 2020). After rare ASVs and singletons were filtered, 1,512 bacterial ASVs and 1,204 fungal ASVs remained.

Statistical analysis

First, differences in microbial biomass, alpha diversity, island attributes, and soil abiotic factors among mainland and island area types were examined using Bayesian-ANOVA based on the independent variances jags model *via* 'rjags' packages (Kruschke, 2014). The posterior distribution of response variables in each group and the differences between two groups were estimated using Markov Chain Monte Carlo (MCMC) sampling techniques. When the 95% highest density interval (HDI) of the posterior distribution of the difference between two groups fell above or below zero, we concluded that the means of the groups were different (Kruschke, 2014). Second, differences in microbial composition among mainland and island area types were visualized using principal coordinate analyses (PCoAs) from Bray-Curtis distances. Permutational multivariate analysis of variance (PERMANOVAs) with the *adonis* function in the 'vegan' packages were used to determine whether bacterial and fungal composition differed among mainland and island area types. CoDA method in 'Selbal' package was used to detect microbial signatures (global balance) between mainland and islands (Rivera-Pinto et al., 2018). The correlations between soil properties and relative abundance of dominant bacterial phyla or fungal classes, and microbial signatures were estimated by Pearson correlation analysis. Third, we used structural equation modelling (SEM) to determine the potential direct and indirect effects of long-term habitat subdivision on soil microbial biomass, richness, and dissimilarity *via* response ratio between mainland and islands: $(Variable_{island} - Variable_{mainland})/Variable_{mainland}$. We assumed that habitat fragmentation would first change habitat area and isolation, and indirectly affect habitat heterogeneity, including soil moisture, soil pH, soil nutrient quantity, and soil nutrient quality. Each hierarchical model was simplified by step-wise exclusion of pathways that had non-significant regressions ($p > 0.05$) and was implemented using the maximum likelihood estimation method (Chen et al., 2019). In the SEM, we classified the soil-nutrient explanatory variables into two categories (quantity and quality) based on previous reports (Chen et al., 2016, 2019): (1) soil substrate quantity included SOC, TN, and TP; and (2) soil substrate quality included the soil C:N ratio, C:P ratio, and N:P ratio. The first principal component (PCA1) of two categories explained 66 and 73% of the total variance, respectively. To test island biogeography theory, we used ordinary least squares regression between microbial richness and island area or distance to mainland. Finally, random forest classification analysis and accuracy significance were used to select the most important determinants of microbial biomass, richness, and dissimilarity among island types, and generalized additive models (GAMs) were used *via* the 'mgcv' package in R to investigate natural relationships between determinants and microbial biomass, richness, and dissimilarity. The SEM models were developed with AMOS 21 software (IBM SPSS Inc., Chicago, IL, United States). Other statistical analyses were performed using R version 3.6.3 (R Core Team, R, 2017).

Results

Responses of land-bridge island attributes and soil abiotic variables

Soil abiotic variables substantially differed among mainland sites and the three island-area types (Figure 1; Supplementary Table S1). The soil moisture of islands was lower than that of the mainland sites at least 12% and soil pH of island was higher than that of the mainland sites at least 2 units (Figure 1; Supplementary Table S1). SOC and TP were similar between the mainland sites and each of the three types of islands (Figure 1). The mainland sites had higher TN and soil N:P than small or large islands, but had lower soil C:N and C:P than small or medium islands (Figure 1; Supplementary Table S1). Soil moisture increased, but soil pH, TN, and TP stayed constant as island size increased; SOC, soil C:N, soil C:P, and soil N:P were higher on the medium-sized islands than on small or large islands (Figure 1; Supplementary Table S1). Island area, perimeter, shape index, and nearest distance increased as island size increased, but distance-to-mainland and perimeter: area ratio decreased as island size increased (Supplementary Figure S2, Table S2).

Responses of soil microbial biomass, richness, dissimilarity, and composition

Soil bacterial biomass and B:F ratio were higher on the large-sized islands than on the small or medium islands, but soil fungal biomass did not differ among the three sizes of islands (Figures 2A–C; Supplementary Table S3). Compared with the mainland, each type of islands had higher soil bacterial biomass and fungal biomass but had lower B:F ratio. For example, the increase of bacterial biomass on large island reached to 25% and

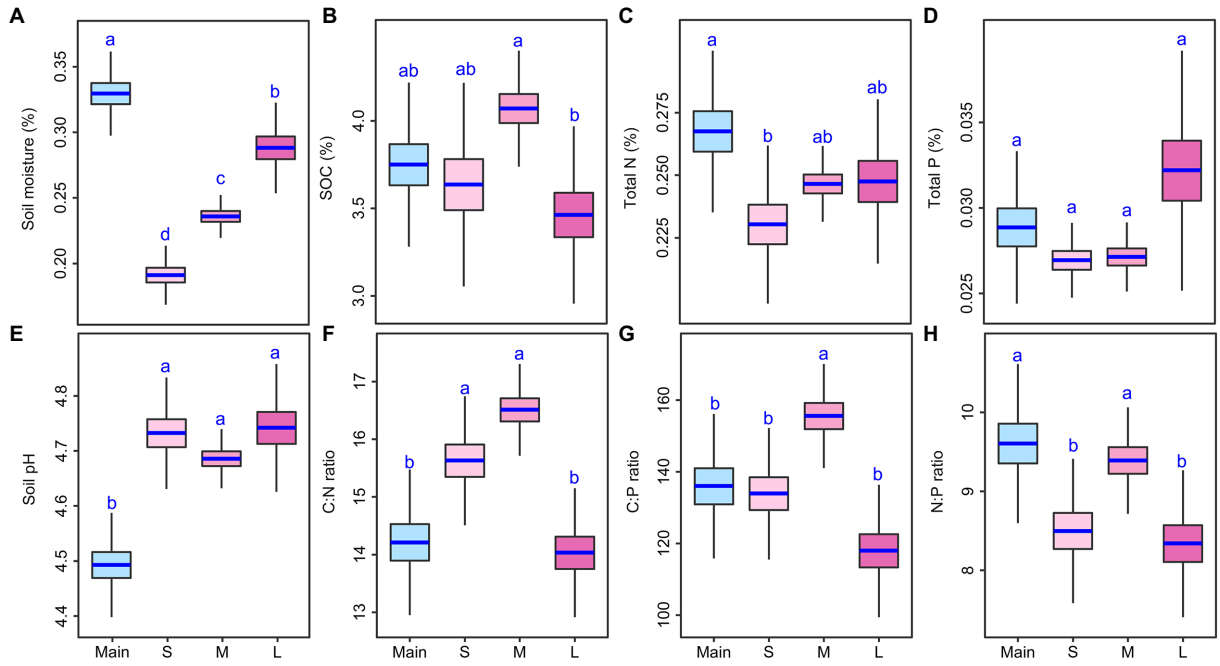

FIGURE 1
Differences in soil abiotic variables **(A–H)** among the mainland (Main) and three island types (S: small islands; M: medium islands; L: large islands). Boxplots indicate the medians and upper and lower quartiles of the posterior distribution. Different letters indicate a credibly different posterior distribution among the mainland and three island types (Bayesian-ANOVA, 95% highest density intervals of the posterior difference between each two groups falls above or below zero).

the increase of fungal biomass on small island reached to 50% (Figures 2A–C; Supplementary Table S3). Soil bacterial richness was higher on the medium-sized islands than on the small or large islands, but soil fungal richness did not differ among the three sizes of islands (Figures 2D,E; Supplementary Table S3). Compared with the mainland, however, medium-sized islands but not small or large islands had higher bacterial and fungal richness (Figures 2D,E; Supplementary Table S3). Among the mainland and three types of islands, the medium islands had the lowest bacterial dissimilarity, but fungal dissimilarity did not differ among the mainland and three types of islands (Figures 2F,G; Supplementary Table S3).

Permutational multivariate analysis of variance analysis showed that the soil bacterial and fungal communities differed among the three types of islands, as well as between each type of islands and the mainland (Figures 3A,B). The relative abundances of *Actinobacteriota* were higher on the islands than on the mainland but decreased from the small to large islands; the relative abundances of *Proteobacteriota* and *Acidobacteriota* were lower on the islands than on the mainland but increased from small to large islands (Figures 3C; Supplementary Tables S4–S6). Although the relative abundance of the dominant fungal class *Agaricomycetes* was constant, the relative abundances of other dominant fungal classes differed among the mainland and three types of islands (Figure 3D; Supplementary Tables S4–S6). In particular, the relative abundance of *Mortierellomycetes* was lower on the three types of islands than on the mainland and decreased from large to small islands. In contrast, the relative abundances of *Tremellomycetes* and *Eurotiomycetes* were higher on small islands than on the mainland or on large islands (Figure 3D; Supplementary Tables S4–S6). Results of microbial balances showed that the bacterial genera *Acidodthermus*, *Pseudonocardia*, and *Bacillus and* fungal genera *Sagenomella*, *Adisciso*, *Clavulina*, and *Trichoderma* were more predictive on three types of islands, while the bacterial genera *Roseiarcus*, *Kitasatospora*, and *Roseiarcus* and fungal genera *Mortierella* were more predictive on mainland (Supplementary Figure S4). Correlation analysis revealed that the relative abundances of dominant phylum/classes and microbial signatures were associated with most soil abiotic variables, especially for soil moisture and soil pH (Supplementary Figure S5; Table S7).

Factors associated with microbial biomass, richness, and dissimilarity

SEM showed that the factors associated with habitat subdivision-induced changes in microbial variables were different among the three types of islands. Compared with mainland, the higher bacterial biomass on the small-sized islands was mainly associated with changes in soil moisture and soil pH, while the higher fungal biomass on the small-sized islands was directly associated with distance-to-mainland (Figures 4A,B). The higher bacterial and fungal biomass on the medium islands than on the

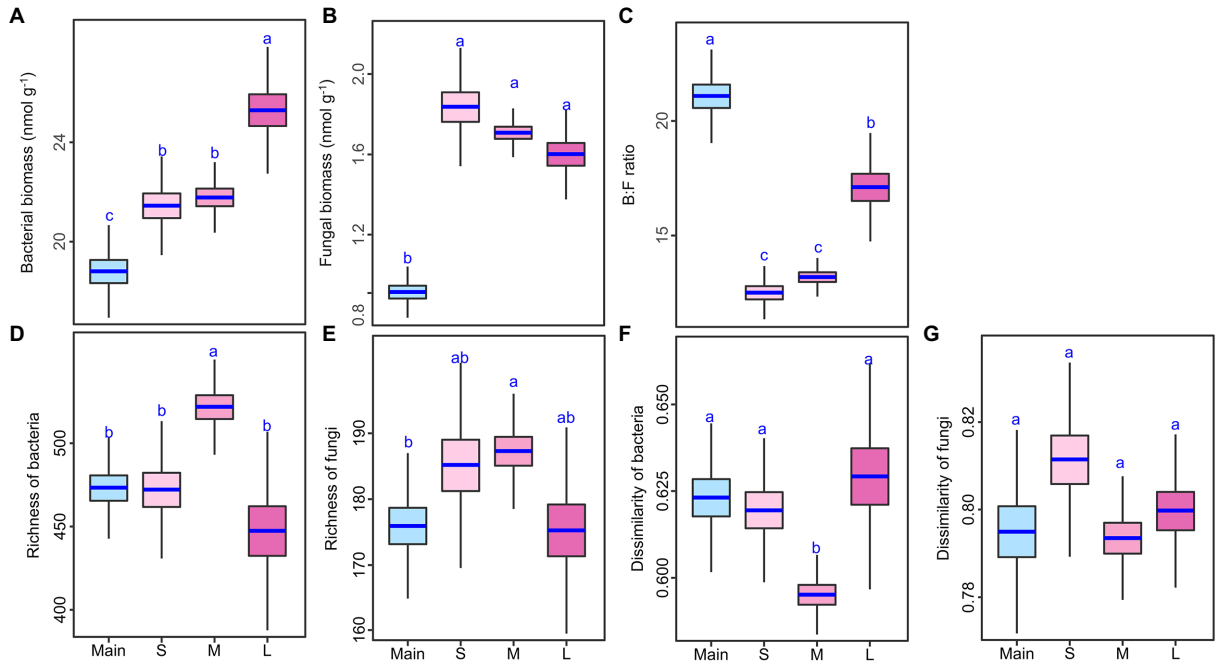

FIGURE 2
Differences in soil bacterial and fungal biomass, amplicon sequencing variant (ASV) richness, and dissimilarity **(A–G)** among the mainland (Main) and three island types (S: small islands; M: medium islands; L: large islands). Boxplots indicate the medians and upper and lower quartile of the posterior distribution. Different letters indicate a credibly different posterior distribution among the mainland and three island types (Bayesian-ANOVA, 95% highest density intervals of the posterior difference between each two groups falls above or below zero).

mainland were mainly associated with changes in soil moisture and soil pH (Figures 4C,D). Compared with mainland, the higher bacterial biomass on the large-sized islands was mainly associated with changes in soil nutrient quality, soil moisture, and soil pH, while the higher fungal biomass was associated with changes in soil moisture (Figures 4E,F). The higher soil bacterial richness on medium islands than on the mainland was mainly associated with soil moisture and direct effect of distance, while the higher fungal richness on the medium islands was mainly associated with soil moisture and pH (Figures 4C,D). The lower soil bacterial dissimilarity on medium islands than on the mainland was mainly associated with bacterial richness and direct effect of distance (Figure 4C).

Across the three island types, regression analyses showed that bacterial richness was not related to island area, but negatively related to distance to mainland, while fungal richness was negatively related to island area, but not related with distance to mainland (Supplementary Figure S6). SEM showed that the bacterial biomass was mainly associated with area-induced changes in soil moisture and soil nutrient quantity and distance-induced changes in soil pH (Supplementary Figures S7A,B). The fungal biomass was mainly associated with area-induced changes in soil moisture and soil nutrient quantity and distance-induced changes in soil pH (Supplementary Figures S7A,B). Soil bacterial richness was mainly associated with distance-induced changes in soil nutrient quantity and soil pH, and direct effect of distance (Supplementary Figures S7A,B). The fungal richness was mainly associated with distance-induced changes in soil pH (Supplementary Figures S7A,B). Soil bacterial or fungal dissimilarity was mainly associated with their richness (Supplementary Figure S7). Further, GAM analysis further showed that soil bacterial biomass was negatively associated with distance to mainland and was positively associated with soil pH; soil fungal biomass was negatively associated with soil moisture and was positively associated with soil substrate quantity (Figures 5A,B; Supplementary Figure S8, Table S8). Soil bacterial richness had unimodal relationship with distance to mainland and had negative linear relationship with soil pH; soil fungal richness had negative relationships with island area and soil pH (Figures 5C,D; Supplementary Figure S8, Table S8). Soil bacterial dissimilarity had negative relationship with soil bacterial richness and distance to mainland; soil fungal dissimilarity had negative relationship with soil fungal richness and had positive relationship with distance to mainland (Figures 5E,F; Supplementary Figure S8, Table S8).

Discussion

We found that both soil bacterial and fungal biomass were higher on islands than that on mainland, but the degree of changes depended on types of subdivision and their associated habitat heterogeneity, which consistent with our first hypothesis. Across three types of islands, area- or distance-induced increase in soil

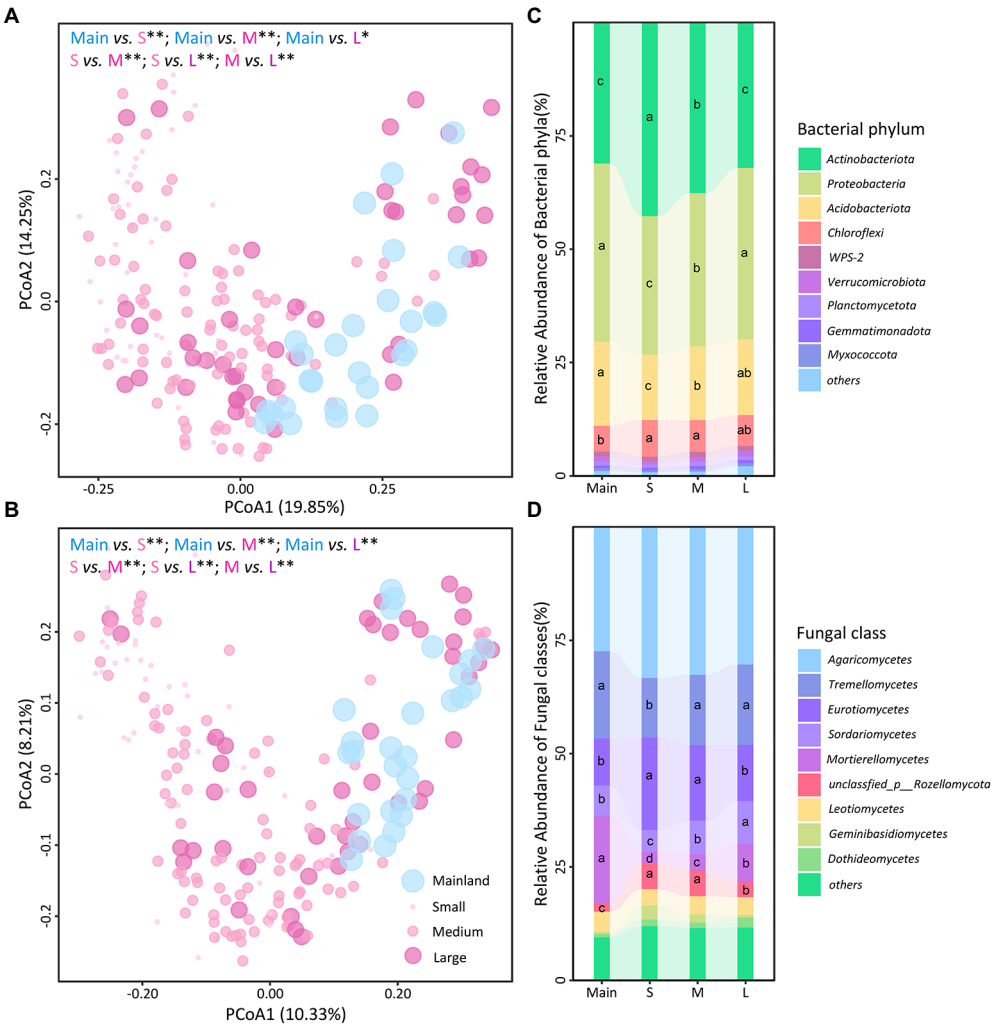

FIGURE 3
Soil bacterial (**A** and **C**) and fungal (**B** and **D**) community composition among the mainland (Main) and three island types (S: small islands; M: medium islands; L: large islands). Community composition was estimated by principal coordinate analysis (PCoA) based on Bray-Curtis dissimilarities **(A,B)**. Differences in community composition between mainland and each island type were assessed using permutational analysis of variance (*, $p \leq 0.05$; **, $p \leq 0.01$). Stacked bar plots indicate relative abundance (%) of bacterial phyla **(C)** and fungal classes **(D)** among the mainland and three island types, respectively. Different letters represent credibly different posterior distributions of relative abundance.

pH consistently enhanced bacterial biomass. The strong and positive associations between soil microbial biomass and soil pH were well reported at different ecosystems due to the narrow pH niche for soil microbial communities (Rousk et al., 2009; Chen et al., 2015). The greatest change in bacterial biomass of large subdivision was attributed to combined effects of soil pH and soil nutrient quality which indicated that higher habitat heterogeneity in larger island may play an important role in bacterial biomass (Li et al., 2020b). In contrast, soil fungal biomass was promoted by distance-induced decrease in soil moisture because the higher soil moisture in the subtropical forests might inhibit the growth of soil fungi (Cruz-Paredes et al., 2021). In addition, habitat subdivision consistently decreased B:F ratio on each type of islands, suggesting that soils on mainland are dominated by bacterial-based energy channels while soils on each of the three types of islands are dominated by fungal-based energy channels. The shift from bacterial-based to fungal-based energy channels resulting from habitat subdivision could result in decreases in soil nutrient losses and CO_2 release, which in turn could cause the fragmented islands to be more resistance to climate changes (de Vries et al., 2013; Chen et al., 2016).

In contrast to our first hypothesis, only on the medium-sized islands, soil bacterial and fungal richness were higher than that on the mainland, which was somewhat consistent with the intermediate disturbance hypothesis (Connell, 1978; Huston, 1979). That is to say, changes in bacterial and fungal richness were mainly derived from extrinsic process and associated intrinsic competition (Raynaud and Nunan, 2014). For example, the increase in bacterial richness was attributed to that lower moisture could promote competition ability of subdominant species

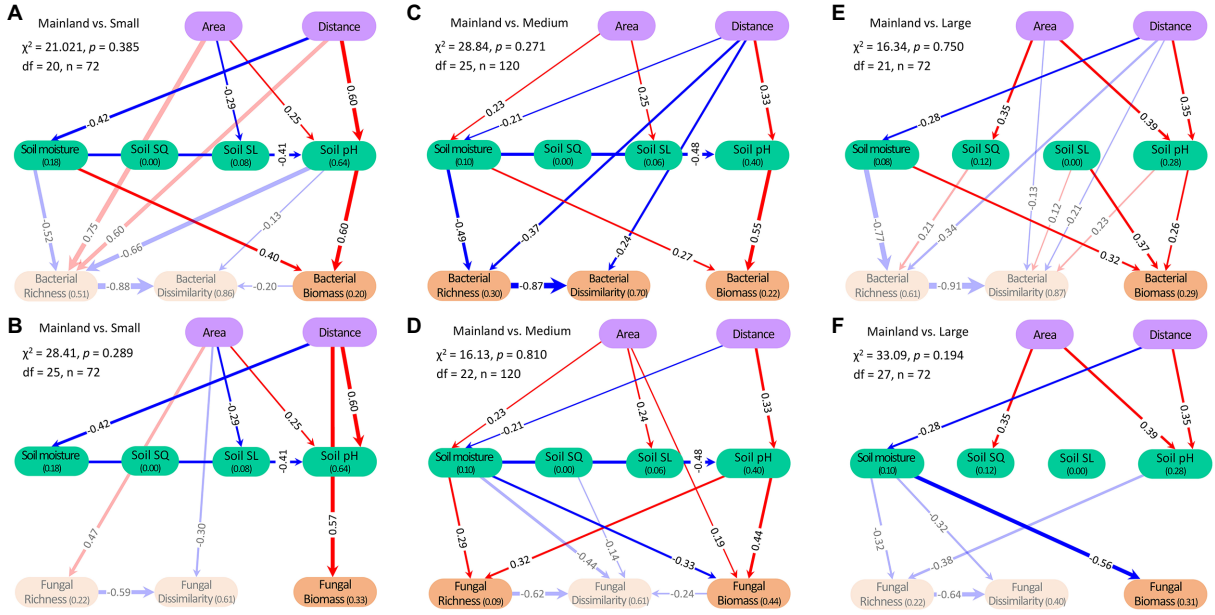

FIGURE 4
Structural equation model (SEM) for the response ratio of soil bacterial and fungal biomass, richness, and dissimilarity under small subdivision **(A,B)**, medium subdivision **(C,D)**, and large subdivision **(E,F)**. Soil SQ, soil substrate quantity; Soil SL, soil substrate quality. Arrows indicate significant ($p \leq 0.05$) effects. Values associated with arrows represent standardized path coefficients; pathways without significant effects ($p > 0.05$) are not shown. Values associated with response variables in brackets indicate the proportion of variation (R^2) explained by relationships with other variables. The variables with light shade in the SEM indicate they are not significantly altered ($p > 0.05$) by habitat fragmentation.

(Carson et al., 2010); the increase in fungal richness was attributed to that higher soil pH could benefit ectomycorrhizal fungi growth and reproduction (Wardle and Lindahl, 2014). The lack differences in microbial richness between mainland and small or large islands could be due to the offset effects among various external environment (Raynaud and Nunan, 2014). The strong differences in microbial biomass between mainland and islands were highly associated changes in habitat heterogeneity resulting from changes in island geometrical properties (Yu et al., 2012). Normally, microbial local interactions are likely to be obscured by relatively large samples which encompass high environmental heterogeneity (Raynaud and Nunan, 2014). The consistent and positive relationships between microbial richness and dissimilarity in any subdivision cases showed that the subdivision process may encounter strong microbial interactions. Bacterial dissimilarity was lowest on medium-sized islands could perhaps be due to the reduced fitness of the original dominant, mainland bacterial taxa on medium-sized islands and to the increased fitness of previously subdominant competitors that were favored by medium-sized islands (Chesson, 2000; Mouquet and Loreau, 2002). The lower sensitive of soil fungal dissimilarity to habitat subdivision than bacterial fungal similarity could be due to the fact that soil fungi have mycelial networks and are more resistant than bacteria to environmental disturbances (Rousk et al., 2010; Wang et al., 2020). The strong negative relationships between microbial richness and dissimilarity without reference to island size suggests that these fragmented habitats may still be experiencing the replacement of the previously most competitive taxa by other competitors (Chesson, 2000; Mouquet and Loreau, 2002).

Our permutational multivariate analysis of variance analysis showed that both soil bacterial and fungal community composition were significantly changed by long-term habitat subdivision. From small to large islands, the relative abundance decreased for the dominant bacterial phylum *Actinobacteriota* but increased for the dominant bacterial phylum *Proteobacteriota*, although both phyla were previously characterized as copiotrophic based on classical life strategy theory (Fierer et al., 2007). The opposite relationships of the relative abundance of *Actinobacteriota* and *Proteobacteriota* with soil nutrients (SOC and TN) on the subtropical land-bridge islands indicates that these taxa still had different preferences for substrates and nutrients, although previous studies showed that the relative abundance of both phyla were positively correlated with soil nutrients (Lauber et al., 2008; Fierer et al., 2011; Laliberté et al., 2017). We also found that the relative abundance of most bacterial phyla and fungal classes were related to soil moisture and soil pH on the subtropical land-bridge islands, which is consistent with previous studies (Rousk et al., 2010; Chen et al., 2016, 2019; Wu et al., 2020). Our research showed that changes in the relationships between the relative abundance of several fungal classes after fragmentation with soil properties (such as the negative relationships between *Agaricomycetes* and soil pH and soil moisture, and the positive relationships between *Eurotiomycetes* and soil pH and total N) were also consistent with other studies (Hartmann et al., 2017; Li

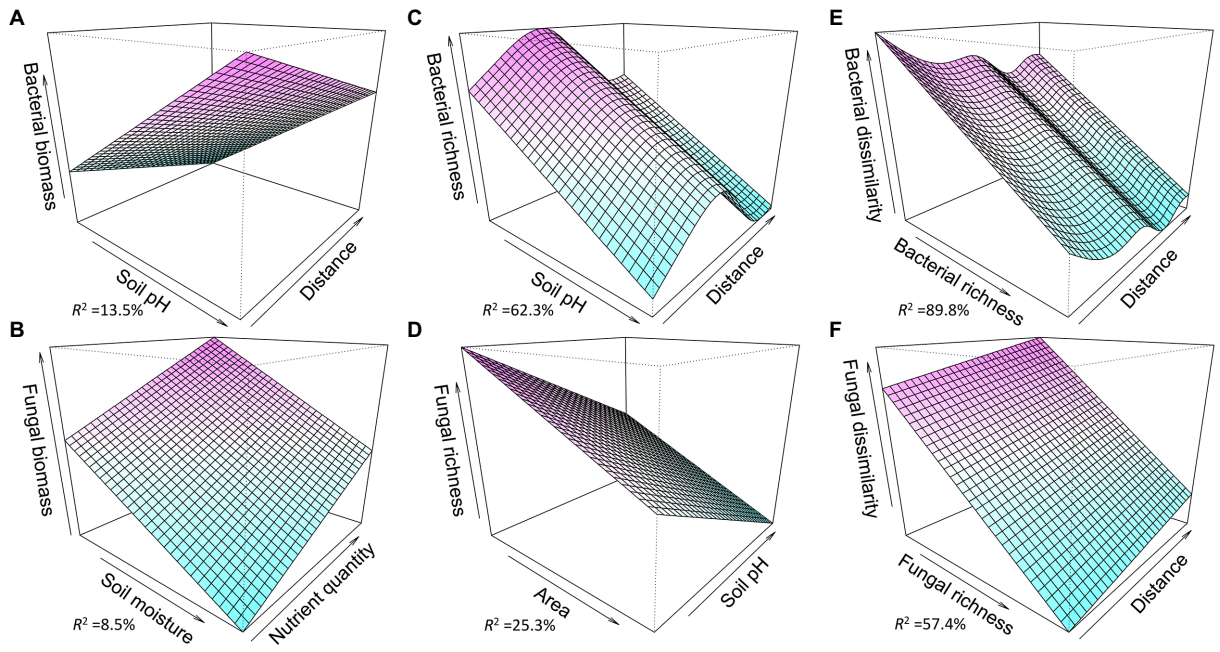

FIGURE 5
Fitted relationships between soil microbial variables (biomass, richness, and dissimilarity) and explanatory variables across the three island types based on generalized additive models. Bacterial biomass **(A)** and bacterial richness **(C)** were explained by distance and soil pH; fungal biomass **(B)** was explained by soil moisture and soil substrate quantity; fungal richness **(D)** was explained by island area and soil pH; bacterial dissimilarity **(E)** and fungal dissimilarity **(F)** were explained by their richness and distance to mainland. The detailed results of generalized additive models were showed in Supplementary Table S8.

et al., 2020a). In addition, based on the reduction in the relative abundance of *Mortierellomycetes*, we infer that fungi are more closely related than bacteria to vegetation (Li et al., 2020a). Differences in microbial signatures between mainland and island also derived from soil properties, especially soil moisture and soil pH (Supplementary Figures S4, S5). For example, bacterial genus *Roseiarcus* and *Kitasatospora* were preferred on mainland due to their negative relationships with soil pH (Kämpfer, 2006; Rezaei et al., 2011; Kulichevskaya et al., 2014; Riahi et al., 2022), and fungal genus *Mortierella* was preferred on mainland due to its close interaction with plant roots (Toju and Sato, 2018). Overall, we found that habitat fragmentation greatly altered the composition of soil bacterial and fungal communities for each island size, and that the soil and plant properties associated with the habitat fragment-induced changes in community composition differed for bacteria and fungi.

Our ordinary least squares regression and structural equation model found only the relationship between bacterial richness and distance to mainland was consistent with species-distance relationships, while microbial richness was completely inconsistent with species-area relationships (MacArthur and Wilson, 2016). In contrast, both microbial biomass and diversity of soil bacteria or fungi were mainly associated with soil abiotic variables. Soil pH was still strongly associated with soil microbial biomass and richness (Rousk et al., 2009), although there were anti-directional responses in bacterial biomass and richness to soil pH might be due to the disproportionate contributions of dominant taxa to biomass than subdominant taxa (Bastida et al., 2021). We found soil fungal biomass decreased with increased soil moisture and increased with soil substrate quantity. The increase of soil carbon and nutrient content could provide more substrates for fungi growth (Bastida et al., 2021), however, negative effects of soil moisture on soil fungal biomass indicated that higher water content may inhibit their mobility to capture soil nutrients (Manzoni et al., 2012). Partly consistent with another land-bridge study (Li et al., 2020b), our results showed the island area had less effects on soil bacterial and fungal richness than distance to the mainland across the three types of islands, and this was especially the case for bacterial richness. Generalized additive model analysis showed that there were unimodal relationships between distance to mainland and bacterial richness across the three types of islands. Based on the coexistence theory of metacommunities (Mouquet and Loreau, 2002; Loreau et al., 2003) and as previously noted the intermediate disturbance hypothesis (Connell, 1978; Huston, 1979), the highest biodiversity may occur at a medium dispersal level because both species homogenization caused by high dispersal and competitive exclusion caused by low dispersal would reduce diversity. Our results also showed that soil bacterial or fungal dissimilarity were mainly associated with their richness and

distance to mainland across the three types of islands. The robust negative relationships between microbial richness and dissimilarity across the three types of islands confirmed that species coexistence was inhibited when the community became more dissimilar (Mouquet and Loreau, 2002). Furthermore, we found that the variables associated with soil fungal richness or dissimilarity had less explanatory power than the variables associated with soil bacteria richness perhaps because some functional groups of soil fungi (e.g., ectomycorrhizal fungi) are more closely related than soil bacteria to the changes in vegetation composition (Peay et al., 2007). Across the three types of islands, we found that the richness of soil microorganisms was mainly associated with island area and distance to the mainland while soil microbial dissimilarity was mainly associated with microbial richness and distance to the mainland.

Conclusion

Using 61 subtropical land-bridge islands with a 50-year history of subdivision and 9 adjacent mainland sites as a model system, we highlight several findings: Firstly, soil bacterial and fungal biomass in different-sized subdivision were higher than that in mainland, while increased the soil bacterial and fungal richness only on the medium-sized islands. These changes were due to subdivision-specified habitat heterogeneity, especial for soil moisture and soil pH. Secondly, soil microbial dissimilarities were robustly and negatively associated with microbial richness suggests that these fragmented habitats may still be experiencing the replacement of the previously most competitive taxa by other competitors. Finally, soil microbial distributions are not consistent with species-area relationships, but determined by habitat heterogeneity and tradeoff between competition and dispersal.

Data availability statement

The datasets presented in this study can be found in online repositories. The names of the repository/repositories and accession number(s) can be found below: https://www.ncbi.nlm.nih.gov/, PRJNA898793. The bacterial and fungal ASV table and relevant environmental variables is available on GitHub at https://github.com/DimaChen-ctgu/Island-2020.

Author contributions

All authors contributed to the article and approved the submitted version, and due care has been taken to ensure the integrity of the work. The accompanying manuscript constitutes original unpublished work and is not under consideration for publication elsewhere.

Funding

This study was supported by the National Natural Science Foundation of China (42177272), and the Youth Innovation Promotion Association of the Chinese Academy of Sciences (2015061).

Conflict of interest

The authors declare that the research was conducted in the absence of any commercial or financial relationships that could be construed as a potential conflict of interest.

Publisher's note

All claims expressed in this article are solely those of the authors and do not necessarily represent those of their affiliated organizations, or those of the publisher, the editors and the reviewers. Any product that may be evaluated in this article, or claim that may be made by its manufacturer, is not guaranteed or endorsed by the publisher.

Supplementary material

The Supplementary material for this article can be found online at: https://www.frontiersin.org/articles/10.3389/fmicb.2022.1063340/full#supplementary-material

References

Abarenkov, K., Zirk, A., Piirmann, T., Pöhönen, R., Ivanov, F., Nilsson, R. H., et al. (2020). *UNITE QIIME release for fungi. Version 04.02. 2020.* London: UNITE community.

Åström, J., and Bengtsson, J. (2011). Patch size matters more than dispersal distance in a mainland–island metacommunity. *Oecologia* 167, 747–757. doi: 10.1007/s00442-011-2024-y

Baas-Becking, L. G. M. (1934). *Geobiologie of inleiding tot de milieukunde.* The Hague, The Netherlands: WP Van Stockum & Zoon NV.

Bastida, F., Eldridge, D. J., García, C., Png, G. K., Bardgett, R. D., and Delgado-Baquerizo, M. (2021). Soil microbial diversity–biomass relationships are driven by soil carbon content across global biomes. *ISME J.* 15, 2081–2091. doi: 10.1038/s41396-021-00906-0

Bru, D., Ramette, A., Saby, N., Dequiedt, S., Ranjard, L., Jolivet, C., et al. (2011). Determinants of the distribution of nitrogen-cycling microbial communities at the landscape scale. *ISME J.* 5, 532–542. doi: 10.1038/ismej.2010.130

Bueno, A. S., and Peres, C. A. (2019). Patch-scale biodiversity retention in fragmented landscapes: reconciling the habitat amount hypothesis with the island biogeography theory. *J. Biogeogr.* 46, 621–632. doi: 10.1111/jbi.13499

Callahan, B. J., Mcmurdie, P. J., Rosen, M. J., Han, A. W., Johnson, A. J. A., and Holmes, S. P. (2016). DADA2: high-resolution sample inference from Illumina amplicon data. *Nat. Methods* 13, 581–588. doi: 10.1038/nmeth.3869

Carson, J. K., Gonzalez-Quiñones, V., Murphy, D. V., Hinz, C., Shaw, J. A., and Gleeson, D. B. (2010). Low pore connectivity increases bacterial diversity in soil. *Appl. Environ. Microbiol.* 76, 3936–3942. doi: 10.1128/AEM.03085-09

Chen, D., Lan, Z., Hu, S., and Bai, Y. (2015). Effects of nitrogen enrichment on belowground communities in grassland: relative role of soil nitrogen availability vs. soil acidification. *Soil Biol. Biochem.* 89, 99–108. doi: 10.1016/j.soilbio.2015.06.028

Chen, D., Pan, Q., Bai, Y., Hu, S., Huang, J., Wang, Q., et al. (2016). Effects of plant functional group loss on soil biota and net ecosystem exchange: a plant removal experiment in the Mongolian grassland. *J. Ecol.* 104, 734–743. doi: 10.1111/1365-2745.12541

Chen, D., Xing, W., Lan, Z., Saleem, M., Wu, Y., Hu, S., et al. (2019). Direct and indirect effects of nitrogen enrichment on soil organisms and carbon and nitrogen mineralization in a semi-arid grassland. *Funct. Ecol.* 33, 175–187. doi: 10.1111/1365-2435.13226

Chesson, P. (2000). Mechanisms of maintenance of species diversity. *Annu. Rev. Ecol. Evol. Syst.* 31, 343–366. doi: 10.1146/annurev.ecolsys.31.1.343

Connell, J. H. (1978). Diversity in tropical rain forests and coral reefs. *Science* 199, 1302–1310. doi: 10.1126/science.199.4335.1302

Cruz-Paredes, C., Tájmel, D., and Rousk, J. (2021). Can moisture affect temperature dependences of microbial growth and respiration? *Soil Biol. Biochem.* 156:108223. doi: 10.1016/j.soilbio.2021.108223

De Vries, F. T., Thébault, E., Liiri, M., Birkhofer, K., Tsiafouli, M. A., Bjørnlund, L., et al. (2013). Soil food web properties explain ecosystem services across European land use systems. *Proc. Natl. Acad. Sci.* 110, 14296–14301. doi: 10.1073/pnas.1305198110

Deane, D. C., Xing, D., Hui, C., Mcgeoch, M., and He, F. (2022). A null model for quantifying the geometric effect of habitat subdivision on species diversity. *Glob. Ecol. Biogeogr.* 31, 440–453. doi: 10.1111/geb.13437

Debinski, D. M., and Holt, R. D. (2000). A survey and overview of habitat fragmentation experiments. *Conserv. Biol.* 14, 342–355. doi: 10.1046/j.1523-1739.2000.98081.x

Delgado-Baquerizo, M., Eldridge, D. J., Hamonts, K., Reich, P. B., and Singh, B. K. (2018). Experimentally testing the species-habitat size relationship on soil bacteria: a proof of concept. *Soil Biol. Biochem.* 123, 200–206. doi: 10.1016/j.soilbio.2018.05.016

Delgado-Baquerizo, M., Maestre, F., Reich, P., Jeffries, T., Gaitan, J., Encinar, D., et al. (2016). Microbial diversity drives multifunctionality in terrestrial ecosystems. *Nat. Commun.* 7:10541. doi: 10.1038/ncomms10541

Ewers, R. M., and Didham, R. K. (2006). Confounding factors in the detection of species responses to habitat fragmentation. *Biol. Rev.* 81, 117–142. doi: 10.1017/S1464793105006949

Fanin, N., Gundale, M. J., Farrell, M., Ciobanu, M., Baldock, J. A., Nilsson, M.-C., et al. (2018). Consistent effects of biodiversity loss on multifunctionality across contrasting ecosystems. *Nat. Ecol. Evol.* 2, 269–278. doi: 10.1038/s41559-017-0415-0

Fierer, N. (2017). Embracing the unknown: disentangling the complexities of the soil microbiome. *Nat. Rev. Microbiol.* 15, 579–590. doi: 10.1038/nrmicro.2017.87

Fierer, N., Bradford, M. A., and Jackson, R. B. (2007). Toward an ecological classification of soil bacteria. *Ecology* 88, 1354–1364. doi: 10.1890/05-1839

Fierer, N., Lauber, C. L., Ramirez, K. S., Zaneveld, J., Bradford, M. A., and Knight, R. (2011). Comparative metagenomic, phylogenetic and physiological analyses of soil microbial communities across nitrogen gradients. *ISME J.* 6, 1007–1017. doi: 10.1038/ismej.2011.159

Finlay, B. (2002). Global dispersal of free-living microbial eukaryote species. *Science* 296, 1061–1063. doi: 10.1126/science.1070710

Haddad, N., Brudvig, L., Clobert, J., Davies, K., Gonzalez, A., Holt, R., et al. (2015). Habitat fragmentation and its lasting impact on Earth's ecosystems. *Sci. Adv.* 1:e1500052. doi: 10.1126/sciadv.1500052

Haddad, N. M., Gonzalez, A., Brudvig, L. A., Burt, M. A., Levey, D. J., and Damschen, E. I. (2017). Experimental evidence does not support the habitat amount hypothesis. *Ecography* 40, 48–55. doi: 10.5061/dryad.k88h6

Hartmann, M., Brunner, I., Hagedorn, F., Bardgett, R., Stierli, B., Herzog, C., et al. (2017). A decade of irrigation transforms the soil microbiome of a semi-arid pine forest. *Mol. Ecol.* 26, 1190–1206. doi: 10.1111/mec.13995

Huston, M. (1979). A general hypothesis of species diversity. *Am. Nat.* 113, 81–101. doi: 10.1086/283366

Kämpfer, P. (2006). "The family Streptomycetaceae, Part I: taxonomy," in *The prokaryotes*. eds. M. Dworkin, S. Falkow, E. Rosenberg, K.-H. Schleifer, and E. Stackebrandt (New York, NY: Springer).

Kardol, P., Fanin, N., and Wardle, D. A. (2018). Long-term effects of species loss on community properties across contrasting ecosystems. *Nature* 557, 710–713. doi: 10.1038/s41586-018-0138-7

Kruschke, J. (2014). *Doing Bayesian data analysis: A tutorial with R, Jags, and Stan*. Cambridge, MA: Academic Press.

Kulichevskaya, I., Danilova, O., Tereshina, V., Kevbrin, V., and Dedysh, S. (2014). Descriptions of Roseiarcus fermentans gen. Nov., sp. nov., a bacteriochlorophyll a-containing fermentative bacterium related phylogenetically to alphaproteobacterial methanotrophs, and of the family Roseiarcaceae fam. Nov. *Int. J. Syst. Evol. Microbiol.* 64, 2558–2565. doi: 10.1099/ijs.0.064576-0

Laliberté, E., Kardol, P., Didham, R. K., Teste, F. P., Turner, B. L., and Wardle, D. A. (2017). Soil fertility shapes belowground food webs across a regional climate gradient. *Ecol. Lett.* 20, 1273–1284. doi: 10.1111/ele.12823

Lauber, C. L., Strickland, M. S., Bradford, M. A., and Fierer, N. (2008). The influence of soil properties on the structure of bacterial and fungal communities across land-use types. *Soil Biol. Biochem.* 40, 2407–2415. doi: 10.1016/j.soilbio.2008.05.021

Li, S., Huang, X., Shen, J., Xu, F., and Su, J. (2020a). Effects of plant diversity and soil properties on soil fungal community structure with secondary succession in the Pinus yunnanensis forest. *Geoderma* 379:114646. doi: 10.1016/j.geoderma.2020.114646

Li, S., Wang, P., Chen, Y., Wilson, M., Yang, X., Ma, C., et al. (2020b). Island biogeography of soil bacteria and fungi: similar patterns, but different mechanisms. *ISME J.* 14, 1886–1896. doi: 10.1038/s41396-020-0657-8

Lindenmayer, D. B., and Fischer, J. (2007). Tackling the habitat fragmentation panchreston. *Trends Ecol. Evol.* 22, 127–132. doi: 10.1016/j.tree.2006.11.006

Loreau, M., Mouquet, N., and Gonzalez, A. (2003). Biodiversity as spatial insurance in heterogeneous landscapes. *Proc. Natl. Acad. Sci.* 100, 12765–12770. doi: 10.1073/pnas.2235465100

Losos, J. B., and Ricklefs, R. E. (2009). Adaptation and diversification on islands. *Nature* 457, 830–836. doi: 10.1038/nature07893

Lu, B., Li, K., Zhang, H., Wang, W., and Gu, H. (2013). Study on the optimal hydropower generation of Zhelin reservoir. *J. Hydrol. Res.* 7, 270–278. doi: 10.1016/j.jher.2013.01.002

Macarthur, R. H., and Wilson, E. O. (1963). An equilibrium theory of insular zoogeography. *Evolution* 17, 373–387. doi: 10.2307/2407089

Macarthur, R. H., and Wilson, E. O. (2016). *The theory of island biogeography*. United States: Princeton university press.

Manzoni, S., Schimel, J. P., and Porporato, A. (2012). Responses of soil microbial communities to water stress: results from a meta-analysis. *Ecology* 93, 930–938. doi: 10.1890/11-0026.1

May, F., Rosenbaum, B., Schurr, F. M., and Chase, J. M. (2019). The geometry of habitat fragmentation: effects of species distribution patterns on extinction risk due to habitat conversion. *Ecol. Evol.* 9, 2775–2790. doi: 10.1002/ece3.4951

Mouquet, N., and Loreau, M. (2002). Coexistence in metacommunities: the regional similarity hypothesis. *Am. Nat.* 159, 420–426. doi: 10.1086/338996

Peay, K., Bruns, T., Kennedy, P., Bergemann, S., and Garbelotto, M. (2007). A strong species-area relationship for eukaryotic soil microbes: island size matters for ectomycorrhizal fungi. *Ecol. Lett.* 10, 470–480. doi: 10.1111/j.1461-0248.2007.01035.x

R Core Team, R. (2017). "*R: A language and environment for statistical computing*". R foundation for statistical computing Vienna, Austria.

Raynaud, X., and Nunan, N. (2014). Spatial ecology of bacteria at the microscale in soil. *PLoS One* 9:e87217. doi: 10.1371/journal.pone.0087217

Rezaei, F., Joh, L. D., Kashima, H., Reddy, A. P., and Vandergheynst, J. S. (2011). Selection of conditions for cellulase and xylanase extraction from switchgrass colonized by Acidothermus cellulolyticus. *Appl. Biochem. Biotechnol.* 164, 793–803. doi: 10.1007/s12010-011-9174-6

Riahi, H. S., Heidarieh, P., and Fatahi-Bafghi, M. (2022). Genus Pseudonocardia: what we know about its biological properties, abilities and current application in biotechnology. *J. Appl. Microbiol.* 132, 890–906. doi: 10.1111/jam.15271

Rivera-Pinto, J., Egozcue, J. J., Pawlowsky-Glahn, V., Paredes, R., Noguera-Julian, M., and Calle, M. L. (2018). Balances: a new perspective for microbiome analysis. *mSystems* 3, e00053–e00018. doi: 10.1128/mSystems.00053-18

Rousk, J., Bååth, E., Brookes, P. C., Lauber, C. L., Lozupone, C., Caporaso, J. G., et al. (2010). Soil bacterial and fungal communities across a pH gradient in an arable soil. *ISME J.* 4, 1340–1351. doi: 10.1038/ismej.2010.58

Rousk, J., Brookes, P. C., and Baath, E. (2009). Contrasting soil pH effects on fungal and bacterial growth suggest functional redundancy in carbon mineralization. *Appl. Environ. Microbiol.* 75, 1589–1596. doi: 10.1128/AEM.02775-08

Si, X., Baselga, A., Leprieur, F., Song, X., and Ding, P. (2016). Selective extinction drives taxonomic and functional alpha and beta diversities in island bird assemblages. *J. Anim. Ecol.* 85, 409–418. doi: 10.1111/1365-2656.12478

Sonnier, G., Jamoneau, A., and Decocq, G. (2014). Evidence for a direct negative effect of habitat fragmentation on forest herb functional diversity. *Landsc. Ecol.* 29, 857–866. doi: 10.1007/s10980-014-0022-2

Toju, H., and Sato, H. (2018). Root-associated fungi shared between arbuscular mycorrhizal and ectomycorrhizal conifers in a temperate forest. *Front. Microbiol.* 9:433. doi: 10.3389/fmicb.2018.00433

Van Der Heijden, M., Bardgett, R., and Van Straalen, N. (2007). The unseen majority: soil microbes as drivers of plant diversity and productivity in terrestrial ecosystems. *Ecol. Lett.* 11, 296–310. doi: 10.1111/j.1461-0248.2007.01139.x

Vannette, R. L., Leopold, D. R., and Fukami, T. (2016). Forest area and connectivity influence root-associated fungal communities in a fragmented landscape. *Ecology* 97, 2374–2383. doi: 10.1002/ecy.1472

Villard, M. A., and Metzger, J. P. (2014). Beyond the fragmentation debate: a conceptual model to predict when habitat configuration really matters. *J. Appl. Ecol.* 51, 309–318. doi: 10.1111/1365-2664.12190

Wang, B., Wu, L. J., Chen, D. M., Wu, Y., Hu, S. J., Li, L. H., et al. (2020). Grazing simplifies soil micro-food webs and decouples their relationships with ecosystem functions in grasslands. *Glob. Chang. Biol.* 26, 960–970. doi: 10.1111/gcb.14841

Wardle, D. A., and Lindahl, B. D. (2014). Disentangling global soil fungal diversity. *Science* 346, 1052–1053. doi: 10.1126/science.aaa1185

Wardle, D. A., Zackrisson, O., Hörnberg, G., and Gallet, C. (1997). The influence of island area on ecosystem properties. *Science* 277, 1296–1299. doi: 10.1126/science.277.5330.1296

Wilson, M. C., Chen, X.-Y., Corlett, R. T., Didham, R. K., Ding, P., Holt, R. D., et al. (2016). Habitat fragmentation and biodiversity conservation: key findings and future challenges. *Landsc. Ecol.* 31, 219–227. doi: 10.1007/s10980-015-0312-3

Wu, Y., Wu, J., Saleem, M., Wang, B., Hu, S., Bai, Y., et al. (2020). Ecological clusters based on responses of soil microbial phylotypes to precipitation explain ecosystem functions. *Soil Biol. Biochem.* 142:107717. doi: 10.1016/j.soilbio.2020.107717

Yu, M., Hu, G., Feeley, K. J., Wu, J., and Ding, P. (2012). Richness and composition of plants and birds on land-bridge islands: effects of island attributes and differential responses of species groups. *J. Biogeogr.* 39, 1124–1133. doi: 10.1111/j.1365-2699.2011.02676.x

Zeng, D., Swihart, R. K., Zhao, Y., Si, X., and Ding, P. (2019). Cascading effects of forested area and isolation on seed dispersal effectiveness of rodents on subtropical islands. *J. Ecol.* 107, 1506–1517. doi: 10.1111/1365-2745.13122

frontiers | Frontiers in Microbiology

TYPE Original Research
PUBLISHED 22 December 2022
DOI 10.3389/fmicb.2022.1042944

OPEN ACCESS

EDITED BY
Muhammad Saleem,
Alabama State University,
United States

REVIEWED BY
Qing Yao,
South China Agricultural University, China
Yanfen Zheng,
Tobacco Research Institute (CAAS), China
Xingang Zhou,
Northeast Agricultural University,
China

*CORRESPONDENCE
Hui Guo
guohuiya@126.com

†These authors have contributed equally to this work

SPECIALTY SECTION
This article was submitted to Microbe and Virus Interactions With Plants, a section of the journal Frontiers in Microbiology

RECEIVED 13 September 2022
ACCEPTED 28 November 2022
PUBLISHED 22 December 2022

CITATION
Li M, Song Z, Li Z, Qiao R, Zhang P, Ding C, Xie J, Chen Y and Guo H (2022) *Populus* root exudates are associated with rhizosphere microbial communities and symbiotic patterns.
Front. Microbiol. 13:1042944.
doi: 10.3389/fmicb.2022.1042944

Populus root exudates are associated with rhizosphere microbial communities and symbiotic patterns

Mengjie Li[1†], Zhen Song[2†], Zhanbiao Li[1], Rongye Qiao[1], Pingdong Zhang[1], Changjun Ding[3], Jianbo Xie[1], Yinglong Chen[4] and Hui Guo[1,5*]

[1]College of Biological Sciences and Technology, Beijing Forestry University, Beijing, China, [2]Institute of Environment and Sustainable Development in Agriculture, Chinese Academy of Agricultural Sciences, Beijing, China, [3]State Key Laboratory of Tree Genetics and Breeding, Key Laboratory of Tree Breeding and Cultivation of State Forestry Administration, Research Institute of Forestry, Chinese Academy of Forestry, Beijing, China, [4]UWA School of Agriculture and Environment, UWA Institute of Agriculture, Perth, WA, Australia, [5]National Engineering Research Center of Tree Breeding and Ecological Restoration, Beijing, China

Introduction: Microbial communities in the plant rhizosphere are critical for nutrient cycling and ecosystem stability. However, how root exudates and soil physicochemical characteristics affect microbial community composition in *Populus* rhizosphere is not well understood.

Methods: This study measured soil physiochemistry properties and root exudates in a representative forest consists of four *Populus* species. The composition of rhizosphere bacterial and fungal communities was determined by metabolomics and high-throughput sequencing.

Results: Luvangetin, salicylic acid, gentisic acid, oleuropein, strigol, chrysin, and linoleic acid were the differential root exudates extracted in the rhizosphere of four *Populus* species, which explained 48.40, 82.80, 48.73, and 59.64% of the variance for the dominant and key bacterial or fungal communities, respectively. Data showed that differential root exudates were the main drivers of the changes in the rhizosphere microbial communities. *Nitrosospira*, *Microvirga*, *Trichoderma*, *Cortinarius*, and *Beauveria* were the keystone taxa in the rhizosphere microbial communities, and are thus important for maintaining a stable *Populus* microbial rhizosphere. The differential root exudates had strong impact on key bacteria than dominant bacteria, key fungi, and dominant fungi. Moreover, strigol had positively effects with bacteria, whereas phenolic compounds and chrysin were negatively correlated with rhizosphere microorganisms. The assembly process of the community structure (keystone taxa and bacterial dominant taxa) was mostly determined by stochastic processes.

Discussion: This study showed the association of rhizosphere microorganisms (dominant and keystone taxa) with differential root exudates in the rhizosphere of *Populus* plants, and revealed the assembly process of the dominant and keystone taxa. It provides a theoretical basis for the identification and utilization of beneficial microorganisms in *Populus* rhizosphere.

KEYWORDS

dominant taxa, keystone taxa, differential root exudates, phenolic compounds, interactive effect

Introduction

Soil microorganisms play an important role in plant growth. Beneficial microbial population can effectively promote the nutrient utilization, growth, and development of plants, and improve plant stress resistance (Song et al., 2020; Gupta et al., 2021). Early studies revealed more abundant microbial density, species richness, and metabolic activity in the rhizosphere than in the bulk soil, which has been regarded as "rhizosphere effect" (Ma et al., 2021). Various rhizosphere microorganisms, such as *Pseudomonas*, *Streptomyces*, and *Fusarium*, are common in the plant habitat (Wu N. et al., 2021). Microbe-microbe interactions sustain ecological balance. Network comprises the various interactions, including complex positive (e.g., commensalism and mutualism) and negative (e.g., predation and competition) interactions (Jiang Y. et al., 2017). For example, reconstructing a consortium of *Chitinophaga* and *Flavobacterium* consistently suppresses root disease caused by *Rhizoctonia solani* (Carrión et al., 2019). *Pseudomonas* interacts with *Lysobacter* and *Bacillus* to colonize the plant rhizosphere, where they supply nutrients for plant growth (Jiang Y. et al., 2017). In-depth research of co-occurrence networks is essential to understand the underlying interactive effect of the microbial communities, and to identify possible keystone populations in the communities.

Microbial groups (dominant and key microorganisms) play essential roles in promoting the utilization of nutrient elements by plant. Rhizosphere microorganisms are affected by soil nutrients and pH, electrical conductivity (EC), and soil moisture (Jiang J. et al., 2017; Bahram et al., 2018; Bai et al., 2020; Zhou et al., 2020). The composition, diversity, and dominance of bacteria vary among soils with different pH and soil organic carbon content (Sui et al., 2021). Basal microbial respiration depends strongly on soil moisture because of the water's crucial role in substrate diffusion (Kundel et al., 2020); in turn, this directly affects the cycling of nutrients to microbes in forest ecosystems, including carbon cycling and nitrogen transformation (Wagg et al., 2014).

In addition to soil physicochemical properties, root exudates also affect the composition of the rhizosphere microbial communities. Root exudates account for 5–21% of the total photosynthetically fixed carbon, including organic acids, fatty acids, phenolics, amino acids, polysaccharides, and other secondary metabolites. The microbes make use of root exudates as nitrogen and carbon sources, and as signal stimuli (Ma et al., 2021). Phenolics are the most abundant plant metabolites and have been used as a slow carbon pool in soil dynamics models (Min et al., 2015). In *Populus*, the phenol salicylic acid acts as an inducible defense chemical that varies with tree genotype (Veach et al., 2019). Several microbial groups interact with salicylic acid, including Chloroflexi and the Basidiomycete family Hymenogastraceae (Veach et al., 2019). Strigol stimulates spore germination and hyphal growth of arbuscular mycorrhizal fungi (AMF). A positive correlation was detected between the capacity of a microbe to utilize compounds exuded by roots and its relative abundance therein (Rozpądek et al., 2018). During plant evolution, rhizosphere microorganisms affected root exudation. Beneficial microorganisms promote the accumulation of organic and amino acids, or produce peroxidase, which improves *Populus* plant growth under stress (Veach et al., 2020). Auxin produced by plant rhizosphere microbiota modulates flowering time and further stimulates exudation *via* a positive feedback mechanism (Lu et al., 2018). Therefore, root exudates affect the microbial community structure and microbial interactions. However, compared to the well-studied effect of nutrients on microorganisms, the role of the interaction between root metabolites and rhizosphere microorganisms in maintaining the stability of the ecosystem is not understood.

Populus is a genus of the Northern Hemisphere willow family (Salicaceae), and is the model organism for the study of woody perennials that may serve as an ideal model for understanding plant-microbe interactions (Feng et al., 2013). The growth and development of *Populus* are partially dependent on the functional microbial communities in the rhizosphere, which is the critical root-soil interface for plant growth (Song et al., 2020). Research on *Populus* has focused on plant aboveground traits, such as photosynthetic characteristics, carbon and nitrogen storage, and circulation, or focused on single factor on the belowground traits (Hogan et al., 2021; Wu X. et al., 2021; Wang et al., 2022). While research on the belowground traits, including dominant combined keystone taxa in the rhizosphere of *Populus* and the regulatory effects of differential root exudates on dominant and keystone taxa is lacking. Thus, this study used multi-omics technique (genomic-metabolomics) to explore microbial communities (dominant and key microorganisms) and differential root exudates in rhizosphere microecology of *Populus* in this ecological niche. The objectives of this study were to (i) identify the major factors influencing microbial communities; (ii) identify the key rhizosphere microorganisms in *Populus*; and (iii) examine the relationships between the exudates and rhizosphere microorganisms in the *Populus* microecosystem. The findings will lay a theoretical foundation for the screening and identification of key rhizosphere growth promoting microorganisms and the development and application of growth promoting agents for *Populus*.

Materials and methods

Study site and sample collection

The soil was sampled at the Research Base of Beijing Forestry University in Guanxian, Shandong Province, China (115°22′10.5″E, 36°30′56″N). The main cultivars of the experimental forests are *Populus tomentosa* (LM), *Populus nigra* (HY), *Populus alba* var. *pyramidalis* Bge. (XJ), and *Populus simonii* Carr (XY). Therefore, four *Populus* species (14 years old) were selected for study. They are widely distributed and cultivated in China and has been widely used in the numerous labs for diverse studies (Song et al., 2016, 2021; Ma et al., 2018; Sun et al., 2021). In this study, soil samples were randomly collected using the

five-point sampling method with three replicates, five-point sampling (1 m × 1 m) was carried out using the diagonal principle. Plant fine roots (< 2 mm) were collected from each point within the root zone at a depth of 10–30 cm. The root samples were divided into two parts. For one part, the root-attached soil was shake off as bulk soils, and the soils tightly adhering to the roots were collected with a hairbrush as rhizosphere soil (Edwards et al., 2015; Zhu et al., 2022). Then, the soil sample was stored at 4°C until the physicochemical parameters were measured. For the other part, the samples were washed in 10 mM PBS buffer for 10 min on a shaking platform (120 rpm) and then transferred to clean 50 ml plastic tubes. Sterile tweezers were used to remove roots from the 50 ml plastic tubes, the soil particles directly centrifuged (6,000× *g*, 4°C, 20 min) from the remaining suspension represented the rhizosphere samples (Beckers et al., 2016, 2017; Qin et al., 2018). And then the samples were stored at −20°C for later DNA extraction.

Soil physicochemical parameters

The soil pH and the electric conductivity (EC) value were tested using a glass electrode meter in a suspension of 1 g of soil in 5 ml of distilled water by pH meter and conductivity meter. Moisture content was determined by the oven dry-weight method. Available phosphorus (AP), available potassium (AK), available nitrogen (AN), and organic matter (OM) were separately measured by the molybdenum blue, flame photometry, potassium persulfate oxidation, and dichromate oxidation method, respectively (Lu, 1999). Each measurement had three replicates. Furthermore, Tukey's test was performed to evaluate the distribution of the soil physicochemical parameters. A p-value <0.05 was considered significant.

Liquid chromatography with tandem mass spectrometry untargeted metabolomic analysis

After homogenization, a 1 g soil sample was put in a 5 ml Eppendorf tube, to which 3 ml of methanol was then added. The mixture was sonicated for 30 min in an ultrasonic bath. The supernatant was collected by centrifugation. These steps were repeated twice. Freeze-dried samples from exudates were resuspended in 150 µl methanol and then sonicated for 5 min in an ultrasonic bath. An aliquot of the supernatant was passed through a 0.22-µm (micropore) organic filter membrane and transferred to vials for subsequent analysis. The supernatant underwent high-performance liquid chromatography/triple time-of-flight mass spectrometry (Sciex TripleTOF 5600+, Framingham, MA, United States) analysis; an electron spray ionization (ESI) source was equipped. Separation was achieved on an HSS T3 column (100 mm × 2.1 mm, 1.7 µm; Waters, Milford, MA, United States). A gradient elution conditions were presented in Supplementary Table S1. The mass spectrometer was operated in both negative and positive ionization modes, and full scan mass spectra were recorded across the range of m/z 50–1,200. The curtain gas, gas 1, and gas 2 of the mass spectrometer were set to 35, 60, and 60 psi, respectively. The ESI temperature and spray voltage were 550°C and 4,500 V (negative)/5,500 V (positive), respectively. The differential metabolites with significant differences between any two of the four *Populus* samples were screened and identified by plant exudates databases (KEGG, PlantCyc, GMD; Wanichthanarak et al., 2020; Hawkins et al., 2021; Duan et al., 2022).

DNA extraction and high-throughput sequencing

Total microbial genomic DNA was extracted from 0.1 g of soil sample using the DNeasy PowerSoil DNA Isolation kit (Qiagen, Hilden, Germany). The V3–V4 regions of the bacterial 16S rRNA genes for the entire bacterial communities were amplified using the 338F/806R primers and the following temperature cycling conditions described by literature (Song et al., 2020). Fungal internal transcribed spacer (ITS1) genes were amplified using the ITS1F and ITS2R barcode primers, with the amplification program according to the reference description (Zhou et al., 2021).

The purified PCR amplified products were paired-end sequenced (2 × 300) on the Illumina MiSeq platform (Illumina, San Diego, CA, United States). The raw data were first screened and sequences were removed from consideration if they were shorter than 120 bp, had a low quality score (≤20), contained ambiguous bases or did not exactly match to primer sequences and barcode tags, and separated using the sample-specific barcode sequences. Qualified reads were clustered into operational taxonomic units (OTUs) at a similarity level of 97% use Uparse algorithm of Vsearch (v2.7.1) software. The Ribosomal Database Project (RDP) Classifier tool was used to classify all sequences (16S rRNA genes) into different taxonomic groups against SILVA128 database. The BLAST tool was used to classify all sequences (ITS1 genes) into different taxonomic groups against Unite database. Sequences belonging to archaea, mitochondria, and chloroplasts were also removed. To avoid potential bias caused by differences in sequencing depth, the number of sequences in each sample was rarefied to 56,232 (16S rRNA genes) and 29,376 (ITS1 genes) sequences per sample (Zhou et al., 2022). The raw sequencing data were deposited in the Sequence Read Archive at NCBI with the accession number PRJNA888251.

Statistical analysis

SPSS software (var. 17.0) was used for the data analysis. One-way ANOVA was used to detect differences among samples. Tukey's test was performed to evaluate the distribution of the data. A value of $p < 0.05$ was considered significant. Metabolites with

value of $p < 0.05$ and fold change >1.20 were considered as differential root exudates by SIMCA software (14.1), the fold change was compared with any two of four *Populus* species in pairs. Redundancy analysis (RDA) was performed using Canoco (v.5.0). A variation partitioning analysis (VPA) was applied to quantify the contributions of the environmental variables to the microbial communities, and the correlations between the microbes and metabolites, using R software 3.6.3. Interactions between microbial composition were studied through network analysis. The Gephi software 9.2 was used to visualize the network. The high values of topological features (degree, betweenness, and closeness centrality) suggest a core position of a node in the network (Jiao et al., 2017, 2020), and the high values of the above three parameters can jointly reflect the importance of key microbial flora (nodes in the network; Xing et al., 2021). Therefore, we choose high values of the topological parameters (degree, betweenness, and closeness centrality) as keystone taxa in this study.

The normalized stochasticity ratio (NST) was quantitated with the "NST" R package, which is assembly with 50% as the boundary point between more deterministic (NST < 50%) and more stochastic (NST > 50%) assembly (Ning et al., 2019). Levin's niche breadth values of the dominant and keystone taxa were performed to illustrate community sensitivity to the environment, using the beta diversity "niche width" function within the R package "spaa" (Levins, 1968).

Results

Soil physicochemical characteristics and composition of root exudates

Most soil properties, including pH, moisture, OM, AN, AP, and AK, differed among the four *Populus* species (Table 1). The pH and EC values among HY, LM, XJ, and XY were 8.03–8.13 and 117.10–124.57 μs/cm, respectively. The moisture values of HY, LM, XJ, and XY were 2.00, 4.00, 4.00, and 3.00%, respectively. The average OM content was in the following order: LM (11.19 g/kg) > HY (9.98 g/kg) > XJ (7.74 g/kg) > XY (7.43 g/kg). The average AP contents of HY, LM, XJ, and XY were 4.34, 32.83, 11.50, and 2.90 mg/kg, respectively. The mean AN value were LM (38.93 mg/kg) > XJ (35.33 mg/kg) > HY (33.92 mg/kg) > XY (28.09 mg/kg). The AK values among HY, LM, XJ, and XY were 9.67, 10.50, 26.48, and 10.87 mg/kg, respectively. OM and AN content were significantly higher in LM than in the others. XJ had the highest AK content among the four *Populus* cultivars.

TABLE 1 Soil properties in the rhizosphere of four *Populus* species.

Soil properties	LM	XJ	HY	XY
pH	8.12 ± 0.04^{a}	8.03 ± 0.03^{b}	8.13 ± 0.02^{a}	8.06 ± 0.03^{ab}
Moisture	$4.00\% \pm 0.00^{a}$	$4.00\% \pm 0.00^{a}$	$2.00\% \pm 0.00^{b}$	$3.00\% \pm 0.00^{a}$
EC(μs/cm)	121.80 ± 0.70^{a}	124.57 ± 0.74^{a}	119.93 ± 0.32^{a}	117.10 ± 6.90^{a}
OM(g/kg)	11.19 ± 0.40^{a}	7.74 ± 0.17^{c}	9.98 ± 0.08^{b}	7.43 ± 0.34^{c}
AP(mg/kg)	32.83 ± 0.02^{a}	11.50 ± 0.03^{b}	4.34 ± 0.00^{c}	2.90 ± 0.01^{c}
AK(mg/kg)	10.50 ± 0.16^{c}	26.48 ± 0.06^{a}	9.67 ± 0.15^{d}	10.87 ± 0.12^{b}
AN(mg/kg)	38.93 ± 0.20^{a}	35.33 ± 0.91^{b}	33.92 ± 1.38^{b}	28.09 ± 1.07^{c}

Different lower letters mean significant differences ($p < 0.05$) between the properties of different samples. *Populus* species: LM (*P. tomentosa*), XJ (*P. alba* var. pyramidalis Bge.), HY (*P. nigra*), and XY (*P. simonii* Carr).

Thirty-nine differential metabolites with significant differences between any two of the four samples (LM, HY, XY, and XJ) were obtained ($p < 0.05$, fold change > 1.20). These metabolites predominantly consisted of fatty acyls, prenol lipids, carboxylic acids and derivatives, benzene and substituted derivatives, organooxygen compounds, and flavonoids. Seven plant root exudates were then identified from them, including coumarins (luvangetin), phenolic compounds (salicylic acid, gentisic acid, and oleuropein), a phytohormone (strigol), a flavonoid compound (chrysin), and fatty acids (linoleic acid; Table 2).

XY had higher contents of chrysin, luvangetin, and gentisic acid compared to the other *Populus* cultivars, and the contents of luvangetin and gentisic acid in XY were 5.67 and 11.88 times higher than in XJ. Relatively high oleuropein content was detected in XJ. The salicylic acid content in HY was 1.37–2.15 times higher than that in LM, XJ, and XY. In this study, LM had the highest strigol content (approximately 168-fold change).

Microbial diversity analysis

The Chao1 and Shannon diversity indices were used to measure the microbial alpha-diversity of each soil sample; the highest bacterial Chao1 and Shannon indices were observed in the LM sample, followed by the HY and XJ samples; the XY sample had the lowest index values (Figure 1A), showing that the sum of bacterial species was the highest in the LM rhizosphere sample. Among the rhizosphere fungal community samples (Figure 1B), the HY cultivar harbored more diverse communities than the LM, XJ, and XY cultivars. Bray-Curtis analysis showed that bacterial and fungal diversity differed among the four *Populus* cultivars (Figures 1C,D).

Microbial community composition

At the bacterial level, the communities were composed of the top 15 phyla and genera (dominant taxa) in each sample (Figure 2). Proteobacteria was the dominant phylum (25–28%), followed by Actinobacteria (18–21%), Acidobacteria (14–21%), Gemmatimonadetes (7–11%), Bacteroidetes (4–7%), and Chloroflexi (6–8%). At the genus level, soil beneficial bacteria included *RB41* and *H16*, with mean relative abundances of 2.9–4.9 and 1.3–1.9%, respectively, followed by *Sphingomonas, Gaiella, Haliangium*, and *Bacillus*.

At the fungal level, the communities were composed of the top 15 phyla and 10 genera (dominant taxa) in each sample

TABLE 2 The peak area of differential root exudates in the rhizosphere of four *Populus* species.

Differential root exudates	Mean value in each type of *Populus*				Pair-wise test (*P*-value)					
	LM	XJ	HY	XY	LM vs. XJ	LM vs. HY	LM vs. XY	XJ vs. HY	XJ vs. XY	HY vs. XY
Chrysin	0.000 ± 0.000	1.250 ± 0.170	29.348 ± 20.686	362.294 ± 176.755	0.041	0.028	0.001	0.045	0	0.001
Luvangetin	8463.262 ± 791.139	4171.554 ± 161.516	11513.344 ± 750.233	23666.135 ± 1231.016	0	0.001	0	0	0	0
Oleuropein	17.356 ± 5.709	435.355 ± 22.632	79.344 ± 5.573	104.369 ± 9.892	0	0	0	0	0	0.011
Salicylic acid	213.105 ± 11.562	275.985 ± 40.937	458.952 ± 38.372	336.125 ± 1.119	0.006	0	0	0	0.013	0.004
Strigol	261.810 ± 26.201	1.558 ± 0.404	7.565 ± 0.481	3.890 ± 0.782	0	0	0	0	0.01	0
Gentisic acid	59.848 ± 2.256	23.370 ± 3.041	155.988 ± 24.740	277.597 ± 77.996	0	0.001	0	0	0	0.02
Linoleic acid	77.894 ± 10.874	29.017 ± 0.545	21.263 ± 2.651	14.891 ± 2.451	0	0	0	0.004	0	0.019

$p < 0.05$, fold change > 1.20; *Populus* species: LM (*P. tomentosa*), XJ (*P. alba* var. pyramidalis Bge.), HY (*P. nigra*), and XY (*P. simonii* Carr).

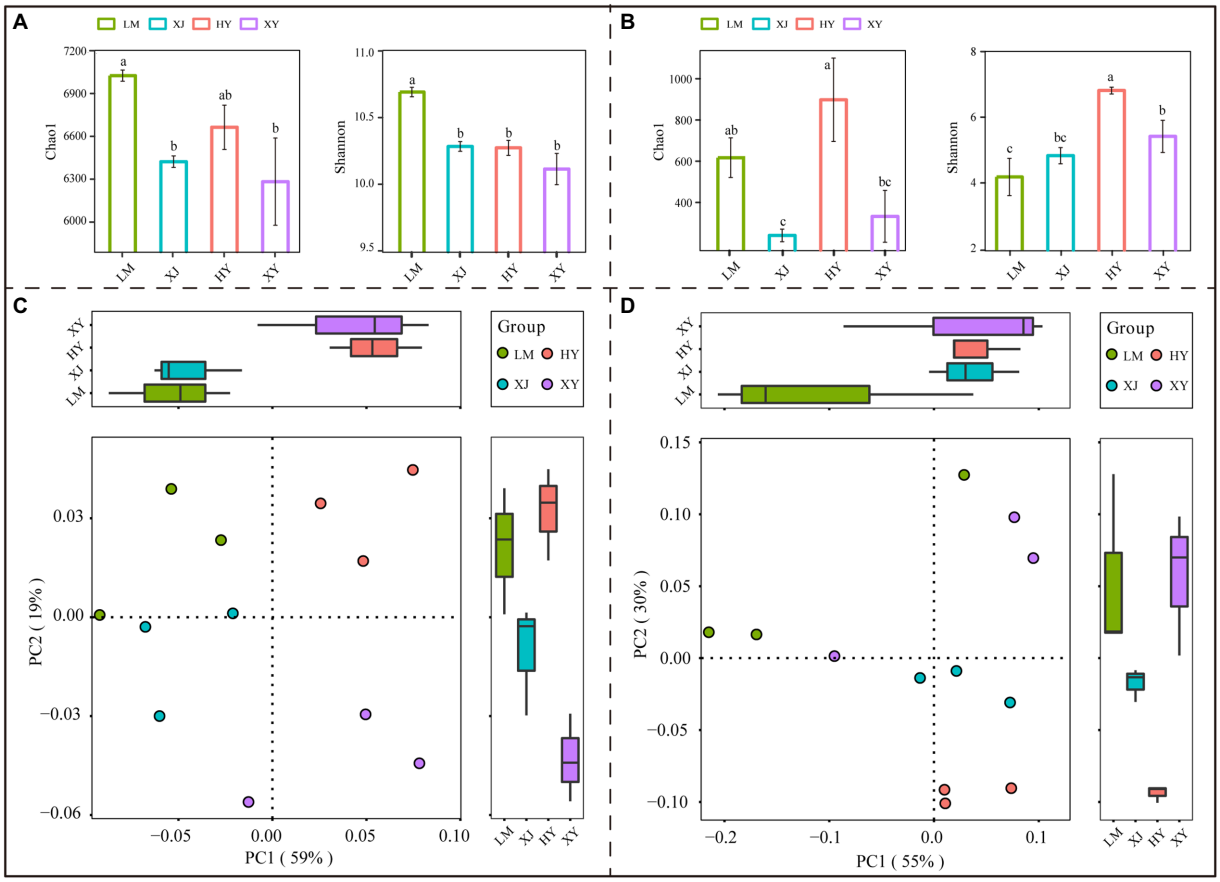

FIGURE 1
Chao1 index, Shannon index, and principal-coordinate analysis (PCoA) of bacteria and fungi from four *Populus* species. **(A)** The bacterial alpha diversity. **(B)** The fungal alpha diversity. **(C)** The bacterial principal component analysis. **(D)** The fungal principal component analysis. Different lower letters mean significant differences ($p < 0.05$). The same lowercase letters mean that the difference is not significant in four *Populus* species ($p > 0.05$).

(Figure 2). Ascomycota, Basidiomycota, and Mortierellomycota were the dominant fungal phyla, accounting for 50–63, 16–34, and 4–16%, respectively. At the genus level, the fungal communities were primarily composed of *Geopora*, *Chrysosporium*, *Mortierella*, and *Tomentella*. *Coprinopsis* was the most abundant fungal genus in LM. *Mortierella* dominated, with an abundance of 30–40% in HY and XY.

Co-occurrence network of rhizosphere microorganisms

The bacterial co-occurrence network composed of 132 nodes (genus) and 103 edges (links) was shown in Figure 3, which included 82 (79.61%) positive and 21 (20.39%) negative interactions. Positive relationships between microbial populations

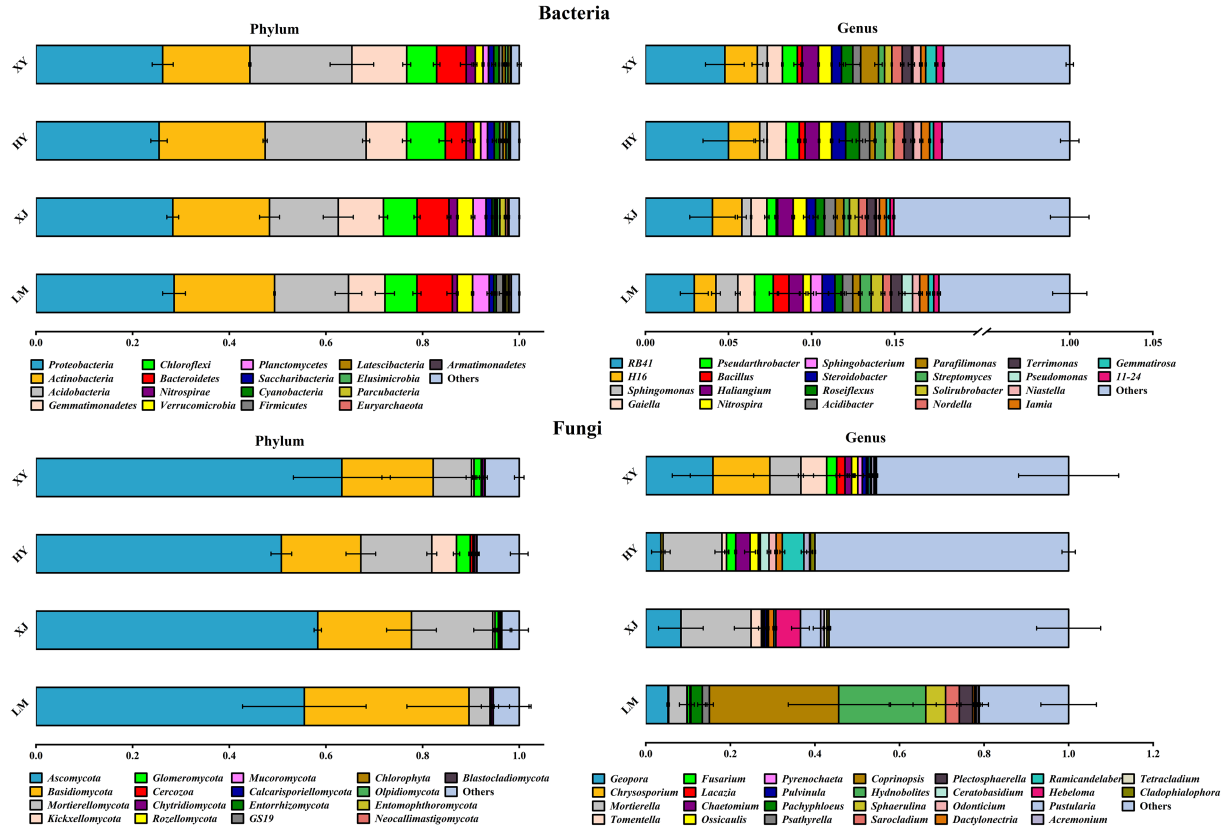

FIGURE 2
Rhizosphere microbial community compositions of four *Populus* species.

show the occurrence of a mutualistic interaction, while negative relationships indicate competition for hosts or a predacious relationship between microorganisms (Chow et al., 2014; Jiang J. et al., 2017). These interactions are strongly associated with important soil processes. The network had a modularity index of 0.94, the modularity index exceeded 0.4, suggesting a modular structure of the micro-network (Liu et al., 2020; Ye et al., 2020). Keystone taxa are the taxa which have major influence on microbiome composition and function at a particular space or time (Banerjee et al., 2018). The high values of the topological parameters (degree, betweenness, and closeness centrality) in the network were considered the keystone taxa (Jiao et al., 2017, 2020; Xing et al., 2021). The key bacteria were *Flavihumibacter*, *Blastocatella*, *Adhaeribacter*, *Microvirga*, *Agromyces*, and *Nitrosospira*. *Flavihumibacter* was positively correlated with *Microvirga*, indicating commensalism or a mutualistic relationship. The changes directly linked with the nodes (*Nitrosospira*) were all positive interactions.

The fungal co-occurrence network composed of 182 genera and 232 links was shown in Figure 3, which included 215 (92.67%) positive and 17 (7.33%) negative interactions. The network had a diameter of 13, average clustering coefficient of 0.33, average path length of 4.32, and modularity index of 0.88. The key microorganisms were mainly *Myrmecridium*, *Trichomerium*, *Absidia*, *Neopaxillus*, *Trichoderma, Pluteus*, *Periconia*, *Cortinarius*, *Beauveria*, *Talaromyces*, and *Arnium*. All of these taxa positively interacted with the *Beauveria* nodes. Eight genera, including *Apodus*, *Laetisaria*, *Racocetra*, *Funneliformis*, *Erysiphe*, *Dentiscutata*, *Colacogloea*, and *Papiliotrema*, were positively correlated with the keystone taxa *Cortinarius*, indicating their similarity or cooperation in ecological functions. There were two positive edges and one negative edge directly associated with *Trichoderma* hubs, including *Lophiotrema*, *Hebeloma*, and *Phakopsora*. *Trichoderma* was negatively correlated with *Fusarium* indirectly. Furthermore, key microorganisms generally have lower relative abundances than dominant microorganisms (Supplementary Table S1).

Relationship between the microbial communities, soil properties, and differential root exudates

Redundancy analysis and VPA were performed to study the relationships between the environmental factors and abundance of microbes (dominant taxa and keystone taxa). The RDA results shown in Figure 4A (dominant bacteria) indicated that OM, AN, AP, and moisture were positively correlated with the abundance

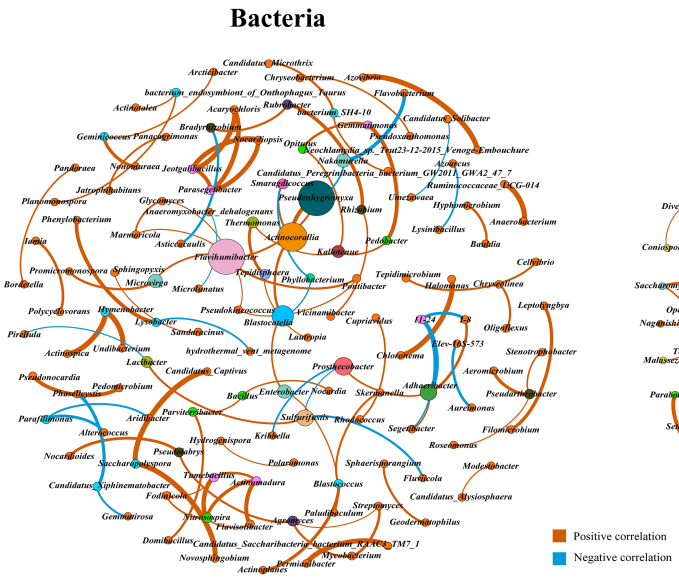

FIGURE 3
Co-occurrence networks of bacterial and fungal communities based on Spearman correlation.

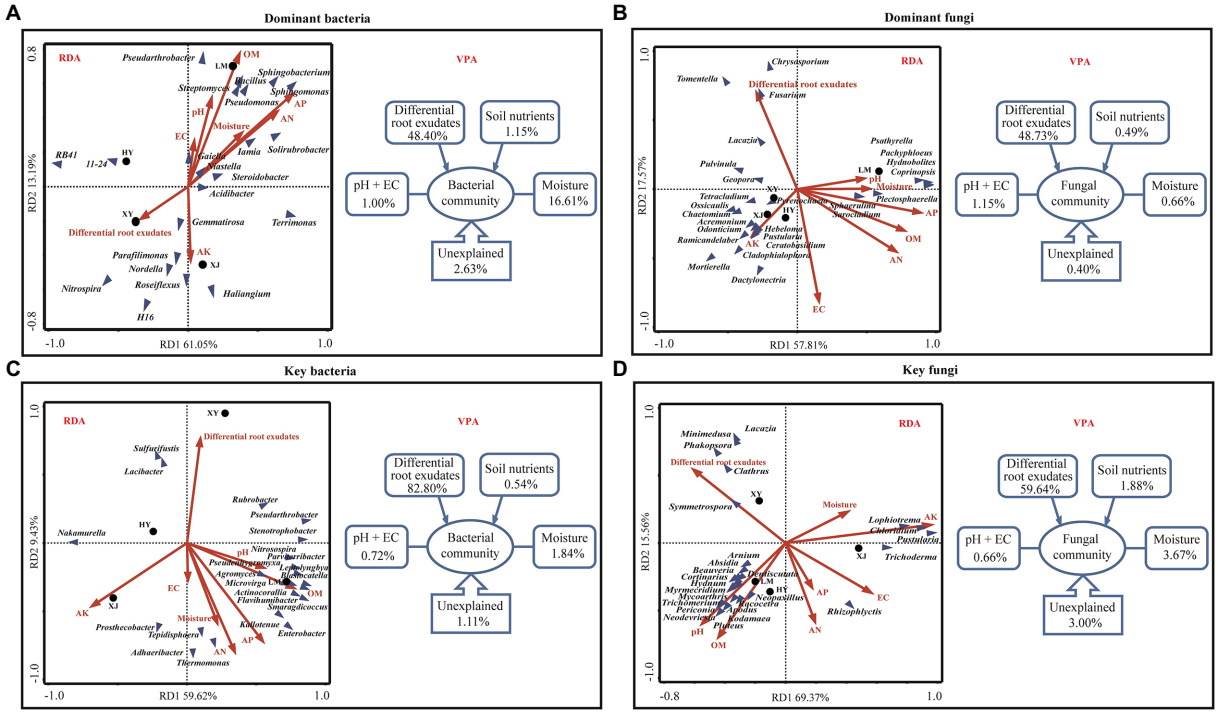

FIGURE 4
Redundancy analysis and variation partitioning analysis of microorganisms and soil properties. **(A)** Dominant bacteria and soil properties. **(B)** Dominant fungi and soil properties. **(C)** Key bacteria and soil properties. **(D)** Key fungi and soil properties. Red arrow: soil properties, blue triangle: microorganisms (In RDA).

of *Sphingomonas*, *Streptomyces*, *Bacillus*, and *Pseudomonas*, suggesting that bacteria were favored in rich nutritional conditions where they play important roles in soil C-, N- and P-cycling. AK and the differential root exudates negatively affected bacterial community composition. AP and AK had contrasting effects on the rhizosphere microbial population, indicating that they play a crucial role in the distribution of the microbial communities. The contribution of environmental factors was further quantified by

VPA, which showed that differential root exudates explained 48.40%, soil nutrients explained 1.15%, pH and EC explained 1.00%, and moisture explained 16.61% of the dominant bacterial variance. The RDA results for dominant fungi (Figure 4B) showed that *Hebeloma* and *Mortierella* were positively correlated with AK, while the most dominant fungi had a negative association with soil nutrients (AP, AN, and OM) and differential root exudates, suggesting that fungi may be more suitable for oligotrophic environments. Differential root exudates had negatively correlation with most of the fungi (Figure 4B). VPA revealed that the differential root exudates explained 48.73% of the variance, soil nutrients explained 0.49%, pH and EC explained 1.15%, and moisture explained 0.66%.

The RDA results shown in Figures 4C,D indicated that OM and pH were positively correlated with the great majority of key microorganisms mainly include *Microvirga*, *Agromyces*, *Blastocatella*, *Apodus*, *Pluteus*, and *Trichomerium*, while the most key microorganisms had a negative association with AK and differential root exudates. VPA revealed that the differential root exudates explained 82.80% of the variance for key bacteria and 59.64% of the variance for key fungi, soil nutrients explained 0.54% (key bacteria) and 1.88% (key fungi), pH and EC explained 0.72% (key bacteria) and 0.66% (key fungi), and moisture explained 1.84% (key bacteria) and 3.67% (key fungi). Differential root exudates explained more of the variance in the bacterial and fungal communities than environmental factors, such as pH, EC, moisture, and soil nutrients. This finding indicates that the differential root exudates played the dominant role in shaping the *Populus* rhizosphere microbial communities and the differential root exudates had more effect on keystone taxa than dominant taxa.

Correlations between the differential root exudates and microbial communities and microbial community assembly processes

Variation partitioning analysis showed that differential root exudates had largest contributions to the changes in the rhizosphere microbial communities (Figure 4), we further focused on analyzing the relationships between differential root exudates and microbes (dominant and key microorganisms) in the rhizosphere by Spearman's correlation analysis. The correlation analysis revealed that strigol was positively correlated with the dominant bacteria *Bacillus* (Figure 5). Phenolic compounds (oleuropein, gentisic acid, and salicylic acid) were negatively correlated with two dominant taxa (*Bacillus* and *Hebeloma*) and positively associated with two genera (*Ossicaulis* and *Ramicandelaber*). Luvangetin showed negatively relationship with *Hebeloma*. The abundances of dominant fungi (*Pachyphloeus* and *Coprinopsis*) had negatively relationship with chrysin and positively relationship with linoleic acid.

The correlation analysis indicated that strigol positively correlated with the abundances of the key bacteria *Microviga*, *Pseudenhygromyxa*, *Flavihumibacter*, and *Actinocorallia*. Oleuropein and other phenolic compounds had significantly negative correlation with the key microorganisms. Negative correlations were detected between the phenolics and abundances of bacteria (*Flavihumibacter*, *Pseudenhygromyxa*, *Actinocorallia*, *Microviga*, *Kallotenue,* and *Thermomonas*) and fungi (*Trichoderma*). Gentisic acid (a phenolic compound) was negatively correlated with *Trichoderma*. Chrysin (flavonoid compounds) was negatively correlated with three keystone taxa (*Kallotenue*, *Thermomonas,* and *Rhizophlyctis*). *Kallotenue* was positively associated with linoleic acid. In general, strigol was positively correlated with key bacteria, whereas phenolic compounds showed a negative correlation, which indicated the response of keystone taxa and dominant taxa were different to the same variables.

To study more in depth the differences in community structure, we further calculated the community-level habitat niche breadths (Bcom). Bacterial keystone taxa exhibited higher Bcom value than dominant taxa, fungal dominant taxa showed higher Bcom value than keystone taxa. Subsequently, we further employed NST to elucidate the assembly processes. The NST value was above the 50% boundary point accounted for both dominant taxa and keystone taxa (for 90.91%), suggesting that stochastic process played a more important role than deterministic process during the bacterial assembly. Additionally, NST value was observed in bacterial keystone communities with an average of 81.69% than that in bacterial dominant communities with an average of 79.43%. The dominant fungi accounted for 42.43% and key fungi accounted for 68.18% in the NST values above 50%, implying that fungal dominant taxa were dominated by deterministic process.

Discussion

Rhizosphere characteristics of *Populus*

Many studies have suggested that soil properties are the basic factors affecting the soil microbial communities (Li X. et al., 2021). The basic metabolism of microorganisms depends strongly on soil moisture (Kundel et al., 2020; Su et al., 2020). Soil OM is the main substrate and energy source for soil microbes (Wang J. et al., 2021). A previous report showed that AK alters the microbial communities and improves soil metabolic activities and functional diversity (Li H. et al., 2021). In the present study, we found that LM and XJ had high trophic level soils (Table 1).

Moreover, root exudates also affect the formation and structure of rhizosphere microbiome (Czarnota et al., 2003; Vives-Peris et al., 2020). Here we found seven differential root exudates. Oleuropein and gentisic acid are phenolic compounds, and gentisic acid is one of the most common aromatic acids in plants (Zhang et al., 2017; Catinella et al., 2022). Salicylic acid content

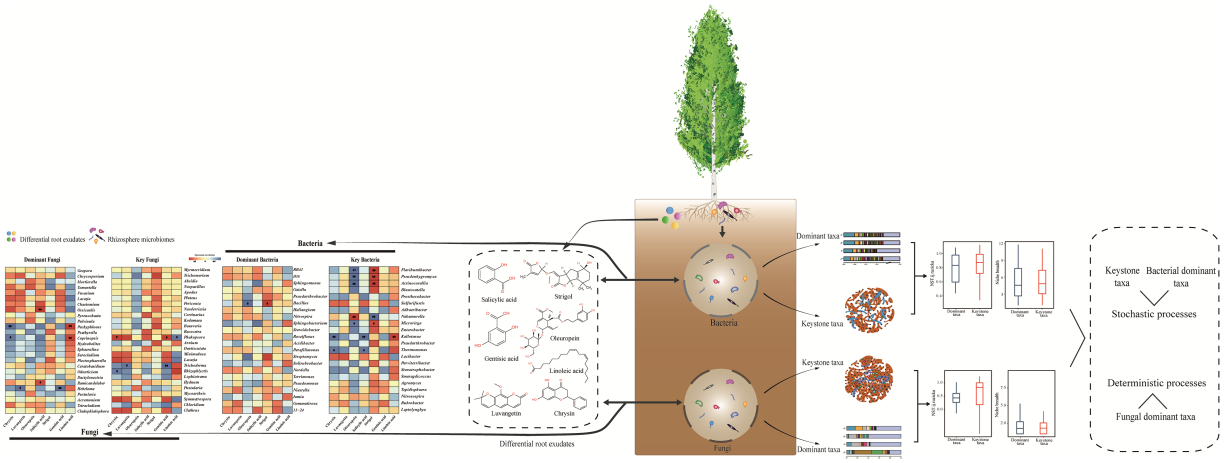

FIGURE 5
Diagram of microbial assembly process. Significance of each exudate: *$p \leq 0.05$. **$p \leq 0.01$.

can vary with genotype and the developmental stage of the plants (Veach et al., 2019). Salicylic acid regulates plant growth and development that as a common plant phenolic compound in Salicaceae, and acts as an inducible defense chemical expressed in response to a pathogen. However, some researches have showed that salicylic acid reduces soil microbial diversity and significantly affects the carbon metabolism capacity and genetic structure of microbial communities. Strigol is a carotenoid-derived signaling molecule that communicates with parasites in the rhizosphere, and regulates plant growth and development by crosstalk with other hormones (Wakabayashi et al., 2021). Strigol is chemically unstable and decomposes rapidly in the soil, but exudates can protect strigol from rapid degradation (Yoneyama, 2020). The linoleic acid level was higher in LM than in the others significantly. Linoleic acid is a major component of biomembranes; it functions as a signaling molecule and directly participates in development (Huang et al., 2021). The changes of some specific compounds in root exudates can affect the dynamics of soil microbial communities (Zhao et al., 2021).

Dominant and keystone taxa on *Populus* rhizosphere

We revealed that the dominant phyla such as Proteobacteria, Actinobacteria, Acidobacteria, Ascomycota, and Basidiomycota. The ratio of Proteobacteria to Acidobacteria can be used to measure the level of soil nutrition, favoring Proteobacteria in rich soils and Acidobacteria in poor soils (Castro et al., 2010; Gottel et al., 2011). In our research, LM and XJ had higher ratios than HY and XY. Bacteroidetes is usually not a dominant bacterial phylum in soil (Song et al., 2020), but was highly abundant in the rhizosphere. *Sphingomonas*, a Gram-negative bacterium and rhizosphere biomarker that grows under aerobic conditions. The biomarker results indicated that the *Populus* rhizosphere environment can provide sufficient air and organic nutrient conditions for these bacteria (Li J. et al., 2020). *Mortierella* is a plant growth-promoting fungi that enhances plant phosphate nutrition (Li F. et al., 2020). *Geopora* species are common and important ectomycorrhizal fungi that often seen in woody plants rhizosphere, where they can increase the utilization of water and nutrients by hosts. These taxa constituted a high proportion of the microbial communities in the different *Populus* cultivars, and play a notable role in promoting plant growth and degrading refractory pollutants, and protect plants from harmful pathogens (Patterson et al., 2019).

Dominant and key populations affect the composition and structure of the entire microbial communities (Berry and Widder, 2014). The entire communities will crumble without key species (Floc'H et al., 2020); thus, apart from those dominant taxa, identifying the keystone taxa of the plant rhizosphere is essential to optimize plant growth. Modularity, which represents microbial interactions, is vital for microbial community stability and resilience due to the resource allocation, habitat heterogeneity, phylogeny, or niche overlap (Tya et al., 2021). In this research, the modularity index exceeded 0.4, suggesting a modular structure of the real-world network (Liu et al., 2020; Ye et al., 2020). The co-occurrence network composed of 22 bacterial keystone taxa and 26 fungal keystone taxa. The genus *Microvirga* is very common in nature. *Microvirga* sp. participates in the soil nitrogen cycle and provides nitrogen for plants and other microorganisms (Amin et al., 2016; Veyisoglu et al., 2016; Longa et al., 2017). The key genus *Adhaeribacter* exhibits urease and alkaline phosphomonoesterase activities, which help maintain available N and P content in the soil and regulate growth in environments polluted with heavy metals (Lin et al., 2020). *Nitrosospira* are ammonia- and nitrite-oxidizing bacteria, related to the nitrogen metabolic processes that make nutrients available to other community members. Numerous studies have revealed that nitrogen cycling taxa play a key role in a variety of ecosystems

(Rädecker et al., 2015; Che et al., 2018; Dai et al., 2020; Ramond et al., 2022). Therefore, the ecological role and mechanism of nitrogen cycling-related microorganisms in plant growth merit further systematic study.

Beauveria bassiana is widely used as an effective strain for biological control of plant diseases. The BbAFP1 chitinase secreted by *B. bassiana* has good antifungal activity in plants, and its gene expression in Chinese white poplar can well reduce the incidence of diseases caused by *Cytospora chrysosperma* (Tong et al., 2021). Members of the ectomycorrhizal genus *Cortinarius* are often dominant in fungal communities from boreal soils. Some members of this genus may be directly involved in the degradation of soil OM in the humus layers of northern forest ecosystems. This is an active mycorrhizal community with high mycelial turnover rates that successively depletes N humus and minimizes the long-term accumulation of humus layers, which were very important in maintaining the balance of the ecosystem (Bödeker et al., 2014; Clemmensen et al., 2015). The genus *Trichoderma*, a well-known plant growth-promoting microorganism and biological control agent (Fernández-González et al., 2020), activates the plant immune system through induced systemic resistance, which is a priming defense mechanism against pathogens (Gupta et al., 2021). Xylanase secreted by *Trichoderma* promotes systemic resistance of host plants against pathogens, suggesting that *Trichoderma* may have biocontrol abilities in the *Populus* rhizosphere (Guo et al., 2021). Furthermore, key microorganisms generally have lower relative abundances than dominant microorganisms, indicating that species interactions may played a more important role in *Populus* growth than that of species abundance.

Effects of differential root exudates on rhizosphere microbial communities

As shown in RDA, environmental factors such as AN, OM, and pH influence microbial communities. Here, we found by VPA that the differential root exudates explained more of the variability in shaping the *Populus* rhizosphere microbiome than other environmental factors. This result was in agreement with previous reports that root exudates significantly regulate the soil microbial community structure (Gu et al., 2020). We further revealed that the correlations of the differential root exudates and microbiome (dominant taxa and keystone taxa). Our results showed that strigol and phenolic compounds were key factors for rhizosphere microbial communities. Strigol was reported to regulate root architecture and hyphal branching of AMF (Liu et al., 2018). *Bacillus* plays an important mediating role in mycorrhizal symbiosis, which improves the growth and nutrient uptake of plants (Wang Y. et al., 2021; Zhang et al., 2021). Therefore, the positive correlation between strigol and *Bacillus* may have combined action on the development of mycorrhiza, which could promote the growth of *Populus*. Phenolic compounds showed a negative correlation with microbiome, probably because these chemicals are relatively resistant to decomposition by microorganisms and inhibit microbial activity (Gu et al., 2020). Furthermore, phenolic compounds can impair membrane structure and function, or increase the permeability of cell membrane to cause the leakage of cell contents (Mattos et al., 2017). It is reported that salicylic acid modulates root colonization by *Trichoderma*, as exogenous inoculation decreases the multiplication of the fungus on roots. Phenolic compounds extracted from rice straw were also reported to have significant inhibition on the growth of *T. reesei* (Zheng et al., 2017; Macías-Rodríguez et al., 2020). Moreover, the differential root exudates affected the key bacteria more than fungi and the dominant bacteria, and that the keystone taxa maintained the microbial ecology critically. Therefore, the further study on the relationship between specific microorganisms and rhizosphere exudates will provide a theoretical basis for reducing the adverse effects and promoting plant growth.

Differences in community assembly between keystone and dominant taxa

In the present study, we demonstrated that the niche-based stochastic processes determine the assembly of bacterial communities and fungal keystone taxa. Keystone taxa showed higher stochasticity comared dominant taxa, thus demonstrating keystone taxa make more contributions to the stable of community structure under environmental disturbances. In addition, a finding is that the NST value of bacteria was higher than that of fungi, suggesting that stochastic processes contribute more to bacterial communities than to fungal communities. This observation could be due to the size-plasticity hypothesis that smaller organisms (bacteria) are less environment filtered than larger organisms (Liu et al., 2015). Subsequently, we quantified the Bcom value. Bacterial keystone taxa had a higher Bcom value than dominant, which was consistent with previous studies, a previous study reported that organisms with Bcom value might have greater metabolic plasticity and be less influenced by deterministic processes (Pandit et al., 2009). The Bcom value of fungal keystone taxa was lower than that of dominant.

In a word, VPA indicated that the differential root exudates explained a larger proportion of keystone taxa (82.8 and 59.64%) than dominant taxa (48.4 and 48.73%), while NST demonstrated keystone taxa showed higher stochasticity compared dominant taxa. These contrasting results may be due to the unmeasured environmental variables as mentioned above. Thus, more comprehensive data (taxonomic, phylogenetic, environmental, and spatial) and more dimensions should be considered when relating the relative influence of ecological processes to microbial community assembly.

Conclusion

In this study, differential root exudates from four *Populus* cultivars, including luvangetin, salicylic acid, gentisic acid, oleuropein, strigol, chrysin, and linoleic acid, were the major interfering factor of microbial communities' variation. Network

analysis revealed that keystone taxa interactions were very important in maintaining the stability of the *Populus* rhizosphere microorganisms than species abundance. Furthermore, correlation analysis revealed that strigol had positively effects with bacteria, the phenolic compounds and chrysin were negatively correlated with the rhizosphere microorganisms. In general, differential root exudates showed significant relationship with the key bacterial taxa. Community structure (keystone taxa and bacterial dominant taxa) was mostly determined by stochastic processes, keystone taxa showed higher stochasticity compared dominant taxa, thus demonstrating keystone taxa make more contributions to the stable of community structure under environmental disturbances. The results provided a basis for further identification and utilization of important microbes in *Populus* rhizosphere.

Data availability statement

The data presented in the study are deposited in the Sequence Read Archive repository, accession number PRJNA888251, https://www.ncbi.nlm.nih.gov/bioproject/PRJNA888251.

Author contributions

ML and ZS: conceptualization, methodology, investigation, writing—original draft, and writing—review and editing. ZL, PZ, and JX: software and formal analysis. RQ: validation and resources. CD: validation and data curation. HG: conceptualization, methodology, writing—review and editing, supervision, and funding acquisition. All authors contributed to the article and approved the submitted version.

Funding

This work was funded by National Key Research and Development Program of China (2021YFD2201205), National Natural Science Foundation of China (41601513 and 41977203), and Beijing Forestry University Municipal Training Program of Innovation and Entrepreneurship for Undergraduates (202110022017).

Conflict of interest

The authors declare that the research was conducted in the absence of any commercial or financial relationships that could be construed as a potential conflict of interest.

Publisher's note

All claims expressed in this article are solely those of the authors and do not necessarily represent those of their affiliated organizations, or those of the publisher, the editors and the reviewers. Any product that may be evaluated in this article, or claim that may be made by its manufacturer, is not guaranteed or endorsed by the publisher.

Supplementary material

The Supplementary material for this article can be found online at: https://www.frontiersin.org/articles/10.3389/fmicb.2022.1042944/full#supplementary-material

References

Amin, A., Ahmed, I., Habib, N., Abbas, S., Hasan, F., Xiao, M., et al. (2016). *Microvirga pakistanensis* sp. nov., a novel bacterium isolated from desert soil of Cholistan. *Pak. Arch. Microbiol.* 198, 933–939. doi: 10.1007/s00203-016-1251-3

Bahram, M., Hildebrand, F., Forslund, S. K., Anderson, J. L., Soudzilovskaia, N. A., Bodegom, P. M., et al. (2018). Structure and function of the global topsoil microbiome. *Nature* 560, 233–237. doi: 10.1038/s41586-018-0386-6

Bai, Y., Ren, P., Feng, P., Yan, H., and Li, W. (2020). Shift in rhizospheric and endophytic bacterial communities of tomato caused by salinity and grafting. *Sci. Total Environ.* 734:139388. doi: 10.1016/j.scitotenv.2020.139388

Banerjee, S., Schlaeppi, K., and Van, D. (2018). Keystone taxa as drivers of microbiome structure and functioning. *Nat. Rev. Microbiol.* 16, 567–576. doi: 10.1038/s41579-018-0024-1

Beckers, B., Op De Beeck, M., Weyens, N., Boerjan, W., and Vangronsveld, J. (2017). Structural variability and niche differentiation in the rhizosphere and endosphere bacterial microbiome of field-grown poplar trees. *Microbiome* 5:25. doi: 10.1186/s40168-017-0241-2

Beckers, B., Op De Beeck, M., Weyens, N., Van Acker, R., Van Montagu, M., Boerjan, W., et al. (2016). Lignin engineering in field-grown poplar trees affects the endosphere bacterial microbiome. *Proc. Natl. Acad. Sci.* 113, 2312–2317. doi: 10.1073/pnas.1523264113

Berry, D., and Widder, S. (2014). Deciphering microbial interactions and detecting keystone species with co-occurrence networks. *Front. Microbiol.* 5:219. doi: 10.3389/fmicb.2014.00219

Bödeker, I. T. M., Clemmensen, K. E., Boer, W., Martin, F., Olson, Å., and Lindahl, B. D. (2014). Ectomycorrhizal *Cortinarius* species participate in enzymatic oxidation of humus in northern forest ecosystems. *New Phytol.* 203, 245–256. doi: 10.1111/nph.12791

Carrión, V. J., Perez-Jaramillo, J., Cordovez, V., Tracanna, V., de Hollander, M., Ruiz-Buck, D., et al. (2019). Pathogen-induced activation of disease-suppressive functions in the endophytic root microbiome. *Science* 366, 606–612. doi: 10.1126/science.aaw9285

Castro, H. F., Classen, A. T., Austin, E. E., Norby, R. J., and Schadt, C. W. (2010). Soil microbial community responses to multiple experimental climate change drivers. *Appl. Environ. Microbiol.* 76, 999–1007. doi: 10.1128/AEM.02874-09

Catinella, G., Donzella, S., Borgonovo, G., Dallavalle, S., Contente, M. L., and Pinto, A. (2022). Efficient 2-step enzymatic cascade for the bioconversion of oleuropein into hydroxytyrosol. *Antioxidants* 11:260. doi: 10.3390/antiox11020260

Che, R., Qin, J., Tahmasbian, I., Wang, F., Zhou, S., Xu, Z., et al. (2018). Litter amendment rather than phosphorus can dramatically change inorganic nitrogen pools in a degraded grassland soil by affecting nitrogen-cycling microbes. *Soil Biol. Biochem.* 120, 145–152. doi: 10.1016/j.soilbio.2018.02.006

Chow, C.-E. T., Kim, D. Y., Sachdeva, R., Caron, D. A., and Fuhrman, J. A. (2014). Top-down controls on bacterial community structure: microbial network analysis of bacteria, T4-like viruses and protists. *ISME J.* 8, 816–829. doi: 10.1038/ismej.2013.199

Clemmensen, K. E., Finlay, R. D., Dahlberg, A., Stenlid, J., Wardle, D. A., and Lindahl, B. D. (2015). Carbon sequestration is related to mycorrhizal fungal

community shifts during long-term succession in boreal forests. *New Phytol.* 205, 1525–1536. doi: 10.1111/nph.13208

Czarnota, M. A., Rimando, A. M., and Weston, L. A. (2003). Evaluation of root exudates of seven sorghum accessions. *J. Chem. Ecol.* 29, 2073–2083. doi: 10.1023/A:1025634402071

Dai, Z., Yu, M., Chen, H., Zhao, H., Huang, Y., Su, W., et al. (2020). Elevated temperature shifts soil N cycling from microbial immobilization to enhanced mineralization, nitrification and denitrification across global terrestrial ecosystems. *Glob. Chang. Biol.* 26, 5267–5276. doi: 10.1111/gcb.15211

Duan, M., Lu, J., Yang, W., Lu, M., Wang, J., Li, S., et al. (2022). Metabarcoding and metabolome analyses reveal mechanisms of *Leymus chinensis* growth promotion by fairy ring of *Leucocalocybe mongolica*. *J. Fungi.* 8:944. doi: 10.3390/jof8090944

Edwards, J., Johnson, C., Santos-Medellín, C., Lurie, E., Podishetty, N. K., Bhatnagar, S., et al. (2015). Structure, variation, and assembly of the root-associated microbiomes of rice. *Proc. Natl. Acad. Sci.* 112, E911–E920. doi: 10.1073/pnas.1414592112

Feng, J., Jiang, D., Shang, H., Dong, M., Wang, G., He, X., et al. (2013). Barcoding poplars (*Populus L.*) from Western China. *PLoS One* 8:e71710. doi: 10.1371/journal.pone.0071710

Fernández-González, A. J., Cardoni, M., Gómez-Lama Cabanás, C., Valverde-Corredor, A., Villadas, P. J., Fernández-López, M., et al. (2020). Linking belowground microbial network changes to different tolerance level towards *Verticillium* wilt of olive. *Microbiome* 8:11. doi: 10.1186/s40168-020-0787-2

Floc'H, J. B., Hamel, C., Harker, K. N., and St-Arnaud, M. (2020). Fungal communities of the canola rhizosphere: keystone species and substantial between-year variation of the rhizosphere microbiome. *Microb. Ecol.* 80, 762–777. doi: 10.1007/s00248-019-01475-8

Gottel, N. R., Castro, H. F., Kerley, M., Yang, Z., Pelletier, D. A., Podar, M., et al. (2011). Distinct microbial communities within the endosphere and rhizosphere of *Populus deltoides* roots across contrasting soil types. *Appl. Environ. Microbiol.* 77, 5934–5944. doi: 10.1128/AEM.05255-11

Gu, Y., Wang, X., Yang, T., Friman, V., Geisen, S., Wei, Z., et al. (2020). Chemical structure predicts the effect of plant-derived low-molecular weight compounds on soil microbiome structure and pathogen suppression. *Funct. Ecol.* 34, 2158–2169. doi: 10.1111/1365-2435.13624

Guo, R., Ji, S., Wang, Z., Zhang, H., Wang, Y., and Liu, Z. (2021). *Trichoderma asperellum* xylanases promote growth and induce resistance in poplar. *Microbiol. Res.* 248:126767. doi: 10.1016/j.micres.2021.126767

Gupta, R., Keppanan, R., Leibman-Markus, M., Rav David, D., Elad, Y., Ment, D., et al. (2021). The entomopathogenic fungi *Metarhizium brunneum* and *Beauveria bassiana* promote systemic immunity and confer resistance to a broad range of pests and pathogens in tomato. *Phytopathology* 112, 784–793. doi: 10.1094/PHYTO-08-21-0343-R

Hawkins, C., Ginzburg, D., Zhao, K., Dwyer, W., Xue, B., Xu, A., et al. (2021). Plant metabolic network 15: a resource of genome-wide metabolism databases for 126 plants and algae. *J. Integr. Plant Biol.* 63, 1888–1905. doi: 10.1111/jipb.13163

Hogan, J. A., Baraloto, C., Ficken, C., Clark, M. D., Weston, D. J., and Warren, J. M. (2021). The physiological acclimation and growth response of *POPULUS TRICHOCARPA* to warming. *Physiol. Plant.* 173, 1008–1029. doi: 10.1111/ppl.13498

Huang, K. L., Tian, J., Wang, H., Fu, Y.-F., Li, Y., Zheng, Y., et al. (2021). Fatty acid export protein BnFAX6 functions in lipid synthesis and axillary bud growth in *Brassica napus*. *Plant Physiol.* 186, 2064–2077. doi: 10.1093/plphys/kiab229

Jiang, Y., Li, S., Li, R., Zhang, J., Liu, Y., Lv, L., et al. (2017). Plant cultivars imprint the rhizosphere bacterial community composition and association networks. *Soil Biol. Biochem.* 109, 145–155. doi: 10.1016/j.soilbio.2017.02.010

Jiang, J., Song, Z., Yang, X., Mao, Z., Nie, X., Guo, H., et al. (2017). Microbial community analysis of apple rhizosphere around Bohai gulf. *Sci. Rep.* 7:8918. doi: 10.1038/s41598-017-08398-9

Jiao, S., Chen, W., and Wei, G. (2017). Biogeography and ecological diversity patterns of rare and abundant bacteria in oil-contaminated soils. *Mol. Ecol.* 26, 5305–5317. doi: 10.1111/mec.14218

Jiao, S., Yang, Y., Xu, Y., Zhang, J., and Lu, Y. (2020). Balance between community assembly processes mediates species coexistence in agricultural soil microbiomes across eastern China. *ISME J.* 14, 202–216. doi: 10.1038/s41396-019-0522-9

Kundel, D., Bodenhausen, N., Jørgensen, H. B., Truu, J., Birkhofer, K., Hedlund, K., et al. (2020). Effects of simulated drought on biological soil quality, microbial diversity and yields under long-term conventional and organic agriculture. *FEMS Microbiol. Ecol.* 96:fiaa205. doi: 10.1093/femsec/fiaa205

Levins, R. (1968). *Evolution in Changing Environments: Some Theoretical Explorations*. Princeton, NJ: Princeton University Press.

Li, X., Chen, J., Zhang, Q., Li, X. F., Zhou, X., and Tao, Y. (2021). Microbial community responses to multiple soil disinfestation change drivers. *Appl. Microbiol. Biotechnol.* 105, 6993–7007. doi: 10.1007/s00253-021-11528-z

Li, J., Luo, Z., Zhang, C., Qu, X., Chen, M., Song, T., et al. (2020). Seasonal variation in the rhizosphere and non-rhizosphere microbial community structures and functions of *camellia yuhsienensis* Hu. *Microorganisms* 8:1385. doi: 10.3390/microorganisms8091385

Li, H., Qiu, Y., Yao, T., Han, D., Gao, Y., Zhang, J., et al. (2021). Nutrients available in the soil regulate the changes of soil microbial community alongside degradation of alpine meadows in the northeast of the Qinghai-Tibet plateau. *Sci. Total Environ.* 792:148363. doi: 10.1016/j.scitotenv.2021.148363

Li, F., Zhang, S., Wang, Y., Li, Y., Li, P., Chen, L., et al. (2020). Rare fungus, *Mortierella capitata*, promotes crop growth by stimulating primary metabolisms related genes and reshaping rhizosphere bacterial community. *Soil Biol. Biochem.* 151:108017. doi: 10.1016/j.soilbio.2020.108017

Lin, H., Liu, C., Li, B., and Dong, Y. (2020). *Trifolium repens* L. regulated phytoremediation of heavy metal contaminated soil by promoting soil enzyme activities and beneficial rhizosphere associated microorganisms. *J. Hazard. Mater.* 402:123829. doi: 10.1016/j.jhazmat.2020.123829

Liu, K., Ding, X., and Wang, J. (2020). Soil metabolome correlates with bacterial diversity and co-occurrence patterns in root-associated soils on the Tibetan plateau. *Sci. Total Environ.* 735:139572. doi: 10.1016/j.scitotenv.2020.139572

Liu, G., Pfeifer, J., de Brito Francisco, R., Emonet, A., Stirnemann, M., Gübeli, C., et al. (2018). Changes in the allocation of endogenous strigolactone improve plant biomass production on phosphate-poor soils. *New Phytol.* 217, 784–798. doi: 10.1111/nph.14847

Liu, J., Sui, Y., Yu, Z., Shi, Y., Chu, H., Jin, J., et al. (2015). Soil carbon content drives the biogeographical distribution of fungal communities in the black soil zone of Northeast China. *Soil Biol. Biochem.* 83, 29–39. doi: 10.1016/j.soilbio.2015.01.009

Longa, C., Nicola, L., Antonielli, L., Mescalchin, E., Zanzotti, R., Turco, E., et al. (2017). Soil microbiota respond to green manure in organic vineyards. *J. Appl. Microbiol.* 123, 1547–1560. doi: 10.1111/jam.13606

Lu, R.K. (1999). *Soil and Agro-Chemistry Analytical Methods*. Beijing: China Agricultural Science & Technology Press.

Lu, T., Ke, M., Lavoie, M., Jin, Y., Fan, X., Zhang, Z., et al. (2018). Rhizosphere microorganisms can influence the timing of plant flowering. *Microbiome* 6:231. doi: 10.1186/s40168-018-0615-0

Ma, J., Wan, D., Duan, B., Bai, X., Bai, Q., Chen, N., et al. (2018). Genome sequence and genetic transformation of a widely distributed and cultivated poplar. *Plant Biotechnol. J.* 17, 451–460. doi: 10.1111/pbi.12989

Ma, L., Yang, L., Liu, W., Zhang, Y., Zhou, Q., Wu, Z., et al. (2021). Effects of root exudates on rhizosphere bacteria and nutrient removal in pond-ditch circulation systems (PDCSs) for rural wastewater treatment. *Sci. Total Environ.* 785:147282. doi: 10.1016/j.scitotenv.2021.147282

Macías-Rodríguez, L., Contreras-Cornejo, H. A., Adame-Garnica, S. G., Del-Val, E., and Larsen, J. (2020). The interactions of *Trichoderma* at multiple trophic levels: inter-kingdom communication. *Microbiol. Res.* 240:126552. doi: 10.1016/j.micres.2020.126552

Mattos, G. N., Tonon, R. V., Furtado, A. A., and Cabral, L. M. (2017). Grape by-product extracts against microbial proliferation and lipid oxidation: a review: grape by-products with antimicrobial and antioxidant potential. *J. Sci. Food Agric.* 97, 1055–1064. doi: 10.1002/jsfa.8062

Min, K., Freeman, C., Kang, H., and Choi, S.-U. (2015). The regulation by phenolic compounds of soil organic matter dynamics under a changing environment. *Biomed. Res. Int.* 2015, 1–11. doi: 10.1155/2015/825098

Ning, D., Deng, Y., Tiedje, J. M., and Zhou, J. (2019). A general framework for quantitatively assessing ecological stochasticity. *Proc. Natl. Acad. Sci.* 116, 16892–16898. doi: 10.1073/pnas.1904623116

Pandit, S. N., Kolasa, J., and Cottenie, K. (2009). Contrasts between habitat generalists and specialists: an empirical extension to the basic metacommunity framework. *Ecology* 90, 2253–2262. doi: 10.1890/08-0851.1

Patterson, A., Flores-Rentería, L., Whipple, A., Whitham, T., and Gehring, C. (2019). Common garden experiments disentangle plant genetic and environmental contributions to ectomycorrhizal fungal community structure. *New Phytol.* 221, 493–502. doi: 10.1111/nph.15352

Qin, Y., Pan, X. Y., Jin, W., Chen, L. Q., and Yuan, Z. L. (2018). Comparison of four extraction methods of soil microbiome in poplar plantation. *Sci. Silvae Sin.* 9, 169–176. doi: 10.11707/j.1001-7488.20180919

Rädecker, N., Pogoreutz, C., Voolstra, C. R., Wiedenmann, J., and Wild, C. (2015). Nitrogen cycling in corals: the key to understanding holobiont functioning. *Trends Microbiol.* 23, 490–497. doi: 10.1016/j.tim.2015.03.008

Ramond, J. B., Jordaan, K., Díez, B., Heinzelmann, S. M., and Cowan, D. A. (2022). Microbial biogeochemical cycling of nitrogen in arid ecosystems. *Microbiol. Mol. Biol. Rev.* 86:e0010921. doi: 10.1128/mmbr.00109-21

Rozpądek, P., Domka, A. M., Nosek, M., Ważny, R., Jędrzejczyk, R. J., Wiciarz, M., et al. (2018). The role of strigolactone in the cross-talk between *Arabidopsis thaliana* and the endophytic fungus *Mucor* sp. *Front. Microbiol.* 9:441. doi: 10.3389/fmicb.2018.00441

Song, Y., Chen, P., Xuan, A., Bu, C., Liu, P., Ingvarsson, P. K., et al. (2021). Integration of genome wide association studies and co-expression networks reveal roles of *PtoWRKY 42-PtoUGT76C1-1* in *trans*-zeatin metabolism and cytokinin sensitivity in poplar. *New Phytol.* 231, 1462–1477. doi: 10.1111/nph.17469

Song, Y., Ci, D., Tian, M., and Zhang, D. (2016). Stable methylation of a non-coding RNA gene regulates gene expression in response to abiotic stress in Populus simonii. *J. Exp. Bot.* 67, 1477–1492. doi: 10.1093/jxb/erv543

Song, Y., Li, X., Yao, S., Yang, X., and Jiang, X. (2020). Correlations between soil metabolomics and bacterial community structures in the pepper rhizosphere under plastic greenhouse cultivation. *Sci. Total Environ.* 728:138439. doi: 10.1016/j.scitotenv.2020.138439

Su, X., Su, X., Yang, S., Zhou, G., Ni, M., Wang, C., et al. (2020). Drought changed soil organic carbon composition and bacterial carbon metabolizing patterns in a subtropical evergreen forest. *Sci. Total Environ.* 736:139568. doi: 10.1016/j.scitotenv.2020.139568

Sui, X., Zhang, R., Frey, B., Yang, L., Liu, Y., Ni, H., et al. (2021). Soil physicochemical properties drive the variation in soil microbial communities along a forest successional series in a degraded wetland in northeastern China. *Ecol. Evol.* 11, 2194–2208. doi: 10.1002/ece3.7184

Sun, N., Bu, Y., Pan, C., Wu, X., Cao, Y., Jing, Y. (2021). Analyses of microstructure and dynamic deposition of cell wall components in xylem provide insights into differences between two black poplar cultivars. *Forests* 12:972. doi: 10.3390/f12080972

Tong, S., Yuan, M., Liu, Y., Li, X., Jin, D., Cheng, X., et al. (2021). Ergosterol-targeting fusion antifungal peptide significantly increases the Verticillium wilt resistance of cotton. *Plant Biotechnol. J.* 19, 926–936. doi: 10.1111/pbi.13517

Tya, B., Jxab, C., Zzb, C., and Ywa, B. (2021). Biochar-based fertilizer amendments improve the soil microbial community structure in a karst mountainous area. *Sci. Total Environ.* 794:148757. doi: 10.1016/j.scitotenv.2021.148757

Veach, A. M., Chen, H., Yang, Z. K., Labbe, A. D., Engle, N. L., Tschaplinski, T. J., et al. (2020). Plant hosts modify belowground microbial community response to extreme drought. *mSystems* 5:5. doi: 10.1128/mSystems.00092-20

Veach, A. M., Morris, R., Yip, D. Z., Yang, Z. K., Engle, N. L., Cregger, M. A., et al. (2019). Rhizosphere microbiomes diverge among *Populus trichocarpa* plant-host genotypes and chemotypes, but it depends on soil origin. *Microbiome* 7:76. doi: 10.1186/s40168-019-0668-8

Veyisoglu, A., Tatar, D., Saygin, H., Inan, K., Cetin, D., Guven, K., et al. (2016). *Microvirga makkahensis* sp. nov., and *microvirga arabica* sp. nov., isolated from sandy arid soil. *Antonie Van Leeuwenhoek* 109, 287–296. doi: 10.1007/s10482-015-0631-z

Vives-Peris, V., de Ollas, C., Gómez-Cadenas, A., and Pérez-Clemente, R. M. (2020). Root exudates: from plant to rhizosphere and beyond. *Plant Cell Rep.* 39, 3–17. doi: 10.1007/s00299-019-02447-5

Wagg, C., Bender, S. F., Widmer, F., and van der Heijden, M. G. A. (2014). Soil biodiversity and soil community composition determine ecosystem multifunctionality. *Proc. Natl. Acad. Sci.* 111, 5266–5270. doi: 10.1073/pnas.1320054111

Wakabayashi, T., Ishiwa, S., Shida, K., Motonami, N., Suzuki, H., Takikawa, H., et al. (2021). Identification and characterization of sorgomol synthase in sorghum strigolactone biosynthesis. *Plant Physiol.* 185, 902–913. doi: 10.1093/plphys/kiaa113

Wang, Y., Hou, L., Wu, X., Zhu, M., Dai, Y., and Zhao, Y. (2021). Mycorrhiza helper bacterium *Bacillus pumilus* HR10 the improves growth and nutritional status of *Pinus thunbergii* by promoting mycorrhizal proliferation. *Tree Physiol.* 42, 907–918. doi: 10.1093/treephys/tpab139

Wang, J., Liu, L., Gao, X., Hao, J., and Wang, M. (2021). Elucidating the effect of biofertilizers on bacterial diversity in maize rhizosphere soil. *PLoS One* 16:e0249834. doi: 10.1371/journal.pone.0249834

Wang, W., Talide, L., Viljamaa, S., and Niittylä, T. (2022). Aspen growth is not limited by starch reserves. *Curr. Biol.* 32, 3619–3627.e4. doi: 10.1016/j.cub.2022.06.056

Wanichthanarak, K., Boonchai, C., Kojonna, T., Chadchawan, S., Sangwongchai, W., and Thitisaksakul, M. (2020). Deciphering rice metabolic flux reprograming under salinity stress via in silico metabolic modeling. *Comput. Struct. Biotechnol. J.* 18, 3555–3566. doi: 10.1016/j.csbj.2020.11.023

Wu, N., Li, Z., Meng, S., and Wu, F. (2021). Soil properties and microbial community in the rhizosphere of *Populus alba* var. *pyramidalis* along a chronosequence. *Microbiol. Res.* 250:126812. doi: 10.1016/j.micres.2021.126812

Wu, X., Liu, J., Meng, Q., Fang, S., Kang, J., and Guo, Q. (2021). Differences in carbon and nitrogen metabolism between male and female *Populus cathayana* in response to deficient nitrogen. *Tree Physiol.* 41, 119–133. doi: 10.1093/treephys/tpaa108

Xing, M., Wang, Q., Li, X., Li, Y., and Zhou, X. (2021). Selection of keystone species based on stable carbon and nitrogen isotopes to construct a typical food web on the shore of Xingkai Lake, China. *Ecol. Indic.* 132:108263. doi: 10.1016/j.ecolind.2021.108263

Ye, X., Li, Z., Luo, X., Wang, W., Li, Y., Li, R., et al. (2020). A predatory myxobacterium controls cucumber *fusarium* wilt by regulating the soil microbial community. *Microbiome* 8:49. doi: 10.1186/s40168-020-00824-x

Yoneyama, K. (2020). Recent progress in the chemistry and biochemistry of strigolactones. *J. Pestic. Sci.* 45, 45–53. doi: 10.1584/jpestics.D19-084

Zhang, Y., Zhao, L., Zhao, J., Li, Y., Wang, J., Guo, R., et al. (2017). *S5H/DMR6* encodes a salicylic acid 5-hydroxylase that fine-tunes salicylic acid homeostasis. *Plant Physiol.* 175, 1082–1093. doi: 10.1104/pp.17.00695

Zhang, L., Zhou, J., George, T. S., Limpens, E., and Feng, G. (2021). Arbuscular mycorrhizal fungi conducting the hyphosphere bacterial orchestra. *Trends Plant Sci.* 27, 402–411. doi: 10.1016/j.tplants.2021.10.008

Zhao, M., Zhao, J., Yuan, J., Hale, L., Wen, T., Huang, Q., et al. (2021). Root exudates drive soil-microbe-nutrient feedbacks in response to plant growth. *Plant Cell Environ.* 44, 613–628. doi: 10.1111/pce.13928

Zheng, W., Zheng, Q., Xue, Y., Hu, J., and Gao, M.-T. (2017). Influence of rice straw polyphenols on cellulase production by *Trichoderma reesei*. *J. Biosci. Bioeng.* 123, 731–738. doi: 10.1016/j.jbiosc.2017.01.009

Zhou, S., Geng, B., Li, M., Li, Z., Liu, X., and Guo, H. (2021). Comprehensive analysis of environmental factors mediated microbial community succession in nitrogen conversion and utilization of ex situ fermentation system. *Sci. Total Environ.* 769:145219. doi: 10.1016/j.scitotenv.2021.145219

Zhou, X., Wang, J.-T., Zhang, Z.-F., Li, W., Chen, W., and Cai, L. (2020). Microbiota in the rhizosphere and seed of rice from China, with reference to their transmission and biogeography. *Front. Microbiol.* 11:995. doi: 10.3389/fmicb.2020.00995

Zhou, X., Zhang, X., Ma, C., Wu, F., Jin, X., Dini-Andreote, F., et al. (2022). Biochar amendment reduces cadmium uptake by stimulating cadmium-resistant PGPR in tomato rhizosphere. *Chemosphere* 307:136138. doi: 10.1016/j.chemosphere.2022.136138

Zhu, Q., Yan, K., Dong, Y., and Wang, Y. (2022). Rhizosphere bacterial communities and soil nutrient conditions reveal sexual dimorphism of *Populus deltoides*. *J. For. Res.* 33, 1–11. doi: 10.1007/s11676-022-01517-x

frontiers | Frontiers in Microbiology

TYPE Original Research
PUBLISHED 05 January 2023
DOI 10.3389/fmicb.2022.1067939

OPEN ACCESS

EDITED BY
Muhammad Saleem,
Alabama State University,
United States

REVIEWED BY
Jiangbing Xu,
Nanjing University of Information Science and Technology, China
Xianan Xie,
South China Agricultural University, China

*CORRESPONDENCE
Jingrui Chen
✉ chenjr5526@126.com
Changxu Xu
✉ changxux@sina.com

SPECIALTY SECTION
This article was submitted to Microbe and Virus Interactions With Plants, a section of the journal Frontiers in Microbiology

RECEIVED 12 October 2022
ACCEPTED 12 December 2022
PUBLISHED 05 January 2023

CITATION
Lv M, Wang Y, Chen X, Qin W, Shi W, Song W, Chen J and Xu C (2023) The moderate substitution of *Astragalus sinicus* returning for chemical fertilizer improves the N cycle function of key ecological bacterial clusters in soil. *Front. Microbiol.* 13:1067939. doi: 10.3389/fmicb.2022.1067939

The moderate substitution of *Astragalus sinicus* returning for chemical fertilizer improves the N cycle function of key ecological bacterial clusters in soil

Minghao Lv[1,2], Yongdong Wang[2], Xiaofen Chen[1], Wenjing Qin[1], Wencong Shi[2], Weifeng Song[2], Jingrui Chen[1]* and Changxu Xu[1]*

[1]Institute of Soil and Fertilizer and Resources and Environment, Jiangxi Academy of Agricultural Sciences, Nanchang, China, [2]State Key Laboratory of Crop Biology, Shandong Agricultural University, Tai'an, China

Astragalus sinicus (Chinese milk vetch) is a well-established resource of organic fertilizer widely used in paddy soil to partially replace chemical fertilizers. However, the influence of returning *A. sinicus* to fields on the soil bacterial community remains poorly understood. Here, we used different amounts of *A. sinicus* partially replacing chemical fertilizers and investigated the changes in soil physicochemical factors and the soil bacterial community structure responses. Returning *A. sinicus* to the field significantly increased the soil total nitrogen and available phosphorus content ($p<0.05$). Weighted gene correlation network analysis (WGCNA) was applied to detect significant associations between the soil microbiome data and physicochemical factors. Two key ecological bacterial clusters (MEturquoise and MEgreen), mainly containing Acidobacteria, Proteobacteria, and Chloroflexi, were significantly correlated with soil nitrogen (N) levels. *A. sinicus* partially replacing chemical fertilizers reduced the normalized stochasticity ratio (NST) of rare amplicon sequence variants (ASVs), abundant ASVs, MEturquoise, and MEgreen ($p<0.05$). Our results further indicated that a moderate amount of *A. sinicus* returned to the soil effectively mitigated the trend of reduced relative abundance of N fixation function of key ecological clusters caused by chemical fertilizer. However, a large amount of *A. sinicus* led to a significant increase in relative abundance of denitrification function and a significant decrease in relative abundance of N fixation function of key ecological clusters. This implies that the moderate substitution of *A. sinicus* returning for chemical fertilizer improves the N cycling function of key ecological bacterial clusters in soil. From the perspective of the bacterial community in paddy soil, this study provides new insight and a reference on how to find a good balance between the amount of *A. sinicus* returned to the soil and ecological safety.

KEYWORDS

Astragalus sinicus, organic substitution, bacterial community, ecological cluster, nitrogen cycle function

Introduction

The nitrogen (N) cycle is an important biogeochemical cycle, as N is an essential element for all living organisms and is involved in the biosynthesis of important substances such as nucleic acids and proteins (Fan, 2019; Lehnert et al., 2021). Human activity has a profound impact on global biogeochemical N cycling, mainly because of the large amount of N fertilizer inputs required for food production (Kuypers et al., 2018). Especially in terrestrial ecosystems, N is considered a limiting nutrient (Zheng et al., 2020). Therefore, in many areas, farmers apply too much N fertilizer to the soil to meet the needs of plant growth, while often less than half of this N is absorbed and used by plants, which exacerbates global climate warming and ozone depletion (Lehnert et al., 2021).

Microorganisms are important players in the N cycle. Biological N fixation fixes about 100 Tg of N from the atmosphere annually, whereas the N cycling function, represented by denitrification, has also been considered a key process determining N loss in terrestrial ecosystems (Fang et al., 2015; Fan et al., 2019). Thus, there is an urgent need to investigate the response patterns of soil microorganisms in order to understand the effects of *Astragalus sinicus* returned to the soil. Soil microorganisms are sensitive to environmental changes. Different ecosystems may vary greatly in microbial response to environmental changes because of different management practices (Dai et al., 2018). In turn, the diverse metabolism of microbes may result in various changes in soil environmental conditions. The abuse of chemical fertilizers can lead to the destruction of microbial community structures in farmlands and reduce the abundance of some microorganisms related to maintaining soil health (Rahman, 2021). The comprehensive application of chemical fertilizer and organic fertilizer can affect many vital paddy ecosystem processes by regulating the soil microbial communities (Oladele et al., 2019). A recent study showed that long-term organic substitution increases rice yield by improving soil properties and regulating soil bacteria (Liu et al., 2021). Song et al. (2022) found that the organic substitution can reduce soil acidification, improve soil physicochemical properties and microbial communities, and enhance soil metabolism (Song et al., 2022). As an ideal source of organic fertilizer, *A. sinicus* can improve the nutrient cycle in soil and affect the fertilizer use efficiency of the soil (Yang W. et al., 2022). Ecological clusters are important ecological units, and microorganisms in the same ecological cluster have strong co-occurrence relationships (Heleno et al., 2012; Guidi et al., 2016). They provide an opportunity to investigate highly connected and identifiable taxa, and recent studies have concluded that ecological clusters and soil nutrient changes are closely related (Fan et al., 2021). Hence, to further understand the mechanism of paddy ecosystem changes, it is essential to study the response of soil microbial communities to *A. sinicus*.

Rice is one of the major food crops in the world (Kusano et al., 2015). According to the latest statistics from the Food and Agriculture Organization,[1] rice ranks third in global food crop output. Thus, to meet the demand for food crops for a growing population, it is particularly important to maintain and ensure the health and stability of the rice field ecosystem. Chemical fertilizer application is one of the important ways to supply N nutrients to crops and enhance crop yield (Qian et al., 2016). However, the phenomenon of chemical fertilizer abuse is common, which endangers soil health and causes problems such as soil acidification, hardening, and fertilizer nutrient loss, which are not conducive to the sustainable development of agriculture (Liu et al., 2021; Song et al., 2022). The damage to soil health by unreasonable fertilization methods has caused widespread concern.

Organic fertilizer is rich in organic matter, which can effectively alleviate the soil problems caused by chemical fertilizer abuse and improve soil health (Jia et al., 2020; Yang W. et al., 2022). However, if only organic fertilizer is applied, its fertilizer effect will be exerted slowly, and it will be difficult to meet the expected crop yield increase in a short time (Garzón et al., 2011). Comprehensive application of organic and inorganic fertilizers may be an important measure to maintain the stability of the farmland ecosystem. Oladele's et al. (2019) study showed that the combined application of carbon and organic fertilizer can improve the productivity of rice and the level of soil available nutrients. Liu et al. (2021) found that long-term organic substitution increases rice yield by improving soil properties and regulating soil bacteria. These studies show that organic substitution effectively alleviates the continuous deterioration of soil quality. Compared with the application of chemical fertilizer alone, organic substitution can significantly improve the utilization rate of N in fertilizer by crops (Cheng et al., 2021). However, excessive N fertilizer input may reduce the nutrient utilization rate of N input in the ecosystem, leading to N loss from soil to other environments and causing potential damage to the

Abbreviations: AHN, alkali-hydrolyzable nitrogen; AK, available potassium; AN, ammonia nitrogen; AP, available phosphorus; NN, nitrate nitrogen; SMC, soil moisture content; TK, total potassium; TN, total nitrogen; TOM, total organic matter; TP, total phosphorus.

1 https://www.fao.org/home/en

ecosystem (Zhao et al., 2019). *A. sinicus* is a well-established green manure for paddy soil in southern China. The moderate amount of *A. sinicus* returned to the soil can improve the protein content and overall quality of rice (Tong et al., 2022; Yang H. et al., 2022). A recent study showed that replacing urea-N with *A. sinicus* can mitigate N_2O emissions in rice paddy (Yang W. et al., 2022). However, the influence of returning *A. sinicus* to paddy soil on the bacterial community remains poorly understood.

Here, 16S rRNA gene high-throughput sequencing technology was used to compare the bacterial community compositions (both taxonomic and functional diversity) between control and *A. sinicus* deposited samples. This study is based on a nine-year paddy field experiment performed by the Jiangxi Academy of Agricultural Sciences in 2008 with the objectives of determining (1) the bacterial community composition, structure, and assembly mechanism of paddy soil under different fertilization treatments; (2) the effects of fertilization on the correlations between microbes and environmental factors; and (3) the effects of different fertilization treatments on soil bacterial community function.

Materials and methods

Experimental design and sample collection

The experiment was set up in 2008 in Dengjiabu Rice Seed Farm, Yujiang County, Jiangxi Province, China (28°12′ E, 116°47′ N) with paddy soil formed by river alluvium. The annual temperature is 17.6°C, and the annual precipitation is 1788.8 mm. Four fertilization treatments with continuous rice cropping were compared in a completely randomized block design with three replicates (each plot was 20 m^2): (1) CK: non-fertilization; (2) CF: 100% chemical fertilizer; (3) LA: 80% chemical fertilizer + moderate amount of *A. sinicus* (15,000 kg/hm^2); and (4) HA: 80% chemical fertilizer + high amount of *A. sinicus* (37,500 kg/hm^2). Generally, N fertilizer is urea, phosphate fertilizer is superphosphate, and potassium fertilizer is potassium chloride (N-P-K). The 100% chemical fertilizer comprised N (150 kg/hm^2), P_2O_5 (75 kg/hm^2), and K_2O (120 kg/hm^2). The equivalent N input of 15,000 kg/hm^2 and 37,500 kg/hm^2 of *A. sinicus* treated with LA and HA was 39.1 kg/hm^2 and 97.8 kg/hm^2, respectively.

After the rice harvest (April 2017), equal amounts of topsoil (0–20 cm) were collected from three experimental areas set in each treatment by multi-point mixed sampling. During soil collection, the soil moisture content was measured on the spot. The collected soil samples were temporarily stored in an ice box and immediately transported to the laboratory. Stones and weeds were removed from the sample as soon as possible, and the soil was passed through a 2-mm sieve. Each sample was then divided into two parts; one part was frozen at −80°C to be used later for DNA extraction, and the other was stored at 4°C for the determination of various physicochemical factors.

Soil physicochemical analysis

Soil pH was measured by potentiometry (Coleman et al., 1951). The total organic matter (TOM) content was measured using the potassium dichromate volumetric method (Cai et al., 2011). Total nitrogen (TN) was determined by the Kjeldahl method (Craft et al., 1991). Alkali-hydrolyzable nitrogen (AHN) was determined by the diffusion method (Yang and Yang, 2020). Nitrate nitrogen (NN) was determined by ultraviolet (UV) spectrophotometry (Cawse, 1967). Ammonia nitrogen (AN) was determined by indophenol blue colorimetry (Kanda, 1995). Total phosphorus (TP) was determined by the molybdenum antimony colorimetric method (Wieczorek et al., 2022). Available phosphorus (AP) was determined by the sodium bicarbonate method (De Silva et al., 2015). Total potassium (TK) and available potassium (AK) were determined by flame spectrophotometry (Hald and Mason, 1958; Liu et al., 2021). To ensure the reliability of the experimental data, three independent measurements of these indicators were made for each sample.

High-throughput sequencing and bioinformatics analysis

DNA was extracted from the samples using a MagPure Stool DNA LQ Kit (Magen, D6358-03, Guangzhou, China). To eliminate interference from external bacteria and impurities during the extraction, all experimental operations were performed according to the kit instructions at a UV-sterilized ultraclean bench (Bolyen et al., 2019). The V3–V4 regions of the bacterial 16S rRNA gene were amplified using the primers 341F (5′-CCTACGGGNGGCWGCAG-3′) and 805R (5′-GACTACHVGGGTATCTAATCC-3′). Amplification was performed with pre-denaturation for 3 min at 95°C, followed by 25 cycles of 30 s at 95°C, 30 s at 55°C, and 45 s at 72°C, and a final extension for 5 min at 72°C. PCR amplicons were detected by electrophoresis on 1.5% (w/v) agarose gels. The purified amplicons were sequenced on an Illumina MiSeq platform.

After sequencing, Quantitative Insights into Microbial Ecology 2 (QIIME2, v2020.8[2]) was used to process the offline data (original data) of different fertilization treatments under long-term unbalanced fertilization (Bolyen et al., 2019). Both ends of the original data were imported into QIIME2 as an input FASTQ file, and the semantic type of bacteria was specified as the single-end sequence. The quality of the raw sequence was evaluated, and low-quality cut-offs for forward and reverse reads were determined. QIIME2 was used to perform quality control and generate an ASV feature table. The quality control function in DADA2 was used for denoising and chimera detection and removal (Callahan et al., 2016). In addition, ASVs present in only one sample and a total relative abundance of less than five in all

2 https://qiime2.org/

samples were removed. Subsequently, the ASV representative sequences were aligned with the SILVA database 138.[3] To accurately assess the diversity of microbial communities, all samples were rarefied to the same depth based on the minimum sequence number (32,781). Subsequent analyzes performed in this study were based on the above normalized data.

Statistical analysis

The 'vegan' package in R software was used to calculate the α-diversity (Chao1, abundance-based coverage estimator (ACE), Shannon, etc.) of the bacterial community. The ß-diversity (Bray–Curtis distance) of the bacterial community was calculated using the 'betapart' package. The 'hmisc' package was used to calculate Spearman correlation coefficients between the bacterial community and environmental factors or ecological niche width. The 'NST' package was used to quantify the assembly process of the bacterial community. The 'rdacca' package was used for hierarchical partitioning analysis. Origin software was used to draw box plots, scatter plots, and stacked histograms. The circular heatmap was visualized using the Tutools platform.[4] The nonparametric factorial Kruskal–Wallis sum-rank test and linear discriminant analysis (LDA > 2.0) were used to identify biomarkers in the different treatments and were performed using the LEfSe tool in Galaxy/Hutlab.[5] Partial least squares-discriminant analysis was performed using an online analysis platform.[6] Based on the methods mentioned in previous studies (Langfelder and Horvath, 2008; Guidi et al., 2016; Chen et al., 2022), weighted gene correlation network analysis (WGCNA) was performed on the relative abundance bacterial community table. An online analysis platform[7] was used to infer community assembly mechanisms by phylogenetic bin-based null model analysis (iCAMP). We assessed the normality of the distribution of indicators such as diversity using the Shapiro–Wilk index in IBM SPSS Statistics software and performed analysis of variance (ANOVA) and Duncan honestly significant difference test ($p < 0.05$) for data that conformed to a normal distribution and Kruskal–Wallis test ($p < 0.05$) for data that did not conform to a normal distribution.

Results

Soil physicochemical properties

Different fertilization treatments significantly affected the soil physicochemical properties such as TN, AHN, NN, AP, and TK (Table 1). The HA treatment significantly increased TN and AP in soil ($p < 0.05$). TN showed a significant increasing trend with the increase in *A. sinicus* returned to the soil ($p < 0.05$). Although the content of AHN, NN, and TK in soil also increased with the increase in *A. sinicus* returned to the soil, no significant difference was observed among treatments ($p > 0.05$). The AP content in soil of the LA treatment was the highest, which was significantly higher than the CK treatment ($p < 0.05$).

Bacterial α- and β-diversity

The bacterial community in the various fertilization treatments showed different structural characteristics. Compared with the CK treatment, the CF treatment significantly increased α-diversity (ACE and Chao1) of the soil bacterial community ($p < 0.05$; Figures 1A, B). However, the Shannon index of the soil bacterial community did not change significantly ($p > 0.05$; Supplementary Table S1). The first two coordinates of the principal coordinate analysis (PC1 = 23% and PC2 = 13%) based on Bray–Curtis distance explained 36% of the variation in bacterial β-diversity. Principal coordinate analysis showed that ASVs were separated in overall treatment (Adonis test, $p < 0.05$; Figure 1C), implying that different fertilization treatments had significant effects on the bacterial structure. Regression analysis showed that with the increase in the input proportion of *A. sinicus* (the ratio of the N content of *A. sinicus* to total fertilizer N, AIP), the soil bacterial α-diversity (ACE and Chao1) significantly decreased ($p < 0.05$; Figures 1D, E). Differences in the bacterial community composition for all treatments were dominated by species replacement processes, which contributed 94.5%; whereas the contribution of richness difference to β-diversity was smaller (5.5%; Supplementary Table S2). With the increase in total inorganic N input, eigenvalues of the bacterial community structure (PC1) significantly increased ($p < 0.001$; Figure 1F).

Composition of the soil bacterial community

In all samples, 40 phyla and 501 genera had certain taxonomic statuses. Among these, the average relative abundance of 12 phyla and 16 genera exceeded 1%, and were the dominant phyla and genera in this study. Acidobacteria (24.56%) and Proteobacteria (24.51%) were the dominant phyla in the soil bacterial community, followed by Chloroflexi (15.93%), Nitrospirota (8.16%), Bacteroides (5.79%), Myxococcota (4.24%), *Actinobacteria* (3.48%), Desulfobacterota (2.41%), Verrucomicrobia (2.07%), Gemmatimonadota (1.72%), Sva0485 (1.39%), and Firmicutes (1.18%). The relative abundance of Acidobacteria in the CK treatment was the highest. Compared with the other three treatments, the relative abundance of Proteobacteria and Firmicutes in HA treatment was significantly increased ($p < 0.001$; Supplementary Table S3).

3 http://www.arb-silva.de/
4 http://www.cloudtutu.com/
5 http://huttenhower.sph.harvard.edu/galaxy/
6 http://www.biomicroclass.com/
7 http://ieg3.rccc.ou.edu:8080/

TABLE 1 Effects of different fertilization treatments on soil physicochemical properties.

	CK	CF	LA	HA
pH	4.797 ± 0.039	4.767 ± 0.074	4.743 ± 0.077	4.713 ± 0.037
SMC (%)	28.287 ± 0.901	28.077 ± 0.676	30.023 ± 2.095	30.233 ± 1.946
TOM (g/kg)	35.056 ± 2.18	36.603 ± 0.244	35.916 ± 1.199	35.419 ± 0.983
TN (g/kg)	1.879 ± 0.039d	1.93 ± 0.110c	2.01 ± 0.114b	2.086 ± 0.007a
AHN (mg/kg)	135.771 ± 4.042b	144.346 ± 16.169ab	155.779 ± 16.169ab	167.213 ± 0a
NN (mg/kg)	3.284 ± 0.673b	3.389 ± 0.805ab	3.645 ± 0.852ab	4.038 ± 0.321a
AN (mg/kg)	5.939 ± 0.815	5.647 ± 0.742	5.191 ± 0.31	5.051 ± 0.497
TP (g/kg)	0.402 ± 0.023	0.434 ± 0.051	0.502 ± 0.059	0.64 ± 0.149
AP (mg/kg)	1.643 ± 0.466b	4.091 ± 3.254ab	7.811 ± 4.995a	10.4 ± 2.171ab
TK (g/kg)	34.665 ± 2.092b	34.54 ± 2.166ab	36.125 ± 2.107ab	37.359 ± 3.335a
AK (mg/kg)	67.669 ± 13.057	69.092 ± 11.91	68.968 ± 11.996	59.961 ± 0.743

Different lowercase letters indicate differences among different treatments (ANOVA and Duncan's test ($p < 0.05$) or Kruskal–Wallis test ($p < 0.05$)). pH, hydrogen ion concentration index; SMC, soil moisture content; TOM, total organic matter; TN, total nitrogen; AHN, alkali-hydrolyzable nitrogen; NN, nitrate nitrogen; AN, ammonia nitrogen; TP, total phosphorus; AP, available phosphorus; TK, total potassium; AK, available potassium.

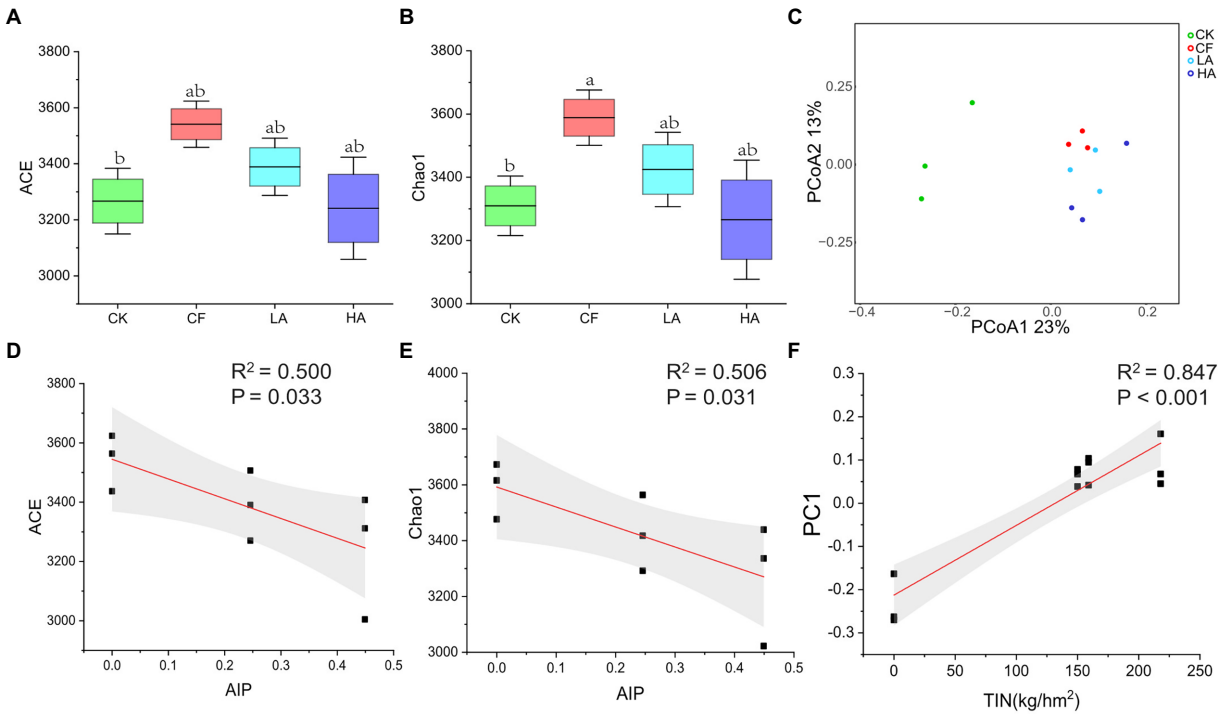

FIGURE 1
Soil bacterial community diversity and structure among different fertilization treatments. **(A)** Chao1 index of the bacterial community. **(B)** ACE index of the bacterial community. **(C)** ß-Diversity of the bacterial community. **(D)** Correlation analysis between AIP and Chao1. **(E)** Correlation analysis between AIP and ACE. **(F)** Correlation analysis between total inorganic N (kg/hm2) and ß-diversity. Different labeled letters indicate significant differences between different treatments according to one-way ANOVA with Duncan's multiple range tests ($p<0.05$).

Correlations between environmental factors and bacterial community

Redundancy analysis was performed to reveal the effects of environmental factors on all bacterial ASVs (Figure 2A), and hierarchical partitioning was used to obtain the explanation rate of each explanatory variable (Lai et al., 2022). The first two axes of the redundancy analysis accounted for 45.59% of the total variation in the bacterial community (PC1 = 27.22%, PC2 = 28.37%). The hierarchical partitioning

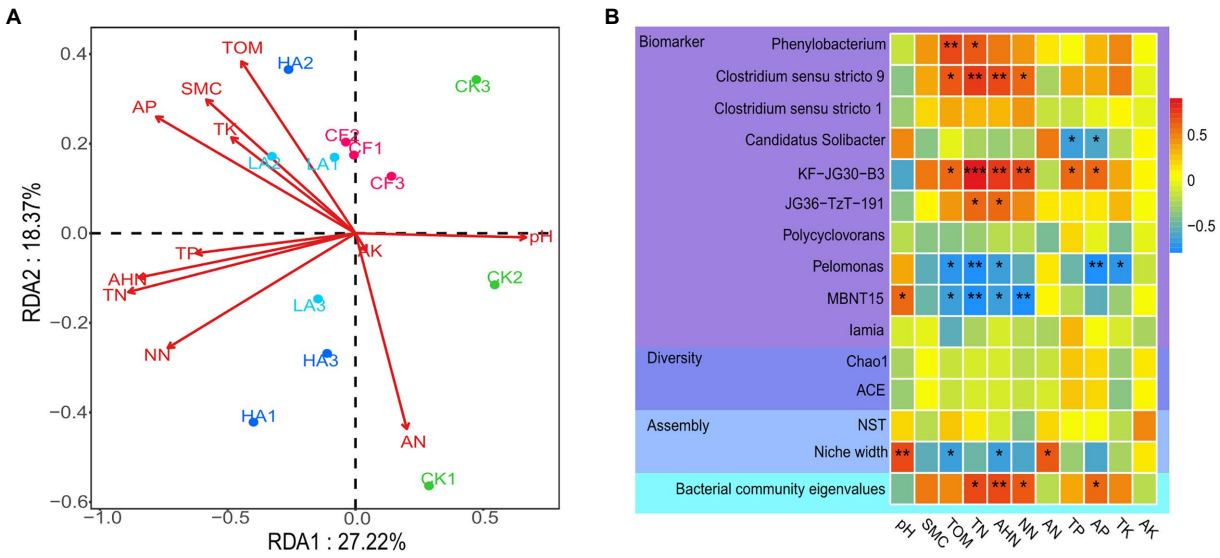

FIGURE 2
Relationships between the soil bacterial community and environmental factors. **(A)** Redundancy analysis between soil microorganisms and environmental factors. **(B)** Spearman correlation heatmaps of environmental factors and bacterial diversity, dominant genera, and bacterial community assembly. Red represents a positive correlation, and blue represents a negative correlation.

analysis showed that among all environmental factors, AP (explanation rate = 12.55%) had the greatest influence on the bacterial community structure, followed by TN (explanation rate = 10.20%) and AHN (explanation rate = 10.20%; Supplementary Table S4). At the genus level, biomarkers that showed significant differences in the abundance between the different treatments were identified using the nonparametric factorial Kruskal–Wallis sum-rank test and linear discriminant analysis (LDA > 2.0; Liu et al., 2021). Spearman correlation analysis was performed to further characterize the relationships between biomarkers, bacterial diversity, bacterial community assembly, bacterial community eigenvalues, and environmental factors. Spearman correlations showed that TOM, TN, AHN, and NN had a significant positive correlation with *Clostridium sensu stricto 9*, *JG36-TzT-191*, and *KF-JG30-B3,* and a significant negative correlation with *MBNT15* ($p < 0.05$). TP and AP had a significant positive correlation with *KF-JG30-B3*, and a significant negative correlation with *Candidatus* Solibacter ($p <$ 0.05). Furthermore, bacterial α-diversity (ACE and Chao1) and normalized stochasticity ratio (NST) did not show a significant relationship with each environmental factor. However, the niche width of the bacterial community was significantly positively correlated with pH and AN and negatively correlated with TOM and AHN. The content of AP, TN, AHN, and NN in soil was the most strongly correlated with bacterial community eigenvalues, which was consistent with the hierarchical partitioning analysis result (Figure 2B).

Construction of ecological clusters

Ecological clusters represent important ecological units that provide the opportunity to identify the highly connected and identifiable taxa (Heleno et al., 2012; Guidi et al., 2016; Fan et al., 2021). Here, WGCNA was applied to the relative abundance tables of prokaryotes, and the bacterial community was divided into 15 ecological clusters (Figure 3A). Pearson correlation analysis was performed to further investigate the relationships within different ecological clusters and between ecological clusters and physicochemical factors (Figures 3B, C). Two ecological clusters (MEturquoise and MEgreen) were strongly correlated with N levels in soil, with MEturquoise showing a significant positive correlation and MEgreen showing a significant negative correlation with soil N levels. Pearson correlation analysis between different ecological clusters showed that these two modules were significantly negatively correlated. The circular heatmap shows the distribution of the relative abundance of bacteria in MEturquoise and MEgreen across treatments. The relative abundance of bacteria in MEturquoise was lower in the *A. sinicus* return treatments (LA and HA), whereas the relative abundance of bacteria in MEturquoise was higher in the *A. sinicus* return treatments (Figures 3D, E). We then analyzed the species composition of the two ecological clusters and found that the bacteria were mainly from the phyla Proteobacteria, Acidobacteria, Myxococcota, Chloroflexi, Bacteroides, and Verrucomicrobia. Acidobacteria had the highest relative abundance in MEgreen, and Proteobacteria had the highest relative abundance in MEturquoise (Figure 3F).

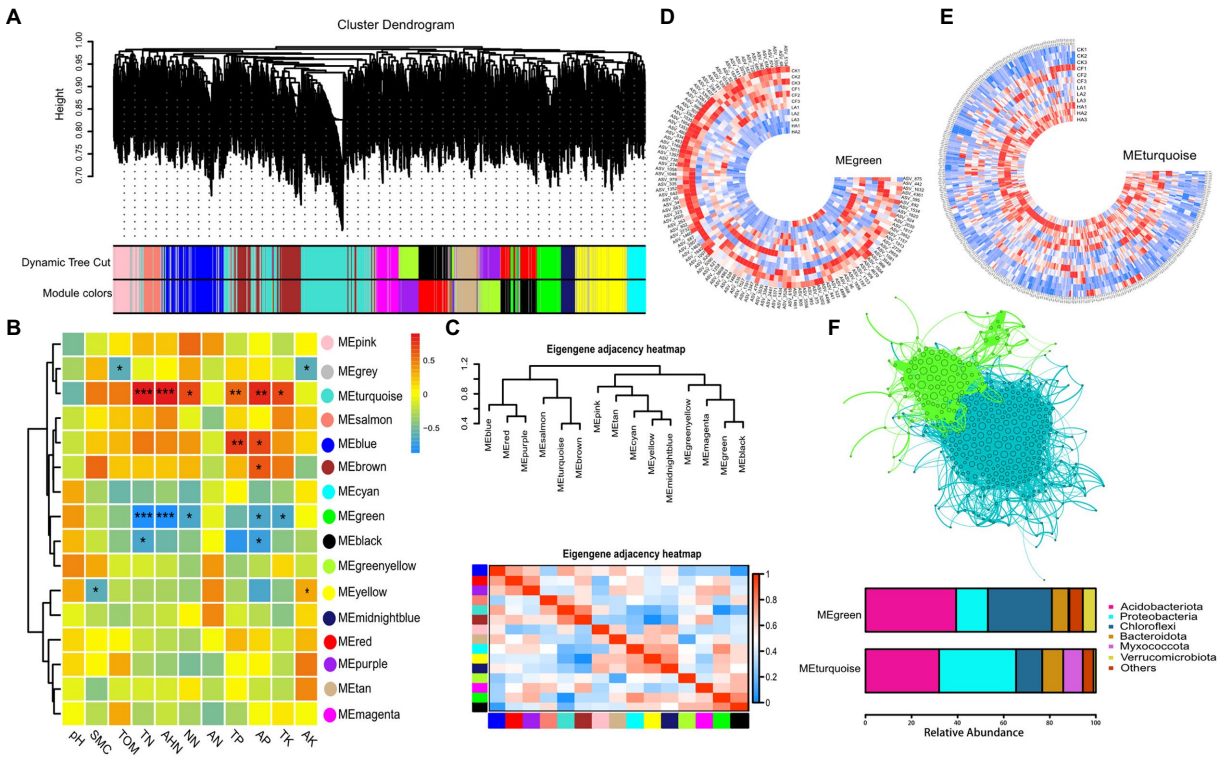

FIGURE 3
Ecological clusters generated by WGCNA. **(A)** WGCNA module plot. Dynamic tree cut represents initial clusters. Module colors represent final clusters. Each branch in the hierarchical tree or each vertical line in color bars represents one gene. Genes not attributed to any module are colored gray. **(B)** Pearson correlation heatmap between ecological clusters and physicochemical factors. **(C)** Pearson correlation heatmap between different ecological clusters. **(D)** Distribution of MEgreen in each treatment. Each color represents one module. **(E)** Distribution of MEturquoise in each treatment. **(F)** Network and species composition of MEgreen and MEturquoise.

Assembly mechanisms of the bacterial community

NST of all ASVs did not differ significantly in different treatments; thus, we further investigated NST of abundant ASVs (relative abundance ≥1% in all samples), rare ASVs (relative abundance <0.01% in all samples), MEturquoise, and MEgreen. The results indicated that NST of rare ASVs was higher than that of abundant ASVs, which meant that rare ASVs were more inclined to stochastic assembly. In contrast, deterministic processes contributed more to the assembly of abundant ASVs. NST of abundant and rare ASVs showed opposite variation trends, which explained why NST of all ASVs did not differ significantly. The LA and HA treatments decreased NST of abundant ASVs, rare ASVs, MEturquoise, and MEgreen. This, to some extent, implies that the stochastic assembly of rare and abundant ASVs in soil could be reduced by *A. sinicus* return to fields (Figure 4).

Functional genes of ecological clusters

Functional annotation of prokaryotic taxa (FAPROTAX) is widely used for predicting functional profiles of biogeochemical cycling processes (especially C, H, N, P, and S cycling) in environmental samples (Xu et al., 2021; Sun et al., 2023). In this study, FAPROTAX was used to predict the function of key soil ecological clusters (MEturquoise and MEgreen). The relative abundance of denitrification function of MEturquoise significantly varied (Figure 5A), whereas the relative abundance of N fixation function did not vary significantly. The relative abundance of N fixation function of MEgreen significantly varied among treatments (Figure 5B). The results of the functional analysis showed that treatment without any fertilizer addition (CK) had the lowest relative abundance of denitrification function of MEturquoise and had the highest relative abundance of N fixation function of MEgreen (Figures 5A, B). Compared with CK, the relative abundance of N fixation function of key ecological clusters in the CF treatment was significantly reduced, and a moderate amount of *A. sinicus* returned to the soil instead of chemical fertilizer could effectively alleviate this process. The HA treatment caused a significant increase in the relative abundance of denitrification function of MEturquoise and a significant decrease in the relative abundance of N fixation function of MEgreen. A moderate amount of *A. sinicus* returned to the soil is more beneficial for key ecological clusters to increase the relative abundance of soil N retention function.

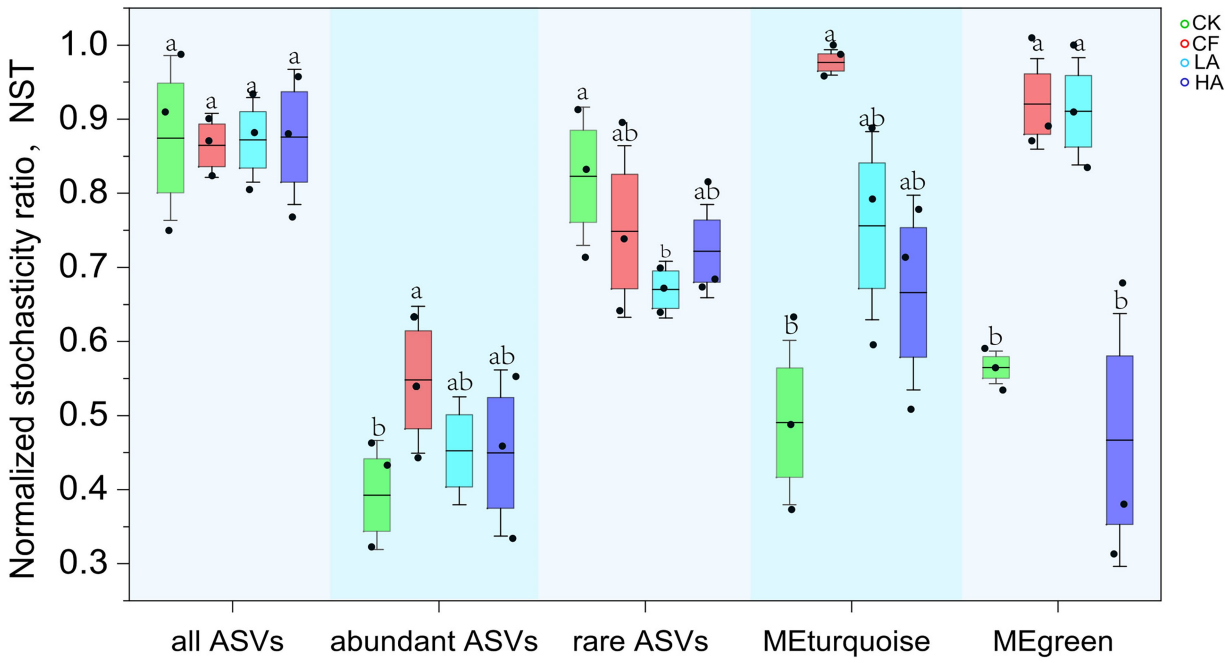

FIGURE 4
Normalized stochasticity ratio of all ASVs, abundant ASVs, rare ASVs, MEturquoise, and MEgreen in different treatments. Different labeled letters indicate significant differences between different treatments according to one-way ANOVA with Duncan's multiple range tests (p<0.05).

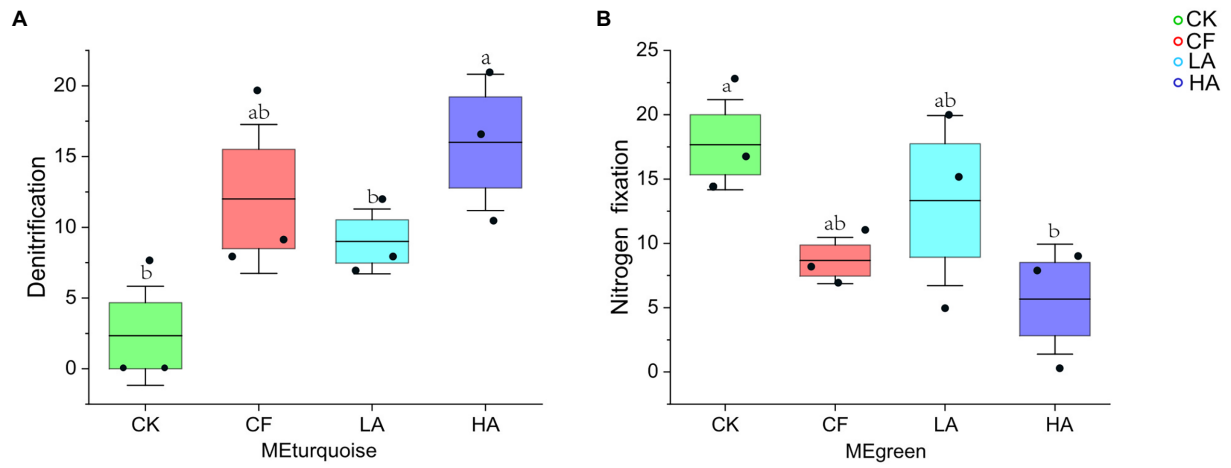

FIGURE 5
Functional abundance of ecological clusters. **(A)** Abundance of denitrification function in MEturquoise. **(B)** Abundance of N fixation function in MEgreen. Different labeled letters indicate significant differences between different treatments according to one-way ANOVA with Duncan's multiple range tests (p<0.05).

Discussion

Astragalus sinicus is widely considered a well-established resource of organic fertilizer with high N content, and its partial replacement of chemical fertilizers can help improve the soil N pool (Yang W. et al., 2022), which was corroborated in this study. Partial replacement of chemical fertilizers by *A. sinicus* significantly increased soil *N* levels (TN, AHN, and AN) in

addition to causing a significant increase in physicochemical indicators such as AP in soil. Increasing soil N and P levels is considered effective in improving crop yield and quality (Table 1; van Bruggen et al., 2015; Song et al., 2022). Although extensive *A. sinicus* returned to the soil plays an important role in improving soil nutrients, previous studies still poorly understood the changes in the bacterial community. Therefore, we focused on the effects of *A. sinicus* on the soil bacterial community, soil key ecological clusters, and functional abundance.

Microbial diversity is an essential feature of soil ecosystems, as microorganisms play a crucial role in nutrient cycling and maintenance of soil structure (Dai et al., 2018). The biodiversity of key ecological clusters was found to determine crop production in a 35-year fertilization experiment (Fan et al., 2021). Replacing chemical fertilizers with *A. sinicus* could lead to a decrease in α-diversity of the soil bacterial community (Figure 1) and an increase in the relative abundance of Proteobacteria (Supplementary Table S3). This conclusion was similarly confirmed by a previous meta-analysis, which concluded that N fertilizer application reduced bacterial diversity in global agroecosystems and favored the growth of Proteobacteria (Dai et al., 2018). Furthermore, the relative abundance of Acidobacteria was the highest in the CK treatment, which might be because of the oligotrophic state of the soil. These oligotrophic bacteria are thought to have the potential ability to break down nutrient-poor and refractory substrates, thereby promoting the growth of copiotrophic bacteria such as Alphaproteobacteria (Zhou et al., 2015). This also implies that *A. sinicus* returned to the soil may have shifted microbial life-history strategies, which transitioned from the K-strategy to the r-strategy (Shi et al., 2022). Therefore, the changes in the soil environment brought about by *A. sinicus* preferentially supported the growth of copiotrophic bacteria (e.g., some Proteobacteria) rather than oligotrophic bacteria (e.g., some Acidobacteria).

Soil physicochemical properties have long been recognized as important mediating factors in agricultural management (e.g., fertilization regimes) affecting soil microbial N response processes. Soil physicochemical conditions and N cycling processes of soil microorganisms are closely related. Compared with acidic and alkaline soils, neutral soils are of great positive significance for N-fixing microbial community structure stability and connectivity (Fan et al., 2018). Structural equation model analysis showed that soil total N and pH could indirectly regulate the primary N fixation rate and nitrification of soils by affecting soil microbial biomass C and increasing soil microbial biomass N, respectively (Lugtenberg, 2015). For denitrification, a high soil C/N content could promote the reduction of NO_3^- to NH_4^+, while suppressing the N flow during denitrification to reduce soil N loss (Putz et al., 2018). The N content of soils is a good predictor of the soil denitrification function and volatilization of soil NH_3 (Li Z. et al., 2022). Among the numerous soil physicochemical factors, some indicators (e.g., pH, N content) exhibited stronger influences on soil microbial N cycling process. Soil microbial communities are closely related to soil health, and the diversity and composition of microbial communities, in turn, can be largely influenced by environmental factors (Li M. et al., 2022). Therefore, it is important to study the relationship between microbial communities and environmental factors. Hierarchical partitioning can be used to solve the problem of covariance to obtain the contribution of individual explanatory variables to response variables (Lai et al., 2022). In hierarchical partitioning, N levels (TN, AHN, and NN) and AP in soil had the highest explanation rates for the bacterial community (Supplementary Table S4), implying that these indicators may be important environmental factors influencing the community structure. N and P are important environmental factors regulating the structure of soil microbial communities in rice fields, which have been widely verified in previous studies (Dong et al., 2014; Wang et al., 2021).

Ecological clusters are considered important ecological units, and microorganisms in the same ecological cluster have strong co-occurrence relationships, which provides an opportunity to investigate and explore highly related taxa within the total microbial community (Fan et al., 2021). Key ecological clusters are closely associated with ecosystems (de Menezes et al., 2015). To further investigate if ecological clusters of the bacterial community are more closely related to the soil environment, we applied the systems biology approach WGCNA to detect significant associations between the soil microbiome data and physicochemical factors. This method delineates clusters that are most associated with physicochemical factors (Langfelder and Horvath, 2008; Heleno et al., 2012; Guidi et al., 2016). Briefly, the WGCNA approach constructed a network and then clustered the network into modules (hereafter ecological clusters) that can be examined to find important ecological cluster–feature relationships (de Menezes et al., 2015). In this study, WGCNA was used to classify the bacterial community into 15 ecological clusters (Figure 3A). We found two ecological clusters (MEturquoise and MEgreen) that were most strongly correlated with soil N levels, with MEturquoise showing a significant positive correlation and MEgreen showing a significant negative correlation with soil N levels (Figure 3B). MEturquoise and MEgreen mainly contain Acidobacteria, Proteobacteria, and Chloroflexi (Figure 3F). We found a higher relative abundance of Proteobacteria in MEturquoise compared to MEgreen, which implies that *A. sinicus* returned to the soil may have shifted bacterial life-history strategies. The importance of these two ecological clusters among different treatments was further confirmed by partial least squares-discriminant analysis (Supplementary Table S5). In addition, the relative abundance of MEturquoise in soil gradually increased and that of MEgreen gradually decreased as the amount of *A. sinicus* returned to the soil increased (Figures 3D, E). This indicates that *A. sinicus* contributes to the growth of MEturquoise bacteria but inhibits the growth of MEgreen bacteria.

Investigating how microbial communities are assembled is crucial for understanding the response processes of microbial communities under organic substitution (Ning et al., 2020; Jiao et al., 2022). NST was used to quantify the extent of the

contribution of stochastic assembly processes in the assembly of the bacterial community under different fertilizer application measures (Ning et al., 2019). Stochastic assembly is the dominant process driving the assembly of the entire soil bacterial community in our study. A higher contribution of stochastic assembly processes promotes the positive effect of microbial community diversity on multifunctionality (Li et al., 2021; Zhou et al., 2022). We further found that NST of rare ASVs was higher than that of abundant ASVs, implying that rare ASVs were more inclined to stochastic assembly processes. In contrast, the deterministic assembly process contributes more to the assembly of abundant ASVs. NSTs of abundant and rare ASVs showed opposite trends. The two parts of all ASVs (abundant and rare) reflected opposite trends, partially explaining why there was no significant difference in NST of total ASVs. Compared with the CF treatment, the *A. sinicus* return treatments (LA and HA) reduced NST of rare taxa, abundant taxa, MEturquoise, and MEgreen. This implies that the stochastic assembly process in the clusters could be reduced by *A. sinicus*. The relative contribution of deterministic and stochastic assembly processes may be related to the niche width of microbial communities. Microbial communities with larger niche widths may have greater metabolic plasticity and can utilize resources in the environment in a more balanced manner, less affecting the microbial communities by deterministic assembly processes (Chen et al., 2021). In addition, the contribution of processes such as homogeneous selection, heterogeneous selection, homogenizing dispersal, dispersal limitation, and 'drift' to the assembly process can be considered (Ning et al., 2020). Thus, we explored the factors that may contribute to differences in the stochastic assembly process between treatments by iCAMP analysis, but there was no significant variation in these indicators between treatments (Supplementary Table S6).

Microorganisms are important players influencing the biogeochemical N cycle (Guidi et al., 2016). Denitrification is one of the important biological processes for the removal of N in the biosphere. Denitrification by microorganisms dominates N loss in ecosystems and that N loss in soils due to denitrification cannot be ignored (Fang et al., 2015; Pan et al., 2022). Biological N fixation is a crucial ecological process and fixes up to 100 Tg N $year^{-1}$ from the atmosphere on a global scale (Fan et al., 2019). Both denitrification function and N fixation function of microorganisms participate in determining the retention and removal of N in soil. We found that not all bacteria in ecological clusters significantly associated with the soil N level had N-related functions. Combined with the strong co-occurrence of bacteria in ecological clusters, we speculate whether there are "functional helpers" in the same ecological cluster that do not have the corresponding functions in the N cycle but can help N-cycling microorganisms to perform their functions and change the relative abundance of functional bacteria or influence their functions. The concept of microbial helpers has been mentioned in recent studies (Pan et al., 2022). However, the presence of functional helpers in the N cycle needs to be investigated and verified in more depth.

The application type of fertilizer can greatly affect the N response patterns of soil microorganisms (Lehnert et al., 2021). Compared with only N fertilization, N-P-K mixed fertilization can effectively alleviate the negative effect of N fertilization on soil bacterial diversity and is beneficial in promoting the mutualistic relationship between microorganisms and plants (Dai et al., 2018). In addition, straw returning is a common strategy to replace chemical fertilizers in agricultural systems and is essential for modulating the N response of the microbial community of agricultural systems. Straw return to fields can promote microbial contributions to soil N accumulation (Xia et al., 2021). Organic manure replacement mediated the contribution of soil microbial residues to the maintenance of soil N pools and enhanced soil microbial N fixation capacity, while competitively suppressing nitrification and reducing the risk of N loss (Ma et al., 2022). Thus, the type of fertilization largely influenced the N response processes of soil microbial communities and caused significant differences in the microbial communities in various ecosystems (Lugtenberg, 2015). Combined with these findings, the high N environment of the soil caused by returning *A. sinicus* might have caused the regulation of key ecological clusters for influencing the soil N content. Among all treatments, the CK treatment had the highest relative abundance of N fixation function of key ecological clusters, and when fertilizer was added to the soil, we found a significant increase in the relative abundance of the denitrification function and a significant decrease in the relative abundance of N fixation function of key ecological clusters, implying that the addition of fertilizer reduced the relative abundance of N fixation function of key ecological clusters. We continued to focus on the LA treatment and found that the application of a moderate amount of *A. sinicus* partially replacing chemical fertilizers could effectively alleviate the decrease in the relative abundance N fixation function of key ecological clusters. In contrast, if we continued to apply large amounts of *A. sinicus* to the field, the relative abundance in key soil ecological clusters (MEturquoise and MEgreen) for denitrification function was higher than the CF treatment, whereas that for N fixation function was lower than the CF treatment. This implies that a moderate amount of *A. sinicus* returned to the soil may be more beneficial for the key ecological clusters to maintain the soil N content, whereas a large amount of *A. sinicus* returned to the soil may promote N loss from the soil. In addition, these findings may explain, to some extent, why the TN content of LA and HA treatments significantly differed, whereas the NN content did not differ significantly. This may be because the HA treatment enriched the denitrification function, which promoted the conversion of NN to the other N forms. Previous studies using isotope labeling have observed that compared with chemical fertilizers, *A. sinicus* can significantly enhance the soil N pool to supply nutrients for the next crop round (Zhu et al., 2014; Yang W. et al., 2022). However, the fraction of N fertilizer inputs to the agroecosystem that exceeds the appropriate amount may have a significant impact on N emissions without contributing significantly to crop yield, which exacerbates global climate warming and ozone depletion (Rosas

et al., 2015; Lehnert et al., 2021). A recent global meta-analysis showed that the increase in temperature changes the N cycle from microbial immobilization to nitrification and denitrification (Dai et al., 2020; Sun et al., 2022). This should make us realize that greenhouse gas emissions due to unreasonable farmland management will influence the N response of soil microorganisms, which may further promote the increase in NO_2 emission factors and cause more serious N loss. The accumulative effect of this continuous cycling undoubtedly brings great pressure to the maintenance of the N fixation function of terrestrial ecosystems.

In brief, our study revealed the N response patterns of soil key ecological bacterial clusters in rice field ecosystems. In addition, it is worth noting that some recent studies have demonstrated that some beneficial soil fungi, such as arbuscular mycorrhizal fungi, can obtain NO_3^-, NH_4^+ and organic N from the surrounding soil and contribute to rice biomass (Panneerselvam et al., 2017; Wang et al., 2020; Das et al., 2022). These studies enlighten future research of plant-microbial interactions in rice field ecosystems. How to further optimize the ratio and input strategy of organic and inorganic fertilizers and find a good balance between fertilizer input benefit and ecological safety remains an extremely important research topic.

Conclusion

This study focused on the response patterns of the soil bacterial community (especially key ecological clusters) to the *A. sinicus* returned to the soil. Soil N levels and AP were important environmental factors affecting the soil bacterial community in this study. We identified key ecological clusters (MEturquoise and MEgreen) by WGCNA. Partial replacement of fertilizer by *A. sinicus* had no effect on the assembly process of total ASVs ($p > 0.05$) but significantly enhanced the deterministic assembly process of abundant ASVs, rare ASVs, MEturquoise, and MEgreen ($p < 0.05$). The partial replacement of chemical fertilizers by moderate amounts of *A. sinicus* effectively mitigated the decrease in the relative abundance of N fixation function of key ecological clusters caused by chemical fertilizer application. However, an excessive amount of *A. sinicus* returned to the soil resulted in a significant increase in the relative abundance of denitrification function and a significant decrease in the relative abundance of N fixation function in key ecological clusters. In conclusion, our results imply that a moderate amount of *A. sinicus* returned to the soil can effectively mitigate the trend of reduced relative abundance of N fixation function of key ecological clusters caused by chemical fertilizer application.

Data availability statement

The datasets presented in this study can be found in online repositories. The names of the repository/repositories and accession number(s) can be found at: https://www.ncbi.nlm.nih.gov/, PRJNA889571.

Author contributions

JC, CX, and ML contributed to conception and design of the study. ML and YW performed the statistical analysis. WCS and WFS provided advice and guidance on the idea of bioinformatics analysis. XC and WQ participated in the sample collection. ML wrote the first draft of the manuscript. All authors contributed to the manuscript revision, read, and approved the submitted version.

Funding

This study was funded by the National Key Research and Development Program of China (2021YFD1700203), the National Natural Science Foundation of China (31860592), the Innovation Fund of Jiangxi Academy of Agricultural Sciences, China (20182CBS002 and JXXTCXQN202008), and the National Industrial Technology System of Green Manure (CARS-22-Z-06).

Acknowledgments

We would like to thank TopEdit (www.topeditsci.com) for linguistic assistance during the preparation of this manuscript.

Conflict of interest

The authors declare that the research was conducted in the absence of any commercial or financial relationships that could be construed as a potential conflict of interest.

Publisher's note

Supplementary material

The Supplementary material for this article can be found online at: https://www.frontiersin.org/articles/10.3389/fmicb.2022.1067939/full#supplementary-material

References

Bolyen, E., Rideout, J. R., Dillon, M. R., Bokulich, N. A., Abnet, C. C., Al-Ghalith, G. A., et al. (2019). Reproducible, interactive, scalable and extensible microbiome data science using QIIME 2. *Nat. Biotechnol.* 37, 852–857. doi: 10.1038/s41587-019-0209-9

Cai, Y., Peng, C., Qiu, S., Li, Y., and Gao, Y. (2011). Dichromate digestion–spectrophotometric procedure for determination of soil microbial biomass carbon in association with fumigation–extraction. *Commun. Soil Sci. Plant Anal.* 42, 2824–2834. doi: 10.1080/00103624.2011.623027

Callahan, B. J., McMurdie, P. J., Rosen, M. J., Han, A. W., Johnson, A. J. A., and Holmes, S. P. (2016). DADA2: high-resolution sample inference from Illumina amplicon data. *Nat. Methods* 13, 581–583. doi: 10.1038/nmeth.3869

Cawse, P. A. (1967). The determination of nitrate in soil solutions by ultraviolet spectrophotometry. *Analyst* 92:311. doi: 10.1039/an9679200311

Chen, Q.-L., Hu, H.-W., Yan, Z.-Z., Li, C.-Y., Nguyen, B.-A. T., Sun, A.-Q., et al. (2021). Deterministic selection dominates microbial community assembly in termite mounds. *Soil Biol. Biochem.* 152:108073. doi: 10.1016/j.soilbio.2020.108073

Chen, T., Liu, Y., and Huang, L. (2022). ImageGP: an easy-to-use data visualization web server for scientific researchers. *iMeta* 1:1. doi: 10.1002/imt2.5

Cheng, B., Jiang, Y., and Cao, C. (2021). Balance rice yield and eating quality by changing the traditional nitrogen management for sustainable production in China. *J. Clean. Prod.* 312:127793. doi: 10.1016/j.jclepro.2021.127793

Coleman, N. T., Williams, D. E., Nielsen, T. R., and Jenny, H. (1951). On the validity of interpretations of Potentiometrically measured soil pH. *Soil Sci. Soc. Am. J.* 15, 106–114. doi: 10.2136/sssaj1951.036159950015000C0022x

Craft, C. B., Seneca, E. D., and Broome, S. W. (1991). Loss on ignition and Kjeldahl digestion for estimating organic carbon and Total nitrogen in estuarine marsh soils: calibration with dry combustion. *Estuaries* 14:175. doi: 10.2307/1351691

Dai, Z., Su, W., Chen, H., Barberán, A., Zhao, H., Yu, M., et al. (2018). Long-term nitrogen fertilization decreases bacterial diversity and favors the growth of *Actinobacteria* and Proteobacteria in agro-ecosystems across the globe. *Glob. Change Biol.* 24, 3452–3461. doi: 10.1111/gcb.14163

Dai, Z., Yu, M., Chen, H., Zhao, H., Huang, Y., Su, W., et al. (2020). Elevated temperature shifts soil N cycling from microbial immobilization to enhanced mineralization, nitrification and denitrification across global terrestrial ecosystems. *Glob. Change Biol.* 26, 5267–5276. doi: 10.1111/gcb.15211

Das, D., Paries, M., Hobecker, K., Gigl, M., Dawid, C., Lam, H.-M., et al. (2022). Phosphate starvation response transcription factors enable arbuscular mycorrhiza symbiosis. *Nat. Commun.* 13:477. doi: 10.1038/s41467-022-27976-8

de Menezes, A. B., Prendergast-Miller, M. T., Richardson, A. E., Toscas, P., Farrell, M., Macdonald, L. M., et al. (2015). Network analysis reveals that bacteria and fungi form modules that correlate independently with soil parameters: network analysis of microbial community structure. *Environ. Microbiol.* 17, 2677–2689. doi: 10.1111/1462-2920.12559

De Silva, C. S., Koralage, I. S. A., Weerasinghe, P., and Silva, N. R. N. (2015). The determination of available phosphorus in soil: a quick and simple method. *OUSL J.* 8:1. doi: 10.4038/ouslj.v8i0.7315

Dong, W.-Y., Zhang, X.-Y., Dai, X.-Q., Fu, X.-L., Yang, F.-T., Liu, X.-Y., et al. (2014). Changes in soil microbial community composition in response to fertilization of paddy soils in subtropical China. *Appl. Soil Ecol.* 84, 140–147. doi: 10.1016/j.apsoil.2014.06.007

Fan, K. (2019). Suppressed N fixation and diazotrophs after four decades of fertilization. *Microbiome* 7:143. doi: 10.1186/s40168-019-0757-8

Fan, K., Delgado-Baquerizo, M., Guo, X., Wang, D., Zhu, Y., and Chu, H. (2021). Biodiversity of key-stone phylotypes determines crop production in a 4-decade fertilization experiment. *ISME J.* 15, 550–561. doi: 10.1038/s41396-020-00796-8

Fan, K., Weisenhorn, P., Gilbert, J. A., Shi, Y., Bai, Y., and Chu, H. (2018). Soil pH correlates with the co-occurrence and assemblage process of diazotrophic communities in rhizosphere and bulk soils of wheat fields. *Soil Biol. Biochem.* 121, 185–192. doi: 10.1016/j.soilbio.2018.03.017

Fang, Y., Koba, K., Makabe, A., Takahashi, C., Zhu, W., Hayashi, T., et al. (2015). Microbial denitrification dominates nitrate losses from forest ecosystems. *Proc. Natl. Acad. Sci. U. S. A.* 112, 1470–1474. doi: 10.1073/pnas.1416776112

Garzón, E., González-Andrés, F., García-Martínez, V. M., and de Paz, J. M. (2011). Mineralization and nutrient release of an organic fertilizer made by flour, meat, and crop residues in two vineyard soils with different pH levels. *Commun. Soil Sci. Plant Anal.* 42, 1485–1496. doi: 10.1080/00103624.2011.581719

Guidi, L., Chaffron, S., Bittner, L., Eveillard, D., Larhlimi, A., Roux, S., et al. (2016). Plankton networks driving carbon export in the oligotrophic ocean. *Nature* 532, 465–470. doi: 10.1038/nature16942

Hald, P. M., and Mason, W. B. (1958). "Sodium and potassium by flame photometry" in *Standard Methods of Clinical Chemistry* (Amsterdam: Elsevier), 165–185.

Heleno, R., Devoto, M., and Pocock, M. (2012). Connectance of species interaction networks and conservation value: is it any good to be well connected? *Ecol. Indic.* 14, 7–10. doi: 10.1016/j.ecolind.2011.06.032

Jia, X., Yang, Q., Dong, S.-T., Zhang, J.-W., Zhao, B., and Liu, P. (2020). Using manure for improving nitrogen fertilization and maize yield. *Exp. Agric.* 56, 901–914. doi: 10.1017/S0014479720000393

Jiao, S., Chu, H., Zhang, B., Wei, X., Chen, W., and Wei, G. (2022). Linking soil fungi to bacterial community assembly in arid ecosystems. *iMeta* 1:e2. doi: 10.1002/imt2.2

Kanda, J. (1995). Determination of ammonium in seawater based on the indophenol reaction with o-phenylphenol (OPP). *Water Res.* 29, 2746–2750. doi: 10.1016/0043-1354(95)00149-F

Kusano, M., Yang, Z., Okazaki, Y., Nakabayashi, R., Fukushima, A., and Saito, K. (2015). Using Metabolomic approaches to explore chemical diversity in Rice. *Mol. Plant* 8, 58–67. doi: 10.1016/j.molp.2014.11.010

Kuypers, M. M. M., Marchant, H. K., and Kartal, B. (2018). The microbial nitrogen-cycling network. *Nat. Rev. Microbiol.* 16, 263–276. doi: 10.1038/nrmicro.2018.9

Lai, J., Zou, Y., Zhang, J., and Peres-Neto, P. R. (2022). Generalizing hierarchical and variation partitioning in multiple regression and canonical analyses using the rdacca.Hp R package. *Methods Ecol. Evol.* 13, 782–788. doi: 10.1111/2041-210X.13800

Langfelder, P., and Horvath, S. (2008). WGCNA: an R package for weighted correlation network analysis. *BMC Bioinformatics* 9:559. doi: 10.1186/1471-2105-9-559

Lehnert, N., Musselman, B. W., and Seefeldt, L. C. (2021). Grand challenges in the nitrogen cycle. *Chem. Soc. Rev.* 50, 3640–3646. doi: 10.1039/D0CS00923G

Li, D., Ni, H., Jiao, S., Lu, Y., Zhou, J., Sun, B., et al. (2021). Coexistence patterns of soil methanogens are closely tied to methane generation and community assembly in rice paddies. *Microbiome* 9:20. doi: 10.1186/s40168-020-00978-8

Li, M., Pommier, T., Yin, Y., Wang, J., Gu, S., Jousset, A., et al. (2022). Indirect reduction of *Ralstonia solanacearum* via pathogen helper inhibition. *ISME J.* 16, 868–875. doi: 10.1038/s41396-021-01126-2

Li, Z., Tang, Z., Song, Z., Chen, W., Tian, D., Tang, S., et al. (2022). Variations and controlling factors of soil denitrification rate. *Glob. Chang. Biol.* 28, 2133–2145. doi: 10.1111/gcb.16066

Liu, J., Shu, A., Song, W., Shi, W., Li, M., Zhang, W., et al. (2021). Long-term organic fertilizer substitution increases rice yield by improving soil properties and regulating soil bacteria. *Geoderma* 404:115287. doi: 10.1016/j.geoderma.2021.115287

Lugtenberg, B. Ed. (2015). *Principles of Plant-Microbe Interactions*. Cham: Springer International Publishing. doi: 10.1007/978-3-319-08575-3

Ma, X., Zhang, W., Zhang, X., Bao, X., Xie, H., Li, J., et al. (2022). Dynamics of microbial necromass in response to reduced fertilizer application mediated by crop residue return. *Soil Biol. Biochem.* 165:108512. doi: 10.1016/j.soilbio.2021.108512

Ning, D., Deng, Y., Tiedje, J. M., and Zhou, J. (2019). A general framework for quantitatively assessing ecological stochasticity. *Proc. Natl. Acad. Sci. U. S. A.* 116, 16892–16898. doi: 10.1073/pnas.1904623116

Ning, D., Yuan, M., Wu, L., Zhang, Y., Guo, X., Zhou, X., et al. (2020). A quantitative framework reveals ecological drivers of grassland microbial community assembly in response to warming. *Nat. Commun.* 11:4717. doi: 10.1038/s41467-020-18560-z

Oladele, S. O., Adeyemo, A. J., and Awodun, M. A. (2019). Influence of rice husk biochar and inorganic fertilizer on soil nutrients availability and rain-fed rice yield in two contrasting soils. *Geoderma* 336, 1–11. doi: 10.1016/j.geoderma.2018.08.025

Pan, B., Xia, L., Lam, S. K., Wang, E., Zhang, Y., Mosier, A., et al. (2022). A global synthesis of soil denitrification: driving factors and mitigation strategies. *Agric. Ecosyst. Environ.* 327:107850. doi: 10.1016/j.agee.2021.107850

Panneerselvam, P., Kumar, U., Sugitha, T. C. K., Parameswaran, C., Sahoo, S., Binodh, A. K., et al. (2017). "Arbuscular mycorrhizal fungi (AMF) for sustainable Rice production" in *Advances in Soil Microbiology: Recent Trends and Future Prospects Microorganisms for Sustainability*. eds. T. K. Adhya, B. B. Mishra, K. Annapurna, D. K. Verma and U. Kumar (Singapore: Springer Singapore), 99–126.

Putz, M., Schleusner, P., Rütting, T., and Hallin, S. (2018). Relative abundance of denitrifying and DNRA bacteria and their activity determine nitrogen retention or loss in agricultural soil. *Soil Biol. Biochem.* 123, 97–104. doi: 10.1016/j.soilbio.2018.05.006

Qian, C., Yu, Y., Gong, X., Jiang, Y., Zhao, Y., Yang, Z., et al. (2016). Response of grain yield to plant density and nitrogen rate in spring maize hybrids released from 1970 to 2010 in Northeast China. *Crop J.* 4, 459–467. doi: 10.1016/j.cj.2016.04.004

Rahman, M. M. (2021). Effect of pesticides and chemical fertilizers on the nitrogen cycle and functional microbial communities in Paddy soils: Bangladesh perspective. *Bull. Environ. Contam. Toxicol.* 106, 243–249. doi: 10.1007/s00128-020-03092-5

Rosas, F., Babcock, B. A., and Hayes, D. J. (2015). Nitrous oxide emission reductions from cutting excessive nitrogen fertilizer applications. *Clim. Chang.* 132, 353–367. doi: 10.1007/s10584-015-1426-y

Shi, J., Gong, J., Li, X., Zhang, Z., Zhang, W., Li, Y., et al. (2022). Plant–microbial linkages regulate soil organic carbon dynamics under phosphorus application in a typical temperate grassland in northern China. *Agric. Ecosyst. Environ.* 335:108006. doi: 10.1016/j.agee.2022.108006

Song, W., Shu, A., Liu, J., Shi, W., Li, M., Zhang, W., et al. (2022). Effects of long-term fertilization with different substitution ratios of organic fertilizer on paddy soil. *Pedosphere* 32, 637–648. doi: 10.1016/S1002-0160(21)60047-4

Sun, M., Li, M., Zhou, Y., Liu, J., Shi, W., Wu, X., et al. (2023). Nitrogen deposition enhances the deterministic process of the prokaryotic community and increases the complexity of the microbial co-network in coastal wetlands. *Sci. Total Environ.* 856:158939. doi: 10.1016/j.scitotenv.2022.158939

Sun, Y., Wang, C., Chen, H. Y. H., Liu, Q., Ge, B., and Tang, B. (2022). A global meta-analysis on the responses of C and N concentrations to warming in terrestrial ecosystems. *Catena* 208:105762. doi: 10.1016/j.catena.2021.105762

Tong, B., Hou, Y., Wang, S., and Ma, W. (2022). Partial substitution of urea fertilizers by manure increases crop yield and nitrogen use efficiency of a wheat–maize double cropping system. *Nutr. Cycl. Agroecosyst.* 2022, 1–11. doi: 10.1007/s10705-022-10219-z

van Bruggen, A. H. C., Sharma, K., Kaku, E., Karfopoulos, S., Zelenev, V. V., and Blok, W. J. (2015). Soil health indicators and *Fusarium* wilt suppression in organically and conventionally managed greenhouse soils. *Appl. Soil Ecol.* 86, 192–201. doi: 10.1016/j.apsoil.2014.10.014

Wang, S., Chen, A., Xie, K., Yang, X., Luo, Z., Chen, J., et al. (2020). Functional analysis of the OsNPF4.5 nitrate transporter reveals a conserved mycorrhizal pathway of nitrogen acquisition in plants. *Proc. Natl. Acad. Sci. U. S. A.* 117, 16649–16659. doi: 10.1073/pnas.2000926117

Wang, J. L., Liu, K. L., Zhao, X. Q., Zhang, H. Q., Li, D., Li, J. J., et al. (2021). Balanced fertilization over four decades has sustained soil microbial communities and improved soil fertility and rice productivity in red paddy soil. *Sci. Total Environ.* 793:148664. doi: 10.1016/j.scitotenv.2021.148664

Wieczorek, D., Żyszka-Haberecht, B., Kafka, A., and Lipok, J. (2022). Determination of phosphorus compounds in plant tissues: from colourimetry to advanced instrumental analytical chemistry. *Plant Methods* 18:22. doi: 10.1186/s13007-022-00854-6

Xia, Y., Chen, X., Zheng, S., Gunina, A., Ning, Z., Hu, Y., et al. (2021). Manure application accumulates more nitrogen in paddy soils than rice straw but less from fungal necromass. *Agric. Ecosyst. Environ.* 319:107575. doi: 10.1016/j.agee.2021.107575

Xu, Z., Ma, Y., Zhang, L., Han, Y., Yuan, J., Li, G., et al. (2021). Relating bacterial dynamics and functions to gaseous emissions during composting of kitchen and garden wastes. *Sci. Total Environ.* 767:144210. doi: 10.1016/j.scitotenv.2020.144210

Yang, H., Li, Y., Cao, Y., Shi, W., Xie, E., Mu, N., et al. (2022). Nitrogen nutrition contributes to plant fertility by affecting meiosis initiation. *Nat. Commun.* 13:485. doi: 10.1038/s41467-022-28173-3

Yang, L., and Yang, K. (2020). Biological function of *Klebsiella variicola* and its effect on the rhizosphere soil of maize seedlings. *PeerJ* 8:e9894. doi: 10.7717/peerj.9894

Yang, W., Yao, L., Zhu, M., Li, C., Li, S., Wang, B., et al. (2022). Replacing urea-N with Chinese milk vetch (*Astragalus sinicus* L.) mitigates CH4 and N_2O emissions in rice paddy. *Agric. Ecosyst. Environ.* 336:108033. doi: 10.1016/j.agee.2022.108033

Zhao, H., Li, X., and Jiang, Y. (2019). Response of nitrogen losses to excessive nitrogen fertilizer application in intensive greenhouse vegetable. *Production* 11:1513. doi: 10.3390/su11061513

Zheng, Z., Lu, J., Su, Y., Yang, Q., Lin, Y., Liu, H., et al. (2020). Differential effects of N and P additions on foliar stoichiometry between species and community levels in a subtropical forest in eastern China. *Ecol. Indic.* 117:106537. doi: 10.1016/j.ecolind.2020.106537

Zhou, J., Guan, D., Zhou, B., Zhao, B., Ma, M., Qin, J., et al. (2015). Influence of 34-years of fertilization on bacterial communities in an intensively cultivated black soil in Northeast China. *Soil Biol. Biochem.* 90, 42–51. doi: 10.1016/j.soilbio.2015.07.005

Zhou, Z., Zheng, M., Xia, J., and Wang, C. (2022). Nitrogen addition promotes soil microbial beta diversity and the stochastic assembly. *Sci. Total Environ.* 806:150569. doi: 10.1016/j.scitotenv.2021.150569

Zhu, B., Yi, L., Hu, Y., Zeng, Z., Lin, C., Tang, H., et al. (2014). Nitrogen release from incorporated 15N-labelled Chinese milk vetch (*Astragalus sinicus* L.) residue and its dynamics in a double rice cropping system. *Plant Soil* 374, 331–344. doi: 10.1007/s11104-013-1808-8

frontiers | Frontiers in Microbiology

TYPE Original Research
PUBLISHED 05 January 2023
DOI 10.3389/fmicb.2022.1106254

OPEN ACCESS

EDITED BY
Ming Liu,
Institute of Soil Science (CAS), China

REVIWED BY
Shuhe Wei,
Institute of Applied Ecology (CAS), China
Fulai Liu,
University of Copenhagen, Denmark
Yuanwang Liu,
Yanshan University, China

*CORRESPONDENCE
Weidong Cao
✉ caoweidong@caas.cn
Hongli Fan
✉ fanhongli@caas.cn

SPECIALTY SECTION
This article was submitted to Microbe and Virus Interactions With Plants, a section of the journal Frontiers in Microbiology

RECEIVED 23 November 2022
ACCEPTED 12 December 2022
PUBLISHED 05 January 2023

CITATION
You M, Wang L, Zhou G, Wang Y, Wang K, Zou R, Cao W and Fan H (2023) Effects of microbial agents on cadmium uptake in *Solanum nigrum* L. and rhizosphere microbial communities in cadmium-contaminated soil. *Front. Microbiol.* 13:1106254. doi: 10.3389/fmicb.2022.1106254

Effects of microbial agents on cadmium uptake in *Solanum nigrum* L. and rhizosphere microbial communities in cadmium-contaminated soil

Meng You[1], Li Wang[1,2], Guopeng Zhou[1], Yikun Wang[1], Kai Wang[1], Rong Zou[1,3], Weidong Cao[1]* and Hongli Fan[1]*

[1]Key Laboratory of Plant Nutrition and Fertilizer, National Engineering Research Center of Arable Land Protection, Ministry of Agriculture and Rural Affairs, Institute of Agricultural Resources and Regional Planning, Chinese Academy of Agricultural Sciences, Beijing, China, [2]Institute of Soil and Fertilizer, Guizhou Academy of Agricultural Sciences, Guiyang, Guizhou, China, [3]College of Forestry, Guizhou University, Guiyang, Guizhou, China

Solanum nigrum L. (*S. nigrum*) and microbial agents are often used for the remediation of cadmium (Cd)-contaminated soil; however, no studies to date have examined the efficacy of using various microbial agents for enhancing the remediation efficiency of Cd-contaminated soil by *S. nigrum*. Here, we conducted greenhouse pot experiments to evaluate the efficacy of applying *Bacillus megaterium* (BM) along with citric acid (BM+CA), *Glomus mosseae* (BM+GM), and *Piriformospora indica* (BM+PI) on the ability of *S. nigrum* to remediate Cd-contaminated soil. The results showed that BM+GM significantly increased the Cd accumulation of each pot of *S. nigrum* by 104% compared with the control. Application of microbial agents changed the soil microbial communities. Redundancy analysis showed that the activities of Catalase (CAT) and urease (UE), soil organic matter, available N and total Cd were the main influencing factors. By constructing the microbial co-occurrence networks, the soil microbe was divided into four main Modules. BM+GM and BM+PI significantly increased the relative abundance of Module#1 and Module#3, respectively, when compared with the control. Additionally, Module#1 showed a significant positive correlation with translocation factor (TF), which could be regarded as the key microbial taxa. Further research found that *Ascomycota*, *Glomeromycota*, *Proteobacteria*, and *Actinobacteria* within Module#1 were also significantly correlated with TF, and these key species enriched in BM+GM. Overall, our findings indicate that the BM+GM treatment was the most effective for the remediation of Cd pollution. This treatment method may further affect the rhizosphere microbial community by affecting soil indicators, which might drive the formation of Module#1, thus greatly enhancing the Cd remediation capacity of *S. nigrum*.

KEYWORDS

phytoremediation, cadmium, *Solanum nigrum L.*, microbial agent, rhizosphere microbe

1. Introduction

Industrial activities are a major source of heavy metal (HM) pollution in farmland; mining, nickel-cadmium (Cd) battery manufacturing, and other anthropogenic activities are some of the major contributors to HM pollution, which has become a global environmental problem that affects more than 200 million hectares of arable land (Mani et al., 2015; Pramanik et al., 2018). Cd can have deleterious effects on the growth of plants, and Cd contamination can pose major risks to human health as it bioaccumulates in the food chain (Zhang et al., 2018). Cd has been classified as a hazardous chemical of global significance by the United Nations Environment Programme, and an increasing number of studies have examined the remediation of Cd-contaminated soils, especially in developing countries (Peng et al., 2014).

Physical, chemical and biological methods for remediation of cadmium pollution have various disadvantages, some of which include high costs, easy to produce secondary pollutants, and their inability to be applied for long periods (Baker et al., 2000). The phytoremediation is a cost-effective, eco-friendly and promising approach (Abdelkrim et al., 2020), this approach includes phytoextraction, rhizofiltration, phytostabilization and phytovolatilization (Saha et al., 2017). Among them, phytoextraction is based on the capacity of the roots to absorb, translocate, and concentrate toxic metals from soil to the shoot harvestable plant tissues (Girdhar et al., 2014). The use of accumulators is an effective method for the phytoextraction of HM-contaminated soils that is low-cost and environmentally friendly (Robinson et al., 1998; Fan and Zhou, 2009). *Solanum nigrum* L. (*S. nigrum*) grows rapidly and has a high reproductive capacity; its antioxidant defense system makes it highly resistant to HMs. However, some of the drawbacks of using *S. nigrum* are its long growing period and low environmental adaptability, which reduces its remediation efficiency (Wang L. et al., 2020; Khalid et al., 2021). The use of plant microbes and chelating agents along with *S. nigrum* can enhance the remediation efficiency of Cd-contaminated soil, and this approach has received increased interest from various researchers (Sheng et al., 2012).

Plant growth-promoting rhizobacteria (PGPR) are highly tolerant to Cd due to their physical isolation and detoxification capacity (Rasouli-Sadaghiani et al., 2019). When they are colonized in the rhizosphere of plants, they can assist plant to detoxify Cd by altering antioxidant enzyme activity and phytohormone secretion in plant (Ashraf et al., 2017), and promoting plant growth and development *via* nitrogen (N) fixation and siderophore production. *Bacillus megaterium* (Bm) is a common, aerobic, and gram-positive PGPR. A previous study showed that inoculation of Bm promoted production of organic acids to enhance the Cd bioavailability in soil, and promoting plant growth (Jeong et al., 2012). Additionally, it is safe to use on food crops and does not pose any harm to humans and animals. Thus, it is a promising microbe for promoting the efficiency of phytoremediation. Inoculation of arbuscular mycorrhizal fungi (AMF) is also a common measure to promote the efficiency of phytoremediation, which are widespread in ecosystem. They can colonize the roots of plants and form symbiosis with nearly 90% of land plant species. AMF thus play key roles in the cycling of plant nutrients, soil conservation, and plant–soil interactions. Some investigations have demonstrated that AMF can ameliorates growth of plants by enhancement of productivity and nutrient acquisition and increase Cd bioavailability in the soil, and mediate the absorption and transfer of metals (Luo et al., 2017; Wang G. et al., 2020). *Glomus mosseae* (Gm) is an AMF that can enhance the ability of plants to acquire nutrients and promote plant growth. And it can also alter the form of HMs to enhance the HM tolerance of host plants, thereby improving the remediation efficiency of HM pollution (Mani et al., 2015; Yang et al., 2016). Scientists in northwestern India discovered *Piriformospora indica* (Pi) in 1998 (Verma et al., 1998; Mao, 2016). Pi is a mycorrhizal-like fungus that is morphologically similar to AMF; it also has some of the same ecological roles as AMF and can enhance the resistance of plants to HM pollution by increasing the activity of antioxidant enzymes. Previous studies have shown that Pi plays a key role in stabilizing concentrations of Cd in the roots and decreasing concentrations of Cd in the stems and leaves (Shahabivand et al., 2017; Khalid et al., 2022; Li et al., 2022). In recent years, chelating agents have been employed to enhance the efficiency of phytoremediation in soil, because they have relatively strong complexing ability with HM (Huang G. et al., 2020). Among them, citric acid (Ca) can dissolve HMs in soil, enhance their bioavailability, and promote the absorption, transport, and enrichment of HMs by plants (Nowack et al., 2008). A previous study has shown that the addition of Ca increases root biomass and the concentration of Cd in *S. nigrum* (Rehman et al., 2017).

Several studies have identified functional strains that enhance plant growth and stress resistance in plant–microbe systems. Although many studies have evaluated the efficacy of using single microbial strains for HM-contaminated soil remediation by plants, few studies have evaluated the efficiency of using microbes combined with other microbes or low-molecular-weight organic acids for the remediation of Cd-contaminated soil. The results of recent studies indicate that the co-inoculation of several microbes can increase the dry weight and stem height of oat plants (*Avena sativa*; Xun et al., 2015). The concentration and removal rate of HMs are increased in Indian mustard following inoculation with Bm and Ca (Wang et al., 2014). The findings of these studies suggest that additional investigation of the effects of the application of several microbes or chelating agents on phytoremediation efficiency is needed. However, the nutrient uptake ability of plants can vary, and HMs might affect the relationships between microbes and host plants. In addition, HM tolerance varies greatly among plant species, even under the same stress conditions. The effects of microbes combined with other microbes or Ca on the efficiency of Cd remediation by *S. nigrum* have not yet been explored.

Here, we conducted pot experiments in a greenhouse to evaluate the effects of Bm combined with Ca, Gm, and Pi on the

ability of *S. nigrum* to remediate Cd-contaminated soil. Our specific aims were to (1) characterize the effects of different additives on Cd accumulation in *S. nigrum*, (2) clarify the effects of different additives on the diversity and structure of rhizosphere microbial communities, (3) explore the relationship between changes in microbial structure and Cd-contaminated soil remediation by *S. nigrum*, and (4) identify the most optimal combination of different additives for the remediation of Cd pollution.

2. Materials and methods

2.1. Experimental materials and design

Solanum nigrum, Bm and Pi, and Gm were obtained from the Agro-environmental Protection Institution, Ministry of Agriculture and Rural Affairs; the Agricultural Culture Collection of China; and the Institute of Plant Nutrition, Resources and Environment, Beijing Academy of Agriculture and Forestry Sciences, respectively.

Cultivated soil (depth of 0–20 cm) was collected from farmland polluted with Cd in Anyang, Henan Province (36°05′N, 114°23′E) and used in the greenhouse pot experiments; the concentration of Cd in this soil was 2.12 mg/kg. The basic physical and chemical properties of the soil were as follows: pH, 8.26; soil organic matter (SOM), 28.2 g·kg^{-1}; available N (AN), 115 mg·kg^{-1}; available phosphorus (AP), 12.1 mg·kg^{-1}; available potassium (AK), 222 mg·kg^{-1}; cation exchange capacity (CEC), 12.5 cmol·kg^{-1}; available Cd (ACd), 0.870 mg·kg^{-1}; and total Cd (TCd), 2.12 mg·kg^{-1}. The experiment comprised five treatments with three replicates for each treatment: *S. nigrum* (CK), Bm addition (BM), Bm + Ca (BM + CA), Bm + Gm (BM + GM), and Bm + Pi (BM + PI). In the BM and BM + CA treatments, 20 ml of Bm bacterial solution was added to each plot when plants were transplanted, and 20 ml of Bm and 10 mmol/kg Ca were added to each pot after 15 days. Gm (30 g) and Pi (5 ml) were added to each pot in the BM + GM and BM + PI treatments, respectively, when plants were transplanted, and Bm (20 ml) was added to each pot 15 days later.

Solanum nigrum seeds were treated with 0.5% (v/v) NaClO for 15 min; they were then washed with deionized water several times and placed in a constant-temperature water bath at 40°C for 6 h. The seeds were cultivated in a sterilized nutrient substrate, placed in a light incubator, and then transplanted to pots until *S. nigrum* plants had five leaves. A total of 1.5 kg of soil was added to each pot. A layer of soil was applied to cover the strains. No fertilizer was added, and plants were watered with distilled water once a week during the experiments. The experiments were performed in a greenhouse with an 8-h/16-h light/dark photoperiod (25/20°C day/night temperature) at 65–75% relative humidity. All plant and soil samples were collected after plants matured at 45 days of growth.

2.2. Collection of samples and measurements

Root and shoot samples of *S. nigrum* were collected and rinsed with tap water and deionized water, respectively. Cd^{2+} attached to the surface of roots was removed by immersing root samples in 20 mmol·L^{-1} Na_2-EDTA for 15 min; these samples were then washed with deionized water several times. All plant samples were dried at 105°C for 30 min and then kept at 80°C until a constant weight was achieved. A ball mill was used to grind the samples; the samples were then filtered through a 0.25-mm sieve. HNO_3 + $HClO_4$ (4:1) was used to digest the plant samples, and inductively coupled plasma mass spectrometry (ICP–MS; 7,700x, Agilent, Foster City, United States) was used to estimate Cd concentrations (Huo et al. 2018). Citrus leaves were used as the reference material [GBW10020 (GSB-11), 0.17 ± 0.02 mg·kg^{-1} Cd] for assessing the quality of the Cd concentration data.

The root shaking method was used to collect rhizosphere soil samples, and these samples were stored at −80°C for subsequent determination of soil microbial diversity. High-throughput sequencing was conducted by Shanghai Meiji Biotechnology Co., Ltd., and these data were used to estimate microbial diversity. According to the Closing Report from Majorbio, a FastDNA Spin Kit for Soil (MP Biomedicals, Santa Ana, CA, United States) was applied for sediment DNA extraction. Then, a NanoDrop 2000 spectrophotometer (Thermo Fisher Scientific, Wilmington, DE, United States) was used for the extracted DNA quantification. Before PCR amplification, all of the DNA samples were stored at −80°C.The bacterial and fungal communities in different samples were analyzed using Illumina MiSeq sequencing. The primers 338F (5′-ACTCCTACGGGAGGCAGCAG-3′)/806R (5′-GGACTACHVGGGTWTCTAAT-3′) and ITS1F (5′-CTTGGTCATTTAGAGGAAGTAA-3′)/ITS2R (5′-GCTGCGTTCTTCATCGATG C-3′) were used to amplify the V3–V4 region of the bacterial 16S rRNA gene and the fungal ITS1 region, respectively. All the forward primers were tagged with a 5-nucleotide barcode to distinguish different samples. After verification by agarose gel electrophoresis, the purification of amplicons was processed with EZNA Cycle-Pure Kit (Omega Bio-tek Inc., Doraville, GA, United States). The purified amplicons were next pooled by normalizing in equimolar numbers and subjected to high-throughput sequencing (Illumina MiSeq PE300 platform; Majorbio Bio-pharm Technology, Shanghai, China). All analyses were performed in triplicate.

After crushing the remaining air-dried soil samples, they were filtered through 2-mm and 0.25-mm sieves for subsequent determination of the TCd and available ACd content of the soil and the physical and chemical properties of the soil. Sulfuric acid, nitric acid, and hydrogen peroxide were used for the microwave digestion samples, and the TCd concentration was measured using ICP–MS. Diethylene triamine pentaacetic acid (DTPA) was used to extract ACd, and ICP–MS (7,700X, Agilent, United States) was used to measure the concentration of ACd. Various kits (Suzhou Keming Biotech, China) were used to determine the

activity of catalase (CAT), urease (UE), and alkaline phosphatase (ALP) in the soil samples. The methods described in a previous study were used to determine the basic physical and chemical properties of the soil samples (Xu et al., 2020). The ammonium acetate method (1 M CH_3COONH_4) at pH 7.0 was used to determine the CEC.

2.3. Data analysis

SPSS 20 was used to conduct statistical analyses. Analysis of variance (ANOVA), followed by Duncan's tests, was used to evaluate the significance of differences between groups; the threshold for statistical significance was $p < 0.05$. Figures of the data were created using Origin (2019) software:

1. Bioaccumulation factor (BCF) = Cd concentration in the shoot/TCd concentration in soil.
2. Translocation factor (TF) = Cd concentration in the shoot/Cd concentration in the roots.

[Cd] indicates the content of Cd in a specific part of the plant in $mg \cdot kg^{-1}$.

The Majorbio Cloud platform[1] was used to create a series of maps of microbial diversity and community composition. The R packages "WGCNA" and "igraph" were used to conduct symbiotic network analysis, and 15 samples with a combined number of operational taxonomic units (OTUs) of less than 150 were excluded from analyses. A total of 638 bacterial and 167 fungal OTUs were used to construct nodes and edge files for the symbiotic network graph. Gephi software was used to divide the taxa in the network into different modules using default parameters. The main modules were retained, and they were visualized and highlighted in different colors using Gephi. The OTUs of each Module were zero-mean normalized, and correlation analyses of sample means with the BCF and TF of shoots were performed to identify the key modules. Correlations between bacterial genera and the BCF and TF of shoots in the key Modules were determined to identify the bacteria associated with the BCF and TF.

3. Results

3.1. Uptake and transport of cadmium in *Solanum nigrum*

The Cd concentrations in the root, stem, and leaf tissues of *S. nigrum* were 124, 84.4, and 64.6% higher in the BM + CA treatment (Figure 1A) than in the CK, and these differences were significant. The BCF of *S. nigrum* shoots was 80.6% higher in the BM + CA treatment than in the CK (Figure 1C). There were no significant differences in Cd accumulation in the roots, shoots, and entire *S. nigrum* plants between the BM + CA treatment and the CK (Figure 1B). The TF of *S. nigrum* shoots was 33.1% lower in the BM + CA treatment than in the CK (Figure 1D). The Cd concentration in each part of *S. nigrum* was higher in the BM + GM treatment than in the CK (Figure 1A), but these differences were not significant. The accumulation of Cd in each part of *S. nigrum* was higher in the BM + GM treatment than in the CK; Cd accumulation was 108 and 104% higher in the shoots and entire plants in the BM + GM treatment than in the CK, respectively, and these differences were significant (Figure 1B). The BCF and TF of *S. nigrum* shoots was 46.9 and 21.6% higher in the BM + GM treatment than in the CK, respectively (Figures 1C, D); the difference in BCF between the BM + GM treatment and the CK was significant. These findings indicate that the Cd uptake and accumulation capacity of *S. nigrum* were higher in the BM + GM treatment than in the CK.

3.2. Microbial diversity and community composition in the rhizosphere

The Ace and Chao indices of bacteria varied among the BM, BM + CA, and CK treatments; specifically, the Ace and Chao indices of bacteria were greater in the BM treatment than in the CK and lower in the BM + CA treatment than in the CK, which suggests that the BM and BM + CA treatments had opposite effects on the species richness of bacteria (Table 1). The Ace and Chao indices of fungi were higher in the BM and BM + CA treatments than in the CK. These findings indicate that the BM and BM + CA treatments had a significant effect on the species richness of bacteria and fungi. Similar findings were obtained from Venn diagrams (Supplementary Figure S1).

We conducted community heatmap analysis and community bar plot analysis of bacteria and fungi to clarify the composition of microbial species in the soil. The relative richness of *Proteobacteria* was the highest among all bacterial communities. The relative richness of *Patescibacteria*, *Gemmatimonadetes*, *Bacteroidetes*, *Firmicutes*, *Acidobacteria*, *Chloroflexi*, and *Actinobacteria* was also high (Figure 2A). The dominant fungal phyla were *Ascomycota*, and *Mortierellomycota*, and the abundance of *Glomeromycota* was significantly higher in the BM + GM treatment than in the CK (Figure 2B). The abundances of *Proteobacteria* and *Actinobacteria* were higher in the BM + GM treatment than in the CK (Figure 2C). The relative abundance of *MortieRellomycot* was higher in the BM + GM and BM + PI treatments than in the CK (Figure 2D).

RDA1 explained 56.92 and 80.52% of the total variation in bacterial and fungal communities, and RDA2 explained 21.76 and 11.58% of the total variation in bacterial and fungal communities, respectively (Figures 3A, B), which suggests that soil properties had a major effect on the structure of microbial communities. AN and SOM explained 28.1 and 25.0% of the

1 www.majorbio.com

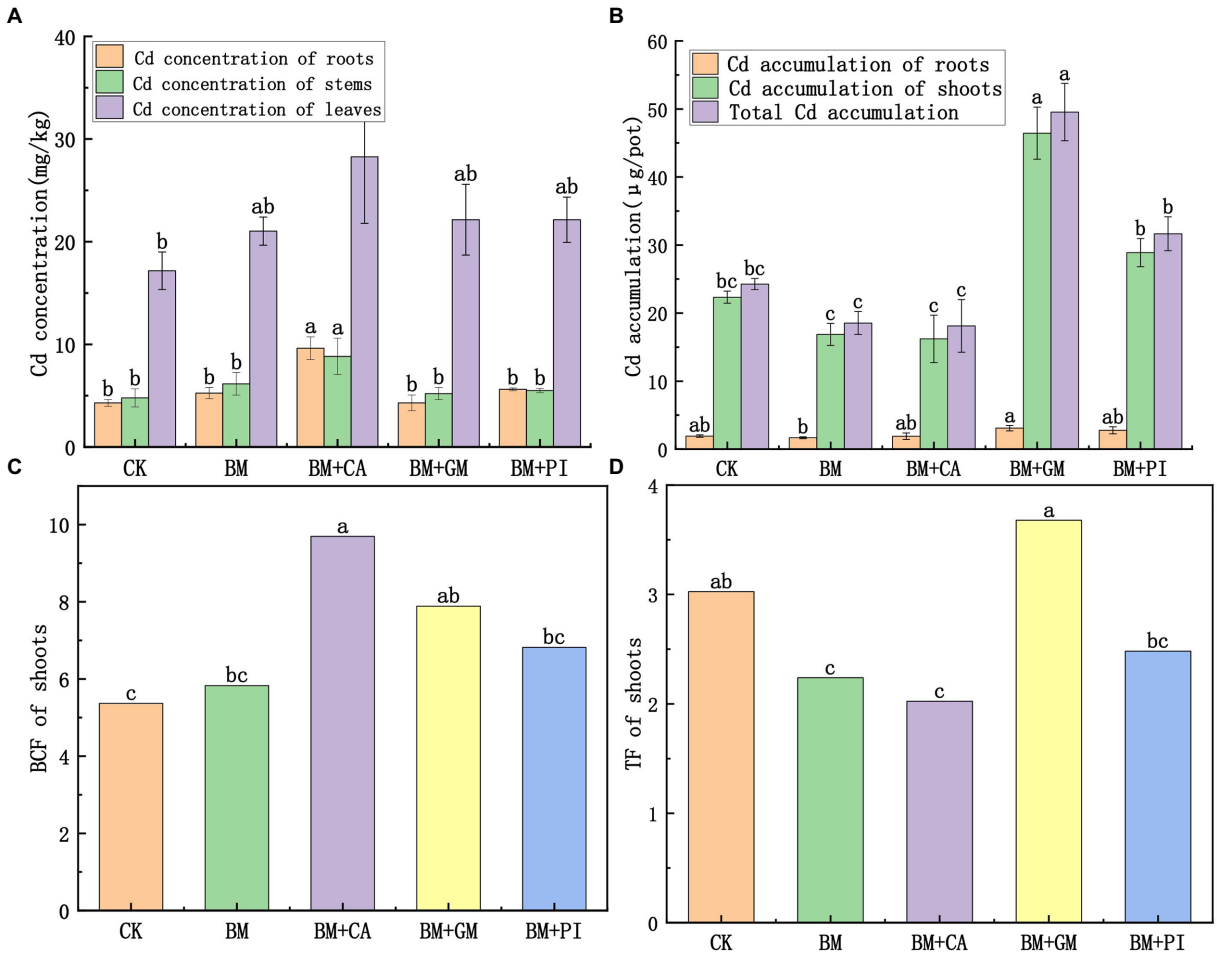

FIGURE 1
The effects of different treatments (*S. nigrum* (CK), *Bacillus megaterium* (BM) along with citric acid (BM+CA), *Glomus mosseae* (BM+GM), and *Piriformospora indica* (BM+PI)) on the Cd concentrations **(A)** and accumulation of Cd **(B)** in *S. nigrum*. Variation in BCF and TF of the shoots of *S. nigrum* in different treatments **(C,D)**. Error bars show the standard deviation of triplicate samples, and columns with different letters are significantly different according to one-way ANOVA, followed by Duncan's test (p <0.05).

TABLE 1 Diversity indexes of bacteria and fungi in different treatments.

	Bacteria			Fungi		
Treatments	Shannon	Ace	Chao1	Shannon	Ace	Chao1
CK	6.67 ± 0.02a	3,754 ± 124ab	3,776 ± 138ab	3.00 ± 0.41a	518.2 ± 8.1a	509.0 ± 6.2a
BM	6.77 ± 0.05a	3,903 ± 107a	3,929 ± 109a	3.07 ± 0.72a	544.2 ± 50.0a	553.1 ± 48.1a
BM + CA	6.59 ± 0.13a	3,387 ± 246b	3,402 ± 251b	2.98 ± 0.47a	562.5 ± 54.0a	569.0 ± 49.4a
BM + GM	6.71 ± 0.03a	3,613 ± 77ab	3,683 ± 65ab	3.32 ± 0.24a	511.7 ± 15.2a	520.0 ± 27.6a
BM + PI	6.69 ± 0.07a	3,742 ± 243ab	3,803 ± 287ab	2.71 ± 0.41a	510.4 ± 46.4a	518.3 ± 57.4a

CK, BM, BM + CA, BM + GM, BM + PI represent *S. nigrum*, *Bacillus megaterium*, and *Bacillus megaterium* along with citric acid, *Glomus mosseae*, and *Piriformospora indica*, respectively. The error bars show the standard deviation of triplicate samples, and values with different letters are significantly different according to one-way ANOVA followed by Duncan's test (P < 0.05).

change in bacterial communities, respectively, and their effects on the composition of bacterial communities were significant (p < 0.05). CAT, SOM, TCd, and UE explained 64.4, 10.3, 7.70, and 4.30% of the change in fungal communities, respectively, suggesting that they were the key environmental factors affecting the composition of fungal communities (p < 0.05). The correlations of bacterial and fungal communities with soil properties also varied.

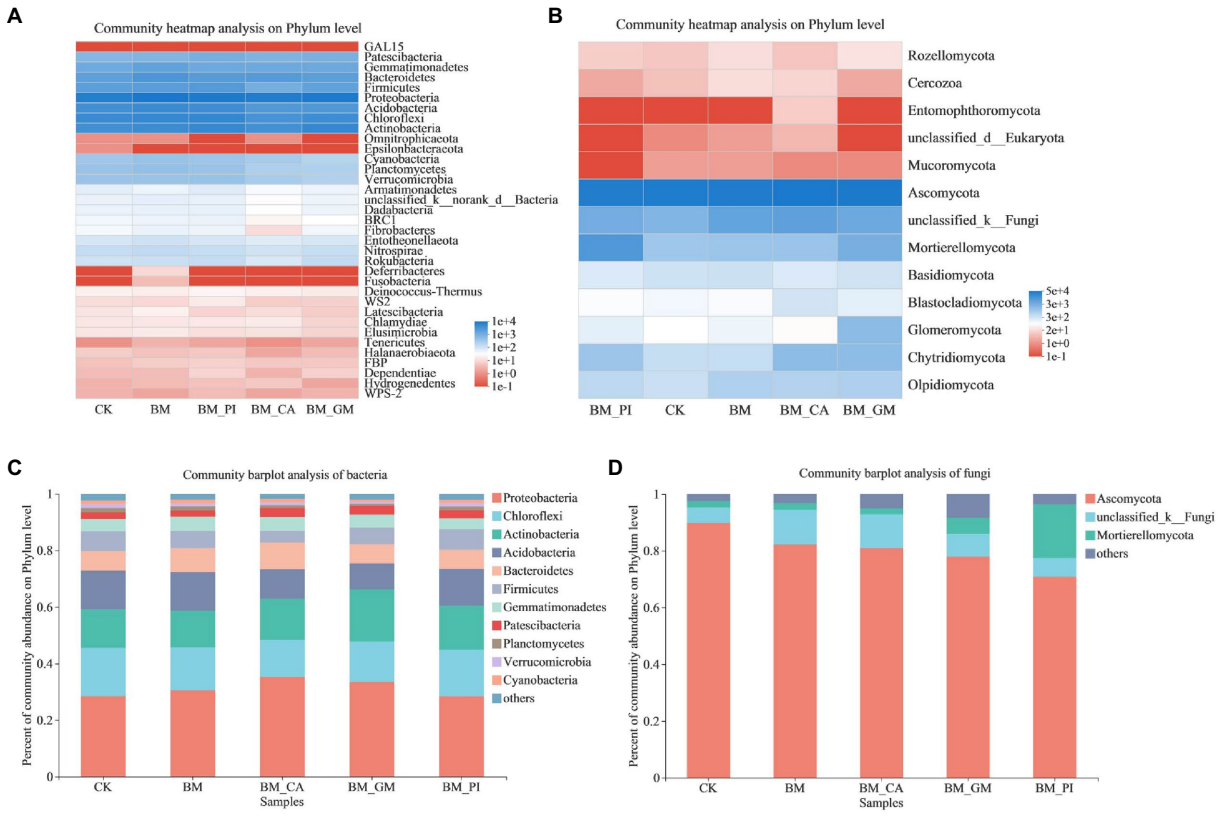

FIGURE 2
The community heatmap analysis **(A,B)** and abundances of communities **(C,D)** of bacteria and fungi in the different treatments [*S. nigrum* (CK), *Bacillus megaterium* (BM) along with citric acid (BM+CA), *Glomus mosseae* (BM+GM), and *Piriformospora indica* (BM+PI)].

3.3. Network analysis and keystone microbial taxa

We constructed a bacterial and fungal network to identify key microbial groups (Figure 4A). The network was divided into four major microbial taxa, which were referred to as modules 1 to 4, and these four modules accounted for 93.98% of the total nodes. After other modules were removed, we constructed a microbial network for modules 1, 2, 3, and 4 (Figure 4B), which accounted for 29.34, 25.90, 24.66, and 20.11% of the nodes, respectively. Modules 1–4 all comprised bacteria and fungi, but the relative abundances of bacteria and fungi in each Module differed (Module#1: 81.36% bacteria and 18.64% fungi; Module#2: 77.60% bacteria and 22.40% fungi; Module#3: 77.78% bacteria and 22.22% fungi; and Module#4: 87.33% bacteria and 12.67% fungi; Figure 4E). Microbial diversity in Module#3 was significantly higher in the BM + GM treatment than in the CK; however, microbial diversity was significantly lower in Module#2 in the BM + CA treatment than in the CK (Figure 4C). The abundances of microbes were significantly higher in Module#1 in the BM + GM treatment and in Module#3 in the BM + PI treatment than in the CK (Figure 4D). We also compared variation in the composition of microbes among modules (Figure 4F). There was substantial variation in the composition of microbes among modules; the dominant bacteria and fungi previously mentioned accounted for 92.56, 92.15, 89.95, and 93.88% of all microbes in Module#1, 2, 3, and 4, respectively (Figures 2C, D). *Actinobacteria*, *Ascomycota*, *Chloroflexi*, and *Proteobacteria* accounted for 18.60, 11.63, 14.42, and 29.30% of all microbes in Module#1, respectively. *Bacteroidetes*, *Proteobacteria*, and unclassified _ k _ Fungi accounted for 16.23, 28.27, and 12.04% of all microbes in Module#2, respectively. *Actinobacteria*, *Ascomycota*, and *Proteobacteria* accounted for 24.34, 11.11, and 24.87% of the microbes in Module#3, respectively. In Module#4, *Acidobacteria* and *Chloroflexi* accounted for 49.66 and 19.05% of all.

3.4. Associations of keystone microbial taxa with Bioaccumulation factor and translocation factor

We evaluated relationships of the standardized mean OTU values of microbial taxa (modules 1–4) with the BCF and TF of shoots (Figure 5A). Module#1 was significantly positively correlated with the TF of shoots, and the coefficient of determination of this correlation was high ($R^2 = 0.4985$)

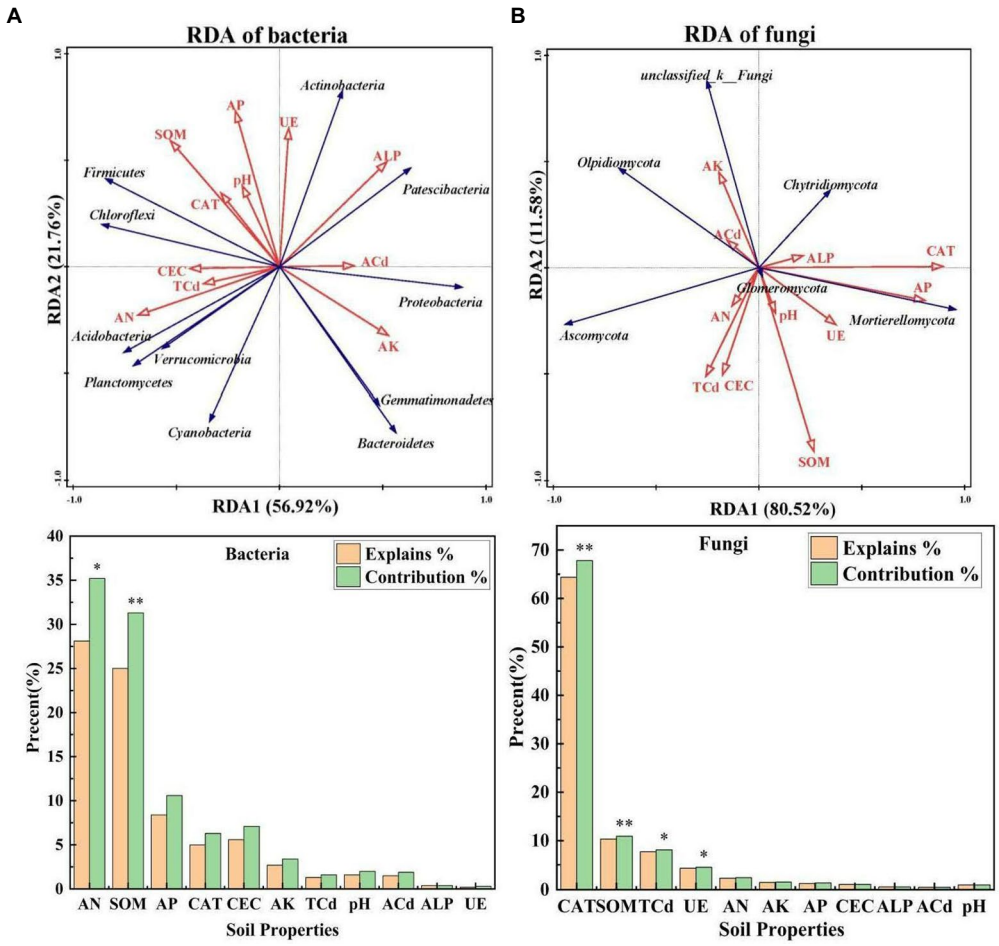

FIGURE 3
(A,B) Redundancy analysis of the dominant bacteria, dominant fungi, and environmental factors under different treatments [*S. nigrum* (CK), *Bacillus megaterium* (BM) along with citric acid (BM+CA), *Glomus mosseae* (BM+GM), and *Piriformospora indica* (BM+PI)]. The blue arrows indicate microbial communities, and the red arrows indicate soil properties. ALP, CAT, and UE indicate alkaline phosphatase activity, catalase activity, and urease activity, respectively; AN, AP, and AK indicate available nitrogen, available phosphorus, and available potassium, respectively; SOM and CEC indicate soil organic matter and cation exchange capacity, respectively; and TCd and ACd indicate total cadmium and available cadmium, respectively. Values marked with * indicate significant differences at $p<0.05$, and values marked with ** indicate significant differences at $p<0.01$.

(Figure 5B). Thus, Module#1 comprises key microbial taxa in our study. *Acidobacteria*, *Actinobacteria*, *Ascomycota*, *Chloroflexi*, *Glomeromycota*, and *Proteobacteria* in Module#1 were significantly positively correlated with the TF of shoots (Figure 5C). An ANOVA of the number of bacterial and fungal OTUs in different treatments was conducted. The number of *Ascomycota*, *Glomeromycota*, *Proteobacteria*, and *Actinobacteria* OTUs was significantly higher in the BM + GM treatment than in the CK (Figure 5D), suggesting that these taxa might enhance the translocation of HMs in *S. nigrum*.

4. Discussion

Phytoremediation is an environmentally friendly and widely used approach to remediate HM-contaminated soil (Yan et al., 2020). Plant biomass is an important factor that affects the success of phytoremediation. Both plant biomass and the concentration of HMs in plants affect the efficiency of phytoremediation (Zhiguo and Qixing, 2009; Jeong et al., 2012; Hou et al., 2017). Soil microbes are abundant and play key roles in the growth and development of plants (Kloepper and Schroth, 1978); however, their precise effects depend on the plant species, microbial species, and the type of HM (Khalid et al., 2021). Bm is a typical PGPR, and previous studies indicate that Bm can secrete organic acids, such as indole acetic acid, to activate Cd and acidify soil (Jeong et al., 2012; Huang H. et al., 2020). In our study, the accumulation of Cd in *S. nigrum* was lower in the BM than in the CK treatment. This might stem from the activation of Cd due to the secretion of organic acids by Bm; this excess Cd is then absorbed by *S. nigrum*, which causes the concentration of Cd in *S. nigrum* to exceed the range that it can tolerate. Consequently, the growth of *S. nigrum* was inhibited following exposure to high levels of Cd, and the biomass (Supplementary Figure S2) and accumulation of Cd were

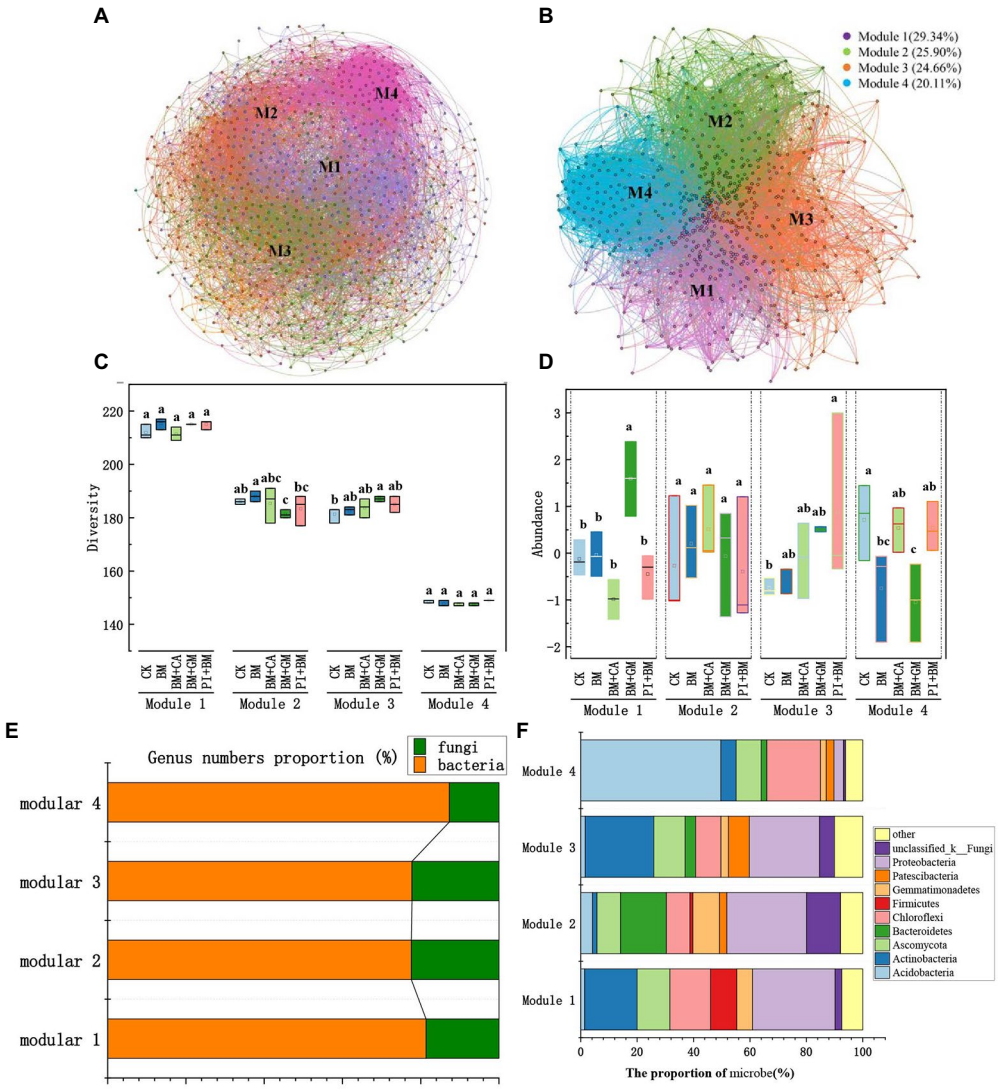

FIGURE 4
Keystone microbial taxa. **(A)** Network map of bacterial and fungal genera; microbial kingdoms in the network are indicated by the colors of the node. **(B)** Network map of microbial taxa from modules 1–4; modules in the network are indicated by different colors. **(C)** Microbial diversity in modules 1–4. **(D)** Microbial abundance in modules 1–4; the data were zero-mean normalized. **(E,F)** Composition of microbes in modules 1–4. CK，BM，BM+CA，BM+GM，BM+PI represent *S. nigrum*, *Bacillus megaterium*, and *Bacillus megaterium* along with citric acid, *Glomus mosseae*, and *Piriformospora indica*, respectively. The error bars show the standard deviation in triplicate samples, and values with different letters significantly differ according to one-way ANOVA followed by Duncan's test.

lower in *S. nigrum* in the BM treatment than in the CK. The activity of HM ions is increased by Ca, as it reduces the pH of soil and promotes the absorption of N, P, K, and other nutrient elements by plants. Thus, Ca can promote the growth and development of plants and the absorption of HM ions (Huang G. et al., 2020; Han R. et al., 2021). The findings of our study indicate that the combined application of Bm and Ca significantly decreased the biomass of *S. nigrum*. The Cd concentration was significantly higher in the BM + CA treatment than in the CK， and the accumulation of Cd was lower in the BM + CA treatment than in the CK; this might stem from the increase in the bioavailability of Cd, which suppressed the growth of *S. nigrum*. The fact that the Cd concentration in *S. nigrum* was highest in the BM + CA treatment is also consistent with these findings. Gm is a common arbuscular mycorrhizal fungus, and Pi is a mycorrhizal-like fungus; they have been previously shown to enhance the resistance of plants to HMs (Dabral et al., 2019). In our study, the biomass of *S. nigrum* was significantly higher in the BM + GM treatment than in the CK; although the Cd concentration in *S. nigrum* was only slightly higher in the BM + GM treatment than in the CK, Cd accumulation was significantly higher in the BM + GM treatment than in the CK. This finding indicates that the concentrations of HMs were diluted in *S. nigrum* in the BM + GM treatment, and this primarily stemmed from increases

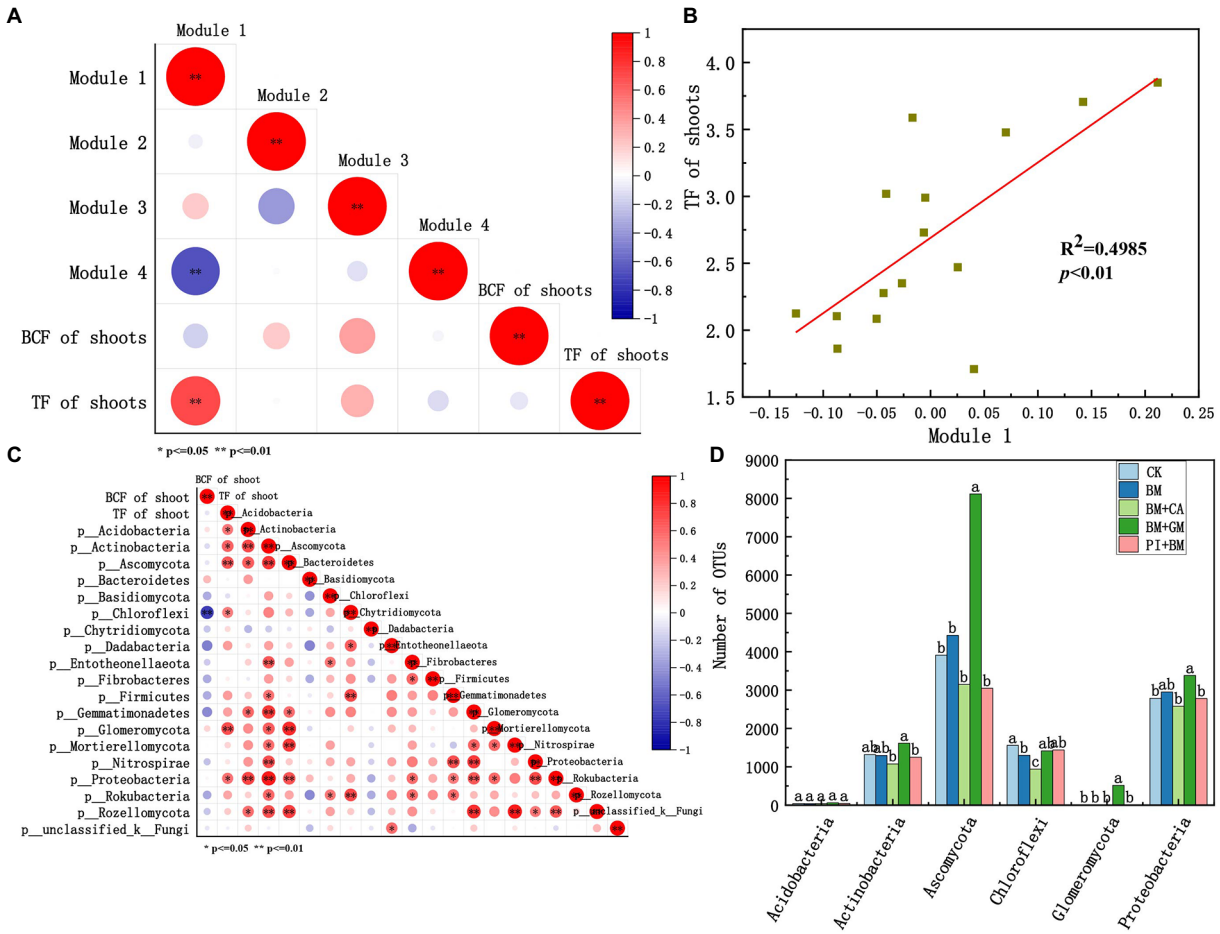

FIGURE 5
(A) Correlations of modules 1–4 with the BCF and TF of the shoots according to Pearson correlation analysis. **(B)** Linear regression analysis between Module#1 and the TF of shoots. **(C)** Correlation of microbes in Module#1 with the TF of shoots according to Pearson correlation analysis. **(D)** Number of bacterial OTUs in Module#1. Asterisks indicate statistically significant differences according to Student's t-test (*p<0.05, **p<0.01). CK，BM，BM+CA，BM+GM，BM+PI represent *S. nigrum*, *Bacillus megaterium*, and *Bacillus megaterium* along with citric acid, *Glomus mosseae*, and *Piriformospora indica*, respectively.

in the growth and biomass of *S. nigrum*, which enhanced the remediation efficiency of Cd-contaminated soil (Yang et al., 2021). Bm can activate a large number of Cd ions and increase the concentrations of N, P, K, and other nutrient elements, which increases the uptake of Cd and nutrient elements by *S. nigrum*. However, Gm alleviated the toxicity of Cd to *S. nigrum*, which enhanced its growth; this indicates that BM and GM had synergistic effects. Pi promotes the growth of plants under both normal and stress conditions (Verma et al., 1998). Pi mitigates the deleterious effects of oxidative stress by enhancing the antioxidant defense system and regulating antioxidant levels in plants, which increases the resistance of plants to stress (Vadassery et al., 2009). Pi has been used to mitigate HM stress in wheat, sunflower, *Nicotiana tabacum* L., and other plants (Shahabivand et al., 2012; Hui et al., 2015; Shahabivand et al., 2017). Previous studies have shown that Pi can increase the yield of *Hordeum vulgare* L. and *Brassica napus* L.; it can also enhance tolerance to water stains and the production of *Brassica pekinensis* (Lour.) Rupr (Waller et al., 2005). Following inoculation with Pi, the resistance of *Arabidopsis thaliana* seedlings to drought is significantly enhanced (Sherameti et al., 2008). The results of our study indicate that co-inoculation of Bm and Pi increased the biomass of *S. nigrum* and increased Cd accumulation in *S. nigrum*, which suggests that Pi enhanced the resistance of *S. nigrum* to the deleterious effects of Cd; however, the protective effects of Gm were stronger than those of Pi.

During the phytoremediation of HM-contaminated soil, plants absorb HMs from the soil and the HMs are transported from the roots to the shoots is a key component.The phytoremediation efficiency can be evaluated according to three criteria: the tolerance of plants to HMs, the ability of plants to absorb HMs, and the ability of plants to transport HMs from the roots to the shoots (Rajkumar et al., 2009; Chen et al., 2014). BCF is an indicator of the ability of plants to absorb HMs from soil; plants with higher BCF values have a stronger ability to absorb and accumulate HMs (Zhou X. et al., 2020; Liu et al., 2022). In our

study, the BCF was higher in the four treatments than in the CK, suggesting that the uptake of Cd in *S. nigrum* was promoted in the four treatments. The most significant increase in Cd uptake was observed in the BM + CA treatment, which suggests that the BM + CA treatment had the most significant effect on the efficacy of phytoremediation. This might be explained by the fact that Bm plays an important role in promoting the activation of soil Cd; Ca also promotes the activation of soil Cd (Marques et al., 2013; Yang et al., 2022). TF is an indicator of the ability of plants to transport HMs from the roots to the shoots (Chi et al., 2022). In our study, the TF of *S. nigrum* was significantly lower in the BM and BM + CA treatments than in the CK. The TF of *S. nigrum* was significantly higher in the BM + GM treatment than in the CK. There was no difference in the TF of *S. nigrum* between the BM + PI treatment and the CK. Some studies have indicated that Cd is stabilized by AMF through mycelia or *via* adsorption by chitin cell walls, which impedes the transport of HMs from the roots to the shoots; this regulates the distribution of HMs in plants, reduces the toxicity of HMs, and promotes plant growth (Christie et al., 2004; Wang et al., 2007; Hui et al., 2015; Wu et al., 2015). The inoculation of Pi under Cd stress limits the movement of HMs to the shoots of the plant and promotes the accumulation of Cd in the roots. Fungi can mitigate the toxicity of HMs in host plants (Hui et al., 2015; Shahabivand et al., 2017). The results of our study indicate that the ability of *S. nigrum* to transport Cd from the roots to the shoots was enhanced in the BM + GM treatment compared with the CK; this might stem from the fact that the toxicity of Cd was reduced and the growth of *S. nigrum* was promoted in the presence of Gm， which could lead to higher phytoextraction efficiency (Han Y. et al., 2021). The effects of the BM + PI and BM + GM treatments on *S. nigrum* might be similar. The protective effects of Pi were weaker than those of Gm, so the ability of *S. nigrum* to transport HMs was weaker in the BM + PI treatment than in the BM + GM treatment. High concentrations of Cd had a toxic effect on *S. nigrum* in the BM and BM + CA treatments, and this affected the normal physiological metabolism of *S. nigrum*. Although the roots absorbed a large number of Cd ions, they were not transported to the shoots.

Phytoremediation is a promising technique for the remediation of HM-contaminated soils, and it might affect the diversity and structure of rhizosphere microbes. During the remediation process, the rhizosphere microbial community plays a role in energy transfer, nutrient circulation, HM resistance, and HM detoxification in soil (Guo et al., 2019). We conducted various analyses to clarify the effects of different treatments on rhizosphere microbes. The effects of different treatments on fungi and bacteria varied, which suggests that changes in rhizosphere microbes are affected by changes in the surrounding environment. *Proteobacteria*, *Acidobacteria*, *Actinobacteria*, and *Bacteroidetes* are the most common bacterial phyla in the rhizosphere (Guo et al., 2019). In our study, *Patescibacteria*, *Chloroflexi*, *Actinobacteria*, *Acidobacteria*, and *Bacteroidetes* were the dominant bacterial phyla, and *Ascomycota*, unclassified _ k _ fungi, *Mortierellomycota*, *Glomomycota*, *Chytridiomycota*, and *Oldiomycota* were the dominant fungal phyla. Variation in the abundances of bacteria might stem from variation in soil type; the factors that explain variation in the abundance of fungi remain unclear because few relevant studies have been conducted. The most significant differences in bacteria and fungi among treatments were observed in *Proteobacteria*, *Actinobacteria*, *Ascomycota*, unclassified _ k _ fungi, and *MortieRellomycot*. Some studies have shown that *Proteobacteria* are highly resistant to HM pollution because they are capable of adapting to environments with high concentrations of HMs (Spain et al., 2009; Wang X. et al., 2021). In our study, the relative abundance of *Proteobacteria* was higher in the BM + CA and BM + GM treatments than in the CK; consequently, the concentrations of Cd were higher in the BM + CA and BM + GM treatments than in the CK. The accumulation of Cd was particularly pronounced in *S. nigrum* in the BM + GM treatment, and the concentration of Cd in the roots of *S. nigrum* was particularly high in the BM + CA treatment. *Actinobacteria* can enhance the resistance of plants to disease (Tang et al., 2016). In our study, the relative abundance of *Actinobacteria* was highest in the BM + GM treatment, which provided further support for this conclusion. Other studies have explored the relationship between CAT activity and the resistance of plants to disease. CAT can mitigate damage induced by Cd stress by scavenging reactive oxygen species (Pramanik et al., 2018; Khalid et al., 2022); thus, CAT might explain why *Actinobacteria* enhance the disease resistance of plants. *MortieRellomycot* has been shown to alleviate the deleterious effects of stress and increase the bioavailability of HMs (Xun et al., 2017). In our study, the abundance of *MortieRellomycot* was significantly higher in the BM + PI treatment than in the other treatments; this might explain why Cd accumulation was higher in the BM + PI treatment. Other dominant microbial communities play key roles in soils; for example, *Acidobacteria* play an important role in the decomposition of organic matter in poor soils, and *Bacteroidetes* mediate the decomposition of macromolecular organic matter (Naumoff and Dedysh, 2012; Rawat et al., 2012). Thus, changes in rhizosphere microbes during the remediation of contaminated soils can be marked. Various environmental factors affect the relative abundances of bacteria and fungi. In our study, AN and SOM were the main factors affecting the relative abundances of bacteria, and CAT, SOM, TCd, and UE were the main factors affecting the relative abundances of fungi; this suggests that microbial diversity and community composition were mainly affected by environmental factors in the rhizosphere.

Microbial taxa constructed based on the microbial co-occurrence networks reflect habitat heterogeneity, different selection regimes and phylogenetically closely related species clusters (Shi et al., 2016), which were shown to be composed of interactions between co-existing microbial species and plant-induced changes in nutrient status, HM behavior, etc. in the immediate soil environment (Chen et al., 2018; Hassani et al., 2018).The microbial co-occurrence networks that we established contained four main modules that differed significantly in

microbial composition, and the percentage distribution of bacterial and fungal phyla varied considerably among modules. Variation in the diversity of OTUs among modules was not as pronounced as variation in the abundances of microbial taxa among modules; this indicates that environmental factors had a greater effect on the abundances of microbes rather than the composition of microbes. The abundances of OTUs in Module#1 were significantly higher in the BM + GM treatment than in the CK, and the abundances of OTUs in Module#3 were significantly higher in the BM + PI treatment than in the CK. OTUs in Module#1 were considered key microbial taxa given that there was a significant correlation between Module#1 and shoot TF. *Acidobacteria*, *Actinobacteria*, *Ascomycota*, *Chloroflexi*, *Glomeromycota*, and *Proteobacteria* in Module#1 were also significantly positively correlated with shoot TF. Given that Cd accumulation and the OTUs numbers of *Ascomycota*, *Glomeromycota*, *Proteobacteria*, and Actinobacteria were higher in the BM + GM treatment than in the CK, these taxa likely enhance the ability of *S. nigrum* to transport Cd. In fact, *Proteobacteria*, *Actinobacteria* have been shown to have high adaptability to Cd and protective ability for plants (DeAngelis et al., 2009; Luo et al., 2021), which suggests that they might contribute to the hyperaccumulation of Cd in plants. *Glomeromycota* could also significantly increase plant resistance and biomass under HM stress condition (Amna et al., 2015). Similarly, *Ascomycota* might enhance the ability of plants to absorb Cd, as well as plant growth. The specific effects need to be further studied and added. It is worth mentioning that *Glomeromycota*, although not a dominant fungal phylum, its abundance in BM + GM treatment was particularly noticeable. It was likely to be a change caused by Gm, which may be related to the improvement of host tolerance by Gm.

In our study, high Cd concentrations were a major stress for *S. nigrum* and soil microbes. Under stress conditions, plants engage in cooperative interactions with microbes in the environment, and this results in changes in the rhizosphere environment, which in turn alters the structure of microbial communities (Liu et al., 2020; Tang et al., 2020). Only microorganisms that can tolerate Cd stress are able to survive, and microbial communities might affect plants by affecting phytohormones, signaling, and nutrient acquisition, which can alter the efficiency of phytoremediation (Yergeau et al., 2014; Zhou F. et al., 2020; Wang G. et al., 2021). In our study, Module#1 taxa played a key role in phytoremediation, and a network of functionally complementary microbes was formed that enhanced phytoremediation efficiency. The BM + GM treatment might drive the formation of this network, which greatly enhanced the Cd remediation capacity of *S. nigrum*.

5. Conclusion

In Cd-contaminated soil, co-inoculation of Bm and Gm significantly enhanced the growth of *S. nigrum* and the accumulation of Cd. The inoculation of different agents further influenced the soil microbial community by affecting soil AN, CAT, SOM, TCd, and UE. By constructing the microbial co-occurrence networks, the soil microbe was divided into four main Modules. BM + GM and BM + PI significantly increased the relative abundance of Module#1 and Module#3, respectively, when compared with the control. Additionally, Module#1 was considered as the key microbial taxon by response to TF of *S. nigrum*, in which *Ascomycota*, *Glomeromycota*, *Proteobacteria*, *Actinobacteria* were identified in close relationship with TF of *S. nigrum*, demonstrating their ability to enhance phytoremediation efficiency. Totally, Bm and Gm can be used for phytoremediation of Cd-contaminated soils, and the importance of key microbial taxa in phytoremediation was emphasized. Additional studies are needed to clarify the mechanisms underlying the interactions among *S. nigrum*, microbes, and soil properties in HM-contaminated soils.

Data availability statement

The datasets presented in this study can be found in online repositories. The names of the repository/repositories and accession number(s) can be found at: https://www.ncbi.nlm.nih.gov/, PRJNA905327; https://www.ncbi.nlm.nih.gov/, PRJNA905569.

Author contributions

MY: conceptualization, investigation, validation, methodology, formal analysis, writing-original draft, and writing-review and editing. LW: conceptualization, resources, data curation, and performing the experiment. GZ and YW: software and writing-review and editing. KW: resources, data curation, and software. RZ: resources, data curation, and performing the experiment. WC: supervision, project administration, and writing-review and editing. HF: supervision, funding acquisition, project administration, and writing-review and editing. All authors contributed to the article and approved the submitted version.

Funding

This work was supported by the National Key Research and Development Program of China (Nos. 2021YFD1700200 and 2016YFD0800800).

Acknowledgments

We thank TopEdit (www.topeditsci.com) for linguistic assistance during the preparation of this manuscript.

Conflict of interest

The authors declare that the research was conducted in the absence of any commercial or financial relationships that could be construed as a potential conflict of interest.

Publisher's note

All claims expressed in this article are solely those of the authors and do not necessarily represent those of their affiliated organizations, or those of the publisher, the editors and the reviewers. Any product that may be evaluated in this article, or claim that may be made by its manufacturer, is not guaranteed or endorsed by the publisher.

Supplementary material

The Supplementary material for this article can be found online at: https://www.frontiersin.org/articles/10.3389/fmicb.2022.1106254/full#supplementary-material

References

Abdelkrim, S., Jebara, S. H., Saadani, O., Abid, G., Taamalli, W., Zemni, H., et al. (2020). In situ effects of Lathyrus sativus-PGPR to remediate and restore quality and fertility of Pb and cd polluted soils. *Ecotoxicol. Environ. Saf.* 192:110260. doi: 10.1016/j.ecoenv.2020.110260

Amna, A. N., Masood, S., Mukhtar, T., Kamran, M. A., Rafique, M., Munis, M. F. H., et al. (2015). Differential effects of cadmium and chromium on growth, photosynthetic activity, and metal uptake of Linum usitatissimum in association with Glomus intraradices. *Environ. Monit. Assess.* 187:311. doi: 10.1007/s10661-015-4557-8

Ashraf, M. A., Hussain, I., Rasheed, R., Iqbal, M., Riaz, M., and Arif, M. S. (2017). Advances in microbe-assisted reclamation of heavy metal contaminated soils over the last decade: a review. *J. Environ. Manag.* 198, 132–143. doi: 10.1016/j.jenvman.2017.04.060

Baker, A., Mcgrath, S. P., Reeves, R. D., and Smith, J. (2000). "Metal hyperaccumulator plants: A review of the ecology and physiology of a biochemical resource for phytoremediation of metal-polluted soils" in *Phytoremediation of Contaminated Soil & Water*. eds. T. Norman, and G. Banuelos. Florida: Lewis Publishers, 85–107.

Chen, Y., Ding, Q., Chao, Y., Wei, X., Wang, S., and Qiu, R. (2018). Structural development and assembly patterns of the root-associated microbiomes during phytoremediation. *Sci. Total Environ.* 644, 1591–1601. doi: 10.1016/j.scitotenv.2018.07.095

Chen, B., Shen, J., Zhang, X., Pan, F., Yang, X., and Feng, Y. (2014). The endophytic bacterium, Sphingomonas SaMR12, improves the potential for zinc phytoremediation by its host *Sedum alfredii*. *Plos One* 9:e106826. doi: 10.1371/journal.pone.0106826

Chi, Y., You, Y., Wang, J., Chen, X., Chu, S., Wang, R., et al. (2022). Two plant growth-promoting bacterial bacillus strains possess different mechanisms in affecting cadmium uptake and detoxification of *Solanum nigrum* L. *Chemosphere* 305:135488. doi: 10.1016/j.chemosphere.2022.135488

Christie, P., Li, X. L., and Chen, B. D. (2004). Arbuscular mycorrhiza can depress translocation of zinc to shoots of host plants in soils moderately polluted with zinc [article]. *Plant Soil* 261, 209–217. doi: 10.1023/B:PLSO.0000035542.79345.1b

Dabral, S., Yashaswee, V. A., Choudhary, D. K., Bahuguna, R. N., and Nath, M. (2019). Biopriming with *Piriformospora indica* ameliorates cadmium stress in rice by lowering oxidative stress and cell death in root cells. *Ecotoxicol. Environ. Saf.* 186:109741. doi: 10.1016/j.ecoenv.2019.109741

DeAngelis, K. M., Brodie, E. L., DeSantis, T. Z., Andersen, G. L., Lindow, S. E., and Firestone, M. K. (2009). Selective progressive response of soil microbial community to wild oat roots. *ISME J.* 3, 168–178. doi: 10.1038/ismej.2008.103

Fan, H.-L., and Zhou, W. (2009). Screening of Amaranth cultivars (*Amaranthus mangostanus* L.) for cadmium Hyperaccumulation. *Agric. Sci. China* 8, 342–351. doi: 10.1016/s1671-2927(08)60218-7

Girdhar, M., Sharma, N. R., Rehman, H., Kumar, A., and Mohan, A. (2014). Comparative assessment for hyperaccumulatory and phytoremediation capability of three wild weeds. *3 Biotech* 4, 579–589. doi: 10.1007/s13205-014-0194-0

Guo, D., Fan, Z., Lu, S., Ma, Y., Nie, X., Tong, F., et al. (2019). Changes in rhizosphere bacterial communities during remediation of heavy metal-accumulating plants around the Xikuangshan mine in southern China. *Sci. Rep.* 9:1947. doi: 10.1038/s41598-018-38360-2

Han, R., Dai, H., Skuza, L., and Wei, S. (2021). Comparative study on different organic acids for promoting Solanum nigrum L. hyperaccumulation of cd and Pb from the contaminated soil. *Chemosphere* 278:130446. doi: 10.1016/j.chemosphere.2021.130446

Han, Y., Zveushe, O. K., Dong, F., Ling, Q., Chen, Y., Sajid, S., et al. (2021). Unraveling the effects of arbuscular mycorrhizal fungi on cadmium uptake and detoxification mechanisms in perennial ryegrass (Lolium perenne). *Sci. Total Environ.* 798:149222. doi: 10.1016/j.scitotenv.2021.149222

Hassani, M. A.DurÃ¡n, P, and Hacquard, S. P. (2018). Microbial interactions within the plant holobiont. *Microbiome* 6:58. doi: 10.1186/s40168-018-0445-0

Hou, D., Wang, K., Liu, T., Wang, H., Lin, Z., Qian, J., et al. (2017). Unique Rhizosphere micro-characteristics facilitate phytoextraction of multiple metals in soil by the Hyperaccumulating plant sedum alfredii. *Environ. Sci. Technol.* 51, 5675–5684. doi: 10.1021/acs.est.6b06531

Huang, G., You, J., Zhou, X., Ren, C., Islam, M. S., and Hu, H. (2020). Effects of low molecular weight organic acids on cu accumulation by castor bean and soil enzyme activities. *Ecotoxicol. Environ. Saf.* 203:110983. doi: 10.1016/j.ecoenv.2020.110983

Huang, H., Zhao, Y., Fan, L., Jin, Q., Yang, G., and Xu, Z. (2020). Improvement of manganese phytoremediation by Broussonetia papyrifera with two plant growth promoting (PGP) bacillus species. *Chemosphere* 260:127614. doi: 10.1016/j.chemosphere.2020.127614

Huo, W., Zou, R., Wang, L., Guo, W., Zhang, D., and Fan, H. (2018). Effect of different forms of N fertilizers on the hyperaccumulator *Solanum nigrum L.* and maize in intercropping mode under Cd stress. *RSC Adv.* 8, 421–4218. doi: 10.1039/c8ra07151a

Hui, F., Liu, J., Gao, Q., and Lou, B.Biotechnology, I. O., University, Z., Co., C., Ltd., & Sciences, A. E (2015). *Piriformospora indica* confers cadmium tolerance in Nicotiana tabacum. *J. Environ. Sci.* 37, 184–191. doi: 10.1016/j.jes.2015.06.005

Jeong, S., Moon, H. S., Nam, K., Kim, J. Y., and Kim, T. S. (2012). Application of phosphate-solubilizing bacteria for enhancing bioavailability and phytoextraction of cadmium (cd) from polluted soil. *Chemosphere* 88, 204–210. doi: 10.1016/j.chemosphere.2012.03.013

Khalid, M., Ur-Rahman, S., Hassani, D., Hayat, K., Zhou, P., and Hui, N. (2021). Advances in fungal-assisted phytoremediation of heavy metals: a review. *Pedosphere* 31, 475–495. doi: 10.1016/s1002-0160(20)60091-1

Khalid, M., Ur-rahman, S., Tan, H., Su, L., Zhou, P., and Hui, N. (2022). Mutualistic fungus *Piriformospora indica* modulates cadmium phytoremediation properties of host plant via concerted action of enzymatic and non-enzymatic biochemicals. *Pedosphere* 32, 256–267. doi: 10.1016/s1002-0160(21)60014-0

Kloepper, J. W., and Schroth, M. N. (1978). *Plant growth-promoting rhizobacteria on radishes*. IV international conference on plant pathogenic bacteria. *In: Proceedings of the 4th international conference on plant pathogenic bacteria, Angers, France 1978*. 879–882.

Li, D., Zheng, X., Lin, L., An, Q., Jiao, Y., Li, Q., et al. (2022). Remediation of soils co-contaminated with cadmium and dichlorodiphenyltrichloroethanes by king grass associated with *Piriformospora indica*: insights into the regulation of root excretion and reshaping of rhizosphere microbial community structure. *J. Hazard. Mater.* 422:126936. doi: 10.1016/j.jhazmat.2021.126936

Liu, H., Brettell, L. E., Qiu, Z., and Singh, B. K. (2020). Microbiome-mediated stress resistance in plants. *Trends Plant Sci.* 25, 733–743. doi: 10.1016/j.tplants.2020.03.014

Liu, A., Wang, W., Zheng, X., Chen, X., Fu, W., Wang, G., et al. (2022). Improvement of the cd and Zn phytoremediation efficiency of rice (Oryza sativa) through the inoculation of a metal-resistant PGPR strain. *Chemosphere* 302:134900. doi: 10.1016/j.chemosphere.2022.134900

Luo, J., Guo, X., Tao, Q., Li, J., Liu, Y., Du, Y., et al. (2021). Succession of the composition and co-occurrence networks of rhizosphere microbiota is linked to cd/Zn hyperaccumulation. *Soil Biol. Biochem.* 153:108120. doi: 10.1016/j.soilbio.2020.108120

Luo, N., Li, X., Chen, A. Y., Zhang, L. J., Zhao, H. M., Xiang, L., et al. (2017). Does arbuscular mycorrhizal fungus affect cadmium uptake and chemical forms in rice at different growth stages? *Sci. Total Environ.* 599–600, 1564–1572. doi: 10.1016/j.scitotenv.2017.05.047

Mani, D., Kumar, C., and Patel, N. K. (2015). Integrated micro-biochemical approach for phytoremediation of cadmium and zinc contaminated soils. *Ecotoxicol. Environ. Saf.* 111, 86–95. doi: 10.1016/j.ecoenv.2014.09.019

Mao, L. (2016). Research overview on *Piriformospora indica* and its interaction effect with plants. *Anhui Agric. Sci. Bullet.* 22, 47–50,99. doi: 10.3969/j.issn.1007-7731.2016.11.019

Marques, A. P. G. C., Moreira, H., Franco, A. R., Rangel, A. O. S. S., and Castro, P. M. L. (2013). Inoculating Helianthus annuus (sunflower) grown in zinc and cadmium contaminated soils with plant growth promoting bacteria – effects on phytoremediation strategies. *Chemosphere* 92, 74–83. doi: 10.1016/j.chemosphere.2013.02.055

Naumoff, D. G., and Dedysh, S. N. (2012). Lateral gene transfer between the Bacteroidetes and Acidobacteria: The case of α-l-rhamnosidases. *FEBS Lett.* 586, 3843–3851. doi: 10.1016/j.febslet.2012.09.005

Nowack, B., Schwyzer, I., and Schulin, R. (2008). Uptake of Zn and Fe by wheat (Triticum aestivum var. Greina) and transfer to the grains in the presence of chelating agents (ethylenediaminedisuccinic acid and ethylenediaminetetraacetic acid). *J. Agric. Food Chem.* 56, 4643–4649. doi: 10.1021/jf800041b

Peng, S., Le, C., and Li, S. (2014). Remediation methods of cadmium contaminated soil and research progress on bioremediation. *Environ. Dev.* 26, 86–90. doi: 10.3969/j.issn.1007-0370.2014.03.030

Pramanik, K., Mitra, S., Sarkar, A., and Maiti, T. K. (2018). Alleviation of phytotoxic effects of cadmium on rice seedlings by cadmium resistant PGPR strain Enterobacter aerogenes MCC 3092. *J. Hazard. Mater.* 351, 317–329. doi: 10.1016/j.jhazmat.2018.03.009

Rajkumar, M., Ae, N., and Freitas, H. (2009). Endophytic bacteria and their potential to enhance heavy metal phytoextraction. *Chemosphere* 77, 153–160. doi: 10.1016/j.chemosphere.2009.06.047

Rasouli-Sadaghiani, M. H., Barin, M., Khodaverdiloo, H., Moghaddam, S. S., Damalas, C. A., and Kazemalilou, S. (2019). *Arbuscular mycorrhizal fungi and rhizobacteria promote growth of Russian knapweed (Acroptilon repens L.) in a cd-contaminated soil*. Springer: United States, *38*.

Rawat, S. R., Mnnist, M. K., Bromberg, Y., and Hggblom, M. M. (2012). Comparative genomic and physiological analysis provides insights into the role of acidobacteria in organic carbon utilization in Arctic tundra soils. *FEMS Microbiol. Ecol.* 82, 341–355. doi: 10.1111/j.1574-6941.2012.01381.x

Rehman, M. Z. U., Rizwan, M., Ali, S., Ok, Y. S., Ishaque, W., Saifullah, , et al. (2017). Remediation of heavy metal contaminated soils by using *Solanum nigrum*: a review. *Ecotoxicol. Environ. Saf.* 143, 236–248. doi: 10.1016/j.ecoenv.2017.05.038

Robinson, B. H., Leblanc, M., Petit, D., Brooks, R. R., Kirkman, J. H., and Gregg, P. E. H. (1998). The potential of *Thlaspi caerulescens* for phytoremediation of contaminated soils. *Plant Soil* 203, 47–56. doi: 10.1023/A:1004328816645

Saha, P., Shinde, O., and Sarkar, S. (2017). Phytoremediation of industrial mines wastewater using water hyacinth. *Int. J. Phytoremediation* 19, 87–96. doi: 10.1080/15226514.2016.1216078

Shahabivand, S., Maivan, H. Z., Goltapeh, E. M., Sharifi, M., and Aliloo, A. A. (2012). The effects of root endophyte and arbuscular mycorrhizal fungi on growth and cadmium accumulation in wheat under cadmium toxicity. *Plant Physiol. Biochem.* 60, 53–58. doi: 10.1016/j.plaphy.2012.07.018

Shahabivand, S., Parvaneh, A., and Aliloo, A. A. (2017). Root endophytic fungus *Piriformospora indica* affected growth, cadmium partitioning and chlorophyll fluorescence of sunflower under cadmium toxicity. *Ecotoxicol. Environ. Saf.* 145, 496–502. doi: 10.1016/j.ecoenv.2017.07.064

Sheng, X., Sun, L., Huang, Z., He, L., Zhang, W., and Chen, Z. (2012). Promotion of growth and cu accumulation of bio-energy crop (Zea mays) by bacteria: implications for energy plant biomass production and phytoremediation. *J. Environ. Manag.* 103, 58–64. doi: 10.1016/j.jenvman.2012.02.030

Sherameti, I., Tripathi, S., Varma, A., and Oelmüller, R. (2008). The root-colonizing endophyte Pirifomospora indica confers drought tolerance in Arabidopsis by stimulating the expression of drought stress-related genes in leaves. *Mol. Plant Microbe Interact.* 21, 799–807. doi: 10.1094/MPMI-21-6-0799

Shi, S., Nuccio, E. E., Shi, Z. J., He, Z., Zhou, J., and Firestone, M. K. (2016). The interconnected rhizosphere: high network complexity dominates rhizosphere assemblages. *Ecol. Lett.* 19, 926–936. doi: 10.1111/ele.12630

Spain, A. M., Krumholz, L. R., and Elshahed, M. S. (2009). Abundance, composition, diversity and novelty of soil Proteobacteria. *ISME J.* 3, 992–1000. doi: 10.1038/ismej.2009.43

Tang, L., Hamid, Y., Zehra, A., Sahito, Z. A., He, Z., Beri, W. T., et al. (2020). Fava bean intercropping with sedum alfredii inoculated with endophytes enhances phytoremediation of cadmium and lead co-contaminated field. *Environ. Pollut.* 265:114861. doi: 10.1016/j.envpol.2020.114861

Tang, H., Shi, X., Wang, X., Hao, H., Zhang, X.-M., and Zhang, L.-P. (2016). Environmental controls over Actinobacteria communities in ecological sensitive Yanshan Mountains zone [article]. *Front. Microbiol.* 7:343. doi: 10.3389/fmicb.2016.00343

Vadassery, J., Tripathi, S., Prasad, R., Varma, A., and Oelmüller, R. (2009). Monodehydroascorbate reductase 2 and dehydroascorbate reductase 5 are crucial for a mutualistic interaction between *Piriformospora indica* and Arabidopsis. *J. Plant Physiol.* 166, 1263–1274. doi: 10.1016/j.jplph.2008.12.016

Verma, S., Varma, A., Rexer, K. H., Hassel, A., Kost, G., Sarbhoy, A., et al. (1998). *Piriformospora indica*, gen. Et sp. nov., a new root-colonizing fungus. *Mycologia* 90, 896–903. doi: 10.1080/00275514.1998.12026983

Waller, F., Achatz, B., Baltruschat, H., Fodor, J., Becker, K., Fischer, M., et al. (2005). The endophytic fungus *Piriformospora indica* reprograms barley to salt-stress tolerance, disease resistance, and higher yield [article]. *Proc. Natl. Acad. Sci. U. S. A.* 102, 13386–13391. doi: 10.1073/pnas.0504423102

Wang, X., Fang, L., Beiyuan, J., Cui, Y., Peng, Q., Zhu, S., et al. (2021). Improvement of alfalfa resistance against cd stress through rhizobia and arbuscular mycorrhiza fungi co-inoculation in cd-contaminated soil. *Environ. Pollut.* 277:116758. doi: 10.1016/j.envpol.2021.116758

Wang, X. M., Hong-Wei, J. I., Liu, W. J., Liu, W., and Bo-Wen, L. I. (2014). Effect of bacillus megateriumand Brassica juncea combination on Phytoextraction of cd from polluted soil. *J. Soil Water Conserv.* 28, 232–236. doi: 10.13870/j.cnki.stbcxb.2014.04.043

Wang, F. Y., Lin, X. G., and Yin, R. (2007). Effect of Arbuscular Mycorrhizal fungal inoculation on heavy metal accumulation of maize grown in a naturally contaminated soil. *Int. J. Phytoremed.* 9, 345–353. doi: 10.1080/15226510701476214

Wang, G., Wang, L., Ma, F., You, Y., Wang, Y., and Yang, D. (2020). Integration of earthworms and arbuscular mycorrhizal fungi into phytoremediation of cadmium-contaminated soil by Solanum nigrum L. *J. Hazard. Mater.* 389:121873. doi: 10.1016/j.jhazmat.2019.121873

Wang, G., Zhang, Q., Du, W., Ai, F., Yin, Y., Ji, R., et al. (2021). Microbial communities in the rhizosphere of different willow genotypes affect phytoremediation potential in cd contaminated soil. *Sci. Total Environ.* 769:145224. doi: 10.1016/j.scitotenv.2021.145224

Wang, L., Zou, R., Li, Y. C., Tong, Z., You, M., Huo, W., et al. (2020). Effect of wheat-Solanum nigrum L. intercropping on cd accumulation by plants and soil bacterial community under cd contaminated soil. *Ecotoxicol. Environ. Saf.* 206:111383. doi: 10.1016/j.ecoenv.2020.111383

Wu, S., Xin, Z., Chen, B., Wu, Z., and Wang, Y. (2015). Chromium immobilization by extraradical mycelium of arbuscular mycorrhiza contributes to plant chromium tolerance. *Environ. Exp. Bot.* 122, 10–18. doi: 10.1016/j.envexpbot.2015.08.006

Xu, L., Dai, H., Skuza, L., and Wei, S. (2020). The effects of different electric fields and electrodes on *Solanum nigrum* L Cd hyperaccumulation in soil. *Chemosphere* 246:125666. doi: 10.1016/j.chemosphere.2019.125666

Xun, W., Huang, T., Li, W., Ren, Y., Xiong, W., Ran, W., et al. (2017). Alteration of soil bacterial interaction networks driven by different long-term fertilization management practices in the red soil of South China. *Appl. Soil Ecol.* 120, 128–134. doi: 10.1016/j.apsoil.2017.08.013

Xun, F., Xie, B., Liu, S., and Guo, C. (2015). Effect of plant growth-promoting bacteria (PGPR) and arbuscular mycorrhizal fungi (AMF) inoculation on oats in saline-alkali soil contaminated by petroleum to enhance phytoremediation. *Environ. Sci. Pollut. Res.* 22, 598–608. doi: 10.1007/s11356-014-3396-4

Yan, A., Wang, Y., Tan, S. N., Mohd Yusof, M. L., Ghosh, S., and Chen, Z. (2020). Phytoremediation: a promising approach for Revegetation of heavy metal-polluted land. *Front. Plant Sci.* 11:359. doi: 10.3389/fpls.2020.00359

Yang, Y., Liang, Y., Han, X., Chiu, T.-Y., Ghosh, A., Chen, H., et al. (2016). The roles of arbuscular mycorrhizal fungi (AMF) in phytoremediation and tree-herb interactions in Pb contaminated soil. *Sci. Rep.* 6:469. doi: 10.1038/srep20469

Yang, X., Qin, J., Li, J., Lai, Z., and Li, H. (2021). Upland rice intercropping with Solanum nigrum inoculated with arbuscular mycorrhizal fungi reduces grain cd while promoting phytoremediation of cd-contaminated soil. *J. Hazard. Mater.* 406:124325. doi: 10.1016/j.jhazmat.2020.124325

Yang, Z., Xue, B., Song, G., and Shi, S. (2022). Effects of citric acid on antioxidant system and carbon-nitrogen metabolism of Elymus dahuricus under cd stress. *Ecotoxicol. Environ. Saf.* 233:113321. doi: 10.1016/j.ecoenv.2022.113321

Yergeau, E., Sanschagrin, S., Maynard, C., St-Arnaud, M., and Greer, C. W. (2014). Microbial expression profiles in the rhizosphere of willows depend on soil contamination. *ISME J.* 8, 344–358. doi: 10.1038/ismej.2013.163

Zhang, H., Xu, N., Li, X., Long, J., Sui, X., Wu, Y., et al. (2018). Arbuscular Mycorrhizal fungi (Glomus mosseae) improves growth, photosynthesis and protects photosystem II in leaves of Lolium perenne L. in cadmium contaminated soil. *Front. Plant* 9:1156. doi: 10.3389/fpls.2018.01156

Zhiguo, Y., and Qixing, Z. (2009). Growth responses and cadmium accumulation of Mirabilis Jalapa L. under interaction between cadmium and phosphorus. *J. Hazard. Mater.* 167, 38–43. doi: 10.1016/j.jhazmat.2008.12.082

Zhou, F., Emonet, A., Dénervaud Tendon, V., Marhavy, P., Wu, D., Lahaye, T., et al. (2020). Co-incidence of damage and microbial patterns controls localized immune responses in roots. *Cells* 180, 440–453.e18. doi: 10.1016/j.cell.2020.01.013

Zhou, X., Wang, S., Liu, Y., Huang, G., Yao, S., and Hu, H. (2020). Coupling phytoremediation efficiency and detoxification to assess the role of P in the cu tolerant Ricinus communis L. *Chemosphere* 247:125965. doi: 10.1016/j.chemosphere.2020.125965

frontiers | Frontiers in Microbiology

TYPE Original Research
PUBLISHED 03 February 2023
DOI 10.3389/fmicb.2023.1104077

OPEN ACCESS

EDITED BY
Muhammad Saleem,
Alabama State University,
United States

REVIEWED BY
Kailou Liu,
Jiangxi Institute of Red Soil,
China
Jiang Nan,
China National Rice Research Institute (CAAS),
China
Ruibo Sun,
Chinese Academy of Sciences,
China

*CORRESPONDENCE
Jie Zhang
✉ mn_zhangjie@163.com
Yanli Li
✉ yanli202211@126.com

SPECIALTY SECTION
This article was submitted to
Microbe and Virus Interactions with Plants,
a section of the journal
Frontiers in Microbiology

RECEIVED 21 November 2022
ACCEPTED 10 January 2023
PUBLISHED 03 February 2023

CITATION
Sun L, Zhang J, Zhao J, Lu X, Xiao C, Xiao Z, Zhang T, Gu Y, Sun H, Liu H and Li Y (2023) Effects of *Cinnamomum camphora* coppice planting on soil fertility, microbial community structure and enzyme activity in subtropical China.
Front. Microbiol. 14:1104077.
doi: 10.3389/fmicb.2023.1104077

Effects of *Cinnamomum camphora* coppice planting on soil fertility, microbial community structure and enzyme activity in subtropical China

Luyuan Sun[1,2], Jie Zhang[1]*, Jiao Zhao[1], Xianghui Lu[1], Changlong Xiao[1], Zufei Xiao[1], Ting Zhang[3], Yueqi Gu[1], He Sun[1], Han Liu[2] and Yanli Li[2]*

[1]Jiangxi Provincial Engineering Research Center for Seed-Breeding and Utilization of Camphor Trees, School of Hydraulic and Ecological Engineering, Nanchang Institute of Technology, Nanchang, China, [2]College of Agriculture, Yangtze University, Jingzhou, China, [3]Jiangxi Academic of Forestry, Nanchang, China

Cinnamomum camphora (*C. camphora*) is a broad-leaved evergreen tree cultivated in subtropical China. Currently, the use of *C. camphora* clonal cuttings for coppice management has become popular. However, the effects of *C. camphora* coppice planting on soil abiotic and biotic variances remained unclear. In this study, we collected soil from three points in the seven-year *C. camphora* coppice planting land: under the tree canopy (P15), between trees (P50), and abandoned land (Control) to investigate the effects of *C. camphora* coppice planting on soil fertility, microbial community structure and enzyme activity. The results revealed that *C. camphora* coppice planting significantly increased soil fertility in the point under the tree canopy (P15) and point between trees (P50), and P15 had more significant effects than P50. Meanwhile, in P15 and P50, soil bacterial, fungal alpha-diversity were improved and microbial community structures were also changed. And the changes of soil organic carbon and total nitrogen promote the transformation of soil bacterial, fungal community structures, respectively. In addition, *C. camphora* coppice planting significantly ($p<0.05$) increased soil urease (UE), polyphenol oxidase, and peroxidase activities, while significantly decreased soil ACP activity. This study demonstrated that the *C. camphora* coppice planting could improve soil fertility in subtropical China, which promoted the transformation of soil microbial community from *oligotrophs* (*K*-strategist) to *copiotrophs* (*r*-strategist). Thus, this work can provide a theoretical basis for soil nutrient variation and productive management of *C. camphora* coppice plantation in subtropical China.

KEYWORDS

***Cinnamomum camphora* coppice planting, soil fertility, bacterial community structure, fungal community structure, enzyme activity**

Introduction

Tree planting has been proposed as a practical method to prevent soil degradation. It can increase vegetation coverage, reduce rain erosion and enhance soil water and fertilizer retention ability (Speranza et al., 2019; Kumar et al., 2021). Meanwhile, the litterfall will return generous amounts of organic matter to the soil and the well-developed roots can activate the soil nutrients elements (Asigbaase et al., 2021). All of these are vital in the formation and evolution of planting land soil fertility (Feng et al., 2019). Various studies proved that tree planting can improve the soil nutrient

stocks and availabilities in the wasteland and farmland (Zarafshar et al., 2020). For instance, relative to the abandoned land, *Robinia pseudoacacia* planting significantly increased the soil total C, N, and P nutrients in Calcaric Cambisol of the Loess Plateau (Zhang et al., 2019). And *Shorea robusta* planting significantly enhanced the available N and P contents in the topsoil compared with the agricultural land used for *Oryza sativa* L. cultivation in tropical areas (Ahirwal and Maiti, 2016). Nevertheless, some researches declared that tree planting has the negative impact on soil fertility. Teng et al. (2020) summarized that the 19-year-old *Pinus sylvestris* var. *mongolica* planting decreased the soil organic carbon (SOC) and TN contents in aeolian sandy soil of northern China. Xu et al. (2021a) also recorded that in subtropical China, the *Manglietia glauca Blume* planting reduced the soil TN and AP contents relative to the abandoned land with 10.42 and 58.77%, respectively. Thus, soil fertility under tree planting may vary with tree species, soil types, and so on.

Soil microorganisms are highly sensitive to changes in soil nutrients and are regarded as one critical biological indicator of soil fertility (Carrara et al., 2018; Liu et al., 2018a; Sun et al., 2020). Tree planting will exert extensive and profound impacts on soil microorganisms (Thoms et al., 2010). A previous study recorded that 20-year-old *Ormosia hosiei* planting obviously improved the soil microbial (bacterial and fungal) biomass and diversity in red-yellow soil (Wan et al., 2021). While the rubber plantation caused the degradation of the soil microbial community structure relative to the natural forests in Latosols and Ferralsols in tropical regions (Monkai et al., 2018). The soil fertility variations caused by tree planting are the dominant factors that drive variations in soil microbial community (Pereira et al., 2019). Xu et al. (2021b) believed that the increase of SOC and TN in *R. pseudoacacia* planting improved the microbial biomass and nutrients metabolism capability. On the contrary, Wu et al. (2015) discovered that with the increase of stand age in *Pinus elliottii* planting, decreased soil fertility leads to the decline of total PLFA amounts and carbon metabolic capability. Hence, to verify the changes of soil microbial community and determine their driving factors after tree planting are conducive to timely and efficiently adjusting the management strategies, thereby maintaining the stability of the forest ecosystems and promoting the sustainable development of forest resources.

Soil enzymes are secreted by soil microorganisms, and they have a pivotal influence on biochemical processes such as litter decomposition and element cycling (Rosinger et al., 2019). Tree planting induces strong effects on soil enzyme activities, and their activities may vary among different tree species (Bueno de Mesquita et al., 2017). Chen et al. (2022) reported that the *Hippophae rhamnoides* (broadleaf) planting increased enzyme activities of soil catalase, urease, and polyphenol oxidase (PPO) compared with the *Larix gmelina* (conifer) planting. Wang et al. (2020) proved that broadleaved tree planting increased soil PPO and peroxidase (POD) activities, while coniferous tree planting increased soil acid phosphatase activity (Moghimian et al., 2017). Cause broadleaved trees have higher litterfall quantity and quality (with low carbon to nitrogen ratio), which can produce large amounts of easily decomposed organic matter to stimulate microbial reproduction and thus secrete more extracellular enzymes (Nakayama et al., 2019). On the contrary, coniferous trees have lower litterfall quantity and quality (with high carbon to nitrogen ratio) with a great deal of hardly decomposed tannin, resin, and wax, which is unfavorable for metabolism of soil microorganisms (Ushio et al., 2008). Therefore, effects on soil enzyme activities will influence by different tree species.

Cinnamomum camphora (L.) Presl is a broad-leaved evergreen tree belonging to the Lauraceae family, which is widely distributed in subtropical China (Liu et al., 2022). *C. camphora* tree can produce large amounts of secondary metabolites such as essential oil (Zhong et al., 2022). Traditionally, the whole *C. camphora* tree was cut down to extract essential oil from its roots, stems, and leaves, and this disposable production method will cause great damage to the ecological environment (Liu et al., 2018b). Currently, using the *C. camphora* clonal cuttings for coppice management has become popular in southern China (Zhao, 2021). From the second year after transplanting, its aerial parts are felled down at 20 cm away from the ground to extract essential oil during July to September every year. Then the remaining *C. camphora* tree stump will sprout year after year, so as to realize the circular production. This management method is similar to regular harvest of crops, which is fundamentally different from traditional tree planting. However, the effects of *C. camphora* coppice planting patterns on soil quality and its ecological effects are still unclear.

In this study, one 5-year-old camphor coppice plantation land was selected to compare with the adjacent abandoned land in subtropical China. We further chose the point under the tree canopy and the point between trees. The former is greatly affected by nutrients transfer and tree growth, while the latter is the opposite. The major objectives of the present study were: (1) to determine how the *C. camphora* coppice planting affected soil fertility. (2) To reveal how the soil microbial community structure varied with the *C. camphora* coppice planting, and confirm the key driving factors. (3) To explore how soil enzyme activity responded to the *C. camphora* coppice planting and clarify the main reasons. This study can offer a theoretical basis for scientifically guiding the production and management of *C. camphora* coppice plantations in subtropical China.

Materials and methods

Study area

The field experiment was conducted on *C. camphora* coppice plantation land in Guixi City, Jiangxi Province, southern China (28°17′46″ N, 117°13′28″E). This research region has the subtropical monsoon climate in which the mean annual temperature precipitation and sunlight hours are 18.8°C, 1980.8 mm, and 1611.5 h at this site, respectively. The soils derived from the quaternary red clay, was abandoned land before the experiment. The initial properties of the topsoil (0–15 cm) with soil pH of 4.83, and with SOC, total nitrogen (TN), available nitrogen (AN), available phosphorus (AP) of 12.95, 0.96, 102.93, 5.21 g·kg^{-1}, respectively.

Experiment design and soil sampling

The 5,000 m^2 *C. camphora* coppice plantation land selected for this study was established in 2015. In early September of each year since 2016, the aboveground part of the *C. camphora* tree was felled at 20 cm away from the ground for essential oil extraction. The row and inter-plant spacings of the *C. camphora* tree are 1 m × 1 m, and the planting density is 10,000 tree·hm^{-2}. Urea (contains 46% N), calcium magnesium phosphate (contains 12% P_2O_5) and potassium chloride (contains 60% K_2O) were used for the nitrogen, phosphorus, potassium fertilizers respectively, and their application rate were all 150 g tree^{-1} year^{-1}. 50% of the fertilizers were applied in early March and the remaining 50% were applied in late September after the *C. camphora* tree felling. The fertilization point (FP) was a 15 cm deep circle 25 cm from the center of the tree (Supplementary Figure S1).

In this study, we selected three different points as three treatments, each with four replicates: (1) Point under the tree canopy, 15 cm from the center of the tree (P15, inside the fertilization point); (2) point between trees, 50 cm from the center of the tree (P50, outside the fertilization point); (3) point in the abandoned land (control, next to the selected *C. camphora* coppice). The specific sampling scheme is shown (Supplementary Figure S1). Soil samples were randomly collected using the S-shaped sampling method after the *C. camphora* tree felling on September 12th, 2021. Each sample was carried out using a soil core sampler (diameter of 2.0 cm) from the depth of 0–15 cm. Each core was taken in 50 m^2 areas, and twenty cores were mixed into one soil sample. Then pass the soils through the 2 mm sieve to remove the impurities and divided into three parts: one part was air-dried for soil fertility measurement, the second part was preserved at 4°C for enzyme activity measurement, and the remaining part was kept at −80°C for DNA extraction.

Soil properties and enzyme activity

Soil pH value (soil to water ratio of 1:2.5) was measured with a pH meter (FE28-Standard, METTLER-TOLEDO, Switzerland; Sun et al., 2022). SOC was determined by dichromate oxidation and titration with ferrous sulfate. TN was determined using the Kjeldahl digestion distillation method. Available nitrogen (AN) and phosphorus (AP) were measured using alkali hydrolyzation and Bray method, respectively (Akhtar et al., 2018). Soil enzyme activities of invertase (INV), urease (UE), acid phosphatase (ACP), catalase (CAT), PPO, and POD were determined using kits from Beijing Solarbio Technology Co. Ltd. according to the test instructions (Tabatabai, 1994; Saiya-Cork et al., 2002).

Soil microbial DNA extraction and Illumina MiSeq sequencing

DNA was extracted from half a gram of fresh soil using the FastDNA® SPIN Kit for soil. The purification of DNA was tested by Power Clean DNA Clean-Up Kit to remove PCR inhibitors. The eluted DNA was examined by 1% (m/v) agarose gel electrophoresis and quantified with NanoDrop® 2000 spectrophotometer. Aliquots of the DNA were stored in a −20°C freezer for subsequent analyses. Primer sets Eub338 and Eub518 were used to determine the bacterial biomass by quantitative real-time PCR (qPCR) on the ABI Prism® 7300 Real-Time detection system. Fungal abundance was determined by Primer set SSU_0817 and SSU_1196 of the 18S rRNA gene in the same method with bacteria. The V4-V5 highly variable regions of the bacterial 16S rRNA genes were amplified with barcoded universal primers 515F (5′-GTGCCAGCMGCCGCGGTAA-3′) and 907R (5′-CCGTCAATTC CTTTGAGTTT-3′; Biddle et al., 2008). And the ITS regions of the fungal rRNA genes were amplified by primer sets ITS1F (5'-CTTGGTCATTTAGAGGAAGTAA-3′) and ITS2R (5-GCTGC GTTCTTCATCGATGC-3′; Adams et al., 2013). The qPCR parameters were referred to Xiang et al. (2021) and Jin et al. (2021) methods.

Bioinformatics analysis for raw sequences

The original raw sequences were analyzed using the QIIME v.1.91 pipeline (Caporaso et al., 2010). And short (<200 bp) and low quality (average scores <25) or sequences were removed before downstream analysis (Magoč and Salzberg, 2011). High-quality sequences at a 3% dissimilarity level were selected as OTUs using UNOISE algorithm (Edgar, 2016). Representative set sequences were analyzed by RDP classifier using the SILVA 132 database with a confidence threshold of 80% (Wang et al., 2007). The representative sequences of ITS were annotated for species using the UNITE database with the blast method (Kõljalg et al., 2013). For downstream analyses, the number of bacterial and fungal sequences was rarefied to 30, 772 and 36, 205 for each sample to uniform the sequencing depths, respectively. A total of 4,427 bacteria OTUs and 1,690 fungal OTUs were identified for subsequent analysis.

Statistical analysis

Firstly, we distinguished whether the initial data were accord with the normal distribution. The non-normally distributed data were logarithm or square root-transformed to make them close to normal distribution. And the mean and standard deviations (e.g., soil fertility indexes and enzyme activities, microbial abundance, and alpha diversity indexes) of different treatments were calculated. One-way analysis of variance (ANOVA) by Duncan's HSD test ($p < 0.05$) was used for multiple comparisons. Pearson correlation analysis was used to test the relationship between soil microbial abundance and alpha diversity indexes or enzyme activities and the soil fertility indexes. Constrained Principal of Coordinate Analysis (CAP) with Bray-Curtis distance was used to distinguish the differences of soil microbial communities or the enzyme profiling in different treatments, and analysis of similarity (ANOSIM) test was performed to verify whether the difference between treatments is significant. Using an Bray-Curtis distance matrix, the correlation between the soil microbial community structure or the enzyme profiling and soil fertility indexes was calculated using Mantel test with 999 permutations. The relationships between the soil microbial community composition or the enzyme profiling and soil fertility indexes were determined by redundancy analysis (RDA). Multivariate regression tree (MRT) was used to identify the key factors that shift the soil microbial community composition. Procrustes analysis was used to confirm the correlation between the soil enzyme profiling and microbial community composition in different treatments.

ANOVA and Pearson correlation analysis were conducted using the statistical software SPSS 20.0. ANOSIM, CAP, Mantel test, RDA, and Procrustes analysis were all done using the "vegan" package (Dixon, 2003), and MRT analysis was performed using the "mvpart" package of the R software (ver. 4.0.1; De'ath, 2003). The differences in soil microbial taxon and enzyme activities were assessed using STAMP software (Parks and Beiko, 2010).

Results

Soil fertility

Significant differences ($p < 0.05$) in soil fertility among different treatments were tested (Table 1). Compared with the Control, soil pH, SOC, TN, AN, and AP of the P15 were increased by 12.96% ($p < 0.05$), 44.29, 80.06% ($p < 0.05$), 79.46% ($p < 0.05$), and 560.16% ($p < 0.05$), respectively. Moreover, soil AN in P50 was significantly greater than Control with 33.99% ($p < 0.05$) increase, but there were no significant changes with other soil fertility indexes. Therefore,

TABLE 1 Soil fertility in the *Cinnamomum camphora* coppice planting.

Variables	P15	P50	Control
pH	5.51 ± 0.68a	4.72 ± 0.17b	4.88 ± 0.10b
SOC (g kg^{-1})	19.56 ± 1.55a	12.60 ± 1.62b	13.55 ± 0.50ab
TN (g kg^{-1})	1.78 ± 0.21a	1.14 ± 0.11b	0.99 ± 0.04b
AN (g kg^{-1})	212.62 ± 24.96a	158.75 ± 18.79b	118.48 ± 9.60c
AP (g kg^{-1})	32.54 ± 6.42a	6.86 ± 0.65b	4.93 ± 0.54b

P15, point under the tree canopy; P50, point between trees; Control, point in the abandoned land; SOC, soil organic carbon; TN, total nitrogen; AN, alkaline nitrogen; AP, available phosphorus. Values (mean ± S.D.) in the same column followed by different letters are significantly different from Duncan's HSD comparisons ($p < 0.05$).

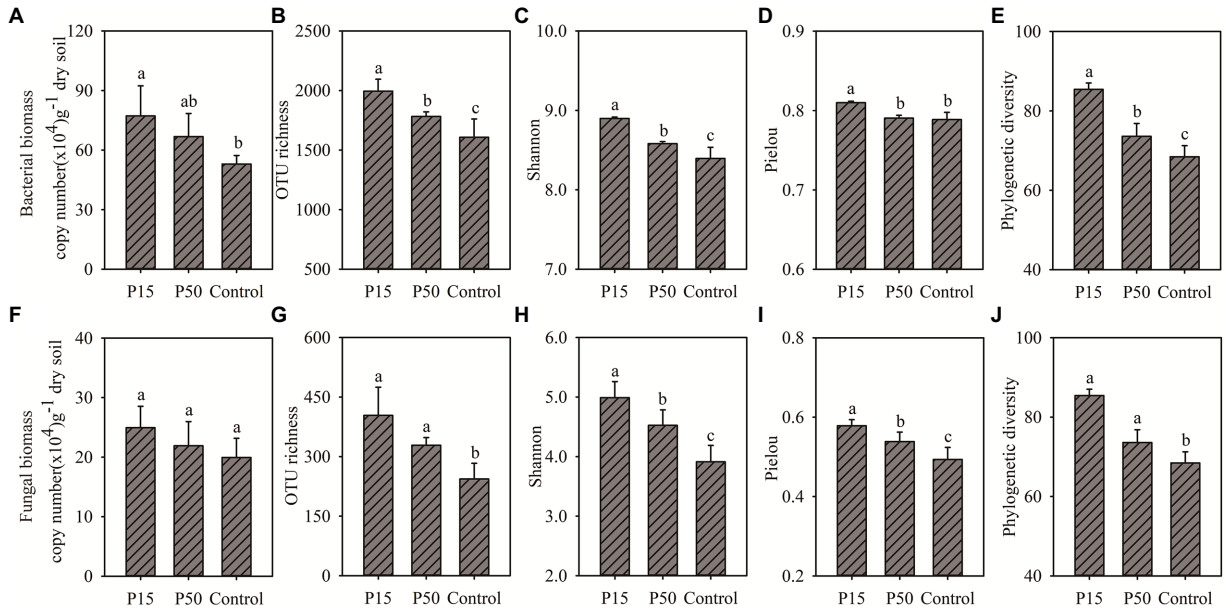

FIGURE 1
(A) Bacterial biomass, **(B)** Bacterial OTU richness, **(C)** Bacterial Shannon index, **(D)** Bacterial Pielou index, **(E)** Bacterial Phylogenetic diversity, **(F)** Fungal biomass, **(G)** Fungal OTU richness, **(H)** Fungal Shannon index, **(I)** Fungal Pielou index, **(J)** Fungal Phylogenetic diversity. Soil bacterial, fungal abundance and alpha-diversity under different treatments in the *Cinnamomum camphora* coppice planting. P15, point under the tree canopy; P50, point between trees; Control, point in the abandoned land. Bars represent mean; error bars denote standard deviation. Letters above bars represent differences from Duncan's HSD comparisons ($p<0.05$).

C. camphora coppice planting can increase soil fertility to a certain extent.

Soil bacterial and fungal community structure

Cinnamomum camphora coppice planting can increase the soil microbial biomass and alpha-diversity (Figure 1). Soil bacterial biomass in P15 and P50 increased by 45.68% ($p < 0.05$) and 26.05% ($p > 0.05$) in comparison with Control, respectively (Figure 1A). The soil bacterial alpha-diversity in P15 and P50 were significantly higher relative to Control, except the pielou index in P50 (Figures 1B–D). Similarly, the P15 and P50 increased soil fungal biomass by 25.00 and 9.79% compared with the Control (Figure 1F). Furthermore, the four fungal alpha-diversity indexes increased significantly ($p < 0.05$) in P15 and P50 relative to the control (Figures 1G–J). The increase of bacterial or fungal biomass and diversity indexes in P15 was greater than that in P50.

For bacterial, in comparison with the Control, the P15 and P50 significantly ($p < 0.05$) improved relative abundance of Proteobacteria (from 29.35 to 40.95 and 36.82%, respectively), Bacteroidetes (from 1.30 to 5.33 and 5.68%, respectively) and Gemmatimonadetes (from 1.26 to 2.51 and 1.47%, respectively). Adversely, relative abundance of Chloroflexi in P15 and P50 was significantly ($p < 0.05$) decreased by 71.49 and 59.46% relative to the Control (Supplementary Figure S2). STAMP analysis was used to analyze significantly differentiated bacterial genera between treatments (Supplementary Figure S3). There were thirteen bacterial genera in P15 and six bacterial genera in P50 significant differential with Control ($p < 0.05$, effect size >1). Specifically, relative to Control, P15 reduced relative abundance of *Conexibacter*, *Ktedonobacter*, *Edaphobacter*, *Fimbriiglobus*, *Rhodanobacter* and so forth, but enhanced relative abundance of *Gaiella* and GP6. Similarly, in comparison with Control, the P50 decreased relative abundance of *Conexibacter* and *Ktedonobacter*, whereas increased relative abundance of *Flavitalea* and *Chryseolinea*.

For fungal, in comparison with Control, the P15 ($p < 0.05$) and P50 increased relative abundance of Zygomycota (by 61.31 and 34.70%) and Basidiomycota (by 149.59 and 36.60%), but reduced the relative abundance of Ascomycota by 35.37 and 18.54% (Supplementary Figure S2). Significantly differentiated fungal genera between treatments were also analyzed (Supplementary Figure S3). Correspondingly, four fungal genera in P15 and five fungal genera in

TABLE 2 Soil enzyme activity in the *Cinnamomum camphora* coppice planting.

Variables	P15	P50	Control
INV ($mg\,g^{-1}\,24\,h^{-1}$)	6.56 ± 1.97a	6.10 ± 1.30a	4.43 ± 0.66a
UE ($\mu g\,g^{-1}\,24\,h^{-1}$)	342 ± 35a	247 ± 18b	212 ± 10b
ACP ($\mu mol\,g^{-1}\,24\,h^{-1}$)	20.48 ± 1.85b	18.97 ± 1.49b	23.53 ± 0.81a
CAT ($mg\,g^{-1}\,24\,h^{-1}$)	1.14 ± 0.07a	0.70 ± 0.08b	1.05 ± 0.03a
PPO ($mg\,g^{-1}\,24\,h^{-1}$)	30.06 ± 4.24a	23.88 ± 0.64b	14.74 ± 3.90c
POD ($mg\,g^{-1}\,24\,h^{-1}$)	25.36 ± 5.35a	16.58 ± 4.45b	2.68 ± 0.01c

P15, point under the tree canopy; P50, point between trees; Control, point in the abandoned land; INV, invertase; UE, urease; ACP, acid phosphatase; CAT, catalase; PPO, polyphenol oxidase; POD, peroxidase. Values (mean ± S.D.) in the same column followed by different letters are significantly different from Duncan's HSD comparisons ($p < 0.05$).

P50 were significantly different with the Control ($p < 0.05$, effect size >1). The relative abundance of *Talaromyces* and *Hyaloscyphaceae* were reduced in both the P15 and P50 relative to Control. In addition, compared with Control, P15 increased relative abundance of *Westerdykella* and *Trichocomaceae*, whereas P50 enhanced relative abundance of *Fusarium*, *Archaeorhizomyces* and *Flagellospora*.

Soil enzyme activities

Cinnamomum camphora coppice planting significantly affected the soil enzyme activities (Table 2). Soil UE, PPO, and POD activities were significant ($p < 0.05$) increased in P15 and P50 relative to Control, except the soil UE activity in the P50 ($p > 0.05$). Compared with Control, soil INV activity in P15 and P50 was increased ($p > 0.05$) by 47.98 and 37.58%. In addition, P15 and P50 significantly ($p < 0.05$) decreased the soil ACP activity, and P50 significantly ($p < 0.05$) decreased soil CAT activity in comparison with Control. STAMP analysis ($p < 0.05$, effect size >1) analyzed significantly different soil enzymes between treatments (Supplementary Figure S3). Specifically, in comparison with Control, P15 and P50 reduced the soil ACP activity, but enhanced the soil UE activity. Moreover, P15 also enhanced the soil POD activity.

Correlations between soil microbial community composition or enzyme activities and soil fertility indexes

Pearson correlation analysis was performed to further characterize the relationships between the soil microbial biomass, alpha-diversity, and dominant genera with soil fertility (Figure 2). The soil bacterial biomass was significantly positive correlated to SOC ($r = 0.705$, $p < 0.05$) and AP ($r = 0.687$, $p < 0.05$). As a whole, the four bacterial alpha-diversity indexes had significant positive correlation with all the soil fertility indexes ($p < 0.01$). For the dominant bacteria phyla, the Proteobacteria was significantly positive correlated with all the soil fertility indexes except pH, and the Gemmatimonadetes had significantly positive correlation with soil pH, SOC, TN and AP. However, the Chloroflexi was significantly negative correlated with soil TN ($r = -0.701$, $p < 0.05$), AN ($r = -0.795$, $p < 0.01$) and AP ($r = -0.645$, $p < 0.05$).

Further analyses illustrated that the soil fungal biomass only had a significant positive correlation with AN (Figure 2; $r = 0.659$, $p < 0.05$). Notably, the fungal OTU richness, Shannon index, and pielou indexes were all significantly positively correlated with all the soil fertility indexes except pH, whereas phylogenetic diversity was only significantly positively correlated with AN ($r = 0.696$, $p < 0.05$) and AP ($r = 0.632$, $p < 0.05$). And the Zygomycota was only significantly positive correlated with AN ($r = 0.651$, $p < 0.05$). Overall, the Basidiomycota was positively correlated with all the soil fertility indexes, while the Ascomycota showed the opposite trend.

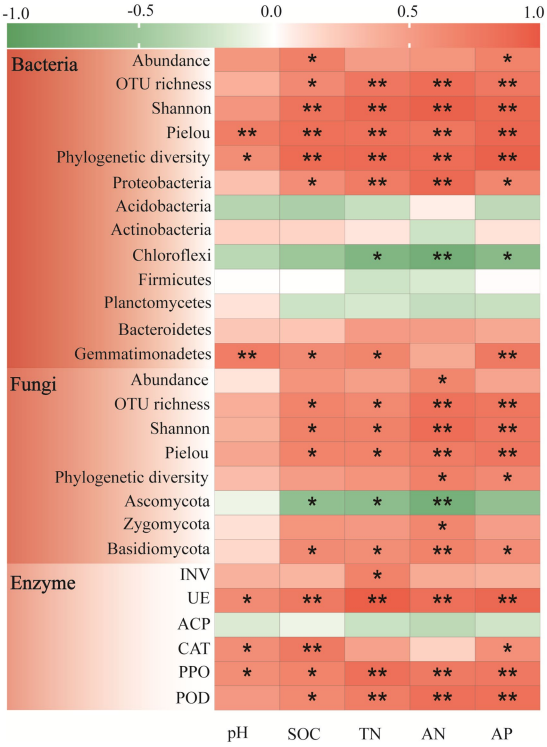

FIGURE 2
Pearson correlation analysis of soil fertility indexes with microbial community composition (abundance, alpha-diversity and dominant phyla) and enzyme activities in the *Cinnamomum camphora* coppice planting. Red represents a positive correlation, and green represents a negative correlation. (*p<0.05; **p<0.01).

Correlation analysis was also detected between soil enzyme activities and soil fertility (Figure 2). In general, the activities of soil UE, PPO, and POD were significantly positive correlated to all the soil fertility indexes. The soil CAT activity had significant positive correlation with pH ($r = 0.599$, $p < 0.05$), SOC ($r = 0.751$, $p < 0.01$), and AP ($r = 0.584$, $p < 0.05$), while the soil INV activity only positive correlated with TN ($r = 0.677$, $p < 0.05$). Nevertheless, the soil ACP activity was slightly negative correlated with all the soil fertility indexes.

Primary factors for changes in soil microbial community and the enzyme profiling

The CAP analysis showed significant differences in soil microbial community between treatments (Supplementary Figure S4). Remarkably, we found that the soil bacterial community clearly separated ($p = 0.001$) among the three treatments (Supplementary Figure 4A; 43.1% of total variance was explained, $p = 0.001$). ANOSIM tests (Supplementary Table S1) revealed significantly ($p < 0.05$) different soil bacterial community among each other. Mantel test exhibited that soil bacterial community had significant ($p < 0.01$) correlation with all the soil

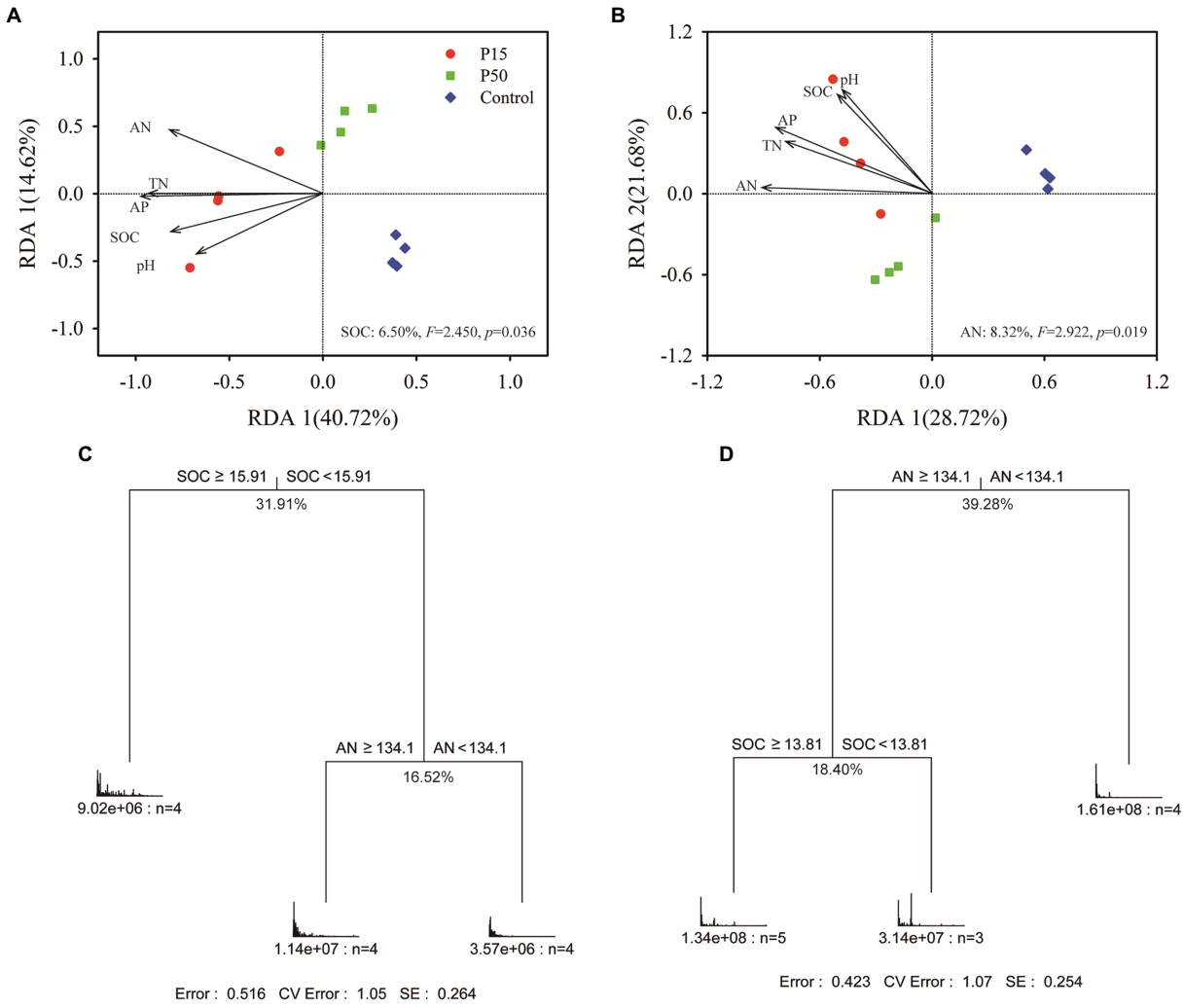

FIGURE 3
Redundancy analysis (RDA) between the soil bacterial **(A)**, fungal **(B)** community and fertility indexes at the OTU level in the *Cinnamomum camphora* coppice planting. P15, point under the tree canopy; P50, point between trees; Control, point in the abandoned land. Multivariate regression trees (MRT) of soil bacteria **(C)**, fungi **(D)** community composition and fertility indexes. Numbers under the crosses of each split indicate percentages of variance explained by the split.

fertility indexes (Supplementary Figure S5). In addition, RDA analysis pointed that the SOC ($F = 2.450$, $p = 0.036$) significantly affected soil bacterial community composition (Figure 3A). Furthermore, the MRT analysis performed that the SOC produced the largest deterministic effects on soil bacterial community variation (31.91%), with a threshold of 15.91 g kg^{-1} (Figure 3C).

Correspondingly, the CAP analysis corroborated obvious differences in soil fungal community (Supplementary Figure S4B, 39.6% of total variance was explained, $p = 0.001$), and the ANOSIM tests indicated there were significantly different ($p < 0.05$) between treatments (Supplementary Table S1). Mantel test (Supplementary Figure S5) further verified that soil fungal community had significant correlation with soil fertility indexes ($p < 0.05$), especially the soil AN and AP ($p < 0.01$). Similarly, RDA analysis suggested that the soil AN ($F = 2.922$, $p = 0.019$) was the primary factor shifting the fungal community composition. And MRT analysis showed that the soil AN produced the largest deterministic effects on soil fungal community variation (39.28%), with a threshold of 134.1 g kg^{-1} (Figure 3D).

In addition, CAP plot demonstrated that the soil enzyme profiling was also clearly segregated ($p = 0.007$) in three different treatments, which explains 50.4% of the variance in the data (Supplementary Figure 4C). ANOSIM tests pointed that the soil enzyme profiling in P15 and P50 were altered significantly ($p < 0.05$) compared with Control, but there was insignificant difference between P15 and P50 ($r = 0.0625$, $p = 0.318$). Unlike the soil microbial community, Mantel test (Supplementary Figure S5) revealed that there were no significant relationships between the soil enzyme profiling and fertility indexes.

Correlations between soil enzyme activities and microbial community

Due to the fact that there had no significant correlation between the soil enzyme profiling and fertility indexes, we further performed our analysis with Procrustes tests to find the linkages between the soil enzyme profiling and microbial community. Procrustes tests corroborated that the soil enzyme profiling had significant correlation

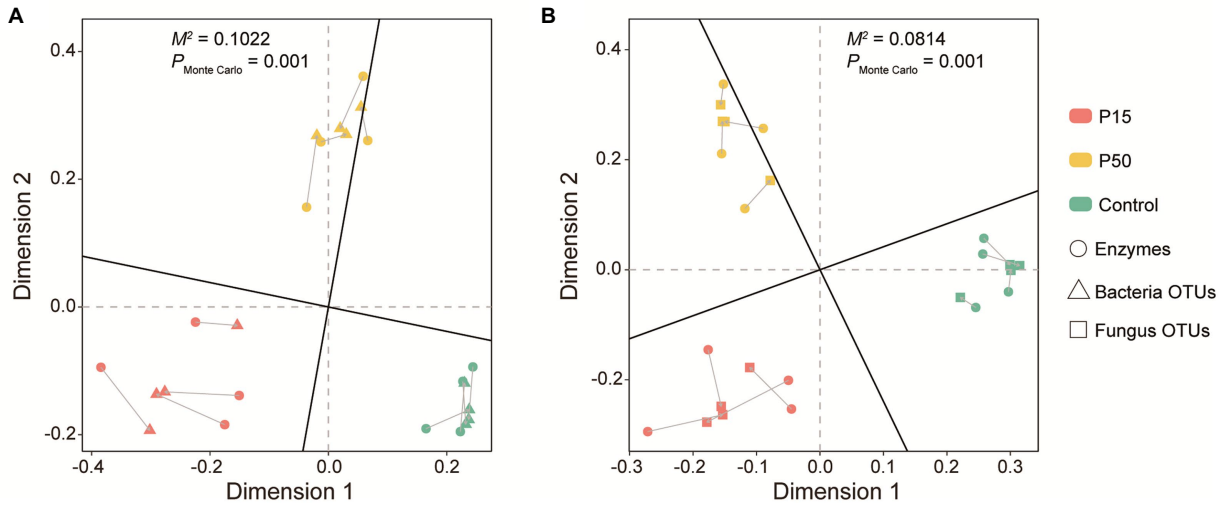

FIGURE 4
Procrustes analysis between soil bacterial **(A)**, fungal **(B)** community composition and enzyme profiling in the *Cinnamomum camphora* coppice planting. P15, point under the tree canopy; P50, point between trees; Control, point in the abandoned land. The lengths of connecting lines represent the dissimilarities of soil bacterial, fungal community composition and enzyme profiling.

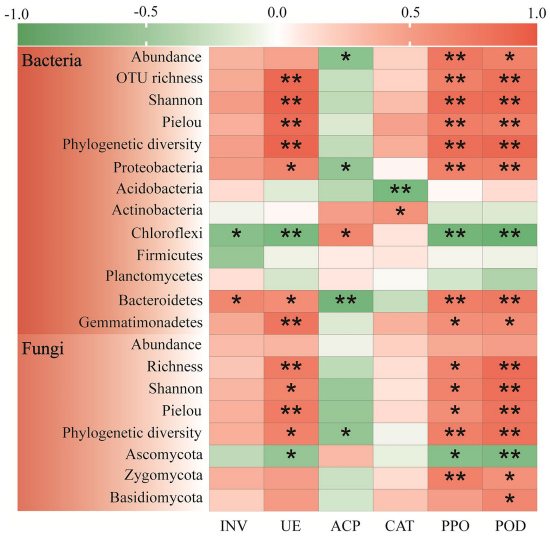

FIGURE 5
Pearson correlation heat maps between soil bacterial, fungal community composition (abundance, alpha-diversity and dominant phyla) and enzyme profiling in the *Cinnamomum camphora* coppice planting. Red represents a positive correlation, and green represents a negative correlation. (*p<0.05; **p<0.01).

with the soil bacterial (Figure 4A, Correlation r = 0.9475, M^2 = 0.1022, p = 0.001) and fungal community (Figure 4B, Correlation r = 0.9584, M^2 = 0.0814, p = 0.001).

Furthermore, relationships between soil enzyme activity and microorganism properties were testified by Pearson correlation analysis (Figure 5). In general, the soil UE, PPO, and POD activities had significantly positive correlation with soil bacterial biomass and alpha diversity, whereas the soil INV and CAT activities had no significant correlation with the above indexes. Notably, soil ACP activity only had significant negative relevance with the bacterial biomass (r = −0.635, p < 0.05). The soil UE, PPO, and POD activities were significantly positive connected with Proteobacteria, Bacteroidetes and Gemmatimonadetes, but negative connected with Chloroflexi. While the soil ACP activity showed the completely opposite tendency. Meanwhile, the soil INV activity had significantly positive relationship with Bacteroidetes (r = 0.665, p < 0.05) and significantly negative relationship with Chloroflexi (r = −0.665, p < 0.05). And the soil CAT activity was significant and positive connected with Actinobacteria (r = 0.579, p < 0.05) whereas significant and negative connected with Acidobacteria (r = −0.773, p < 0.01).

Correspondingly, the soil UE, PPO, and POD activities were significant and positive related to the four fungal alpha-diversity indexes, while the soil ACP activity was only significantly negative related to fungal phylogenetic diversity (r = −0.596, p < 0.05). The soil UE, PPO, and POD activities had significantly negative correlation with Ascomycota. In the meantime, the soil POD activity had significantly positive correlation with Zygomycota (r = 0.593, p < 0.05) and Basidiomycota (r = 0.661, p < 0.05), whereas the soil PPO activity only significantly positively correlated with Zygomycota (r = 0.713, p < 0.01). Remarkably, the soil INV and CAT activities had no significant correlation with all the soil fungal properties.

Discussion

Effects of *Cinnamomum camphora* coppice planting on soil fertility

In this study, the *C. camphora* tree was cultivated as coppice and its aerial part were annually cut down to extract the essential oil. This will inevitably take away nutrients from the soil. However, we found that relative to the abandoned land, the point under the tree canopy (P15) substantially increased the soil pH and N, P contents. Firstly, fertilization can compensate for the high quantities of soil nutrients consumed by the *C. camphora* trees (Selvaraj et al., 2017). Secondly, though *C. camphora* coppices were felled during July to September every year, they sprouted and form the canopy rapidly, which can

effectively reduce the erosion caused by the concentrated rainfall season (March to July) in south China (Hinojosa et al., 2021; Tang et al., 2021). Moreover, the continuously growing roots of the *C. camphora* tree can promote the activation and transportation of soil mineral elements (Männistö et al., 2016). Earlier study had suggested that the soil nutrients content under the tree canopy was higher than the point outside the tree canopy in the *Artemisia ordosica* Krasch planting (Qi et al., 2010). On account of the "fertility islands" effects that the soil fertility gradually decreased from the inside to the outside under the tree canopy (San Emeterio et al., 2021). Nevertheless, our research revealed that even the point between trees (P50), which was weakly affected by fertilization and tree growth, can somehow enhance the soil nutrients availability (Han et al., 2021). This further corroborated that the *C. camphora* tree planting can improve the soil fertility.

Effects of *Cinnamomum camphora* coppice planting on soil microbial structure

Soil microorganisms are important regulatory factors in soil organic matter transformation, and they may influence by changes in soil fertility after tree planting (Thébault et al., 2014). Huang et al. (2022) recorded that tree planting enhanced the SOC and TN contents, and they had notable correlation with soil microbial biomass and diversity. A previous study on *Cryptomeria japonica* also verified that the increase of the soil C and N nutrients stimulated the improvement of soil microbial biomass, OTU richness, and Shannon index (Sawada et al., 2021). Likewise, our results proved that the *C. camphora* tree coppice planting enhanced the bacterial, fungal biomass and diversity (Figure 1), and their change was induced by increased soil fertility (Figure 2). One possible reason was that the *C. camphora* tree coppice planting can produce a large amount of soil N, P nutrients and C substratum, which in turn provide more diverse niches available for microorganisms (Pereira et al., 2019; Asigbaase et al., 2021).

Alterations in soil microorganisms after tree planting were closely correlated with their ecological strategies (Fierer et al., 2007). The *C. camphora* coppice planting significantly influenced the soil microbial dominant phyla (Supplementary Figure S2). Proteobacteria was the typical *copiotrophs* (*r*-strategist), which generally exists in high C and N soils (Trivedi et al., 2013). An earlier study indicated that mixed *Eucalyptus grandis* plantings significantly improved soil fertility, and relative abundance of Proteobacteria increased from 14.29 to 27.90% (Zhang et al., 2022). In the present study, relative abundance of Proteobacteria increased significantly by 7.47 and 11.60% in P15 and P50, respectively. This also reflected that the *C. camphora* coppice planting can increase soil fertility. Similarly, Zygomycota and Basidiomycota were also *copiotrophs*, which can form the mycorrhiza with tree roots and use readily available nutrients in a short period (Wang et al., 2017; Zhu et al., 2019). Their relative abundance was also significantly improved in the *C. camphora* coppice planting (Supplementary Figure S2). And the correlation analysis further identified that Proteobacteria, Zygomycota, and Basidiomycota were significantly positively correlated with soil fertility indexes (Figure 2).

On the contrary, Chloroflexi and Ascomycota were the typical *oligotrophs* (*K*-strategist), early studies reported that with increase of soil fertility, relative abundance of Chloroflexi and Ascomycota were decreased (Zhu et al., 2019; Idbella et al., 2022). This further confirmed by our research that relative abundance of Chloroflexi and Ascomycota were significantly negative correlated with soil fertility indexes in general (Figure 2). Additionally, *Ktedonobacter* was the member of Chloroflexi, and *Talaromyces* and *Hyaloscyphaceae* were the members of Ascomycota. STAMP analysis indicated that their relative abundance was declining when soil fertility was improved. And in the low fertile soil, such as P15 *vs* Control, *Ktedonobacter*, *Talaromyces* and *Hyaloscyphaceae* were the significantly different species between treatments (Supplementary Figure S3). In conclusion, the *C. camphora* coppice planting shifted the soil microbial community from *oligotrophs* to *copiotrophs*, and relative abundance of *copiotrophs* microorganisms in P15 were increased from 37.78% (bacteria), 18.09% (fungi) to 53.80% (bacteria), 29.24% (fungi), respectively (Supplementary Table S2).

Various studies have summarized that soil microbial community compositions changed under tree planting. The conversion from natural forest to tree planting had significantly changed the community of soil bacteria (Jiang et al., 2021; Li et al., 2022), and SOC was the primary factor for its change (Zhang et al., 2016). This was consistent with our results, indicating that SOC can provide resources for soil bacterial community and modify its ecological strategy, thus affecting soil bacterial community composition (Qu et al., 2020; Yang et al., 2021a). Additionally, soil fungal community significantly shifted in the *C. camphora* coppice planting (Supplementary Figure S4), and RDA, MRT analysis exhibited that AN produced the largest deterministic effects to them (Figure 3). This had also confirmed by Wang et al. (2021) who recorded that soil fungal community composition had significant positive relation to soil AN content in *Cunninghamia lanceolate* (Lamb.) Hook plantings.

Effects of *Cinnamomum camphora* coppice planting on soil enzyme activities

Soil enzymes, as the participants in soil organic matter transformation, can also make vital functions in carbon (C), nitrogen (N), and phosphorus (P) cycling of soil ecosystems (Feyissa et al., 2022). our results declared the *C. camphora* coppice planting significantly enhanced the soil INV, UE, PPO and POD activities (Table 2). And correlation analysis suggested that soil enzyme activities except soil ACP showed positive relationship with soil pH and fertility indexes in general (Figure 2). Many previous studies pointed out that soil INV and UE activities were involved in soil C and N transformation, respectively (Boughattas et al., 2019; Zhu et al., 2019). Wang et al. (2018) acknowledge that *Camellia sinensis* L. planting increased soil C, N concentration, and soil INV, UE activities were also improved with the stand age. Moreover, soil PPO and POD were involved in the oxidation and degradation of soil lignin and SOM (Sinsabaugh, 2010), and their increase illustrated that *C. camphora* coppice planting can improve soil nutrients availability. Nevertheless, in the present study, soil ACP activity under the tree canopy (P15) and between the trees (P50) was significantly decreased. Though the soil ACP is involved in the decomposition of soil organic phosphorus to promote its metabolic turnover and reuse efficiency, the increasing soil available phosphorus content will reduce the ACP activity (Tran et al., 2010). In other words, high nutrient availability may inhibit soil ACP activity (Janes-Bassett et al., 2022), and we also found that there were negative correlations between soil ACP activity and soil fertility (Figure 2). And STAMP analysis further revealed that soil ACP activity was higher in the low fertility soil (Supplementary Figure S3).

Our work corroborated that soil enzyme profiling was weakly ($p > 0.05$) affected by soil fertility (Supplementary Figure S5), while they were highly connected with soil bacterial and fungal community (Figure 4). Further correlation analysis identified that soil UE, PPO, and POD activity was significantly positively correlated with soil microbial biomass and diversity (Figure 5). Earlier studies declared that soil microbial biomass, diversity (e.g., OTUs, Shannon) and enzyme activities (e.g., UE and POD) were all significantly increased after afforestation. (Thoms et al., 2010; Huang et al., 2022). For one thing, soil microorganisms have their unique ecological functions, and the increasing soil microbial diversity may enhance the quantities of specific-species involved in soil nutrient cycling (Weand et al., 2010). For another, the enhancement of soil microbial biomass will promote the secretion of soil extracellular enzymes (van der Heijden et al., 2008). As for the dominant microbial phylum, we found that soil UE, PPO, and POD activities had significantly positive correlation with *copiotrophs* (e.g., Proteobacteria, Bacteroidetes and Gemmatimonadetes), while they had significantly negative correlation with *oligotrophs* (e.g., Chloroflexi and Ascomycota). As soil UE, PPO and POD were conducive to recalcitrant carbon decomposition, their increase may signify the enhancement of soil nutrient supplying capacity (Yang et al., 2021b). This also confirmed that the *C. camphora* coppice planting can improve soil fertility. Conversely, soil ACP activity was significantly positive connected with Chloroflexi (*oligotrophs*), whereas significantly negatively related to Proteobacteria (*copiotrophs*). These findings suggested that Chloroflexi have more survival advantages in low soil fertility (abandoned land), which may promote the secretion of soil ACP (Kaiser et al., 2010; Gong et al., 2019).

Conclusion

The present study indicated that the *C. camphora* coppice planting significantly increased the soil fertility, and therefore cause a corresponding alteration in soil microbial community composition. Compared with the abandoned land, the microbial biomass and diversity were significantly higher under the tree canopy (P15) and between the trees (P50). The *C. camphora* coppice planting shifted the soil microbial community from *oligotrophs* (*K*-strategist) to *copiotrophs* (*r*-strategist). SOC and AN were the primary factors that drive changes in soil bacterial, fungal community composition, respectively. In addition, soil UE, PPO, and POD activities were significantly increased, while soil ACP activity was significantly decreased. And soil bacterial and fungal community significantly influenced the soil enzyme profiling. Soil UE, PPO, and POD activities were significantly positive correlated with *copiotrophic* microorganisms, while significantly negative correlated with *oligotrophic* microorganisms, and soil ACP activity show the opposite trend. Overall, the *C. camphora* coppice planting led to significant changes in soil fertility, microbial community structure, and enzyme activities, at which the point under the tree canopy (P15) had more significant effects than the point between trees (P50). This work can provide a theoretical basis for soil sustainable utilization and productive management of *C. camphora* coppice plantation in subtropical China.

Data availability statement

The original contributions presented in the study are included in the article/Supplementary material, further inquiries can be directed to the corresponding authors.

Author contributions

LS, JieZ, and YL contributed to conception and design of the study. LS, JieZ, JiaZ, XL, YG, HS, HL, and YL completed the field sampling. LS, JieZ, CX, ZX, TZ, and YL performed the statistical analysis. LS, JieZ, and YL wrote the manuscript. LS, JieZ, JiaZ, XL, CX, ZX, TZ, and YL contributed to the revision of manuscript. All authors contributed to the article and approved the submitted version.

Funding

This study is supported by Jiangxi Provincial Science and Technology Program (20204BCJL23046, 20181ACF60002), the National Natural Science Foundation of China (32060333, 52269013), and the National Key Research and Development Program of China (no. 2021YFD1901201-05).

Acknowledgments

We thank the reviewers and editors for their helpful comments regarding the manuscript.

Conflict of interest

The authors declare that the research was conducted in the absence of any commercial or financial relationships that could be construed as a potential conflict of interest.

Publisher's note

Supplementary material

The Supplementary material for this article can be found online at: https://www.frontiersin.org/articles/10.3389/fmicb.2023.1104077/full#supplementary-material

References

Adams, R. I., Miletto, M., Taylor, J. W., and Bruns, T. D. (2013). Dispersal in microbes: fungi in indoor air are dominated by outdoor air and show dispersal limitation at short distances. *ISME J.* 7, 1262–1273. doi: 10.1038/ismej.2013.28

Ahirwal, J., and Maiti, S. K. (2016). Assessment of soil properties of different land uses generated due to surface coal mining activities in tropical Sal (*Shorea robusta*) forest, India. *Catena* 140, 155–163. doi: 10.1016/j.catena.2016.01.028

Akhtar, K., Wang, W. Y., Ren, G. X., Khan, A., Feng, Y. Z., and Yang, G. H. (2018). Changes in soil enzymes, soil properties, and maize crop productivity under wheat straw mulching in Guanzhong, China. *Soil Tillage Res.* 182, 94–102. doi: 10.1016/j.still.2018.05.007

Asigbaase, M., Dawoe, E., Sjogersten, S., and Lomax, B. H. (2021). Decomposition and nutrient mineralisation of leaf litter in smallholder cocoa agroforests: a comparison of organic and conventional farms in Ghana. *J. Soils Sediments* 21, 1010–1023. doi: 10.1007/s11368-020-02844-4

Biddle, J. F., Fitz-Gibbon, S., Schuster, S. C., Brenchley, J. E., and House, C. H. (2008). Metagenomic signatures of the Peru margin subseafloor biosphere show a genetically distinct environment. *PNAS Nexus* 105, 10583–10588. doi: 10.1073/pnas.0709942105

Boughattas, I., Hattab, S., Alphonse, V., Livet, A., Giusti-Miller, S., Boussetta, H., et al. (2019). Use of earthworms *Eisenia andrei* on the bioremediation of contaminated area in north of Tunisia and microbial soil enzymes as bioindicator of change on heavy metals speciation. *J. Soils Sediments* 19, 296–309. doi: 10.1007/s11368-018-2038-8

Bueno de Mesquita, C. P., Knelman, J. E., King, A. J., Farrer, E. C., Porazinska, D. L., Schmidt, S. K., et al. (2017). Plant colonization of moss-dominated soils in the alpine: microbial and biogeochemical implications. *Soil Biol. Biochem.* 111, 135–142. doi: 10.1016/j.soilbio.2017.04.008

Caporaso, J. G., Kuczynski, J., Stombaugh, J., Bittinger, K., Bushman, F. D., Costello, E. K., et al. (2010). QIIME allows analysis of high-throughput community sequencing data. *Nat. Methods* 7, 335–336. doi: 10.1038/nmeth.f.303

Carrara, J. E., Walter, C. A., Hawkins, J. S., Peterjohn, W. T., Averill, C., and Brzostek, E. R. (2018). Interactions among plants, bacteria, and fungi reduce extracellular enzyme activities under long-term N fertilization. *Glob. Chang. Biol.* 24, 2721–2734. doi: 10.1111/gcb.14081

Chen, Y. X., Wei, T. X., Sha, G. L., Zhu, Q. K., Liu, Z., Ren, K., et al. (2022). Soil enzyme activities of typical plant communities after vegetation restoration on the loess plateau, China. *Appl. Soil Ecol.* 170:104292. doi: 10.1016/j.apsoil.2021.104292

De'ath, G. (2003). Multivariate regression trees: a new technique for modeling species–environment relationships. *Ecology* 14, 927–930. doi: 10.1111/j.1654-1103.2003.tb02228.x

Dixon, P. (2003). VEGAN, a package of R functions for community ecology. *J. Veg. Sci.* 14, 927–930. doi: 10.1111/j.1654-1103.2003.tb02228.x

Edgar, R. C. (2016). UNOISE2: improved error-correction for Illumina 16S and ITS amplicon sequencing. *BioRxiv.*:081257. doi: 10.1101/081257

Feng, J. X., Cui, X. W., Zhou, J., Wang, L. M., Zhu, X. S., and Lin, G. H. (2019). Effects of exotic and native mangrove forests plantation on soil organic carbon, nitrogen, and phosphorus contents and pools in Leizhou, China. *Catena* 180, 1–7. doi: 10.1016/j.catena.2019.04.018

Feyissa, A., Gurmesa, G. A., Yang, F., Long, C. Y., Zhang, Q., and Cheng, X. L. (2022). Soil enzyme activity and stoichiometry in secondary grasslands along a climatic gradient of subtropical China. *Sci. Total Environ.* 825:154019. doi: 10.1016/j.scitotenv.2022.154019

Fierer, N., Bradford, M. A., and Jackson, R. B. (2007). Toward an ecological classification of soil bacteria. *Ecology* 88, 1354–1364. doi: 10.1890/05-1839

Gong, X. W., Liu, C. J., Li, J., Luo, Y., Yang, Q. H., Zhang, W. L., et al. (2019). Responses of rhizosphere soil properties, enzyme activities and microbial diversity to intercropping patterns on the loess plateau of China. *Soil Tillage Res.* 195:104355. doi: 10.1016/j.still.2019.104355

Han, Z. Q., Wang, J. Y., Xu, P. S., Sun, Z. R., Ji, C., Li, S. Q., et al. (2021). Greater nitrous and nitric oxide emissions from the soil between rows than under the canopy in subtropical tea plantations. *Geoderma* 398:115105. doi: 10.1016/j.geoderma.2021.115105

Hinojosa, M. B., Albert-Belda, E., Gómez-Muñoz, B., and Moreno, J. M. (2021). High fire frequency reduces soil fertility underneath woody plant canopies of Mediterranean ecosystems. *Sci. Total Environ.* 752:141877. doi: 10.1016/j.scitotenv.2020.141877

Huang, H. Y., Tian, D., Zhou, L. H., Su, H. J., Ma, S. H., Feng, Y. H., et al. (2022). Effects of afforestation on soil microbial-diversity and enzyme activity: a meta-analysis. *Geoderma* 423:115961. doi: 10.1016/j.geoderma.2022.115961

Idbella, M., De Filippis, F., Zotti, M., Sequino, G., Abd-ElGawad, A. M., Fechtali, T., et al. (2022). Specific microbiome signatures under the canopy of Mediterranean shrubs. *Appl. Soil Ecol.* 173:104407. doi: 10.1016/j.apsoil.2022.104407

Janes-Bassett, V., Blackwell, M. S. A., Blair, G., Davies, J., Haygarth, P. M., Mezeli, M. M., et al. (2022). A meta-analysis of phosphatase activity in agricultural settings in response to phosphorus deficiency. *Soil Biol. Biochem.* 165:108537. doi: 10.1016/j.soilbio.2021.108537

Jiang, S., Xing, Y. J., Liu, G. C., Hu, C. Y., Wang, X. C., Yan, G. Y., et al. (2021). Changes in soil bacterial and fungal community composition and functional groups during the succession of boreal forests. *Soil Biol. Biochem.* 161:108393. doi: 10.1016/j.soilbio.2021.108393

Jin, L. L., Xiang, X. J., Zhang, J. Y., Zhang, J., Liu, M., Qin, W. J., et al. (2021). Dramatic shifts in fungal communities following application of hairy vetch (*Vicia villosa Roth* L.) in upland of Ultisol. *Eur. J. Soil Biol.* 106:103349. doi: 10.1016/j.ejsobi.2021.103349

Kaiser, C., Koranda, M., Kitzler, B., Fuchslueger, L., Schnecker, J., Schweiger, P., et al. (2010). Belowground carbon allocation by trees drives seasonal patterns of extracellular enzyme activities by altering microbial community composition in a beech forest soil. *New Phytol.* 187, 843–858. doi: 10.1111/j.1469-8137.2010.03321.x

Kõljalg, U., Nilsson, R. H., Abarenkov, K., Tedersoo, L., Taylor, A. F. S., Bahram, M., et al. (2013). Towards a unified paradigm for sequence-based identification of fungi. *Mol. Ecol.* 22, 5271–5277. doi: 10.1111/mec.12481

Kumar, R., Bhardwaj, A. K., Rao, B. K., Vishwakarma, A. K., Kakade, V., Dinesh, D., et al. (2021). Soil loss hinders the restoration potential of tree plantations on highly eroded ravine slopes. *J. Soils Sediments* 21, 1232–1242. doi: 10.1007/s11368-020-02833-7

Li, J., Li, S. F., Huang, X. B., Tang, R., Zhang, R., Li, C., et al. (2022). Plant diversity and soil properties regulate the microbial community of monsoon evergreen broad-leaved forest under different intensities of woodland use. *Sci. Total Environ.* 821:153565. doi: 10.1016/j.scitotenv.2022.153565

Liu, Z. Z., Deng, B. Q., Li, S. L., and Zou, Z. R. (2018b). Optimization of solvent-free microwave assisted extraction of essential oil from *Cinnamomum camphora* leaves. *Ind. Crop. Prod.* 124, 353–362. doi: 10.1016/j.indcrop.2018.08.016

Liu, Z. Z., Li, H. L., Zhu, Z., Huang, D., Qi, Y. L., Ma, C. H., et al. (2022). *Cinnamomum camphora* fruit peel as a source of essential oil extracted using the solvent-free microwave-assisted method compared with conventional hydrodistillation. *Lebensm. Wiss. Technol.* 153:112549. doi: 10.1016/j.lwt.2021.112549

Liu, J., Liu, M., Wu, M., Jiang, C. Y., Chen, X. F., Cai, Z. J., et al. (2018a). Soil pH rather than nutrients drive changes in microbial community following long-term fertilization in acidic Ultisols of southern China. *J. Soils Sediments* 18, 1853–1864. doi: 10.1007/s11368-018-1934-2

Magoč, T., and Salzberg, S. L. (2011). FLASH: fast length adjustment of short reads to improve genome assemblies. *Bioinformatics* 27, 2957–2963. doi: 10.1093/bioinformatics/btr507

Männistö, M., Ganzert, L., Tiirola, M., Häggblom, M. M., and Stark, S. (2016). Do shifts in life strategies explain microbial community responses to increasing nitrogen in tundra soil? *Soil Biol. Biochem.* 96, 216–228. doi: 10.1016/j.soilbio.2016.02.012

Moghimian, N., Hosseini, S. M., Kooch, Y., and Darki, B. Z. (2017). Impacts of changes in land use/cover on soil microbial and enzyme activities. *Catena* 157, 407–414. doi: 10.1016/j.catena.2017.06.003

Monkai, J., Goldberg, S. D., Hyde, K. D., Harrison, R. D., Mortimer, P. E., and Xu, J. C. (2018). Natural forests maintain a greater soil microbial diversity than that in rubber plantations in Southwest China. *Agric. Ecosyst. Environ.* 265, 190–197. doi: 10.1016/j.agee.2018.06.009

Nakayama, M., Imamura, S., Taniguchi, T., and Tateno, R. (2019). Does conversion from natural forest to plantation affect fungal and bacterial biodiversity, community structure, and co-occurrence networks in the organic horizon and mineral soil? *For. Ecol. Manag.* 446, 238–250. doi: 10.1016/j.foreco.2019.05.042

Parks, D. H., and Beiko, R. G. (2010). Identifying biologically relevant differences between metagenomic communities. *Bioinformatics* 26, 715–721. doi: 10.1093/bioinformatics/btq041

Pereira, A. P. A., Durrer, A., Gumiere, T., Gonçalves, J. L. M., Robin, A., Bouillet, J. P., et al. (2019). Mixed *eucalyptus* plantations induce changes in microbial communities and increase biological functions in the soil and litter layers. *For. Ecol. Manag.* 433, 332–342. doi: 10.1016/j.foreco.2018.11.018

Qi, Y. C., Dong, Y. S., Jin, Z., Peng, Q., Xiao, S. S., and He, Y. T. (2010). Spatial heterogeneity of soil nutrients and respiration in the Desertified grasslands of Inner Mongolia, China. *Pedosphere* 20, 655–665. doi: 10.1016/S1002-0160(10)60055-0

Qu, Z. L., Liu, B., Ma, Y., Xu, J., and Sun, H. (2020). The response of the soil bacterial community and function to forest succession caused by forest disease. *Funct. Ecol.* 34, 2548–2559. doi: 10.1111/1365-2435.13665

Rosinger, C., Rousk, J., and Sandén, H. (2019). Can enzymatic stoichiometry be used to determine growth-limiting nutrients for microorganisms? - a critical assessment in two subtropical soils. *Soil Biol. Biochem.* 128, 115–126. doi: 10.1016/j.soilbio.2018.10.011

Saiya-Cork, K. R., Sinsabaugh, R. L., and Zak, D. R. (2002). The effects of long term nitrogen deposition on extracellular enzyme activity in an *Acer saccharum* forest soil. *Soil Biol. Biochem.* 34, 1309–1315. doi: 10.1016/S0038-0717(02)00074-3

San Emeterio, L., Durán, M., Múgica, L., Jiménez, J. J., and Canals, R. M. (2021). Relating the spatial distribution of a tall-grass to fertility islands in a temperate mountain grassland. *Soil Biol. Biochem.* 163:108455. doi: 10.1016/j.soilbio.2021.108455

Sawada, K., Inagaki, Y., Sugihara, S., Funakawa, S., Ritz, K., and Toyota, K. (2021). Impacts of conversion from natural forest to cedar plantation on the structure and diversity of root-associated and soil microbial communities. *Appl. Soil Ecol.* 167:104027. doi: 10.1016/j.apsoil.2021.104027

Selvaraj, S., Duraisamy, V., Huang, Z. J., Guo, F. T., and Ma, X. Q. (2017). Influence of long-term successive rotations and stand age of Chinese fir (*Cunninghamia lanceolata*) plantations on soil properties. *Geoderma* 306, 127–134. doi: 10.1016/j.geoderma.2017.07.014

Sinsabaugh, R. L. (2010). Phenol oxidase, peroxidase and organic matter dynamics of soil. *Soil Biol. Biochem.* 42, 391–404. doi: 10.1016/j.soilbio.2009.10.014

Speranza, C. I., Adenle, A., and Boillat, S. (2019). Land degradation neutrality—potentials for its operationalisation at multi-levels in Nigeria. *Environ. Sci. Pol.* 94, 63–71. doi: 10.1016/j.envsci.2018.12.018

Sun, R. B., Chen, Y., Han, W. X., Dong, W. X., Zhang, Y. M., Hu, C., et al. (2020). Different contribution of species sorting and exogenous species immigration from manure to soil fungal diversity and community assemblage under long-term fertilization. *Soil Biol. Biochem.* 151:108049. doi: 10.1016/j.soilbio.2020.108049

Sun, R. B., Zhang, W. J., Liu, Y. B., Yun, W. J., Luo, B. B., Chai, R. S., et al. (2022). Changes in phosphorus mobilization and community assembly of bacterial and fungal communities in rice rhizosphere under phosphate deficiency. *Front. Microbiol.* 13:953340. doi: 10.3389/fmicb.2022.953340

Tabatabai, M. A. (1994). "Soil enzymes" in *Methods of Soil Analysis: Part 2 Microbiological and Biochemical Properties*. ed. A. L. Page, vol. *5* (Madison, WI: The American Society of Agronomy), 775–833.

Tang, C. J., Liu, Y., Li, Z. W., Guo, L. P., Xu, A. Z., and Zhao, J. D. (2021). Effectiveness of vegetation cover pattern on regulating soil erosion and runoff generation in red soil environment, southern China. *Ecol. Indic.* 129:107956. doi: 10.1016/j.ecolind.2021.107956

Teng, Y. M., Zhan, J. Y., Liu, W., Zhang, F., Wang, C., and Dong, S. K. (2020). Larch or Mongolian pine? Effects of tree species on soil properties and microbial biomass with the consideration of afforestation time. *Ecol. Eng.* 158:106074. doi: 10.1016/j.ecoleng.2020.106074

Thébault, A., Clément, J. C., Ibanez, S., Roy, J., Geremia, R. A., Pérez, C. A., et al. (2014). Nitrogen limitation and microbial diversity at the treeline. *Oikos* 123, 729–740. doi: 10.1111/j.1600-0706.2013.00860.x

Thoms, C., Gattinger, A., Jacob, M., Thomas, F. M., and Gleixner, G. (2010). Direct and indirect effects of tree diversity drive soil microbial diversity in temperate deciduous forest. *Soil Biol. Biochem.* 42, 1558–1565. doi: 10.1016/j.soilbio.2010.05.030

Tran, H. T., Hurley, B. A., and Plaxton, W. C. (2010). Feeding hungry plants: the role of purple acid phosphatases in phosphate nutrition. *Plant Sci.* 179, 14–27. doi: 10.1016/j.plantsci.2010.04.005

Trivedi, P., Anderson, I. C., and Singh, B. K. (2013). Microbial modulators of soil carbon storage: integrating genomic and metabolic knowledge for global prediction. *Trends Microbiol.* 21, 641–651. doi: 10.1016/j.tim.2013.09.005

Ushio, M., Wagai, R., Balser, T. C., and Kitayama, K. (2008). Variations in the soil microbial community composition of a tropical montane forest ecosystem: does tree species matter? *Soil Biol. Biochem.* 40, 2699–2702. doi: 10.1016/j.soilbio.2008.06.023

Van Der Heijden, M. G., Bardgett, R. D., and Van Straalen, N. M. (2008). The unseen majority: soil microbes as drivers of plant diversity and productivity in terrestrial ecosystems. *Ecol. Lett.* 11, 296–310. doi: 10.1111/j.1461-0248.2007.01139.x

Wan, P., Peng, H., Ji, X. L., Chen, X. L., and Zhou, H. M. (2021). Effect of stand age on soil microbial communities of a plantation *Ormosia hosiei* forest in southern China. *Ecol. Inform.* 62:101282. doi: 10.1016/j.ecoinf.2021.101282

Wang, Q., Garrity, G. M., Tiedje, J. M., and Cole, J. R. (2007). Naïve Bayesian classifier for rapid assignment of rRNA sequences into the new bacterial taxonomy. *Appl. Environ. Microbiol.* 73, 5261–5267. doi: 10.1128/AEM.00062-07

Wang, S. Q., Li, T. X., and Zheng, Z. C. (2018). Effects of tea plantation age on soil aggregate-associated C-and N-cycling enzyme activities in the hilly areas of Western Sichuan, China. *Catena* 171, 145–153. doi: 10.1016/j.catena.2018.07.010

Wang, J. C., Song, Y., Ma, T. F., Raza, W., Li, J., Howland, J. G., et al. (2017). Impacts of inorganic and organic fertilization treatments on bacterial and fungal communities in a paddy soil. *Appl. Soil Ecol.* 112, 42–50. doi: 10.1016/j.apsoil.2017.01.005

Wang, C. Q., Xue, L., Dong, Y. H., and Jiao, R. Z. (2021). Effects of stand density on soil microbial community composition and enzyme activities in subtropical *Cunninghamia lanceolate* (lamb.) hook plantations. *For. Ecol. Manag.* 479:118559. doi: 10.1016/j.foreco.2020.118559

Wang, J. C., Zou, Y. K., Gioia, D. D., Singh, B. K., and Li, Q. F. (2020). Conversion to agroforestry and monoculture plantation is detrimental to the soil carbon and nitrogen cycles and microbial communities of a rainforest. *Soil Biol. Biochem.* 147:107849. doi: 10.1016/j.soilbio.2020.107849

Weand, M. P., Arthur, M. A., Lovett, G. M., McCulley, R. L., and Weathers, K. C. (2010). Effects of tree species and N additions on forest floor microbial communities and extracellular enzyme activities. *Soil Biol. Biochem.* 42, 2161–2173. doi: 10.1016/j.soilbio.2010.08.012

Wu, Z. Y., Haack, S. E., Lin, W. X., Li, B. L., Wu, L. K., Fang, C. X., et al. (2015). Soil microbial community structure and metabolic activity of *Pinus elliottii* plantations across different stand ages in a subtropical area. *PLoS One* 10:e0135354. doi: 10.1371/journal.pone.0135354

Xiang, X. J., Adams, J. M., Qiu, C. F., Qin, W. J., Chen, J. R., Jin, L. L., et al. (2021). Nutrient improvement and soil acidification inducing contrary effects on bacterial community structure following application of hairy vetch (*Vicia villosa Roth* L.) in Ultisol. *Agric. Ecosyst. Environ.* 312:107348. doi: 10.1016/j.agee.2021.107348

Xu, M. P., Jian, J. N., Wang, J. Y., Zhang, Z. J., Yang, G. H., Han, X. H., et al. (2021b). Response of root nutrient resorption strategies to rhizosphere soil microbial nutrient utilization along *Robinia pseudoacacia* plantation chronosequence. *For. Ecol. Manag.* 489:119053. doi: 10.1016/j.foreco.2021.119053

Xu, Y. X., Ren, S. Q., Liang, Y. F., Du, A. P., Li, C., Wang, Z. C., et al. (2021a). Soil nutrient supply and tree species drive changes in soil microbial communities during the transformation of a multi-generation *eucalyptus* plantation. *Appl. Soil Ecol.* 166:103991. doi: 10.1016/j.apsoil.2021.103991

Yang, Y., Li, T., Wang, Y. Q., Cheng, H., Chang, S. X., Liang, C., et al. (2021b). Negative effects of multiple global change factors on soil microbial diversity. *Soil Biol. Biochem.* 156:108229. doi: 10.1016/j.soilbio.2021.108229

Yang, C. B., Zhang, X. P., Ni, H. J., Gai, X., Huang, Z. C., Du, X. H., et al. (2021a). Soil carbon and associated bacterial community shifts driven by fine root traits along a chronosequence of Moso bamboo (*Phyllostachys edulis*) plantations in subtropical China. *Sci. Total Environ.* 752:142333. doi: 10.1016/j.scitotenv.2020.142333

Zarafshar, M., Bazot, S., Matinizadeh, M., Bordbar, S. K., Rousta, M. J., Kooch, Y., et al. (2020). Do tree plantations or cultivated fields have the same ability to maintain soil quality as natural forests? *Appl. Soil Ecol.* 151:103536. doi: 10.1016/j.apsoil.2020.103536

Zhang, D. J., Li, J. J., Huang, Y. M., Gao, S., and Zhang, J. (2022). Root-soil facilitation in mixed *Eucalyptus grandis* plantations including nitrogen-fixing species. *For. Ecol. Manag.* 516:120215. doi: 10.1016/j.foreco.2022.120215

Zhang, C., Liu, G. B., Xue, S., and Wang, G. L. (2016). Soil bacterial community dynamics reflect changes in plant community and soil properties during the secondary succession of abandoned farmland in the loess plateau. *Sci. Total Environ.* 97, 40–49. doi: 10.1016/j.soilbio.2016.02.013

Zhang, W., Xu, Y., Gao, D., Wang, X., Liu, W., Deng, J., et al. (2019). Ecoenzymatic stoichiometry and nutrient dynamics along a revegetation chronosequence in the soils of abandoned land and *Robinia pseudoacacia* plantation on the loess plateau, China. *Soil Biol. Biochem.* 134, 1–14. doi: 10.1016/j.soilbio.2019.03.017

Zhao, J. (2021). Dynamic changes of the contents of essential oil and nutrients of *Cinnamomum camphora* var. *linaloolifera* and their correlation. *Scientia Silvae Sinicae* 57, 57–67. doi: 10.11707/j.1001-7488.20211206

Zhong, Y., Chen, C., Gong, X., Luan, X., Wu, Z., Li, H., et al. (2022). Transcriptome and metabolome analyses reveal a key role of the anthocyanin biosynthetic pathway cascade in the pigmentation of a *Cinnamomum camphora* red bark mutant ('Gantong 1'). *Ind. Crop. Prod.* 175:114236. doi: 10.1016/j.indcrop.2021.114236

Zhu, L. Y., Wang, X. H., Chen, F. F., Li, C. H., and Wu, L. C. (2019). Effects of the successive planting of *Eucalyptus urophylla* on soil bacterial and fungal community structure, diversity, microbial biomass, and enzyme activity. *Land Degrad. Dev.* 30, 636–646. doi: 10.1002/ldr.3249

frontiers | Frontiers in Microbiology

TYPE Original Research
PUBLISHED 16 February 2023
DOI 10.3389/fmicb.2023.1072228

OPEN ACCESS

EDITED BY
Jesús Navas-Castillo,
IHSM La Mayora (CSIC), Spain

REVIEWED BY
Arturo Fabiani,
Agricoltura e Ambiente (CREA-AA), Italy
Guangbin Zhang,
Institute of Soil Science (CAS), China

*CORRESPONDENCE
Lifen Huang
✉ lfhuang@yzu.edu.cn

†These authors have contributed equally to this work and share first authorship

SPECIALTY SECTION
This article was submitted to Microbe and Virus Interactions with Plants, a section of the journal Frontiers in Microbiology

RECEIVED 17 October 2022
ACCEPTED 31 January 2023
PUBLISHED 16 February 2023

CITATION
Xu C, Chen Y, Zang Q, Li Y, Zhao J, Lu X, Jiang M, Zhuang H and Huang L (2023) The effects of cultivation patterns and nitrogen levels on fertility and bacterial community characteristics of surface and subsurface soil. *Front. Microbiol.* 14:1072228. doi: 10.3389/fmicb.2023.1072228

The effects of cultivation patterns and nitrogen levels on fertility and bacterial community characteristics of surface and subsurface soil

Chengyu Xu[1,2†], Yuanjie Chen[1,2†], Qian Zang[1,2], Yulin Li[1,2], Jinbiao Zhao[1,2], Xuanrui Lu[1,2], Min Jiang[1,2], Hengyang Zhuang[1,2] and Lifen Huang[1,2*]

[1]Jiangsu Key Laboratory of Crop Genetics and Physiology/Jiangsu Key Laboratory of Crop Cultivation and Physiology, Agricultural College of Yangzhou University, Yangzhou, China, [2]Jiangsu Co-Innovation Center for Modern Production Technology of Grain Crops, Yangzhou University, Yangzhou, China

The cropping system affects the physicochemical property and microbial community of paddy soil. Previous research mostly focused on the study of soil 0–20cm underground. However, there may be difference in the laws of nutrient and microorganism distribution at different depths of arable soil. In surface (0–10cm) and subsurface (10–20cm) soil, a comparative analysis including soil nutrients, enzymes, and bacterial diversity was carried out between the organic and conventional cultivation patterns, low and high nitrogen levels. Analysis results suggested that under the organic farming pattern, the contents of total nitrogen (TN), alkali-hydrolyzable nitrogen (AN), available phosphorus (AP), and soil organic matter (SOM) as well as alkaline phosphatase and sucrose activity increased in surface soil, but the SOM concentration and urease activity decreased in subsurface soil. A moderate reduction of nitrogen applied to soil could enhance soil enzyme activity. It was demonstrated by α diversity indices that high nitrogen levels remarkably undermined soil bacterial richness and diversity. Venn diagrams and NMDS analysis manifested great difference in bacterial communities and an apparent clustering tendency under different treatment conditions. Species composition analysis indicated that the total relative abundance of Proteobacteria, Acidobacteria, and Chloroflexi retained stable in paddy soil. LEfSe results revealed that a low nitrogen organic treatment could elevate the relative abundance of Acidobacteria in surface soil and Nitrosomonadaceae in subsurface soil, thereby tremendously optimizing the community structure. Moreover, Spearman's correlation analysis was also performed, which proved the significant correlation of diversity with enzyme activity and AN concentration. Additionally, redundancy analysis disclosed that the Acidobacteria abundance in surface soil and Proteobacteria abundance in subsurface soil exerted conspicuous influence on environmental factors and the microbial community structure. According to the findings of this study, it was believed that reasonable nitrogen application together with an organic agriculture cultivation system could effectively improve soil fertility in Gaoyou City, Jiangsu Province, China.

KEYWORDS

organic farming, nitrogen level, soil depth, soil nutrient, soil enzyme, soil microorganism

1. Introduction

Organic food emerges as a new consumption fashion and arouses increasing attention due to its merits of natural ingredients, good quality, high safety, and hygiene. The whole world has witnessed the swift growth of its consumption (Pimentel et al., 2005; Mäder et al., 2007). As one of the competitive organic agricultural specialties in China, organic rice plays an essential part in the organic agricultural product industry. Organic agriculture is instrumental in ecosystem stability. To achieve sustainable development of organic rice, it is urgent to develop complete sets of technical measures appropriate for organic farming. In recent years, China's rice planting has still been dominated by traditional heavy nitrogen fertilizer application. Although the conventional cultivation mode boosts the short-term yield of rice, the long-term excessive application of single nitrogen fertilizer not only lowers the utilization rate of fertilizer but also brings about severe environmental issues such as soil degradation, groundwater pollution, nitrogen loss, etc. (Ju et al., 2009; Guo et al., 2010). Taking measures to control the amount of nitrogen fertilizer used can save resources, abate pollution, ameliorate soil and water systems, and improve rice quality (Wang H. Y. et al., 2017).

Being critical to material circulating, nutrient transformation, and the mineralization-fixation process of organic carbon, soil microorganisms act as sensitivity indicators of soil quality (Zelles, 1999; Shi et al., 2015). It was established by Gunapala and Scow (1998) that the quantity of soil microorganisms was negatively related to the soil mineral nitrogen content under conventional cultivation, but the two were positively correlated under organic farming. Zhao et al. (2016) noticed that applying pig manure organic–inorganic compound fertilizer while reducing the use of chemical fertilizer could enrich microorganisms related to the carbon-nitrogen cycle, promote nitrification and conversion of organic matter, raise enzyme activity and the amount of microorganisms, and boost plant growth and grain yield. A comparative test conducted by Takahashi et al. (2018) showed that compared with conventional cultivation, organic farming was more capable of diversifying and stabilizing the bacterial population in soil, which greatly suppressed rice diseases. All the above-mentioned results testify the advantage of organic farming. That is, it can recruit effective microorganisms to form a soil environment favorable to crop growth (Wang L. et al., 2017).

The partial factor productivity of nitrogen fertilizer of China is 34 $kg{\cdot}kg^{-1}$, which is far lower than that of Japan (73 $kg{\cdot}kg^{-1}$), the Philippines (49 $kg{\cdot}kg^{-1}$), and Thailand (43 $kg{\cdot}kg^{-1}$; FAO, 2001). Nitrogen is the main component of crop protein, having vital influence on grain yield. Therefore, clarifying the effect of different nitrogen levels on soil microorganisms can facilitate the development of the optimal crop nutrient management strategy from the perspective of soil ecology. Besides, owing to the high spatial heterogeneity of soil (Imhoff et al., 2000; Critchley et al., 2002) as well as dissimilar soil types, geological features, and climates in different areas, the heterogeneity degree and main driving mechanism of soil vary (Begum et al., 2010). Microorganisms in the arable layer (0–20 cm underground) of rice under organic planting systems were extensively studied previously. However, there are few reports comparing the surface soil (0–10 cm) and subsurface soil (10–20 cm) of the arable layer. More research on vertical heterogeneity of paddy field soil should aid in the knowledge of the change law of soil nutrient uptake and microbial distribution in the arable layer.

An organic farming system of milk vetch-straw-rapeseed cake-San'an bio-organic fertilizer was developed by our research team through a 10-year plot test in Gaoyou, Jiangsu. Given the importance of developing efficient fertilizer application approaches in the future, a comparative test was conducted between conventional and organic farming patterns in this study. Under different management modes of nitrogen levels, the variations of characteristics of bacterial communities (accounting for 70–90% of total microorganisms) in surface and subsurface paddy soil were analyzed *via* high-throughput sequencing. The aim of this study is firstly to discuss the influence of the interaction between cultivation patterns and nitrogen levels on nutrient contents, enzyme activity, and bacterial diversity in paddy soil. Secondly, the change law of soil microbial community characteristics is also clarified by the correlation analysis between soil nutrient indicators and bacteria. Thirdly, the mechanism of microbial communities in paddy soil responding to cultivation patterns is revealed. At last, a reasonable organic agricultural planting system is sought based on soil microorganisms, so as to provide a theoretical foundation for sustainable farming of paddy fields.

2. Materials and methods

2.1. Plot location and test materials

The experiment was conducted in the experimental plot of Mapengwan Ecological Agriculture Technology Co., Ltd., Gaoyou City, Jiangsu Province, China (119° 25′ east longitude, 32° 47′ northern latitude) from 2020 to 2021 (Figure 1A). The plot has a northern subtropical monsoon climate, with a mean annual temperature of 16.2°C, annual precipitation of 1341.5 mm, annual sunshine hours of 2100 h, and a frost-free period of 221 days. The plot has long been designated to organic farming research since 2012. The soil property is stable and the texture is clay loam. The soil sample collected in June 2021 contained 27.70 $g{\cdot}kg^{-1}$ organic matter, 112.24 $mg{\cdot}kg^{-1}$ alkali-hydrolyzable nitrogen, 7.54 $mg{\cdot}kg^{-1}$ available phosphorus, 61.16 $mg{\cdot}kg^{-1}$ available potassium, and 1.32 $g{\cdot}kg^{-1}$ total nitrogen. The pH of the sample was 8.15. The test rice was of Nanjing 46 brand, with a whole growth period of 165 days. Figure 1B shows the mean daily temperature, daily sunshine hours, and daily precipitation of rice during the period from sowing to harvesting.

2.2. Experimental design

The experiment involved farming pattern (*CF* and OF) and nitrogen level (N12 and N18) managements combined into four treatments, including the conventional farming with low nitrogen treatment (CFN12), conventional farming with high nitrogen treatment (CFN18), organic farming with low nitrogen treatment (OFN12), and organic farming with high nitrogen treatment (OFN18), respectively. These treatments were randomly arranged within each zone, and each treatment was repeated 3 times. There were 12 zones, each having an area of 49 m^2 (7 m × 7 m). Previous

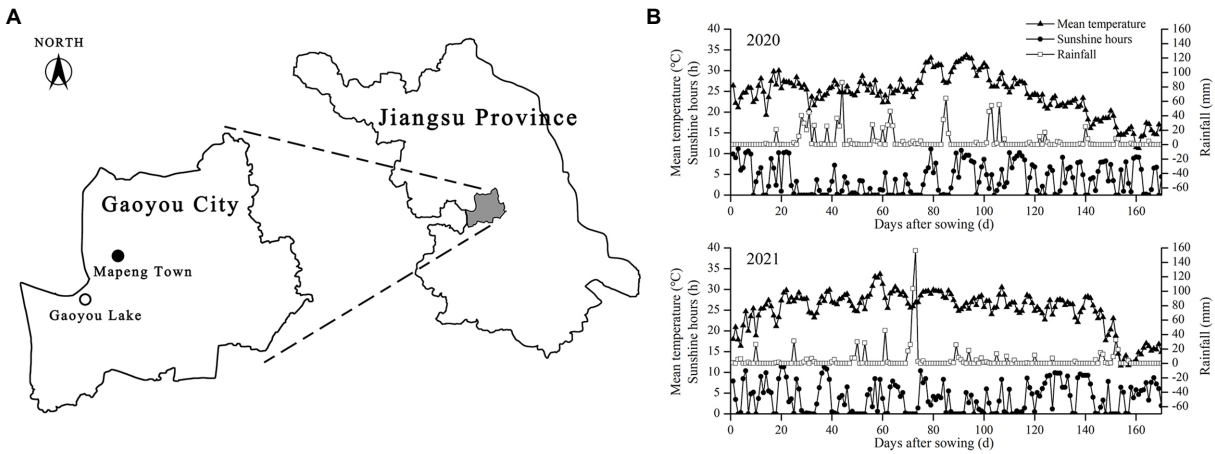

FIGURE 1
The location of the experimental site **(A)** and meteorological conditions during the whole growth period of rice **(B)**.

TABLE 1 Fertilizer application rates under two nitrogen levels of conventional and organic cultivation (kg·hm^{-2}).

Treatment	Basal fertilizer				Topdressing fertilizer	
	Compound fertilizer	Milk vetch	Rapeseed cake	San'an bio-organic fertilizer	Urea	San'an bio-organic fertilizer
CFN12	500	/	/	/	235	/
CFN18	750	/	/	/	352	/
OFN12	/	12,000	1,200	1,200	/	930
OFN18	/	12,000	2,400	1,200	/	1800

The nutrient contents of various fertilizers are: compound fertilizer: 15%N, 15% P_2O_5 and 15% K_2O; Milk vetch: 0.33% N, 0.08% P_2O_5 and 0.23% K_2O; Rapeseed cake: 4.60% N, 0.80% P_2O_5, 1.04% K_2O, 0.80% Ca, 0.48% Mg and various trace elements; San'an bio-organic fertilizer: 4.00% N, 1.87% P_2O_5, 2.28% K_2O, Various organic acids, peptides and rich nutrient elements including 53% organic matter.

crops were wheat, and straw returning was conducted in all the zones. The test rice was sown on 17th May and transplanted by hand on 9th June with row spacing of 30.0 cm × 12.5 cm. Three seedlings were planted per hole.

Conventional farming (CF) was subjected to the high yield cultivation management according to local production rules. 45% compound fertilizer (containing 15%N) was applied as basal fertilizer 1 day before rice transplanting. Taking urea as topdressing nitrogen fertilizer, urea was applied 3 times as the first tillering fertilizer, the second tillering fertilizer and panicle fertilizer at a ratio of 1:2:3.

Organic farming (OF) was performed as per the National Standards for Organic Product Production (GB/T19630.1). The milk vetch-rice planting model was adopted. Milk vetch (containing 0.33% N) was applied as basal fertilizer 2 weeks before rice transplanting *via* once turning-over of soil. Rapeseed cake (containing 4.60% N) and San'an bio-organic fertilizer (containing 4.00% N; Ling et al., 2010) were applied as basal fertilizer 1d before rice transplanting. Subsequently, San'an bio-organic fertilizer was top-dressed as panicle fertilizer in mid-July. The application amount is given in Table 1. N18 is equivalent to 270 kg·hm^{-2} pure nitrogen, which is the local conventional application amount of nitrogen. N12 corresponds to 180 kg·hm^{-2} pure nitrogen, which is a reduced amount of nitrogen for experiment purpose.

2.3. Sample collection

The 0–20 cm deep topsoil in each zone was collected by a soil extractor according to the five-point sampling method on October 21, 2021. Four types of soil were obtained, including CFN12, CFN18, OFN12, and OFN18. Each treatment was carried out 3 times. The soil samples were divided into surface soil (0–10 cm) and subsurface soil (10–20 cm). The samples were mixed evenly, from which sundries like rice root residues and stones were removed. A part of the samples (dry soil) were then air-dried and ground prior to filtering through 20-mesh and 100-mesh sieves. Lately, nutrients and enzyme activity of the samples were measured. The other part of the samples (fresh soil) were put into a sealed bag and stored in a refrigerator at −70°C for subsequent analysis of soil microorganisms.

2.4. Determination of sample nutrients and enzyme activity

The content of each soil nutrient was measured by the conventional analysis method (Bao, 2000). The alkali-hydrolyzable nitrogen in soil was determined by the alkaline hydrolysis diffusion method. The total nitrogen in soil was detected by the H_2SO_4-mixed

accelerator distillation method. Soil organic matter was measured by the $K_2Cr_2O_7$-H_2SO_4 external heating approach. The available phosphorus in soil was detected using $NaHCO_3$ extraction spectrophotometry. The available potassium in soil was detected by CH_3COONH_4 extraction flame spectrophotometry. The soil pH was measured manually by the COMBI 5000 gauge in accordance with operation manual.

The enzyme activity of soil was detected using the method proposed by Guan (1986). The 3,5-dinitrosalicylic acid colorimetric method, indophenol blue colorimetry method, and disodium phenyl phosphate colorimetry method were used to measure the activity of soil sucrose, urease, and alkaline phosphatase, respectively.

2.5. DNA extraction, PCR amplification, and high-throughput sequencing

0.5 g soil was taken from each sample and the microorganism DNA was extracted from the soil using the Omega soil DNA kit. The quantity and quality of the DNA extracted were assessed by ultraviolet spectrophotometer (NanoDrop, Thermo Scientific, NC2000), while the DNA integrity was determined by 1.2% agarose gel electrophoresis. The target DNA sequence of bacteria for amplification was the 16S_V3V4 region. PCR amplification of 16S rDNA was carried out with 338F (5′-ACTCCTACGGGAGGCAGCA-3′) as the forward primer and 806R (5′-GGACTACHVGGGTWTCTAAT-3′) as the reverse primer. The amplification system (25 μL) consisted of 5 × reaction buffer 5 μL, 5 × GC buffer 5 μL, dNTP (2.5 mM) 2 μL, forward primer (10 uM) 1 μL, reverse primer (10 uM) 1 μL, DNA template 2 μL, ddH2O 8.75 μL, and Q5 DNA polymerase 0.25 μL. The amplification conditions were pre-denaturation at 98°C for 2 min, denaturation at 98°C for 15 s, annealing at 55°C for 30 s, extension at 72°C for 30 s, final extension at 72°C for 5 min, and heat preservation at 10°C. The process was repeated for 25–30 cycles. After amplification, gel electrophoresis was conducted and 2% agarose was prepared to detect the PCR amplification products. Following QIIME2 dada2 analysis process, Illumina MiSeq sequencing was performed for quality control, denoise, mergence, and chimera removal. Shanghai Personalbio Technology Co., Ltd. was entrusted to conduct high-throughput sequencing of soil.

2.6. Data analysis

Data were sorted and analyzed by Microsoft Excel 2019 and SPSS 23.0 software and mapped by Origin 8.5. Soil nutrients and enzyme activity data of various treatment modes were analyzed by the univariate method. Differences in data among groups were compared by LSD. Microbial community characteristics were mapped on the Genescloud platform. According to the distribution of amplicon sequence variants or operational taxonomic units (ASV/OTU) in different treatment modes, Alpha diversity of each treatment was calculated, and a rarefaction curve was drawn to assess whether the sequencing depth was reasonable. The Venn diagram was used to count the number of exclusive and shared ASV/OTU of different treatment methods based on ASV/OTU richness. Species composition analysis was made through assessing the feature table with singletons removed, and the phylum-level diversity was shown by a histogram. In non-metric multidimensional scaling (NMDS) analysis, the Bray–Curtis distance matrix was used for dimension reduction and decomposition, and differences in bacterial community composition were described with a two-dimension distribution figure. In LEfSe analysis, with the linear discriminant analysis (LDA) threshold set at 3.5, Kruskal-Wallis test was conducted to analyze simultaneously the difference among varied groups and identify notable biomarkers in each treatment. The correlation of α diversity indices with nutrients and enzyme activity was investigated by Spearman's method. The relevance of dominant phyla with nutrients and enzyme activity was examined by redundancy method.

3. Results

3.1. The influence of organic and conventional farming modes and two nitrogen levels on soil nutrient and enzyme activity

3.1.1. Soil nutrients

As is shown in Table 2, organic farming surface soil contained more TN, AN, AP, and SOM than conventional farming surface soil. The content of the above-mentioned four nutrients in OFN12 type soil was higher than that in CFN12 type soil by 8.46, 9.23, 8.99, and 4.55%, respectively. The content of the four nutrients in OFN18 type soil was higher than that in CFN18 type soil by 7.39, 15.21, 12.63, and 2.84%, respectively. High nitrogen application raised the concentration of AN. The content of AN in CFN18 type soil was 4.06% higher than that in CFN12 type soil, and the content of AN in OFN18 type soil was 9.76% higher than that in OFN12 type soil. As for subsurface soil, conventional farming soil contained more SOM than organic farming soil. The content of SOM in CFN12 type soil was 6.66% higher than that in OFN12 type soil, and the content of SOM in CFN18 type soil was 11.18% higher than that in OFN18 type soil. The AP and AK content in conventional farming soil was significantly lower than those in organic farming soil. Their concentrations in CFN12 type soil were reduced by 15.27 and 5.29%, respectively, compared with those in OFN12 type soil. Their concentrations in CFN18 type soil were reduced by 12.92 and 7.04%, respectively, compared with those in OFN18 type soil. Generally, the surface soil contained more nutrients than subsurface soil, while the pH of surface soil was lower than that of subsurface soil. Whether it was surface soil or subsurface soil, the pH of organic farming soil was remarkably lower than that of conventional farming soil under the same nitrogen level condition. Under the same farming pattern, the pH of soil treated by high nitrogen was lower than that treated by low nitrogen, and the difference was notable in the pH of subsurface soil.

3.1.2. Soil enzyme activity

As shown in Figure 2, the activity of 3 enzymes in surface soil was all apparently higher than that in subsurface soil. The farming methods and nitrogen levels had great impact on soil enzyme activity, but the interaction between the two was slight in general. Three enzymes in both surface and subsurface soil were found more active at low nitrogen levels than at high nitrogen levels. At the same nitrogen level, the activity of alkaline phosphatase and sucrase in organic farming surface soil was tremendously higher than that in

10.3389/fmicb.2023.1072228

TABLE 2 Effects of two nitrogen levels under organic and conventional cultivation on soil nutrients.

Layer(cm)	Treatment	ω(TN)/ (g·kg^{-1})	ω(AN)/ (mg·kg^{-1})	ω(AP)/ (mg·kg^{-1})	ω(AK)/ (mg·kg^{-1})	ω(SOM)/ (g·kg^{-1})	pH
0–10	CFN12	2.01 ± 0.03 b	155.97 ± 2.21 c	12.12 ± 0.23 b	110.5 ± 1.5 a	39.76 ± 0.02 bc	8.33 ± 0.02 a
	CFN18	2.03 ± 0.03 b	162.30 ± 1.25 c	12.11 ± 0.04 b	105.5 ± 0.5 bc	39.43 ± 0.01 c	8.32 ± 0.01 ab
	OFN12	2.18 ± 0.03 a	170.36 ± 1.01 b	13.21 ± 0.04 a	103.5 ± 0.5 c	41.57 ± 0.09 a	8.25 ± 0.02 bc
	OFN18	2.18 ± 0.01 a	186.98 ± 0.56 a	13.64 ± 0.08 a	109.5 ± 0.5 ab	40.55 ± 0.35 ab	8.24 ± 0.02 c
10–20	CFN12	1.49 ± 0.01 ab	106.93 ± 2.00 a	8.38 ± 0.21 b	98.5 ± 1.5 c	26.42 ± 0.19 b	8.73 ± 0.01 a
	CFN18	1.52 ± 0.00 a	110.00 ± 1.07 a	8.09 ± 0.18 b	99.0 ± 1.0 bc	27.05 ± 0.01 a	8.64 ± 0.01 b
	OFN12	1.42 ± 0.01 ab	101.33 ± 3.49 a	9.89 ± 0.07 a	104.0 ± 0.0 ab	24.77 ± 0.01 c	8.65 ± 0.02 b
	OFN18	1.41 ± 0.04 b	102.03 ± 0.09 a	9.29 ± 0.09 a	106.5 ± 0.5 a	24.33 ± 0.03 c	8.57 ± 0.02 c

Data are presented by mean value ± SD. Different lower case letters in the same column indicate significant differences among the four treatments at $p < 0.05$. TN, total nitrogen; AN, alkali-hydrolyzable nitrogen; AP, available phosphorus; AK, available potassium; SOM, soil organic matter. The same below.

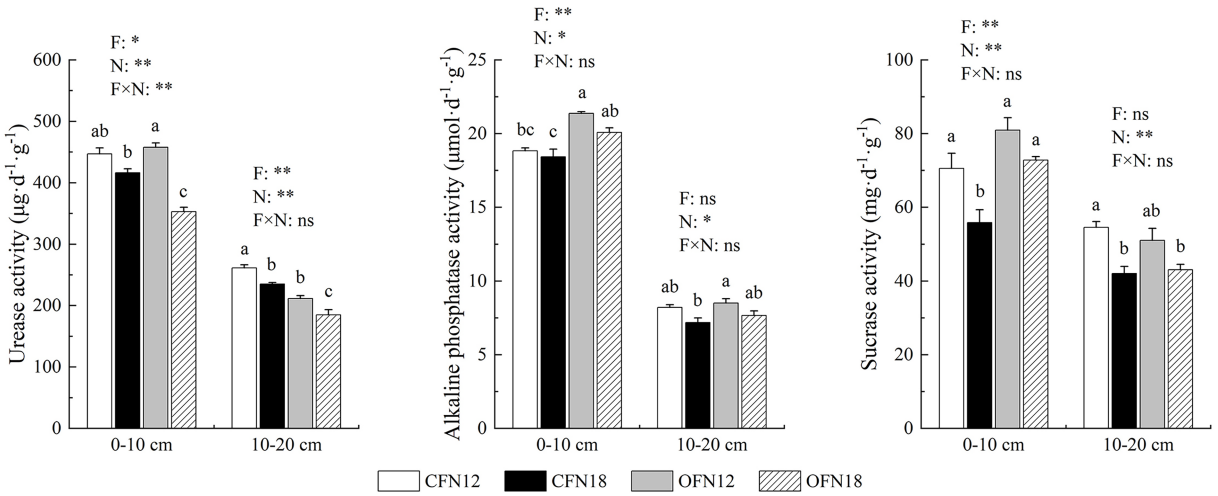

FIGURE 2
Effects of two nitrogen levels under organic and conventional cultivation on soil enzyme activities. F, Cultivation Pattern; N, Nitrogen Level; F×N, interaction between F and N. *$p < 0.05$, **$p < 0.01$, ns $p > 0.05$. Different lower case letters indicate significant differences among the four treatments at $p<0.05$.

conventional farming surface soil. Compared with that in conventional farming soil, the activity of alkaline phosphatase in organic farming soil was promoted by 13.44 and 8.96% at low and high nitrogen levels, respectively, and the activity of sucrase in organic farming soil was improved by 14.67 and 30.31% at low and high nitrogen levels, respectively. Nevertheless, organic farming greatly reduced the activity of urease in subsurface soil. The activity of urease in organic farming subsurface soil was 19.14 and 21.37% lower than that in conventional farming subsurface soil at low and high nitrogen levels, respectively.

3.2. The influence of organic and conventional farming modes and two nitrogen levels on characteristics of bacterial communities in soil

3.2.1. Alpha diversity index

Bacterial richness was represented by Chao1 and Observed species indices, while bacterial diversity was denoted by Shannon and Simpson indices in this paper. Figure 3 shows the indices. For surface soil, the Chao1 and Observed species indices of the CFN12 group were significantly higher than those of the other three groups. Compared with low nitrogen application, high nitrogen application reduced bacterial richness and diversity. Chao1, Observed species, Shannon, and Simpson indices of CFN18 type surface soil were remarkably lower than those of CFN12 type surface soil by 16.34, 15.05, 2.82, and 0.04%, respectively. Chao1, Observed species, Shannon, and Simpson indices of OFN18 type surface soil were lower than those of OFN12 type surface soil by 1.82, 6.83, 2.44, and 0.04%, respectively. For subsurface soil, Chao1 index of the OFN12 group was lower than that of other three groups. Under both organic and conventional cultivation patterns, Observed species, Shannon, and Simpson indices at high nitrogen levels were slightly higher than those at low nitrogen levels.

3.2.2. Bacterial community difference

To investigate the exclusive and shared species of different treatment groups, the Venn diagram (Figure 4) was plotted for

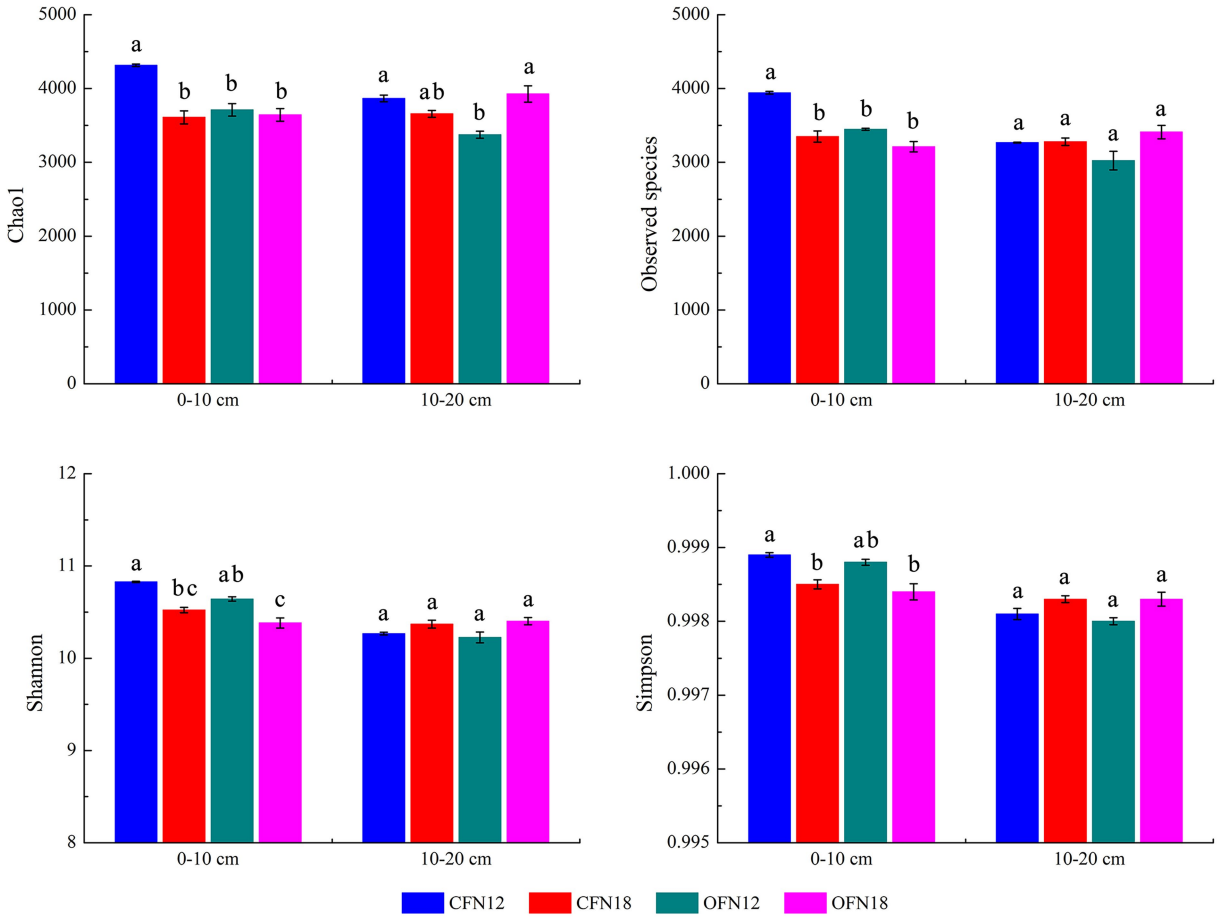

FIGURE 3
Alpha diversity of bacteria under two nitrogen levels of conventional and organic cultivation. Different lower case letters indicate significant differences among the four treatments at $p<0.05$.

community analysis. In general, the farming methods and nitrogen levels affected notably the species in soil. There were obviously more species in surface soil than in subsurface soil. As shown in Figure 4A, the number of OTU in surface soil of the CFN12, CFN18, OFN12, and OFN18 groups was 8,957, 7,666, 8,102, and 7,766, respectively. The number of exclusive OTU in surface soil of the above four groups was 4,753, 3,727, 4,089, and 3,968, respectively. There were 1,503 shared OTU in total. The bacterial richness and number of exclusive species in CFN12 type surface soil were especially higher than those in other three types of surface soil. As is shown in Figure 4B, there were 7,205, 6,986, 6,671, and 7,301 OTU in subsurface soil of the CFN12, CFN18, OFN12, and OFN18 groups, respectively. There were 3,673, 3,559, 3,116, and 3,691 exclusive OTU in subsurface soil of the above four groups, respectively. The share OTU of the four groups was 1,312. The treatment of OFN12 reduced the bacterial richness and the number of exclusive species in subsurface soil.

3.2.3. NMDS analysis

NMDS analysis can simplify the data structure, describe the distribution of samples at a given distance metric, and represent clearly the difference in the bacterial community structure among varied treatment groups. As shown in Figure 5, dots of different colors denote different treatment groups, and a closer distance between two dots indicates more similarities in the bacterial community between two groups. The stress of NMDS analysis is 0.0558 (<0.2), proving that NMDS fitting can accurately measure the bacterial community structure of different treatment groups. For surface soil, the bacterial community structures of CFN18 and CFN12 groups were quite similar, while the bacterial community structures of OFN18 and OFN12 groups were greatly dissimilar. For subsurface soil, the bacterial community of the CFN12 group notably resembled that of the OFN12 group, while the bacterial community of the CFN18 group greatly differed from that of the OFN18 group. Significant differences were found in the bacterial community between surface and subsurface soil. Soil has high heterogeneity and the bacterial community varies in soil at different depths.

3.2.4. Species composition analysis

The relative abundance of phyla in each treatment group was analyzed after high-throughput sequencing of the bacterial community. The top 5 dominant phyla were compared among different groups. Figure 6 shows top 20 species with the highest relative abundance, and the relative abundance of remaining species was combined and classified as Others. In surface soil (Figure 6A), the top 5 phyla with the highest relative abundance were Proteobacteria,

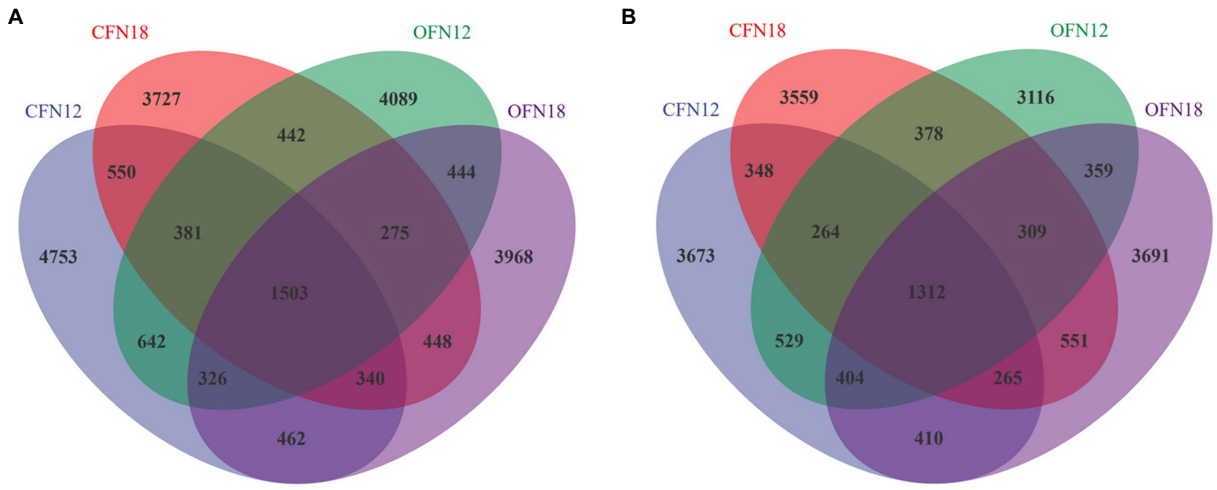

FIGURE 4
OTUs Venn Diagram of soil bacteria. **(A)** 0–10cm; **(B)** 10–20cm.

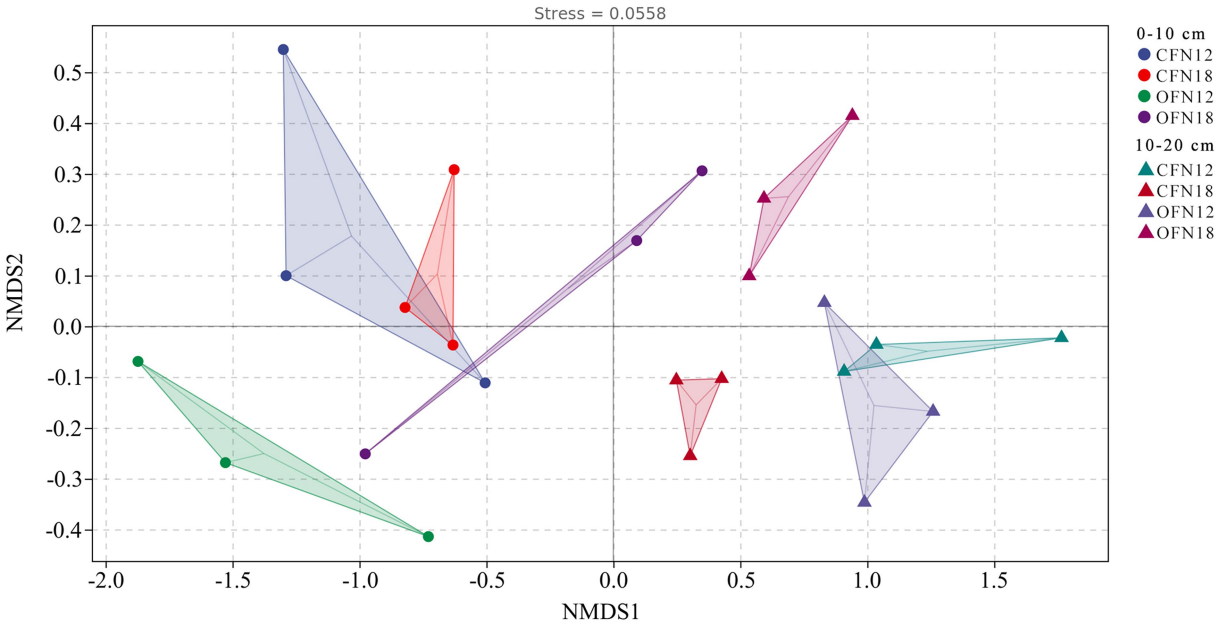

FIGURE 5
Non-metric multidimensional scaling analysis score plots of bacteria based on the Bray–Curtis distance.

Acidobacteria, Chloroflexi, Nitrospirae, and Actinobacteria. Proteobacteria (34.46–40.93%), Acidobacteria (17.07–20.72%), and Chloroflexi (13.77–21.99%) phyla predominated in surface soil, accounting for 75% of the total phyla. Among the four different treatment groups, the relative abundance of Proteobacteria was the lowest and the relative abundance of Chloroflexi was the highest in the OFN18 group. Compared with the low nitrogen treatment, high nitrogen application reduced the relative abundance of Proteobacteria, Acidobacteria, and Actinobacteria. Their relative abundance in CFN18 type soil was lower than that in CFN12 type soil by 0.20, 9.89, and 26.80%, respectively. Their relative abundance in OFN18 type soil was lower than that in OFN12 type soil by 15.81, 14.23, and 31.39%, respectively. However, the relative abundance of Chloroflexi in CFN18 and OFN18 groups was higher than that in CFN12 and OFN12 groups by 7.30 and 59.74%, respectively. High nitrogen application abated the total ratio of dominant phyla but enlarged the total ratio of rare phyla.

In subsurface soil (Figure 6B), the top 5 phyla with the highest relative abundance were Proteobacteria, Chloroflexi, Acidobacteria, Gemmatimonadetes, and Rokubacteria. The dominant phyla were Proteobacteria (32.77–39.31%), Chloroflexi (18.52–22.66%), and Acidobacteria (15.37–16.15%), which occupied 70% of the total phyla. The relative abundance of Proteobacteria and Rokubacteria in CFN18 type soil was 19.98% higher and 40.84% lower than that of CFN12 type soil, respectively, and the differences were significant. The relative

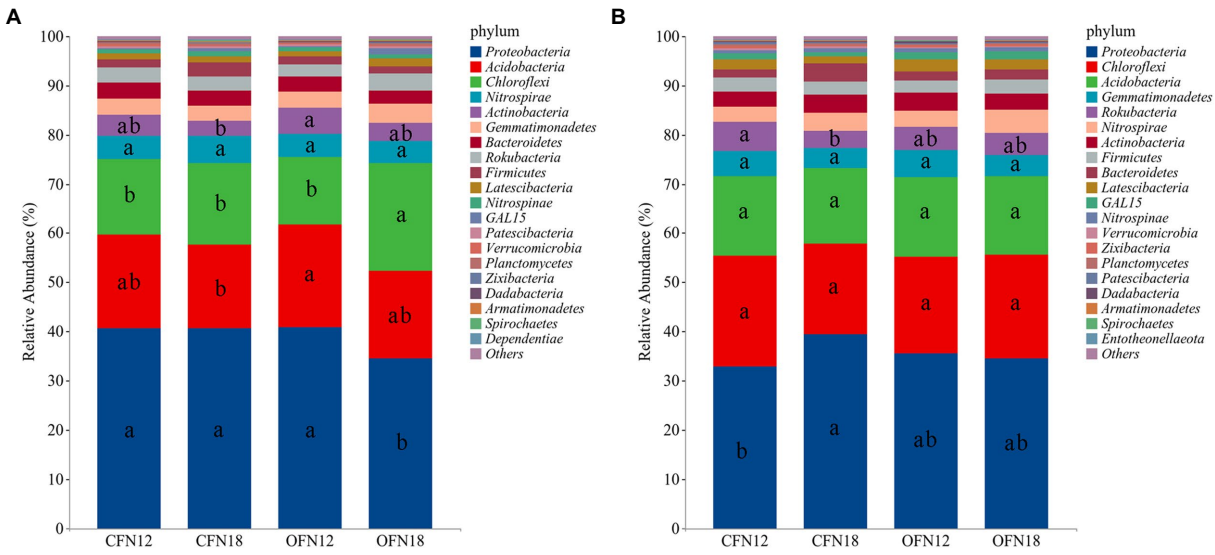

FIGURE 6
Relative Abundance of bacteria on phylum level. **(A)** 0–10cm; **(B)** 10–20cm. Different lower case letters indicate significant differences among the four treatments at $p<0.05$.

abundance of Chloroflexi, Acidobacteria, and Gemmatimonadetes maintained stable and showed little difference among four groups. On the whole, the ratio of dominant phyla in surface soil was larger than that in subsurface soil, while there were more rare phyla in subsurface soil than in surface soil.

3.2.5. LEfSe analysis

Biomarkers that were tremendously different among four treatment groups were identified by LEfSe analysis (species with abundance lower than 0.0015 were removed). Results were concluded in a cladogram and a histogram of the LDA scores. The cladogram represents the phylum to genus from the innermost ring to the outermost ring. The diameter of small circles is proportional to the relative abundance of the species, and the biomarkers with significant difference are colored the same as the group. The length of a row in the histogram represents the LDA score, namely, the influence of the biomarker. It was found that in surface soil (Figure 7A), f_SC_I_84 was notably enriched in the CFN12 group, p_Acidobacteria and f_Rhodospirillaceae were remarkably enriched in the OFN12 group, and p_GAL15 was significantly enriched in the OFN18 group. No biomarkers were observed in the CFN18 group. According to the LDA histogram, when the LDA value was greater than 3.5, all the four groups had 13 biomarkers in total and there were more biomarkers in OF groups than in *CF* groups. The most influenced species in CFN12, OFN12, and OFN18 type soil were g_SC_I_84, p_Acidobacteria, and f_GAL15, respectively.

In subsurface soil (Figure 7B), the enriched species in CFN12, OFN12, and OFN18 groups were c_Dehalococcoidia, p_Latescibacteria and f_Nitrosomonadaceae, c_Thermodesulfovibrionia and o_SJA_15, respectively. No biomarkers were found in the CFN18 group. There were totally 14 biomarkers in four groups when the LDA value was larger than 3.5, as is shown in the LDA histogram. The OFN12 group had the most biomarkers. c_Dehalococcoidia in the CFN12 group, f_Latescibacteria in the OFN12 group, and c_Thermodesulfovibrionia in the OFN18 group were subjected to the greatest impact.

It is noteworthy that among all biomarkers, p_Acidobacteria with the highest relative richness in surface soil and f_Nitrosomonadaceae with the highest relative abundance in subsurface soil were both present in the OFN12 group.

3.3. Relevance between soil nutrients and microbial communities

3.3.1. Correlation between environmental factors and diversity indices

The relationship between soil environmental factors and bacterial α diversity was analyzed by the Spearman's algorithm (Figure 8). The results suggested that in surface soil (Figure 8A), four α diversity indices were significantly related with each other. Observed species, Shannon, and Simpson indices were positively correlated to Urease, while Shannon was negatively correlated to AN. What's more, a negative connection was observed between pH values and AN, TN, AP, SOM, and Alkaline phosphatase. SOM was positively associated with TN, Alkaline phosphatase, and Sucrase. Besides, AN was positively correlated to TN and AP, and Alkaline phosphatase was positively connected to TN and Sucrase. All the correlations were notable.

In subsurface soil (Figure 8B), a significant association was also observed among four α diversity indices. Simpson was negatively related to Alkaline phosphatase and Sucrase. AK was positively correlated with AN, TN, SOM, pH, and Urease. SOM was positively connected to AN, TN, and Urease. AN was positively correlated with TN and Urease. AP was negatively related to AN and TN. Moreover, a positive connection was found between Alkaline phosphatase and Sucrase as well as between pH values and Urease. All the correlations were significant.

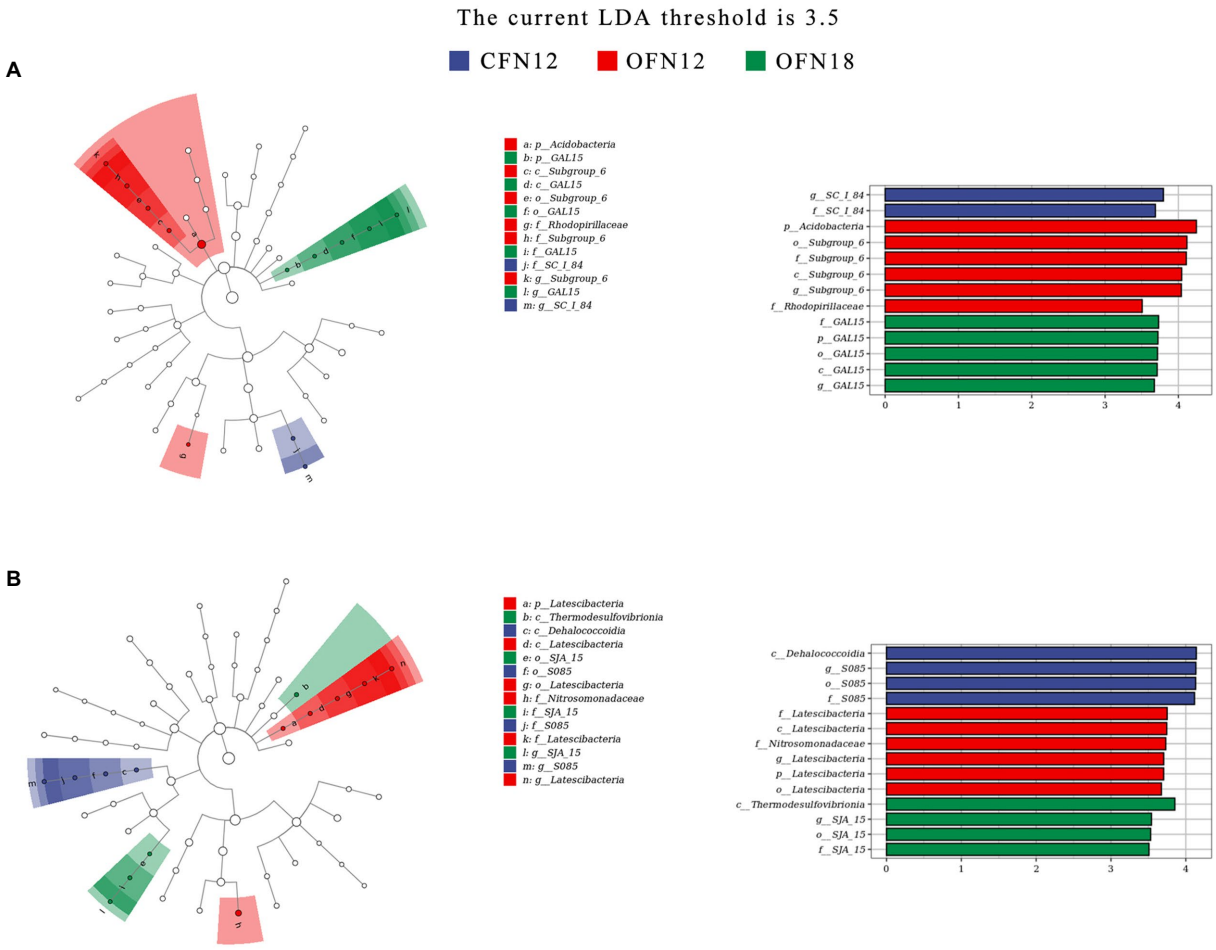

FIGURE 7
LEfSe analysis of bacterial community. **(A)** 0–10cm; **(B)** 10–20cm. p, phylum; c, class; o, order; f, family; g, genus.

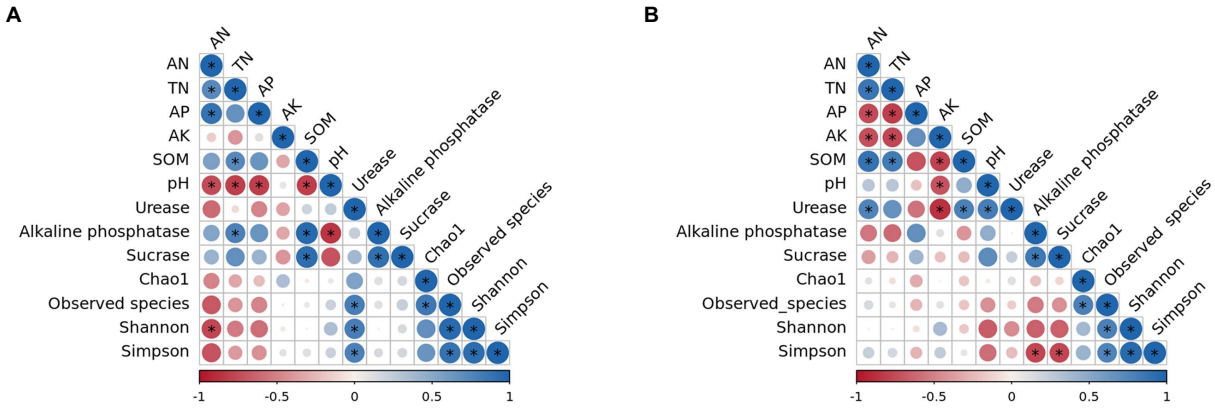

FIGURE 8
Correlation analysis of soil nutrients, enzyme activities and diversity index. **(A)** 0–10cm; **(B)** 10–20cm. *$p < 0.01$.

3.3.2. Redundancy analysis of environmental factors and dominant phyla

The relationship of top 10 phyla with environmental factors was investigated by redundancy analysis. The results are summarized in Figure 9. In surface soil (Figure 9A), RDA1 and RDA2 accounted for 79.29 and 9.16% variations of the bacterial community, respectively. AK (r2 = 0.18, $p = 0.39$) had small influence on community composition. Acidobacteria was positively associated with AN, TN, AP, SOM, Alkaline phosphatase, and Sucrase (AN: r2 = 0.67, $p = 0.01$; TN: r2 = 0.55, $p = 0.02$; AP: r2 = 0.67, $p = 0.00$; SOM: r2 = 0.60, p = 0.01;

Alkaline phosphatase: r2 = 0.55, $p = 0.03$; Sucrase: r2 = 0.75, p = 0.00), while Proteobacteria was negatively related to these factors. There was slight correlation between Chloroflexi and most environmental factors.

In subsurface soil (Figure 9B), RDA1 and RDA2 explained 69.81 and 11.82% variations of the bacterial community, respectively. Alkaline phosphatase (r2 = 0.45, $p = 0.07$) might impact community composition, but all the other environmental factors had little effect on community composition, with r2 ranging between 0.01 ~ 0.37 and p between 0.13 ~ 0.98. Proteobacteria was positively correlated to AN, TN and SOM, but negatively correlated to other environmental factors. Chloroflexi was not related to a majority of the environmental factors.

4. Discussion

4.1. Effects of cultivation patterns and nitrogen levels on nutrients in surface and subsurface soil

Organic fertilizer can ameliorate physicochemical properties of soil, raise the amount of SOM and renovate SOM, lessen nutrient loss, and enhance fertilizer utilization efficiency (Rahman et al., 2011; Hou et al., 2016; Du et al., 2020). In this study, the content of TN, AN, AP, and SOM in surface soil and the content of AP and AK in subsurface soil were notably elevated under the organic farming pattern. This finding is consistent with the conclusion of previous studies. The content of nutrients in soil at different depths increased in varying degrees. Dislike TN, AN can represent the capacity of soil to supply nitrogen available to rice in a short term. In the organic farming system, planting milk vetch increased the concentration of available (potentially mineralizable) nitrogen of the paddy field ecosystem. Such legume fertilizer released nitrogen in synchrony with the nitrogen uptake of plants, and meanwhile reduced nitrogen loss through leaching and volatilization (Askegaard and Eriksen, 2007; Suja et al., 2012). Results of this study revealed that AN content in surface soil with high nitrogen applied was higher than that with low nitrogen applied, indicating that an increased nitrogen application amount directly led to ascending AN content. Nevertheless, the content of SOM in subsurface soil did not rise under the organic farming pattern. The reason might be that under the conventional farming mode, soil microorganisms decomposed subsurface SOM at a slow rate, but the microorganisms tended to be more active and disintegrated the original SOM in soil under the organic farming mode. It requires some time to transform organic matter into SOM. As a result, the SOM content in subsurface soil was lower under the organic farming pattern than under the conventional farming mode. Soil nutrient stratification can be observed on the section of the upper layer of soil undergoing long-term farming, and generally, the nutrient content descends as the depth increases (Gwenzi et al., 2009). In our experiment, nutrient stratification of paddy soil was also noticed because of fertilizer application, and there were more nutrients in surface soil than in subsurface soil. Previous researchers have already confirmed that application of a large amount of nitrogen fertilizer over a long period can bring about soil acidification (Bowman et al., 2008). This conclusion corresponded to a slight decrease in pH under high nitrogen treatment. Meanwhile, the pH of surface soil was greatly lower than that of subsurface soil owing to nitrogen stratification. Most notably, the pH of organic farming soil was lower than that of conventional farming soil. Two reasons might be accountable. One is that organic fertilizer used induces nitrification and the release of H^+ (Xun et al., 2016), and the other is organic acid accumulation in organic fertilizer (Liang et al., 2012). It is thus evident that organic farming has a latent capacity to reduce the pH level of alkaline soil in Gaoyou, Jiangsu Province.

Niemi et al. (2005) claimed that root biomass and enzyme activity declined as soil depth increased. It was also found in our study that enzyme activity in surface soil was more intense than in subsurface soil, which might be attributed to an increased bulk density and decreased metabolic diversity of soil (Li et al., 2002; Griffiths et al.,

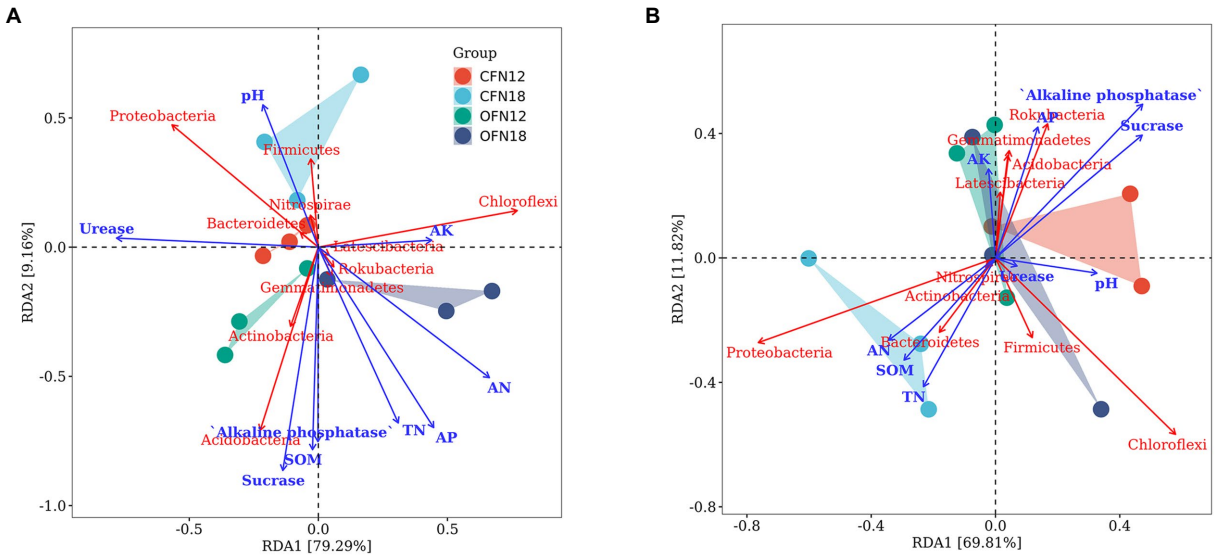

FIGURE 9
Redundancy analysis of soil nutrients, enzyme activities and abundant phyla. **(A)** 0–10cm; **(B)** 10–20cm.

2003). Remarkable changes in enzyme activity were also related to the amount of nitrogen applied (Corrales et al., 2017). In this paper, nitrogen reduction was suggested to boost enzyme activity. It was because low nitrogen application limited the supply of nitrogen needed by soil microorganisms (Mooshammer et al., 2014), which thereby had to secret more enzymes to acquire more nitrogen (Olander and Vitousek, 2000). It has been proven by a large number of studies that organic fertilizer promotes enzyme activity (Ye et al., 2014; Wang N. et al., 2020; Li et al., 2022). Results of this study also indicated that organic farming greatly activated alkaline phosphatase and sucrase in surface soil. The reason was that organic fertilizer increased the SOM content and stabilized the aggregates in surface soil, provided soil microorganisms with adequate carbon sources and a good environment, and enriched the substrates needed by soil enzymes. However, urease activity in subsurface soil was reduced under the organic farming mode. The proximate cause for why urease in organic farming soil was less active than that in conventional farming soil might be that urease could catalyze the hydrolysis of urea, and urea applied as topdressing in convention farming increased urease activity notably.

4.2. The impact of cultivation patterns and nitrogen levels on microorganisms in surface and subsurface soil

The present study results showed that bacterial diversity indices were subject to nitrogen levels in a short term. Campbell et al. (2010) noticed a decrease in bacterial diversity of Arctic tundra soil with an increased nitrogen application amount. Nevertheless, Fierer et al. (2012) reported no association between the nitrogen application amount and bacterial diversity of grassland and farmland soil in the United States. It is clear that effects of nitrogen levels on bacterial communities vary in different regions. The study of Liu et al. (2011) on paddy soil in southeastern China suggested that applying an appropriate amount of nitrogen could increase microbial biomass and respiration activity of paddy soil, but excessive nitrogen would impede soil bacterial diversity. The findings of the present study proved that low nitrogen levels could improve bacterial richness and diversity of surface soil, especially under the conventional farming pattern (Figures 3, 4). There are long-standing issues such as excessive application of industrial nitrogen fertilizer and a lack of awareness of soil conservation in rice cropping regions in Jiangsu Province. An excessive supplement of external nitrogen fertilizer would result in extremely low soil C/N. Without sufficient carbon sources, soil microorganism growth is restricted and soil microbial biomass is thus greatly reduced (Fontaine et al., 2003). Therefore, a proper reduction of nitrogen may increase microbial diversity of surface soil. A previous study established that microbial communities had stable and strong adaptability to the increasing depth of paddy soil (Yu et al., 2020). In this experiment, Observed species, Shannon, and Simpson indices of subsurface soil under high nitrogen levels were just slightly larger than those under low nitrogen levels, and the difference was not significant. It indicated that a proper reduction of nitrogen could improve nitrogen fertilizer use efficiency and reduce nitrogen loss resulted from leaching without damnifying microbial diversity in subsurface soil.

Both the Venn diagram and nonmetric multidimensional scaling analysis results suggested that microbial communities varied greatly and tended to cluster under different treatment conditions (Figures 4, 5). It was indicated in a study that the difference in soil microbial communities was ascribed to the mutual selection of plants and environmental factors (Mendes et al., 2014). Different from that in a natural ecosystem, the microbial community in the paddy field ecosystem under human control is more susceptible to environmental changes (Xu et al., 2019). Environmental factors of this test included farming patterns, nitrogen levels, and soil depth. These factors increased the exclusive species of different treatment groups and remarkably affected the microbial community composition of paddy soil. Bacteria in subsurface soil showed an obvious tendency to cluster. In contrast, bacteria in surface soil were distributed in a more scattered manner (Figure 5). A possible reason was the influence of bacterial community competition, artificial disturbance and climate change.

The cultivation patterns had little influence on bacterial diversity but great impact on the bacterial community structure. Proteobacteria, Acidobacteria, and Chloroflexi were the top dominant phyla in paddy soil. This finding conformed to that of previous research (Huang et al., 2019; Li et al., 2019). Significantly decreased Proteobacteria and remarkably increased Chloroflexi in surface soil of the OFN18 group (Figure 6) were attributed to the competition of dominant phyla. Though there were changes in the proportion of dominant phyla among different treatment groups, the total relative abundance of the above 3 dominant phyla remained unchanged. The total relative abundance of surface soil was 5% higher than that of subsurface soil, which was probably because some aerobic bacteria in the dominant phyla proliferated rapidly in surface soil with good permeability and high nutrient and O_2 content. Ramirez et al. (2012) carried out a series of tests to study the effect of different application amounts of nitrogen, and they found that high nitrogen levels reduced the relative abundance of Acidobacteria. Their finding was in agreement with the result of this study that Acidobacteria was tremendously enriched in surface soil of the OFN12 group (Figures 6, 7). However, Acidobacteria did not become a biomarker in CFN12 treatment. The reason might be that some species in Acidobacteria with genes encoding cellulase and hemicellulos (Kanokratana et al., 2011) participated in degrading a large number of milk vetch and rapeseed meal residues under the organic farming pattern. Oxidation of ammonium to nitrites by ammonia-oxidizing bacteria (AOB) is an essential part of nitrification (Chen et al., 2010). The amoA gene involved in catalytic nitrification is closely related to Nitrosospira and Nitrosomonas in AOB (Hussain et al., 2011). The results of this paper showed that Nitrosomonadaceae, to which Nitrosomonas belongs, was the biomarker of subsurface soil under the OFN12 treatment (Figure 7). Previous researchers have established that the AOB community in the rice rhizosphere was highly responsive to soil depth and nitrogen fertilizer application (Wang et al., 2009; Hussain et al., 2011). This study implied that under the organic farming pattern, low nitrogen treatment could increase the quantity of Nitrosomonas in subsurface soil, thereby improving nitrification efficiency and nitrogen fixation activity. To conclude, organic farming has the merit of optimizing the community structure.

4.3. Connection between soil nutrients and microbial community

The Spearman's correlation test revealed a correlation between diversity indices and enzyme activity. In surface soil, Shannon was significantly positively related to urease but negatively related to AN. It was inferred that nitrogen application easily led to changes in bacterial diversity. As the mount of nitrogen fertilizer applied increased, AN lifted greatly, resulting in unbalanced C/N. Low carbon induced declined bacterial diversity in surface soil. Under high nitrogen levels, urease maintained low activity and thus prevented severe imbalance of C/N (Mooshammer et al., 2014; Chen et al., 2018). In subsurface soil, Simpson was significantly negatively correlated with alkaline phosphatase. The reason might be that the amount of nitrogen flowing from surface soil into subsurface soil was moderate, which unexpectedly increased bacterial diversity. Subsurface soil of Gaoyou city is prone to phosphorus deficiency, and applying nitrogen fertilizer (compound fertilizer and San'an bio-fertilizer) added phosphorus into soil and alleviated phosphorus shortage, which therefore reduced phosphatase activity (Marklein and Houlton, 2012). To conclude, the interaction between bacterial diversity and enzyme activity was determined by nitrogen fertilizer application and affected by factors including soil physicochemical properties, soil types, climate, and farming patterns. The specific mechanism requires further investigation.

A majority of species of Acidobacteria are acidophilic. Redundancy analysis results showed that the relative abundance of Acidobacteria in surface soil was notably negatively correlated to the soil pH, which was confirmed by a previous study (Jones et al., 2009; Chu et al., 2010; Griffiths et al., 2011). The research of Wang H. et al. (2020) proved a significant positive connection between Acidobacteria and SOM, AP, and AN. Zhang et al. (2014) concluded that some subspecies of Acidobacteria were positively related to the activity of several key soil enzymes. In this paper, Acidobacteria in surface soil was found positively associated with AN, TN, AP, SOM, Alkaline phosphatase, and Sucrase. It was speculated that the positive relationship was originated from straw incorporation of previous crops prior to rice transplanting. Acidobacteria degraded straw as nutrients of soil, and the application of milk vetch in the organic farming pattern intensified the degradation activity of Acidobacteria. In subsurface soil, Proteobacteria was positively related to AN, TN, and SOM, which might be ascribed to the participation of nitrogen-fixing bacteria of Proteobacteria in the biochemical cycling of various nutrients in soil such as mineral carbon and nitrogen. Organic matter mineralization and degradation adds to the nitrogen source and thereby increases the relative abundance of nitrogen-fixing microorganisms in Proteobacteria (Chaudhry et al., 2012). However, Proteobacteria in surface soil was negatively related to most nutrients in this study. It was conjectured that some species of Proteobacteria were either adverse or unrelated to nutrient promotion. Further studies should focus more on specific bacterial communities of Proteobacteria since this phylum had the largest relative abundance in paddy soil. What's more, this experiment also indicated that Chloroflexi was not relevant to most environmental factors despite its huge influence on bacterial community composition. It was probably due to high stability of Chloroflexi in paddy soil. Some species of Chloroflexi are well known because of their unique 3-HP structure, which is capable of fixing CO_2 (Shih et al., 2017). Nevertheless, the genotype and phenotype of Chloroflexi vary greatly, and research on Chloroflexi strains is warranted to make up for the lack of knowledge of Chloroflexi.

5. Conclusion

Soil nutrients and enzyme activity decrease with the increasing soil depth. Organic farming can effectively improve soil nutrients and reduce nutrient loss, and has the potentiality to neutralize the alkaline soil in Gaoyou of Jiangsu Province. However, the organic farming mode will reduce the SOM content and urease activity in subsurface soil. Increased application of nitrogen fertilizer directly induces rising AN content and lowered pH values, while nitrogen reduction can activate a variety of enzymes. Besides, the overuse of nitrogen fertilizer will damage the diversity of soil microorganisms, while a proper reduction of nitrogen can improve the utilization rate of nitrogen fertilizer without affecting soil microbial diversity. The correlation analysis reveals a significant relationship of AN with diversity indices and enzyme activity. Organic farming upgrades markedly the community structure. Low nitrogen treatment under the organic farming mode can increase the relative abundance of Acidobacteria in surface soil and Nitrosomonadaceae in subsurface soil, thereby promoting the degradation of plant residues and boosting nitrification. Proteobacteria, Acidobacteria and Chloroflexi were the top 3 dominant phyla in paddy soil, and their total relative richness maintains stable. Proteobacteria and Acidobacteria play a critical part in the generation of soil nutrients. Therefore, we recommend an organic farming system with reduced application of nitrogen fertilizer for restoring fertility levels of soil in Gaoyou, Jiangsu Province.

Data availability statement

The datasets presented in this study can be found in online repositories. The names of the repository/repositories and accession number(s) can be found at: https://www.ncbi.nlm.nih.gov/sra/PRJNA890158.

Author contributions

CX: validation, formal analysis, investigation, data curation, and writing – original draft. YC: validation, investigation, and data curation. QZ: investigation. YL: methodology and investigation. JZ: investigation. XL: investigation. MJ: supervision. HZ: resources and project administration. LH: term, conceptualization, methodology, resources, and writing – review and editing. All authors contributed to the article and approved the submitted version.

Funding

This study was financially supported by the National Key R&D Program of China Under Grant, projects number 2017YFD0300102. Modern Agricultural Development Projects of Jiangsu Province, projects number 2019-SJ-039-08-11.

Acknowledgments

The Project was Funded by the Priority Academic Program Development of Jiangsu Higher Education Institutions (PAPD), and we thank the staff of Mapengwan Ecological Agriculture Technology Co., for their great support in the experiments.

Conflict of interest

The authors declare that the research was conducted in the absence of any commercial or financial relationships that could be construed as a potential conflict of interest.

Publisher's note

All claims expressed in this article are solely those of the authors and do not necessarily represent those of their affiliated organizations, or those of the publisher, the editors and the reviewers. Any product that may be evaluated in this article, or claim that may be made by its manufacturer, is not guaranteed or endorsed by the publisher.

Supplementary material

The Supplementary material for this article can be found online at: https://www.frontiersin.org/articles/10.3389/fmicb.2023.1072228/full#supplementary-material

References

Askegaard, M., and Eriksen, J. (2007). Growth of legume and nonlegume catch crops and residual-N effects in spring barley on coarse sand. *J. Plant Nutr. Soil Sci.* 170, 773–780. doi: 10.1002/jpln.200625222

Bao, S.D. (2000). *Agriculture and Chemistry Analysis of Soil*. Beijing China Agricultural Press.

Begum, F., Bajracharya, R. M., Sharma, S., and Sitaula, B. K. (2010). Influence of slope aspect on soil physico-chemical and biological properties in the mid hills of central Nepal. *Int J Sust Dev World* 17, 438–443. doi: 10.1080/13504509.2010.499034

Bowman, W. D., Cleveland, C. C., Halada, L., Hresko, J., and Baron, J. S. (2008). Negative impact of nitrogen deposition on soil buffering capacity. *Nat. Geosci.* 1, 767–770. doi: 10.1038/ngeo339

Campbell, B. J., Polson, S. W., Hanson, T. E., Mack, M. C., and Schuur, E. (2010). The effect of nutrient deposition on bacterial communities in Arctic tundra soil. *Environ. Microbiol.* 12, 1842–1854. doi: 10.1111/j.1462-2920.2010.02189.x

Chaudhry, V., Rehman, A., Mishra, A., Chauhan, P. S., and Nautiyal, C. S. (2012). Changes in bacterial community structure of agricultural land due to long-term organic and chemical amendments. *Microb. Ecol.* 64, 450–460. doi: 10.1007/s00248-012-0025-y

Chen, H., Li, D. J., Zhao, J., Zhang, W., Xiao, K. C., and Wang, K. L. (2018). Nitrogen addition aggravates microbial carbon limitation: evidence from ecoenzymatic stoichiometry. *Geoderma* 329, 61–64. doi: 10.1016/j.geoderma.2018.05.019

Chen, X., Zhang, L. M., Shen, J. P., Xu, Z. H., and He, J. Z. (2010). Soil type determines the abundance and community structure of ammonia-oxidizing bacteria and archaea in flooded paddy soils. *J. Soils Sediments* 10, 1510–1516. doi: 10.1007/s11368-010-0256-9

Chu, H. Y., Fierer, N., Lauber, C., Caporaso, J. G., Knight, R., and Grogan, P. (2010). Soil bacterial diversity in the Arctic is not fundamentally different from that found in other biomes. *Environ. Microbiol.* 12, 2998–3006. doi: 10.1111/j.1462-2920.2010.02277.x

Corrales, A., Turner, B. L., Tedersoo, L., Anslan, S., and Dalling, J. W. (2017). Nitrogen addition alters ectomycorrhizal fungal communities and soil enzyme activities in a tropical montane forest. *Fungal Ecol.* 27, 14–23. doi: 10.1016/j.funeco.2017.02.004

Critchley, C., Chambers, B. J., Fowbert, J. A., Sanderson, R. A., Bhogal, A., and Rose, S. C. (2002). Association between lowland grassland plant communities and soil properties. *Biol. Conserv.* 105, 199–215. doi: 10.1016/S0006-3207(01)00183-5

Du, Y. D., Cui, B. J., Zhang, Q., Wang, Z., Sun, J., and Niu, W. Q. (2020). Effects of manure fertilizer on crop yield and soil properties in China: a meta-analysis. *Catena* 193:104617. doi: 10.1016/j.catena.2020.104617

FAO. (2001). Statistical databases, food and agriculture organization (FAO) of the United Nations. Available at: http://www.fao.org

Fierer, N., Lauber, C. L., Ramirez, K. S., Zaneveld, J., Bradford, M. A., and Knight, R. (2012). Comparative metagenomic, phylogenetic and physiological analyses of soil microbial communities across nitrogen gradients. *ISME J.* 6, 1007–1017. doi: 10.1038/ismej.2011.159

Fontaine, S., Mariotti, A., and Abbadie, L. (2003). The priming effect of organic matter: a question of microbial competition? Soil biol. *Biochemist* 35, 837–843. doi: 10.1016/S0038-0717(03)00123-8

Griffiths, R. I., Thomson, B. C., James, P., Bell, T., Bailey, M., and Whiteley, A. S. (2011). The bacterial biogeography of British soils. *Environ. Microbiol.* 13, 1642–1654. doi: 10.1111/j.1462-2920.2011.02480.x

Griffiths, R. I., Whiteley, A. S., O'Donnell, A. G., and Bailey, M. J. (2003). Influence of depth and sampling time on bacterial community structure in an upland grassland soil. *FEMS Microbiol. Ecol.* 43, 35–43. doi: 10.1111/j.1574-6941.2003.tb01043.x

Guan, S.Y. (1986). *Soil Enzyme and Its Study Method*. Beijing China Agriculture Press.

Gunapala, N., and Scow, K. M. (1998). Dynamics of soil microbial biomass and activity in conventional and organic farming systems. *Soil Biol. Biochem.* 30, 805–816. doi: 10.1016/S0038-0717(97)00162-4

Guo, J. H., Liu, X. J., Zhang, Y., Shen, J. L., Han, W. X., Zhang, W. F., et al. (2010). Significant acidification in major Chinese croplands. *Science* 327, 1008–1010. doi: 10.1126/science.1182570

Gwenzi, W., Gotosa, J., Chakanetsa, S., and Mutema, Z. (2009). Effects of tillage systems on soil organic carbon dynamics, structural stability and crop yields in irrigated wheat (*Triticum aestivum* L.)-cotton (*Gossypium hirsutum* L.) rotation in semi-arid Zimbabwe. *Nutr. Cycl. Agroecosys.* 83, 211–221. doi: 10.1007/s10705-008-9211-1

Hou, M. M., Chen, D. Y., Shao, X. H., and Zhai, Y. M. (2016). Mulching and organic-inorganic fertilizer application reduce runoff losses of nitrogen from tobacco fields. *Fresenius Environ. Bull.* 25, 5542–5554.

Huang, Q., Wang, J. L., Wang, C., and Wang, Q. (2019). The 19-years inorganic fertilization increased bacterial diversity and altered bacterial community composition and potential functions in a paddy soil. *Appl. Soil Ecol.* 144, 60–67. doi: 10.1016/j.apsoil.2019.07.009

Hussain, Q., Liu, Y. Z., Jin, Z. J., Zhang, A. F., Pan, G. X., Li, L. Q., et al. (2011). Temporal dynamics of ammonia oxidizer (amoA) and denitrifier (nirK) communities in the rhizosphere of a rice ecosystem from tai Lake region, China. *Appl. Soil Ecol.* 48, 210–218. doi: 10.1016/j.apsoil.2011.03.004

Imhoff, S., Da Silva, A. P., and Tormena, C. A. (2000). Spatial heterogeneity of soil properties in areas under elephant-grass short-duration grazing system. *Plant Soil* 219, 161–168. doi: 10.1023/A:1004770911906

Jones, R. T., Robeson, M. S., Lauber, C. L., Hamady, M., Knight, R., and Fierer, N. (2009). A comprehensive survey of soil acidobacterial diversity using pyrosequencing and clone library analyses. *ISME J.* 3, 442–453. doi: 10.1038/ismej.2008.127

Ju, X. T., Xing, G. X., Chen, X. P., Zhang, S. L., Zhang, L. J., Liu, X. J., et al. (2009). Reducing environmental risk by improving N management in intensive Chinese agricultural systems. *Proc. Natl. Acad. Sci. U. S. A.* 106, 3041–3046. doi: 10.1073/pnas.0813417106

Kanokratana, P., Uengwetwanit, T., Rattanachomsri, U., Bunterngsook, B., Nimchua, T., Tangphatsornruang, S., et al. (2011). Insights into the phylogeny and metabolic potential of a primary tropical peat swamp Forest microbial community by metagenomic analysis. *Microb. Ecol.* 61, 518–528. doi: 10.1007/s00248-010-9766-7

Li, T. F., Liu, C. Y., Jin, X. M., Cao, X. Y., Lin, Z. Q., Lu, Q., et al. (2022). Effects of different cultivation strategies on soil nutrients and bacterial diversity in kiwifruit orchards. *Eur. J. Hortic. Sci.* 87, 1–8. doi: 10.17660/eJHS.2022/005

Li, C. H., Ma, B. L., and Zhang, T. Q. (2002). Soil bulk density effects on soil microbial populations and enzyme activities during the growth of maize (*Zea mays* L.) planted in large pots under field exposure. Can. J. *Soil Sci.* 82, 147–154. doi: 10.4141/S01-026

Li, X., Wang, H. H., Li, X., Li, X. Y., and Zhang, H. W. (2019). Shifts in bacterial community composition increase with depth in three soil types from paddy fields in China. *Pedobiologia* 77:150589. doi: 10.1016/j.pedobi.2019.150589

Liang, Q., Chen, H. Q., Gong, Y. S., Fan, M. S., Yang, H. F., Lal, R., et al. (2012). Effects of 15 years of manure and inorganic fertilizers on soil organic carbon fractions in a wheat-maize system in the North China Plain. *Nutr. Cycl. Agroecosys.* 92, 21–33. doi: 10.1007/s10705-011-9469-6

Ling, Q. H., Zhang, H. C., Ju, Z. W., Dai, Q. G., and Huo, Z. Y. (2010). Effects of different application rates of San'an bio-organic fertilizer on yield, quality and nitrogen absorption and utilization of organic Rice. *China Rice* 16, 17–22.

Liu, M., Ekschmitt, K., Zhang, B., Holzhauer, S., Li, Z. P., Zhang, T. L., et al. (2011). Effect of intensive inorganic fertilizer application on microbial properties in a paddy soil of subtropical China. *Agric. Sci. China* 10, 1758–1764. doi: 10.1016/S1671-2927(11)60175-2

Mäder, P., Hahn, D., Dubois, D., Gunst, L., Alfoldi, T., Bergmann, H., et al. (2007). Wheat quality in organic and conventional farming: results of a 21 year field experiment. *J. Sci. Food Agr.* 87, 1826–1835. doi: 10.1002/jsfa.2866

Marklein, A. R., and Houlton, B. Z. (2012). Nitrogen inputs accelerate phosphorus cycling rates across a wide variety of terrestrial ecosystems. *New Phytol.* 193, 696–704. doi: 10.1111/j.1469-8137.2011.03967.x

Mendes, L. W., Kuramae, E. E., Navarrete, A. A., van Veen, J. A., and Tsai, S. M. (2014). Taxonomical and functional microbial community selection in soybean rhizosphere. *ISME J.* 8, 1577–1587. doi: 10.1038/ismej.2014.17

Mooshammer, M., Wanek, W., Hammerle, I., Fuchslueger, L., Hofhansl, F., Knoltsch, A., et al. (2014). Adjustment of microbial nitrogen use efficiency to carbon: nitrogen imbalances regulates soil nitrogen cycling. *Nat. Commun.* 5:3694. doi: 10.1038/ncomms4694

Niemi, R. M., Vepsalainen, M., Wallenius, K., Simpanen, S., Alakukku, L., and Pietola, L. (2005). Temporal and soil depth-related variation in soil enzyme activities and in root growth of red clover (*Trifolium pratense*) and timothy (*Phleum pratense*) in the field. *Appl. Soil Ecol.* 30, 113–125. doi: 10.1016/j.apsoil.2005.02.003

Olander, L. P., and Vitousek, P. M. (2000). Regulation of soil phosphatase and chitinase activity by N and P availability. *Biogeochemistry* 49, 175–190. doi: 10.1023/A:1006316117817

Pimentel, D., Hepperly, P., Hanson, J., Douds, D., and Seidel, R. (2005). Environmental, energetic, and economic comparisons of organic and conventional farming systems. *Bioscience* 55, 573–582. doi: 10.1641/0006-3568(2005)055[0573:EEAECO]2.0.CO;2

Rahman, L., Whitelaw-Weckert, M. A., and Orchard, B. (2011). Consecutive applications of brassica green manures and seed meal enhances suppression of *Meloidogyne javanica* and increases yield of *Vitis vinifera* cv Semillon. *Appl. Soil Ecol.* 47, 195–203. doi: 10.1016/j.apsoil.2010.12.006

Ramirez, K. S., Craine, J. M., and Fierer, N. (2012). Consistent effects of nitrogen amendments on soil microbial communities and processes across biomes. *Glob. Chang. Biol.* 18, 1918–1927. doi: 10.1111/j.1365-2486.2012.02639.x

Shi, Y., Grogan, P., Sun, H. B., Xiong, J. B., Yang, Y. F., Zhou, J. Z., et al. (2015). Multi-scale variability analysis reveals the importance of spatial distance in shaping Arctic soil microbial functional communities. *Soil Biol. Biochem.* 86, 126–134. doi: 10.1016/j.soilbio.2015.03.028

Shih, P. M., Ward, L. M., and Fischer, W. W. (2017). Evolution of the 3-hydroxypropionate bicycle and recent transfer of anoxygenic photosynthesis into the Chloroflexi. *Proc. Natl. Acad. Sci. U. S. A.* 114, 10749–10754. doi: 10.1073/pnas.1710798114

Suja, G., Sundaresan, S., John, K. S., Sreekumar, J., and Misra, R. S. (2012). Higher yield, profit and soil quality from organic farming of elephant foot yam. *Agron. Sustain. Dev.* 32, 755–764. doi: 10.1007/s13593-011-0058-5

Takahashi, H., Matsushita, Y., Ito, T., Nakai, Y., Nanzyo, M., Kobayashi, T., et al. (2018). Comparative analysis of microbial diversity and bacterial seedling disease-suppressive activity in organic-farmed and standardized commercial conventional soils for rice nursery cultivation. *J. Phytopathol.* 166, 249–264. doi: 10.1111/jph.12682

Wang, H. Y., Hu, R. F., Chen, X. X., Zhong, X. H., Zheng, Z. T., Huang, N. R., et al. (2017). Reduction in nitrogen fertilizer use results in increased rice yields and improved environmental protection. *Int. J. Agr. Sustain.* 15, 681–692. doi: 10.1080/14735903.2017.1398627

Wang, Y. A., Ke, X. B., Wu, L. Q., and Lu, Y. H. (2009). Community composition of ammonia-oxidizing bacteria and archaea in rice field soil as affected by nitrogen fertilization. *Syst. Appl. Microbiol.* 32, 27–36. doi: 10.1016/j.syapm.2008.09.007

Wang, L., Li, J., Yang, F., E, Y., Raza, W., Huang, Q. W., et al. (2017). Application of bioorganic fertilizer significantly increased apple yields and shaped bacterial community structure in Orchard Soil. *Microb. Ecol.* 73, 404–416. doi: 10.1007/s00248-016-0849-y

Wang, N., Nan, H. Y., and Feng, K. Y. (2020). Effects of reduced chemical fertilizer with organic fertilizer application on soil microbial biomass, enzyme activity and cotton yield. *Chin. J. Appl. Ecol.* 31, 173–181. doi: 10.13287/j.1001-9332.202001.022

Wang, H., Wang, S. L., Wang, R., Wang, X. L., and Li, J. (2020). Conservation tillage increased soil bacterial diversity and improved soil nutrient status on the Loess Plateau in China. *Arch. Agron. Soil Sci.* 66, 1509–1519. doi: 10.1080/03650340.2019.1677892

Xu, S. Q., Tian, L., Chang, C. L., Li, X. J., and Tian, C. J. (2019). Cultivated rice rhizomicrobiome is more sensitive to environmental shifts than that of wild rice in natural environments. *Appl. Soil Ecol.* 140, 68–77. doi: 10.1016/j.apsoil.2019.04.006

Xun, W. B., Zhao, J., Xue, C., Zhang, G. S., Ran, W., Wang, B. R., et al. (2016). Significant alteration of soil bacterial communities and organic carbon decomposition by different long-term fertilization management conditions of extremely low-productivity arable soil in South China. *Environ. Microbiol.* 18, 1907–1917. doi: 10.1111/1462-2920.13098

Ye, X. F., Liu, H. E., Li, Z., Wang, Y., Wang, Y. Y., Wang, H. F., et al. (2014). Effects of green manure continuous application on soil microbial biomass and enzyme activity. *J. Plant Nutr.* 37, 498–508. doi: 10.1080/01904167.2013.867978

Yu, H., Xue, D. M., Wang, Y. D., Zheng, W., Zhang, G. L., and Wang, Z. L. (2020). Molecular ecological network analysis of the response of soil microbial communities to depth gradients in farmland soils. *Microbiology* 9:e983. doi: 10.1002/mbo3.983

Zelles, L. (1999). Fatty acid patterns of phospholipids and lipopolysaccharides in the characterisation of microbial communities in soil: a review. *Biol. Fert. Soils* 29, 111–129. doi: 10.1007/s003740050533

Zhang, Y. G., Cong, J., Lu, H., Li, G. L., Qu, Y. Y., Su, X. J., et al. (2014). Community structure and elevational diversity patterns of soil Acidobacteria. *J. Environ. Sci.* 26, 1717–1724. doi: 10.1016/j.jes.2014.06.012

Zhao, J., Ni, T., Li, J., Lu, Q., Fang, Z. Y., Huang, Q. W., et al. (2016). Effects of organic-inorganic compound fertilizer with reduced chemical fertilizer application on crop yields, soil biological activity and bacterial community structure in a rice-wheat cropping system. *Appl. Soil Ecol.* 99, 1–12. doi: 10.1016/j.apsoil.2015.11.006

frontiers | Frontiers in Microbiology

TYPE Original Research
PUBLISHED 23 February 2023
DOI 10.3389/fmicb.2023.1034761

OPEN ACCESS

EDITED BY
Ming Liu,
Institute of Soil Science (CAS), China

REVIEWED BY
Pengfa Li,
Nanjing Agricultural University, China
Robert Larkin,
New England Plant, Soil and Water Research Laboratory, Agricultural Research Service (USDA), United States

*CORRESPONDENCE
Jie-hua Zhu
✉ zhujiehua356@126.com
Ji-zong Zhang
✉ nxyzjz@163.com

SPECIALTY SECTION
This article was submitted to Microbe and Virus Interactions with Plants, a section of the journal Frontiers in Microbiology

RECEIVED 02 September 2022
ACCEPTED 10 January 2023
PUBLISHED 23 February 2023

CITATION
Li Q-m, Zhang D, Zhang J-z, Zhou Z-j, Pan Y, Yang Z-h, Zhu J-h, Liu Y-h and Zhang L-f (2023) Crop rotations increased soil ecosystem multifunctionality by improving keystone taxa and soil properties in potatoes.
Front. Microbiol. 14:1034761.
doi: 10.3389/fmicb.2023.1034761

Crop rotations increased soil ecosystem multifunctionality by improving keystone taxa and soil properties in potatoes

Qing-mei Li[1,2], Dai Zhang[1,2], Ji-zong Zhang[3]*, Zhi-jun Zhou[4], Yang Pan[1,2], Zhi-hui Yang[1,2], Jie-hua Zhu[1,2]*, Yu-hua Liu[3] and Li-feng Zhang[3]

[1]Technological Innovation Center for Biological Control of Crop Diseases and Insect Pests of Hebei Province, Baoding, China, [2]College of Plant Protection, Hebei Agricultural University, Baoding, China, [3]College of Agronomy, Hebei Agricultural University, Baoding, China, [4]Practice and Training Center, Hebei Agricultural University, Baoding, China

Continuous cropping of the same crop leads to soil degradation and a decline in crop production, and these impacts could be mitigated through rotation cropping. Although crop rotation enhances soil fertility, microbial community diversity, and potato yield, its effects on the soil ecosystem multifunctionality (EMF) remain unclear. In the present research, we comparatively examined the effects of potato continuous cropping (PP) and rotation cropping [potato–oat rotation (PO) and potato–forage maize rotation (PFM)] on the soil EMF as well as the roles of keystone taxa, microbes abundance, and chemical properties in EMF improvement. It was demonstrated that soil EMF is increased in rotation cropping (PO and PFM) than PP. Soil pH was higher in rotation cropping (PO and PFM) than in PP, while total phosphorus (TP) and available phosphorus (AP) were significantly decreased than that in PP. Rotation cropping (PO and PFM) markedly changed the bacterial and fungal community compositions, and improved the potential plant-beneficial fungi, e.g., *Schizothecium* and *Chaetomium*, while reducing the abundances of the potentially phytopathogenic fungi, e.g., *Alternaria*, *Fusarium*, *Verticillium dahiae*, *Gibberella*, *Plectosphaerella*, *Colletotrichum*, *Phoma*, and *Lectera* in comparison with PP. Also, co-occurrence patterns for bacteria and fungi were impacted by crop rotation, and keystone taxa, e.g., *Nitrospira*.1, *Lysinibacillus*, *Microlunatus*.1, *Sphingomonas*.3, *Bryobacter*.1, *Micromonospora*, and *Schizothecium,* were enriched in PO and PFM than PP. The structural equation model (SEM) further demonstrated that cropping systems increased soil ecosystem multifunctionality through regulating SOM and keystone taxa (*Schizothecium*1), and keystone taxa were mediated by soil pH. This study suggested that rotation cropping might contribute to the improvement of soil ecosystem multifunctionality as well as the development of disease-suppressive soils in comparison with potato continuous cropping.

KEYWORDS

rotation cropping, soil ecosystem multifunctionality, microbial community composition, keystone taxa, chemical properties, potato

1. Introduction

Potato (*Solanum tuberosum*), one of the most important crops in the world, plays an irreplaceable role in ensuring world food security and promoting economic development (Gustavsen, 2021). Because of the limited cultivated area and economic interest, potato continuous cropping within the same field has become a very widespread problem (Zhou et al., 2019). Long-term continuous potato cropping results in soil-borne diseases, including common scab, black scurf disease, blackleg, and fusarium wilt, which lead to a reduction in potato productivity and sustainable health development (Xu et al., 2022), and biotic factors are the major causes for soil-borne diseases (Dias et al., 2015). In order to control these diseases, fungicides are extensively used in potato production to prevent and control those soil-borne diseases and maintain sufficient crop yield and product quality (Al-Mughrabi et al., 2015), while they can also cause serious risks to the environment and human health (Tan et al., 2020).

Rotation cropping is a safe and effective measure that can improve soil productivity, reduce pathogens, control plant soil-borne diseases, and increase yields in comparison with continuous cropping (Larkin and Halloran, 2014; Ashworth et al., 2020). Previous studies have suggested that potato–corn/green manure rotation provided higher tuber yield *via* enhancing abundances of some beneficial microbes (e.g., *Sphingomonas*, *Haliangium*, *Gemmatimonas*, and *Pseudogymnoascus*), while decreasing the abundances of pathogenic microbes (e.g., *Fusarium*, *Stagonosporopsis, Alternaria*, *Lectera, Fusaria*, and *Mortierell*) and autotoxic substances (Qin et al., 2017; Wang et al., 2022). Long-time rotation cropping improved microbial community composition and enhanced soil health which eventually contributed to improved plant growth. Thus, maintaining the potato production system is closely associated with improving diverse and functional soil microbial communities (Hiltunen et al., 2021).

Soil microbes (bacteria and fungi) play a crucial role in the agroecosystem, as they participate in material cycling and organic matter decomposition (Liu et al., 2019), and are vital and decisive factors in plant health and productivity (Guo et al., 2021). Keystone taxa play a role in biological connectivity and may be considered indicative markers of community migration and compositional rollover, which have the largest influence on microbial community and ecosystem functionality (Vick-Majors et al., 2014; Banerjee et al., 2016a, 2018). Previous studies have demonstrated that keystone taxa can have significant effects on soil quality improvement, carbon transformation, and organic compound degradation (Banerjee et al., 2016b; Yan et al., 2019; Liu et al., 2022). Agricultural management, e.g., tillage practices, that effectively affect keystone taxa, also influence soil quality and ecosystem multifunctionality (Liu et al., 2022). However, the responses of soil ecosystem multifunctionality, microbial co-occurrence network, patterns, and keystone taxa to different cropping systems remain unclear.

Soil ecosystem multifunctionality motivated by soil microbes is important for maintaining the cycling of nutrients, the decomposition of organic matter, and plant productivity (Bardgett and van der Putten, 2014; Delgado-Baquerizo et al., 2016). Previous studies have shown that soil multifunctionality (e.g., C and N cycling) was affected by microbial community composition, diversity, and soil environment (e.g., pH and SOC) (Zheng et al., 2019). Agricultural management practices can enhance ecosystem services function and maintain ecosystem multifunctionality (Ryan et al., 2018). Recent studies have shown that intercropping can increase the soil ecosystem multifunctionality by improving available nutrients (Ma et al., 2022). It remains incompletely understood, however, whether the alterations in soil chemical properties affected by crop rotation affect the co-occurrence patterns of microbes and the relationship between keystone taxa and soil ecosystem multifunctionality.

In the present research, we comparatively explored the differences in soil chemical properties [pH, total nitrogen (TN), alkali hydrolyzable nitrogen (AN), organic matter (SOM), total phosphorus (TP), and available phosphorus (AP)], bacterial and fungal community compositions, co-occurrence patterns, keystone taxa, and ecosystem multifunctionality between potato continuous cropping (PP) and rotation cropping [potato–oat rotation (PO) and potato–forage maize rotation (PFM)]. The aims of the present study were to (1) investigate the responses of soil ecosystem multifunctionality, microbial community composition, co-occurrence network patterns, and keystone taxa to different cropping systems; (2) determine how the keystone taxa, microbes abundance, and chemical properties affect soil ecosystem multifunctionality under different cropping systems.

2. Materials and methods

2.1. Study site description

The study was conducted at the Zhangbei Agricultural Resource and Ecological Environment Key Field Research Station, Ministry of Agriculture and Rural Affairs, Zhangjiakou, Hebei, China (41°09'N, 114°42'E). The study site is situated at an elevation of 1,420 m, with a mean annual temperature of 3.9°C and a mean annual precipitation record of 382.5 mm. The soil type is meadow chestnut soil with a pH of 7.7, organic matter 18.53 g kg^{-1}, alkaline hydrolysis nitrogen 80.68 mg kg^{-1}, total nitrogen 1.09 g kg^{-1}, available phosphorus 34.10 mg kg^{-1}, total phosphorus 0.54 g kg^{-1}, available potassium 76.63 mg kg^{-1}, and total potassium 22.03 g kg^{-1} (Yao et al., 2020).

Three treatments were used during the growing seasons from 2015 to 2021. Treatments used in this study include potato (*Solanum tuberosum*) continuous cropping (PP), potato–oat (*Avena sativa*) rotation (PO), and potato–forage maize (*Zea mays*) rotation (PFM). Three 20 m × 6 m experimental plots were established and treated as the three treatments described earlier. There were five pseudo-replicates within each experimental plot, and the size of each replicate plot was 4 m × 6 m. Fertilizers were used as basal fertilizers before sowing, with no irrigation throughout the crop growth period. The detailed experimental treatments are shown in **Figure 1**.

2.2. Soil sampling

After the harvest of potatoes, a total of 15 bulk soil samples (three treatments × five replicates) were collected with a 2-cm-diameter auger on 14 October 2021. For the bulk soils, 10 topsoil samples (0–20 cm) were randomly collected from each replicate plot and combined into a single sample (a replicate). Each composite sample (a replicate) was divided into two parts, where the first part was stored at −80°C before DNA extraction, and the second part was air-dried at room temperature for determining soil chemical properties [pH, total nitrogen (TN), alkali hydrolyzable nitrogen (AN), organic matter (SOM), total phosphorus (TP), and available phosphorus (AP)], enzyme activities [β-1,4-N-acetyl-glucosaminidase (NAG), β-1,4-glucosidase (β-GC), and alkaline phosphatase (ALP)].

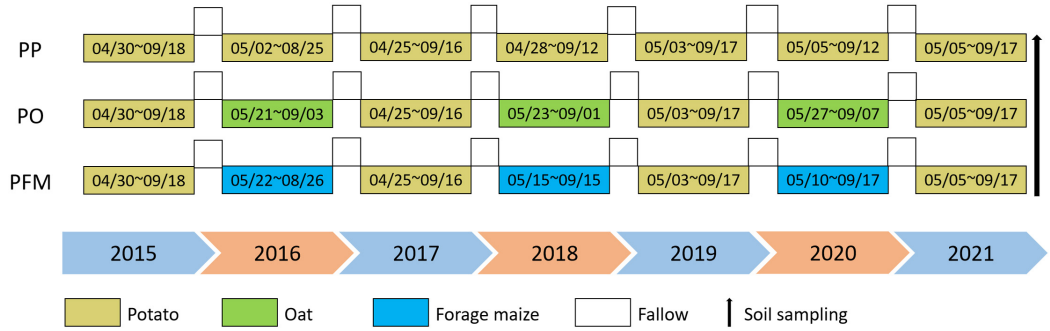

FIGURE 1
Schematic diagram of three experimental planting patterns.

2.3. Microbial DNA extraction, PCR amplification, and Illumina MiSeq

Total soil genomic DNA was extracted from 0.5 g of soil using the E.Z.N.A.® soil DNA kit (Omega Bio-Tek, Norcross, GA, USA). The DNA extract was checked on 1% agarose gel, and DNA concentration and purity were determined with NanoDrop 2000 UV–vis spectrophotometer (Thermo Scientific, Wilmington, USA). Bacterial 16S rRNA gene fragments were performed using the general bacterial primers 338F–806R, which are specific to the V3–V4 hypervariable region (Wang et al., 2018). The ITS region was targeted with the primers ITS1F–ITS2R (Kerfahi et al., 2016). The adaptor and primer sequences were trimmed using the cutadapt plugin. The quality control and identification of amplicon sequence variants were performed using the DADA2 plugin (Callahan et al., 2016) according to the standard protocols by Majorbio Bio-Pharm Technology Co., Ltd. (Shanghai, China). Through quality trimming (using Btrim to remove sequencing adaptors and low-quality regions), merging, and clustering (using the CD-HIT algorithm), samples were rarefied to a depth of 52,460 and 38,494 sequences per sample of bacterial and fungal communities, respectively, and clustered into 47,678 and 38,064 operational taxonomic units (OTUs) of bacterial and fungal communities, respectively, by a 97% similarity cutoff using UPARSE version 7.1 (Edgar, 2013). The taxonomy of each OTU representative sequence was analyzed by RDP Classifier version 2.2 (Wang et al., 2007) using a confidence threshold of 0.7. The raw data of bacterial and fungal sequences were deposited into the NCBI Sequence Read Archive (SRA) database under the following accession numbers: SRR22669278-22669292 (bacteria), and SRR22703913-22703927 (fungi).

2.4. Soil chemical properties, enzyme activities, and soil ecosystem multifunctionality analysis

Soil pH was determined in a mixture of water and soil suspension (2.5:1) with an electrode method. TN was done by measuring the residual ammonia by the Kjeldahl method. AN was determined by the alkaline diffusion method. TP was determined by Mo–Sb anti-spectrophotometric method. AP was extracted by the diacid method and determined by the molybdenum–antimony colorimetry. SOM was measured by the potassium dichromate external heating method. Soil analyses (pH, TN, AN, TP, AP, and SOM) procedures were conducted as detailed by Bao (2000).

Enzymatic activities of NAG and β-GC were determined by the colorimetric method, and ALP was measured using the disodium phenyl phosphate colorimetric method (Sinsabaugh et al., 2008).

Soil multifunctionality was assessed based on three soil functional attributes associated with the carbon (C), nitrogen (N), and phosphorus (P) cycles. NAG, TN, and AN for the N cycle; β-GC and organic matter for the C cycle; ALP, TP, and AP for the P cycle. Single soil functions were normalized with Z-score transformation and averaged to calculate the multifunctionality (Guo et al., 2021).

2.5. Statistical analyses

One-way ANOVA was employed to determine the effects of different cropping systems (PP, PO, and PFM) on the soil chemical properties, multifunctionality, and the abundance of the potential plant-beneficial and phytopathogenic microbes, and significant differences were analyzed by Duncan's new multiple differences test at a P-value of < 0.05. Data were tested for normality and homogeneity of variance before conducting ANOVA and were log-transformed when needed. The Pearson correlation coefficient was used to determine the possible association among soil microbes, soil chemical properties, and ecosystem multifunctionality. SPSS 22.0 software was used for statistical analyses.

Principal coordinate analysis (PCoA) was calculated by the "vegan 3.3.1" package in R. Linear discriminant analysis (LDA) effect size (LEfSe) was conducted to illustrate the biomarkers in each treatment. Those with an LDA score of ≥ 2.5 for bacteria and ≥ 4.0 for fungi were considered to be important biomarkers in each treatment.

Co-occurrence network analysis of microbial communities at the genus level using high-throughput sequencing data and the relative abundance of a genus of $> 0.1\%$ was used in the analyses. A correlation matrix was analyzed using the "psych" package in the R environment and the co-occurrence network visualization was achieved *via* Gephi (version 0.9.2). Spearman correlations between genera were performed, and the correlations with a coefficient of more than 0.6 and a P-value of less than 0.05 were applied. Microbial community networks were built according to MENAP

(Wu et al., 2021a).[1] The topological roles of individual nodes in the network were decided by the threshold values of *Zi* and *Pi* (Ling et al., 2016; Han et al., 2022). Nodes were classified into four categories: peripherals ($Zi < 2.5$ and $Pi < 0.62$), connectors ($Zi < 2.5$ and $Pi > 0.62$), module hubs ($Zi > 2.5$ and $Pi < 0.62$), and network hubs ($Zi > 2.5$ and $Pi > 0.62$). The nodes assigned to the network connector, module hub, and hub were the generalists that may be paralleled to key organisms in the microbial community as predicted by the network theory (Han et al., 2022).

A structural equation model was performed to assess the direct and indirect effects of cropping systems, soil pH, SOM, keystone taxa (*Schizothecium*1 abundance), and potentially phytopathogenic microbes on the soil ecosystem multifunctionality (C and N cycling) using IBM SPSS AMOS 21. Before the SEM analysis, we integrated the relative abundances of potentially phytopathogenic fungi [*Alternaria* (Wang et al., 2022; Xu et al., 2022), *Fusarium* (Zhang et al., 2017), *Verticillium dahliae* (Zhao et al., 2021), *Gibberella* (Li et al., 2022), *Plectosphaerella* (Xu et al., 2014), *Colletotrichum* (Cuevas-Fernández et al., 2022), *Phoma* (Wunsch and Bergstrom, 2011), and *Lectera* (Cannon et al., 2012)] through the principal component analyses (PCA). The first principal component (PC1) was used in the subsequent SEM analysis to represent soil pathogenic microbe abundance. Sufficient model fits of the structural equation models by χ^2/df ($1 \leq \chi^2/df \leq 3$ and $0.05 < P \leq 1.00$) and root mean square error of approximation ($0 \leq \text{RMSEA} \leq 0.08$) were used (Delgado-Baquerizo et al., 2016). The standardized total effect of each variable on the soil ecosystem multifunctionality was also determined for the structural equation model.

3. Results

3.1. Soil ecosystem multifunctionality and chemical properties

The response of the changes in soil ecosystem multifunctionality to different cropping systems is presented in **Table 1**. Soil multifunctionality of crop rotation (PO and PFM) soils was higher than those of PP soils ($P = 0.069$). Specifically, soil multifunctionality related to the C cycle ($P < 0.001$) and single soil functions β-GC ($P < 0.001$) were increased in the crop rotation (PO and PFM) soils than those of PP soils. Soil multifunctionality related to the N cycle ($P = 0.002$) and single soil functions NAG ($P < 0.001$) were increased in the crop rotation (PO and PFM) soils than those of PP soils. In contrast, single functions TP ($P < 0.001$) and AP ($P < 0.001$) relating to the soil P cycle were decreased in the crop rotation (PO and PFM) soils than the PP soils. Compared to PP, crop rotation increased soil pH ($P < 0.001$), and PFM also increased pH relative to PO. PO, but not PFM, also increased SOM ($P = 0.002$), TN ($P = 0.055$), and C/N ($P = 0.029$) than PP.

3.2. Composition of microbial community

We sequenced the V3–V4 region of the 16S rRNA gene for 15 samples and obtained a total of 980,851 high-quality sequence reads that ranged from 52,460 to 80,674, with an average read length of 417 bp. The fungal ITS sequences totaled 754,215, and the number of sequences obtained from each sample ranged from 38,494 to 73,983, with an average read length of 237 bp (**Supplementary Table 1**).

The disparities in the structures of soil bacterial and fungal communities from different cropping systems were analyzed by PCoA, and the structures of the microbial communities among continuous cropping and rotational cropping were significantly different (**Figure 2**). The first two principal component axes explained 18.67% (PC1) and 11.72% (PC2) of the variation in the bacterial community. The PO and PFM were clustered together, and were separated from PP along the PC2 axis (ANOSIM $R = 0.2418$, $P = 0.001$) (**Figure 2A**). Similar to the soil bacterial community, crop rotation also changed the fungal community structure. The first two principal component axes explained 17.15% (PC1) and 12.94% (PC2) of the variation in the fungal community. The fungal communities in soil from the PP treatment were separated from that of the PO and PFM treatments along the PC1 axis, and the PO was separated from the PFM along the PC2 axis (ANOSIM $R = 0.7769$, $P = 0.001$) (**Figure 2C**).

For the bacterial community, nine groups were described with an average relative abundance of > 1% at the phylum level. The dominant taxa in soil mainly included *Actinobacteriota* (33.32%), *Proteobacteria* (19.79%), *Chloroflexi* (13.20%), *Acidobacteriota* (10.40%), *Firmicutes* (6.79%), *Gemmatimonadota* (5.11%), *Bacteroidota* (3.20%), *Myxococcota* (2.37%), and *Methylomirabilota* (1.05%) (**Figure 2B**). Crop rotation shifted the dominant bacterial groups in comparison with PP. Dominant groups were displayed in cladograms, and LDA scores greater than or equal to 2.5 were confirmed by LEfSe (**Figure 3A** and **Supplementary Figure 1A**). *Cyanobacteria*, *Gemmatimonadetes*, and *Bacilli* performed major roles in PP, PO, and PFM, respectively. In addition, potential plant-beneficial bacteria *Bacillus* ($P = 0.008$) and *Pseudomonas* ($P = 0.001$), which are widely used for controlling plant diseases (Jiang et al., 2017; Wei et al., 2018), were in greater abundance in PFM than in PP and PO. In contrast, *Streptomyces scabiei*, which causes potato scab, was lower in abundance in PFM than in PP and PO, but there was no significant change between PP and PO (**Table 2**).

For the fungal community, the dominant phyla predominantly consisted of *Ascomycota* (81.36%), *Mortierellomycota* (10.30%), and *Basidiomycota* (6.19%) (**Figure 2D**). Crop rotation also shifted the dominant fungal groups in comparison with PP. Dominant groups were revealed in cladograms, and LDA scores greater than or equal to 4.0 were determined by LEfSe (**Figure 3B** and **Supplementary Figure 1B**). *Nectriaceae*, *Chaetomium*, and *Basidiomycota,* as the main dominant taxa, play key roles in PP, PO, and PFM, respectively. In addition, rotation cropping increased the potential plant-beneficial fungi abundance in comparison with PP (**Table 2**). Specifically, PO and PFM increased the abundance of *Schizothecium* ($P = 0.001$) and *Chaetomium* ($P < 0.001$) than PP, with PFM increasing *Schizothecium* to a greater degree, and PO increasing *Chaetomium* to a greater degree. Conversely, rotation cropping (PO and PFM) decreased the abundance of potentially phytopathogenic fungi than PP (**Table 2**). Specifically, the relative abundances of *Verticillium dahliae* ($P = 0.009$), *Alternaria* ($P = 0.004$), *Fusarium* ($P = 0.007$), *Gibberella* ($P = 0.002$), *Plectosphaerella* ($P < 0.001$), *Phoma* ($P < 0.001$), *Lectera* ($P < 0.001$), and *Colletotrichum* ($P = 0.019$) were significantly higher in PP than in PO and PFM but were insignificantly higher in PO and PFM.

1 http://ieg2.ou.edu/MENA/main.cgi

TABLE 1 The soil chemical properties, enzyme activities, and multifunctionality under different crop rotations.

Soil properties	PP	PO	PFM	*F*	*P*
EMF	−0.25 ± 0.08a	0.12 ± 0.12a	0.13 ± 0.12a	3.365	0.069
C cycle	−0.97 ± 0.11b	0.65 ± 0.18a	0.32 ± 0.09a	33.522	<0.001
β-GC (nmol g^{-1} h^{-1})	0.4867 ± 0.0005b	0.4915 ± 0.0009a	0.4937 ± 0.0006a	20.285	<0.001
SOM (g kg^{-1})	20.78 ± 0.54b	23.52 ± 0.21a	21.56 ± 0.31b	11.098	0.002
N cycle	−0.75 ± 0.17b	0.37 ± 0.17a	0.38 ± 0.17a	10.719	0.002
NAG (nmol g^{-1} h^{-1})	229.33 ± 14.09b	396.44 ± 8.19a	444.44 ± 23.45a	37.526	<0.001
TN (g kg^{-1})	1.22 ± 0.01b	1.27 ± 0.01a	1.26 ± 0.01*ab*	3.739	0.055
AN (mg kg^{-1})	109.13 ± 3.63a	111.37 ± 2.54a	110.89 ± 2.19a	0.136	0.874
P cycle	0.96 ± 0.12a	−0.65 ± 0.06a	−0.31 ± 0.21a	2.666	0.110
ALP (nmol g^{-1} h^{-1})	479.39 ± 11.89a	466.26 ± 4.91a	479.39 ± 3.98a	2.666	0.110
TP (g kg^{-1})	0.78 ± 0.02a	0.64 ± 0.02b	0.65 ± 0.01b	17.668	<0.001
AP (mg kg^{-1})	50.59 ± 1.38a	35.09 ± 1.96b	34.56 ± 2.09b	19.736	<0.001
pH	7.73 ± 0.02*c*	7.82 ± 0.01b	7.87 ± 0.00a	16.851	<0.001
C/N	9.85 ± 0.27b	10.73 ± 0.16a	9.93 ± 0.15b	4.802	0.029

SOM, soil organic matter; TN, total nitrogen; AN, alkali-hydrolysable nitrogen; TP, total phosphorus; AP, available phosphorus; C/N, organic carbon/total nitrogen; β-GC, β-1, 4-glucosidase; NAG, β-1, 4-N-acetyl-glucosaminidase; ALP, alkaline phosphatase; C cycle, carbon cycle; N cycle, nitrogen cycle; P cycle, phosphorus cycle; EMF, soil ecosystem multifunctionality; PP, potato continuous cropping; PO, potato–oat rotation; PFM, potato–forage maize rotation. Data represent the mean ± *SD* ($n = 5$). The different lowercase letters in the same rows indicate significant differences among treatments at the $P < 0.05$ level (one-way ANOVA).

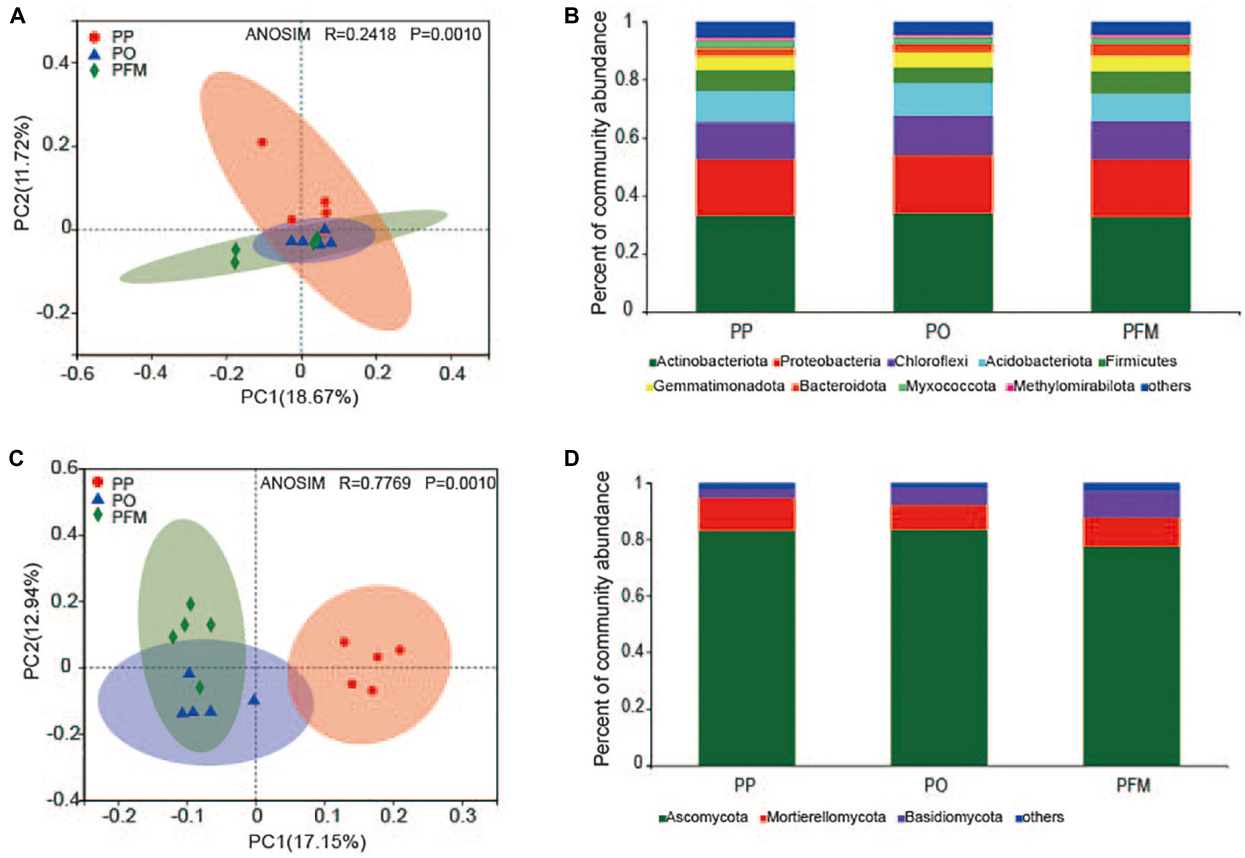

FIGURE 2
Principal coordinate analysis (PCoA) showing the changes in bacterial **(A)** and fungal **(C)** community composition. The abundances of total bacterial **(B)** and fungal **(D)** communities are based on the proportional frequencies of 16S rRNA and ITS sequences. PP, potato continuous cropping; PO, potato–oat rotation; PFM, potato–forage maize rotation.

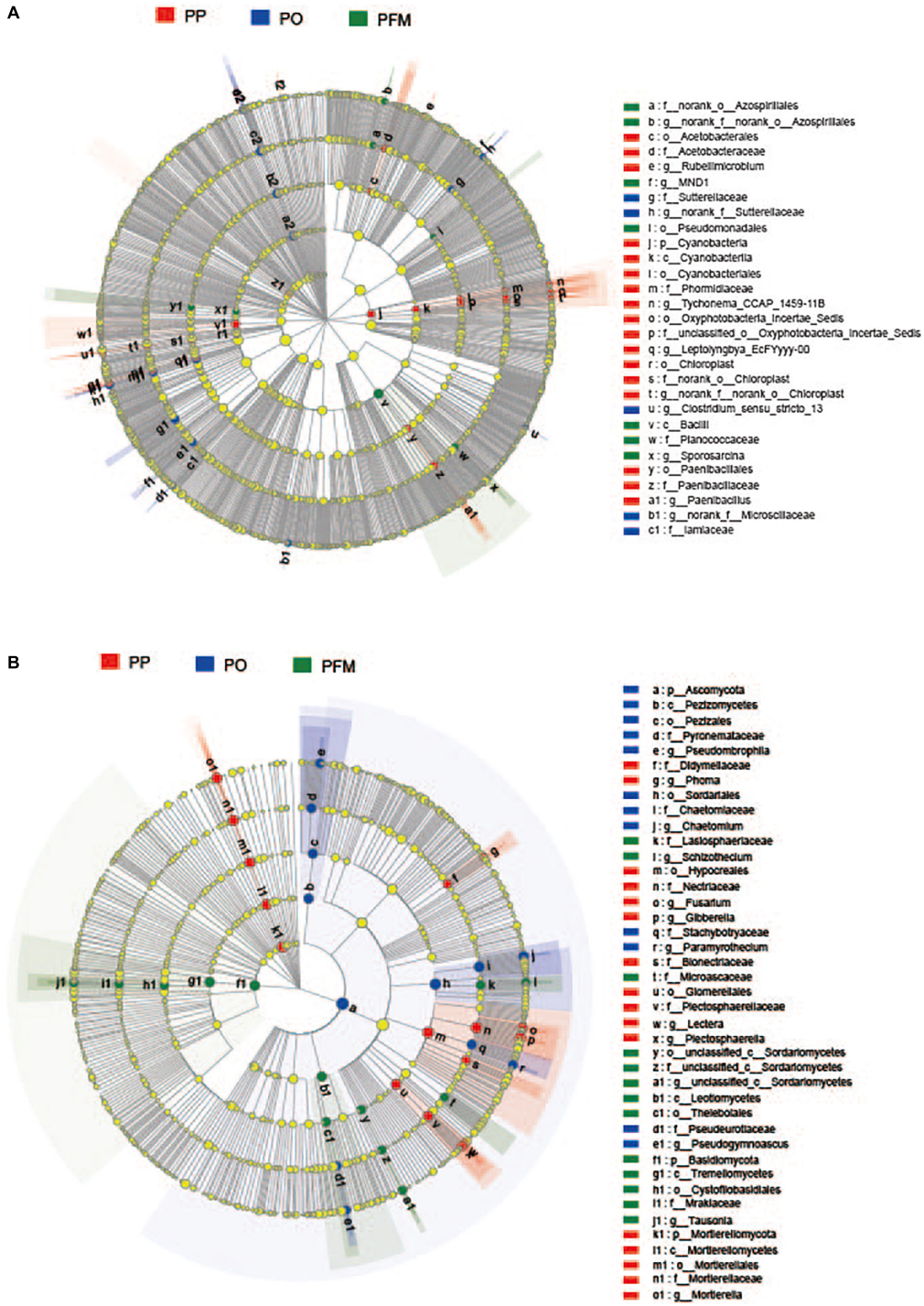

FIGURE 3
Cladogram showing the phylogenetic distribution of the bacterial **(A)** and fungal **(B)** lineages associated with soil from different crop rotations. Circles indicate phylogenetic levels from domain to genus. PP, potato continuous cropping; PO, potato–oat rotation; PFM, potato–forage maize rotation.

3.3. Co-occurrence network patterns and keystone taxa analysis of soil microbial community

In the present study, the interactions and differences of soil bacterial and fungal communities among different cropping systems were investigated at the genus level through co-occurrence networks (Figure 4), and the resulting complex pattern of the associations between nodes was depicted *via* calculating the topological properties (Supplementary Table 2). Significant differences in topological properties within bacterial and fungal networks were observed among the different cropping systems. For the bacterial community, the edges number, network density, modularity, and average clustering coefficient increased in PO and PFM than PP. The average path length decreased in PO and PFM than in PP. For the fungal community, compared with PP, the number of edges was increased in

PFM and decreased in PO. The PO and PFM increased the network density while decreasing the modularity and average clustering coefficient than PP.

To determine keystone taxa in the networks, the connectivity of genera (nodes) was computed within (*Zi*) and among (*Pi*) modules. In this study, most genera were connectors with more links to the nodes within modules (**Figure 5**). Compared with PP, rotation cropping engaged more generalists, which connect different nodes within their modules. In the bacterial networks, 75.77% of genera for the PP network, 95.65% for the PO network, and 89.69% for the PFM network had connections with other nodes within and among modules (**Supplementary Table 3**). In the fungal networks, 93.58% of genera for the PP network, 95.16% for the PO network, and 95.24% for the PFM network had links to other nodes within and among modules (**Supplementary Table 3**). Crop rotation altered the keystone taxa in comparison with PP. Nodes, such as *Nitrospira*.1, *Lysinibacillus*, *Microlunatus*.1, *Sphingomonas*.3, *Bryobacter*.1 and *Micromonospora*, and *Schizothecium* were classified as network connectors (generalists) within crop rotation but peripherals (specialists) in PP (**Figure 5** and **Supplementary Table 4**). In addition, one node (*Cystofilobasidium*) was classified as a network hub (supergeneralist) in the PFM network, whereas there were no nodes as supergeneralists in the PP network (**Figure 5B** and **Supplementary Table 4**).

Pearson's correlation coefficient examined the relationships between the relative abundance of keystone taxa and soil properties (**Supplementary Table 5**). *Nitrospira*1 and *Sphingomonas*3 were significantly related to TN, while *Bryobacter*1 and *Cystofilobasidium* were closely correlated to C/N, and *Schizothecium*1 was significantly associated with pH, TN, TP, and AP.

3.4. Direct and indirect effects of soil biotic and abiotic factors on soil ecosystem multifunctionality

The relationships between soil biotic, abiotic factors, and soil ecosystem multifunctionality are shown in **Supplementary Table 6**. The soil ecosystem multifunctionality was strongly positively associated with pH ($r = 0.64$, $P < 0.05$), TN ($r = 0.54$, $P < 0.05$), AN ($r = 0.62$, $P < 0.05$), NAG ($r = 0.66$, $P < 0.01$), SOM ($r = 0.68$, $P < 0.01$), β-GC ($r = 0.57$, $P < 0.05$), *Chaetomiun* ($r = 0.56$, $P < 0.05$), *Schizothecium*1 ($r = 0.53$, $P < 0.05$), N cycle ($r = 0.87$, $P < 0.01$), and C cycle ($r = 0.80$, $P < 0.01$). The structural equation modeling (SEM) also estimated the association between cropping systems, soil chemical properties, microbes abundance (keystone taxa and potentially phytopathogenic microbes), and soil ecosystem multifunctionality (**Figure 6** and **Supplementary Table 7**). The results indicated that the cropping systems had significant and direct positive effects on soil pH ($r = 0.79$, $P < 0.001$) and SOM ($r = 0.58$, $P < 0.01$), and significant and negative effects on potentially phytopathogenic microbes ($r = -0.85$, $P < 0.001$). However, the cropping systems had no direct effects on the keystone taxa and soil ecosystem multifunctionality. We observed that the pH ($r = 0.78$, $P < 0.001$) affected the keystone taxa abundance directly. Also, SOC ($r = 0.66$, $P < 0.001$) and keystone taxa abundance ($r = 0.49$, $P < 0.001$) were positively and closely linked with soil ecosystem multifunctionality, whereas the abundance of potentially phytopathogenic microbes was negatively associated with soil ecosystem multifunctionality ($r = -0.16$, $P = 0.118$).

4. Discussion

4.1. Effect of crop rotation on soil chemical properties and multifunctionality

The long-term continuous monocropping of crops such as potatoes, and soybean can cause severe soil degradation and nutrient imbalance (Liu et al., 2012; Wang et al., 2022). In the current research, as the years of potato continuous cropping increased, soil pH noticeably decreased due to the accumulation of phenolic acids that were beyond the processing capacity of soil microbes (Li et al., 2016; Liu et al., 2020). In addition, the composition of phenolic acids in root exudates or rhizosphere soils differed among different rotation crops (Zhou and Wu, 2018), this may be a possible reason leading to the pH difference between PO and PFM. SOM and TN remarkably increased in PO soil likely resulted due to larger root systems returning more residues to the soil in potato–oat rotation cropping system than in potato continuous cropping. Moreover, the nutrient uptake of different rotation crops and their utilization ability significantly differed. Plants with greater aboveground biomass often require more nutrients for growth than smaller plants. This may be a possible reason leading to the SOM and TN being higher in PO than that in PFM. Wu et al. (2021b) reported that the SOM and TN were higher in the wheat season (SOM 27.94∼30.31 g kg^{-1} and TN 0.92∼1.16 g kg^{-1}) than that in the maize season (SOM 20.00∼24.26 g kg^{-1} and TN 0.89∼1.03 g kg^{-1}). Conversely, the results of soil TP and AP were remarkably lower in crop rotation systems than that in continuous cropping of potatoes. The reason for this result may be due to different requirements of phosphorus among different crops and that the phosphorus requirement in maize and oats is greater than in potatoes.

4.2. Effect of crop rotation on soil microbial community composition

The microbial community structure was markedly affected by rotation cropping based on the PCoA. We found that the communities of bacteria and fungi were predominantly subdivided into two groups, and PP varied from those of PO and PFM. The result indicates that rotation cropping is a major reason for determining the changes in bacterial and fungal community composition (Liu et al., 2020). This is possibly attributed to crop root exudates and residual accumulation differences in a soil environment with different cropping systems because crop root exudates and residues can impact the structure of microbial communities by providing different nutritional substances for microbes. In addition, communities in the soil of the PO and PFM clustered together for bacteria but were separated by the PC2 axis for fungi. This result indicated that different rotation crops affected the fungal community structures. Rotation cropping changed the dominant microbes in comparison with potato continuous cropping. LEfSe analysis suggested that the variation in the bacterial community structure was mainly driven by 26 taxa, among which *Cyanobacteria*, *Gemmatimonadetes*, and *Bacilli* performed a major role in PP, PO, and PFM,

10.3389/fmicb.2023.1034761

TABLE 2 Relative abundance (%) of beneficial and pathogenic microbes in different crop rotation systems.

Taxonomy	PP	PO	PFM	F	*P*
Beneficial microbes					
Bacillus	2.9011 ± 0.0989b	2.9087 ± 0.1194b	3.4885 ± 0.1419a	4.848	0.008
Pseudomonas	0.0306 ± 0.0019b	0.0306 ± 0.0023b	0.0461 ± 0.0024a	12.676	0.001
Schizothecium	0.7587 ± 0.0439c	0.9302 ± 0.1228b	1.4102 ± 0.1218a	12.924	0.001
Chaetomium	2.1264 ± 0.0779c	4.6924 ± 0.1191a	3.6452 ± 0.1547b	104.444	< 0.001
Pathogenic microbes					
Streptomyces scabiei	0.1493 ± 0.0105ab	0.1808 ± 0.0089a	0.1211 ± 0.0058b	7.840	0.008
Verticillium dahliae	0.1941 ± 0.0988a	0.0147 ± 0.0035b	0.0286 ± 0.0109b	7.204	0.009
Alternaria	1.2973 ± 0.0775a	0.6367 ± 0.1258b	0.8080 ± 0.0975b	9.000	0.004
Fusarium	3.1790 ± 0.6834a	1.0360 ± 0.0448b	1.0591 ± 0.0792b	7.647	0.007
Gibberella	4.7892 ± 0.7523a	1.9392 ± 0.1791b	1.5714 ± 0.2114b	11.583	0.002
Plectosphaerella	2.1767 ± 0.3430a	0.2462 ± 0.0310b	0.1654 ± 0.0188b	26.156	< 0.001
Phoma	0.9969 ± 0.1812a	0.0143 ± 0.0076b	0.0116 ± 0.0041b	23.548	< 0.001
Lectera	1.4917 ± 0.1317a	0.5599 ± 0.0549b	0.4197 ± 0.0574b	34.440	< 0.001
Colletotrichum	0.0576 ± 0.0144a	0.0096 ± 0.0043b	0.0238 ± 0.0059b	5.606	0.019

The relative species abundances were calculated as percentages of the total species abundances. Data represent the mean ± *SD* ($n = 5$). The different lowercase letters in the same rows indicate significant differences among treatments at the $P < 0.05$ level (one-way ANOVA). PP, potato continuous cropping; PO, potato–oat rotation; PFM, potato–forage maize rotation.

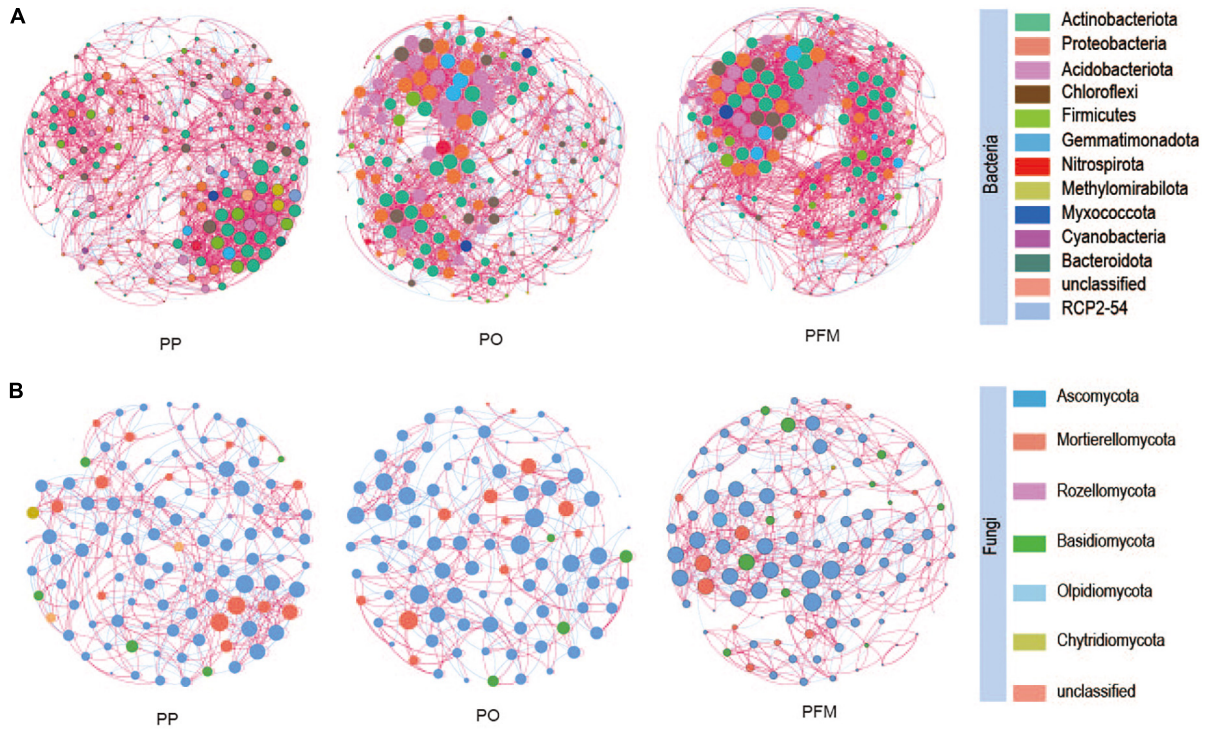

FIGURE 4
Co-occurrence network of soil bacteria **(A)** and fungi **(B)** in soil based on correlation analysis. A connection stands for a strong (Spearman's $r > 0.6$) and significant ($P < 0.05$) correlation. The nodes represent a unique genus. The size of each node is proportional to the degree. The nodes are colored by taxonomy. PP, potato continuous cropping; PO, potato–oat rotation; PFM, potato–forage maize rotation.

respectively. *Gemmatimonadetes* are copiotrophic populations and prefer decomposing labile organic carbon fractions with rich nutrients (Ghosh et al., 2016; Clocchiatti et al., 2020) and then obtained higher abundance in PO soil with greater TN and SOM. In this study, the abundance of *Gemmatimonadetes* showed a significant and positive association with TN (**Supplementary Table 5**). The C/N increased in the soil after the maize straw returned. The *Bacillaceae* family that belongs to the class *Bacilli* had strong resistance to harmful external factors, and the *Bacillus* genus can effectively decompose organic matter, playing an important role in the element cycle in ecosystems (Wu et al., 2021a). In this study, the abundance of *Bacilli* showed a significant and positive association with C/N

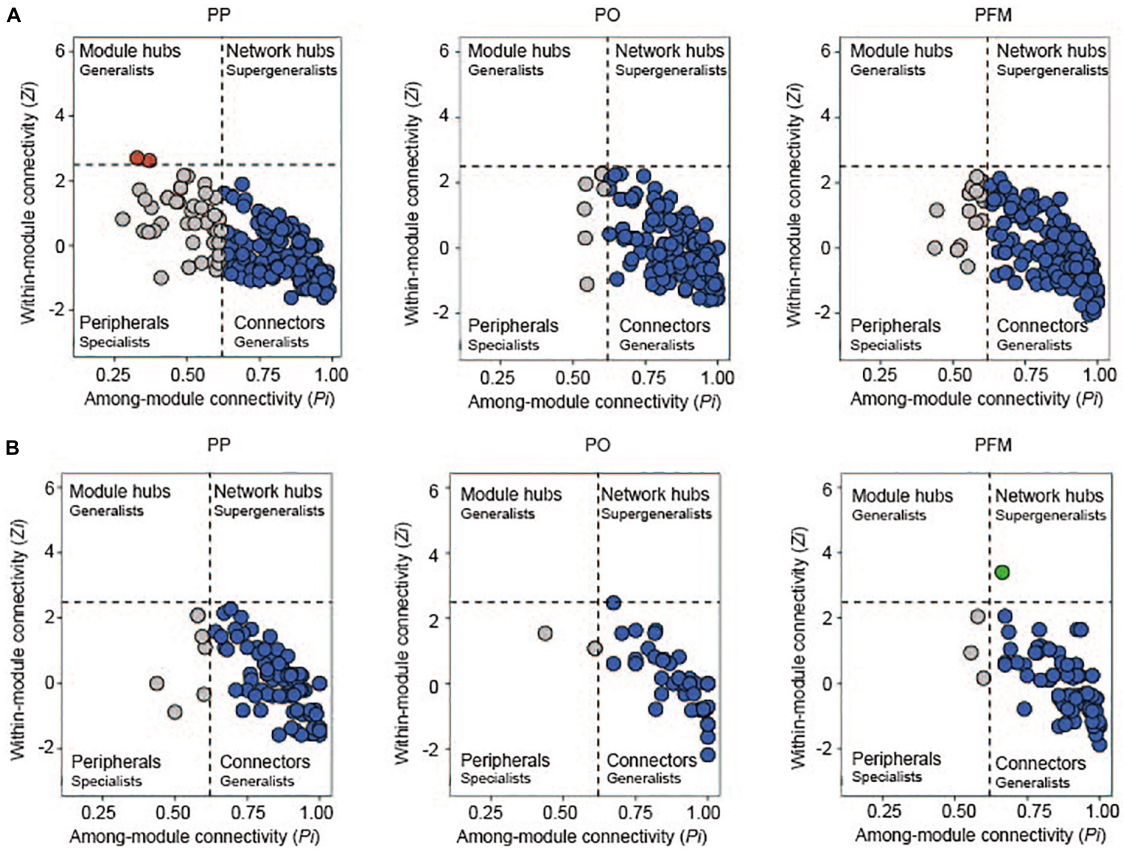

FIGURE 5
Zi–*Pi* plots of bacteria **(A)** and fungi **(B)** based on genus topological roles in bacterial and fungal networks. The threshold values of *Zi* and *Pi* for categorizing genus were 2.5 and 0.62, respectively. PP, potato continuous cropping; PO, potato–oat rotation; PFM, potato–forage maize rotation.

(**Supplementary Table 5**). In addition, the abundance of *Bacillus* and *Pseudomonas* increased in PFM than PP and PO, and some species within *Bacillus* and *Pseudomonas* are antagonistic strains to plant pathogens, allowing potato and banana to suppress common scab and fusarium wilt disease (Lin et al., 2018; Tao et al., 2020). Li et al. (2022) documented that, compared with peanut continuous cropping, rape–peanut–winter wheat–summer maize rotation increased *Bacillus* abundance, which has biological control activities. However, the pathogenic bacteria *Streptomyces scabiei,* which causes potato scab diseases, was slightly decreased in PFM than PP and PO. This result may be associated with the increased abundance of potential plant-beneficial bacteria, which inhibit the growth and sporulation of *Streptomyces scabiei* within PFM. Previous studies reported that both *Pseudomonas fluorescens* and *Bacillus amyloliquefaciens* can inhibit the growth of *Streptomyces scabiei* and reduce the occurrence of potato common scab in potato production (Arseneault et al., 2015; Lin et al., 2018).

With regards to fungi, *Nectriaceae*, *Chaetomium*, and *Basidiomycota,* as the main dominant taxa, performed major roles in PP, PO, and PFM, respectively. *Nectriaceae* contain pathogens that cause the rotting of plant roots (Toju et al., 2018). Species of *Chaetomium* are important agents of cellulose degradation (Wu et al., 2021a); the degradation of oat residues may lead to a higher abundance of *Chaetomium*. *Basidiomycota* contains many saprotrophic soil fungi that are involved in aerobic cellulose degradation (Boer et al., 2005), which may improve soil fertility. In addition, the abundance of *Schizothecium* was significantly higher in PFM than that in PP and PO, *Chaetomium* was significantly higher in PO than that in PP and PFM, and these genera can protect crops and vegetables from diseases (Zhao et al., 2013; Nong et al., 2017). There were significant differences in soil environment among different cropping ecosystems. This could be a reason to explain the fungal community composition differences among different cropping ecosystems. Soil pH and nutrients are important factors affecting fungal community composition (Wang et al., 2022). In this study, the abundance of *Chaetomium*, *Schizothecium*, and *Basidiomycota* showed significant and positive associations with pH and TN, respectively, while significant negative correlations between the abundance of *Nectriaceae* and pH and TN were observed (**Supplementary Table 5**). Other studies demonstrated that the difference in the fungal community composition among different treatments is also caused by the root exudates (e.g., sugars, organic acids, aromatics, and enzymes) of the rotation crops (Lang et al., 2019). Conversely, the abundance of potentially phytopathogenic fungi was significantly enriched in PP. *Alternaria* is a potentially phytopathogenic fungus that causes potato early blight disease, potato brown spot, and soybean black spot, and was significantly richer in PP compared with that in PO and PFM (Wang et al., 2022; Xu et al., 2022). *Fusarium* can infect a wide variety of crops and lead to corresponding diseases, such as potato dry rot disease and potato fusarium wilt (Zhang et al., 2017), which was higher in PP than that in PO and PFM. *Verticillium dahliae* can cause verticillium wilt in the potato during growth (Zhao et al., 2021) and was enriched in PP than PO and PFM.

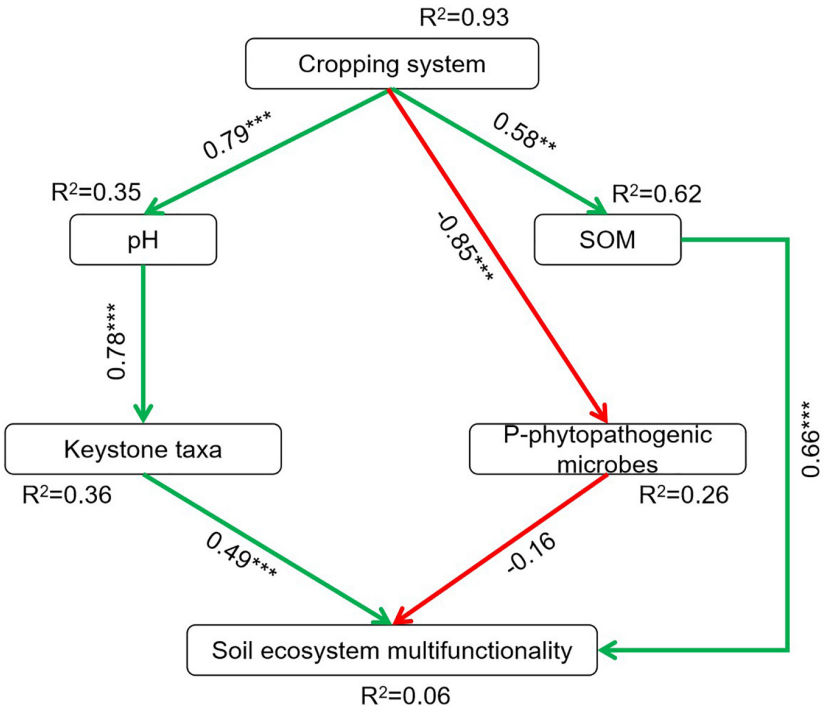

FIGURE 6
Structural equation modeling for the direct and indirect relationships of cropping systems on soil ecosystem multifunctionality. SOC, soil organic carbon. Red and green lines indicate significant negative and positive path coefficients, respectively; $^{**}P < 0.01$, $^{***}P < 0.001$. $\chi^2/df = 1.096$, $P = 0.362$, RMSEA = 0.071. P-phytopathogenic microbes, potentially phytopathogenic microbes.

These results suggested that continuous potato cropping promotes the growth and proliferation of specific pathogenic microbes in the soil, enhances disease infection risk, and disturbs the balance of the microbial community structure, while the rotation cropping of potato and oat (PO) and potato and forage maize (PFM) reduced potentially phytopathogenic microbes but increased potential plant-beneficial microbes. This may be the major reason that rotation cropping increased the yield and decreased the diseases of potatoes than continuous cropping of potatoes (Yao et al., 2020). Variations of soil microbial community composition in response to different cropping systems also revealed that rotation cropping in comparison with continuous cropping of potatoes can maintain soil ecosystem health.

4.3. Effect of crop rotation on co-occurrence network patterns and keystone taxa

Core microbes may represent coevolution with plants, which may be significant for plant health and productivity (Cúcio et al., 2016). In the current study, we further explored the interactions and differences in both bacterial and fungal co-occurrence patterns under different cropping systems by analyzing co-occurrence networks. Network topological properties displayed obvious distinctions in both bacterial and fungal co-occurrence patterns among PP, PO, and PFM. The number of edges for bacterial communities in rotation cropping soils was dramatically greater than those in potato continuous cropping soils. This finding is in line with Liu et al. (2020), who reported that the number of edges increased in the network of maize–soybean rotation than soybean continuous cropping. This result indicated that rotation cropping exhibits a larger network size and recruits more microbes participating in the bacteria–bacteria interactions than those in potato continuous cropping (Karimi et al., 2019). The PO and PFM microbial networks had larger network densities and lower average path lengths than the network of PP. This indicated that, compared with potato continuous cropping, rotation cropping enhanced the bacteria–bacteria interactions in terms of exchanges of nutrients, information, and energy among different communities (Chen et al., 2018; Yan et al., 2021). In addition, the average clustering coefficient and modularity were greater in PO and PFM networks than that in the PP network, indicating that bacteria in rotation cropping soils are more sensitive to the disturbance of external environmental factors and respond more rapidly, and community structure is more prone to change (de Araujo et al., 2019). These findings are in line with Chen et al. (2018), who reported that there were higher connectivity and clustering coefficient in the tobacco–corn rotation network than in tobacco continuous cropping. For the fungal community, changes in the number of edges and network density as well as average path length were consistent with alterations in the bacterial communities. However, the average clustering coefficient and modularity showed contrary changes in the bacterial community. This may be primarily attributed to the slow responses of soil fungi to external environmental change and may have less influence on the whole ecological network of fungi within brief periods (Wu et al., 2021a).

Rotation cropping altered the keystone taxa in both bacterial and fungal co-occurrence networks, which play important roles in the structure of the microbial community. In networks, generalists are beneficial for sustaining the microbial community balance and

are emerging as essential players in enhancing the exchanges of information, materials, and energy among species in networks (Chen et al., 2018; Yan et al., 2021). For bacterial networks, the *Zi–Pi* relationship of every individual genus demonstrated that 95.65 and 89.69% of generalists existed in the networks of PO and PFM, respectively. However, in the PP network, the relative abundance of generalists decreased to 75.77% (74.74% connectors and 1.03% module hubs). For fungal networks, generalists that existed in the networks of PO and PFM were 95.16 and 95.24%, respectively. In addition, 1.19% of supergeneralists existed in the PFM network, whereas the relative abundance of generalists decreased to 93.58% in the PP network. Chen et al. (2018) reported that there were more generalists in the tobacco–corn rotation network than in tobacco continuous cropping. Yang et al. (2021) found that the number of connectors increased under pulse frequency (e.g., pea–pea–pea–wheat) than low-pulse frequency (e.g., pea–wheat–wheat–wheat) in crop rotations. The higher number of generalists under rotation cropping networks indicated that soil microbes were more active within their own modules under continuous cropping, but tended to establish connections with genera located at different modules under crop rotation. These results revealed that rotation cropping enhanced the interactions of soil microbes and altered the roles of some nodes and modified the ecological functions of key microbes in soils in comparison with potato continuous cropping. Thus, the reduction in the number of generalists and supergeneralists after potato continuous cropping could be perceived as a major reason causing the problems associated with continuous cropping in potatoes.

Crop rotation altered the distribution of keystone taxa (**Supplementary Table 4**). Specifically, *Nitrospira*.1 was the node with a maximum degree and was determined as a generalist in the PO and PFM networks, but was determined as a specialist in the PP network. *Nitrospira* plays an important role in nitrogen cycling (Daims et al., 2015; Ochieno et al., 2021). In this study, *Nitrospira*.1 was positively associated with TN (**Supplementary Table 5**). Some nodes that were identified as generalists [*Lysinibacillus* (*Firmicutes*), *Microlunatus*.1 (*Actinobacteriota*), and *Sphingomonas*.3 (*Proteobacteria*)] in the PO and PFM networks but as specialists in the PP network play key roles in the degradation of pesticide and organic pollutants (Li et al., 2007, 2018). Species of *Firmicutes* and *Actinobacteriota* could produce antibacterial and nematocidal compounds to prevent some soil-borne diseases, such as soybean root rot and potato scab (Qi et al., 2010; Sugiyama et al., 2014; Shi et al., 2019). Phyla *Proteobacteria* is a copiotrophic population and prefer decomposing labile organic C fractions with rich nutrients (Ghosh et al., 2016; Clocchiatti et al., 2020). Previous studies demonstrated that the phylum *Actinobacteriota* was the most important keystone member in potato soils (Gu et al., 2022). Chen et al. (2018) reported that microbes belonging to *Firmicutes* and *Proteobacteria* were enriched in the tobacco–corn rotation network. Oberholster et al. (2018) found that members of the *Proteobacteria* are the most prominent keystone taxa in the sunflower–sorghum rotation networks. In this study, *Sphingomonas*.3 belonging to *Proteobacteria* was positively associated with TN (**Supplementary Table 5**). *Bryobacter*.1 was the node with a maximum degree and was classified as a generalist in the PO network, but was classified as a specialist in the PP network. Liu et al. (2020) reported that *Bryobacter aggregates*, which have the ability to decompose organic matter in the soil, were classified as keystone taxa in maize–soybean rotation. In this study, *Bryobacter*.1 was positively associated with C/N (**Supplementary Table 5**). *Micromonospora* (*Actinobacteriota*) and *Schizothecium* (*Ascomycota*) were the nodes with maximum degrees and were classified as generalists in the PFM network, but were classified as specialists in the PP network. In addition, one node [*Cystofilobasidium* (*Basidiomycota*)] was classified as a network hub (supergeneralist) in the PFM network, whereas was not classified as a supergeneralist in the PP network. All those genera are considered beneficial microbes and have been used to control crop diseases in agricultural production (Hirsch and Valdés, 2010; Garat et al., 2010; Liu et al., 2020). This result is contrary to a previous study, which reported that *Actinobacteriota*, *Basidiomycota*, and *Ascomycota* were the most important keystone taxa in soils with potatoes cropping (Hou et al., 2020). This may be related to the difference in soil environment and nutrient resources. Correlation analysis indicated that significant positive associations occur among *Schizothecium*1, pH, and TN (**Supplementary Table 5**), and negative correlations among *Schizothecium*1, TP, AP (**Supplementary Table 5**), *Alternaria*, and other potentially phytopathogenic fungi (**Supplementary Table 8**). In addition, keystone taxa *Cystofilobasidium* exhibited a significantly negative correlation with *Streptomyces scabiei* (**Supplementary Table 8**). Therefore, these keystone functional taxa in PO and PFM may be beneficial for improving soil ecosystem environments and enhancing soil disease-suppression ability after long-term rotation cropping in comparison with continuous cropping of potatoes.

4.4. Factors mediating soil ecosystem multifunctionality under cropping systems

Soil chemical properties not only affected microbial community compositions but also the soil ecosystem multifunctionality. In this study, soil ecosystem multifunctionality was increased in crop rotation than PP, mainly driven by pH, TN, AN, SOM, N cycle, and C cycle. This indicates that higher carbon and nitrogen resource availability favors the growth of microbes, eventually promotes biogeochemical cycles, and enhances ecological functions (Geyer et al., 2016; Han et al., 2021). Also, soil biotic factors affect soil ecosystem multifunctionality. A previous study has demonstrated that microbes play critical roles in supporting ecosystem functioning (Delgado-Baquerizo et al., 2016). In this study, positive links among keystone taxa, potential plant-beneficial microbes, and soil ecosystem multifunctionality are conspicuous. *Schizothecium*1 and *Chaetomium* were positively related to C and N cycling as well as soil ecosystem multifunctionality (**Supplementary Table 6**), and the potential phytopathogenic microbes were negatively associated with C and N cycling as well as soil ecosystem multifunctionality (**Supplementary Table 6**). SEM also suggested that pH and SOC were abiotic factors affecting soil ecosystem multifunctionality (**Figure 6**), and that pH indirectly affected soil ecosystem multifunctionality by mediating keystone taxa, and SOC directly affected soil ecosystem multifunctionality. Soil pH decreased with the increasing years of continuous cropping (Li et al., 2016), which is an important factor significantly influencing soil microbial community composition (Wang et al., 2019), and subsequently affecting soil ecosystem multifunctionality. Rotation crop residues are a source of organic carbon and can increase organic carbon input (Rao et al., 2021), and then promote soil biochemistry processes and ecosystem multifunctionality (Ma et al., 2022).

5. Conclusion

Our experimental findings demonstrated that rotation cropping (PO and PFM) altered soil ecosystem multifunctionality, chemical properties, microbial community compositions, and keystone taxa in comparison with potato continuous cropping. In addition, compared with potato continuous cropping, rotation cropping increased the abundance of potential plant-beneficial bacteria and fungi but reduced potentially phytopathogenic bacteria and fungi, indicating that rotation cropping causes a more healthy microflora, and is beneficial to soil health and sustainable use of soil. Furthermore, co-occurrence networks of bacteria within rotation cropping (PO and PFM) and co-occurrence networks of fungi within PFM were more complex than potato continuous cropping. Keystone taxa were related to bacterial and fungal functional groups that may play underlying roles in the nutrient cycling, toxic material degradation, and prevention and control of soil-borne disease, suggesting that these keystone taxa may play vital roles in improving the soil environment and ecosystem multifunctionality and may make it possible to develop disease-suppressive soils in rotation cropping systems. Collectively, rotation cropping is an effective practice to improve soil ecosystem multifunctionality in agroecosystems and relieve continuous cropping obstacles in comparison with potato continuous cropping, and this study provides a scientific basis for the selection of rotation crops in potato continuous cropping.

Data availability statement

The original contributions presented in this study are included in the article/**Supplementary material**, further inquiries can be directed to the corresponding authors.

Author contributions

J-HZ: conceptualization, funding acquisition, project administration, supervision, and validation. Q-ML: data curation, formal analysis, software, and writing—original draft. Q-ML, J-ZZ, Y-HL, and L-FZ: investigation. J-HZ, Q-ML, and Z-JZ: methodology. DZ, YP, and Z-HY: resources. Q-ML, J-HZ, and J-ZZ: writing—review and editing. All authors contributed to the article and approved the submitted version.

Funding

This work was funded by the Key Research and Development Program of Hebei Province (grant no. 21326515D).

Conflict of interest

The authors declare that the research was conducted in the absence of any commercial or financial relationships that could be construed as a potential conflict of interest.

Publisher's note

All claims expressed in this article are solely those of the authors and do not necessarily represent those of their affiliated organizations, or those of the publisher, the editors and the reviewers. Any product that may be evaluated in this article, or claim that may be made by its manufacturer, is not guaranteed or endorsed by the publisher.

Supplementary material

The Supplementary Material for this article can be found online at: https://www.frontiersin.org/articles/10.3389/fmicb.2023.1034761/full#supplementary-material

References

Al-Mughrabi, K. I., Vikram, A., Poirier, R., Jayasuriya, K., and Moreau, G. (2015). Management of common scab of potato in the field using biopesticides, fungicides, soil additives, or soil fumigants. *Biocontrol Science and Technology* 26, 125–135. doi: 10.1080/09583157.2015.1079809

Arseneault, T., Goyer, C., and Filion, M. (2015). *Pseudomonas* fluorescens LBUM223 increases potato yield and reduces common scab symptoms in the field. *Phytopathology* 105, 1311–1317. doi: 10.1094/PHYTO-12-14-0358-R

Ashworth, A., Owens, P., and Allen, F. (2020). Long-term cropping systems management influences soil strength and nutrient cycling. *Geoderma* 361, 114062. doi: 10.1016/j.geoderma.2019.114062

Banerjee, S., Baah-Acheamfour, M., Carlyle, C. N., Bissett, A., Richardson, A. E., Siddique, T., et al. (2016a). Determinants of bacterial communities in C anadian agroforestry systems. *Environmental Microbiology* 18, 1805–1816. doi: 10.1111/1462-2920.12986

Banerjee, S., Kirkby, C. A., Schmutter, D., Bissett, A., Kirkegaard, J. A., and Richardson, A. E. (2016b). Network analysis reveals functional redundancy and keystone taxa amongst bacterial and fungal communities during organic matter decomposition in an arable soil. *Soil Biology and Biochemistry* 97, 188–198. doi: 10.1016/j.soilbio.2016.03.017

Banerjee, S., Schlaeppi, K., and van der Heijden, M. G. (2018). Keystone taxa as drivers of microbiome structure and functioning. *Nat Rev Microbiol* 16, 567–576. doi: 10.1038/s41579-018-0024-1

Bao, S. (2000). *Soil agro-chemistries analysis*. Beijing: Agricultural Press.

Bardgett, R. D., and van der Putten, W. H. (2014). Belowground biodiversity and ecosystem functioning. *Nature* 515, 505–511. doi: 10.1038/nature13855

Boer, W. D., Folman, L. B., Summerbell, R. C., and Boddy, L. (2005). Living in a fungal world: impact of fungi on soil bacterial niche development. *FEMS microbiology reviews* 29, 795–811. doi: 10.1016/j.femsre.2004.11.005

Callahan, B. J., McMurdie, P. J., Rosen, M. J., Han, A. W., Johnson, A. J. A., and Holmes, S. P. (2016). DADA2: High-resolution sample inference from Illumina amplicon data. *Nat. Methods* 13, 581–583. doi: 10.1038/nmeth.3869

Cannon, P., Buddie, A., Bridge, P., de Neergaard, E., Lübeck, M., and Askar, M. (2012). Lectera, a new genus of the Plectosphaerellaceae for the legume pathogen Volutella colletotrichoides. *MycoKeys* 3, 23–36. doi: 10.3897/mycokeys.3.3065

Chen, S., Qi, G., Luo, T., Zhang, H., Jiang, Q., Wang, R., et al. (2018). Continuous-cropping tobacco caused variance of chemical properties and structure of bacterial network in soils. *Land Degrad Dev* 29, 4106–4120. doi: 10.1002/ldr.3167

Clocchiatti, A., Hannula, S. E., van den Berg, M., Korthals, G., and De Boer, W. (2020). The hidden potential of saprotrophic fungi in arable soil: Patterns of short-term stimulation by organic amendments. *Applied Soil Ecology* 147, 103434. doi: 10.1016/j.apsoil.2019.103434

Cúcio, C., Engelen, A. H., Costa, R., and Muyzer, G. (2016). Rhizosphere microbiomes of European seagrasses are selected by the plant, but are not species specific. *Front Microbiol* 7:440. doi: 10.3389/fmicb.2016.00440

Cuevas-Fernández, F. B., Robledo-Briones, A. M., Baroncelli, R., Trkulja, V., Thon, M. R., Buhinicek, I., et al. (2022). First report of Colletotrichum graminicola causing maize anthracnose in Bosnia and Herzegovina. *Plant Disease* 103, 3281. doi: 10.1094/PDIS-06-19-1224-PDN

Daims, H., Lebedeva, E. V., Pjevac, P., Han, P., Herbold, C., Albertsen, M., et al. (2015). Complete nitrification by Nitrospira bacteria. *Nature* 528, 504–509. doi: 10.1038/nature16461

de Araujo, A. S. F., Miranda, A. R. L., Sousa, R. S., Mendes, L. W., Antunes, J. E. L., de Souza Oliveira, L. M., et al. (2019). Bacterial community associated with rhizosphere of maize and cowpea in a subsequent cultivation. *Appl Soil Ecol* 143, 26–34. doi: 10.1016/j.apsoil.2019.05.019

Delgado-Baquerizo, M., Maestre, F. T., Reich, P. B., Jeffries, T. C., Gaitan, J. J., Encinar, D., et al. (2016). Microbial diversity drives multifunctionality in terrestrial ecosystems. *Nature Communications* 2016, 7. doi: 10.1038/ncomms10541

Dias, T., Dukes, A., and Antunes, P. M. (2015). Accounting for soil biotic effects on soil health and crop productivity in the design of crop rotations. *J. Sci. Food Agric.* 95, 447–454. doi: 10.1002/jsfa.6565

Edgar, R. C. (2013). UPARSE: highly accurate OTU sequences from microbial amplicon reads. *Nat Methods* 10, 996–998. doi: 10.1038/nmeth.2604

Garat, M., de Aurrecoechea, I., Wisniewski, M., Vero, S., and Garmendia, G. (2010). Cystofilobasidium infirmominiatum as a biocontrol agent of postharvest diseases on apples and citrus. *International Symposium on Biological Control of Postharvest Diseases: Challenges and Opportunities* 905, 169–180. doi: 10.17660/ActaHortic.2011.905.18

Geyer, K. M., Kyker-Snowman, E., Grandy, A. S., and Frey, S. D. (2016). Microbial carbon use efficiency: accounting for population, community, and ecosystem-scale controls over the fate of metabolized organic matter. *Biogeochemistry* 127, 173–188. doi: 10.1007/s10533-016-0191-y

Ghosh, A., Bhattacharyya, R., Dwivedi, B., Meena, M., Agarwal, B., Mahapatra, P., et al. (2016). Temperature sensitivity of soil organic carbon decomposition as affected by long-term fertilization under a soybean based cropping system in a sub-tropical Alfisol. *Agriculture, Ecosystems & Environment* 233, 202–213. doi: 10.1016/j.agee.2016.09.010

Gu, S., Xiong, X., Tan, L., Deng, Y., Du, X., Yang, X., et al. (2022). Soil microbial community assembly and stability are associated with potato (Solanum tuberosum L.) fitness under continuous cropping regime. *Frontiers in Plant Science* 13:1000045. doi: 10.3389/fpls.2022.1000045

Guo, Y., Luo, H., Wang, L., Xu, M., Wan, Y., Chou, M., et al. (2021). Multifunctionality and microbial communities in agricultural soils regulate the dynamics of a soil-borne pathogen. *Plant Soil* 461, 309–322. doi: 10.1007/s11104-020-04826-4

Gustavsen, G. W. (2021). Sustainability and potato consumption. *Potato Res.* 64, 571–586. doi: 10.1007/s11540-021-09493-1

Han, H., Hwang, J., and Kim, G. (2021). Characterizing the origins of dissolved organic carbon in coastal seawater using stable carbon isotope and light absorption characteristics. *Biogeosciences* 18, 1793–1801. doi: 10.5194/bg-18-1793-2021

Han, Z., Xu, P., Li, Z., Lin, H., Zhu, C., Wang, J., et al. (2022). Microbial diversity and the abundance of keystone species drive the response of soil multifunctionality to organic substitution and biochar amendment in a tea plantation. *GCB Bioenergy* 14, 481–495. doi: 10.1111/gcbb.12926

Hiltunen, L. H., Tarvainen, O., Kelloniemi, J., Tanskanen, J., Karhu, J., and Valkonen, J. P. T. (2021). Soil bacterial community in potato tuberosphere following repeated applications of a common scab suppressive antagonist. *Applied Soil Ecology* 2021, 167. doi: 10.1016/j.apsoil.2021.104096

Hirsch, A. M., and Valdés, M. (2010). Micromonospora: an important microbe for biomedicine and potentially for biocontrol and biofuels. *Soil Biol Biochem* 42, 536–542. doi: 10.1016/j.soilbio.2009.11.023

Hou, Q., Wang, W., Yang, Y., Hu, J., Bian, C., Jin, L., et al. (2020). Rhizosphere microbial diversity and community dynamics during potato cultivation. *European Journal of Soil Biology* 98, 103176. doi: 10.1016/j.ejsobi.2020.103176

Jiang, J., Song, Z., Yang, X., Mao, Z., Nie, X., Guo, H., et al. (2017). Microbial community analysis of apple rhizosphere around Bohai Gulf. *Sci Rep-Uk* 7, 1–9. doi: 10.1038/s41598-017-08398-9

Karimi, B., Dequiedt, S., Terrat, S., Jolivet, C., Arrouays, D., Wincker, P., et al. (2019). Biogeography of soil bacterial networks along a gradient of cropping intensity. *Sci Rep-Uk* 9, 1–10. doi: 10.1038/s41598-019-40422-y

Kerfahi, D., Tripathi, B. M., Dong, K., Go, R., and Adams, J. M. (2016). Rainforest conversion to rubber plantation may not result in lower soil diversity of bacteria, fungi, and Nematodes. *Microbial Ecology* 72, 359–371. doi: 10.1007/s00248-016-0790-0

Lang, M., Bei, S., Li, X., Kuyper, T. W., and Zhang, J. (2019). Rhizoplane bacteria and plant species co-determine phosphorus-mediated microbial legacy effect. *Frontiers in microbiology* 10:2856. doi: 10.3389/fmicb.2019.02856

Larkin, R. P., and Halloran, J. M. (2014). Management effects of disease-suppressive rotation crops on potato yield and soilborne disease and their economic implications in potato production. *Am J Potato Res* 91, 429–439. doi: 10.1007/s12230-014-9366-z

Li, H., Li, C., Song, X., Liu, Y., Gao, Q., Zheng, R., et al. (2022). Impacts of continuous and rotational cropping practices on soil chemical properties and microbial communities during peanut cultivation. *Scientific reports* 12, 1–12. doi: 10.1038/s41598-022-06789-1

Li, J., Luo, C., Zhang, D., Song, M., Cai, X., Jiang, L., et al. (2018). Autochthonous bioaugmentation-modified bacterial diversity of phenanthrene degraders in PAH-contaminated wastewater as revealed by DNA-stable isotope probing. *Environ Sci Technol* 52, 2934–2944. doi: 10.1021/acs.est.7b05646

Li, X., Jia, K., He, J., and Li, S. (2007). Isolation and identification of chlorpyrifos degrading strain Sphingomonas sp. Dsp-2 and its chlorpyrifos degradation characteristics. *Acta Pedologica Sinica* 44, 734–739.

Li, X., Lewis, E. E., Liu, Q., Li, H., Bai, C., and Wang, Y. (2016). Effects of long-term continuous cropping on soil nematode community and soil condition associated with replant problem in strawberry habitat. *Sci Rep* 6, 30466. doi: 10.1038/srep30466

Lin, C., Tsai, C.-H., Chen, P.-Y., Wu, C.-Y., Chang, Y.-L., Yang, Y.-L., et al. (2018). Biological control of potato common scab by Bacillus amyloliquefaciens Ba01. *PLoS One* 13:e0196520. doi: 10.1371/journal.pone.0196520

Ling, N., Zhu, C., Xue, C., Chen, H., Duan, Y., Peng, C., et al. (2016). Insight into how organic amendments can shape the soil microbiome in long-term field experiments as revealed by network analysis. *Soil Biol Biochem* 99, 137–149. doi: 10.1016/j.soilbio.2016.05.005

Liu, H., Pan, F., Han, X., Song, F., Zhang, Z., Yan, J., et al. (2019). Response of soil fungal community structure to long-term continuous soybean cropping. *Front Microbiol* 9:3316. doi: 10.3389/fmicb.2018.03316

Liu, X., Li, Y., Han, B., Zhang, Q., Zhou, K., Zhang, X., et al. (2012). Yield response of continuous soybean to one-season crop disturbance in a previous continuous soybean field in Northeast China. *Field Crops Research* 138, 52–56. doi: 10.1016/j.fcr.2012.09.012

Liu, X., Liu, H., Ren, D., Liu, C., Zhang, Y., Wang, S., et al. (2022). Interlinkages between soil properties and keystone taxa under different tillage practices on the North China Plain. *Applied Soil Ecology* 178, 104551. doi: 10.1016/j.apsoil.2022.104551

Liu, Z., Liu, J., Yu, Z., Yao, Q., Li, Y., Liang, A., et al. (2020). Long-term continuous cropping of soybean is comparable to crop rotation in mediating microbial abundance, diversity and community composition. *Soil Till Res* 197, 104503. doi: 10.1016/j.still.2019.104503

Ma, H., Zhou, J., Ge, J., Nie, J., Zhao, J., Xue, Z., et al. (2022). Intercropping improves soil ecosystem multifunctionality through enhanced available nutrients but depends on regional factors. *Plant and Soil* 2022, 1–14. doi: 10.1007/s11104-022-05554-7

Nong, Q., Zhang, W., Lan, T., Su, Q., Chen, Y., Zhang, Y., et al. (2017). Screening and identification of dark septate Endophytestrain L-14 and its mechanism of banana fusarium Wilt disease resistance. *Chinese J Tropical Crops* 38, 559–564.

Oberholster, T., Vikram, S., Cowan, D., and Valverde, A. (2018). Key microbial taxa in the rhizosphere of sorghum and sunflower grown in crop rotation. *Science of the total environment* 624, 530–539. doi: 10.1016/j.scitotenv.2017.12.170

Ochieno, D. M., Karoney, E. M., Muge, E. K., Nyaboga, E. N., Baraza, D. L., Shibairo, S. I., et al. (2021). Rhizobium-linked nutritional and phytochemical changes under multitrophic functional contexts in Sustainable Food Systems. *Front Sustain Food Syst* 4:604396. doi: 10.3389/fsufs.2020.604396

Qi, G., Zhu, F., Du, P., Yang, X., Qiu, D., Yu, Z., et al. (2010). Lipopeptide induces apoptosis in fungal cells by a mitochondria-dependent pathway. *Peptides* 31, 1978–1986. doi: 10.1016/j.peptides.2010.08.003

Qin, S. H., Yeboah, S., Cao, L., Zhang, J. L., Shi, S. L., and Liu, Y. H. (2017). Breaking continuous potato cropping with legumes improves soil microbial communities, enzyme activities and tuber yield. *Plos One* 12:e0175934. doi: 10.1371/journal.pone.0175934

Rao, D., Meng, F., Yan, X., Zhang, M., Yao, X., Kim, K. S., et al. (2021). Changes in soil microbial activity, bacterial community composition and function in a long-term continuous soybean cropping system after corn insertion and fertilization. *Front. Microbiol.* 12:638326. doi: 10.3389/fmicb.2021.638326

Ryan, M. R., Crews, T. E., Culman, S. W., DeHaan, L. R., Hayes, R. C., Jungers, J. M., et al. (2018). Managing for multifunctionality in perennial grain crops. *Bioscience* 68, 294–304. doi: 10.1093/biosci/biy014

Shi, W. C., Li, M. C., Wei, G. S., Tian, R. M., Li, C. P., Wang, B., et al. (2019). The occurrence of potato common scab correlates with the community composition and function of the geocaulosphere soil microbiome. *Microbiome* 7:14. doi: 10.1186/s40168-019-0629-2

Sinsabaugh, R. L., Lauber, C. L., Weintraub, M. N., Ahmed, B., Allison, S. D., Crenshaw, C., et al. (2008). Stoichiometry of soil enzyme activity at global scale. *Ecology letters* 11, 1252–1264. doi: 10.1111/j.1461-0248.2008.01245.x

Sugiyama, A., Ueda, Y., Zushi, T., Takase, H., Yazaki, K. (2014). Changes in the bacterial community of soybean rhizospheres during growth in the field. *Plos One* 9:e100709. doi: 10.1371/journal.pone.0100709

Tan, H., Li, Q., Zhang, H., Wu, C., Zhao, S., Deng, X., et al. (2020). Pesticide residues in agricultural topsoil from the Hainan tropical riverside basin: Determination, distribution, and relationships with planting patterns and surface water. *Science of the Total Environment* 722, 137856. doi: 10.1016/j.scitotenv.2020.137856

Tao, C., Li, R., Xiong, W., Shen, Z., Liu, S., Wang, B., et al. (2020). Bio-organic fertilizers stimulate indigenous soil *Pseudomonas* populations to enhance plant disease suppression. *Microbiome* 8, 137. doi: 10.1186/s40168-020-00892-z

Toju, H., Tanabe, A. S., and Sato, H. (2018). Network hubs in root-associated fungal metacommunities. *Microbiome* 6, 1–16. doi: 10.1186/s40168-018-0497-1

Vick-Majors, T. J., Priscu, J. C., and Amaral-Zettler, L. (2014). Modular community structure suggests metabolic plasticity during the transition to polar night in ice-covered Antarctic lakes. *The ISME journal* 8, 778–789. doi: 10.1038/ismej.2013.190

Wang, B., Wang, Y., Cui, X., Zhang, Y., and Yu, Z. (2019). Bioconversion of coal to methane by microbial communities from soil and from an opencast mine in the Xilingol grassland of northeast China. *Biotechnology for biofuels* 12, 1–15. doi: 10.1186/s13068-019-1572-y

Wang, Q., Garrity, G. M., Tiedje, J. M., and Cole, J. R. (2007). Naive Bayesian classifier for rapid assignment of rRNA sequences into the new bacterial taxonomy. *Appl Environ Microbiol* 73, 5261–5267. doi: 10.1128/AEM.00062-07

Wang, Q., Wang, C., Yu, W., Ali, T., Chen, D., Huang, Y., et al. (2018). Effects of nitrogen and phosphorus inputs on soil bacterial abundance, diversity, and community composition in Chinese fir plantations. *Frontiers in Microbiology* 9:1543. doi: 10.3389/fmicb.2018.01543

Wang, X., Duan, Y., Zhang, J., Ciampitti, I. A., Cui, J., Qiu, S., et al. (2022). Response of potato yield, soil chemical and microbial properties to different rotation sequences of green manure-potato cropping in North China. *Soil Till Res* 217, 105273. doi: 10.1016/j.still.2021.105273

Wei, W., Yang, M., Liu, Y., Huang, H., Ye, C., Zheng, J., et al. (2018). Fertilizer N application rate impacts plant-soil feedback in a sanqi production system. *Sci Total Environ* 633, 796–807. doi: 10.1016/j.scitotenv.2018.03.219

Wu, X., Hu, H., Wang, R., Zhao, J., Yang, D., Wang, L., et al. (2021a). Effects of reduction of chemical fertilizer and substitution coupled with organic manureon the molecular ecological network of microbial communities in fluvo-aquic soil. *Acta Pedologica Sinica* 59, 545–556.

Wu, X., Zhang, T., Zhao, J., Wang, L., Yang, D., Li, G., et al. (2021b). Variation of soil bacterial and fungal communities from fluvo-aquic soil under chemical fertilizer reduction combined with organic materials in North China Plain. *Journal of Soil Science and Plant Nutrition* 21, 349–363. doi: 10.1007/s42729-020-00365-0

Wunsch, M. J., and Bergstrom, G. C. (2011). Genetic and morphological evidence that Phoma sclerotioides, causal agent of brown root rot of alfalfa, is composed of a species complex. *Phytopathology* 101, 594–610. doi: 10.1094/PHYTO-04-10-0107

Xu, J., Xu, X., Wang, L., Jiang, Y., Zhang, W., and Cao, Y. (2014). Biological characteristics of tomato wilt fungus. *Journal of Shenyang Aricultural University* 6, 673–678.

Xu, X., Zhang, L., Yang, X., Cao, H., Li, J., Cao, P., et al. (2022). Alternaria spp. associated with leaf blight of maize in Heilongjiang Province. *China. Plant Dis* 106, 572–584. doi: 10.1094/PDIS-06-21-1151-RE

Yan, L., Zhang, W., Duan, W., Zhang, Y., Zheng, W., and Lai, X. (2021). Temporal bacterial community diversity in the nicotiana tabacum rhizosphere over years of continuous monocropping. *Front Microbiol* 12:1276. doi: 10.3389/fmicb.2021.641643

Yan, Z., Hao, Z., Wu, H., Jiang, H., Yang, M., and Wang, C. (2019). Co-occurrence patterns of the microbial community in polycyclic aromatic hydrocarbon-contaminated riverine sediments. *Journal of hazardous materials* 367, 99–108. doi: 10.1016/j.jhazmat.2018.12.071

Yang, T., Evans, B., and Bainard, L. D. (2021). Pulse frequency in crop rotations alters soil microbial community networks and the relative abundance of fungal plant pathogens. *Frontiers in microbiology* 12:667394. doi: 10.3389/fmicb.2021.667394

Yao, Z., Zhang, J., Du, Y., Liu, Y., and Zhang, L. (2020). Productivity evaluation of crop rotation in cold and arid region of Northern China. *Acta Agronomica Sinica* 16, 32–34.

Zhang, K., Wang, X., Sun, J., Yang, Q., and Sun, H. (2017). Identification of potato rot disease inner ventilation bank of Huade County, Mongilia during storage period. *J Anhui Sci* 45, 147–151.

Zhao, L., Liu, X., Zhang, B., Zhang, Y., Li, C., and Qi, J. (2013). "A biocontrol strain isolation, identification and antimicrobial activity," in *Proceedings of the Chinese Society for Plant Protection*.

Zhao, W., Guo, Q., Su, Z., Wang, P., Dong, L., Hu, Q., et al. (2021). Characterization of fungal community structure in the rhizosphere soil of healthy and diseased-Verticillium Wilt potato plants and carbon source utilization. *Scientia Agricultura Sinica* 54, 296–309.

Zheng, Q., Hu, Y., Zhang, S., Noll, L., Böckle, T., Dietrich, M., et al. (2019). Soil multifunctionality is affected by the soil environment and by microbial community composition and diversity. *Soil Biology and Biochemistry* 136, 107521. doi: 10.1016/j.soilbio.2019.107521

Zhou, H., Peng, Y., Li, T., Xie, Y., Tang, L., Wang, R., et al. (2019). Effects of potato continuous cropping on soil physicochemical and biological properties. *J. Hunan Agric. Univ.* 45, 611–616.

Zhou, X., and Wu, F. (2018). Vanillic acid changed cucumber (Cucumis sativus L.) seedling rhizosphere total bacterial, *Pseudomonas* and Bacillus spp. communities. *Sci Rep* 8, 1–11. doi: 10.1038/s41598-018-23406-2

frontiers | Frontiers in Microbiology

TYPE Original Research
PUBLISHED 16 March 2023
DOI 10.3389/fmicb.2023.1141585

OPEN ACCESS

EDITED BY
Jesús Navas-Castillo,
IHSM La Mayora, CSIC, Spain

REVIEWED BY
Haoqing Zhang,
Ningbo University, China
Shengen Liu,
Institute of Applied Ecology (CAS), China

*CORRESPONDENCE
Pengfa Li
✉ pfli@njau.edu.cn
Jiandong Jiang
✉ jiang_jjd@njau.edu.cn

SPECIALTY SECTION
This article was submitted to Microbe and Virus Interactions with Plants, a section of the journal Frontiers in Microbiology

RECEIVED 10 January 2023
ACCEPTED 20 February 2023
PUBLISHED 16 March 2023

CITATION
Kuang L, Li T, Wang B, Peng J, Li J, Li P and Jiang J (2023) Diseased-induced multifaceted variations in community assembly and functions of plant-associated microbiomes. *Front. Microbiol.* 14:1141585. doi: 10.3389/fmicb.2023.1141585

Diseased-induced multifaceted variations in community assembly and functions of plant-associated microbiomes

Lu Kuang[1], Ting Li[1], Baozhan Wang[1], Junwei Peng[2], Jiangang Li[2], Pengfa Li[1]* and Jiandong Jiang[1]*

[1]Key Lab of Microbiology for Agricultural Environment, Ministry of Agriculture, College of Life Sciences, Nanjing Agricultural University, Nanjing, China, [2]State Key Laboratory of Soil and Sustainable Agriculture, Institute of Soil Science, Chinese Academy of Sciences, Nanjing, China

Plant-associated microorganisms are believed to be part of the so-called extended plant phenotypes, affecting plant growth and health. Understanding how plant-associated microorganisms respond to pathogen invasion is crucial to controlling plant diseases through microbiome manipulation. In this study, healthy and diseased (bacterial wilt disease, BWD) tomato (*Solanum lycopersicum* L.) plants were harvested, and variations in the rhizosphere and root endosphere microbial communities were subsequently investigated using amplicon and shotgun metagenome sequencing. BWD led to a significant increase in rhizosphere bacterial diversity in the rhizosphere but reduced bacterial diversity in the root endosphere. The ecological null model indicated that BWD enhanced the bacterial deterministic processes in both the rhizosphere and root endosphere. Network analysis showed that microbial co-occurrence complexity was increased in BWD-infected plants. Moreover, higher universal ecological dynamics of microbial communities were observed in the diseased rhizosphere. Metagenomic analysis revealed the enrichment of more functional gene pathways in the infected rhizosphere. More importantly, when tomato plants were infected with BWD, some plant-harmful pathways such as quorum sensing were significantly enriched, while some plant-beneficial pathways such as streptomycin biosynthesis were depleted. These findings broaden the understanding of plant–microbiome interactions and provide new clues to the underlying mechanism behind the interaction between the plant microbiome and BWD.

KEYWORDS

plant microbiome, bacterial wilt disease, assembly mechanism, microbial interactions, microbiome function

Introduction

Plant-associated microorganisms play a major role in affecting plant growth and health (Muller et al., 2016; Theis et al., 2016; Singh et al., 2020; Woodhams et al., 2020). The rhizosphere, a hot spot for plants to exchange substances and energy with the surrounding environment, has drawn the most attention (Li et al., 2020; Li P. et al., 2022). There is an emerging consensus about the dominant role of the rhizosphere microbiome in influencing host performance, especially regarding resistance to disease (Berendsen et al., 2012; Li X. et al., 2019); for example, disrupting the balance between the abundances of *Firmicutes* and *Actinobacteria* in the tomato rhizosphere causes increased incidence of bacterial wilt disease (BWD; Lee et al., 2021). Understanding how the rhizosphere microbiome responds to disease

incidence is fundamental to understanding the microbiome pathways that improve plant health, potentially allowing the favorable manipulation of the microbiome.

Multiple biotic and abiotic factors contribute to plant microbiome assemblies, such as host genotype, plant growth stage, local climates, regional microbial species pool, soil type, and field management strategies (Berendsen et al., 2012; Gao et al., 2020). Apart from these factors, changes in plant performance caused by a pathogen invasion are considered to be some of the most important forces driving microbiome assembly (Carrion et al., 2019). Species composition and community diversity can be greatly influenced by pathogen invasion (Gao et al., 2021); more plant-beneficial microorganisms, especially those that can antagonize phytopathogens, are enriched in diseased plant organs (Gao et al., 2021), and the alpha diversity of the rhizosphere microbiome significantly declined after pathogen invasion (Li et al., 2021). Our knowledge of whether pathogen invasion also affects other aspects of the plant microbiome, such as microbial interactions, community assembly, and metabolic functions, is limited.

In metacommunity ecology, niche and neutral mechanisms are two divergent, but complementary, paradigms that describe the assemblages of the metacommunity (Zhou and Ning, 2017). The niche theory posits that deterministic processes such as competition, facilitation, predation, resource differentiation, and other environmental filters determine community assembly by causing niche differentiation (Dini-Andreote et al., 2015). The neutral theory hypothesizes that stochastic processes such as colonization, dispersal, priority effects, and ecological drift regulate the assembly and functioning of ecological communities (Dini-Andreote et al., 2015). Disease-induced changes in plant performance lead to cascading variations in the rhizosphere environment that greatly influence the deterministic-stochastic balance of the rhizosphere microbiome (Wen et al., 2022; Zhang et al., 2022). Although this is obviously known, it has been rarely tested and examined in detail. It can be hypothesized that pathogen invasion, as a selection pressure acting upon the rhizosphere microbiome by changing plant performance, would deterministically drive the compositional variation of the rhizosphere microbiome. Pathogen invasion is commonly seen alongside changes in rhizosphere microbial diversity (Wei et al., 2018; Yuan et al., 2018; Shi et al., 2019). It can therefore be concluded that pathogen invasion would affect microbial interactions that depend on the types and abundances of microorganisms present (Weiland-Brauer, 2021). In addition, the dynamic universality (whether interactions among microbes and with their environment are consistent across hosts or whether each individual's microbiota follows its own rules) of the plant root's bacterial microbiome is also yet to be assessed (Bashan et al., 2016). These knowledge gaps limited the effective management of soil and plant health through strategies exploiting the plant-associated microbiome. Furthermore, while the community functions of natural microbial communities are always redundant (Louca et al., 2018; Li P. et al., 2019), pathogen invasion would change the functions in rhizosphere microbes, as community function and assembly are tightly coupled (Xun et al., 2019; Luan et al., 2020).

Ralstonia solanacearum is one of the most economically important phytopathogens since the lethal BWD it causes can lead to devastating impacts on many plant species. Tomato (*Solanum lycopersicum* L.) is one of the most widely grown vegetable crops (Fibiani et al., 2022). BWD in tomatoes caused by *R. solanacearum* leads to high annual production losses. A deep understanding of how the plant-associated microbiome responds to BWD may help in the development of environmental-friendly BWD control strategies. In this study, the plant-associated microbiome was investigated using sequencing to determine the differences in the communities of healthy and diseased tomato plants. Plants were harvested and their rhizosphere and root endosphere microbial communities were investigated, examining how plant-associated microbiome assembly, interactions in the plant-associated microbiome, and the functional potentials of plant-associated microbes are affected by pathogen invasion (Figure 1).

Materials and methods

Collection of soil and plant samples

Sampling was performed on 15 September 2021 at plastic greenhouses with tomatoes growing for six contiguous seasons, located in Hengxi Town, Nanjing city, Jiangsu province, China (118°46'E, 31°43'N). The sample site has a typical subtropical monsoon climate with a mean annual precipitation of 1,106 mm and a mean annual temperature of 15.5°C. The typical soil is udic argosol. The cultivars ("Hezuo 908") were infected by the pathogen *R. solanacearum* naturally and randomly. Twelve tomato plants that showed bacterial wilt symptoms (75–100% of leaves wilted or dead) were collected from four plastic greenhouses, and 12 non-infected plants were harvested as controls (Figure 1). Three healthy and three diseased plants were taken from each greenhouse at the setting stage, ensuring the chosen healthy plants were not spatially close to the diseased ones. Rhizosphere soil samples from healthy (RH) and diseased plants (RD) were gently collected; after uprooting the plants, excess soil was first gently shaken from the roots, and then the remaining soil attached to the roots was considered rhizosphere soil (Kibbey and Strevett, 2019). Root tissues of healthy (EH) and diseased plants (ED) were collected to investigate the microbial communities in the root endosphere (Figure 1).

DNA extraction

Total genomic DNA was extracted from both the rhizosphere soil (0.5 g fresh soil from each sample) and the root tissue (1 g fresh plant tissue from each sample) samples using the FastDNA SPIN Kit for Soil (MP Biomedicals, Solon, OH, USA) following the manufacturer's instructions, except for modifications to homogenization when extracting DNA from the endosphere. Before extracting, the surface of the root tissues was sterilized. First, soil on the root surface was removed by rinsing it with water. After this, the tissues were cut into 0.5 cm sections and submerged in 70% ethanol for 5 min, 6% sodium hypochlorite for 3 min, 70% ethanol for 30 s and then washed with sterile H_2O five times (Ruiz-Perez et al., 2016). Liquid nitrogen grinding was done in a sterile mortar and pestle for root tissue homogenization.

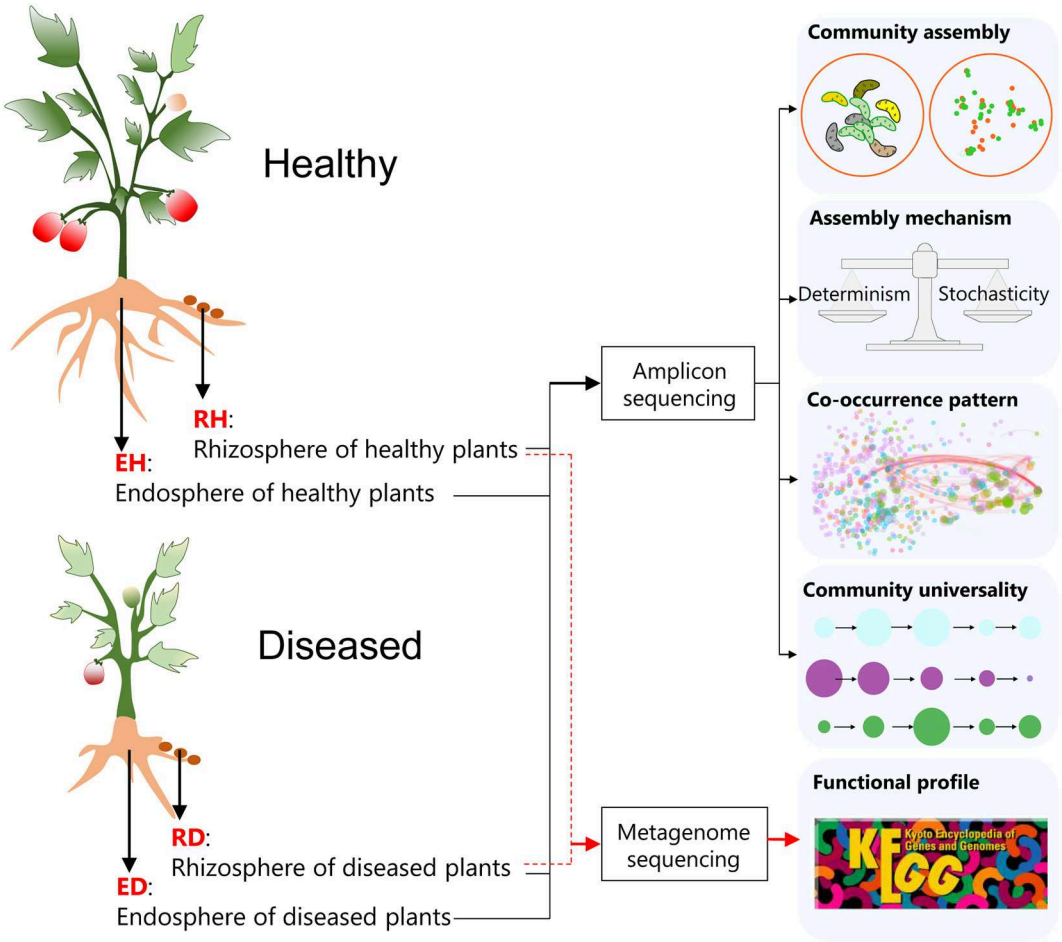

FIGURE 1
A flow diagram of the key experimental settings in the current study. Healthy and diseased (bacterial wilt disease, BWD) tomato (*Solanum Lycopersicum* L.) plants were harvested, and the variations in the rhizosphere and root endosphere microbial communities were subsequently investigated using amplicon sequencing and shotgun metagenome sequencing. RH, rhizosphere of healthy plants; RD, rhizosphere of diseased plants; EH, endosphere of healthy plants; ED, endosphere of diseased plants.

DNA quality and concentration were measured using gel electrophoresis (0.8% agarose gel) and the Qubit dsDNA HS Assay Kit (Thermo Scientific, Rockford, IL, USA), respectively, on a Qubit 3.0 fluorometer.

Amplicon sequencing and data processing

The primers 515F (5′-GTGCCAGCMGCCGCGG-3′) and 907R (5′- CCGTCAATTCMTTTRAGTTT-3′) targeting the V4–V5 region of the 16S rRNA gene were used to analyze the rhizosphere bacterial community. The primers 799F (5′-AACMGGATTAGATACCCKG-3′) and 1193R (5′-ACGTCATCCCCACCTTCC-3′) targeting the bacterial V5–V7 regions of the 16S rRNA gene were used for endosphere bacterial community analysis. For the polymerase chain reaction (PCR), a 20-μL reaction mixture containing 10 μL of 2 × SYBR Premix Ex TaqTM (Takara, Dalian, China), 0.5 μL of each primer (10 μM), and 10 ng of template DNA was cycled as follows: 3 min at 95°C; 27 cycles of 30 s at 95°C, 30 s at 55°C, and 45 s at 72°C; a final extension of 10 min at 72°C. PCR reactions were performed in triplicate. The PCR product was extracted from 2% agarose gel, purified using the AxyPrep DNA Gel Extraction Kit (Axygen Biosciences, Union City, CA, USA) according to manufacturer's instructions, and quantified using a Quantus™ Fluorometer (Promega, USA). The purified amplicons were then sequenced by Majorbio Bio-Pharm Technology Co., Ltd. (Shanghai, China) on Illumina MiSeq PE300.

After sequencing, the raw 16S rRNA gene sequencing reads were demultiplexed, quality-filtered by fastp version 0.20.0 (Chen et al., 2018), and merged using FLASH version 1.2.7 (Magoc and Salzberg, 2011) as described in a previous study (Chu et al., 2020). The resulting data were then processed in the QIIME2 (Quantitative Insight into Microbial Ecology toolkit, version 2021.8) pipeline (Bolyen et al., 2019). DADA2 (Callahan et al., 2016) was deployed to remove noise and obtain absolute sequence variants (ASVs) with *denoise-single* plugin. Considering that the amplicons were obtained from the rhizosphere and endosphere with different primers, operational taxonomic units (OTUs) were chosen from ASVs at 97% sequence identity against the SILVA 138

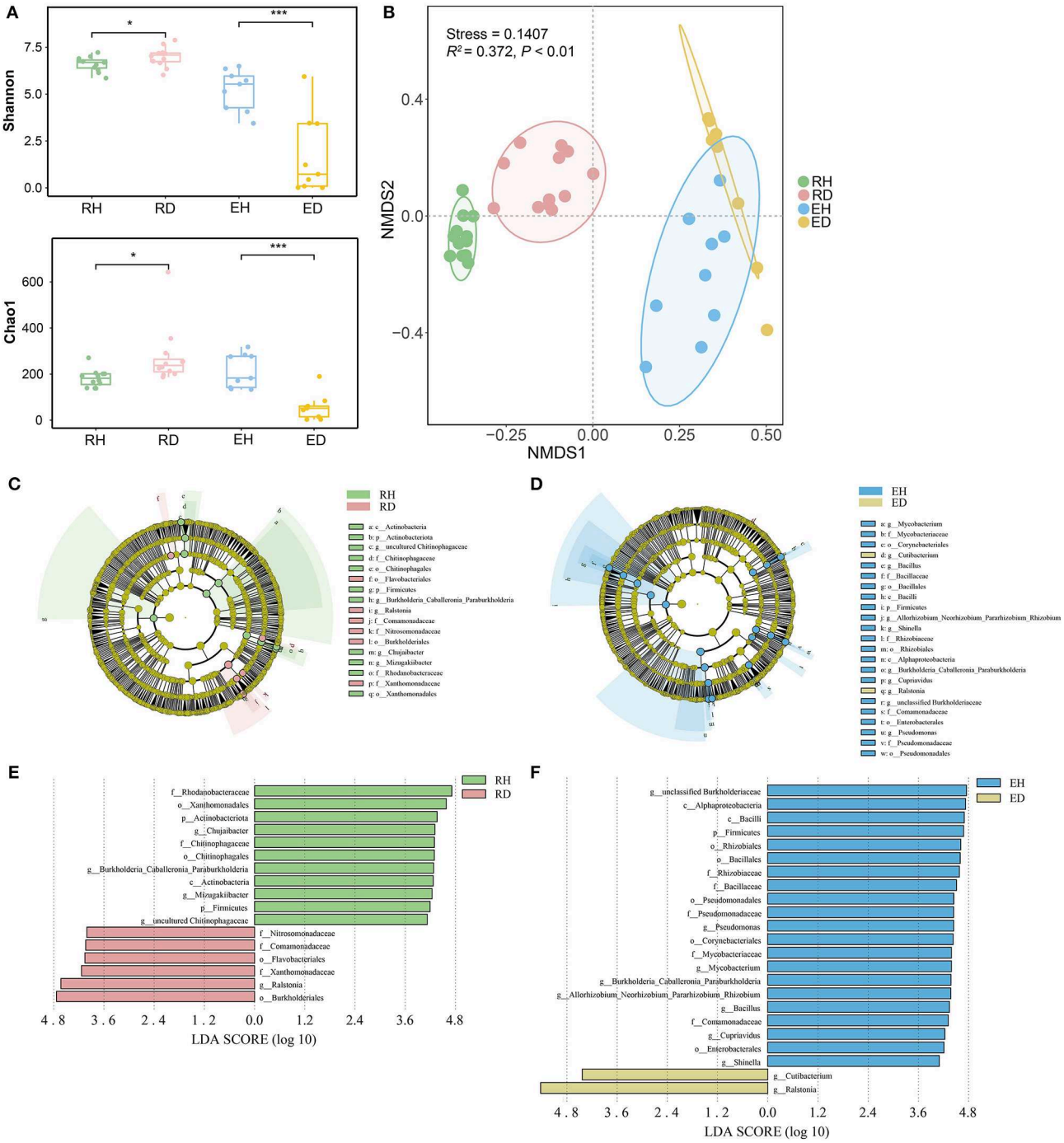

FIGURE 2
Microbiome assembly in plant rhizosphere and endosphere. **(A)** Alpha diversity of microbial communities in rhizosphere and endosphere. Significant differences between different groups were obtained using pairwise Wilcoxon tests with *P*-values. $*P < 0.05$, $***P < 0.001$. **(B)** Non-metric multidimensional scaling (NMDS) ordinations of Bray–Curtis dissimilarity matrices with permutational analysis of variance (PERMANOVA, $R^2 = 0.372$, $P < 0.001$). The potential biomarkers were defined by LEfSe. Cladogram for taxonomic representation of significant differences between **(C)** RH and RD, and **(D)** EH and ED. The colored nodes from the inner to the outer circles represent taxa from the phylum to the genus level. The significantly different taxa are signified by different colors representing the four groups. Histogram of the LDA scores for differentially abundant features between **(E)** RH and RD, and **(F)** EH and ED. The threshold on the logarithmic LDA score for discriminative features was set to 4.0. RH, rhizosphere of healthy plants; RD, rhizosphere of diseased plants; EH, endosphere of healthy plants; ED, endosphere of diseased plants.

SSURef NR 99 full-length sequences database (Quast et al., 2013) using the vsearch *cluster-features-closed-reference* plugin. OTUs assigned to chloroplasts, mitochondria, or archaea were removed, and the corresponding representative sequences were also filtered. After quality filtering, a total of 1,688,642 high-quality 16S rRNA reads were generated, which were finally clustered into 3,331 OTUs.

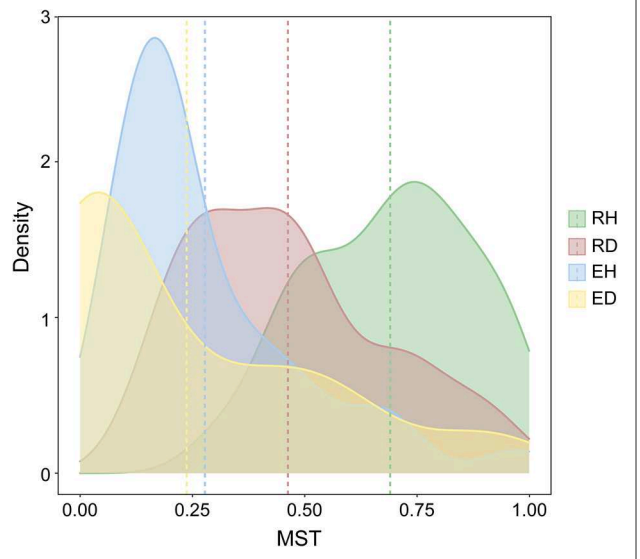

FIGURE 3
Modified normalized stochasticity (MST) ratios estimated for bacterial community assembly mechanism. The four groups are represented by different colors. The vertical dashed lines represent the mean MST values of different groups. RH, rhizosphere of healthy plants; RD, rhizosphere of diseased plants; EH, endosphere of healthy plants; ED, endosphere of diseased plants.

Shotgun metagenome sequencing and data processing

To evaluate the impact of BWD on the community function of tomato bacterial microbiomes, rhizosphere DNA samples were mixed for shotgun metagenome sequencing. The construction of metagenome libraries was performed using the NEB Next® Ultra™ DNA Library Prep Kit for Illumina® (New England Biolabs, MA, USA). Eight DNA samples were sequenced as 150 bp paired-end reads on the Illumina NovaSeq 6000 platform at Houze Biological Technology Co. (Hangzhou, China) with an average of 20 Gb raw data per sample. Trimming and quality filtering were performed using Trimmomatic 0.39 (Bolger et al., 2014). To avoid any disturbance, reads mapped to the host reference genome (*Solanum lycopersicum*, RefSeq ID GCF_000188115.5) were removed by Bowtie 2 (version 2.4.1; Langmead and Salzberg, 2012). The remaining reads were *de novo* assembled into contigs using metaSPAdes v.3.13.0 (parameters: K-mer Sizes = 21, 33, 55; Nurk et al., 2017). Generated contigs longer than 800 bp were selected to obtain the coding sequences (CDSs) and corresponding amino acid (AA) sequences using the predicting function of Prodigal (version 2.6.1, Hyatt et al., 2010). All predicted genes were then clustered to a non-redundant gene catalog by using CD-HIT version 4.8.1 (Li and Godzik, 2006) with the identity cutoff at 0.95. The quantification of 12,594,607 non-redundant genes in each sample was performed using Salmon (Patro et al., 2017). Functional annotation was carried out with DIAMOND (Buchfink et al., 2015) against the Kyoto Encyclopedia of Genes and Genomes (KEGG, version 94.2) database (Kanehisa et al., 2012), resulting in 8,040 KEGG orthology (KO) functional categories and 501 KEGG pathways.

Statistical analysis

To determine the diversity in the four groups of samples (RH, RD, EH, and ED), the alpha (Shannon and Chao1 index) and beta (Bray–Curtis dissimilarities) diversity indices were calculated with the "vegan" package in R (Dixon, 2003) using the rarefied microbial abundance table. The differences in alpha diversity were tested using the Wilcoxon rank-sum tests using the base R package "stats" (version 4.1.1) wilcox.test function. Non-metric multidimensional scaling (NMDS) and non-parametric multivariate analysis of variance (ADONIS; Anderson, 2001) were used to examine the microbial community dissimilarity between the four groups. To analyze taxonomic differences in rhizosphere and endosphere bacterial abundance, a linear discriminant analysis (LDA) effect size (LEfSe) analysis was performed on the amplicon dataset at the genus level (Galaxy web application, http://huttenhower.sph.harvard.edu/galaxy/; Segata et al., 2011). NMDS was also applied to determine whether the microbiomes were functionally distinct between different groups.

The modified normalized stochasticity ratio (MST) based on Bray–Curtis dissimilarity was used to identify the bacterial community assembly processes, with 50% as the threshold for determining the dominance of deterministic (MST $<$ 50%) or stochastic processes (MST $>$ 50%; Ning et al., 2019). A neutral community model (NCM, Sloan et al., 2006) was also used to cross-check the results of the MST analysis. To assess the universality of microbial dynamics, a dissimilarity–overlap curve (DOC) analysis was conducted using the R package "DOC" with a bootstrap value of 200 (Bashan et al., 2016). The overlap was defined as the fraction of shared taxa between two communities in the same group. Dissimilarity refers to differences in shared taxa relative abundance. The dissimilarity and overlap of all sample pairs were plotted to generate a dissimilarity–overlap curve (DOC) with a non-parametric regression and bootstrap sampling procedure. Universal dynamics exist only when a negative correlation is detected between dissimilarity and overlap and the DOC inflection point occurs where the slope is negative. The fraction of points after the inflection point is termed *Fns*.

To infer the co-occurrence and mutual exclusion patterns, the CoNet plugin in Cytoscape version 3.7.1 (Shannon et al., 2003) was used to calculate multiple correlations and similarities between the microbial OTUs. To decrease the number of false positives, all taxa below a minimum occurrence of six were combined across the samples into a garbage taxon, and the Benjamini–Hochberg procedure was adopted to adjust the *P*-values. The co-occurrence between taxa was considered valid when the *P*-value (adjusted) was below 0.05 (Benjamini and Hochberg, 1995) and the correlation threshold was above 0.7. Network images were generated with Gephi (version 0.9.2; Heymann, 2009) with the Fruchterman-Reingold layout. Topological parameters of networks were also calculated with Gephi.

Functional diversity, including alpha and beta diversity, was also calculated using the "vegan" package in R. Principal coordinate analysis (PCoA) combined with ADONIS was applied to examine functional gene dissimilarity between RH and RD using "vegan" with the Bray–Curtis dissimilarity metric. Differential analysis of functional genes and KEGG pathways was carried out using a generalized linear model (GLM) in R package "edgeR"

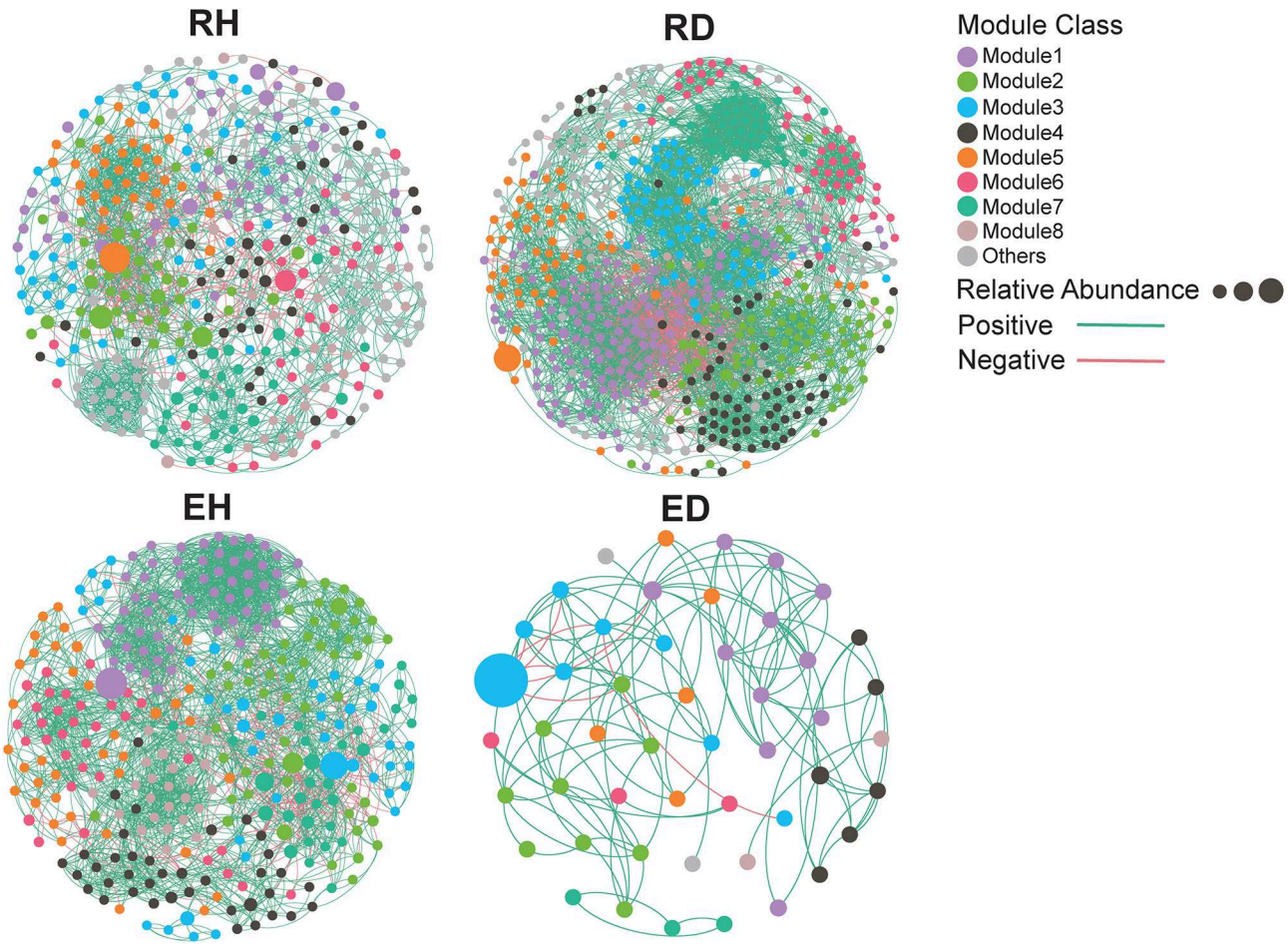

FIGURE 4
Co-occurrence network for bacterial communities. Each node represents an OTU, and the relationship between two OTUs in the network was shown by an edge (Coefficient $R \geq 0.7$, significant $P \leq 0.01$). The nodes are colored according to module classes. Node size reflects the relative abundance of an OTU. The edge color represents positive (green) or negative (red) correlation. RH, rhizosphere of healthy plants; RD, rhizosphere of diseased plants; EH, endosphere of healthy plants; ED, endosphere of diseased plants.

(Robinson et al., 2010) and STAMP (Parks et al., 2014) with Welch's *t-test*, and all *P*-values were corrected for a false discovery rate (*FDR*) of 0.01 using the Benjamini–Hochberg algorithm.

Results

Diversity and community composition

At the phylum level, *Proteobacteria*, *Bacteroidota*, and *Actinobacteriota* were dominant across all rhizosphere and endosphere samples (Supplementary Figure 1). Bacterial alpha diversity in RH (Shannon index/Chao1 index: 6.70/183.0) was significantly lower than that in RD (Shannon index/ Chao1 index: 7.08/237.5, $P < 0.001$), while bacterial diversity in EH (Shannon index/Chao1 index: 5.52/184.5) was significantly higher than that in ED (Shannon index/Chao1 index: 0.71/52.0, $P < 0.01$, Figure 2A). Non-metric NMDS analysis based on Bray–Curtis dissimilarity showed that the samples clustered well and separated according to the different sample groups (Figure 2B). The ordination plot indicated that microbial community composition was distributed according to the groups (Figure 2B). ADONIS further demonstrated that there was a significant difference in community composition between different groups ($R^2 = 0.372$, $P < 0.001$). ANOSIM analysis indicated that the compositional variation (indicated by Bray–Curtis dissimilarity) was lower in both RH and EH compared to RD ($R = 0.469$, $P = 0.001$) and RH ($R = 0.424$, $P = 0.002$; Supplementary Figure 2).

LEfSe analysis was conducted to explore the indicator taxa in the four groups. In the rhizosphere, the phyla *Actinobacteriota* and *Firmicutes*, orders *Xanthomonadales* and *Chitinophagales*, and genera *Chujaibacter*, *Burkholderia, Caballeronia, Paraburkholderia*, *Mizugakiibacter,* and uncultured *Chitinophagaceae* were enriched in RH. Orders *Burkholderiales* and *Flavobacteriales*, family *Xanthomonadaceae*, and genus *Ralstonia* were greatly enriched in RD compared to RH (Figures 2C, E). In EH, the most significantly different taxa were phylum *Firmicutes*, classes *Alphaproteobacteria* and *Bacilli*, orders *Rhizobiales*, *Bacillales*, *Pseudomonadales, Corynebacteriales,* and *Enterobacterales*, families *Rhizobiaceae, Bacillaceae*, *Pseudomonadaceae*, *Mycobacteriaceae,* and *Comamonadaceae*, and genera *unclassified Burkholderiaceae,*

TABLE 1 Topology properties of the RH, RD, EH, and ED networks.

Parameter	RH	RD	EH	ED
No. of nodes	381	621	322	49
No. of edges	3,654	11,958	5,478	260
Linkage density	4.8	9.63	8.51	2.65
No. of positive edges/proportion (%)	3,458 (86%)	10,678 (89%)	5,126 (94%)	246 (95%)
No. of negative edges/proportion (%)	496 (14%)	1,280 (11%)	352 (6%)	14 (5%)
Clustering coefficient	0.466	0.567	0.63	0.8
Avg. degree	9.591	19.256	17.012	5.306
Betweeness centrality	0.0017	0.0012	0.0026	0.0525
Closeness centrality	0.2587	0.2829	0.3001	0.5765
Modularity	0.673	0.65	0.67	0.624
Network density	0.025	0.031	0.053	0.111
Average path length	4.11	3.68	3.38	2.61

RH, rhizosphere of healthy plants; RD, rhizosphere of diseased plants; EH, endosphere of healthy plants; ED, endosphere of diseased plants.

Pseudomonas, Mycobacterium, Burkholderia Caballeronia Paraburkholderia, Allorhizobium, Neorhizobium, Pararhizobium, Rhizobium, Bacillus, Cupriavidus, and *Shinella*. Compared to EH, genera *Ralstonia* and *Cutibacterium* were significantly enriched in ED (Figures 2D, F).

Community assembly mechanisms

The modified normalized stochasticity ratio (MST) index was calculated to evaluate the importance of stochasticity and determinism for bacterial community assembly. The average MST values in RH, RD, EH, and ED were 0.690, 0.462, 0.278, and 0.238, respectively (Figure 3). In addition, we further assessed the contribution of the stochastic process to community assembly by the neutral community model (NCM). The NCM model performance was indicated by R^2, where a higher R^2 (close to 1) indicates a better neutral fitting (more stochastically assembled). RH had a higher NCM model R^2 in comparison with RD ($R^2 = 0.607$ vs. $R^2 = 0.475$, Supplementary Figure 3).

Microbial co-occurrence patterns

To determine the effect of BWD on microbial co-occurrence patterns, networks based on correlation relationships were constructed (Figure 4). Based on complexity-denoting network topological parameters, higher node (RH/RD: 381/621) and edge (RH/RD: 3654/11958) numbers and smaller betweenness centrality (RH/RD: 0.0017/0.0012) were identified in the RD network compared to the RH network (Table 1). In contrast, higher node (EH/ED: 322/49) and edge (EH/ED: 5478/260) numbers and smaller betweenness centrality (EH/ED: 0.0026/0.0525) were recorded in the EH network compared to that recorded in the ED network (Table 1). The topological parameters, clustering coefficient (RH/RD: 0.466/0.567), average degree (RH/RD: 9.591/19.256), and average path length (RH/RD: 4.11/2.68), were also assessed, and a higher clustering coefficient and average degree but lower average path length were observed in the RD network compared to that in the RH network (Table 1).

Effects of BWD on community universality

Universal dynamics denotes when communities in the same group share the same interaction rules. The rules are supported only if the shared taxa have the same relative abundances (Bashan et al., 2016). To assess whether there are universal dynamics in samples that belonged to the same group, we performed a dissimilarity–overlap curve (DOC) analysis. Here, the overlap indicates the fraction of the shared taxa between two communities in the same group. Dissimilarity refers to differences in the composition of the shared taxa based on relative abundance. The dissimilarity and overlap of all sample pairs are then plotted to generate a DOC with a non-parametric regression and a bootstrap sampling procedure. Universal dynamics were determined only when a negative correlation was detected between dissimilarity and overlap, and the inflection point occurred in DOC where the slope was negative. The fraction of points after the inflection point is termed as *Fns*.

The DOCs had significant negative slopes, with an *Fns* of 6.1% for RH community comparisons (Figures 5A, B); this was lower than that of the RD community comparisons (9.1%). Similarly, the DOCs for EH comparisons had significant negative slopes with an *Fns* of 5.6%, which was also lower than those observed for the diseased ED community comparisons (8.3%; Figures 5C, D).

Determining the functional profile of the rhizosphere microbiome

The metagenomic functional profiling yielded a total of 8,040 KO functional categories. PCoA and Adonis reflected significant differences in microbiome functional profiles between RH and RD ($R^2 = 0.71$, $P < 0.05$, Supplementary Figure 4D). A total of 1,015 significantly different KOs were detected, of which 391 were found to be significantly enriched in RH and 624 were enriched in RD (Figure 6A).

To clarify which significant KOs were predominant, KOs with relative abundance >0.08% were used for statistical analysis. This resulted in 48 KOs, four of which were significantly enriched in RH; the remaining 44 were significantly enriched in RD. K01156 (*res*, type III restriction enzyme [EC:3.1.21.5], prokaryotic defense system, mean 0.055%) was most abundant in RH, followed by K12526 (*lysAC*, bifunctional diaminopimelate decarboxylase/aspartate kinase, mean 0.026%), K05998

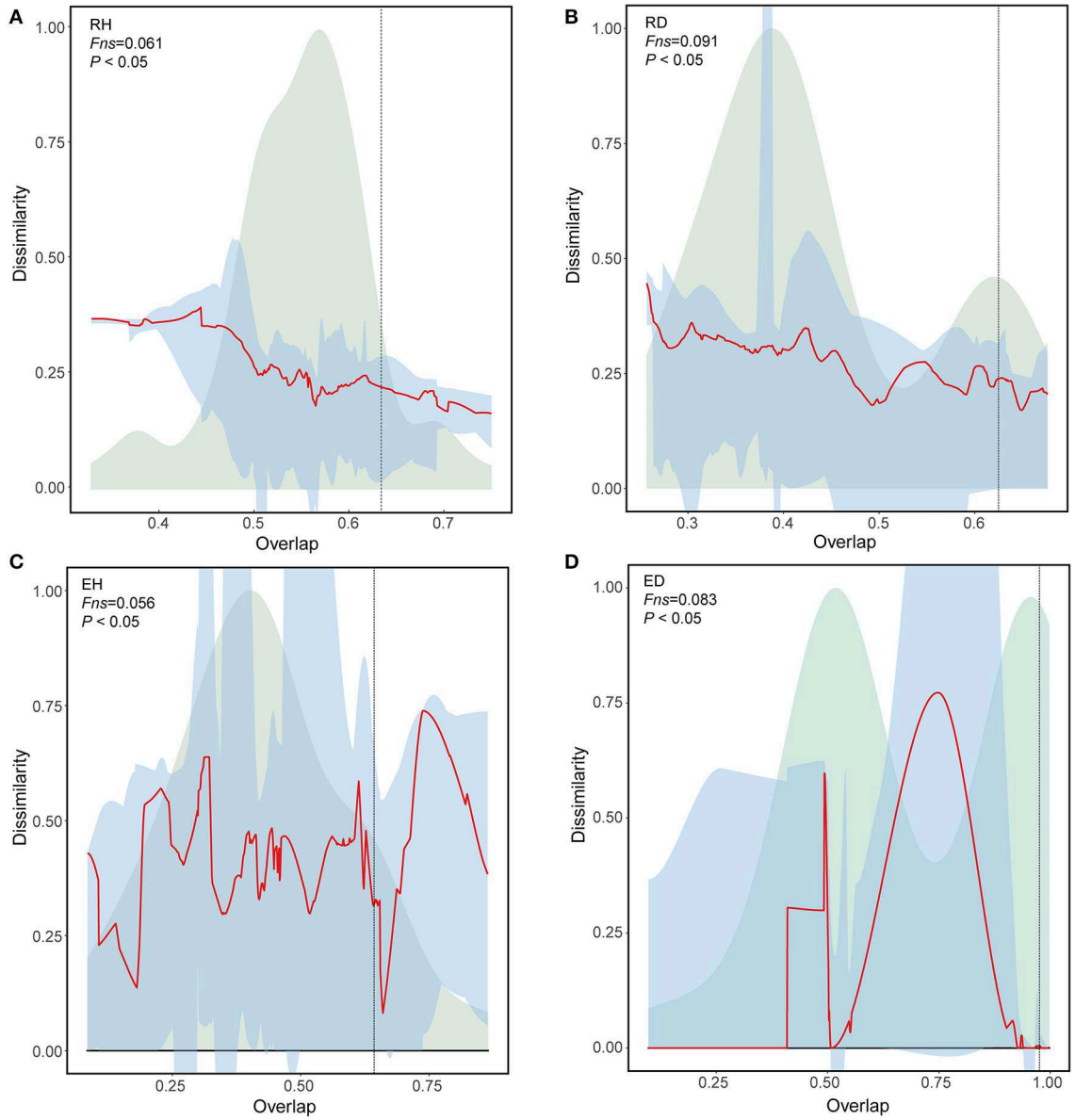

FIGURE 5
Universal ecological dynamics of RH **(A)**, RD **(B)**, EH **(C)**, and ED **(D)** microbiome. The ecological universality of microbiome was assessed using dissimilarity-overlap curves (DOC). DOCs are in red, the distribution density of sample pair overlap is in light green, and the point at which the DOC first becomes negative is marked by a vertical dashed line (chosen by median of 200 bootstraps). A higher *Fns* value indicates higher ecological universality (host-independent) of the metacommunity. RH, Rhizosphere of healthy plants; RD, Rhizosphere of diseased plants; EH, Endosphere of healthy plants; ED, Endosphere of diseased plants.

(pseudomonalisin [EC:3.4.21.100], peptidases, and inhibitors, mean 0.022%), and K09704 (mean 0.018%; Figure 6B). In RD, the top three KOs were K07481 (transposase, IS5 family, mean 0.287%), K15125 (*fhaB*, filamentous hemagglutinin, glycosaminoglycan binding proteins, mean 0.235%), and K11904 (*vgrG*, type VI secretion system secreted protein VgrG, mean 0.166%). When the pathways involved with these significantly differential KOs were mapped, KOs enriched in RH were mainly assigned to KEGG pathways "Prokaryotic defense system," "Peptidases and inhibitors," "Monobactam biosynthesis," "Glycine, serine, and threonine metabolism," and "cysteine and methionine metabolism." Except for pathway "Metabolic pathways," which was shared with RH, KOs enriched in RD mainly mapped into pathways "Transporters," "ABC transporters," "Enzymes with EC numbers," "Two-component system," "Secretion system," "Replication and repair," and "biosynthesis of siderophore group non-ribosomal peptide" (Figure 6B).

A total of 19 enriched KEGG pathways were detected in RH and seven were enriched in RD. Despite the pathways enriched in RH exhibiting a diversified pattern, pathways with high relative abundance were principally those involved in metabolism and human diseases (vancomycin resistance). In RD, the pathway "Two-component system" involved in environmental information processing was most abundant, followed by "Quorum

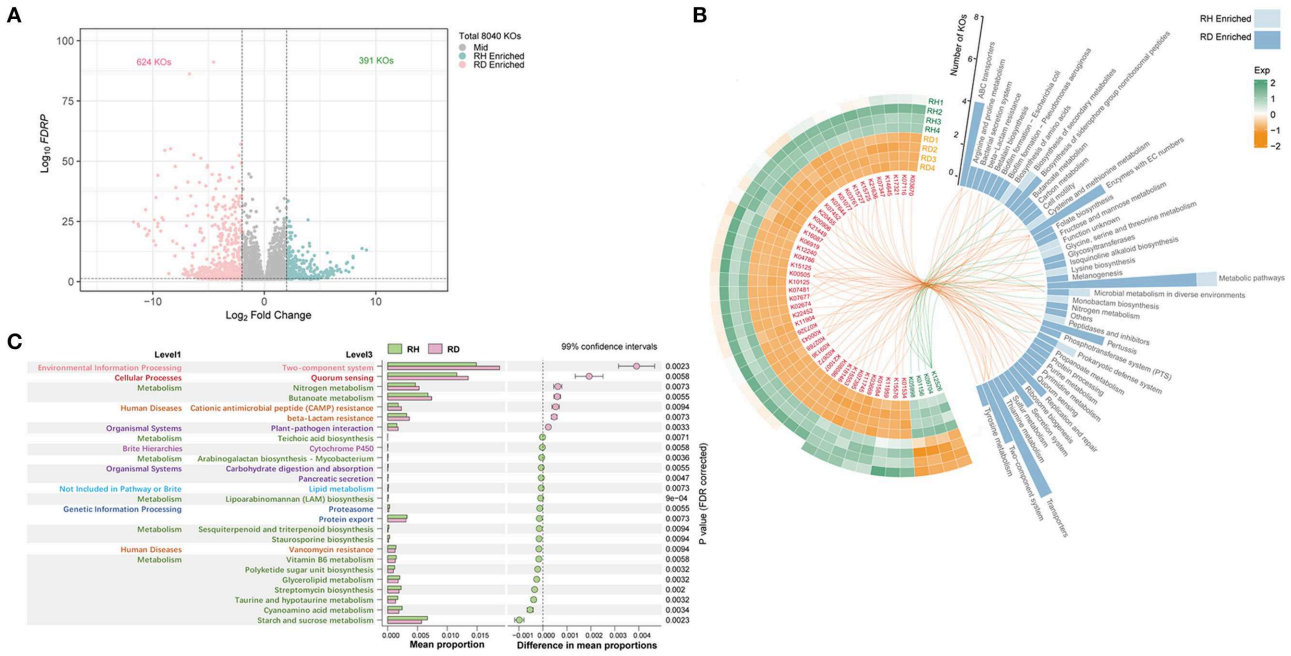

FIGURE 6
Functional profile of rhizosphere microbiome. Significantly ($P < 0.01$) different A, B KO functional categories and C pathways between RH and RD. All KO functional categories are depicted in **(A)**, and the differential KO functional categories were evaluated using the generalized linear model (GLM) edgeR approach. The abundant differential KO functional categories (relative abundance > 0.08%) are described in the heatmap **(B)**, and the involved pathways are counted in the histogram and are linked by lines. KO functional categories that were significantly enriched in RH or RD were separately analyzed for KEGG pathway enrichment; those pathways that did not belong to microorganisms were removed; all significantly enriched pathways are described in **(C)**. The pathway difference between RH and RD was quantified using a two-tailed Wilcoxon test, and the corrected *P*-values were shown. RH, rhizosphere of healthy plants; RD, rhizosphere of diseased plants.

sensing" involved in cellular processes. Pathways "Nitrogen metabolism" and "Butanoate metabolism" were more abundant in RD than in RH. Furthermore, pathways "Cationic antimicrobial peptide (CAMP) resistance"/"beta-Lactam resistance" involved in human diseases and "Butanoate metabolism" and "Plant–pathogen interaction" involved in organismal systems also showed significantly higher relative abundance in the RD samples (Figure 6C).

Discussion

Using a field sampling approach, the present study revealed multifaceted disease-induced variations in the community assembly and functions of plant-associated microbiomes, which may provide new insights into the role of pathogen invasion in altering the functioning of plant-associated microbiomes in soil ecosystems.

BWD increased diversity of the rhizosphere microbiome

The disease occurs commonly alongside changes in microbial diversity in the rhizosphere (Wei et al., 2018; Yuan et al., 2018; Shi et al., 2019). Contrasting previous reports showing pathogen invasion led to a decline in microbial diversity, the results of this study showed that the alpha diversity of diseased plants (RD) was significantly higher than that of healthy ones (RH; Figure 2A). This demonstrated that pathogen invasion may not necessarily suppress microbial diversity in the rhizosphere (Gibbons et al., 2016); on the contrary, the diverse nutrients released by the damaged roots may have the potential to feed more microbial species in the rhizosphere, leading to a diversity increase after pathogen invasion. Similarly, beta diversity also increased with pathogen infection (Figure 2B), indicating that pathogen invasion disrupted host control of the rhizosphere microbiome (Wei et al., 2018; Wen et al., 2020). This is inconsistent with the prediction of the Anna Karenina principle, which suggested that the microbiome of diseased hosts may display greater compositional or functional variation compared to healthy ones (Arnault et al., 2023). Environmental perturbations such as pathogen invasion could lead to the development of new niches, and microbes nearby could then colonize the rhizosphere opportunistically, resulting in higher beta diversity (Macke et al., 2017; Yu et al., 2020; Lin et al., 2022).

BWD promoted microbial co-occurrence complexity and altered the relative contribution of deterministic processes

Using the ecological null model, the relative contribution of deterministic processes in influencing bacterial community assembly increased under diseased conditions (Figure 3 and

Supplementary Figure 3B). The deterministic process is mainly derived from environmental filtering and species competition that influence the occurrence and abundance of species (Zhou and Ning, 2017). The enhanced deterministic processes observed after pathogen invasion may be jointly attributed to the drastic environmental changes as well as to different biological interactions that then occurred (Zhang et al., 2022). Roots damaged by pathogen invasion can release rich nutrients into the rhizosphere; consequently, many microbial species that favor copiotrophic conditions would be subsequently enriched, while some oligotrophic species would be selectively excluded. For example, the genus *Ralstonia* is mainly composited of copiotrophic species that prefer nutrient-rich conditions and was found to be significantly enriched in diseased plants (Li et al., 2021). The "cry for help" hypothesis suggests that many plant-beneficial microbial species, especially those with the ability to antagonize pathogens, would be selectively recruited by plants after pathogen invasion, contributing to the deterministic processes in the diseased plant rhizosphere (Gao et al., 2021; Arnault et al., 2023).

While co-occurrence does not directly reflect interaction, it allows the construction of a linkage between community assembly processes and co-occurrence patterns. Using the co-occurrence network analysis, pathogen invasion was found to increase the network complexity of the plant-associated microbiome (Table 1), implying that pathogen invasion potentially promoted microbial interactions. In addition to network analysis, the universal dynamics of the plant-associated microbiome were analyzed using DOCs, which can also reflect microbial interactions (Bashan et al., 2016). A higher *Fns* value was found for diseased plants than for healthy plant-associated microbiomes, suggesting that microbes in diseased plants interacted more closely. These results consistently indicated that pathogen invasion promoted microbial interactions in the rhizosphere and endosphere (Figure 5), which may contribute to the deterministic assembly. It should be noted that the tightened microbial interactions may also be linked to plant disease. A community with tight and complex interactions always has lower community stability, since resonance is more likely to occur (Coyte et al., 2015; de Vries et al., 2018). As a consequence, it can be inferred that pathogens may have better chances to colonize and proliferate in these less stable environments. Therefore, future experiments testing plant disease incidence and community stability in complex microbial communities will be necessary to discern their relative importance in soil and plant health.

BWD induced changes in microbiome functions

Using shotgun metagenome sequencing, we investigated how pathogen invasion affects the functioning profile of the rhizosphere microbiome. Metagenomic analysis indicated that several genes essential for the pathogenicity of *R. solanacearum* involved in pathways "Two-component system" and "Secretion system" (Genin and Denny, 2012), such as *fhaB and vgrG,* were enriched in RD (Figure 6B). A higher relative abundance of K05998 (pseudomonalisin [EC:3.4.21.100], peptidases, and inhibitors) was found in RH. Peptidases have been reported to be potential biocontrol factors participating in the predation of *Myxococcus xanthus* on *R. solanacearum* (Dong et al., 2022; Figure 6B). An important differential pathway worth noting is "Quorum sensing," which was found to be significantly enriched in the diseased rhizosphere (Figure 6C). Quorum sensing can coordinate the expression of specific genes in multiple pathogens and regulate pathogenic performance (Bassler, 1999). It can therefore be speculated that other microorganisms may induce pathogenic *Ralstonia* to cause plant disease, although this needs to be demonstrated by further experimentation (Shi et al., 2019; Li M. et al., 2022). In contrast, some plant-beneficial pathways such as "streptomycin biosynthesis" were found to be significantly enriched in the healthy plant rhizosphere (Figure 6C). Streptomycin is an aminoglycoside antibiotic that inhibits protein synthesis and targets the 30S ribosomal protein RpsL. Streptomycin has been used to control multiple plant bacterial diseases and can antagonize multiple phytopathogens such as *Pseudomonas aeruginosa* and *R. solanacearum* (Lee et al., 2018; Attia et al., 2022).

Conclusion

This study aimed to reveal how plant-associated microbiomes respond to plant disease. The results demonstrated that pathogen invasion enhanced the bacterial deterministic processes, promoted microbial co-occurrence complexity and ecological universality, and modified the functional profile of the plant-associated microbiome. This study broadens the understanding of the relationships between plant disease and the plant microbiome and provides novel insights into BWD occurrence.

Data availability statement

The data presented in the study are deposited in the NCBI's archival repository, accession number PRJNA917505.

Author contributions

PL and JJ designed the work. LK and TL conducted the experiments. LK analyzed the data and wrote the manuscript. BW participated in revising the manuscript. JP and JL took part in sample collection. All authors contributed to the study and approved the final submitted version.

Funding

This study was supported by the Fundamental Research Funds for the Central Universities (680-ZJ21195006), the National Natural Science Foundation of China (42207349), the Natural Science Foundation of Jiangsu Province (BK20221005), the China Postdoctoral Science Foundation (2022M711653), and the Jiangsu Funding Program for Excellent Postdoctoral Talent (2022ZB331).

Conflict of interest

The authors declare that the research was conducted in the absence of any commercial or financial relationships that could be construed as a potential conflict of interest.

Publisher's note

All claims expressed in this article are solely those of the authors and do not necessarily represent those of their affiliated organizations, or those of the publisher, the editors and the reviewers. Any product that may be evaluated in this article, or claim that may be made by its manufacturer, is not guaranteed or endorsed by the publisher.

Supplementary material

The Supplementary Material for this article can be found online at: https://www.frontiersin.org/articles/10.3389/fmicb.2023.1141585/full#supplementary-material

References

Anderson, M. J. (2001). A new method for non-parametric multivariate analysis of variance. *Austral. Ecol.* 26, 32–46. doi: 10.1046/j.1442-9993.2001.01070.x

Arnault, G., Mony, C., and Vandenkoornhuyse, P. (2023). Plant microbiota dysbiosis and the Anna Karenina Principle. *Trends Plant Sci.* 28, 18–30. doi: 10.1016/j.tplants.2022.08.012

Attia, M. S., Balabel, N. M., Ababutain, I. M., Osman, M. S., Nofel, M. M., Abd Elkodous, M., et al. (2022). Protective role of copper oxide-streptomycin nano-drug against potato brown rot disease caused by *Ralstonia solanacearum*. *J. Clust. Sci.* 33, 1373–1386. doi: 10.1007/s10876-021-02048-x

Bashan, A., Gibson, T. E., Friedman, J., Carey, V. J., Weiss, S. T., Hohmann, E. L., et al. (2016). Universality of human microbial dynamics. *Nature* 534, 259–262. doi: 10.1038/nature18301

Bassler, B. L. (1999). How bacteria talk to each other: regulation of gene expression by quorum sensing. *Curr. Opin. Microbiol.* 2, 582–587. doi: 10.1016/S1369-5274(99)00025-9

Benjamini, Y., and Hochberg, Y. (1995). Controlling the false discovery rate – a practical and powerful approch to mutiple testing. *J. R. Stat. Soc. B* 57, 289–300. doi: 10.1111/j.2517-6161.1995.tb02031.x

Berendsen, R. L., Pieterse, C. M. J., and Bakker, P. A. H. M. (2012). The rhizosphere microbiome and plant health. *Trends Plant Sci.* 17, 478–486. doi: 10.1016/j.tplants.2012.04.001

Bolger, A. M., Lohse, M., and Usadel, B. (2014). Trimmomatic: a flexible trimmer for Illumina sequence data. *Bioinformatics* 30, 2114–2120. doi: 10.1093/bioinformatics/btu170

Bolyen, E., Rideout, J. R., Dillon, M. R., Bokulich, N., Abnet, C. C., Al-Ghalith, G. A., et al. (2019). Reproducible, interactive, scalable and extensible microbiome data science using QIIME 2. *Nat. Biotechnol.* 37, 852–857. doi: 10.1038/s41587-019-0209-9

Buchfink, B., Xie, C., and Huson, D. H. (2015). Fast and sensitive protein alignment using DIAMOND. *Nat. Methods* 12, 59–60. doi: 10.1038/nmeth.3176

Callahan, B. J., McMurdie, P. J., Rosen, M. J., Han, A. W., Johnson, A. J. A., and Holmes, S. P. (2016). DADA2: High-resolution sample inference from Illumina amplicon data. *Nat. Methods* 13, 581–589. doi: 10.1038/nmeth.3869

Carrion, V. J., Perez-Jaramillo, J., Cordovez, V., Tracanna, V., de Hollander, M., Ruiz-Buck, D., et al. (2019). Pathogen-induced activation of disease-suppressive functions in the endophytic root microbiome. *Science* 366, 606–612. doi: 10.1126/science.aaw9285

Chen, S., Zhou, Y., Chen, Y., and Gu, J. (2018). fastp: an ultra-fast all-in-one FASTQ preprocessor. *Bioinformatics* 34, 884–890. doi: 10.1093/bioinformatics/bty560

Chu, B., Zhu, Y., Su, J., Xia, B., Zou, Y., Nie, J., et al. (2020). Butyrate-mediated autophagy inhibition limits cytosolic *Salmonella* Infantis replication in the colon of pigs treated with a mixture of *Lactobacillus* and *Bacillus*. *Vet. Res.* 51, 99–117. doi: 10.1186/s13567-020-00823-8

Coyte, K. Z., Schluter, J., and Foster, K. R. (2015). The ecology of the microbiome: networks, competition, and stability. *Science* 350, 663–666. doi: 10.1126/science.aad2602

de Vries, F. T., Griffiths, R. I., Bailey, M., Craig, H., Girlanda, M., Gweon, H. S., et al. (2018). Soil bacterial networks are less stable under drought than fungal networks. *Nat. Commun.* 9, 3033–3045. doi: 10.1038/s41467-018-05516-7

Dini-Andreote, F., Stegen, J. C., van Elsas, J. D., and Salles, J. F. (2015). Disentangling mechanisms that mediate the balance between stochastic and deterministic processes in microbial succession. *Proc. Natl. Acad. Sci. U.S.A.* 112, 1326–1332. doi: 10.1073/pnas.1414261112

Dixon, P. (2003). VEGAN, a package of R functions for community ecology. *J. Veg. Sci.*14, 927–930. doi: 10.1111/j.1654-1103.2003.tb02228.x

Dong, H., Xu, X., Gao, R., Li, Y., Li, A., Yao, Q., et al. (2022). *Myxococcus xanthus* R31 suppresses tomato bacterial wilt by inhibiting the pathogen *Ralstonia solanacearum* with secreted proteins. *Front. Microbiol.* 12:801091. doi: 10.3389/fmicb.2021.801091

Fibiani, M., Paolo, D., Leteo, F., Campanelli, G., Picchi, V., Bianchi, G., et al. (2022). Influence of year, genotype and cultivation system on nutritional values and bioactive compounds in tomato (*Solanum lycopersicum* L.). *Food. Chem.* 30, 133090–133101. doi: 10.1016/j.foodchem.2022.133090

Gao, C., Montoya, L., Xu, L., Madera, M., Hollingsworth, J., Purdom, E., et al. (2020). Fungal community assembly in drought-stressed sorghum shows stochasticity, selection, and universal ecological dynamics. *Nat. Commun.* 11:34. doi: 10.1038/s41467-019-13913-9

Gao, M., Xiong, C., Gao, C., Tsui, C. K. M., Wang, M. M., Zhou, X., et al. (2021). Disease-induced changes in plant microbiome assembly and functional adaptation. *Microbiome* 9:187. doi: 10.1186/s40168-021-01138-2

Genin, S., and Denny, T. P. (2012). Pathogenomics of the *Ralstonia solanacearum* species complex. *Annu. Rev. Phytopathol.* 50, 67–89. doi: 10.1146/annurev-phyto-081211-173000

Gibbons, S. M., Scholz, M., Hutchison, A. L., Dinner, A. R., Gilbert, J. A., and Coleman, M. L. (2016). Disturbance regimes predictably alter diversity in an ecologically complex bacterial system. *mBio* 7, e01372–e01316. doi: 10.1128/mBio.01372-16

Heymann, M. B. (2009). Gephi : an open source software for exploring and manipulating networks. *ICWSM* 3, 361–362. doi: 10.1609/icwsm.v3i1.13937

Hyatt, D., Chen, G.-L., LoCascio, P. F., Land, M. L., Larimer, F. W., and Hauser, L. J. (2010). Prodigal: prokaryotic gene recognition and translation initiation site identification. *BMC Bioinformatics* 11:119. doi: 10.1186/1471-2105-11-119

Kanehisa, M., Goto, S., Sato, Y., Furumichi, M., and Tanabe, M. (2012). KEGG for integration and interpretation of large-scale molecular data sets. *Nucleic Acids Res.* 40, D109–D114. doi: 10.1093/nar/gkr988

Kibbey, T. C. G., and Strevett, K. A. (2019). The effect of nanoparticles on soil and rhizosphere bacteria and plant growth in lettuce seedlings. *Chemosphere* 221, 703–707. doi: 10.1016/j.chemosphere.2019.01.091

Langmead, B., and Salzberg, S. L. (2012). Fast gapped-read alignment with Bowtie 2. *Nat. Methods* 9, 354–357. doi: 10.1038/nmeth.1923

Lee, L.-H., Chan, K.-G., Stach, J., Wellington, E. M. H., and Goh, B.-H. (2018). Editorial: The search for biological active agent(s) from *Actinobacteria*. *Front. Microbiol.* 9:824. doi: 10.3389/fmicb.2018.00824

Lee, S. M., Kong, H. G., Song, G. C., and Ryu, C. M. (2021). Disruption of *Firmicutes* and *Actinobacteria* abundance in tomato rhizosphere causes the incidence of bacterial wilt disease. *ISME J.* 15, 330–347. doi: 10.1038/s41396-020-00785-x

Li, M., Pommier, T., Yin, Y., Wang, J., Gu, S., Jousset, A., et al. (2022). Indirect reduction of Ralstonia solanacearum via pathogen helper inhibition. *ISME J.* 16, 868–875. doi: 10.1038/s41396-021-01126-2

Li, P., Liu, J., Jiang, C., Wu, M., Liu, M., and Li, Z. (2019). Distinct successions of common and rare bacteria in soil under humic acid amendment - A microcosm study. *Front. Microbiol.* 10:2271. doi: 10.3389/fmicb.2019.02271

Li, P., Liu, J., Saleem, M., Li, G., Luan, L., Wu, M., et al. (2022). Reduced chemodiversity suppresses rhizosphere microbiome functioning in the mono-cropped agroecosystems. *Microbiome* 10:108. doi: 10.1186/s40168-022-01287-y

Li, P., Liu, M., Li, G., Liu, K., Liu, T., Wu, M., et al. (2021). Phosphorus availability increases pathobiome abundance and invasion of rhizosphere microbial networks by *Ralstonia*. *Environ. Microbiol.* 23, 5992–6003. doi: 10.1111/1462-2920.15696

Li, W., and Godzik, A. (2006). Cd-hit: a fast program for clustering and comparing large sets of protein or nucleotide sequences. *Bioinformatics* 22, 1658–1659. doi: 10.1093/bioinformatics/btl158

Li, X., Jousset, A., de Boer, W., Carrion, V. J., Zhang, T., Wang, X., et al. (2019). Legacy of land use history determines reprogramming of plant physiology by soil microbiome. *ISME J.* 13, 738–751. doi: 10.1038/s41396-018-0300-0

Li, X., Yao, S., Bian, Y., Jiang, X., and Song, Y. (2020). The combination of biochar and plant roots improves soil bacterial adaptation to PAH stress: insights from soil enzymes, microbiome, and metabolome. *J. Hazard. Mater.* 400:123227. doi: 10.1016/j.jhazmat.2020.123227

Lin, L., Xu, E. G., Liu, M., Yang, Y., Zhou, A., Suyamud, B., et al. (2022). Microbiological processes of submicrometer plastics affecting submerged plant growth in a chronic exposure microcosm. *Environ. Sci. Tech. Lett.* 10, 33–39. doi: 10.1021/acs.estlett.2c00789

Louca, S., Polz, M. F., Mazel, F., Albright, M. B. N., Huber, J. A., O'Connor, M. I., et al. (2018). Function and functional redundancy in microbial systems. *Nat. Ecol. Evol.* 2, 936–943. doi: 10.1038/s41559-018-0519-1

Luan, L., Liang, C., Chen, L., Wang, H., Xu, Q., Jiang, Y., et al. (2020). Coupling bacterial community assembly to microbial metabolism across soil profiles. *mSystems* 5, e00298–e00220. doi: 10.1128/mSystems.00298-20

Macke, E., Tasiemski, A., Massol, F., Callens, M., and Decaestecker, E. (2017). Life history and eco-evolutionary dynamics in light of the gut microbiota. *Oikos* 126, 508–531. doi: 10.1111/oik.03900

Magoc, T., and Salzberg, S. L. (2011). FLASH: fast length adjustment of short reads to improve genome assemblies. *Bioinformatics* 27, 2957–2963. doi: 10.1093/bioinformatics/btr507

Muller, D. B., Vogel, C., Bai, Y., and Vorholt, J. A. (2016). The plant microbiota: systems-level insights and perspectives. *Annu. Rev. Genet.* 50, 211–234. doi: 10.1146/annurev-genet-120215-034952

Ning, D., Deng, Y., Tiedje, J. M., and Zhou, J. (2019). A general framework for quantitatively assessing ecological stochasticity. *Proc. Natl. Acad. Sci. U.S.A.* 116, 16892–16898. doi: 10.1073/pnas.1904623116

Nurk, S., Meleshko, D., Korobeynikov, A., and Pevzner, P. A. (2017). metaSPAdes: a new versatile metagenomic assembler. *Genome Res.* 27, 824–834. doi: 10.1101/gr.213959.116

Parks, D. H., Tyson, G. W., Hugenholtz, P., and Beiko, R. G. (2014). STAMP: statistical analysis of taxonomic and functional profiles. *Bioinformatics* 30, 3123–3124. doi: 10.1093/bioinformatics/btu494

Patro, R., Duggal, G., Love, M. I., Irizarry, R. A., and Kingsford, C. (2017). Salmon provides fast and bias-aware quantification of transcript expression. *Nat. Methods* 14, 417–419. doi: 10.1038/nmeth.4197

Quast, C., Pruesse, E., Yilmaz, P., Gerken, J., Schweer, T., Yarza, P., et al. (2013). The SILVA ribosomal RNA gene database project: improved data processing and web-based tools. *Nucleic Acids Res.* 41, 590–596. doi: 10.1093/nar/gks1219

Robinson, M. D., McCarthy, D. J., and Smyth, G. K. (2010). edgeR: a Bioconductor package for differential expression analysis of digital gene expression data. *Bioinformatics* 26, 139–140. doi: 10.1093/bioinformatics/btp616

Ruiz-Perez, C. A., Restrepo, S., and Zambrano, M. M. (2016). Microbial and functional diversity within the phyllosphere of espeletia species in an andean high-mountain ecosystem. *Appl. Environ. Microbiol.* 82, 1807–1817. doi: 10.1128/AEM.02781-15

Segata, N., Izard, J., Waldron, L., Gevers, D., Miropolsky, L., Garrett, W. S., et al. (2011). Metagenomic biomarker discovery and explanation. *Genome Biol.* 12:R60. doi: 10.1186/gb-2011-12-6-r60

Shannon, P., Markiel, A., Ozier, O., Baliga, N. S., Wang, J. T., Ramage, D., et al. (2003). Cytoscape: a software environment for integrated models of biomolecular interaction networks. *Genome Res.* 13, 2498–2504. doi: 10.1101/gr.1239303

Shi, W. C., Li, M. C., Wei, G. S., Tian, R. M., Li, C. P., Wang, B., et al. (2019). The occurrence of potato common scab correlates with the community composition and function of the geocaulosphere soil microbiome. *Microbiome* 7:14. doi: 10.1186/s40168-019-0629-2

Singh, B. K., Liu, H., and Trivedi, P. (2020). Eco-holobiont: a new concept to identify drivers of host-associated microorganisms. *Environ. Microbiol.* 22, 564–567. doi: 10.1111/1462-2920.14900

Sloan, W. T., Lunn, M., Woodcock, S., Head, I. M., Nee, S., and Curtis, T. P. (2006). Quantifying the roles of immigration and chance in shaping prokaryote community structure. *Environ. Microbiol.* 8, 732–740. doi: 10.1111/j.1462-2920.2005.00956.x

Theis, K. R., Dheilly, N. M., Klassen, J. L., Brucker, R. M., Baines, J. F., Bosch, T. C., et al. (2016). Getting the hologenome concept right: an eco-evolutionary framework for hosts and their microbiomes. *mSystems* 2, e00028–e00016. doi: 10.1128/mSystems.00028-16

Wei, Z., Hu, J., Gu, Y. A., Yin, S., Xu, Y., Jousset, A., et al. (2018). *Ralstonia solanacearum* pathogen disrupts bacterial rhizosphere microbiome during an invasion. *Soil Biol. Biochem.* 118, 8–17. doi: 10.1016/j.soilbio.2017.11.012

Weiland-Brauer, N. (2021). Friends or foes-microbial interactions in nature. *Biology* 10:496. doi: 10.3390/biology10060496

Wen, T., Xie, P., Penton, C. R., Hale, L., Thomashow, L. S., Yang, S., et al. (2022). Specific metabolites drive the deterministic assembly of diseased rhizosphere microbiome through weakening microbial degradation of autotoxin. *Microbiome* 10:177. doi: 10.1186/s40168-022-01375-z

Wen, T., Zhao, M., Liu, T., Huang, Q., Yuan, J., and Shen, Q. (2020). High abundance of *Ralstonia solanacearum* changed tomato rhizosphere microbiome and metabolome. *BMC Plant Biol.* 20:166. doi: 10.1186/s12870-020-02365-9

Woodhams, D. C., Bletz, M. C., Becker, C. G., Bender, H. A., Buitrago-Rosas, D., Diebboll, H., et al. (2020). Host-associated microbiomes are predicted by immune system complexity and climate. *Genome Biol.* 21:23. doi: 10.1186/s13059-019-1908-8

Xun, W., Li, W., Xiong, W., Ren, Y., Liu, Y., Miao, Y., et al. (2019). Diversity-triggered deterministic bacterial assembly constrains community functions. *Nat. Commun.* 10, 3833–3843. doi: 10.1038/s41467-019-11787-5

Yu, Y., Dunaway, S., Champer, J., Kim, J., and Alikhan, A. (2020). Changing our microbiome: probiotics in dermatology. *Br. J. Dermatol.* 182, 39–46. doi: 10.1111/bjd.18659

Yuan, J., Zhao, J., Wen, T., Zhao, M. L., Li, R., Goossens, P., et al. (2018). Root exudates drive the soil-borne legacy of aboveground pathogen infection. *Microbiome* 6:156. doi: 10.1186/s40168-018-0537-x

Zhang, H., Wu, C., Wang, F., Wang, H., Chen, G., Cheng, Y., et al. (2022). Wheat yellow mosaic enhances bacterial deterministic processes in a plant-soil system. *Sci. Total Environ.* 812:151430. doi: 10.1016/j.scitotenv.2021.151430

Zhou, J. Z., and Ning, D. L. (2017). Stochastic community assembly: does it matter in microbial ecology? *Microbiol. Mol. Biol. R.* 81:e00002-17. doi: 10.1128/MMBR.00002-17

frontiers | Frontiers in Microbiology

TYPE Original Research
PUBLISHED 12 May 2023
DOI 10.3389/fmicb.2023.1155088

OPEN ACCESS

EDITED BY
Jesús Navas-Castillo,
IHSM La Mayora, CSIC, Spain

REVIEWED BY
Jia Liu,
Jiangxi Academy of Agricultural Sciences (CAAS), China
Jianping Wu,
Yunnan University, China

*CORRESPONDENCE
Yuji Jiang
✉ yjjiang@issas.ac.cn

†These authors have contributed equally to this work

RECEIVED 31 January 2023
ACCEPTED 19 April 2023
PUBLISHED 12 May 2023

CITATION
Shi G, Luan L, Zhu G, Zeng Z, Zheng J, Shi Y, Sun B and Jiang Y (2023) Interaction between nematodes and bacteria enhances soil carbon sequestration under organic material amendments.
Front. Microbiol. 14:1155088.
doi: 10.3389/fmicb.2023.1155088

Interaction between nematodes and bacteria enhances soil carbon sequestration under organic material amendments

Guangping Shi[1,2†], Lu Luan[1,3†], Guofan Zhu[1,2], Zhaoyang Zeng[1,2], Jie Zheng[1,3], Yue Shi[1,4], Bo Sun[1] and Yuji Jiang[1,3*]

[1]State Key Laboratory of Soil and Sustainable Agriculture, Institute of Soil Science, Chinese Academy of Sciences, Nanjing, China, [2]University of Chinese Academy of Sciences, Beijing, China, [3]Ecological Experimental Station of Red Soil, Chinese Academy of Sciences, Yingtan, China, [4]College of Land Resources and Environment, Jiangxi Agricultural University, Nanchang, China

The process of carbon (C) sequestration plays an important role in soil fertility and productivity, yet most studies have focused on the individual role of the bacterial community. However, an in-depth mechanistic understanding of how soil nematodes interact with the bacterial community to regulate soil C accumulation is still lacking. We conducted a 10-year field experiment to explore the nematode and bacterial communities and determine the influence of nematode-bacteria interactions on C mineralization, microbial metabolic quotient (qCO_2), and carbon use efficiency (CUE) under the organic material amendments, including chemical fertilizers with straw (NS), chemical fertilizers with straw and pig manure (NSM), and chemical fertilizer with straw biochar (NB). Here, our results showed the abundance of bacterial and nematode communities was significantly higher under NS, NSM, and NB treatments than under chemical fertilizers (N) treatment, with the highest abundance under the NSM treatment. The enrichment index and functional dispersion index were significantly higher under NSM treatment than under N, NS, and NB treatments, while the channel index followed the opposite pattern. Structural equation modeling indicated that the potential predation pressure induced by nematodes may improve bacterial abundance, with positive cascading effects on C sequestration. Collectively, our study highlights the functional importance of nematode-microorganism interactions in mediating C dynamics under organic material amendments.

KEYWORDS

bacterial community, nematode assemblage, nematode indices, carbon mineralization, microbial metabolic quotient, organic material amendments

Introduction

Soil organic carbon (SOC) reservoir is the major component of the carbon (C) pool in terrestrial ecosystems and plays an important role in soil fertility and crop yield (Cook-Patton et al., 2020). Excessive use of chemical fertilizers degrades soil structure and reduces C content, while the application of organic materials, especially straw and manure, is considered an effective measure to improve soil quality and C sequestration (Wei et al., 2021). Straw itself is rich in mineral elements and nutrients and is often combined with chemical fertilizers to simultaneously improve C turnover and accumulation (Berhane et al., 2020). Pig manure efficiently increases

easily decomposable particulate organic carbon due to its high nitrogen content and low carbon to nitrogen ratio (Gross and Glaser, 2021). A comprehensive understanding of the biological mechanisms of C turnover is paramount to quantifying C accumulation potential in agricultural ecosystems.

Microorganisms are the primary C decomposers in agricultural ecosystems (Zechmeister-Boltenstern et al., 2015). External carbon sources cause a series of changes in the abundance and composition of the soil microbial community, thereby affecting microbial metabolic quotient and C mineralization. Microbial biomass carbon is an essential component of the C pool (Fan et al., 2021). Microorganisms alter the amount and chemical composition of soil organic matter through decomposition, respiration, growth, and death (Min et al., 2021). While C measurements can represent changes in the magnitude of C storage, indicators related to microbial biomass and respiration can predict long-term trends in C sequestration (Zhou et al., 2017). The ratio of soil microbial respiration to growth (qCO_2) indicates the energy required to maintain microbial biomass (Fließbach et al., 2000), with the higher qCO_2 indicating faster nutrient turnover and lower carbon use efficiency (CUE) (Wardle and Ghani, 1995). It is generally accepted that increasing microbial CUE can enhance C sequestration (Sinsabaugh et al., 2013). However, the potential mechanism by which CUE varies with substrate quality and predation pressure needs to be further investigated (Dijkstra et al., 2015; Kane et al., 2022).

Traditional research has mainly focused on the individual role of the soil microbial community in C turnover and accumulation, but the understanding of how the interactions between soil animals and microorganisms affect C dynamics under the organic material amendments is still emerging (Van Den Hoogen et al., 2019). Nematodes are widely known as the most abundant soil invertebrates and contribute significantly to C decomposition and cycling through their interactions with the bacterial community (Jiang et al., 2013; Pausch et al., 2016; Zhang et al., 2021). Nematode predation alters the diversity and structure of the bacterial community and limits bacterial community size and physiology, thereby affecting C-related microbial functions (Grandy et al., 2016; Wang et al., 2021) A global-scale study further highlights the importance of nematode assemblages in soil food webs, nutrient cycling, and ecosystem functioning (Van Den Hoogen et al., 2019). Based on their board distribution and feeding traits, the ecological indices of nematode communities are well established as indicators of soil environmental conditions and food web status (Ferris et al., 2001). Although a rapidly growing literature has investigated the nematode-microbe interactions, there is still insufficient research on the direction and strength of nematode-microbe interactions on the regulation of C dynamics at different fertility levels (Grandy et al., 2016). Therefore, it is necessary to explore the role of nematodes on microorganisms to better understand the ecological role of nematode predation in mediating C dynamics.

Here, we aimed to examine how the influence of nematode predation affects C mineralization and sequestration by affecting the bacterial community in response to the organic material amendments. We used a field experiment under five fertilization treatments, and focused on answering the following two questions: (1) how the diversity, abundance, and composition of bacterial and nematode communities varied with the addition of different organic materials? and (2) whether and to what extent the nematode-bacteria interactions mediated C sequestration subject to organic material amendments? To address these questions, we examined the bacterial community structure by using Illumina sequencing, identified nematodes under a microscope, and determined qCO_2 and CUE. We hypothesized that the nematode predation on bacterial community would improve C turnover and accumulation under organic material amendments.

Materials and methods

Description of the field experiment

The long-term experiment was established at the Yingtan National Agro-Ecosystem Observation and Research Station of the Chinese Academy of Sciences, Jiangxi Province (E116°55′30″, N28°15′20″). The climate of the region is characterized as warm and monsoon with a mean annual temperature of 17.6°C and a mean annual precipitation of 1795 mm. The soil is an acid loamy clay derived from Ferric Acrisols in the FAO classification system and Udic Ferralsols in the Chinese Soil Taxonomy.

The field experiment was initiated in 2011, and included five treatments with three replications in a randomized design: (1) no fertilizer (CK); (2) NPK chemical fertilizers (N); (3) NPK chemical fertilizers with straw (NS); (4) NPK chemical fertilizers with straw and pig manure (NSM); and (5) NPK chemical fertilizers with straw biochar (NB). Each of the 15 plots was applied to 20 m long and 5 m wide. The monoculture corn (cultivar Suyu 24) was annually planted in April and harvested in July. Except for CK, urea (N 150 kg hm^{-2}, Shanxi Weihe Heavy Chemical Co., Ltd.), calcium–magnesium-phosphate fertilizer (P_2O_5 75 kg hm^{-2}, Yifeng Fertilizer Co. Ltd.), and potassium fertilizer (K_2O 60 kg hm^{-2}, Mosaic Potash Esterhazy LP.) were once applied in each treatment. The amount of corn straw, pig manure, and straw biochar was applied as 1,000 kg C hm^{-2} $year^{-1}$.

Soil sampling and chemical analysis

Soil samples were collected after the corn harvest at the end of July 2020. A total of 10 sampling points were taken from 0 to 20 cm topsoil samples using an S-shaped sampling method, and 1 kg soil samples were taken using the quartering method after evenly mixing. After that, fresh soil samples were placed in clean bags on ice and immediately transported to the laboratory. Soil samples in each treatment were separated into two subsamples for analysis of soil chemical properties, and the bacterial and nematode communities, respectively.

Soil pH was determined using a glass electrode at a water: soil ratio of 2.5:1 (v/w). Soil organic carbon (SOC) and total potassium (TK) were measured by the Walkley-Black wet digestion method and flame photometry, respectively (Jackson, 1958). Total phosphorus (TP) and total nitrogen (TN) were determined by molybdenum-blue colorimetry and Kjeldahl digestion, respectively (Zheng et al., 2009). Cation exchange capacity (CEC) was determined by the ammonium acetate saturation method (Kitsopoulos, 1999). Microbial biomass carbon (MBC) was measured by the chloroform fumigation incubation method (Vance et al., 1987).

Quantitative PCR and illumina sequencing

The DNA from the soil sample was extracted following standard procedures of the DNeasy PowerSoil Extraction Kit (MoBio Laboratories, Carlsbad, CA, USA). DNA quality and content were checked using a NanoDrop spectrophotometer. The copy number of the bacterial community was determined by quantitative PCR (*q*PCR) using universal primers 515F and 907R (Biddle et al., 2008). Each sample was amplified in a 30 μl reaction mix containing 15 μL 2 × qPCR Mix, 0.5 μl forward primer (10 μM), 0.5 μl reverse primer (10 μM), and 2 μL template DNA. The *q*PCR conditions were: initial denaturation at 95°C for 10 min, followed by 40 cycles of 95°C for 30 s, 60°C for 30 s, 72°C for 30 s, and a final extension at 72°C for 10 min. The *q*PCR amplification was performed in triplicate with efficiencies >95% and r^2 values >0.99.

The amplicon fragments using the same primer pairs were subjected to high-throughput sequencing on the Illumina MiSeq. Raw sequencing data were processed using the Quantitative Insights into Microbial Ecology (QIIME) pipeline (version 1.9.1). Sequences with masses less than 20 and lengths less than 300 bp were removed, matched to different samples based on specific tags, and assigned to separate files for the bacterial 16S *rRNA* gene. The remaining sequences were chimera removed and clustered into operational taxonomic units (OTUs) at 97% similarity using the Usearch algorithm. The representative sequence for each OTU with the highest abundance was then chosen. Taxonomic assignments were performed against the Silva database (version 138) for the bacteria community. The command "alpha_diversity.py" of the QIIME software was used to calculate the Shannon index of bacterial alpha-diversity after the rarefaction of all samples to the same sequencing depth of 28,883 sequences.

Carbon use efficiency and microbial metabolic quotient

Soil microbial growth rate and respiration rate were determined by the ^{18}O labeling method to determine carbon use efficiency (CUE) (Zheng et al., 2019). Briefly, 1 g of precultured soil sample was added into a 2 mL injection bottle, three replicates were set for each sample, and $H_2{}^{18}O$ (97.0%, ABX, Israel) was added to one of them to label the soil with ^{18}O. The abundance was adjusted to 20%, and an equal volume of deionized water was added to another portion as a natural ^{18}O natural abundance control. After the added water was thoroughly mixed with the soil, the sample was placed in a 50 mL headspace vial, and aluminum caps were crimped on to seal the headspace vials. The headspace vial gas was then immediately replaced with CO_2-free air to limit the CO_2 concentration in the vial. A blank headspace vial without soil was used as a blank control throughout the experiment. After all manipulations, the incubation vials were incubated at 15°C for 24 h. After the incubation, the gas in the headspace vial was collected using a syringe with a three-way valve, and the CO_2 concentration was measured using a gas chromatograph (GC-7890B, Agilent, USA). After freeze-drying the soil samples in the injection vials, the DNA was extracted and transferred to a silver cup, and then dried at 45°C. The ^{18}O abundance and oxygen content were determined by an elemental analyzer coupled to an isotope ratio mass spectrometer using the EA-IRMS system (Thermo Scientific, TX, USA). The newly produced DNA content ($DNA_{produced}$, μg) of the soil samples during the 24-h incubation period was calculated as follows:

$$DNA_{produced} = O_{total} \times \frac{at\%excess}{100} \times \frac{100}{at\%label} \times \frac{100}{31.21}$$

In the formula, O_{total} (μg) is the oxygen content in the dried sample DNA; $at\%_{excess}$ is the difference between the abundance of ^{18}O in the labeled and unlabeled samples; $at\%_{label}$ is the abundance of ^{18}O in the final soil solution.

The ratio of MBC to DNA content of each precultured sample was calculated as a conversion factor (*fDNA*), and *fDNA* was used to convert the newly generated DNA content in the sample during the culture period into MBC content, thereby calculating the microbial growth rate (*Growth*, ng C· g^{-1} h^{-1}) formula is as follows:

$$\text{Growth} = \frac{\text{fDNA} \times \text{DNAproduced} \times 1000}{\text{DW} \times \text{t}}$$

In the formula, *DW* (g) is soil dry weight; *t* (h) is cultivation time.

The calculation formula of microbial respiration rate (*Respiration*, ng C g^{-1} h^{-1}) is as follows:

$$\text{Respiration} = \frac{\Delta\text{CO2}}{22.4 \times \text{DW} \times \text{t}} \times M \times V \times 1000$$

where ΔCO_2 (ppm) is the increase in CO_2 concentration in the closed headspace vessel during the incubation period of the soil sample; *M* is the molar mass of carbon (12.01 g mol^{-1}); *V* (l) is the total volume of gas; *DW* (g) is the soil dry weight; *t* (h) is incubation time.

The formula for calculating the metabolic entropy (qCO_2, ng C μg MBC^{-1} h^{-1}) is as follows:

$$q\text{CO2} = \frac{\text{Respiration}}{\text{MBC}}$$

The formula for calculating CUE is as follows:

$$\text{CUE} = \frac{\text{Growth}}{\text{Growth} + \text{Respiration}}$$

Carbon mineralization

The determination of C mineralization adopts an indoor constant temperature culture, and C mineralization was determined by the alkali absorption technique: weigh 100 g of fresh soil in a 500 mL culture bottle and spread it on the bottom of the bottle. The water holding capacity is calculated when the maximum water holding capacity is 60%. Then, an absorption bottle containing 20 mL of NaOH solution at a concentration of 0.5 mol L^{-1} was placed in the culture bottle, the culture bottle was sealed with a cap, and placed in a constant temperature incubator at 25°C for 30 days under dark conditions. The solution in the absorption bottle was taken out,

washed completely into the conical flask, and 20 mL of 1 mol L^{-1} $BaCl_2$ solution and two drops of phenolphthalein indicator were added. The remaining NaOH was titrated and neutralized with 0.4 mol L^{-1} HCl solution until the red color disappeared, and the CO_2 release by HCl consumption was calculated.

$$\text{Soil C mineralization}\left(\text{calculated as } CO_2 \text{ release}\right) = c_{HCl} \times \left(V_0 - V_1\right) \times 22 / 0.1,$$

where c_{HCl} is the concentration of hydrochloric acid (mol l^{-1}), V_0 is the volume of the blank titration, and V_1 is the volume of hydrochloric acid consumed.

Nematode community and ecological indices

Baermann funnel method was used to extract nematodes (Cesarz et al., 2019). Briefly, 100 g of soil was spread evenly on the funnel device and then water was added to submerge the soil. The spring clip was opened to obtain an aqueous solution of nematodes after 72 h. The nematodes were killed at 60°C and stored in a 4% formalin solution. At least 150 nematodes per sample were collected and placed under a light microscope for nematode identification. Nematodes were classified into four trophic guilds based on morphology (Yeates, 1998), including bacterivores (Ba), fungivores (Fu), plant-parasites (Pp), and omnivores-predators (OP). Predation pressure of nematodes on bacteria was calculated as the ratio of the number of nematodes to bacterial copy number (Mathisen et al., 2016). Furthermore, we selected the nematode indices to indicate the food web status, including Shannon–Wiener index, channel index (CI), enrichment index (EI), structure index (SI), functional dispersion index (FDis), and free-living nematode maturity index (MI) (Ferris et al., 2001). The corresponding calculation formulas are as follows:

$$H = -\Sigma p_i \left(lnp_i\right)$$

$$MI = \Sigma\left(c - p_i\right) \mathrm{p_i}\left(\text{free} - \text{living nematode}\right)$$

$$CI = 100\left(0.8 \times \mathrm{Fu2} / \left(3.2 \times \mathrm{Ba1} + 0.8 \times \mathrm{Fu}\right)\right)$$

$$EI = 100 \times \left(e / \left(e + b\right)\right)$$

$$SI = 100 \times \left(s / \left(s + b\right)\right)$$

$$\text{Predation pressure} = \mathrm{Ba} / \text{bacterial copies}$$

In these formulas, p_i is the proportion of individuals of the ith taxon in the total number of nematodes; Ba, Fu, and PP represent the number of bacterivorous, fungivorous, and plant-parasitic nematodes, respectively; *e*, *b*, and *s* are enriched components (Ba1 and Fu2), basic components (Ba2 and Fu2), structural components (Ba3-Ba5, Fu3-Fu5, Om3-Om5, and Ca2-Ca5), respectively. The CI is between 0 and 100, greater than 50 indicates that the fungal degradation pathway is dominant, and less than 50 indicates that the bacterial degradation pathway is dominant. EI and SI vary from 0 to 100, with higher EI and SI indicating better nutritional status and better food web connectivity, respectively. Predation pressure refers to the predation pressure of bacterivorous nematodes on bacteria.

Statistical analyses

Significant difference analysis of the data was performed using one-way ANOVA with SPSS 24.0 (Kim, 2017). Spearman's rank correlation test was used to measure the correlations between soil properties, bacterial and nematode communities, and C mineralization (Sedgwick, 2014). The varpart function in the "vegan" package was used to determine the contribution of different types of factors to bacterial diversity, community composition, and C mineralization. Non-metric multidimensional scaling (NMDS) analysis based on Bray-Curtis distance was conducted to characterize differences in the structure of bacterial and nematode communities (Cox and Ferry, 1993). Redundancy analysis was used to estimate the relationships between soil variables, bacterial community, and nematode assemblage (Capblancq et al., 2018). The envfit function in the "vegan" package was used to perform a permutation test to test for potentially significant effects of soil properties and nematode index on community structure (Oksanen, 2015). The random forest model was constructed using the package "randomForest" of the R software (Liaw and Wiener, 2002). The "rfUtilities" and "rfPermute" packages were used to test the *p* value of each variable and the model, and to check the effect of each factor on the C mineralization. Structural equation modeling (SEM) was constructed to assess the potential effects of soil factors, and the bacterial and nematode communities on C mineralization. The R-packaging "lavan" was used for SEM analysis, and the data used in the model were standardized (Mamet et al., 2019).

Results

Soil chemical properties and carbon mineralization

One-way ANOVA showed that soil chemical properties were significantly changed under different organic material amendments (Figure 1). Soil pH ranged from 4.4 to 4.8, and was significantly ($p = 0.048$) higher under NB treatment than under the other four treatments. Soil organic carbon (SOC) was significantly increased ($p < 0.001$) under NS, NSM, and NB treatments compared to CK and N treatments. Total phosphorus (TP) and total nitrogen (TN) were the highest under the NSM treatment and the lowest under CK treatment. There was no significant ($p > 0.05$) difference in cation-exchange capacity (CEC) and total potassium (TK) among all treatments. Carbon mineralization (CM) under NSM treatment was significantly ($p < 0.05$) higher than that under N, NS, and NB treatments (Supplementary Figure S1A). Carbon use efficiency (CUE) under N and NSM treatments was significantly ($p < 0.05$)

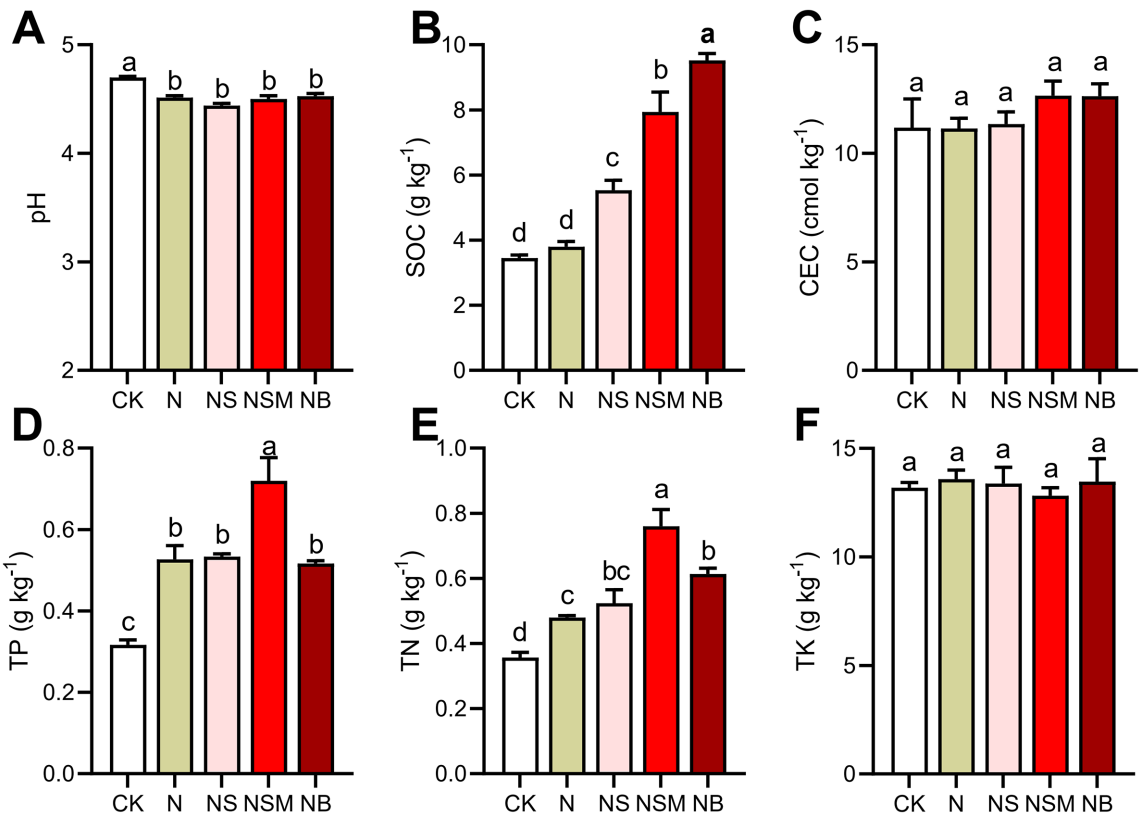

FIGURE 1
Soil chemical properties under the five fertilization treatments, including **(A)** pH, **(B)** soil organic carbon (SOC), **(C)** cation-exchange capacity (CEC), **(D)** total phosphorus (TP), **(E)** total nitrogen (TN), **(F)** total potassium (TK). Different lowercase letters indicate significant differences based on Tukey's HSD test (p <0.05). CK, no fertilizer; N, chemical fertilizers; NS, chemical fertilizers with straw; NSM, chemical fertilizers with straw and pig manure; NB, chemical fertilizers with biochar.

improved compared to CK, NS, and NB treatments (Supplementary Figure S1B).

Nematode community composition and ecological indices

Among all treatments, the dominant trophic guilds of the nematode community were bacterivores (Ba, 47.6%), followed by fungivores (Fu, 25.7%), omnivores-predators (OP, 13.2%) and plant parasites (PP, 13.3%) (Figure 2A). The dominant genus of bacterivorous nematodes was *Cephalobus*, followed by *Eucephalobus* and *Protorhabditis* (Figure 2A). Nonmetric multidimensional scale (NMDS) analysis showed that the fertilization treatments significantly changed the composition of the nematode community (Figure 2B). Nematode community compositions showed that nematode assemblages under organic treatments were significantly (p < 0.05) distinct from that under CK treatment (Figure 2B). The numbers of total nematodes and bacterivores were significantly (p < 0.05) increased under NSM treatment than other treatments (Supplementary Figure S2A). Metabolic footprints of bacterivores and omnivores-predators were significantly (p < 0.05) increased under NSM treatment than N, NS, and NB treatments, while there was no significant difference in metabolic footprints of fungivores among different treatments (Supplementary Figure S2B). We further found that the ecological indices of the nematode community significantly (p < 0.05) varied among fertilization treatments. Nematode diversity, as indicated by the Shannon index, was significantly (p < 0.05) higher under NSM treatments than under N treatment (Figure 3A). Functional dispersion index (FDis) was significantly (p < 0.05) improved by NS and NSM treatments compared to CK treatment, while channel index (CI) followed the opposite trend (Figures 3B,C). The maturity index (MI) of free-living nematodes under NS and NB treatments was significantly (p < 0.05) higher than that under CK and N treatments (Figure 3D). The enrichment index (EI) and structure index (SI) were significantly (p < 0.05) higher under NSM treatment than under CK and N treatments (Figures 3E,F).

Bacterial community and metabolic activities

Organic material amendments significantly (p < 0.05) differed the bacterial communities from those under CK and N treatments (Figure 4A). Bacterial community compositions showed that bacterial assemblages under four fertilization treatments were significantly (p < 0.05) distinct from that under CK treatment. At the phylum level, the bacterial community was dominated by Chloroflexi (30.5%), Proteobacteria (23.8%), Acidobacteria (15.1%), and Actinobacteria (14.0%) (Figure 4B). The relative abundance of Proteobacteria and

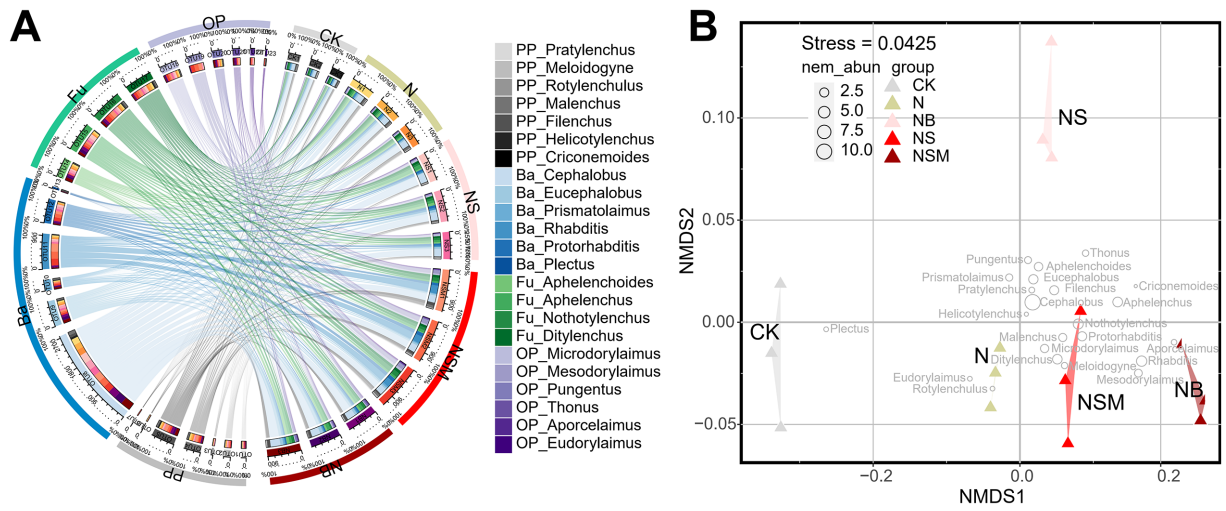

FIGURE 2
Chord diagram showing the relative abundances of nematode at the genus level under different fertilization treatments **(A)**. The non-metric multi-dimensional scaling plot (NMDS) depicts the distance between the samples based on Bray-Curtis similarities **(B)**. Different circle sizes represent the relative abundance of nematodes. CK, no fertilizer; N, chemical fertilizers; NS, chemical fertilizers with straw; NSM, chemical fertilizers with straw and pig manure; NB, chemical fertilizers with biochar.

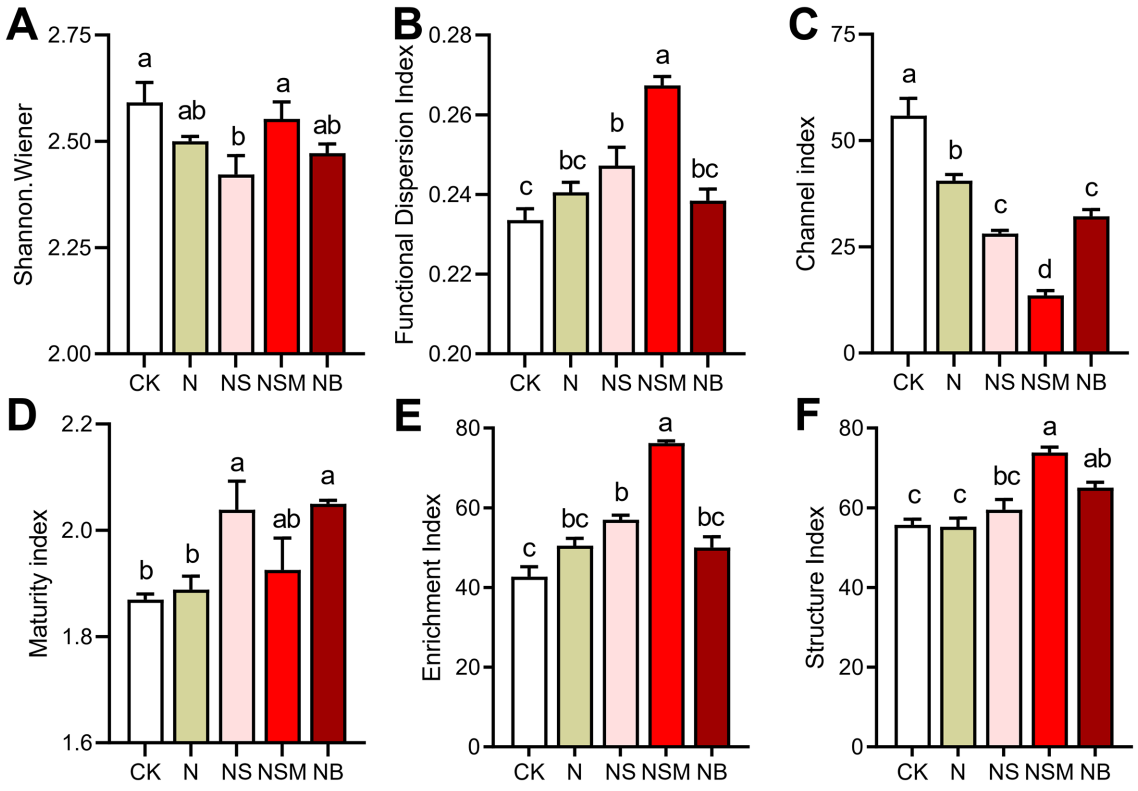

FIGURE 3
Nematode ecological index under the five fertilization treatments, including **(A)** Shannon–Wiener index, **(B)** functional dispersion index (FDis), **(C)** Channel index (CI), **(D)** maturity index (MI) of free-living nematodes, **(E)** Enrichment index (EI) and **(F)** Structure index (SI). Different lowercase letters indicate significant differences based on Tukey's HSD test ($p < 0.05$). CK, no fertilizer; N, chemical fertilizers; NS, chemical fertilizers with straw; NSM, chemical fertilizers with straw and pig manure; NB, chemical fertilizers with biochar.

Actinobacteria was significantly ($p < 0.01$) enriched under NS and NSM treatments compared to CK and NB treatments, while Chloroflexi and Acidobacteria were significantly higher under NB treatment (Figure 4B). The copy number and Shannon index of the bacterial community were significantly increased ($p < 0.05$) under NS, NSM, and NB treatments compared to CK and N treatments, while

the microbial metabolic quotient (qCO_2) followed the opposite trend (Figure 5).

Redundancy analysis showed that all parameters explained 77.8% of the variation in the bacterial communities (Figure 6A). The main grouping factors under NS and NSM treatments were *Protorhabditis* and OP, and Proteobacteria and Actinobacteria were clustered with a high relative abundance of bacterivores and *Protorhabditis*. The envfit test indicated that soil chemical factors (TP, pH, and TN) and nematode assemblage (the numbers of total nematodes, bacterivores, omnivores-predators, *Protorhabditis* and *Cephalobus*, CI, and predation pressure) had significant effects on the bacterial community composition ($r^2 = 0.61$ to 0.87, $p < 0.05$) (Figure 6B). Variance partitioning analyses showed that the interactions between the environmental factors and nematode indices could explain 61% of the variation of bacterial communities, while the two independent explanations were only 6 and 8% (Figure 6C). Environmental factors and nematode indices can independently explain 15 and 17% of the variation of bacterial biomass, respectively, and interactions between the two major components were up to 25% (Figure 6D).

Potential nematode-bacteria interactions affected C sequestration

Correlation heatmap analysis showed that the bacterial diversity and abundance and CM were significantly positively correlated with the numbers of total, bacterivorous and omnivorous-predatory nematodes, predation pressure, EI, and FDis ($r = 0.66$ to 0.89, $p < 0.05$), but negatively correlated with CI ($r = -0.84$ to -0.87, $p < 0.05$) (Figure 7A). In contrast, the bacterial community composition (PCOA1) ($r = -0.76$ to -0.83, $p < 0.05$) and qCO_2 ($r = -0.50$ to -0.64, $p < 0.06$) exhibited negative relationships with the abundance of total and bacterivorous nematodes,

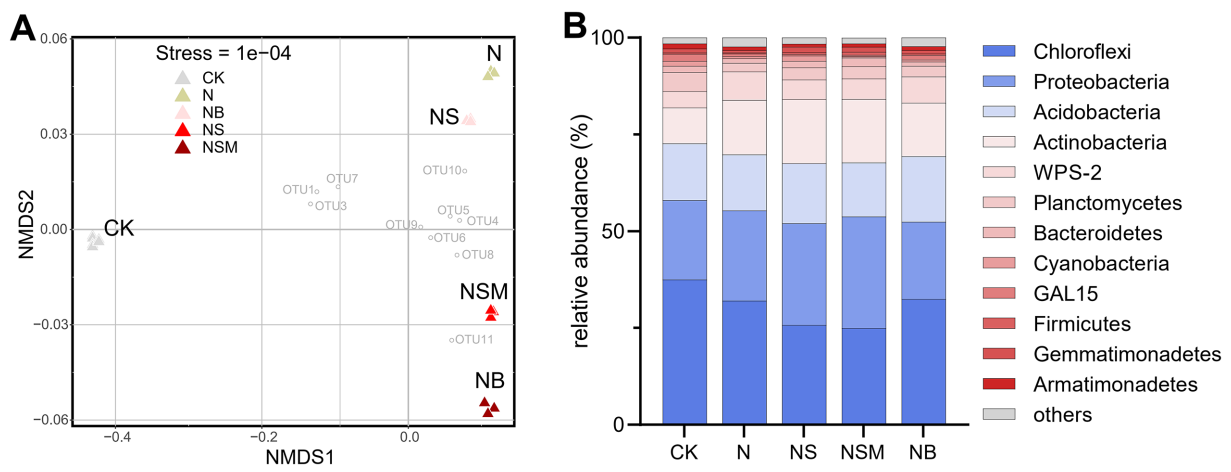

FIGURE 4
The non-metric multi-dimensional scaling plot (NMDS) of bacterial community structures of the five treatments **(A)**. The mean relative abundance of bacterial phyla within each treatment **(B)**. CK, no fertilizer; N, chemical fertilizers; NS, chemical fertilizers with straw; NSM, chemical fertilizers with straw and pig manure; NB, chemical fertilizers with biochar.

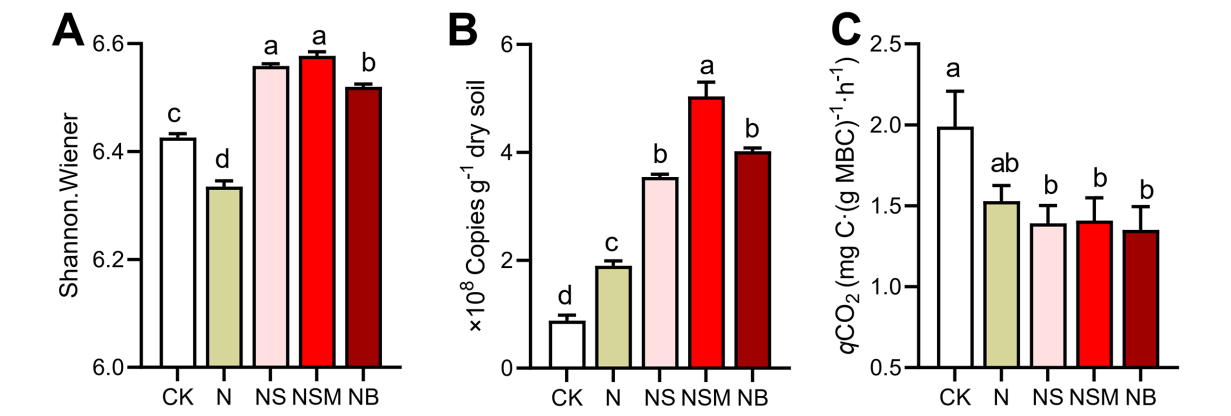

FIGURE 5
The diversity (**A**, Shannon index) and abundance (**B**, copy numbers of 16S *RNA*) of bacterial communities and microbial metabolic quotient (**C**, qCO_2) under the five fertilization treatments. Different lowercase letters indicate significant differences based on Tukey's HSD test ($p < 0.05$). CK, no fertilizer; N, chemical fertilizers; NS, chemical fertilizers with straw; NSM, chemical fertilizers with straw and pig manure; NB, chemical fertilizers with biochar.

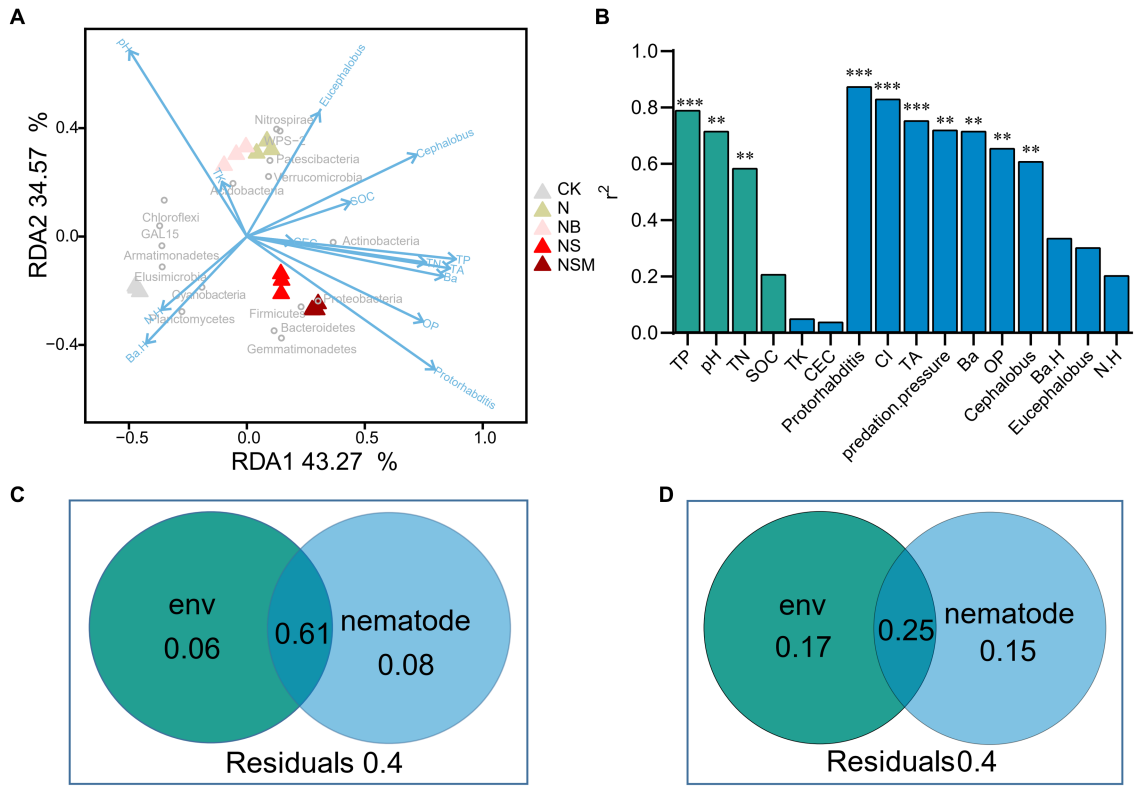

FIGURE 6
Redundancy analysis (RDA) indicates the relationships of soil properties and nematode indices with bacterial community **(A)**. Contributions of each factor to community structure based on envfit test (Monte Carlo permutation test) **(B)**. The proportion of soil chemical properties and nematodes explaining the composition (**C**, first principal coordinates, PCoA1) and abundance (**D**, copy number of 16S *rRNA*) of bacterial community. Soil chemical properties include soil pH, soil organic carbon (SOC), total nitrogen (TN), total phosphorus (TP), total potassium (TK), and cation-exchange capacity (CEC). The nematode community include the number of total nematodes (TA), bacterivores (Ba), and omnivores-predators (OP), and diversity (Shannon index, N.H). *p <0.05, **p <0.01, ***p <0.001.

predation pressure, SI, and FDis. Variance partitioning analyses showed that soil chemical factors, nematode indices, and bacterial characteristics individually explained 36, 15, and 10% of the variances in CM, and interactively contributed to 15% of the observed variation (Figure 7B). Specifically, random forest analysis soil TN (6.5%), TP (7.1%), the abundance (4.7%) and composition (8.6%) of the bacterial community, and the numbers of total nematode (7.6%), bacterivores (7.5%), and omnivores-predators (6.7%) contributed significantly ($p<0.05$) to C mineralization (Figure 7C). Structural equation modeling indicated that the nematode assemblage indirectly affected soil C sequestration by regulating bacterial community structure and biomass (Figure 7D). Specifically, the bacterial community was positively associated with the nematode assemblage ($r=0.42$, $p<0.001$), but negatively associated with qCO_2 ($r=-0.94$, $p<0.001$).

Discussion

Bacterial community varied with organic material amendments

We revealed that organic material amendments could significantly promote soil fertility by improving SOC, TN, and TP. Corn straw and pig manure are rich in soil organic matter and nutrients, and biochar is a carbon-rich material. The addition of these organic materials greatly increases SOC content (Cooper et al., 2011; Sandhu et al., 2017). Notably, SOC, TP, and TN were significantly increased under NSM treatment compared to N treatment, but not significantly increased under NS treatment. The simultaneous utilization of straw and manure reduces the C/N ratio of straw, resulting in faster decomposition and turnover rates of soil nutrients (Zheng et al., 2022a). Compared with corn straw, manure treatments can substantially enhance soil phosphorus content due to the high proportion of phosphorus. The NSM treatment significantly increased the contents of TN and TP by improving the organic N mineralization of straw compared with NS and NB treatments. In particular, the more reasonable ratio of corn straw and pig manure leads to a higher efficiency of the positive priming effect on straw decomposition, and a higher level of soil fertility (Abdalla et al., 2022). Soils treated with straw and pig manure enrich the food resources for microbial growth, and stimulate bacterial biomass and diversity (Hussain et al., 2019). Biochar with a good porous structure may provide habitats for microorganisms that are protected from predators, thereby preserving bacterial biomass within the biochar (Pietikäinen et al., 2000). Compared to NB treatment, we found that lower SOC under NSM treatment was not consistent with the trend of bacterial abundance, which may be partially explained by the alleviation of nutrient limitation (Wei et al., 2020). Organic material amendments promote soil structural complexity and

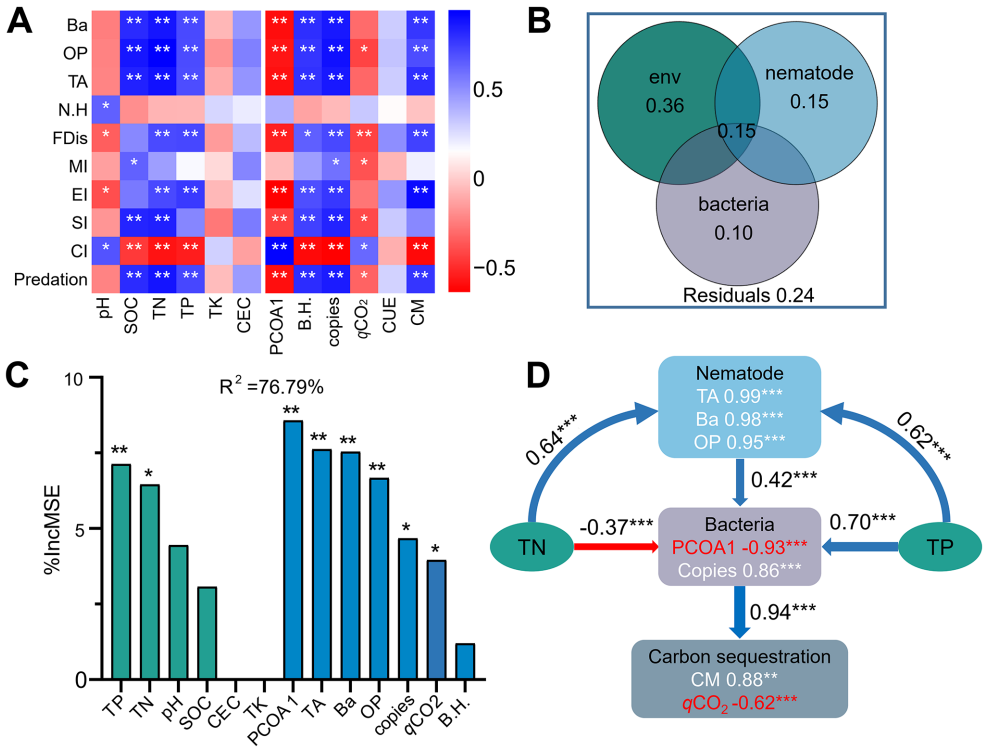

FIGURE 7
Spearman's correlation coefficients between soil properties, the bacterial and nematode communities, and carbon mineralization **(A)**. Blue and red denote positive and negative correlations, respectively. * p <0.05, ** p <0.01, *** p <0.001. Contribution of soil chemical properties and the bacterial and nematode communities to carbon mineralization using variance partitioning analysis **(B)**. Mean predictor importance (% of increased mean square error, MSE) of soil chemical properties and the bacterial and nematode communities on carbon mineralization using random forest modeling **(C)**. Structural equation modeling shows the direct and indirect effects of soil properties and the bacterial and nematode communities on carbon sequestration **(D)**. Soil chemical properties include soil pH, soil organic carbon (SOC), total nitrogen (TN), total phosphorus (TP), total potassium (TK), and cation-exchange capacity (CEC). The bacterial community include diversity (Shannon index, B.H), abundance (copy number of 16S rRNA) and composition (first principal coordinates, PCoA1). The nematode community include the number of total nematodes (TA), bacterivores (Ba), and omnivores-predators (OP), and diversity (Shannon index, N.H), Channel index (CI), Enrichment Index (EI) Structure Index (SI), functional dispersion index (FDis), and free-living nematode maturity index (MI) Carbon sequestration is indicated by carbon mineralization (CM) and microbial metabolic quotient (qCO_2).

heterogeneity, and better soil quality contributes to biodiversity by increasing spatial niches (Bebber and Richards, 2022). Soils with more abundant resources and higher nutrient availability can support higher bacterial diversity (Clarke and Gaston, 2006).

Nematode community affected by organic material amendments

We observed that the numbers of total nematodes, bacterivores, and omnivores-predators were considerably increased under NS, NSM, and NB treatments due to the improved food sources and better habitats. Organic material amendments not only create better habitats for nematodes and facilitate their movement through soil pore water, but also improve the ability of nematodes to capture abundant food resources (bacteria) due to the increased soil organic matter (Liu et al., 2016; Jiang et al., 2018b). In addition, our results determined that fertilization practices increased the metabolic footprint of four nematode groups, suggesting that more carbon flowed into the soil nematode community for nematode reproduction (Zhang et al., 2016). Straw and manure amendments increased the functional dispersion index (FDis), indicating weaker species competition within a community and more complete utilization of available resources (Prada-Salcedo et al., 2021). Organic material amendments result in a more bacterially dominated fast cycle decomposition pathway, as indicated by the high number of bacterial-feeding nematodes and low CI value (Zhong et al., 2017). The interaction between EI and SI has been widely used to indicate resource enrichment and food web status (Ferris et al., 2001). The higher values of EI and SI under NSM treatment represent better nutrient status and a more complex soil food web. The higher MI value supported that the food web was more mature under the NS and NB treatments, whereas the lower MI value under NSM treatment was mainly due to the increased presence of opportunistic bacterivorous nematodes. For example, *Rhabditis* and *Protorhabditis* are capable of rapidly reproducing and responding to bacteria when food resources are abundant at high nutrient levels (Hu and Qi, 2010).

Nematode-bacteria interactions enhanced C sequestration

Microbial metabolic quotient (qCO_2) and carbon use efficiency (CUE) are commonly indicated as the rate of C storage in diverse ecosystems, with lower qCO_2 reflecting better soil biophysical conditions and higher CUE reflecting higher metabolic efficiency (Chavarria et al., 2018; Feng et al., 2021). We suggested that the lower qCO_2 value probably indicates better soil biophysical conditions caused by the organic material amendments (NS, NSM, and NB treatments). The variation of qCO_2 may also be related to microbial community composition and biomass, and the values of lower qCO_2 and higher CUE indicate a higher C sequestration potential (Ros et al., 2006; Liu et al., 2020). Phosphorus (P) limitation may have a greater impact on CUE in red soils (Feng et al., 2021). Since biochar is a reluctant compound with extremely limited P content, bacteria need to secrete more extracellular enzymes to acquire nutrients, resulting in a lower CUE value (Allison, 2005; Spohn, 2016). Biochar amendment can induce competition with potential keystone taxa to promote the abundance and diversity of the bacterial community, thereby reducing carbohydrate catabolism and qCO_2 (Chen et al., 2019).

Soil bacterial community plays a crucial role in organic matter decomposition and nutrient availability (Steenwerth et al., 2002). Our results indicated that the nematode predation may increase the abundance of the bacterial community, with positive cascading effects on C sequestration. Numerous studies have pointed out that the bacterial community composition and biomass can mediate qCO_2 and CUE, leading to variations in C mineralization processes (Spohn and Chodak, 2015; Fanin and Bertrand, 2016). Although the higher bacterial abundance indicates that more microorganisms are involved in the C decomposition, qCO_2 was generally found to decrease with increasing microbial biomass. Nematodes are thought to be functionally critical in microbial food webs. Bacterivorous nematodes are primarily involved in regulating rates of C mineralization and altering pathways of energy flow and nutrient cycling by affecting the abundance and composition of the bacterial community (Hungate et al., 2021; Tian et al., 2022). We found that the bacterial biomass significantly increased with the increased predation pressure, with the highest biomass under NSM treatment. Trophic dynamics suggest that the prey biomass at a given trophic level is maximal at a moderate level of predation (Carpenter et al., 1985). Bacterivores can positively influence the diversity and abundance of the bacterial community by providing new niches for colonization and by creating physical and behavioral refuges for prey (Cressman and Garay, 2009; Zheng et al., 2022b). Selective predation by bacterivorous nematodes alters the bacterial community, specifically promoting the relative abundance of Proteobacteria to alter C mineralization (Neidig et al., 2011). *Protorhabditis* shows a strong effect on Gram-negative bacteria (e.g., Proteobacteria), which may be related to their thinner cell wall that makes them more easily digestible by predators (Wilson, 1993). In this case, nematode-bacteria interactions significantly increase the metabolic capacities of six substrate groups of carbon sources, including carbohydrates, carboxylic acids, amino acids, polymers, phenolic acids, and amines (Jiang et al., 2018b). In addition, bacterivore predation further shows a positive relationship with the size and turnover rate of C pools and contributes positively to C sequestration (Zhang et al., 2013; Jiang et al., 2018a). The C sequestration efficiency was improved under NSM treatment, which could be further explained by the bacterial characteristics and nematode indices. The higher level of SOC and TP implied sufficient nutrient resources, which was supported by the higher EI value under NSM treatment than under CK treatment. However, the lower CI indicates the superiority in ensuring less carbon flux to higher trophic levels and the degradation of more labile carbon in the bacterial decomposition channel (Tabarant et al., 2011).

Conclusion

Our findings indicated that organic material amendments enhanced the abundance of bacterial and nematode communities, and significantly altered the structure of bacterial and nematode communities. The higher values of EI, SI, and MI indicated a more mature and stable food web structure, while the low value of CI indicated dominant bacterial decomposition pathways under organic material amendments. We found that nematode predation could increase bacterial abundance and enhance C sequestration, thereby facilitating C accumulation and storage. Taken together, our research integrates the ecology of nematode assemblages with empirical evidence to provide insights into nematode predation driving C dynamics under organic material amendments. As such, a comprehensive understanding of the biological mechanisms of C sequestration may have important implications for the development of sustainable agroecosystems.

Data availability statement

The datasets presented in this study can be found in online repositories. The names of the repository/repositories and accession number(s) can be found in the article/Supplementary material.

Author contributions

YJ and BS designed all the experiments. GS, LL, and YJ wrote the manuscript. GS, GZ, ZZ, JZ, and YS were responsible for performing the field and lab experiments. All authors analyzed all data, discussed the results, critically reviewed the manuscript, and approved its publication. All authors read and approved the final manuscript.

Funding

This study was supported by the National Key Research and Development Program (2022YFD1900603), National Natural Science Foundation of China (41922048, 42177298, and 42107336), Jiangxi Provincial Natural Science Foundation (20224BAB215054), the Youth Innovation Promotion Association of CAS (Y2021084), Double Thousand Plan of Jiangxi Province, and the Science and Technology Project of Jiangsu Province (BE2022393).

Conflict of interest

The authors declare that the research was conducted in the absence of any commercial or financial relationships that could be construed as a potential conflict of interest.

Publisher's note

All claims expressed in this article are solely those of the authors and do not necessarily represent those of their affiliated organizations, or those of the publisher, the editors and the reviewers. Any product that may be evaluated in this article, or claim that may be made by its manufacturer, is not guaranteed or endorsed by the publisher.

Supplementary material

The Supplementary material for this article can be found online at: https://www.frontiersin.org/articles/10.3389/fmicb.2023.1155088/full#supplementary-material

References

Abdalla, K., Sun, Y., Zarebanadkouki, M., Gaiser, T., Seidel, S., and Pausch, J. (2022). Long-term continuous farmyard manure application increases soil carbon when combined with mineral fertilizers due to lower priming effects. *Geoderma* 428:116216. doi: 10.1016/j.geoderma.2022.116216

Allison, S. D. (2005). Cheaters, diffusion and nutrients constrain decomposition by microbial enzymes in spatially structured environments. *Ecol. Lett.* 8, 626–635. doi: 10.1111/j.1461-0248.2005.00756.x

Bebber, D. P., and Richards, V. R. (2022). A meta-analysis of the effect of organic and mineral fertilizers on soil microbial diversity. *Appl. Soil Ecol.* 175:104450. doi: 10.1016/j.apsoil.2022.104450

Berhane, M., Xu, M., Liang, Z., Shi, J., Wei, G., and Tian, X. (2020). Effects of long-term straw return on soil organic carbon storage and sequestration rate in North China upland crops: a meta-analysis. *Glob. Chang. Biol.* 26, 2686–2701. doi: 10.1111/gcb.15018

Biddle, J. F., Fitz-Gibbon, S., Schuster, S. C., Brenchley, J. E., and House, C. H. (2008). Metagenomic signatures of the Peru margin subseafloor biosphere show a genetically distinct environment. *Proc. Natl. Acad. Sci. U. S. A.* 105, 10583–10588. doi: 10.1073/pnas.0709942105

Capblancq, T., Luu, K., Blum, M. G., and Bazin, E. (2018). Evaluation of redundancy analysis to identify signatures of local adaptation. *Mol. Ecol. Resour.* 18, 1223–1233. doi: 10.1111/1755-0998.12906

Carpenter, S. R., Kitchell, J. F., and Hodgson, J. R. (1985). Cascading trophic interactions and lake productivity. *Bioscience* 35, 634–639. doi: 10.2307/1309989

Cesarz, S., Schulz, A. E., Beugnon, R., and Eisenhauer, N. (2019). Testing soil nematode extraction efficiency using different variations of the Baermann-funnel method. *Soil Org.* 91, 61–72. doi: 10.25674/so91201

Chavarria, D. N., Pérez-Brandan, C., Serri, D. L., Meriles, J. M., Restovich, S. B., Andriulo, A. E., et al. (2018). Response of soil microbial communities to agroecological versus conventional systems of extensive agriculture. *Agric. Ecosyst. Environ.* 264, 1–8. doi: 10.1016/j.agee.2018.05.008

Chen, L., Jiang, Y., Liang, C., Luo, Y., Xu, Q., Han, C., et al. (2019). Competitive interaction with keystone taxa induced negative priming under biochar amendments. *Microbiome* 7:77. doi: 10.1186/s40168-019-0693-7

Clarke, A., and Gaston, K. J. (2006). Climate, energy and diversity. *P. Roy. Soc. B-Biol. Sci.* 273, 2257–2266. doi: 10.1098/rspb.2006.3545

Cook-Patton, S. C., Leavitt, S. M., Gibbs, D., Harris, N. L., Lister, K., Anderson-Teixeira, K. J., et al. (2020). Mapping carbon accumulation potential from global natural forest regrowth. *Nature* 585, 545–550. doi: 10.1038/s41586-020-2686-x

Cooper, J. M., Burton, D., Daniell, T. J., Griffiths, B. S., and Zebarth, B. J. (2011). Carbon mineralization kinetics and soil biological characteristics as influenced by manure addition in soil incubated at a range of temperatures. *Eur. J. Soil Biol.* 47, 392–399. doi: 10.1016/j.ejsobi.2011.07.010

Cox, T. F., and Ferry, G. (1993). Discriminant analysis using non-metric multidimensional scaling. *Pattern Recogn.* 26, 145–153. doi: 10.1016/0031-3203(93)90096-F

Cressman, R., and Garay, J. (2009). A predator–prey refuge system: evolutionary stability in ecological systems. *Theor. Popul. Biol.* 76, 248–257. doi: 10.1016/j.tpb.2009.08.005

Dijkstra, P., Salpas, E., Fairbanks, D., Miller, E. B., Hagerty, S. B., van Groenigen, K. J., et al. (2015). High carbon use efficiency in soil microbial communities is related to balanced growth, not storage compound synthesis. *Soil Biol. Biochem.* 89, 35–43. doi: 10.1016/j.soilbio.2015.06.021

Fanin, N., and Bertrand, I. (2016). Aboveground litter quality is a better predictor than belowground microbial communities when estimating carbon mineralization along a land-use gradient. *Soil Biol. Biochem.* 94, 48–60. doi: 10.1016/j.soilbio.2015.11.007

Fan, X., Gao, D., Zhao, C., Wang, C., Qu, Y., Zhang, J., et al. (2021). Improved model simulation of soil carbon cycling by representing the microbially derived organic carbon pool. *ISME J.* 15, 2248–2263. doi: 10.1038/s41396-021-00914-0

Feng, J., Zeng, X. M., Zhang, Q., Zhou, X. Q., Liu, Y. R., and Huang, Q. (2021). Soil microbial trait-based strategies drive metabolic efficiency along an altitude gradient. *ISME Commun.* 1:71. doi: 10.1038/s43705-021-00076-2

Ferris, H., Bongers, T., and de Goede, R. G. (2001). A framework for soil food web diagnostics: extension of the nematode faunal analysis concept. *Appl. Soil Ecol.* 18, 13–29. doi: 10.1016/S0929-1393(01)00152-4

Fließbach, A., Mäder, P., and Niggli, U. (2000). Mineralization and microbial assimilation of ^{14}C-labeled straw in soils of organic and conventional agricultural systems. *Soil Biol. Biochem.* 32, 1131–1139. doi: 10.1016/S0038-0717(00)00028-6

Grandy, A. S., Wieder, W. R., Wickings, K., and Kyker-Snowman, E. (2016). Beyond microbes: are fauna the next frontier in soil biogeochemical models? *Soil Biol. Biochem.* 102, 40–44. doi: 10.1016/j.soilbio.2016.08.008

Gross, A., and Glaser, B. (2021). Meta-analysis on how manure application changes soil organic carbon storage. *Sci. Rep.* 11:5516. doi: 10.1038/s41598-021-82739-7

Hu, C., and Qi, Y. (2010). Effect of compost and chemical fertilizer on soil nematode community in a Chinese maize field. *Eur. J. Soil Biol.* 46, 230–236. doi: 10.1016/j.ejsobi.2010.04.002

Hungate, B. A., Marks, J. C., Power, M. E., Schwartz, E., van Groenigen, K. J., Blazewicz, S. J., et al. (2021). The functional significance of bacterial predators. *MBio* 12, e00466–e00421. doi: 10.1128/mBio.00466-21

Hussain, A., Zahir, Z. A., Ditta, A., Tahir, M. U., Ahmad, M., Mumtaz, M. Z., et al. (2019). Production and implication of bio-activated organic fertilizer enriched with zinc-solubilizing bacteria to boost up maize (*Zea mays* L.) production and biofortification under two cropping seasons. *Agronomy* 10:39. doi: 10.3390/agronomy10010039

Jackson, M.L. (1958). *Soil chemical analysis*. Prentice-Hall, Inc, Engle-wood Cliffs, NJ. 111–133.

Jiang, Y., Qian, H., Wang, X., Chen, L., Liu, M., Li, H., et al. (2018a). Nematodes and microbial community affect the sizes and turnover rates of organic carbon pools in soil aggregates. *Soil Biol. Biochem.* 119, 22–31. doi: 10.1016/j.soilbio.2018.01.001

Jiang, Y., Zhou, H., Chen, L., Yuan, Y., Fang, H., Luan, L., et al. (2018b). Nematodes and microorganisms interactively stimulate soil organic carbon turnover in the macroaggregates. *Front. Microbiol.* 9:2803. doi: 10.3389/fmicb.2018.02803

Jiang, Y., Sun, B., Jin, C., and Wang, F. (2013). Soil aggregate stratification of nematodes and microbial communities affects the metabolic quotient in an acid soil. *Soil Biol. Biochem.* 60, 1–9. doi: 10.1016/j.soilbio.2013.01.006

Kane, J. L., Kotcon, J. B., Freedman, Z. B., and Morrissey, E. M. (2022). Fungivorous nematodes drive microbial diversity and carbon cycling in soil. *Ecology* 104:e3844. doi: 10.1002/ecy.3844

Kim, T. K. (2017). Understanding one-way ANOVA using conceptual figures. *Korean J. Anesthesiol.* 70, 22–26. doi: 10.4097/kjae.2017.70.1.22

Kitsopoulos, K. P. (1999). Cation-exchange capacity (CEC) of zeolitic volcaniclastic materials: applicability of the ammonium acetate saturation (AMAS) method. *Clay Clay Miner.* 47, 688–696. doi: 10.1346/CCMN.1999.0470602

Liaw, A., and Wiener, M. (2002). Classification and regression by randomForest. *R News* 2, 18–22. doi: 10.1023/A:1010933404324

Liu, T., Chen, X., Hu, F., Ran, W., Shen, Q., Li, H., et al. (2016). Carbon-rich organic fertilizers to increase soil biodiversity: evidence from a meta-analysis of nematode communities. *Agric. Ecosyst. Environ.* 232, 199–207. doi: 10.1016/j.agee.2016.07.015

Liu, Z., Wu, X., Liu, W., Bian, R., Ge, T., Zhang, W., et al. (2020). Greater microbial carbon use efficiency and carbon sequestration in soils: amendment of biochar versus crop straws. *GCB Bioenergy* 12, 1092–1103. doi: 10.1111/gcbb.12763

Mamet, S. D., Redlick, E., Brabant, M., Lamb, E. G., Helgason, B. L., Stanley, K., et al. (2019). Structural equation modeling of a winnowed soil microbiome identifies how

invasive plants re-structure microbial networks. *ISME J.* 13, 1988–1996. doi: 10.1038/s41396-019-0407-y

Mathisen, P., Thelaus, J., de Luna, S. S., and Andersson, A. (2016). Rapid adaptation of predation resistance in bacteria isolated from a seawater microcosm. *Aquat. Microb. Ecol.* 78, 81–92. doi: 10.3354/ame01802

Min, K., Slessarev, E., Kan, M., McFarlane, K., Oerter, E., Pett-Ridge, J., et al. (2021). Active microbial biomass decreases, but microbial growth potential remains similar across soil depth profiles under deeply-vs. shallow-rooted plants. *Soil Biol. Biochem.* 162:108401. doi: 10.1016/j.soilbio.2021.108401

Neidig, N., Paul, R. J., Scheu, S., and Jousset, A. (2011). Secondary metabolites of *Pseudomonas fluorescens* CHA0 drive complex non-trophic interactions with bacterivorous nematodes. *Microb. Ecol.* 61, 853–859. doi: 10.1007/s00248-011-9821-z

Oksanen, J. (2015). Vegan: an introduction to ordination. Available at: https://cran.r-project.org/web/packages/vegan/vignettes/intro-vegan.pdf

Pausch, J., Hofmann, S., Scharroba, A., Kuzyakov, Y., and Ruess, L. (2016). Fluxes of root-derived carbon into the nematode micro-food web of an arable soil. *Food Webs* 9, 32–38. doi: 10.1016/j.fooweb.2016.05.001

Pietikäinen, J., Kiikkilä, O., and Fritze, H. (2000). Charcoal as a habitat for microbes and its effect on the microbial community of the underlying humus. *Oikos* 89, 231–242. doi: 10.1034/j.1600-0706.2000.890203.x

Prada-Salcedo, L. D., Wambsganss, J., Bauhus, J., Buscot, F., and Goldmann, K. (2021). Low root functional dispersion enhances functionality of plant growth by influencing bacterial activities in European forest soils. *Environ. Microbiol.* 23, 1889–1906. doi: 10.1111/1462-2920.15244

Ros, M., Klammer, S., Knapp, B., Aichberger, K., and Insam, H. (2006). Long-term effects of compost amendment of soil on functional and structural diversity and microbial activity. *Soil Use Manag.* 22, 209–218. doi: 10.1111/j.1475-2743.2006.00027.x

Sandhu, S. S., Ussiri, D. A., Kumar, S., Chintala, R., Papiernik, S. K., Malo, D. D., et al. (2017). Analyzing the impacts of three types of biochar on soil carbon fractions and physiochemical properties in a corn-soybean rotation. *Chemosphere* 184, 473–481. doi: 10.1016/j.chemosphere.2017.05.165

Sedgwick, P. (2014). Spearman's rank correlation coefficient. *BMJ* 349:g7327. doi: 10.1136/bmj.g7327

Sinsabaugh, R. L., Manzoni, S., Moorhead, D. L., and Richter, A. (2013). Carbon use efficiency of microbial communities: stoichiometry, methodology and modelling. *Ecol. Lett.* 16, 930–939. doi: 10.1111/ele.12113

Spohn, M., and Chodak, M. (2015). Microbial respiration per unit biomass increases with carbon-to-nutrient ratios in forest soils. *Soil Biol. Biochem.* 81, 128–133. doi: 10.1016/j.soilbio.2014.11.008

Spohn, M. (2016). Element cycling as driven by stoichiometric homeostasis of soil microorganisms. *Basic Appl Ecol.* 17, 471–478. doi: 10.1016/j.baae.2016.05.003

Steenwerth, K. L., Jackson, L. E., Calderón, F. J., Stromberg, M. R., and Scow, K. M. (2002). Soil microbial community composition and land use history in cultivated and grassland ecosystems of coastal California. *Soil Biol. Biochem.* 34, 1599–1611. doi: 10.1016/S0038-0717(02)00144-X

Tabarant, P., Villenave, C., Risede, J. M., Roger-Estrade, J., Thuries, L., and Dorel, M. (2011). Effects of four organic amendments on banana parasitic nematodes and soil nematode communities. *Appl. Soil Ecol.* 49, 59–67. doi: 10.1016/j.apsoil.2011.07.001

Tian, S., Zhu, B., Yin, R., Wang, M., Jiang, Y., Zhang, C., et al. (2022). Organic fertilization promotes crop productivity through changes in soil aggregation. *Soil Biol. Biochem.* 165:108533. doi: 10.1016/j.soilbio.2021.108533

Van Den Hoogen, J., Geisen, S., Routh, D., Ferris, H., Traunspurger, W., Wardle, D. A., et al. (2019). Soil nematode abundance and functional group composition at a global scale. *Nature* 572, 194–198. doi: 10.1038/s41586-019-1418-6

Vance, E. D., Brookes, P. C., and Jenkinson, D. S. (1987). Microbial biomass measurements in forest soils: the use of the chloroform fumigation-incubation method in strongly acid soils. *Soil Biol. Biochem.* 19, 697–702. doi: 10.1016/0038-0717(87)90051-4

Wang, S., Chen, X., Li, D., and Wu, J. (2021). Effects of soil organism interactions and temperature on carbon use efficiency in three different forest soils. *Soil Ecol. Lett.* 3, 156–166. doi: 10.1007/s42832-020-0067-x

Wardle, D. A., and Ghani, A. A. (1995). A critique of the microbial metabolic quotient (qCO_2) as a bioindicator of disturbance and ecosystem development. *Soil Biol. Biochem.* 27, 1601–1610. doi: 10.1016/0038-0717(95)00093-T

Wei, W., Huangfu, C., Jia, Z., and Liu, S. (2021). Long-term organic amendments improved soil carbon sequestration to support crop production. *J. Plant Nutr. Soil Sci.* 184, 678–687. doi: 10.1002/jpln.202100128

Wei, X., Zhu, Z., Liu, Y., Luo, Y., Deng, Y., Xu, X., et al. (2020). C:N:P stoichiometry regulates soil organic carbon mineralization and concomitant shifts in microbial community composition in paddy soil. *Biol. Fertil. Soils* 56, 1093–1107. doi: 10.1007/s00374-020-01468-7

Wilson, J. R. (1993). "Organization of forage plant tissues" in *Forage cell wall structure and digestibility*. ed. H. G. Jung (Madison, WI: American Society of Agronomy Inc), 1–32.

Yeates, G. W. (1998). "Feeding in free-living soil nematodes: a functional approach" in *The physiology and biochemistry of free-living and plant-parasitic nematodes* (Wallingford, UK: CAB international), 245–269.

Zechmeister-Boltenstern, S., Keiblinger, K. M., Mooshammer, M., Peñuelas, J., Richter, A., Sardans, J., et al. (2015). The application of ecological stoichiometry to plant–microbial–soil organic matter transformations. *Ecol. Monogr.* 85, 133–155. doi: 10.1890/14-0777

Zhang, S., Li, Q., Lü, Y., Zhang, X., and Liang, W. (2013). Contributions of soil biota to C sequestration varied with aggregate fractions under different tillage systems. *Soil Biol. Biochem.* 62, 147–156. doi: 10.1016/j.soilbio.2013.03.023

Zhang, Z., Wang, H., Wang, Y., Zhang, X., Zhao, T., and Mahamood, M. (2021). Organic input practice alleviates the negative impacts of elevated ozone on soil microfood-web. *J. Clean. Prod.* 290:125773. doi: 10.1016/j.jclepro.2020.125773

Zhang, Z., Zhang, X., Mahamood, M., Zhang, S., Huang, S., and Liang, W. (2016). Effect of long-term combined application of organic and inorganic fertilizers on soil nematode communities within aggregates. *Sci. Rep.* 6:31118. doi: 10.1038/srep31118

Zheng, J., Tao, L., Dini-Andreote, F., Luan, L., Kong, P., Xue, J., et al. (2022a). Dynamic responses of ammonia-oxidizing archaea and bacteria populations to organic material amendments affect soil nitrification and nitrogen use efficiency. *Front. Microbiol.* 13:911799. doi: 10.3389/fmicb.2022.911799

Zheng, J., Dini-Andreote, F., Luan, L., Geisen, S., Xue, J., Li, H., et al. (2022b). Nematode predation and competitive interactions affect microbial-mediated phosphorus dynamics. *MBio* 13:e0329321. doi: 10.1128/mbio.03293-21

Zheng, Q., Hu, Y., Zhang, S., Noll, L., Böckle, T., Richter, A., et al. (2019). Growth explains microbial carbon use efficiency across soils differing in land use and geology. *Soil Biol. Biochem.* 128, 45–55. doi: 10.1016/j.soilbio.2018.10.006

Zheng, S., Hu, J., Chen, K., Yao, J., Yu, Z., and Lin, X. (2009). Soil microbial activity measured by microcalorimetry in response to long-term fertilization regimes and available phosphorous on heat evolution. *Soil Biol. Biochem.* 41, 2094–2099. doi: 10.1016/j.soilbio.2009.07.019

Zhong, S., Zeng, H. C., and Jin, Z. Q. (2017). Influences of different tillage and residue management systems on soil nematode community composition and diversity in the tropics. *Soil Biol. Biochem.* 107, 234–243. doi: 10.1016/j.soilbio.2017.01.007

Zhou, H., Zhang, D., Wang, P., Liu, X., Cheng, K., Li, L., et al. (2017). Changes in microbial biomass and the metabolic quotient with biochar addition to agricultural soils: a Meta-analysis. *Agri. Ecosyst. Environ.* 239, 80–89. doi: 10.1016/j.agee.2017.01.006

frontiers | Frontiers in Microbiology

TYPE Original Research
PUBLISHED 22 May 2023
DOI 10.3389/fmicb.2023.1150505

OPEN ACCESS

EDITED BY
Xiancan Zhu,
Anhui Normal University, China

REVIEWED BY
Yuji Jiang,
Chinese Academy of Sciences (CAS), China
Hanuman Singh Jatav,
Sri Karan Narendra Agriculture University, India
Sumera Yasmin,
National Institute for Biotechnology and Genetic Engineering, Pakistan

*CORRESPONDENCE
Ming Liu
✉ mliu@issas.ac.cn

†These authors have contributed equally to this work

RECEIVED 24 January 2023
ACCEPTED 28 April 2023
PUBLISHED 22 May 2023

CITATION
Xia M, Ma X, Liu J, Wu M, Li Z and Liu M (2023) Potential effect of key soil bacterial taxa on the increase of rice yield under milk vetch rotation. *Front. Microbiol.* 14:1150505. 10.3389/fmicb.2023.1150505

Potential effect of key soil bacterial taxa on the increase of rice yield under milk vetch rotation

Mingming Xia[1,2†], Xinling Ma[1,2†], Jia Liu[3], Meng Wu[1,2], Zhongpei Li[1,2] and Ming Liu[1,2,4*]

[1]State Key Laboratory of Soil and Sustainable Agriculture, Institute of Soil Science, Chinese Academy of Sciences, Nanjing, China, [2]University of Chinese Academy of Sciences, Beijing, China, [3]National Engineering and Technology Research Center for Red Soil Improvement, Soil and Fertilizer & Resources and Environment Institute, Jiangxi Academy of Agricultural Sciences, Nanchang, China, [4]Ecological Experimental Station of Red Soil Academia Sinica, Nanjing, China

Legume crop rotation is often adopted in rice cultivation to improve soil productivity. However, little is known about the role of microbes under legume rotation in affecting soil productivity. To elucidate this, a long-term paddy cropping experiment was set up to study the relationship between crop yield, soil chemical properties, and key microbial taxa under a double-rice and milk vetch rotation. Milk vetch rotation significantly improved soil chemical properties compared to no fertilization treatment, and soil phosphorus was a major factor correlated with crop yield. Long-term legume rotation increased soil bacterial alpha diversity and changed soil bacterial community. After milk vetch rotation, the relative abundances of *Bacteroidota*, *Desulfobacterota*, *Firmicutes*, and *Proteobacteria* increased while those of *Acidobacteriota*, *Chloroflexi*, and *Planctomycetota* decreased. Moreover, milk vetch rotation increased the relative abundance of phosphorus-related gene K01083 (*bpp*), which was significantly correlated with soil phosphorus content and crop yield. Network analysis showed that taxa of *Vicinamibacterales* were positively correlated with total phosphorus and available phosphorus, which was a potential taxon contributing to the availability of soil phosphorus stock. Our results indicated that milk vetch rotation could enrich key taxa with latent phosphate-solubilizing ability, increase the content of soil available phosphorus, and finally enhance crop yield. This could provide scientific guidance for better crop production.

KEYWORDS

milk vetch rotation, functional genes, phosphorus metabolism, crop yield, latent phosphate-solubilizing microorganisms

1. Background

Rice is a crucial staple crop for more than half of the world's population, and China is a significant producer, responsible for 18.5% of global cultivation area and 28.0% of global production output. Ensuring sustainable rice production is imperative for global food security (Zhou et al., 2020). Increasing demand to feed the huge population is driving the search for more efficient and eco-friendlier cropping regimes (Godfray et al., 2010), and legume rotation is a widely applied measure (Zhao et al., 2022). With a long planting history, legume manure has an

integrative effect on soil abiotic properties and crop production (Yang et al., 2022). The symbiotic legume root nodules with rhizobium are responsible for soil nitrogen fixation, improving soil nitrogen supply (Dong et al., 2021). Additionally, legumes can take up nutrients in deeper soil due to deep roots and supply these nutrients after being plowed into soil (Xue et al., 2016). Milk vetch is an important leguminous crop in traditional agricultural production. It can improve the effectiveness of soil nutrients and promote the absorption and accumulation of nutrients by crops (Solangi et al., 2019). However, there is limited knowledge about the biotic effect of legume rotations. Since soil microbes play crucial roles in soil nutrient cycling (Jiao et al., 2019), determining how soil microbes and their functions respond to legume rotation can help to accurately predict changes in soil productivity.

Crop rotation can regulate the soil microbial community, mainly through specific root exudates and litter input (Panettieri et al., 2020), and consequently enrich specific microbial consortia (Xiong and Lu, 2022) and perform different functions. For example, the selective effect of specific substrates on microbial communities can induce a shift of nutrient metabolism *via* changing the activity of certain enzymes (Peng et al., 2023). Research on community-level sole-carbon-source utilization properties of soil microbes showed that legume rotation altered the carbon source preference of the microbial community (Aschi et al., 2017). However, determining the general function of microbes could mask the heterogeneous roles of key microbes in soil nutrient cycling under crop rotation. The prediction of microbial community genes based on the phylogenetic similarity between taxa and reference sequences could be used to produce a latent abundance table containing information on microbial multiple functions (Czech et al., 2022), thus shedding light on the possible shift in microbial metabolism after legume rotation.

To investigate the selective effect of legume rotation on microbial consortia and their reaction to soil nutrient cycling and crop production, we performed a long-term legume rotation experiment. The relationships between soil key microbial taxa, chemical properties, and rice yield under different cropping regimes were determined. The phylogenetic prediction method for bacterial function genes was also applied to determine the reaction of key taxa to nutrient cycling. We hypothesized that long-term legume rotation would enrich specific microbial groups with specific functions. We further hypothesized that the enriched functional groups have potential to alter soil nutrient cycling after legume rotation.

2. Materials and methods

2.1. Site description and sampling

The samples were collected from a long-term paddy cropping experiment site in Yingtan City (28°15′30″N, 116°55′30″E), Jiangxi Province in China. This site has a subtropical monsoon climate with mean temperature of 17.6°C and mean precipitation of 1795 mm annually. The soil of the site is paddy soil developed on quaternary red clay. Double-cropped rice was cultivated on the site for about 30 years, and all agronomic practices were very similar between treatments except for cropping regime.

Three cropping and fertilization regimes with three replications were applied: (1) CK, double-rice with no fertilization; (2) NPK, double-rice with mineral fertilization (230 kg N, 136 kg P_2O_5, and 84 kg K_2O per ha per year); and (3) NPKGM, double-rice and milk vetch rotation with mineral fertilization (230 kg N, 136 kg P_2O_5, and 84 kg K_2O per ha per year). Milk vetch (*Astragalus sinicus* L.) was planted after harvest of the later rice crop and plowed during flowering stage, where 5,000 kg of fresh milk vetch (dry weight 2,500 kg) ha^{-1} $year^{-1}$ was applied.

The later rice crop was harvested, husked, and weighed in November 2017, and the rice yield of each plot was calculated after measuring the water content. Five surface soil samples (0–20 cm) were collected using an earth-boring auger in a 'X' pattern and merged into one soil sample for each plot after rice harvest. Each soil sample was sieved through 2 mm and divided into two parts: one part was air-dried for physiochemical assay, and the other was stored at −40°C for DNA extraction.

2.2. Soil chemical property measuring

Soil pH was determined using a pH meter in a 1:2.5 of soil and water suspension. The total nitrogen (TN) content in soil was determined using the Kjeldahl method (Pansu and Gautheyrou, 2006). The available nitrogen (AN) was determined using the alkali hydrolysis and micro diffusion method (Pansu and Gautheyrou, 2006). Total phosphorus (TP) and available phosphorus (AP) were determined by vanadium-molybdate photometric method, and total potassium (TK) and available potassium (AK) were determined by inductively coupled plasma-atomic emission spectrometry (Pansu and Gautheyrou, 2006). Soil organic carbon (SOC) was determined using potassium dichromate oxidation with an external heating method (Pansu and Gautheyrou, 2006).

2.3. Soil DNA extraction and sequencing

Each 1 g soil sample was weighed, and soil microbial DNA was extracted according to the manufacturer's instructions using FastDNA™ Spin Kit (MP Biomedicals, Santa Ana, CA, USA). The hyper-variable region (V4–V5) of prokaryotic 16S rRNA was amplified using the primers 515F (5′-GTGCCAGCMGCCGC GGTAA-3′) and 907R (5′-CCGTCAATTCCTTTGAGTTT-3′) with barcodes. All PCR reactions were carried out with 15 μL of Phusion® High-Fidelity PCR Master Mix (New England Biolabs), 0.2 μM of forward and reverse primers, and about 10 ng of template DNA. Thermal cycling consisted of initial denaturation at 98°C for 1 min, followed by 30 cycles of denaturation at 98°C for 10 s, annealing at 50°C for 30 s, and elongation at 72°C for 30 s, with a final step of 72°C for 5 min. The samples after PCR amplification were sequenced on an Illumina NovaSeq platform, and 250-bp paired-end reads were generated. The raw reads were denoised, dereplicated, and clustered using a VSEARCH pipeline. High-quality sequences of 84,811–141,764 reads per sample were obtained, and we finally obtained 12,913 operational taxonomic units (OTUs). A trained Naïve Bayes classifier based on the Silva 138 database was deployed to classify the OTU sequences (Quast et al., 2013; Bolyen et al., 2019). After filtering the non-bacterial sequences, 12,673 OTUs were prepared for downstream analysis. All the raw sequences tested in the study were uploaded to the NCBI SRA database (accession no., PRJNA957222).

Bacterial community gene abundances were predicted using Phylogenetic Investigation of Communities by Reconstruction of Unobserved States (Douglas et al., 2020), and a final list of 7,425 latent function genes and their abundances were obtained. The shifts of three phosphorus-related genes (K00117, *gcd*; K01083, *bpp*; and K06137, *pqqC*) and taxa contributing up to 80% of their abundance were analyzed.

2.4. Data analysis

One-way analysis of variance was applied to the differences between soil chemical properties and crop yields among treatments. Pearson correlations were calculated using function '*rcorr*' of the R package '*Hmisc*.' The bacterial Shannon and richness indices were calculated using functions '*diversity*' and '*estimateR*' of the R package '*vegan*,' respectively. Constrained principal coordinate analysis (CPCoA) was adopted to display the discrepancies of bacterial community structure between treatments using function '*capscale*' of the R package '*vegan*.' A network containing TP, AP, rice yield, and OTUs contributing to the previously selected phosphorus-related genes was constructed based on the Pearson correlations with $p < 0.001$ (Supplementary Figure S1). Subnetworks characterizing correlations per sample were obtained later, and topological indexes of every subnetwork were calculated (Supplementary Table S1). To determine the functional groups related to nutrient cycling, a subnetwork containing TP, AP, rice yield, and taxa directly related to them was obtained from the initial network. The network was constructed using the R package '*igraph*,' and the network graphic was constructed using the Gephi program.

3. Results

3.1. Effect of milk vetch rotation on soil chemical properties and rice yield

The NPK and NPKGM treatments increased soil nutrient content and rice yield. The NPKGM significantly increased pH, SOC, TN, TP, AP, AK, and rice yield compared to CK ($p < 0.05$) (Table 1).

Pearson correlation analysis showed associations between rice yield and soil chemical properties (Figure 1). Among all soil chemical properties, pH, TP, AP, and AK were significantly correlated with crop yield, and pH was significantly correlated with TP, AP, and AK.

3.2. Effect of milk vetch rotation on soil bacterial community structure

Although not significant, the richness and Shannon indices of the bacterial community were higher in the NPKGM than in CK and NPK treatments (Figures 2A,B). The CPCoA showed that the bacterial community changed in the different cropping regimes (Figure 2C), with principal coordinates 1 and 2 explaining 76.62 and 27.38% of the total variance, respectively. Further analysis showed that the legume rotation increased the relative abundances of *Bacteroidota*, *Desulfobacterota*, *Firmicutes*, and *Proteobacteria* but reduced those of *Acidobacteriota*, *Chloroflexi*, and *Planctomycetota* (Figure 2D).

3.3. Effect of milk vetch rotation on phosphorus-related genes

The predicted absolute abundances of the enriched genes were in the following order in all treatments: K00117 (*gcd*) > K06137 (*pqqC*) > K01083 (*bpp*) (Figure 3). The abundance of K00117 was highest in NPK and lowest in CK. The abundance of K06137 was highest in CK and lowest in NPK. Moreover, abundance of K01083 was higher in NPKGM than in CK and NPK. Correlation analysis showed that K00177 had no significant correlation with TP, AP, or crop yield ($p > 0.05$, Supplementary Figure S1); however, K01083 was significantly positively correlated (and K06137 was negatively correlated) with TP, AP, and crop yield ($p < 0.05$).

Bryobacterales, *Solibacterales*, *Vicinamibacterales*, *Rhizobiales*, and *Pedosphaerales* were the top five taxa contributing most to K00117 abundance. *Xanthomonadales*, *Flavobacterales*, *Streptomycetales*, *Gemmatimonadales*, and *Myxococcales* were the top five taxa contributing most to K01083. *Acidobacteriales*, *Rhizobiales*, *Nitrospirales*, *Burkholderiales*, and *Caulobacterales* were the top five taxa contributing most to K06137. *Bryobacterales*, *Solibacterales*, and *Pedosphaerales* contributed more K00117 genes in CK, while *Vicinamibacterales* and *Rhizobiales* contributed more K00117 in NPKGM. *Gemmatimonadales* and *Myxococcales* contributed more K01083 genes in NPK, while *Xanthomonadales*, *Flavobacterales*, and *Streptomycetales* contributed more K01083 in NPKGM. *Acidobacteriales* and *Rhizobiales* contributed more K06137 genes in CK, while *Nitrospirales* contributed more K06137 genes in NPK. *Burkholderiales* and *Caulobacterales* contributed more K06137 in NPKGM.

TABLE 1 Soil physiochemical properties and rice yield after different fertilization treatments.

Treat	pH	SOC	TN	TP	TK	AN	AP	AK	Yield
	1:2.5	gkg^{-1}	gkg^{-1}	gkg^{-1}	gkg^{-1}	$mgkg^{-1}$	$mgkg^{-1}$	$mgkg^{-1}$	kg/ha
CK	5.59 ± 0.03b	7.69 ± 0.88b	0.93 ± 0.07b	0.86 ± 0.07b	15.21 ± 0.71a	77.18 ± 7.35a	44.39 ± 6.13b	92.50 ± 21.36b	4391.08 ± 478.15b
NPK	6.42 ± 0.10a	8.75 ± 1.64ab	1.09 ± 0.26ab	1.41 ± 0.15ab	14.07 ± 1.46a	95.55 ± 24.10a	88.56 ± 9.22a	202.50 ± 19.53a	6692.23 ± 340.47a
NPKGM	6.60 ± 0.10a	10.35 ± 1.26a	1.32 ± 0.11a	1.56 ± 0.04a	14.99 ± 1.19a	101.68 ± 9.25a	99.40 ± 8.07a	237.50 ± 43.37a	7059.08 ± 393.03a

SOC, soil organic carbon; TN, total nitrogen; TP, total phosphorus; TK, total potassium; AN, available nitrogen; AP, available phosphorus; AK, available potassium; CK, double-rice with no fertilization; NPK, double-rice with mineral fertilization (230 kg N, 136 kg P_2O_5, and 84 kg K_2O per ha per year); and NPKGM, double-rice and milk vetch rotation with mineral fertilization (230 kg N, 136 kg P_2O_5, and 84 kg K_2O per ha per year). Different letters indicate a significant difference between treatments at $p < 0.05$.

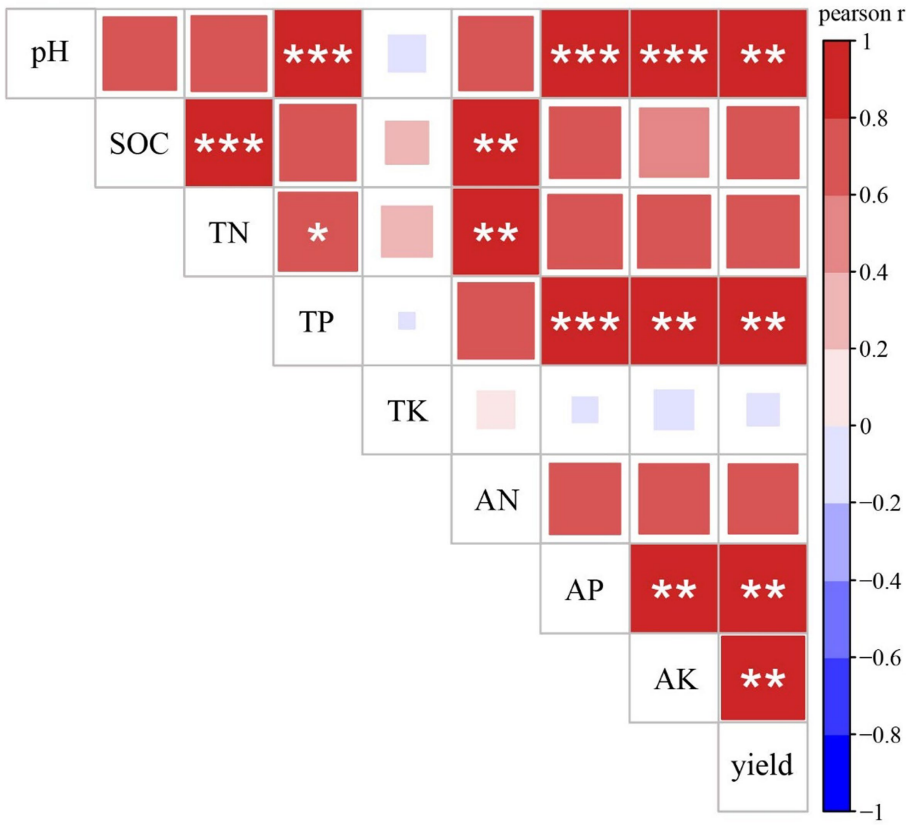

FIGURE 1
Pearson correlations between crop yield and soil properties. SOC, soil organic carbon; TN, total nitrogen; TP, total phosphorus; TK, total potassium; AN, available nitrogen; AP, available phosphorus; AK, available potassium.

3.4. Relationships between soil phosphorus content, crop yield, and phosphorus-related taxa

The Balaban Index and Topological Index showed no significant difference between treatments, while the positive edges/negative edges ratio in CK was significantly higher than other treatments (Supplementary Table S1). Thirteen OTUs belonging to six orders were directly correlated with TP, AP, or crop yield, and four orders were correlated with TP, AP, or both (Figure 4). Nodes belonging to *Gemmatales* were negatively correlated with TP, AP, and crop yield, while nodes belonging to *Vicinamibacterales* were positively correlated with TP and AP. From the order *Polyangiales*, OTU 6233 had a positive correlation with TP and AP, while OTU 8505 was negatively correlated with AP. The OTU 2853 was positively correlated with AP, while another *Acidobacteriales* (OTU 7944) was negatively correlated with AP (Supplementary Figure S2).

4. Discussion

4.1. Rotation of milk vetch changed soil chemical properties and crop yield

Consistent with previous research (Zhang et al., 2023), long-term rotation of milk vetch increased double-rice yield. The significant positive relationship between rice yield and phosphorus content indicates that the higher phosphorus level was responsible for the high productivity of the rotation soil. The research site is subtropical China, which is dominated by phosphorus limitation (Yu et al., 2018), thus, AP supply could enhance crop production. As well as phosphorus content, pH and AK were positively related to crop yield. Soil pH is a crucial factor regulating soil nutrient availability (Xue et al., 2019) and the microbial community (Liu et al., 2018), while the potassium stock in subtropical red soil experiences strong leaching, leading to demand for potassium. Therefore, improving soil pH and K availability likely led to the yield increase.

Milk vetch rotation increased soil phosphorus content, similar to results of Li et al. (2018). Researchers found that legume rotation improved the humification of SOC (Virk et al., 2021) and could inhibit phosphorus migration, activate fixed phosphorus, improve the distance of phosphorus movement, and finally improve the effective phosphorus content in soil (Xu et al., 2017; Wulanningtyas et al., 2021). The higher pH in the rotation treatment also likely improved phosphate availability (Barrow and Lambers, 2022). Moreover, the milk vetch roots could reach deeper soil, providing more phosphorus to the surface soil (Zhang et al., 2022).

4.2. Rotation of milk vetch changed soil bacterial community

Cropping regimes such as legume rotation have important effects on bacterial community diversity and composition (Zheng et al.,

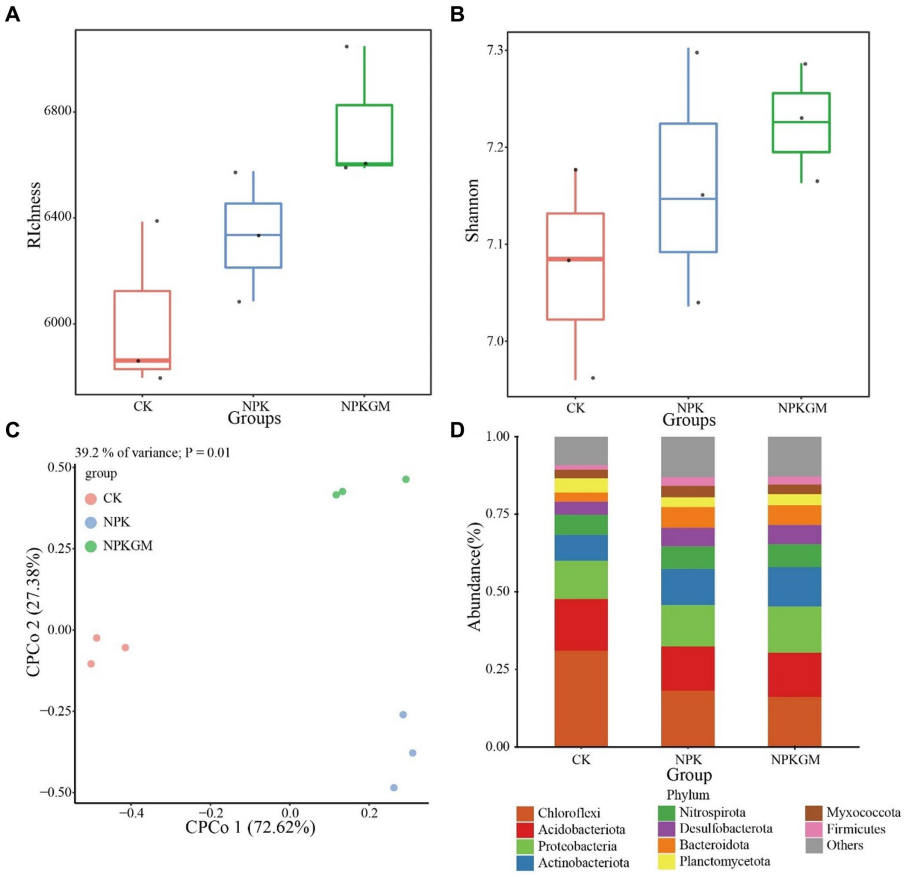

FIGURE 2
Bacterial community **(A,B)** diversity and **(C,D)** structure under different fertilization treatments: **(A)** richness index, **(B)** Shannon index, **(C)** CPCoA of soil bacterial community under different fertilization treatments, and **(D)** soil bacterial composition in phylum level under different fertilization treatments. CK, double-rice with no fertilization; NPK, double-rice with mineral fertilization (230kgN, 136kg P_2O_5, and 84kg K_2O per ha per year); and NPKGM, double-rice and milk vetch rotation with mineral fertilization (230kgN, 136kg P_2O_5, and 84kg K_2O per ha per year).

2021). Similar phenomena were found in our study, and the higher richness and Shannon indices in the NPKGM treatment indicated that the milk vetch rotation increased microbial diversity (Benkwitt et al., 2020). We found that milk vetch rotation increased the relative abundance of high nitrogen affinity taxon *Bacteroidota*, possibly due to the higher TN content in the NPKGM treatment (Li W. L. et al., 2022), and *Proteobacteria*, which is the source of many enzymes and usually participates in the biological cycling of mineral elements in soil to maintain soil fertility (Chaudhry et al., 2012; Li W. L. et al., 2022). In addition, both *Bacteroidota* and *Proteobacteria* are *eutrophic* bacteria, which benefit from eutrophic environments in the NPKGM treatment (Fierer et al., 2007). Related studies show that lower soil pH led to higher *Firmicutes* abundance (Li Y. Z. et al., 2022; Palansooriya et al., 2022), which contrasts with our study in which *Firmicutes* was enriched in NPKGM at higher pH. *Firmicutes* can also benefit from a high source-availability environment, whose content increases with abundance of nutrients (Vanwonterghem et al., 2016; Zhou et al., 2021); in our study, *Firmicutes* may have responded more to nutrients than pH.

Hu et al. (2022) found that *Chloroflexi* was negatively correlated with TN content, consistent with our results of lower *Chloroflexi* abundance in the NPK and NPKGM treatments. As typical *copiotrophic* taxa, both *Acidobacteria* and *Planctomycetota* usually dominate in barren conditions (Fierer et al., 2007; Shelyakin et al., 2022) and thus were enriched in our CK treatment.

4.3. Keystone taxa and their predicted function promoted soil phosphorus metabolism under double-rice and milk vetch rotation

Unlike the recognition that phosphate-solubilizing microorganisms were responsible for soil AP (Chen et al., 2023), K00117 (*gcd*) and K06137 (*pqqC*), known as genes that encode enzymes to mediate the resolving of soil phosphate, had non-significant or even negative correlations with soil AP and TP in CK or NPK in our study. Only K01083 (*bpp*) was positively correlated with AP and TP in NPKGM. A possible mechanism was the phosphate released from soil minerals being easily leached from red paddy soil under high precipitation (Peng et al., 2020), while the organic phosphorus released from milk vetch rotation could remain longer in soil (Zhao et al., 2013), hence we observed a significant positive correlation between K01083 and soil phosphorus content even when the abundance of K01083 was low (Jorquera et al., 2013). In addition, encoding phytases that catalyze the hydrolysis of plant-sourced

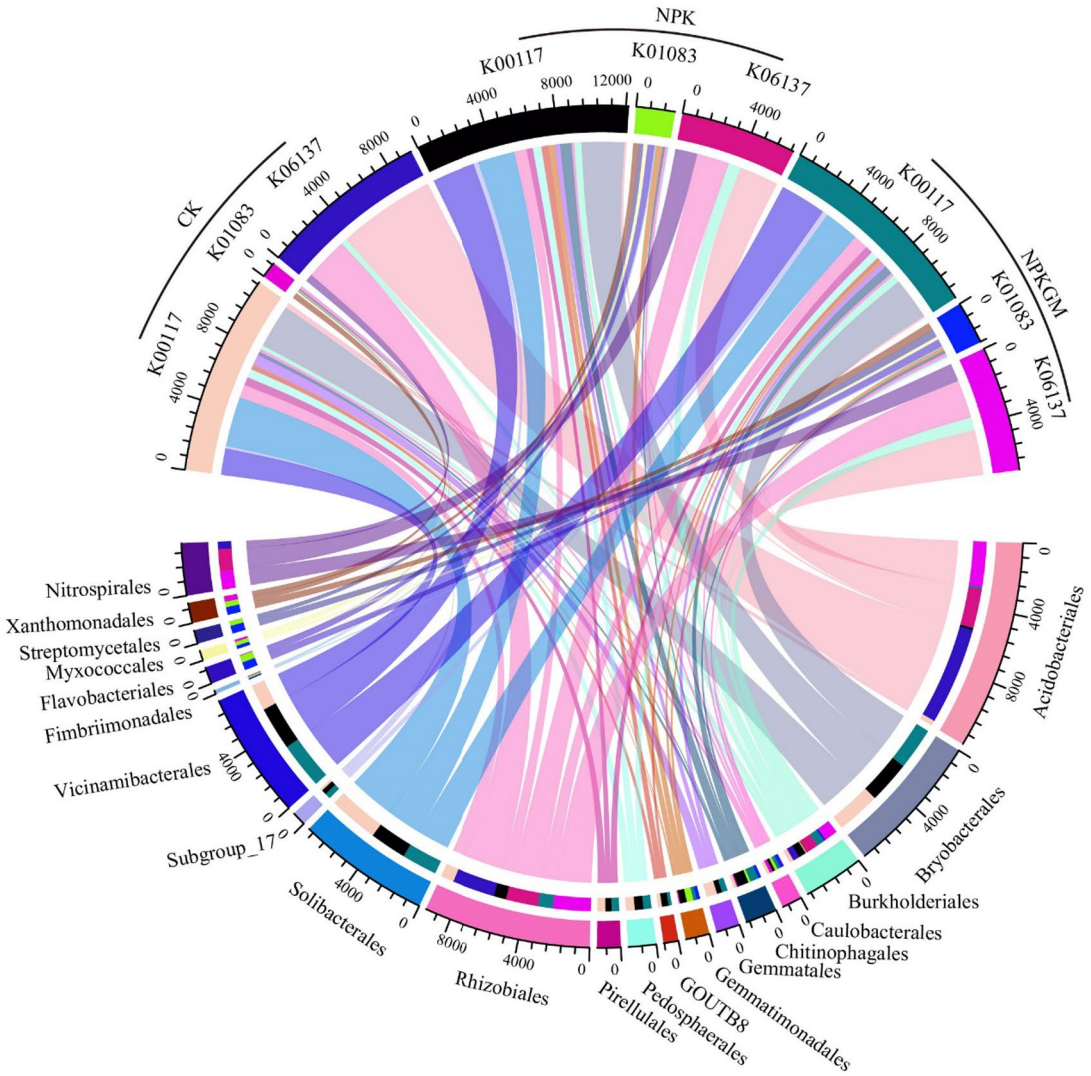

FIGURE 3
Circular plot of abundance of phosphorus-related genes K00117 (*gcd*), K01083 (*bpp*), and K06137 (*pqqC*) and the average abundance of genes contained by taxa. CK, double-rice with no fertilization; NPK, double-rice with mineral fertilization (230kgN, 136kg P_2O_5, and 84kg K_2O per ha per year); and NPKGM, double-rice and milk vetch rotation with mineral fertilization (230kgN, 136kg P_2O_5, and 84kg K_2O per ha per year).

phytate (Lu et al., 2022) and taxa containing *bpp* could benefit in soil with greater plant litter input (Liu X. et al., 2022). This can also further explain the enrichment of *bpp* in the NPKGM treatment.

Moreover, evidence showed that high pH and high AP content could reduce the abundances of taxa with genes encoding *phoD* such as *Gemmatales*, since we found a negative correlation between AP and *Gemmatales*. Nodes belonging to *Acidobacteriales* had an opposite correlation with AP and AP-related taxa, indicating that different specific taxa belonging to *Acidobacteriales* might play different roles in phosphorus metabolism (Cui et al., 2022; Liu H. et al., 2022). Strong correlations were found between *Polyangiales* and AP (Figure 3). As a predator belonging to the phylum *Myxococcota*, it can be inferred that *Polyangiales* might benefit in a high-nutrition environment which provides more microorganisms. Among the taxa concerned with phosphorus content, *Vicinamibacterales* was the only taxon that was purely positively correlated with AP and rice yield in the network analysis. It was reported that *Vicinamibacterales* could encode *pit* that participated in the assimilation of phosphate and prevented the loss of AP in an extreme leaching environment (Wu et al., 2022). Our study indicated that legume rotation may influence soil element cycling, especially phosphorus cycling, by enriching certain key species and key functional genes to increase phosphorus availability and ultimately promote crop yield.

5. Conclusion

Our milk vetch rotation improved the physiochemical properties and crop yield of the paddy soil. In addition, this rotation altered the soil bacterial community, especially some groups closely associated with phosphorus-related functional genes. Network analysis showed that taxa belonging to six phyla were associated with TP, AP, and crop yield. Taken together, milk vetch rotation could enrich key taxa encoding phytase, increase soil AP content, and ultimately improve

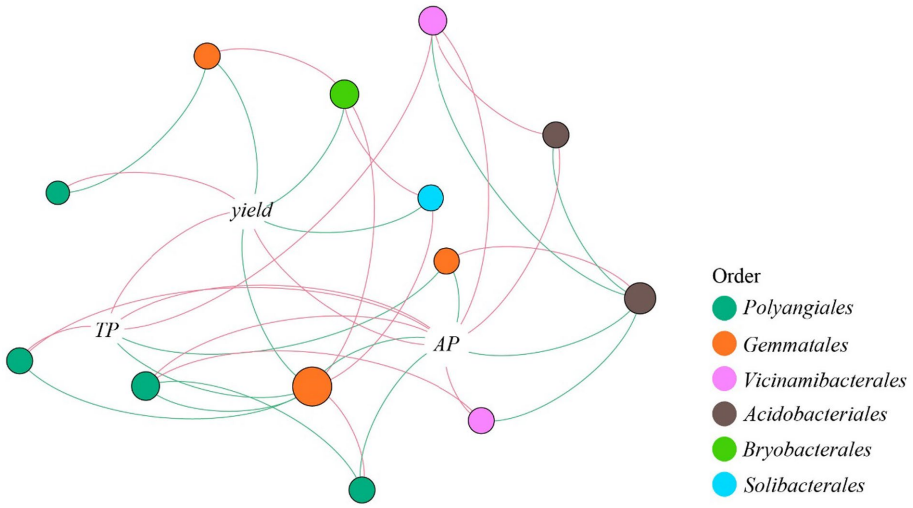

FIGURE 4
Network analysis of correlativity between TP, AP, yield, and phosphorus gene related taxa. Red edges indicate positive correlation, while green edges indicate negative correlation. The size of a node indicates the number of edges it participates in. TP, total phosphorus; AP, available phosphorus.

crop yield. This could provide scientific guidance for better crop production. However, we were mainly interested in the relationship between changes and interactions of soil characteristics and microbial communities and crop yield. In future studies, it is recommended to focus on the expression of relevant functional genes to obtain direct evidence that nutrient cycling is closely related to rice yield.

Data availability statement

The original contributions presented in the study are included in the article/Supplementary materials, further inquiries can be directed to the corresponding author.

Author contributions

MX: measurement and analysis, writing–original draft, and visualization. XM: methodology, data curation, and formal analysis. JL: methodology, review, and editing. MW: software and formal analysis. ZL: funding acquisition and validation. ML: funding acquisition, review, and editing. All authors contributed to the article and approved the submitted version.

Funding

This work was supported by the National Natural Science Foundation of China (42177294), the Key Research and Development Program of Jiangxi Province (20212BBF63007), the Central Guidance for Local Science and Technology Development Projects (20231ZDD02003), China Agriculture Research Systems of MOF and MARA (CARS-22), and the Jiangxi Modern Agricultural Innovation Project (JXXTCXQN202008).

Conflict of interest

The authors declare that the research was conducted in the absence of any commercial or financial relationships that could be construed as a potential conflict of interest.

The reviewer YJ declared a shared affiliation with the authors MX, XM, ML, MW, and ZL to the handling editor at the time of review.

Publisher's note

Supplementary material

The Supplementary material for this article can be found online at: https://www.frontiersin.org/articles/10.3389/fmicb.2023.1150505/full#supplementary-material

References

Aschi, A., Aubert, M., Riah-Anglet, W., Nelieu, S., Dubois, C., Akpa-Vinceslas, M., et al. (2017). Introduction of Faba bean in crop rotation: impacts on soil chemical and biological characteristics. *Appl. Soil Ecol.* 120, 219–228. doi: 10.1016/j.apsoil.2017.08.003

Barrow, N. J., and Lambers, H. (2022). Phosphate-solubilising microorganisms mainly increase plant phosphate uptake by effects of pH on root physiology. *Plant Soil* 476, 397–402. doi: 10.1007/s11104-021-05240-0

Benkwitt, C. E., Wilson, S. K., and Graham, N. A. J. (2020). Biodiversity increases ecosystem functions despite multiple stressors on coral reefs. *Nature Ecol Evol* 4:919. doi: 10.1038/s41559-020-1203-9

Bolyen, E., Rideout, J. R., Dillon, M. R., Bokulich, N., Abnet, C. C., Al-Ghalith, G. A., et al. (2019). Reproducible, interactive, scalable and extensible microbiome data science using QIIME 2. *Nat. Biotechnol.* 37, 852–857. doi: 10.1038/s41587-019-0209-9

Chaudhry, V., Rehman, A., Mishra, A., Chauhan, P. S., and Nautiyal, C. S. (2012). Changes in bacterial community structure of agricultural land due to long-term organic and chemical amendments. *Microb. Ecol.* 64, 450–460. doi: 10.1007/s00248-012-0025-y

Chen, S. Q., Gao, J. S., Chen, H. H., Zhang, Z. Y., Huang, J., Lv, L. F., et al. (2023). The role of long-term mineral and manure fertilization on P species accumulation and phosphate-solubilizing microorganisms in paddy red soils. *Soil-Germany* 9, 101–116. doi: 10.5194/soil-9-101-2023

Cui, J. W., Zhang, S., Wang, X. Y., Xu, X. P., Ai, C., Liang, G. Q., et al. (2022). Enzymatic stoichiometry reveals phosphorus limitation-induced changes in the soil bacterial communities and element cycling: evidence from a long-term field experiment. *Geoderma* 426:116124. doi: 10.1016/j.geoderma.2022.116124

Czech, L., Stamatakis, A., Dunthorn, M., and Barbera, P. (2022). Metagenomic analysis using phylogenetic placement-a review of the first decade. *Front Bioinform* 2:871393. doi: 10.3389/fbinf.2022.871393

Dong, W. T., Zhu, Y. Y., Chang, H. Z., Wang, C. H., Yang, J., Shi, J. C., et al. (2021). An SHR-SCR module specifies legume cortical cell fate to enable nodulation. *Nature* 589:590. doi: 10.1038/s41586-020-3016-z

Douglas, G. M., Maffei, V. J., Zaneveld, J. R., Yurgel, S. N., Brown, J. R., Taylor, C. M., et al. (2020). PICRUSt2 for prediction of metagenome functions. *Nat. Biotechnol.* 38, 685–688. doi: 10.1038/s41587-020-0548-6

Fierer, N., Bradford, M. A., and Jackson, R. B. (2007). Toward an ecological classification of soil bacteria. *Ecology* 88, 1354–1364. doi: 10.1890/05-1839

Godfray, H. C. J., Beddington, J. R., Crute, I. R., Haddad, L., Lawrence, D., Muir, J. F., et al. (2010). Food security: the challenge of feeding 9 billion people. *Science* 327, 812–818. doi: 10.1126/science.1185383

Hu, Y., Chen, M., Yang, Z. L., Cong, M. F., Zhu, X. P., and Jia, H. T. (2022). Soil microbial community response to nitrogen application on a swamp meadow in the arid region of Central Asia. *Front. Microbiol.* 12:797306. doi: 10.3389/fmicb.2021.797306

Jiao, S., Xu, Y. Q., Zhang, J., Hao, X., and Lu, Y. H. (2019). Core microbiota in agricultural soils and their potential associations with nutrient cycling. *Msystems*:4. doi: 10.1128/mSystems.00313-18

Jorquera, M. A., Saavedra, N., Maruyama, F., Richardson, A. E., Crowley, D. E., Catrilaf, R. D., et al. (2013). Phytate addition to soil induces changes in the abundance and expression of Bacillus beta-propeller phytase genes in the rhizosphere. *FEMS Microbiol. Ecol.* 83, 352–360. doi: 10.1111/j.1574-6941.2012.01480.x

Li, Y. Z., Chen, Z., Peng, Y. Y., Huang, W. Z., Liu, J. X., Mironov, V., et al. (2022). Deeper insights into the effects of substrate to inoculum ratio selection on the relationship of kinetic parameters, microbial communities, and key metabolic pathways during the anaerobic digestion of food waste. *Water Res.* 217:118440. doi: 10.1016/j.watres.2022.118440

Li, D. D., Luo, P. Y., Han, X. R., and Yang, J. F. (2018). "Influence of long-term fertilization on soil physicochemical properties in a brown soil" in *2017 3rd international conference on environmental science and material application (Esma2017)*, vol. 1-4, 108.

Li, W. L., Wang, Z. C., Li, W. P., and Li, Z. (2022). Impacts of microplastics addition on sediment environmental properties, enzymatic activities and bacterial diversity. *Chemosphere* 307:135836. doi: 10.1016/j.chemosphere.2022.135836

Liu, X., Han, R., Cao, Y., Turner, B. L., and Ma, L. Q. (2022). Enhancing Phytate availability in soils and Phytate-P acquisition by plants: a review. *Environ. Sci. Technol.* 56, 9196–9219. doi: 10.1021/acs.est.2c00099

Liu, H., Li, S. S., Qiang, R. W., Lu, E. J., Li, C. L., Zhang, J. J., et al. (2022). Response of soil microbial community structure to phosphate fertilizer reduction and combinations of microbial fertilizer. *Front. Environ. Sci.* 10:727. doi: 10.3389/fenvs.2022.899727

Liu, J., Liu, M., Wu, M., Jiang, C. Y., Chen, X. F., Cai, Z. J., et al. (2018). Soil pH rather than nutrients drive changes in microbial community following long-term fertilization in acidic Ultisols of southern China. *J. Soils Sediments* 18, 1853–1864. doi: 10.1007/s11368-018-1934-2

Lu, J. L., Jia, P., Feng, S. W., Wang, Y. T., Zheng, J., Ou, S. N., et al. (2022). Remarkable effects of microbial factors on soil phosphorus bioavailability: a country-scale study. *Glob. Chang. Biol.* 28, 4459–4471. doi: 10.1111/gcb.16213

Palansooriya, K. N., Shi, L., Sarkar, B., Parikh, S. J., Sang, M. K., Lee, S. R., et al. (2022). Effect of LDPE microplastics on chemical properties and microbial communities in soil. *Soil Use Manag.* 38, 1481–1492. doi: 10.1111/sum.12808

Panettieri, M., Guigue, J., Prevost-Boure, N. C., Thevenot, M., Leveque, J., Le Guillou, C., et al. (2020). Grassland-cropland rotation cycles in crop-livestock farming systems regulate priming effect potential in soils through modulation of microbial communities, composition of soil organic matter and abiotic soil properties. *Agric. Ecosyst. Environ.* 299:106973. doi: 10.1016/j.agee.2020.106973

Pansu, M., and Gautheyrou, J., (2006). *Handbook of soil analysis: Mineralogical, organic and inorganic methods*. Springer Berlin, Heidelberg.

Peng, Z., Wu, Y., Guo, L., Yang, L., Wang, B., Wang, X., et al. (2023). Foliar nutrient resorption stoichiometry and microbial phosphatase catalytic efficiency together alleviate the relative phosphorus limitation in forest ecosystems. *New Phytol.* 238, 1033–1044. doi: 10.1111/nph.18797

Peng, L., Xue, X. G., Tang, Q. H., Zhu, Y., Xiao, L. J., Yang, Y., et al. (2020). Phosphorus retention and loss in three types of soils with implications for geographical pattern of eutrophication in China. *Water Environ. J.* 34, 9–18. doi: 10.1111/wej.12490

Quast, C., Pruesse, E., Yilmaz, P., Gerken, J., Schweer, T., Yarza, P., et al. (2013). The SILVA ribosomal RNA gene database project: improved data processing and web-based tools. *Nucleic Acids Res.* 41, D590–D596. doi: 10.1093/nar/gks1219

Shelyakin, P. V., Semenkov, I. N., Tutukina, M. N., Nikolaeva, D. D., Sharapova, A. V., Sarana, Y. V., et al. (2022). The influence of kerosene on microbiomes of diverse soils. *Life Basel* 12:221. doi: 10.3390/life12020221

Solangi, F., Bai, J. S., Gao, S. J., Yang, L., Zhou, G. P., and Cao, W. D. (2019). Improved accumulation capabilities of phosphorus and potassium in green manures and its relationship with soil properties and enzymatic activities. *Agronomy Basel* 9:708. doi: 10.3390/agronomy9110708

Vanwonterghem, I., Jensen, P. D., Rabaey, K., and Tyson, G. W. (2016). Genome-centric resolution of microbial diversity, metabolism and interactions in anaerobic digestion. *Environ. Microbiol.* 18, 3144–3158. doi: 10.1111/1462-2920.13382

Virk, A. L., Liu, W. S., Niu, J. R., Xu, C. T., Liu, Q. Y., Kan, Z. R., et al. (2021). Effects of diversified cropping sequences and tillage practices on soil organic carbon, nitrogen, and associated fractions in the North China plain. *J. Soil Sci. Plant Nutr.* 21, 1201–1212. doi: 10.1007/s42729-021-00433-z

Wu, X. J., Rensing, C., Han, D. F., Xiao, K. Q., Dai, Y. X., Tang, Z. X., et al. (2022). Genome-resolved metagenomics reveals distinct phosphorus acquisition strategies between soil microbiomes. *Msystems* 7:e0110721. doi: 10.1128/msystems.01107-21

Wulanningtyas, H. S., Gong, Y. T., Li, P. R., Sakagami, N., Nishiwaki, J., and Komatsuzaki, M. (2021). A cover crop and no-tillage system for enhancing soil health by increasing soil organic matter in soybean cultivation. *Soil Tillage Res.* 205:104749. doi: 10.1016/j.still.2020.104749

Xiong, C., and Lu, Y. H. (2022). Microbiomes in agroecosystem: diversity, function and assembly mechanisms. *Environ. Microbiol. Rep.* 14, 833–849. doi: 10.1111/1758-2229.13126

Xu, J. S., Zhao, B. Z., Chu, W. Y., Mao, J. D., Olk, D. C., Zhang, J. B., et al. (2017). Evidence from nuclear magnetic resonance spectroscopy of the processes of soil organic carbon accumulation under long-term fertilizer management. *Eur. J. Soil Sci.* 68, 703–715. doi: 10.1111/ejss.12445

Xue, W., Bezemer, T. M., and Berendse, F. (2019). Soil heterogeneity and plant species diversity in experimental grassland communities: contrasting effects of soil nutrients and pH at different spatial scales. *Plant Soil* 442, 497–509. doi: 10.1007/s11104-019-04208-5

Xue, Y. F., Xia, H. Y., Christie, P., Zhang, Z., Li, L., and Tang, C. X. (2016). Crop acquisition of phosphorus, iron and zinc from soil in cereal/legume intercropping systems: a critical review. *Ann. Bot.* 117, 363–377. doi: 10.1093/aob/mcv182

Yang, Z. Y., Zhang, Y. P., Wang, Y. Z., Zhang, H. F., Zhu, Q. R., Yan, B. J., et al. (2022). Intercropping regulation of soil phosphorus composition and microbially-driven dynamics facilitates maize phosphorus uptake and productivity improvement. *Field Crop Res.* 287:108666. doi: 10.1016/j.fcr.2022.108666

Yu, Z. P., Wang, M. H., Huang, Z. Q., Lin, T. C., Vadeboncoeur, M. A., Searle, E. B., et al. (2018). Temporal changes in soil C-N-P stoichiometry over the past 60 years across subtropical China. *Glob. Chang. Biol.* 24, 1308–1320. doi: 10.1111/gcb.13939

Zhang, J. L., Nie, J., Cao, W. D., Gao, Y. J., Lu, Y. H., and Liao, Y. L. (2023). Long-term green manuring to substitute partial chemical fertilizer simultaneously improving crop productivity and soil quality in a double-rice cropping system. *Eur. J. Agron.* 142:126641. doi: 10.1016/j.eja.2022.126641

Zhang, Y. B., Wang, L., Guo, Z. H., Xu, L., Zhao, H. Y., Zhao, P., et al. (2022). Revealing the underlying molecular basis of phosphorus recycling in the green manure crop *Astragalus sinicus*. *J. Clean. Prod.* 341:130924. doi: 10.1016/j.jclepro.2022.130924

Zhao, J., Chen, J., Beillouin, D., Lambers, H., Yang, Y. D., Smith, P., et al. (2022). Global systematic review with meta-analysis reveals yield advantage of legume-based rotations and its drivers. *Nature Commun.* 13:4926. doi: 10.1038/s41467-022-32464-0

Zhao, Y. J., Chen, X., Shi, Y., Lu, C. Y., Bin, H. U. A. N. G., and Zhao, M. Q. (2013). Impact of fertilization and soil phosphorus status on phosphorus leaching from soil in vegetable greenhouse. *Progress Environ. Sci. Eng.* 610-613, 2968–2973. doi: 10.4028/www.scientific.net/AMR.610-613.2968

Zheng, W., Zhao, Z. Y., Lv, F. L., Wang, R. Z., Wang, Z. H., Zhao, Z. Y., et al. (2021). Assembly of abundant and rare bacterial and fungal sub-communities in different soil aggregate sizes in an apple orchard treated with cover crop and fertilizer. *Soil Biol. Biochem.* 156:108222. doi: 10.1016/j.soilbio.2021.108222

Zhou, G. P., Cao, W. D., Bai, J. S., Xu, C. X., Zeng, N. H., Gao, S. J., et al. (2020). Co-incorporation of rice straw and leguminous green manure can increase soil available nitrogen (N) and reduce carbon and N losses: an incubation study. *Pedosphere* 30, 661–670. doi: 10.1016/S1002-0160(19)60845-3

Zhou, G. P., Gao, S. J., Chang, D. N., Rees, R. M., and Cao, W. D. (2021). Using milk vetch (*Astragalus sinicus* L.) to promote rice straw decomposition by regulating enzyme activity and bacterial community. *Bioresour. Technol.* 319:124215. doi: 10.1016/j.biortech.2020.124215

Frontiers in Microbiology

Explores the habitable world and the potential of microbial life

The largest and most cited microbiology journal which advances our understanding of the role microbes play in addressing global challenges such as healthcare, food security, and climate change.

Discover the latest Research Topics

See more →

Frontiers

Avenue du Tribunal-Fédéral 34
1005 Lausanne, Switzerland
frontiersin.org

Contact us

+41 (0)21 510 17 00
frontiersin.org/about/contact